Ricarda Rosemann

Impact of Regulatory Requirements for Emission Trading Systems: An Analysis in a Stochastic Control Model

Datum der Disputation:

25. November 2022

Gutachter

Prof. Dr. Jörn Sass
Technische Universität Kaiserslautern

Prof. Dr. Ralf Wunderlich
Brandenburgische Technische Universität Cottbus – Senftenberg

Vom Fachbereich Mathematik der Technischen Universität Kaiserslautern zur Verleihung des akademischen Grades Doktor der Naturwissenschaften (Doctor rerum naturalium, Dr. rer. nat.) genehmigte Dissertation.

DE-386

Acknowledgments

First of all, I would like to thank Professor Jörn Sass for his dedicated and competent supervision of my thesis. The opportunity to work on a topic that I care so deeply about meant a lot to me. I am grateful for his guidance in choosing my topic and for the many discussions on model design decisions or the caveats of various proofs. His advice – sometimes only consisting of a small hint – was always valuable to point me in the right direction, leading to a significant progress in my work.

This PhD project would not have been possible without the financial support of the German Scholarship Foundation (Studienstiftung des deutschen Volkes), which is gratefully appreciated. At the same time, I am thankful to have been able to participate in various seminars, which were of significant help in my personal development. I was particularly happy to attend a PhD seminar (Doktorandenseminar) in Berlin, providing me with valuable insights on my work from other disciplines.

I thank my colleagues in the financial mathematics group for the always friendly atmosphere, for enriching our weekly breakfast meetings and for diverting breaks enjoyed together. Furthermore, it always was interesting to learn about other PhD students' topics in the weekly PhD seminar.

Finally, I am very thankful that I could always count on the support of my friends and family; and I was happy to see their interest in my work. In particular, I would like to thank Florian, Marek, Steffen and Tobias for their help and their insights on my thesis.

Contents

Introduction

Global warming presents an enormous and unprecedented challenge to humanity: The changes made by mankind to the earth's atmosphere endanger the stability of various natural ecosystems and the health and well-being of the human population all over the world. Greenhouse gases such as carbon dioxide (CO_2), methane, or nitrous oxide keep radiation energy within the atmosphere that would have otherwise escaped out to space. In this way, they contribute to warming the earth's surface. Industrial production and various other human activities led to an increase in greenhouse gas concentrations in the atmosphere, which in turn resulted in higher surface temperatures; by now the global mean temperature is approximately 1°C higher than before the industrialization of the economy. These higher temperatures have severe impacts: They increase the frequency and intensity of weather extremes and they lead to rising sea levels and melting glaciers. In the course of this century, temperatures are projected to increase further, which will aggravate all these effects. However, the extent of future global warming strongly depends on present and future greenhouse gas emissions. Hence emission reductions are crucial to limit the impacts of global warming.

As greenhouse gas emissions take their effect globally, effective emission reductions can only be achieved by international cooperation. The first international agreement to address global warming was reached in form of the Kyoto Protocol, signed in 1997; it has now been replaced by the more extensive Paris Agreement of 2015. These treaties require signatory countries to reduce their emissions by a given amount. To achieve this, many governments have resorted to market mechanisms, with the most prominent option being the introduction of an Emission Trading System (ETS). In an ETS, the regulator fixes the amount of emissions that is supposed to be allowed in a given time period. In accordance with this amount, emission allowances are allocated to companies underlying the system; allowances are tradeable, so that emission reductions take place where it is the cheapest. To enforce compliance with the system, a penalty needs to be paid for any emissions not covered by an allowance. In the European Union such a system (EU ETS) is in operation already since 2005, making it one of the earliest and still one of the largest ETS' worldwide. Despite numerous problems and concerns, studies show that the EU ETS has succeeded in achieving its goals at least partially; at the same time, it has been reformed several times to improve its performance.

To analyze an ETS and to predict the behavior of companies underlying the system, modeling approaches have proven to be an important tool. Early deterministic models of an ETS are presented for example by Montgomery [Mon72] or Rubin [Rub96]. More recently, stochastic models have been introduced to reflect the uncertainty in crucial quantities such as the emissions in the absence of the ETS. At the core of essentially every ETS model, a minimization problem needs to be solved; in a stochastic setting this can be done by applying a stochastic control approach. Carmona, Fehr and Hinz [CFH09] follow this

strategy in a discrete-time setting, while Kollenberg and Taschini [KT16] as well as Seifert, Uhrig-Homburg and Wagner [SUW08] proceed in a similar way in continuous time.

Extending the work of Seifert et al., in this thesis we apply a stochastic control approach to construct a model of the EU ETS. We provide the theoretical foundation of the model; furthermore, we introduce an extension to a multi-period setting and incorporate the auctioning of allowances in the model. In establishing an ETS, the regulator aims to achieve a significant reduction of emissions, while providing a clear price signal to incentivize investments in clean technology. Therefore, our main focus is to study resulting emissions and the allowance price development. In numerical simulations we vary several regulatory settings and analyze their impact on the performance of the ETS.

This thesis is structured as follows. In Chapter 1 we present general background information on global warming and explain the mechanism of an ETS, with a particular focus on the EU ETS. Furthermore, we discuss the literature on various modeling approaches, including all references mentioned above. In Chapter 2 we introduce a model of an ETS with one compliance period, modeling the uncertainty of the emissions by a stochastic differential equation (SDE). For a simple variant of the model we are able to show that the Hamilton-Jacobi-Bellman (HJB) equation arising from the stochastic control approach delivers the optimal emission reduction. Furthermore, we provide a theorem to ensure existence and uniqueness of an SDE solution in a specific setting where the coefficient functions of the SDE are not continuous at final time. Under similar assumptions, we show that the Euler-Maruyama scheme converges to the solution. In our ETS model, we describe the resulting emissions by an SDE with such a discontinuity; these theorems allow us to conclude that this SDE has a solution, which can be approximated by the Euler-Maruyama scheme. We then provide an extension of the model to several time periods in Chapter 3. Here we introduce two different approaches: In a multi-period setting, the allowance price of the next time period needs to be taken into account in the cost minimization problem. In the first approach, we make the simplifying assumption that the value anticipated for this price is constant throughout each time period. This allows us to proceed similarly as in the one-period case and, accordingly, we obtain similar theoretical results. The second approach is to introduce an additional stochastic process enabling us to model the anticipation of the allowance price in the next time period with more precision. In Chapter 4 we include the auctioning of allowances in our model and show that this does not impact the resulting emissions and the allowance price. Chapter 5 discusses the numerical methods applied to solve the model and the parameters chosen in simulations. In Chapter 6 we present numerical results of both the one-period and the multi-period model. We vary several model parameters to study their impact on the outcome in the ETS. Finally, in Chapter 7 we discuss the findings of this thesis. An appendix provides auxiliary computations and further numerical results.

Chapter 1

Emission Trading Systems and Modeling Approaches

The advancement of global warming and the dangers it poses to human societies and the world's ecosystems require a drastic reduction of greenhouse gas emissions all over the world on a comparably short time scale. At the same time, in order to avoid welfare losses, these reductions should be achieved at the lowest possible economic costs. Emission trading systems have become a widely used policy tool to combine these two goals. One of the first and at the same time one of the largest ETS' is the EU ETS of the European Union. While this system has proven to achieve its purpose to some extent, it has also suffered from structural problems and inefficiencies. As a result, the EU ETS has seen several revisions in the course of its existence. Thus the question of how to choose the regulatory framework is still open to debate. ETS models are an important tool to study the impacts of an ETS and to analyze design choices made by the regulator. Since emissions depend on non-deterministic parameters, such as weather or the economy, it is natural to view them as a stochastic quantity. This suggests to employ a stochastic approach in modeling an ETS.

In this chapter, we first present some background information on global warming and its consequences as well as the corresponding political implications. Then we introduce the concept of an ETS; furthermore, we discuss the EU ETS and the evidence on its efficacy in some detail. Finally, we provide an overview on various approaches to formulate a model of an ETS. We specifically focus on models following a stochastic control approach.

1.1 The Advancement of Global Warming

The scientific evidence for global warming and its cause lying in human activity has been strong for decades now. Nevertheless, recent years have seen an increasing public interest in global warming and the need of countermeasures. On the one hand, weather extremes and related catastrophes such as wildfires, heat waves, droughts, but also heavy rainfall and flooding seem to become more and more frequent. On the other hand, especially young people have acknowledged the threat of continuing global warming and have formed a global protest movement demanding immediate action, strongly supported by scientists, environmental organizations and various other social groups.

1.1.1 The Greenhouse Effect

Since the industrial revolution humanity has increasingly influenced the composition of the earth's atmosphere; in particular the concentration of carbon dioxide (CO_2) has drastically increased due to the burning of fossil fuels such as coal, oil, and gas. Since 1958 the CO_2 concentrations have been measured at Mauna Loa in Hawaii, delivering the curve shown in Figure 1.1. The crucial property of CO_2 in this context is its ability to absorb infrared

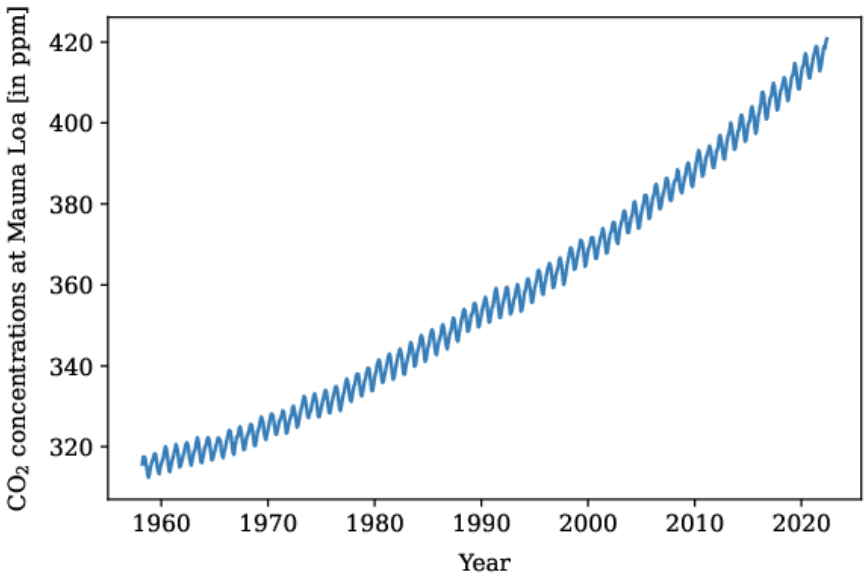

Figure 1.1: CO_2 concentrations measured at Mauna Loa in Hawaii. Source: Scripps Institution of Oceanography [Kee+01].

(IR) radiation. The general mechanism works as follows: Molecules absorb radiation of IR wavelengths by initiating vibrations of the molecule's bonds. This can only occur if the vibration induces a change in the electrical polarization within the molecule, i.e. if the spatial distribution of partial charges is changed. CO_2 is formed by one carbon and two oxygen atoms. Since the oxygen atoms are more electronegative than the carbon atom, the electrons forming the bond between the carbon atom and each of the oxygen atoms are closer to the oxygen atoms, thus they have a negative partial charge whereas the partial charge of the carbon atom is positive. In its ground state the molecule is symmetric, so the charges are equally distributed and thus it is not polar. But vibrations may annihilate this symmetry, inducing a polarization; therefore CO_2 may absorb IR radiation. The main constituents of the atmosphere, oxygen and nitrogen molecules, both cannot absorb IR radiation, since they each consist of two atoms of the same element, thus charges are equally distributed. Other molecules present in the atmosphere that may absorb IR radiation include methane, nitrous oxide, and halogenated gases. Absorption of IR radiation is also the mechanism behind IR spectroscopy, hence this procedure is usually described in physical chemistry textbooks such as [AD13].

Although the percentage of IR absorbing molecules in the atmosphere is comparably low, they have a large impact. This can be seen by computing the theoretical temperature for the earth's surface from the radiation coming in from the sun, as described by Hites

et al. [HRW17][1]: We first need to take into account that a certain percentage of the incoming radiation is directly reflected back to space, in particular from white surfaces such as clouds and ice sheets. This percentage is usually called the albedo and is assumed to be approximately 30% for the earth on average. If we assume that the remaining 70% are absorbed by the earth's surface, we may compute the theoretical temperature from the energy coming from the sun as 255°K or -18°C. This is considerably colder than the actual global mean temperature at about 280°K or 15°C and would have been too cold to support the development of life[2]. The difference between the theoretical and the actual temperature is due to the greenhouse effect: The radiation reaching the earth's surface is absorbed and in accordance with Planck's law emitted largely as IR radiation. Gases like CO_2 then absorb this radiation and emit it again, usually also at IR wavelengths. But this re-emission may occur in any direction; thus, partly this radiation is still directed to space, but partly it is also directed back at the earth. In this way molecules that may absorb IR radiation keep part of the energy that would otherwise have been emitted back to space within the atmosphere, thus warming the earth's surface. This resembles the effect of a greenhouse, therefore this procedure is known as the greenhouse effect and the gases causing it are called greenhouse gases.

1.1.2 Global Warming

While the greenhouse effect was crucial for the development of life in the first place, the increasing concentrations of greenhouse gases such as CO_2, but also methane and nitrous oxide, now cause the global surface temperature to increase further, thus leading to global warming. Since 1990 changes in the earth's climate are reported by the Intergovernmental Panel on Climate Change (IPCC); they regularly assess the physical changes of the climate system, their impacts on human societies and natural ecosystems, and how governments and the public may respond. In their latest report on the physical science basis of global warming [IPC21] they describe that the average CO_2-concentration has reached 410 parts per million (ppm), compared to 280 ppm at pre-industrial levels [IPC92], while the average global surface temperature in the last decade, i.e. between 2011 and 2020 was 1.09°C higher than in the period from 1850–1900, which is the usual temperature reference for pre-industrial levels; this is also illustrated in Figure 1.2. These numbers for the CO_2-concentration and the average surface temperature are unprecedented to the scale of hundreds of thousands of years. The CO_2-concentration is higher than at any time point in the last two million years; the last warm-period of at least several centuries reaching roughly the same temperatures was 125 000 years ago. Moreover, every single one of the last four decades has been warmer than any decade before that since 1850. Additionally, these changes occur at a speed as it possibly was not seen before in human history: Since 1970 the temperature has increased faster than in any comparable time period within the last 2000 years. As a consequence, glaciers have been retreating globally since the 1990s and the area of Arctic sea ice has decreased. The oceans have warmed since the 1970s, they have seen an increase in acidity, and mean sea levels have risen by 0.2 m since 1901, where the speed of sea level rise has drastically increased in the past decades.

These changes have led to more frequent and more intense weather extremes. The

[1] These computations can be found in [HRW17] on pages 77–82.

[2] To be more precise, the formation of life might still have been possible in much lower temperatures. But the development of the species and ecosystems observed today strongly relies on the actual higher temperatures.

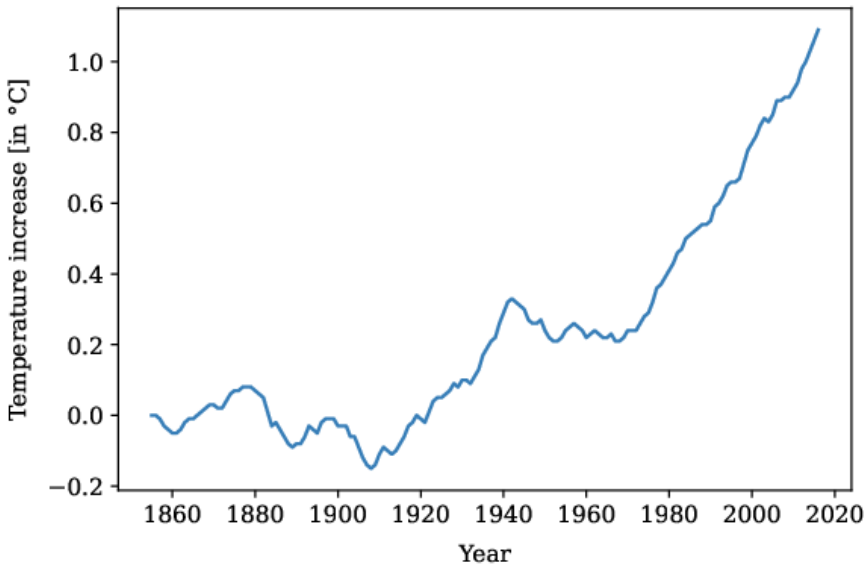

Figure 1.2: Global surface temperature relative to the average in 1850-1900, smoothed per decade. Source: Intergovernmental Panel on Climate Change [Gil+21].

news has reported a large number of such events in the past few years; examples include the wildfires in 2019 in Australia, the Amazonian rain forest, and Siberia, extreme heat waves as this year (2022) in India and Pakistan, and droughts as in East Africa (e.g. reported in [Hor22] and [Hof21]). Very recently, in July this year, Western Europe has suffered from extreme heat, which has caused numerous wildfires [tag22]. Heavy rainfalls and resulting floods have occurred this year in Brazil and in Australia (as reported e.g. in [Bod22]). In Germany the summers have become notably hotter and drier; the most predominant weather extreme in Germany has been the heavy rain and the following flood in the Ahrtal in 2021, which has caused massive damages and claimed more than a hundred lives [Wei22].

These events are in line with the IPCC report [IPC21]. It documents more frequent hot extremes, such as heat waves, and claims that some recently occurring extreme events would have been very unlikely without human influence. According to the report, the frequency and intensity of heavy precipitation events have increased, but on the other hand, some regions have seen an increase in droughts; tropical cyclones have become more dangerous and wildfires more common. A second stream of IPCC reports on the impacts and risks of global warming [IPC22] describes that global warming has already induced severe damages to various ecosystems with more and more irreversible losses. Species have been moving polewards and on land also upwards, the seasonal timing has shifted. Locally, species are lost and in some cases go extinct. The previously seen growth in agricultural productivity has slowed down and warming and acidification of the ocean impact fishery productivity, which presents a threat to food security. Millions of people are already in danger of acute food insecurity. At the same time, diseases transmitted by water, food, or various vectors such as insects occur more often and heat-related mortality is increasing. Moreover, extreme weather increasingly affects displacement and migration.

All these changes are predicted to be aggravated in the future; and the higher the temperatures will rise, the more drastic these effects will be. The IPCC has modeled

several future emission pathways and estimated the corresponding long-term[3] temperature increase. In case of further increasing CO_2-emissions the temperature rise in comparison to pre-industrial levels is predicted to be 4.4°C (if current emissions double by 2050) or 3.7°C (if current emissions double by 2100). In an intermediate scenario of roughly constant emissions until 2050 followed by a decrease the rise in temperature still reaches 2.7°C above pre-industrial levels. If however emissions decrease from now on, global warming can be limited to 1.8°C (if net zero emissions are reached around 2075) or to 1.5°C (if net zero emissions are reached around 2050).

It is predicted that every increase in temperature of 0.5°C increases the intensity and frequency of hot extremes, heavy precipitation, and regional droughts; a higher temperature will also lead to more severe tropical storms with higher wind speeds. Flood damages are expected to be about three times higher at global warming of 3°C than at 1.5°C; warming of more than 2°C will severely endanger food security. Diseases will probably spread further and extend their seasons or their geographic range. Furthermore, cities and infrastructure especially at the coast or in hot areas are threatened; approximately a billion people are expected to be at risk from coastal hazards by 2100 and the continuing rise in sea level is an existential danger to small islands and low-lying coasts. As a result of extreme weather events, people will be forced to migrate.

In addition, tipping points of the climate system may result in greatly accelerated global warming as soon as a certain point is reached. For example, the melting of the large ice sheets in Antarctica would reduce the albedo of the earth, so that less radiation from the sun is reflected, thereby increasing global warming. It is very difficult to predict at which temperature levels these tipping points are reached. The IPCC denotes such a scenario as a low-likelihood event but stresses that higher global warming makes these events more probable. However, some scientists believe that some tipping points might already be close: In a comment, Lenton et al. [Len+19] report that for instance the West Antarctic ice sheet is already in grave danger of collapsing, and they see similar threats to the East Antarctic and the Greenland ice sheet.

1.1.3 International Cooperation against Global Warming

The IPCC reports stress that a reduction of greenhouse gas emissions is of great importance. This can only be achieved by political intervention; however in political debates global warming and possible countermeasures are often met by high controversy. Moreover, the reduction of greenhouse gas emissions requires a global response, thus worldwide cooperation is indispensable.

Global warming became an increasing concern in international politics in the late 1980s. As a consequence, the United Nations Framework Convention on Climate Change (UNFCCC) was initiated on the Earth Summit in 1992 in Rio de Janeiro and came into force in 1994 [Jac07]. One year later, the parties to the convention met for their first conference, the so-called conference of the parties (COP); these conferences have been held yearly[4] since then and are commonly known as the climate conferences. The third of these conferences, COP3 in Kyoto, led to the agreement on the Kyoto Protocol [UN97]. Therein most industrialized countries committed to specific emission reductions for the years 2008 to 2012 in comparison to their emissions in 1990; the parties to the protocol were allowed to trade with their reduction commitments. The overall reduction goal was

[3] Long-term in this case refers to the time period from 2081 until 2100.

[4] with the exception of the year 2020, where the conference was postponed due to the Covid-19 pandemic

satisfied and even over-accomplished [SMB16]; some of the reduction can be attributed to the collapse of heavy industries in former Soviet-Union countries and the economic recession in 2008 probably also had an impact, whereas meaningful efforts were accredited for example to the European Union and Japan [Gru16]. Nevertheless, global emissions have increased in the corresponding time period [WBb]. This might be caused by the fact that the USA have never ratified the protocol and Canada has withdrawn before the end of the commitment period; furthermore, all developing and newly industrialized countries were not assigned a reduction target. The reduction targets for a second commitment period from 2013 to 2020 were negotiated in 2012 at the COP in Doha [UN12]. This agreement only entered into force on December 31, 2020, when finally sufficiently parties to the Kyoto Protocol had accepted it.

As a successor to the Kyoto Protocol, at the COP21 in Paris a new agreement was adopted, which came to be known as the Paris Agreement [UN15]. It formulated the goal of "Holding the increase in the global average temperature to well below 2°C above pre-industrial levels and pursuing efforts to limit the temperature increase to 1.5°C above pre-industrial levels". In contrast to the Kyoto Protocol, the Paris Agreement requires all parties to the agreement to comply with emission goals. These goals are set by the countries themselves in so-called nationally determined contributions, which should "reflect its [the country's] highest possible ambition". The Paris Agreement entered into force on November 4, 2016, when sufficiently many parties had ratified it. The progress of parties within the agreement is evaluated at global stocktakes every five years; the first such stocktake started in June 2022 [UN22].

The inclusion of almost all countries in the world in the Paris Agreement and the resulting commitment to address global warming has been viewed as a milestone by many. On the other hand, concerns have been raised that the reduction targets set by parties to the Paris Agreement are not sufficient to achieve the goal of limiting global warming to "well below 2°C": Rogelj, den Elzen, Höhne, Fransen et al. [Rog+16] assess the nationally determined contributions and find that, in compliance with these, global warming is likely to reach about 3°C.

1.2 Emission Trading Systems

The controversy about mitigation measures to address global warming often arises from adverse economic interests. At the same time, as many other environmental damages, global warming can be seen as an externality and thus represents a market failure: Global warming leads to costs through the effects described above, but these costs are not paid by the agents causing them, i.e. by emitters of greenhouse gases. As a result, market mechanisms as a tool to reduce greenhouse gas emissions have become increasingly popular. The overall idea of such mechanisms is to give emissions a price, thus resolving the externality of unpaid costs. At the same time, the details of where and when emissions are reduced are left to usual mechanisms of free markets. A particular simple approach to this is the so called Pigou tax, as proposed already in 1920 by Pigou [Pig13]: The price of an environmental good – such as CO_2-storage capacities of the atmosphere – is simply set by the government in form of a tax. As soon as emissions have a price, companies have an incentive to reduce their emissions; the reduction of emissions is often referred to as abatement. Of course, in this case the resulting emissions strongly depend on the value chosen for this tax; already intuitively it should be clear that a higher tax leads to less emissions, since companies will put more effort into the abatement of emissions. More

precisely, companies will reduce emissions until their marginal costs of emission abatement are equal to the tax. While this system provides a clear price signal, the resulting emissions are difficult to predict. An alternative avoiding this problem is given by emission trading systems.

1.2.1 Mechanism of an Emission Trading System

Instead of fixing the price of emissions, in an Emission Trading System (ETS) the desired total emissions are fixed, whereas the price is left to develop on the market. The mechanism of an ETS, described for instance by Sturm and Vogt [SV18] or by Siebert [Sie08], is as follows: The government or the corresponding regulatory institution decides on the amount of emissions to be allowed in the course of a certain time period, known as the emission cap. Then, in accordance with this amount, emission allowances are handed out to companies underlying the system; these can be given out for free or they can be sold at an auction. Importantly, the allowances are transferable, so companies may trade with them. In this way a market for emission allowances develops where the price of emissions forms. In the course of the respective time period companies will produce emissions and trade with allowances, where each company will abate emissions until their marginal abatement costs equal the market price of emission allowances. If their allocated emission allowances are insufficient to cover remaining emissions, they will buy additional allowances at the market, whereas if they have allowances they do not need, they will sell at the market. In this way, emission abatement will be shifted to companies where this can be done at lowest costs. At the end of the predefined compliance period the regulator evaluates whether each company holds enough allowances to cover their overall emissions. To enforce the need of having an allowance for emitting CO_2, a penalty needs to be paid for emissions for which this does not hold. A crucial policy decision concerns the transferability of allowances between compliance periods: The transfer of allowances to the subsequent time period is known as banking, whereas transferring allowance from the subsequent period to the current one is called borrowing.

The goal of a policy to address global warming is clearly to reduce greenhouse gas emissions and usually governments set themselves fixed reduction targets as for example given in the Kyoto Protocol but also in the Paris Agreement. Thus ETS' have the definite advantage that they fix the resulting total emissions; therefore the effect of an ETS is easier to predict than of a Pigou tax. On the other hand, in this case it is the allowance price that is not given in advance, resulting in a less clear price signal, which makes it harder for companies to plan for instance their investment in low-carbon technologies. Moreover, also in an ETS it is possible that the actual emissions surpass the predefined amount: If the marginal abatement costs at the abatement level necessary to comply with the emission cap exceed the penalty, then companies will pay the penalty instead.

1.2.2 The Emission Trading System of the European Union

The first ETS was introduced in 1995 in the USA; this was not yet intended to address greenhouse gases but to reduce acid rain: For this purpose, allowances were distributed and traded for the emissions of sulfur dioxide and nitrogen oxides. This system decreased sulfur dioxide emissions in 2016 compared to 1990 by 90% as reported by the US Environmental Protection Agency [EPA16]. A mechanism similar to an ETS applying to greenhouse gases was in principle incorporated in the Kyoto Protocol, whose parties were allowed to trade with the amount of emissions they were entitled to. The first fully operational

ETS, covering CO_2-emissions on the company level, was introduced 2005 in the European Union; still today it is one of the largest ETS' worldwide. As reported by the International Carbon Action Partnership [ICA] there are now 25 ETS' in operation including a fairly recently introduced national ETS in China; in total these systems cover about 17% of the world's greenhouse gas emissions.

Structure of the EU ETS

The EU ETS has initially been established to ensure compliance of the EU member states with the Kyoto Protocol, with its regulatory framework being set up by Directive 2003/87/EC of the European Parliament and of the Council [EU03]. As explained by the Commission [ECa], it is structured in several phases: The first one from 2005 to 2007 served as a pilot phase to gain experience on price formation and set up the required infrastructure to track emissions. At this point, the EU ETS only covered CO_2-emissions from the power sector and energy-intensive industries, amounting to approximately 40% to 50%[5] of total CO_2-emissions in the EU. In the first phase allowances were almost entirely given out for free, following an allocation mechanism which was based on historical emission data of the companies underlying the system. The penalty for a ton of emissions not covered by an allowance was set to 40 Euro. Importantly, in the case of non-compliance companies were obliged to surrender the missing allowances in the subsequent phase. Unused allowances expired at the end of the first phase, thus banking or borrowing was not allowed. A key challenge was to determine the amount of allowances to be handed out such that companies could handle the required abatement, but the system would still lead to a reduction in emissions.

The second phase from 2008 until 2012 was aligned with the first commitment period of the Kyoto Protocol. Based on the experience from the first phase, the amount of emission allowances was reduced; furthermore, the penalty was increased to 100 Euro and a small share of 10% of the allowances was auctioned. At the same time, unused allowances could be transferred to the next phase, so banking was allowed. The third phase lasted from 2013 until 2020 and thus was in line with the second commitment period of the Kyoto Protocol. It saw an extension of the ETS to further sectors such as the chemical industry and the inclusion of the greenhouse gases nitrous oxide and perfluorocarbons (as implemented by Directive 2009/29/EC [EU09]). The fraction of auctioned allowances was increased to 57%. In addition, there was a structural change: In contrast to the previous phases, the allowance cap was no longer set by each member state for itself; instead an EU-wide cap of allowances applied. For the fourth and current phase from 2021 until 2030 the decrease of the cap was accelerated and further adaptations were made to address several of the issues we will discuss below. As a consequence of the EU's commitment to reduce greenhouse gas emissions by 55% in comparison to 1990 by the year 2030, a legislative proposal to further strengthen the EU ETS is currently negotiated among EU institutions. The EU ETS legislation might be again revised in accordance with the results of the global stocktake, conducted in the course of the Paris Agreement [ECd] as mentioned above.

[5] This figure was estimated from total CO_2-emissions in the EU in 2005 as given in [EEA07] and verified emissions in the EU ETS, given by [EEA].

Empirical Evidence on the EU ETS

Being the first fully operational ETS to cover greenhouse gas emissions and at the same time being of remarkable size, the EU ETS naturally has attracted research interests from various directions. Several authors, such as Laing et al. [Lai+14] and Egenhofer et al. [Ege+11], provide a broad literature review to analyze the effects of the EU ETS, as well as the initial issues and structural problems that were observed. One key question surrounding the EU ETS is whether it has indeed led to the abatement of greenhouse gas emissions. Typically, abatement is viewed as the difference between the actual emissions within the EU ETS and the emissions that would have occurred without the EU ETS, usually referred to as the counterfactual or the Business-As-Usual (BAU) emissions. This already highlights the main challenge in assessing abatement: While the actual emissions are verified by the EU and published, the BAU emissions cannot be observed and therefore need to be estimated.

Ellerman and Buchner [EB08] make use of the historic emission baseline data that was collected by member states prior to the start of the EU ETS; this data collection was intended to help set up the initial cap by providing an estimate of emissions from sectors underlying the EU ETS. Ellerman and Buchner remark that this data may be biased, since it was mainly obtained from the greenhouse gas emitting installations themselves, which had an incentive to inflate their actual emissions. From this data, Ellerman and Buchner construct the BAU emissions for the years 2005 and 2006 by computing the effect of economic growth, taking into account the estimated decrease in carbon intensity of economic activity. They obtain an estimate of 50 to 100 mega tons (Mt) of yearly abated emissions in 2005 and 2006, roughly corresponding to 2.5% to 5% of the emission cap[6].

Anderson and Di Maria [AD11] study the first phase of the EU ETS based on sector-wise emission data provided by Eurostat. From this data set they obtain historical emission data for the sectors underlying the EU ETS and fit a regression model describing CO_2-emissions as dependent on the economic activity of the EU ETS sectors, on energy prices and weather factors. They then use this model to estimate the BAU emissions and compare the results with the verified emissions, finding an estimated net abatement between 2005 and 2007 of 173.6 Mt of CO_2. This amounts to 2.8% of the emission cap of the first phase[7].

Again a different approach was taken by Delarue, Ellerman and D'haeseleer [DED10], who restrict themselves to the power sector. They use a European electricity modeling system called "E-Simulate", which they adapt by computing emissions for each modeled power plant based on fuel use and fuel type. Furthermore, they include the price of emissions as additional costs. Then they simulate the electricity system for the years 2005 and 2006 with the actual allowances prices on the one hand and with an allowance price of zero on the other hand, thus obtaining the BAU emissions. By comparing the results, they conclude that the abatement in the power sector was 34 Mt in 2005 and 19 Mt in 2006, corresponding to 1.75% and 1.0% of the total cap and to 3% and 1.7% of emissions in the power sector. They also compare the results from the simulation with verified emissions from the power sector and find very high agreement, supporting the validity of their model. These three early studies on abatement thus reach similar results by very different methodologies.

[6] The cap of 2005 and 2006 amounts to roughly 2100 Mt as given in [AD11].

[7] The emission cap of the years 2005 to 2007 amounts to 6246.6 Mt in total as can be computed from data provided by Anderson and Di Maria [AD11].

For the second phase of the EU ETS an assessment of the abatement is even more difficult, as the recession in the wake of the financial crisis further complicates the estimation of the BAU emissions. Egenhofer et al. [Ege+11] extend the analysis of Ellerman and Buchner [EB08] to the years 2008 and 2009. From a contribution by Ellerman, Convery and Perthuis [ECP10] they take the projected rate of change in emission intensity[8] and compare this to the observed emission intensity, first for the years 2006 and 2007. The difference is then attributed to abatement, amounting to a decrease of emission intensity of 1.1% and 0.9% in 2006 and 2007. For the years 2008 and 2009 they take the rate of change in emission intensity in 2006 and 2007 of about 2% as the projected rate of change in emission intensity; they obtain emission intensity reductions, assumed to be caused by abatement, of 1.3% in 2008 and of 5.4% in 2009.

Another study by Bel and Joseph [BJ15] builds on the work of Anderson and Di Maria [AD11]: By applying a similar regression approach, they aim to separate the effect of the EU ETS from the effects of the recession. They modify the model of Anderson and Di Maria by introducing independent variables accounting for the presence of the EU ETS and the gross domestic product (GDP) or alternatively the occurrence of a crisis; they construct the value of the EU ETS variable from the difference in emissions between EU ETS sectors and sectors not underlying the EU ETS. Based on this model they compute different estimates, partly omitting either the EU ETS variable or the GDP/crisis variable. By comparison they conclude that only a small fraction of total abatement can be attributed to the EU ETS, whereas the remainder was caused by the recession. Importantly, they define abatement as the difference in emissions between 2005 and 2012, thus considering the reduction in yearly emissions rather than the difference to the BAU emissions. Following this definition, total abatement between 2005 and 2012 was 294.5 Mt, of which they only attribute 33 to 41 Mt to the EU ETS.

Next to direct emission reductions, a market based instrument, such as the EU ETS, with a price on emissions aims to provide an incentive to invest in clean technologies, i.e. technologies with low greenhouse gas emissions. As summarized by Laing et al. [Lai+14] several survey-based studies have addressed this issue, typically finding that there is some impact of the EU ETS on investment and innovation but not on a large scale. Rogge and Hoffmann [RH10] analyze the effect of the EU ETS on innovation in the German power sector by conducting 42 interviews with experts from power generators, technology providers, authorities, and other relevant groups. They find that the EU ETS has accelerated the innovation process and in case of coal-fired plants has a main impact on research and development, with a focus on Carbon Capture and Storage technologies[9] and efficiency of energy use. Moreover, the EU ETS has caused companies to take climate policies more seriously and has led to an involvement of the top management in emission-related issues. On the other hand, the allowance price appears to be still too small to motivate large investment decisions like switching to fuels which produce less emissions[10]. Another study conducted by Anderson, Convery and Di Maria [ACD11] on companies in Ireland subject to the EU ETS reports several actions undertaken to reduce emissions. Based on a questionnaire returned by 27 Irish companies with installations underlying the EU ETS and

[8] In this context, the emission intensity is given as the emissions relative to the gross domestic product (GDP).

[9] This technology, which is not yet applied in practice, serves to capture emissions before they are released into the atmosphere and afterwards transfers them to a suitable storage.

[10] Usually this switch is from coal to gas, as the latter causes less emissions for the same amount of energy produced.

interviews with seven of these, they report that 48% of responding companies state that they are using new machinery or equipment that decreases their emissions. Furthermore, 74% claim that they have undertaken procedural or behavioral changes. Notably, the interviewed companies reveal that these adaptions were mostly motivated by rising energy prices, with the allowance price and the presence of the EU ETS playing only a minor role. In addition, 41% of the companies report that they have reduced emissions by fuel switching, contrary to the findings of Rogge and Hoffmann. Moreover, 46% of responses report that the EU ETS has influenced the way investments are analyzed. It should be noted that these studies only cover the early phases of the EU ETS; by now the impact on investment might have increased.

In summary, these results document that the EU ETS has at least to some extent succeeded in reaching its goals, with positive impacts already being observed for the pilot phase from 2005 and 2007. In light of the criticism that the system has faced in particular in its early days and the additional problems caused by the economic crisis, this is almost surprising. As reported by Egenhofer et al. [Ege+11], the EU ETS suffered from initial problems, partly caused by the short time scale in which it was set up, including issues with monitoring and verifying emissions, but also a highly volatile allowance price. As

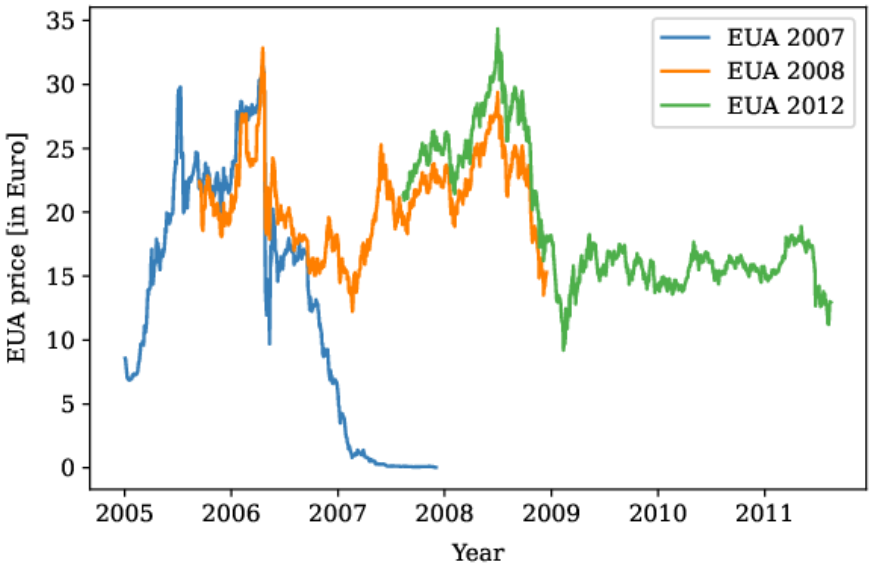

Figure 1.3: Prices of Allowance Futures (EUA) with different maturities. Source: European Environment Agency [EEA11].

can be seen in Figure 1.3, after an increase until early 2006, there was a sharp price drop in April 2006 and eventually a decline to a price of essentially zero for the allowances of phase 1. Moreover, according to Egenhofer et al., the design of the EU ETS led to over-allocation of emission allowances and windfall profits in the power sector. Over-allocation is difficult to quantify: First of all, it is not a priori clear what is meant by over-allocation. As pointed out by Ellerman and Buchner [EB08], this could either refer to having more allowances in the system than BAU emissions; alternatively already the case of an allocation of allowances that does not impose a sufficiently stringent cap can be viewed as over-allocation. While the former definition again requires an estimate of the BAU emissions, the latter would need to be formulated with more precision to be eligible

for analysis. Ellerman and Buchner define over-allocation by considering country-wide net and gross short or long positions of allowances and view over-allocation as the case of a high ratio between the net long and the gross long position in a country. By applying this methodology, they come to the conclusion that over-allocation to the extent of at most 125 million allowances occurred between 2005 and 2006.

Additional profits made by companies due to the presence of the EU ETS are referred to as windfall profits, which are most commonly reported for the power sector. Usually, they are assumed to be generated by passing on the price of allowances to consumers, while the producer has received their allowances for free. The effect of the allowance price on the electricity price has been studied for instance by Sijm, Neuhoff and Chen [SNC06]. They estimate the cost pass-through of allowance prices onto electricity prices by linear regression: They assume that the difference between power price and fuel price depends linearly on the emission-induced costs, i.e. the allowance price multiplied with the emission rate of the respective fuel. By fitting this model to data from the Dutch and the German electricity markets, they obtain a cost pass-through between 60% and 100%. Furthermore, they use a model simulating the behavior of large producers in the electricity market called the COMPETES model to simulate profits with a price of 20 Euro per ton on CO_2-emissions compared to a price of zero. Thus they find additional profits from free allocation of allowances in the range of 5.3 to 7.7 billion Euro generated in Belgium, France, Germany, and the Netherlands. Importantly, the model suggests that companies also make additional profits if all allowances are auctioned instead of allocating them for free.

Lise, Sijm and Hobbs [LSH10] extend this work: They apply the COMPETES EU20 model, an extension of the COMPETES model to 20 EU member states, to various scenarios with either perfect or oligopolistic competition. They use the simulation results to compare the case of no price on CO_2-emissions to the setting with an allowance price of either 20 or 40 Euro per ton. In this way, they obtain cost pass-through rates between 70% and 90%. For an allowance price of 20 Euro per ton they compute that profits increase by 20 billion Euros if 90% of allowances are allocated for free, representing a 27.6% increase compared to the scenario without a price on emissions. As in the previous study by Sijm et al., they find an increase in profits also in case of the auctioning of allowances, amounting to 16 billion Euro, which represents a 21.7% increase. These profits are mainly due to the higher electricity price, which also applies to electricity generators with low emissions.

Revision of the EU ETS

The issues of over-allocation and windfall profits have been addressed in the revisions of the EU ETS for its later phases by increasing the share of auctioned allowances and stricter regulation on allocation. By the start of the third phase the union-wide cap facilitated this; moreover, as pointed out by Egenhofer et al. [Ege+11], from then on the power sector did not receive any allowances for free and had to acquire almost all of its allowances at an auction instead. Nevertheless, also in the third phase some issues remained: Despite the more stringent allocation of allowances in phase 2, the economic crisis has led to a large oversupply of allowances, and since a transfer of these allowances to phase 3 was possible, prices remained low much throughout the third phase, as shown in Figure 1.3; this was also remarked by the European Commission [ECc]. To address this oversupply, the auction of 900 million allowances scheduled for the years 2014 to 2016 was postponed by five years; this procedure was termed “backloading”. Furthermore, a new tool called

the Market Stability Reserve was introduced to be able to handle economic shocks to the system also in the long term [EU15]. The idea is to assess the state of the allowance market via the number of allowances in circulation. If this number is above a certain threshold, allowances are withdrawn from the market and placed in the Reserve; if on the other hand the number of allowances is below another threshold, allowances are released from the Reserve. Thus both an oversupply and an insufficient supply can be addressed. The Market Stability Reserve was revised by introducing a cancellation mechanism which cancels allowances in the Reserve if the amount of allowances stored in the Reserve is too large. Moreover, this revision included a further tightening of the emission cap by increasing the annual reduction to 2.2% [EU18]. The recent price development shown in

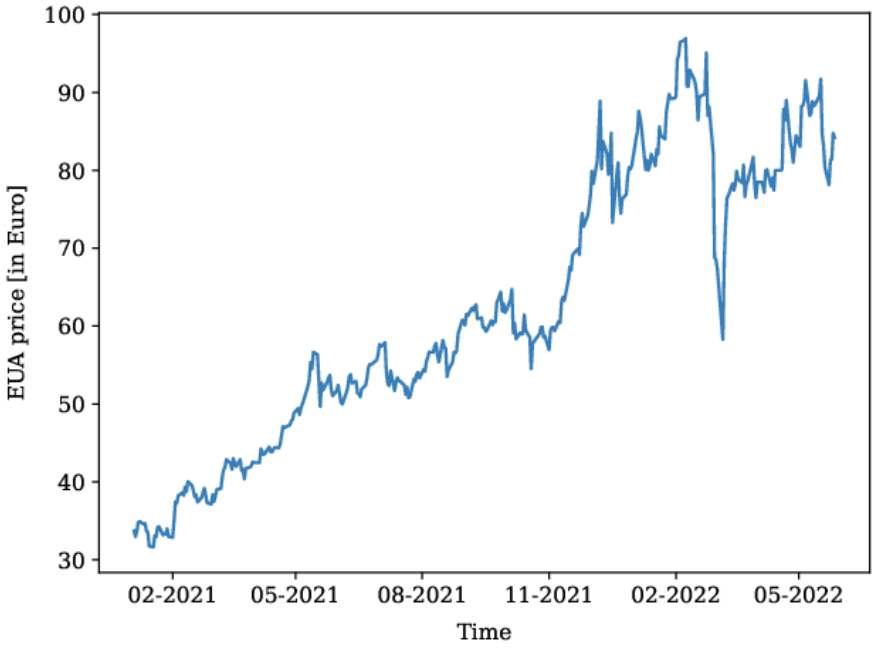

Figure 1.4: Recent price development of an allowance future with maturity in 2022. Source: EMBER [Em22].

Figure 1.4 indicates that these changes probably have been successful: Allowance future prices have risen to a value of about 80 Euro per ton, despite the shocks to the economy caused by the Covid-19 pandemic and the ongoing war of Russia against Ukraine. Due to the resulting shifts in the energy market, the war might on the other hand have been a factor in causing these high prices.

The rise of the allowance price might also be influenced by the ongoing legislative procedure to further revise the EU ETS as a reaction to the EU's raised climate ambitions in course of the European Green Deal. In July 2021 the European Commission proposed a revision of the EU ETS, including a yearly reduction of the cap by 4.2% [EC21]. The European Parliament reached a decision on this proposal in June 2022; the Parliament decided to further tighten the cap by setting a yearly reduction that rises to 4.6% by 2029 [Erb22]. In the next step, an agreement between the Parliament, the Commission, and the Council needs to be found. But already the discussion on a further tightening of the cap may raise the allowance price since it causes agents to expect a shortage of allowances in the future.

1.3 Modeling Approaches to Emission Trading

As explored above, empirical analysis of an ETS – and of many other policy instruments – is challenging, since the case of not implementing the system cannot be observed. Furthermore, before introducing such an influential policy measure, there is a demand for predictions on the impacts that this measure will have. The same applies to any substantial changes in the regulatory framework of the system. Thus ETS models are an important field of research and play a large role in their analysis. We will start by introducing the earliest ETS models; the more recent literature is largely based on this early work. We will then consider three different directions of ETS modeling approaches: The literature on recent developments and adaptations in the EU ETS and on allowance price models will be discussed in brief. We will explain several models based on stochastic control methods in more detail, thus arriving at the work which forms the foundation of this thesis.

1.3.1 Early Models

The first model of an ETS was introduced already in 1972 by Montgomery [Mon72], long before such systems were implemented in practice. He proposes a static and deterministic model of a general pollution control system, which aims to restrict pollution to a certain level at several locations. He considers a finite number of firms and first formulates the problem to minimize total costs of all firms to comply with the pollution constraint; he assumes that the cost of emission abatement is convex. This problem, which he calls the total joint cost minimum problem, can be seen as the minimization performed by a representative agent with full information. He shows that a solution to this problem exists. Then he explores two different approaches to introduce a system of tradeable allowances, which are called licenses in his model: In the first, firms are allocated location-specific licenses to pollute, meaning they are allowed to pollute the given location. Since pollutants can spread, this does not necessarily coincide with producing emissions at that location. Montgomery defines a market equilibrium as the distribution of emissions and licenses among the firms that minimizes costs for each firm under the constraints imposed by their licenses, with the additional condition that the market of licenses clears. He shows that such an equilibrium exists and that it constitutes a solution to the total joint cost minimum problem if the allocation of licenses is chosen in line with the pollution restriction. The second approach is to construct a market of emission licenses, which allow firms to emit pollutants at a given location. In this case the constraints on firms are more complicated since the goal of the system is still to restrict pollution and not emissions. Again an equilibrium is defined as the allocation of emissions and licenses minimizing the cost of each firm individually subject to the constraints derived from the licenses the firm holds, where this allocation is required to satisfy the market clearing condition of the license market. Also in this case it is shown that an equilibrium exists. For appropriately chosen allocation by the regulator, the equilibrium solves the total joint cost minimum problem; but such a suitable allocation does not necessarily exist. In this model the distinction between pollution and emission in order to be able to control pollution at specific locations introduces a challenge. While such a distinction might be reasonable for the examples mentioned by Montgomery, such as air quality or water quality in rivers, this no longer applies in the case of greenhouse gases: They take their effect globally, thus the location of emission is irrelevant.

An extension of this model to a consideration of the development in time is given by Cronshaw and Kruse [CK96]. They construct a very general model with discrete time steps, taking into account also the production decisions of the firm. The time dimension becomes relevant as in their model it is possible to save allowances for future use (i.e. to bank them). This is described by a banking variable, which develops in accordance with the allocation and usage of allowances. The banking variable (or bank for short) represents the number of unused allowances which the corresponding firm holds. This variable is required to be non-negative, thus forbidding the borrowing of allowances from the future. In addition to the environmental constraint, Cronshaw and Kruse study the effect of profit regulation on allowance prices and banking behavior of the firms.

Similarly, Rubin also formulates a model to study banking and borrowing in an ETS [Rub96], but in contrast to Cronshaw and Kruse, his model is set up in continuous time. Thus a firm's bank evolves continuously in time as determined by its allocation rate and its emission rate. Rubin's general approach resembles Montgomery's, with the addition of the time dimension. He first considers a representative agent, who aims to minimize the aggregated costs of all individual firms subject to the constraint that the bank on aggregate cannot be negative. Costs are now given by the integral of the abatement costs over the entire time period considered; as Montgomery, he assumes that the abatement cost function is convex. He calls this problem the joint cost problem and refers to optimal control theory to argue that a solution exists. He continues by formulating the cost minimization problem of the individual firms, where costs now arise both from abatement and from trading with emission allowances. By solving this problem he derives a relation for the development of allowance prices in time: If there is a firm that would desire to borrow emissions from the future, i.e. with a bank of zero allowances, but is not allowed to do so, then the price of allowances grows more slowly than the interest rate; otherwise, it grows with the interest rate. Furthermore, from the optimality conditions it follows that the allowance price is equal to the marginal abatement costs of each firm. Rubin defines an equilibrium as emission rates and trading rates, given as functions in time, that minimize the costs of each firm over the entire time period, subject to the market clearing condition. He then shows that an equilibrium exists under the assumption that there are no binding constraints on the firms' trading rates. Finally, he can show that the market equilibrium is a solution to the joint cost problem. Furthermore, he concludes from his model that if environmental standards are tightening in time, then allowing firms to bank emissions may reduce pollution damage.

All models mentioned so far are purely deterministic. However, many variables influencing emission trading should more realistically be viewed as stochastic. An early model introducing uncertainty is given by Schennach [Sch00], extending on the work of Rubin. In the first part she still considers a deterministic regime: She constructs a two-period model in continuous time with a change in the emission cap between the two periods. As justified by the results of Rubin, she only considers a representative agent instead of individual firms; she assumes that this agent may bank allowances as necessary but is not allowed to borrow. Since in her model setup in the second period the cap tightens, she assumes that there is a banking period in which the bank takes positive values, starting with the first period and ending at some time point in the second. She then formulates the cost minimization problem of the representative agent, which is constrained by the requirement that the bank remains non-negative. From this she derives expressions for the price and the emissions path. In line with Rubin, she finds that the price increases with the interest during the banking period; afterwards it changes in dependence on the

BAU emissions. Moreover, the emissions increase with BAU emissions, whereas discounting effects will eventually cause the emissions to be decreasing in time. In the second part of her work, she introduces uncertainty in the BAU emissions and in the abatement costs but does not specify a precise stochastic model. She reformulates the minimization problem by considering expected costs and adding a risk premium to the interest rate. In order to solve this, she discretizes the problem and makes use of the dynamic programming approach; this is a first application of stochastic control in an ETS model. From the results she concludes that when the bank is non-empty with probability one, the expected allowance price rises with the interest rate plus the risk premium. If the probability of the bank being empty is strictly between zero and one, then the expected price rises at less than that; and if the bank is empty with probability one, the expected allowance price is determined by the marginal abatement costs.

Another contribution with uncertainty in the emissions is given by Innes [Inn03]. He considers a discrete-time model with two time periods and, correspondingly, three time points: At time 0, firms decide on their abatement and production for the first time period. Depending on these decisions and additionally on a random variable to model uncertainty, each firm produces emissions, which are revealed at time 1. Then, at time 2, abatement and production decisions are made for the second time period. Since the resulting emissions of this time period are not considered to be stochastic, they can be given immediately. As a reference scenario, for each time period Innes introduces the problem of a representative agent with perfect information who maximizes aggregate profits at the deficit of expected damage caused by emissions; Innes calls this reference scenario the first-best. The perfect information assumption is highly unlikely, therefore he compares two possible approaches of the regulator to attain this theoretical first-best: The first is to not allow banking or borrowing and impose a penalty on violations of the cap; this is a setting very similar to the first phase of the EU ETS. The second is to allow banking and possibly also borrowing of allowances. If there are no costs of imposing the penalty, then already the first approach yields a first-best solution, even when no allowances are allocated; then the system only consists of the penalty payment and thus corresponds to the case of a Pigou tax. If on the other hand imposing the penalty leads to costs for the regulator, the first approach cannot achieve a first-best solution as long as firms are not assumed to be identical. On the contrary, by the second approach, i.e. with banking and borrowing allowed, a first-best solution is possible if regulatory parameters are chosen correctly; this also includes the adjustment of allowances for the second period based on the observations gained up to that time point. Importantly, achieving the first-best hinges on avoiding penalty payments; thus the penalty needs to be chosen high enough such that firms do not prefer to pay the penalty instead of emission abatement.

Another early contribution to the emission trading literature is the work by Maeda [Mae04]. His main focus is the influence of bankable allowances on spot and forward allowance prices. He considers two points in time, namely time 0 and time 1. Thus he can allow for three different trades: Spot market trades both at time 0 and time 1 and a forward market trade at time 0 with maturity at time 1. Furthermore, he assumes that there are two kinds of market participants: Regulated firms, which need allowances to cover their emissions, and unregulated agents. As Schennach [Sch00] and Innes [Inn03], he assumes that BAU emissions of a firm are uncertain, and he proposes to model them via a normally distributed common risk factor and an idiosyncratic risk factor of the given firm. Based on this, he develops pricing formulas for the forward market and for the time 0 spot price market and studies the effects of several factors, such as uncertainty about

future prices and emissions, or the technological progress on the spot price.

1.3.2 Models to Analyze Recent EU ETS Revisions

The adaptations of the EU ETS in recent years have motivated the development of different models to capture these changes. The Market Stability Reserve (MSR) of the EU ETS, which was introduced in 2019, is studied by Perino and Willner [PW16]. Based on the work by Rubin [Rub96], they construct a deterministic model in continuous time with a continuum of firms, where banking is allowed. Furthermore, they assume that allowances are auctioned continuously in time, with their number decreasing exponentially. Each firm then aims to minimize costs from abatement and trading in allowances under the constraint that their bank remains non-negative. First, Perino and Willner solve this problem for a baseline case without the MSR. Then they introduce the dynamics of the MSR to the model, which means that the aggregate bank now influences the number of auctioned allowances. The optimization problem of the firms remains the same, since they are assumed to be in perfect competition, but could only collectively have an impact on the MSR; the equilibrium conditions on the other hand change. Perino and Willner show that the price and emission paths only change in comparison to the baseline case if due to the MSR there are not enough allowances available to cover the emissions in the baseline emission path; this means that the MSR leads to a scarcity of allowances (in their notion, the baseline emission path is unfeasible under the MSR). In that case, prices first rise above those of the baseline case and then drop below; conversely, emissions first fall below the baseline case and then rise above. This change in behavior is due to the fact that, with the MSR, the aggregate bank is depleted earlier. Perino and Willner modify their model by introducing uncertainty to the BAU emissions. From the work of Schennach [Sch00] they obtain an expression for the expected price path. This allows them to show that the price and emission paths in equilibrium are the same as without the MSR if and only if all emission paths that occur with positive probability are feasible under the MSR. This means that for these paths there are still sufficiently many allowances available with the MSR in operation. Perino and Willner further explore the impact of uncertainty by considering a Bernoulli-distributed shock at a specific time. They show that a shock occurring in the medium term will lead to a smaller price shock with the MSR than in the baseline case under the usual assumption that the abatement cost function is convex. On the other hand, for a shock that occurs early, the presence of the MSR may increase the price response.

Bocklet, Hintermayer, Schmidt and Wildgrube [Boc+19] also study the MSR but in addition, they include further recent EU ETS adaptations in their model. They consider a finite number of firms in a discrete-time deterministic setting, which minimize their costs and may bank their allowances; as borrowing is not allowed, the bank always needs to be non-negative. The volume of allowances issued decreases linearly in time. The equilibrium allowance price is then determined from the optimality conditions of the individual firms and the requirement that cumulated emissions have to be smaller or equal to cumulated allowances. The MSR is modeled in accordance with EU legislation, where the intake of the MSR and the reinjection depends on the allowances in circulation as given by the aggregate bank; intake and reinjection in turn influence the volume of issued allowances. Furthermore, the cancellation of allowances from the MSR is included in the model and its impact analyzed; as a third recent modification to the EU ETS, Bocklet et al. study an increase of the linear reduction factor which determines the number of issued allowances.

From numerical results they obtain that the MSR alone (without cancellation and a higher linear reduction factor) leads to higher allowances prices in the short term, when allowances are withdrawn from auctions, whereas the reinjection at a later stage causes the prices to be lower than without the MSR. The cancellation of allowances from the MSR amounts to 2 billion allowances, which takes place in 2023. Thus the overall cap is reduced and the depletion of the allowances in the MSR is accelerated. The price effects of this are small in the short term but much higher in the long term when the canceled allowances would have been released to the market if the cancellation mechanism had not existed. The increase of the linear reduction factor causes a considerably larger reduction of the cap amounting to 9 billion allowances and has thus a higher effect than the cancellation. Bocklet et al. identify this as the main driver of the allowance price increase which their model predicts due to the reform.

Based on the model by Bocklet et al., Hintermayer [Hin20] studies a further modification of the ETS that is not yet implemented or officially proposed: He considers two separate mechanisms to introduce a price floor for the allowance prices. One way to obtain such a lower bound for the price is a buyback by the regulator, i.e. allowances can always be sold back to the regulator for a fixed price so that the allowance price on the market will not fall below this price. A second approach is a so-called top-up tax. This means that firms need to pay an additional tax on their emissions, amounting to the difference between the desired price floor and the actual market price of allowances. For the buyback approach Hintermayer finds that in the short run it increases prices and decreases emissions, which is reversed at a later stage but to a lesser extent. Since the increased scarcity in the short term leads to a higher cancellation, emissions on aggregate are reduced. In case of the top-up tax, the timing of the announcement to implement such a tax is relevant, since the announcement itself will lead to an increase in emissions. As soon as the tax is implemented, it reduces emissions; thus the overall effect is ambiguous.

1.3.3 Models on Emission Price Development

Another stream of literature has developed with the focus to model the development of the allowance price. This is relevant for example in option pricing and to develop hedging strategies. Hintermann constructs an ETS model with the intent to analyze the behavior of allowance prices [Hin10]. In particular, he studies how well the allowance price is explained by marginal abatement costs and which factors play an important role. In his model he considers finitely many firms in one compliance period with discrete time points. The BAU emissions of a firm are described as a function of a vector of common risk factors and are additionally subject to idiosyncratic uncertainties. He assumes that marginal abatement costs are linear and that they depend explicitly on coal and gas prices; in this way, it is assumed that abatement is performed by switching the fuel used e.g. for energy generation from coal to gas. Firms then choose optimal abatement by equating their marginal abatement costs with the allowance price. In equilibrium, total abatement of all firms needs to be equal to the difference between BAU emissions and the emission cap. From this condition an expression of the allowance price in dependence on the BAU emissions can be derived. Hintermann specifies several factors that may influence the BAU emissions, namely temperature and precipitation, fuel prices, and economic performance. He rewrites the allowance price by specifically using these factors as the common risk factors in his model. Then he performs a regression analysis based on data corresponding to the risk factors and data on the allowance price. He finds that his model cannot provide

an adequate explanation of the allowance price before the price crash in April 2006, thus marginal abatement costs probably were not equal to the allowance price at that time, indicating an inefficient market. After the price crash, the model explains the prices well, pointing to an efficient market. As important price drivers, he identifies the fuel prices, summer temperatures, and precipitation.

Another contribution focusing on price development, but still rooted in an ETS model, is given by Borovkov, Decrouez and Hinz [BDH11]. They construct an equilibrium model of an ETS in discrete time, where they assume that BAU emissions are given by a stochastic process. Firms in the system aim to minimize their costs; from the cost minimization problem an expression for the equilibrium allowance price can be derived. From this result Borovkov et al. conclude that they are looking for a Q-martingale under an equivalent measure Q satisfying the expression derived before. They first assume that the price process is a continuous diffusion process. They show that the price process can then be obtained from a function solving a PDE that they derive. Additionally, they demonstrate how this result can be applied in option pricing. Then they proceed in a similar way for a price process that may exhibit jumps. In this case they derive an integro-differential equation; its solution delivers the desired price process with jumps.

Benz and Trück follow a different approach [BT08]: They fit two time series models to the logarithmic returns of allowance prices. Based on the observation that the variance of the allowance price in the EU ETS seems to vary in time, they propose a Markov switching model with two different regimes, allowing the process to switch between high and low variance periods. As a second approach, they consider a so-called AR-GARCH model, where both the variance and the mean of the process are modeled by autoregressive processes. They compare both of these models to a normal distribution of the logarithmic returns and to an AR model, where the mean is modeled by an autoregressive process but the variance remains constant. They use maximum likelihood estimation to fit these models to allowance price data. As a result, they find that the Markov switching model and the AR-GARCH lead to a better fit than the two models with constant variance. Moreover, they are able to show that the former also outperform the latter in forecasting allowance prices.

A similar strategy is adopted by Cai and Pan [CP17]. They consider five different SDEs and aim to analyze which ones model the allowance price best. By applying the Euler-Maruyama scheme, they discretize each of the SDEs and thus obtain a multiple linear regression model. Using least squares, they estimate the parameters in each of the models from allowance price data. Furthermore, they use their estimation results to forecast prices and compare them with observed actual prices. They obtain that a mean reverting square root process provides the best fit and performs best in forecasting.

1.3.4 Stochastic Control Models

So far we have mainly discussed modeling approaches which are either deterministic or do not provide a thorough stochastic model; instead, uncertainty has been modeled by a single random variable or was not further specified. At the core of most ETS models, an optimization problem needs to be solved. Hence with the introduction of uncertainty to such a model, stochastic control theory provides a powerful tool to solve this optimization problem. In the following, we will introduce three different approaches to applying stochastic control to ETS modeling present in the literature.

Discrete-Time Models

Carmona, Fehr and Hinz [CFH09] propose a discrete-time equilibrium model, intended to represent the EU ETS in its first phase. Initially, they consider each agent i in the system individually. In the case of no abatement, i.e. the BAU case, they introduce a random variable Γ^i to model the emissions which are not covered by an allocated allowance. They assume that allowances are traded in a forward market with prices given by a stochastic process $(A_t)_t$, according to the agent's trading strategy denoted by θ_t^i. Carmona et al. focus on the power sector and on a particular abatement measure, namely fuel switching from coal to gas. This allows them to derive the abatement costs from fuel prices. More precisely, they assume that each agent at each time point may decide to abate an amount $\xi_t^i \in [0, \lambda^i]$ by fuel switching, inducing costs of $\mathcal{E}_t^i$ per unit; the parameter λ^i represents the maximum fuel switching capacity. Importantly, since the abatement costs depend on the fuel prices of coal and gas, they are stochastic and thus $\mathcal{E}_t^i$ is a stochastic process. If the agent's emissions at final time given by Γ^i surpass the units abated and the number of allowances held, the agent needs to pay a penalty given by π. Thus the total profit $I^{A,i}$ (or loss if negative) of agent i is given by her net wealth from trading with allowances at the deficit of abatement costs and penalty payments, resulting in

$$I^{A,i}\left(\theta^i, \xi^i\right) = \sum_{t=0}^{T-1} \theta_t^i \left(A_{t+1} - A_t\right) - \theta_T^i A_T - \pi \left(\Gamma^i - \sum_{t=0}^{T-1} \xi_t^i - \theta_T^i\right)^+ - \sum_{t=0}^{T-1} \xi_t^i \mathcal{E}_t^i.$$

The term $-\theta_T^i A_T$ enters this equation since the expression to determine the net wealth from trading implicitly assumes that the final position is liquidated, which is not the case here, as the agent needs the allowances to cover emissions. Since the agent aims to maximize her profits, her optimization problem is given by

$$\sup_{(\theta^i, \xi^i)} \mathrm{E}\left[I^{A,i}\left(\theta^i, \xi^i\right)\right]$$

where the trading and abatement strategies θ^i and ξ^i are subject to admissibility constraints. Similar to the early equilibrium models, for a given abatement cost process $\mathcal{E}_t$ an equilibrium is defined as trading and abatement strategies θ^i and ξ^i such that profits of all agents are maximized and the allowance market clears.

In the next step, Carmona et al. introduce the global optimization problem of a representative agent. They define $F(\xi)$ as the aggregate fuel switching costs in the course of the entire time period and of all agents. Similarly, $\Pi(\xi)$ represents the total emission abatement and Γ the overall BAU emissions subtracted by the initial allowance allocations, i.e. the sum over all Γ^i. The representative agent aims to minimize total costs by choosing the abatement strategy ξ. Thus she needs to solve

$$\xi^* = \arg\sup_{\xi} \mathrm{E}\left[-\pi \left(\Gamma - \Pi(\xi)\right)^+ - F(\xi)\right].$$

Carmona et al. show that there exists a solution to the global optimization problem. Furthermore, they prove that when imposing a weak assumption on the distribution of Γ, the optimal abatement strategy ξ^* delivers the equilibrium price process as

$$A_t^* = \pi\, \mathrm{E}\left[\mathbf{1}_{\{\Gamma - \Pi(\xi^*) \geq 0\}} \,\middle|\, \mathcal{F}_t\right].$$

For a numerical study, they formulate the model more specifically. The fuel switch price $\mathcal{E}$ – corresponding to the abatement costs – is modeled by an Ornstein-Uhlenbeck process

and a deterministic function to account for seasonality. The BAU emissions Γ are modeled by a Brownian motion with drift. Since the basic model is in discrete time, both these processes need to be discretized. The global optimization problem is then solved by backward induction. Carmona et al. use their numerical results to study the effect of modifying the penalty on the allowance price and the probability of complying with the amount of allocated allowances, i.e. the probability $P(\Gamma \leq \Pi(\xi^*))$. If only a low capacity of fuel switching is expected to be required to comply with the emission constraint, an increase in the penalty increases the compliance probability, but barely influences the allowance price. If on the other hand a high level of fuel switching is needed for compliance, increasing the penalty still increases the compliance probability but also leads to a strong increase in the price.

This work is extended by Carmona, Fehr, Hinz and Porchet [Car+10] to a broad and general model of an economy underlying an ETS. They consider the production of finitely many goods, each with finitely many production technologies available, which differ in cost and resulting emissions. Thus abatement is possible by switching to a different technology with a lower emission level. The case of fuel switching in the power sector, as considered above, thus corresponds to having only one good, namely electricity, and two different technologies. In comparison to their previous work, Carmona et al. now include the profits from selling the produced goods in the expression describing each firm's profit. As a result, they also need to model the prices S of all goods considered. An equilibrium in this market is then defined as a tuple of price processes (A^*, S^*) satisfying similar conditions as before, with the additional requirement that the supply of all goods meets the demand, which is assumed to be independent of the price. In the global optimization problem Carmona et al. now also include the overall production costs and then continue to show that a solution to this problem exists. As in their previous contribution, this solution delivers an equilibrium with the same expression for the allowance price; furthermore, they obtain an expression for the equilibrium price of each good. In course of their analysis, they find that whenever total emissions are below the number of allocated allowances, the allowance price at final time will be zero, whereas it equals the penalty when the total emissions surpass the number of allocated allowances. Carmona et al. modify the setup of the ETS in their model by allowing a dynamic procedure to allocate allowances, which may depend linearly on production. Furthermore, they include a carbon tax or subsidy in the model. By numerical analysis, which is again conducted in the energy sector with fuel switching as abatement measure, they study the effects of different modes of allocation on windfall profits. They find that an allocation of allowances which is proportional to production considerably reduces windfall profits and additionally slightly reduces emissions, while only leading to a small increase in overall costs of emission reduction. A carbon tax high enough to reach the same emission reduction as in the ETS with high probability is a lot more expensive but may also lead to further emission reductions. Finally, they show that there exists an allowance allocation scheme that reduces windfall profits to zero.

Another contribution that is in some aspects similar but also is influenced by the work of Seifert et al. [SUW08], which we will present below, is given by Yu and Mallory [YM15]. They aim to model an ETS with a price ceiling for the allowance price, meaning that if the price reaches a certain value, the regulator sells additional allowances to the market at this price. Their model is also set in discrete time; but in this case, the separate time points each represent one compliance period, so that banking of allowances can be included in the model. Furthermore, the time horizon is chosen to be infinite. Yearly emissions are assumed to be stochastic but bounded. Yu and Mallory first consider the optimization

problem of the regulator, who needs to choose the optimal abatement level minimizing total abatement costs and the damage caused by emissions. The firms underlying the ETS are modeled by a representative agent. Her optimization problem is then to choose the optimal abatement level minimizing her costs that originate from abatement and penalty payment, while taking into account her bank of allowances. Both optimization problems are reformulated as Bellman equations and solved analytically. The regulator then chooses the price ceiling and the cap so that the optimal abatement of the regulator's and of the firm's problem are equal. This delivers the optimal short-term policy; notably, this choice is not unique. By considering average emissions, Yu and Mallory formulate equations to describe the long-term development of the accumulated emissions and the allowances in the bank. Thus they obtain the long-run optimization problem and solve it; again by equating both solutions for the optimal abatement, the long-run optimal regulatory solution can be determined. Their conclusion is that for the purpose of consistency the regulator would usually choose a long-term optimum; but if the present situation makes it necessary, for instance, because allowance prices are too high, the regulator may move to a short-term optimal policy.

Models of the Bank of Allowances

Building on the work of Rubin [Rub96], Kollenberg and Taschini [KT16] follow a second approach to make use of stochastic control in an ETS model. They construct a continuous time model to study a mechanism which allows the regulator to adjust the allocation of allowances based on the number of currently banked allowances; this is similar to the Market Stability Reserve implemented in the EU ETS. Thus, the allowance bank of each agent, as given by a process B^i, is a key feature of the model. Notably, Kollenberg and Taschini assume that there is a continuum of agents in the system. For each agent, the cumulated BAU emissions are modeled by a process $(E^i(0,t))_t$ and the cumulated allowance allocation is modeled by a process $(A^i(0,t))_t$. Furthermore, abatement and trading are represented by the abatement rate α^i and the trading rate β^i. Then the bank is given as

$$B_t^i = B_0^i + A^i(0,t) - E^i(0,t) + \int_0^t \alpha_s^i \mathrm{d}s - \int_0^t \beta_s^i \mathrm{d}s.$$

To enforce compliance with the overall emission cap as determined by aggregate allocation, the bank needs to be zero at final time, i.e. $B_T = 0$. In contrast to Rubin [Rub96], borrowing is allowed, thus the bank may attain negative values before final time. Under the assumption that abatement costs are given by a quadratic cost function $C(t,\alpha)$, each agent's optimization problem is then given by

$$\min_{\alpha^i,\beta^i} \mathrm{E}\left[\int_0^T \mathrm{e}^{-rt}\left(C(t,\alpha_t^i) - P_t\beta_t^i + v\left(\beta_t^i\right)^2\right)\mathrm{d}t\right]$$

under the constraint that $B_T^i = 0$ and with the bank B^i evolving in time as given above. In this expression P_t, denotes the allowance price and the term $v(\beta_t^i)^2$ accounts for transaction costs. Similarly to previously discussed models, a market equilibrium is given by a family of abatement and trading rates $(\alpha_t^i, \beta_t^i)_{t\in[0,T]}$ and a price process P such that all agents minimize their costs and the market clearing condition holds. To determine an equilibrium, Kollenberg and Taschini derive the HJB equation for an individual company and solve it. They obtain explicit expressions for the equilibrium abatement and trading rate as well as

for the price process, where the price process is mainly driven by the difference between BAU emissions and allowance allocation.

In this framework, they introduce a responsive mechanism, which works as follows: If the aggregate bank falls below a given level c, the allocation of allowances is increased by $\delta|B_t - c|\mathrm{d}t$, whereas if the aggregate bank is above the level c, an amount of $\delta|B_t - c|\mathrm{d}t$ allowances is removed from the market; the parameter δ determines the sensitivity of the mechanism. Then, with the allocation schedule prior to adjustment being given by f_t, the authors model the evolution of the bank as

$$\mathrm{d}B_t = f_t\mathrm{d}t + \delta\left(c - B_t\right)\mathrm{d}t - E(t, t+\mathrm{d}t) + \alpha_t\mathrm{d}t,$$

from which a closed-form expression for B is derived. Thus it can be observed that increasing the sensitivity parameter δ leads to less variability in the bank. If $\delta = 0$, the resulting system corresponds to a standard ETS, whereas setting $\delta = 1$ leads to a pure tax system. In this way, the parameter δ introduces a spectrum of policy measures between a Pigou tax and an ETS. Kollenberg and Taschini then formulate an optimization problem to choose δ such that overall costs in the system are minimized. For a set of exemplary parameters, they graphically show that the optimal value δ lies between the two extremes of $\delta = 0$ and $\delta = 1$.

Kollenberg and Taschini [KT19] extend this work to align their model more closely with the EU ETS and its Market Stability Reserve. They no longer allow borrowing, thus requiring that the bank never becomes negative. To do this, they follow the approach introduced by Schennach [Sch00]: They only consider the banking period, i.e. the time until the bank is fully depleted; due to the stochastic setting, they model this via a stopping time τ. In line with their previous result, they show that the aggregate abatement rate and in turn also the price process are driven by the expected required aggregate abatement. This quantity, denoted as $\mathrm{E}_t[Y]$, is given as the expectation of the difference between BAU emissions and allowance allocation, conditional on the information available at time t. By considering risk-averse firms, they argue that a supply management mechanism (SMM, such as the Market Stability Reserve) imposes changes to the distribution of $\mathrm{E}_t[Y]$, which may increase the probability that the firms on aggregate will instantaneously fully deplete the bank. Since this entails lower abatement and low allowance prices, the SMM may increase price volatility and the risk premium of risk-averse firms. Finally, they conclude that the more recently implemented cancellation mechanism of the Market Stability Reserve may increase prices and thus reduce the risk in low carbon investment.

Aid and Biagini model a regulator who aims to choose the allowance allocation in order to minimize social costs in a system of cost minimizing firms with stochastic BAU emissions [AB21]. They model the bank of allowances and formulate the cost minimization problem of firms as in the model of Kollenberg and Taschini [KT16]; they describe the BAU emissions as a Brownian motion with drift, including both idiosyncratic and systemic sources of uncertainty. In contrast to Kollenberg and Taschini, they do not impose a constraint on the final bank position; instead, a value deviating from zero is penalized as part of the cost minimization problem. The regulator then chooses the instantaneous allocation at each point in time and for every firm in order to minimize the aggregate costs in the system. At the same time, the constraint that expected emissions comply with a given reduction goal in comparison to the expected BAU emissions needs to be satisfied. For this, the regulator assumes that the allowance market is in equilibrium. Aid and Biagini determine the unique optimal trading and abatement strategies for each firm and derive an expression for the equilibrium price. Based on this, they derive the optimal

allocation process for the regulator. They show that the optimal allocation annihilates the price volatility, so that in particular the resulting equilibrium price is constant; the same holds for the optimal abatement rate. Notably, the optimal allocation is not unique. The intuition behind this result is the following: The reduction target predefines the average abatement requirement, which in turn determines the average allowance price. But due to stochastically driven variations of the price, the abatement is no longer spread equally in time. This increases the costs of abatement because of the quadratic nature of the abatement cost function. The constant price points to a high similarity to a Pigou tax. However, Aid and Biagini compare their optimal allocation scheme to that of a pure tax and show that for a sufficiently high penalty parameter, the total costs of the optimal allocation scheme are smaller than those of a tax. Furthermore, they conduct a numerical study to compare the optimal allocation scheme to a standard ETS and to the EU ETS with the Market Stability Reserve. They find that the optimal allocation scheme has the lowest costs, while aggregate emissions are below those of the standard ETS and at the same level as the EU ETS with the Market Stability Reserve.

Continuous-Time Models

Seifert, Uhrig-Homburg and Wagner [SUW08] follow a third approach to apply stochastic control in an ETS model. In order to study properties of the allowance spot price, they construct a model of a representative agent in continuous time, minimizing costs by appropriately choosing abatement. Since our model builds on the work by Seifert et al., the details of their modeling approach will be covered in Chapter 2 below. In the interest of clarity and completeness, we will already describe their work here, while using the notation applied throughout this thesis. Seifert et al. model BAU emissions by a diffusion process Y and let u denote the abatement rate, which acts as the control. For a given time period $[0, T]$, they define the total expected emissions X as

$$X_t = -\int_0^t u_s \mathrm{d}s + \mathrm{E}^t\left[\int_0^T Y_s \mathrm{d}s\right],$$

thus representing the emissions expected for the entire time period at a given time t. This construction implicitly allows for banking and borrowing throughout the time period $[0, T]$. From the definition, they derive an SDE describing X as

$$\mathrm{d}X_t = -u_t \mathrm{d}t + G(t)\mathrm{d}W_t,$$

where $G(t)$ denotes the volatility of X, which needs to be computed from the process chosen for Y. In their online appendix, they perform the derivation of $G(t)$ for a Brownian motion with drift and state the result for a white noise and an Ornstein-Uhlenbeck process. The cost minimization problem of the representative agent is formulated as the problem to choose the abatement in order to maximize profits, which in this case only consist of negative costs. These arise from abatement costs given by a quadratic cost function $C(u_t) = -\frac{1}{2}\, c\, u_t^2$ and potential penalty payments given as $P(X_T) = \min(0, p(e_0 - X_T))$, where c is a cost coefficient, e_0 the initial allocation of allowances, and p the penalty. The optimization problem can then be stated as

$$\max_{(u_t)_{t\in[0,T]}} \mathrm{E}^0\left[\int_0^T \mathrm{e}^{-rt}\, C(t, u_t)\mathrm{d}t + \mathrm{e}^{-rT}\, P(X_T)\right].$$

Seifert et al. derive the corresponding HJB equation, from which they obtain an expression for the optimal abatement rate and thus the characteristic PDE. By assuming that the allowance price is given by the marginal abatement costs, they arrive at an expression for the allowance price, which depends on the PDE solution. This result enables them to show that the discounted spot price process $\mathrm{e}^{-rt} S$ is a martingale.

For the particularly simple case of a constant volatility $G(t) = \sigma$, they derive an analytical PDE solution with the help of a symbolic mathematics program and thus obtain the price process as a function of X_t and of time. In the case that Y is a Brownian motion with drift, they solve the PDE numerically. From the results, they observe that the price is bounded in the interval $(0, \mathrm{e}^{-r(T-t)}\, p)$. Furthermore, they study the influence of several parameters on the allowance price at initial time; they find that it has an upper limit even for an increasing value of the penalty p. In addition, they show that in their model expected banking is positive at any point in time. To conduct a numerical sensitivity analysis on the price volatility, they apply Itô's formula to the price function, yielding

$$\mathrm{d}S_t = \left(-u_t\, S_x + S_t + \frac{1}{2}\, G(t)^2\, S_{xx} \right) \mathrm{d}t + G(t)\, S_x \mathrm{d}W_t.$$

Their analysis delivers that the price volatility $G(t)\, S_x$ increases with increasing penalty, cost coefficient and volatility of the emission rate. Finally, they modify their approach to study a risk averse representative agent. In this case, the spot price is no longer bounded.

An extension of the model by Seifert et al. is given by Liang and Huang. In two articles, [LH20] and [LH22], they include auctioning and partly also banking and borrowing across different time periods in the model. In [LH20], they first present a single-period model with auctioning. They assume that the abatement rate u is bounded from above by a constant $\bar{u}$ and they fix the auction price S_0. Furthermore, they only consider the case where $G(t) = \sigma$, i.e. the volatility of the total expected emissions X is constant. By denoting the amount of freely allocated allowances as N_1 and the amount of allowances acquired at the auction as N_2, they formulate the expected costs as

$$U_1(x; u, N_2) = \mathrm{E}\left[\int_0^T \mathrm{e}^{-rs}\, C(u_s) \mathrm{d}s + \mathrm{e}^{-rT}\, p\, (X_T - N_1 - N_2)^+ + S_0\, N_2 \,\middle|\, X_0 = x \right].$$

In comparison to the work by Seifert et al., they reformulate the maximization problem to a minimization problem where the sign of the costs is reversed, i.e. the abatement cost function is now given as $C(u_t) = \frac{1}{2}\, c\, u_t^2$. Due to the inclusion of the auctioning of allowances, the agent needs to solve two optimization problems: On the one hand, she needs to choose her abatement rate in an optimal way; on the other, she also needs to determine the optimal number of allowances N_2 to buy at the auction. This can be done in two different orders[11]. Liang and Huang first determine the optimal value for N_2. They assume that the auction price is higher than the penalty, i.e. $S_0 > p$, and they fix the abatement rate u. By computing the partial derivative of the cost function U_1 with respect to N_2, they show that it is optimal not to purchase allowances at the auction. The remaining problem to find the optimal abatement rate is then the same as the one considered by Seifert et al. By omitting the terms involving N_2, they formulate the value function V_1 and state the HJB equation. For the case that $p < S_0$, the same procedure is

[11] In theory, a simultaneous optimization might also be a viable approach but this is not explored by Liang and Huang.

not applicable. Therefore they conduct the optimization in the other order: For fixed N_2 and with the assumption that $r = 0$, they formulate the value function as

$$\tilde{V}_1(x,t;N_2) = \inf_u \mathrm{E}\left[\int_t^T C(u_s)\mathrm{d}s + p\,(X_T - N_1 - N_2)^+ \,\middle|\, X_t = x\right],$$

hence the term $S_0\,N_2$ reflecting the cost of auctioned allowances in the cost function U_1 is omitted as it is not influenced by u. From the value function, they derive the HJB equation, which allows them to determine the optimal abatement rate and the characteristic PDE. Similar as Seifert et al., they compute an analytical solution of the PDE. The next step is to choose the optimal auctioned amount. For this, they compute the derivative with respect to N_2 of the cost function, now given by $\tilde{V}_1(x,0;N_2) + S_0\,N_2$. In this way, they obtain an implicit equation for the optimal value of N_2, which needs to be solved numerically.

In a second model, Liang and Huang introduce a second time period, given by the interval $[T, T^*]$, to allow for banking and borrowing between the two time periods; they call this model the inheriting period model. They introduce a geometric Brownian motion to model the auction price $(S_t)_t$ and they assume for its drift μ that $r > \mu$. Furthermore, they assume that the auction price and the total expected emissions are uncorrelated. Then the cost function of the first time period is given as

$$\begin{aligned} U_2(x,s;u,N_2) = \mathrm{E}\Bigg[\int_0^T \mathrm{e}^{-rt}\,C(u_t)\mathrm{d}t + \mathrm{e}^{-rT}\,\min\{p,S_T\}\,(X_T - N_1 - N_2)^+ \\ - \mathrm{e}^{-rT}\,S_T\,(X_T - N_1 - N_2)^- + S_0\,N_2 \,\Big|\, X_0 = x, S_0 = s\Bigg]. \end{aligned}$$

If the total emissions X_T surpass the sum of auctioned and freely allocated allowances, the agent needs to either pay the penalty or borrow allowances from the second period, which is reflected in the term $\mathrm{e}^{-rT}\,\min\{p,S_T\}(X_T - N_1 - N_2)^+$. If, on the other hand, total emissions are below the amount of available allowances, the agent has a benefit worth the price of the additional allowances, given by the term $\mathrm{e}^{-rT}\,S_T(X_T - N_1 - N_2)^-$. Again, two optimization problems need to be solved. In [LH22], Liang and Huang first determine the optimal amount of allowances N_2 to be purchased at the auction. As in the single period model – but without the assumption that $P < S_0$ – they compute the partial derivative of the cost function U_2 with respect to N_2 and obtain that it is optimal not to purchase allowances at the auction because the growth rate μ of the auction price is smaller than the interest rate. Then they proceed with the optimization with respect to u by formulating the value function V_2 and deriving the HJB equation. The optimization in reversed order is described in [LH20]. They formulate the value function as

$$\begin{aligned} \tilde{V}_2(x,s,t;N_2) = \inf_{0\le u\le \bar{u}} \mathrm{E}\Bigg[\int_t^T \mathrm{e}^{-r(\xi-t)}\,C(u_\xi)\mathrm{d}\xi + \mathrm{e}^{-r(T-t)}\,\min\{p,S_T\}(X_T - N_1 - N_2)^+ \\ - \mathrm{e}^{-r(T-t)}\,S_T(X_T - N_1 - N_2)^- \,\Big|\, X_t = x, S_t = s\Bigg]. \end{aligned}$$

From the corresponding HJB equation, they derive an expression for the optimal abatement rate and obtain the characteristic PDE, which is now two-dimensional in space. They solve this PDE numerically; from the PDE solution, they determine the total costs by adding the costs of the auction given by $S_0\,N_2$ and thus compute the optimal amount to be purchased at the auction by minimizing this expression. In [LH22], Liang and Huang

also provide a theoretical discussion of their models. For the case of no purchase of allowances at the auction, they show that the value function of determining the optimal abatement rate, given by V_1 in the single period model and by V_2 in the inheriting period model, is a unique viscosity solution.

Both articles conclude with a numerical analysis of these models. In [LH20], they compare the value functions obtained in the second optimization approach, i.e. when first determining the optimal abatement rate, of the single period and the inheriting period model given by $\tilde{V}_1$ and $\tilde{V}_2$. Additionally, they include a two-period model where only banking is allowed with value function

$$\begin{aligned}\tilde{V}_3(x,s,t;N_2) = \inf_{0\le u\le \bar{u}} \mathrm{E}\Bigg[\int_t^T \mathrm{e}^{-r(\xi-t)}\, C(u_\xi)\mathrm{d}\xi + \mathrm{e}^{-r(T-t)}\, p(X_T - N_1 - N_2)^+ \\ - \mathrm{e}^{-r(T-t)}\, S_T(X_T - N_1 - N_2)^- \,\Big|\, X_t = x, S_t = s\Bigg].\end{aligned}$$

Numerical results show that for differing initial expectations on total emissions, the inheriting period model always leads to the lowest costs; this also holds for different amounts of allowances purchased at the auction. Interestingly, in both cases the third model represented by $\tilde{V}_3$ lies between the two other models: For low initially expected emissions, the results for $\tilde{V}_3$ are equal to those of the inheriting period model given by $\tilde{V}_2$, whereas for high initially expected emissions, they are equal to those of the single period model; a similar behavior can be observed when varying the auctioned amount of allowances. Liang and Huang also compare the emission reductions in the three models for varying penalties and find that emission reductions are linearly increasing and the same in all three models if the penalty is not too high, i.e. below 150 Euro. For higher penalties, the emission reduction in the inheriting period model is lower and constant, whereas for the other two models, it still increases linearly.

Contribution of the Present Thesis

The main interest of this thesis is to study the effects of various regulatory changes on the outcome of an ETS. We focus on the ability of the ETS to achieve its goals, namely to reduce emissions and provide an incentive for investment in clean technologies. To this end, we extend the work of Seifert et al. [SUW08] in various ways. Since we are interested in the realized outcome, we use the result for the optimal abatement rate to simulate the process of total expected emissions X by solving the SDE

$$\mathrm{d}X_t = -u(t, X_t)\mathrm{d}t + G(t)\mathrm{d}W_t.$$

In turn, this allows us to compute the corresponding price process S. Furthermore, by applying a suitable verification theorem, we show that the PDE solution V and the abatement rate u derived from the HJB equation indeed provide the optimal costs and the optimal abatement rate. As Liang and Huang [LH20]/[LH22], we extend the model to allow for banking and to introduce auctioning. In contrast to Liang and Huang, we do this separately; moreover, our model allows for arbitrarily many time periods and follows a different approach to reflect the banking of allowance.

Chapter 2

One-Period Model

In this chapter we present our basic model of an Emission Trading System (ETS). This model covers only one compliance period and may serve to represent the EU ETS in its first phase from 2005 to 2007. We first model the development of emissions in the system. To this end we introduce the quantity of total expected emissions, which we describe by a stochastic differential equation (SDE). Then we formulate the cost minimization problem of the companies underlying the system: Companies will try to abate emissions in such a way that their expected costs from penalty payments and from emission abatement are minimized. We apply a stochastic control approach to this problem and thus derive a partial differential equation (PDE). In order to obtain the optimal abatement, we need to solve this PDE; for one particularly simple model variant, this can be done analytically. The optimal abatement enters the SDE, which we then aim to solve. Classical results on existence and uniqueness of a solution as well as on convergence of numerical methods do not apply in our case. Under suitable assumptions, we show that a unique solution exists and that the Euler-Maruyama method converges to this solution.

2.1 Derivation of the Total Expected Emissions

In the formulation of a stochastic continuous-time model of an emission trading system we closely follow the work by Seifert, Uhrig-Homburg and Wagner [SUW08].

We aim to model the development of an emission trading system in the course of a time period from time 0 to some fixed terminal time T given by the interval $[0, T]$. The regulator fixes the amount of emissions in mega tons to be allowed during this time period, which shall be given by the parameter e_0. In accordance with this amount e_0, allowances are distributed to companies underlying the system. The regulator also determines the value of the penalty payment that is due for any ton which is not covered by an allowance, denoted by the parameter p. In order to simplify both notation and computations, we gather all companies subject to the system in one representative agent. This simplification was justified by Seifert et al. [SUW08]: They show that the joint cost problem, which corresponds to considering a representative agent, is equivalent to the cost minimization problem of individual agents[1].

We introduce a stochastic process $Y = (Y_t)_{t\in[0,T]}$ to model the rate at which the representative agent produces emissions prior to any reduction efforts. The agent may put in an effort to abate emissions, which we model by the abatement rate $u = (u_t)_{t\in[0,T]}$.

[1] This result can be found in their online appendix of [SUW08].

Let $(\Omega, \mathcal{A}, \mathcal{P})$ be a probability space. Let furthermore $W = (W_t)_{t\in[0,T]}$ be a standard Brownian motion and let $\mathcal{F} = (\mathcal{F}_t)_{t\in[0,T]}$ be the filtration generated by W and augmented by the null sets, i.e. we have $\mathcal{F}_0 = \sigma\left(\{\emptyset, \Omega\} \cup \mathcal{N}_\mathcal{P}\right)$, where $\mathcal{N}_\mathcal{P}$ denotes the set of all null sets with respect to the probability measure $\mathcal{P}$. Then we assume the emission rate Y to be given by the SDE

$$\mathrm{d}Y_t = \mu(t, Y_t)\mathrm{d}t + \sigma(t, Y_t)\mathrm{d}W_t,$$

where μ and σ are real-valued and measurable functions. The volatility term $\sigma(t, Y_t)\mathrm{d}W_t$ serves to introduce randomness to the evolution of the emission rate; note that this was chosen as a general formulation which does not take into account the nature of realistic sources of randomness for the emission rate. From the processes Y and u, we define the total expected emissions, which will later allow us to determine whether a penalty needs to be paid or not.

Definition 2.1. The total expected emissions for a time period $[0, T]$ are given by the process $X = (X_t)_{t\in[0,T]}$ defined as

$$X_t = -\int_0^t u_s \mathrm{d}s + \mathrm{E}\left[\int_0^T Y_s \mathrm{d}s \,\middle|\, \mathcal{F}_t\right].$$

The total expected emissions therefore represent the total amount of emissions we expect for the entire time period from the perspective of time t, where we take into account the emissions without abatement for the entire time period but we include the abatement only until time t. Note that by this construction, X is adapted to $\mathcal{F}$ as long as u is $\mathcal{F}$-adapted.

Remark 2.2. The definition delivers two very important special cases:

- $X_0 = \mathrm{E}\left[\int_0^T Y_s \mathrm{d}s\right]$ represents the emissions expected at the beginning of the time period without any abatement.
- $X_T = \int_0^T (-u_s + Y_s)\,\mathrm{d}s$ represents the total amount of emissions which are actually produced in the course of the time period.

By specifying the functions μ and σ more explicitly, we rewrite the process X in the form

$$\mathrm{d}X_t = -u_t\mathrm{d}t + G(t)\mathrm{d}W_t;$$

we will proceed to do this for three special cases.

2.1.1 The Simple Model Variant

In order to obtain a very simple variant of our model, which in the following will be called the simple model variant, we do not specify a formulation for Y and model the total expected emissions X explicitly instead. We therefore assume X to be given by

$$\mathrm{d}X_t = -u_t\mathrm{d}t + \sigma\mathrm{d}W_t$$

where $\sigma > 0$ is now a constant. Thus in the general expression above we have $G(t) = \sigma$.

2.1.2 The Brownian Model Variant

A still rather simple approach is to assume μ and σ to be constant, i.e. $\mu(t, Y_t) = \mu \in \mathbb{R}$ and $\sigma(t, Y_t) = \sigma \in \mathbb{R}_+$. Then the emission rate Y is given by

$$\mathrm{d}Y_t = \mu \mathrm{d}t + \sigma \mathrm{d}W_t.$$

With $Y_0 = y_0 \in \mathbb{R}$, we rewrite this as $Y_t = y_0 + \mu\, t + \sigma\, W_t$. Now we can compute

$$\begin{aligned}
\mathrm{E}\left[\int_0^T Y_s \mathrm{d}s \,\middle|\, \mathcal{F}_t\right] &= \int_0^T (y_0 + \mu\, s) ds + \mathrm{E}\left[\int_0^T \sigma W_s \mathrm{d}s \,\middle|\, \mathcal{F}_t\right] \\
&= y_0\, T + \frac{T^2}{2}\mu + \sigma\, \mathrm{E}\left[W_T\, T - \int_0^T s \mathrm{d}W_s \,\middle|\, \mathcal{F}_t\right] \\
&= y_0 T + \frac{T^2}{2}\mu + \sigma\, T\, \mathrm{E}\left[W_T \,\middle|\, \mathcal{F}_t\right] - \sigma\, \mathrm{E}\left[\int_0^T s \mathrm{d}W_s \,\middle|\, \mathcal{F}_t\right] \\
&= y_0\, T + \frac{T^2}{2}\mu + \sigma\, T\, W_t - \sigma \int_0^t s \mathrm{d}W_s
\end{aligned}$$

by using Itô's product rule as well as the martingale property of Brownian motion and of the stochastic integral. We obtain

$$X_t = x_0 - \int_0^t u_s \mathrm{d}s + \sigma\, T\, W_t - \sigma \int_0^t s \mathrm{d}W_s$$

since

$$x_0 \coloneqq X_0 = \mathrm{E}\left[\int_0^T Y_s \mathrm{d}s\right] = y_0\, T + \frac{T^2}{2}\mu + \sigma\, \mathrm{E}\left[\int_0^T W_s \mathrm{d}s\right] = y_0\, T + \frac{T^2}{2}\mu$$

with the computation above. Finally, we arrive at the dynamics of X given by

$$\mathrm{d}X_t = -u_t \mathrm{d}t + \sigma\, T \mathrm{d}W_t - \sigma\, t \mathrm{d}W_t = -u_t \mathrm{d}t + \sigma\,(T - t)\mathrm{d}W_t.$$

Hence in this case we have $G(t) = \sigma\,(T - t)$.

2.1.3 The Ornstein-Uhlenbeck Model Variant

We now assume that Y is an Ornstein-Uhlenbeck process, thus we have

$$\mathrm{d}Y_t = \theta\,(\mu - Y_t)\mathrm{d}t + \sigma \mathrm{d}W_t$$

for constant parameters $\theta, \mu, \sigma \in \mathbb{R}$. Since this SDE is linear, we may apply the variation of constants method (as given e.g. by Korn [Kor14]) to obtain a closed-form expression as

$$\begin{aligned}
Y_t &= \mathrm{e}^{-\theta t}\left[y_0 + \int_0^t \mu\, \theta\, \mathrm{e}^{\theta s} \mathrm{d}s + \int_0^t \sigma\, \mathrm{e}^{\theta s} \mathrm{d}W_s\right] \\
&= y_0\, \mathrm{e}^{-\theta t} + \mu\, \left(1 - \mathrm{e}^{-\theta t}\right) + \sigma \int_0^t \mathrm{e}^{-\theta(t-s)} \mathrm{d}W_s.
\end{aligned}$$

Again we compute

$$\mathrm{E}\left[\int_0^T Y_s \mathrm{d}s \,\middle|\, \mathcal{F}_t\right] = \int_0^T \left[y_0\, \mathrm{e}^{-\theta v} + \mu\, \left(1 - \mathrm{e}^{-\theta v}\right)\right] \mathrm{d}v + \sigma\, \mathrm{E}\left[\int_0^T \int_0^v \mathrm{e}^{-\theta(v-s)} \mathrm{d}W_s \mathrm{d}v \,\middle|\, \mathcal{F}_t\right].$$

The first term can easily be evaluated to result in

$$\int_0^T \left[y_0 \, \mathrm{e}^{-\theta v} + \mu \left(1 - \mathrm{e}^{-\theta v} \right) \right] \mathrm{d}v = \mu \, T + \frac{1}{\theta} \left(1 - \mathrm{e}^{-\theta T} \right) (y_0 - \mu) \, .$$

In order to rewrite the second term, let $Z_v = \int_0^v \mathrm{e}^{\theta s} \mathrm{d}W_s$ and $\tilde{Z}_v = \mathrm{e}^{-\theta v}$. We compute $\frac{\mathrm{d}\left(\mathrm{e}^{-\theta v}\right)}{\mathrm{d}v} = -\theta \mathrm{e}^{-\theta v}$ and therefore we have

$$\begin{aligned} \int_0^T Z_v \mathrm{d}\tilde{Z}_v = \int_0^T \int_0^v \mathrm{e}^{\theta s} \mathrm{d}W_s \mathrm{d}\left(\mathrm{e}^{-\theta v} \right) &= \int_0^T \int_0^v \mathrm{e}^{\theta s} \mathrm{d}W_s \frac{\mathrm{d}\left(\mathrm{e}^{-\theta v} \right)}{\mathrm{d}v} \mathrm{d}v \\ &= -\theta \int_0^T \mathrm{e}^{-\theta v} \int_0^v \mathrm{e}^{\theta s} \mathrm{d}W_s \mathrm{d}v = -\theta \int_0^T \int_0^v \mathrm{e}^{-\theta(v-s)} \mathrm{d}W_s \mathrm{d}v. \end{aligned}$$

In the next step we use this to apply the product rule; note that by definition $Z_0 = 0$ and $\tilde{Z}_0 = 1$, therefore $Z_0 \, \tilde{Z}_0 = 0$. Furthermore, since $\tilde{Z}$ is deterministic, we have for the quadratic covariation that $[Z, \tilde{Z}]_T = 0$. Thus, we compute

$$\begin{aligned} \int_0^T \int_0^v \mathrm{e}^{-\theta(v-s)} \mathrm{d}W_s \mathrm{d}v &= -\frac{1}{\theta} \int_0^T Z_v \mathrm{d}\tilde{Z}_v = -\frac{1}{\theta} \left(Z_T \tilde{Z}_T - \int_0^T \tilde{Z}_v \mathrm{d}Z_v \right) \\ &= -\frac{1}{\theta} \left(\mathrm{e}^{-\theta T} \int_0^T \mathrm{e}^{\theta s} \mathrm{d}W_s - \int_0^T \mathrm{e}^{-\theta v} \mathrm{d} \left(\int_0^v \mathrm{e}^{\theta s} \mathrm{d}W_s \right) \right) \\ &= -\frac{1}{\theta} \left(\mathrm{e}^{-\theta T} \int_0^T \mathrm{e}^{\theta s} \mathrm{d}W_s - \int_0^T \mathrm{e}^{-\theta v} \, \mathrm{e}^{\theta v} \mathrm{d}W_v \right) \\ &= -\frac{1}{\theta} \left(\mathrm{e}^{-\theta T} \int_0^T \mathrm{e}^{\theta s} \mathrm{d}W_s - \int_0^T \mathrm{d}W_s \right). \end{aligned}$$

Now we compute the conditional expectation by applying the martingale property of the stochastic integral as

$$\begin{aligned} \mathrm{E}\left[\int_0^T \int_0^v \mathrm{e}^{-\theta(v-s)} \mathrm{d}W_s \mathrm{d}v \,\middle|\, \mathcal{F}_t \right] &= -\frac{1}{\theta} \mathrm{e}^{-\theta T} \mathrm{E}\left[\int_0^T \mathrm{e}^{\theta s} \mathrm{d}W_s \,\middle|\, \mathcal{F}_t \right] + \frac{1}{\theta} \mathrm{E}\left[\int_0^T \mathrm{d}W_s \,\middle|\, \mathcal{F}_t \right] \\ &= -\frac{1}{\theta} \mathrm{e}^{-\theta T} \int_0^t \mathrm{e}^{\theta s} \mathrm{d}W_s + \frac{1}{\theta} \int_0^t \mathrm{d}W_s \\ &= \int_0^t \frac{1 - \mathrm{e}^{-\theta(T-s)}}{\theta} \mathrm{d}W_s. \end{aligned}$$

Altogether we have

$$\mathrm{E}\left[\int_0^T Y_s \mathrm{d}s \,\middle|\, \mathcal{F}_t \right] = \mu T + \frac{1}{\theta} \left(1 - \mathrm{e}^{-\theta T} \right) (y_0 - \mu) + \sigma \int_0^t \frac{1 - \mathrm{e}^{-\theta(T-s)}}{\theta} \mathrm{d}W_s$$

and therefore

$$X_t = -\int_0^t u_s \mathrm{d}s + \mu \, T + \frac{1}{\theta} \left(1 - \mathrm{e}^{-\theta T} \right) (y_0 - \mu) + \sigma \int_0^t \frac{1 - \mathrm{e}^{-\theta(T-s)}}{\theta} \mathrm{d}W_s.$$

With

$$x_0 \coloneqq X_0 = \mu \, T + \frac{1}{\theta} \left(1 - \mathrm{e}^{-\theta T} \right) (y_0 - \mu),$$

we simplify this to

$$X_t = x_0 - \int_0^t u_s \mathrm{d}s + \sigma \int_0^t \frac{1 - \mathrm{e}^{-\theta(T-s)}}{\theta} \, \mathrm{d}W_s$$

and rewrite in differential form as

$$\mathrm{d}X_t = -u_t \mathrm{d}t + \sigma \, \frac{1 - \mathrm{e}^{-\theta(T-t)}}{\theta} \, \mathrm{d}W_t.$$

Thus, we obtain

$$G(t) = \sigma \, \frac{1 - \mathrm{e}^{-\theta(T-t)}}{\theta}.$$

It should be noted that

$$\frac{1 - \mathrm{e}^{-\theta(T-t)}}{\theta} \approx T - t,$$

therefore the volatility functions G of the Brownian and the Ornstein-Uhlenbeck model variants are similar.

Summary

In this section, we introduced three different ways to model the emission rate Y and in each case, we derived an SDE to describe the total expected emissions X.

2.2 Cost Minimization

The next step is to model the optimization problem of the representative agent. She aims to choose her abatement rate in such a way that her total costs originating in the emission trading system are minimized. There are two sources of costs in the system: If the total amount of emissions surpasses the number of distributed allowances e_0, the agent needs to pay a penalty p for each surplus ton of emissions. We introduce a penalty function P to represent this given by

$$P(x) = \begin{cases} p\,(x - e_0) & \text{if} \quad x > e_0, \\ 0 & \text{if} \quad x \leq e_0. \end{cases}$$

Since the total emissions resulting in the system are given by X_T, we obtain the penalty payment as $P(X_T)$. On the other hand, abatement of emissions also induces costs. We assume that abatement costs are quadratic in the abatement rate and therefore define the cost function as

$$C(u) = \frac{1}{2} \, c \, u^2,$$

where c is a constant cost coefficient. Thus the overall costs of the agent for a fixed abatement rate u, discounted to time 0, are given by

$$\mathrm{e}^{-rT} \, P(X_T) + \int_0^T \mathrm{e}^{-rt} \, C(u_t) \mathrm{d}t.$$

The agent now aims to minimize expected costs by choosing the abatement rate u. Since a negative abatement rate would not be plausible both from a technical and from an

economical perspective, we assume that u takes values in $\mathcal{U} = [0, \infty)$. We furthermore define all admissible abatement rates by the admissibility set

$$\mathcal{A}(t) = \Big\{ u = (u_s)_{s\in[t,T]} \text{ a progressively measurable process into } \mathcal{U} \text{ with } \mathrm{E}\left[\int_t^T |u_s|^2 \mathrm{d}s\right] < \infty \Big\}.$$

Then the optimization problem of the agent can be stated as

$$\inf_{u\in\mathcal{A}(0)} \mathrm{E}\left[\mathrm{e}^{-rT} P(X_T) + \int_0^T \mathrm{e}^{-rs} C(u_s)\mathrm{d}s\right].$$

In order to solve this problem, we will follow a stochastic control approach. In the next steps we will motivate the Hamilton-Jacobi-Bellman equation by applying the Bellman principle; note that since we cannot ensure at this point that the Bellman principle holds, the following derivation is only heuristic. We define the value function as

$$V(t,x) = \inf_{u\in\mathcal{A}(t)} \mathrm{E}^{t,x}\left[\mathrm{e}^{-rT} P(X_T) + \int_t^T \mathrm{e}^{-rs} C(u_s)\mathrm{d}s\right].$$

In this expression and in the remainder of the thesis, we use the notation $\mathrm{E}^{t,x}[Z]$ to denote the factorized conditional expectation

$$\mathrm{E}^{t,x}[Z] = \mathrm{E}[Z \mid X_t = x]$$

for any random variable Z. We let $\tau \in \mathbb{R}$ with $\tau > t$ and apply the Bellman principle to yield

$$V(t,x) = \inf_{u\in\mathcal{A}(t)} \mathrm{E}^{t,x}\left[\int_t^\tau e^{-rs} C(u_s)\mathrm{d}s + V(\tau, X_\tau)\right].$$

Then we apply the Itô-formula to $V(\tau, X_\tau)$, using the relation $\mathrm{d}X_t = -u_t\mathrm{d}t + G(t)\mathrm{d}W_t$ as derived above, to arrive at

$$\begin{aligned} V(t,x) = \inf_{u\in\mathcal{A}(t)} \mathrm{E}^{t,x}\Bigg[&\int_t^\tau e^{-rs} C(u_s)\mathrm{d}s + V(t,x) - \int_t^\tau G(s)\, V_x(s, X_s)\mathrm{d}W_s \\ &+ \int_t^\tau \left(V_t(s,X_s) - u_s\, V_x(s,X_s) + \frac{1}{2} G(t)^2\, V_{xx}(s,X_s)\right)\mathrm{d}s\Bigg]. \end{aligned}$$

We assume that $G(s)V_x(s, X_s)$ is integrable with respect to Brownian motion such that the stochastic integral is a martingale. Then it follows that

$$\begin{aligned} &\mathrm{E}\left[\int_t^\tau G(s)\, V_x(s,X_s)\mathrm{d}W_s \,\middle|\, \mathcal{F}_t\right] \\ &\quad = \mathrm{E}\left[\int_0^\tau G(s)\, V_x(s,X_s)\mathrm{d}W_s \,\middle|\, \mathcal{F}_t\right] - \mathrm{E}\left[\int_0^t G(s)\, V_x(s,X_s)\mathrm{d}W_s \,\middle|\, \mathcal{F}_t\right] \\ &\quad = \int_0^t G(s) V_x(s,X_s)\mathrm{d}W_s - \int_0^t G(s) V_x(s,X_s)\mathrm{d}W_s = 0, \end{aligned}$$

thus we can omit the stochastic integral from the expression above. We subtract $V(t,x)$, divide by $\tau - t$ and let $\tau \downarrow t$, then

$$\begin{aligned} 0 = \inf_{u\in\mathcal{A}(t)} \mathrm{E}^{t,x}\Bigg[\lim_{\tau\downarrow t} \frac{1}{\tau - t}\int_t^\tau \Bigg(e^{-rs}\, C(u_s) + V_t(s,X_s) - u_s\, V_x(s,X_s) \\ + \frac{1}{2}\, G(t)^2\, V_{xx}(s,X_s)\Bigg)\,\mathrm{d}s\Bigg] \\ = \inf_{u\in\mathcal{A}(t)} \mathrm{E}^{t,x}\left[e^{-rt}\, C(u_t) - u_t\, V_x(t,X_t) + V_t(t,X_t) + \frac{1}{2}\, G(t)^2\, V_{xx}(t,X_t)\right]. \end{aligned}$$

Since X_t is $\mathcal{F}_t$-measurable and we may now choose $u \in \mathcal{U}$, we eliminate the conditional expectation and set $X_t = x$ to result in the HJB equation

$$0 = \inf_{u\in\mathcal{U}} \left\{e^{-rt}\, C(u) - u\, V_x(t,x) + V_t(t,x) + \frac{1}{2}\, G(t)^2\, V_{xx}(t,x)\right\}.$$

We minimize with respect to u by computing the first order condition

$$\mathrm{e}^{-rt}\,\frac{\partial C}{\partial u}(t,u) - V_x(t,x) = \mathrm{e}^{-rt}\, c\, u - V_x(t,x) \stackrel{!}{=} 0,$$

which delivers

$$u(t,x) = \frac{V_x(t,x)}{c}\,\mathrm{e}^{rt}.$$

Note that since the second derivative is given by

$$\mathrm{e}^{-rt}\, c > 0,$$

we directly see that u as determined above is indeed a minimum. We therefore obtain the characteristic PDE

$$V_t = \frac{1}{2c}\,\mathrm{e}^{rt}\,(V_x)^2 - \frac{1}{2}\, G(t)^2\, V_{xx}.$$

We then determine a final condition by setting $t = T$ in the value function, which results in

$$V(T,x) = \inf_{u_T\in\mathcal{U}} \mathrm{E}^{T,x}\left[\mathrm{e}^{-rT}\, P(X_T)\right] = \mathrm{e}^{-rT}\, P(x).$$

We now require the verification theorem for the HJB equation to make sure that the characteristic PDE provides us with the desired result.

Verification Theorem for the HJB Equation

We will introduce a slightly more general control problem to be able to state the result more generally; the problem formulation and the theorem are largely taken from Pham [Pha09]. We consider the SDE

$$\mathrm{d}X_t = b(t,X_t,u)\mathrm{d}t + \sigma(t,X_t,u)\mathrm{d}W_t$$

where u denotes the control, which maps into a set $\mathcal{U} \subseteq \mathbb{R}^m$, and $b : [0,T]\times\mathbb{R}^d\times\mathcal{U} \to \mathbb{R}^d$ and $\sigma : [0,T]\times\mathbb{R}^d\times\mathcal{U} \to \mathbb{R}^d$ are measurable functions. We assume that the coefficient functions b and σ are Lipschitz continuous in x, uniformly in t and u, i.e. there exists a constant L such that

$$\|b(t,x,u) - b(t,y,u)\| + \|\sigma(t,x,u) - \sigma(t,y,u)\| \le L\|x - y\|$$

for any $t \in [0,T]$, $x \in \mathbb{R}^d$ and $u \in \mathcal{U}$. Furthermore we assume that the coefficient functions satisfy a linear growth bound in x and in u, uniformly in t, i.e. there exists a constant K such that

$$\|b(t,x,u)\| + \|\sigma(t,x,u)\| \leq K(1 + \|x\| + \|u\|)$$

for any $t \in [0,T]$, $x \in \mathbb{R}^d$ and $u \in \mathcal{U}$.

Let $f : [0,T] \times \mathbb{R}^d \times \mathcal{U} \to \mathbb{R}$ and $g : \mathbb{R}^d \to \mathbb{R}$ be measurable functions which satisfy a quadratic growth condition, i.e. there exists a constant K such that

$$|f(t,x,u)| + |g(x)| \leq K(1 + \|x\|^2 + \|u\|^2)$$

for any $t \in [0,T]$, $x \in \mathbb{R}^d$ and $u \in \mathcal{U}$. As above, we define the admissibility set for the control u as

$$\mathcal{A}(t) = \Big\{ u = (u_s)_{s\in[t,T]} \text{ a progressively measurable process into } \mathcal{U} \text{ with } \mathrm{E}\left[\int_t^T \|u_s\|^2 \mathrm{d}s\right] < \infty \Big\}.$$

Then we may state the generalized control problem by defining the value function

$$V(t,x) = \inf_{u\in\mathcal{A}(t)} \mathrm{E}^{t,x}\left[g(X_T) + \int_t^T f(s, X_s, u)\mathrm{d}s \right];$$

we will discuss below why the assumptions made so far suffice to ensure the existence of this conditional expectation. Finally, we define the infinitesimal generator of the process X for a given control u as

$$\mathcal{L}^u V(t,x) = b(t,x,u)^\top V_x(t,x) + \frac{1}{2}\operatorname{Tr}\left(\sigma(t,x,u)\sigma(t,x,u)^\top V_{xx}(t,x)\right),$$

where $\operatorname{Tr}(\cdot)$ denotes the trace of a square matrix, i.e. for $A \in \mathbb{R}^{d\times d}$ we have

$$\operatorname{Tr}(A) = \sum_{i=1}^d a_{ii}.$$

We now continue to formulate the verification theorem.

Proposition 2.3. *Let V be the value function as defined above. Let $\hat{V}$ be a function with $\hat{V} \in C^{1,2}\left([0,T)\times\mathbb{R}^d\right)$ and $\hat{V} \in C\left([0,T]\times\mathbb{R}^d\right)$ satisfying a quadratic growth condition, i.e. there exists a constant K such that*

$$|\hat{V}(t,x)| \leq K\left(1 + |x|^2\right) \quad \textit{for any } (t,x) \in [0,T]\times\mathbb{R}^d.$$

(i) Suppose that

$$-\hat{V}_t(t,x) - \inf_{u\in\mathcal{U}}\left\{\mathcal{L}^u\hat{V}(t,x) + f(t,x,u)\right\} \leq 0$$

for all $(t,x) \in [0,T)\times\mathbb{R}^d$ and $\hat{V}(T,x) \leq g(x)$ for all $x \in \mathbb{R}^d$. Then $\hat{V} \leq V$.

(ii) Suppose that $\hat{V}(T,x) = g(x)$ *for all* $x \in \mathbb{R}$ *and there exists a measurable function* $\hat{u} : [0,T) \times \mathbb{R}^d \to \mathbb{R}^d$ *such that*

$$\begin{aligned} 0 &= -\hat{V}_t(t,x) - \inf_{u \in \mathcal{U}} \left\{ \mathcal{L}^u \hat{V}(t,x) + f(t,x,u) \right\} \\ &= -\hat{V}_t(t,x) + \mathcal{L}^{\hat{u}} \hat{V}(t,x) + f(t,x,\hat{u}). \end{aligned}$$

In addition suppose that the SDE

$$\mathrm{d}X_s = b(s, X_s, \hat{u}(s, X_s))\mathrm{d}s + \sigma(s, X_s, \hat{u}(s, X_s))\mathrm{d}W_s$$

has a unique solution, which we denote by $\hat{X}_s^{t,x}$ *for a given initial condition* $X_t = x$*, and suppose furthermore that* $\left\{ \hat{u}\left(s, \hat{X}_s^{t,x}\right) : t \le s \le T \right\} \in \mathcal{A}(t)$*. Then*

$$\hat{V} = V \quad \text{on } [0,T] \times \mathbb{R}^d$$

and $\hat{u}$ *is an optimal control.*

Proof. We will refer to the proof by Pham[2] [Pha09] and argue why this applies to our setting despite having modified assumptions and a slightly different formulation of the result. First we note that by the linear growth bound on the coefficient functions we have

$$\begin{aligned} \mathrm{E}\left[\int_0^T \left(\|b(t,0,u_t)\|^2 + \|\sigma(t,0,u_t)\|^2 \right) \right] &\le \mathrm{E}\left[\int_0^T K(1 + \|0\|^2 + \|u_t\|^2)\mathrm{d}t \right] \\ &\le K + K\,\mathrm{E}\left[\int_0^T \|u_t\|^2 \mathrm{d}t \right] < \infty \end{aligned}$$

for any control $u \in \mathcal{A}(0)$, which ensures that the first assumption in the work by Pham that we did not make here also holds in our case. Pham uses this to conclude with the Lipschitz continuity of the coefficient functions that for a given control $u \in \mathcal{A}(t)$, given initial value x and starting time t the SDE has a unique solution, which we will denote by $X^{t,x,u}$. Furthermore, the solution satisfies

$$\mathrm{E}\left[\sup_{t \le s \le T} \left\| X_s^{t,x,u} \right\|^2 \right] < \infty.$$

With the quadratic growth condition on f this implies

$$\begin{aligned} \mathrm{E}\left[\int_t^T |f(s, X_s^{t,x,u}, u_s)| \mathrm{d}s \right] &\le \mathrm{E}\left[\int_t^T K(1 + \|X_s^{t,x,u}\|^2 + \|u\|^2)\mathrm{d}s \right] \\ &\le K\,T + K\,T\,\mathrm{E}\left[\sup_{t \le s \le T} \|X_s^{t,x,u}\|^2 \right] + \mathrm{E}\left[\int_t^T \|u_s\|^2 \mathrm{d}s \right] < \infty, \end{aligned}$$

corresponding to the second assumption of Pham that is not contained in our assumptions above. In a similar way, we have

$$\mathrm{E}\left[\left| g(X_T^{t,x,u}) \right| \right] \le \mathrm{E}\left[K\left(1 + \|X_T^{t,x,u}\|^2 \right) \right] \le K + K\,\mathrm{E}\left[\sup_{t \le s \le T} \left\| X_s^{t,x,u} \right\|^2 \right] < \infty,$$

[2] The theorem and the proof can be found as Theorem 3.5.2 on page 47 in [Pha09].

which together with the above ensures existence of the conditional expectation

$$\mathrm{E}^{t,x}\left[g(X_T) + \int_t^T f(s, X_s, u)\mathrm{d}s\right].$$

Finally, note that although Pham works with a time-homogenous SDE, his results can still be applied in our setting, since the structure of the SDE only plays a role in assuring the existence of a solution, which also holds in the time-inhomogenous case.

(i) We consider $-\hat{V}$. By the assumptions on $\hat{V}$ we have that $-\hat{V} \in C^{1,2}\left([0,T)\times\mathbb{R}^d\right)$, $-\hat{V} \in C\left([0,T]\times\mathbb{R}^d\right)$ and $-\hat{V}$ satisfies a quadratic growth condition. By assumption and by the duality of the supremum and the infimum[3] we have for any $(t,x) \in [0,T)\times\mathbb{R}^d$ that

$$-\hat{V}_t(t,x) + \sup_{u\in\mathcal{U}}\left\{-\mathcal{L}^u\hat{V}(t,x) - f(t,x,u)\right\} = -\hat{V}_t(t,x) - \inf_{u\in\mathcal{U}}\left\{\mathcal{L}^u\hat{V}(t,x) + f(t,x,u)\right\} \leq 0,$$

which is equivalent to

$$-\left(-\hat{V}_t(t,x)\right) - \sup_{u\in\mathcal{U}}\left\{\mathcal{L}^u\left(-\hat{V}(t,x)\right) - f(t,x,u)\right\} \geq 0.$$

Furthermore, $-\hat{V}(T,x) \geq -g(x)$ for any $x \in \mathbb{R}^d$. We define

$$v(t,x) = \sup_{u\in\mathcal{A}(t)} \mathrm{E}^{t,x}\left[-g(X_T) - \int_t^T f(s, X_s, u)\mathrm{d}s\right]$$

and by the verification theorem of Pham we obtain $-\hat{V} \geq v$. Then again by the duality of the supremum and the infimum, we have $v = -V$ and therefore $\hat{V} \leq V$.

(ii) In the computations in (i), we have equality if $u = \hat{u}$, i.e.

$$-\left(-\hat{V}_t(t,x)\right) - \mathcal{L}^{\hat{u}}\left(-\hat{V}(t,x)\right) - f(t,x,\hat{u}) = 0$$

for any $(t,x) \in [0,T)\times\mathbb{R}^d$ and $-\hat{V}(T,x) = -g(x)$ for all $x \in \mathbb{R}^d$. Then by the verification theorem of Pham we have that $-\hat{V} = v$ and therefore $\hat{V} = V$. Furthermore, $\hat{u}$ is optimal. □

We now embed our control problem in this general framework. Clearly the coefficient functions satisfy the Lipschitz condition, since $b(t,x,u) = -u$ does not depend on x and the same holds for all volatility functions $\sigma(t,x,u) = G(t)$ in the different model variants. We also directly obtain the linear growth bound of b. Furthermore, the volatility functions of the model variants are continuous in t and do not depend on x and the control u. Thus they are bounded on the interval $[0,T]$ and therefore satisfy the linear growth bound.

In addition, the cost function C satisfies $C(u) = \frac{1}{2}\,c\,u^2 \leq K(1+|u|^2)$ for some constant K and the terminal condition function is linear for $x > e_0$ and constant for $x \leq e_0$ and therefore clearly $|\mathrm{e}^{-rT}P(x)| \leq K(1+|x|^2)$, again for a constant K. Thus we conclude that the verification theorem in Proposition 2.3 applies to our model. If we find a solution $\hat{V}$ of the PDE that satisfies the requirements of this theorem and if furthermore for $\hat{u}$ computed as $\hat{u}_t = \hat{u}(t, X_t) = \frac{\hat{V}_x(t,X_t)}{c}\,\mathrm{e}^{rt}$ we have that $\hat{u} \in \mathcal{A}(t)$ and the SDE

$$\mathrm{d}X_t = -\hat{u}(t, X_t)\mathrm{d}t + G(t)\mathrm{d}W_t$$

[3]For any set $B \subset \mathbb{R}$ it holds that $\inf\{B\} = -\sup\{-B\}$ where $-B \coloneqq \{-b : b \in B\}$.

has a unique solution, then the verification theorem delivers that $\hat{V}$ indeed gives us the minimum costs and that $\hat{u}$ represents the optimal control. We will assess these requirements once we have solved the PDE.

Remark 2.4. Note that although the set $\mathcal{U}$ into which all controls map is unbounded, in our case the infimum in the HJB equation is always finite: The term in the infimum given by

$$e^{-rt}\,C(u) - u\,V_x(t,x) + \frac{1}{2}\,G(t)^2\,V_{xx}(t,x) = \frac{1}{2}\,e^{-rt}\,c\,u^2 - u\,V_x(t,x) + V_t(t,x) + \frac{1}{2}\,G(t)^2\,V_{xx}(t,x)$$

is quadratic in u with positive coefficient for the term of second order and is thus for each $(t,x) \in [0,T) \times \mathbb{R}$ bounded from below.

Summary

We formulated the HJB equation for the cost minimization problem of the representative agent and we derived the characteristic PDE. Furthermore, we stated a verification theorem for the HJB equation, which will allow us to show that the solution of the characteristic PDE delivers a solution to the cost minimization problem.

2.3 Solution of the PDE

In this section, we will derive an analytical solution in the simple model; we will prove several properties of this solution. In the Brownian and in the Ornstein-Uhlenbeck model, the PDE needs to be solved numerically. Importantly, the solution of the PDE also supplies us with a function to compute the allowance price: By modeling individual agents separately, Seifert et al. [SUW08] have shown[4] that the price of an allowance, denoted by S, is given by the marginal abatement costs, i.e.

$$S(t,x) = \frac{\partial C}{\partial u} = c\,u(t,x).$$

2.3.1 Analytical Solution in the Simple Model Variant

We consider the simple model, i.e. $G(t) = \sigma$. In addition, we impose that $r = 0$; note that due to the currently very low interest rates, this is a realistic assumption. Then the characteristic PDE simplifies to

$$V_t = \frac{1}{2c}\,(V_x)^2 - \frac{1}{2}\,\sigma^2\,V_{xx}$$

with final condition

$$V(T,x) = P(x).$$

Thus the coefficients in the PDE are no longer time-dependent, which will enable us to derive an analytical solution. First, we perform a time reversion to transform the problem into an initial value problem. We substitute $t = T - \tilde{t}$ and define $\tilde{V}(\tilde{t},x) = V(T-\tilde{t},x)$. Then

$$V_t(t,x) = V_t(T-\tilde{t},x) = -V_{\tilde{t}}(T-\tilde{t},x) = -\tilde{V}_{\tilde{t}}(\tilde{t},x)$$

[4] This result can be found in their online appendix.

and $V_{xx}(T-\tilde{t},x) = \tilde{V}_{xx}(\tilde{t},x)$ and $V_x(T-\tilde{t},x) = \tilde{V}_x(\tilde{t},x)$. Therefore we obtain

$$\begin{aligned}\tilde{V}_{\tilde{t}} &= -\frac{1}{2c}\,(\tilde{V}_x)^2 + \frac{1}{2}\,\sigma^2\,\tilde{V}_{xx}\\ V(T,x) &= \tilde{V}(0,x) = P(x).\end{aligned}$$

For ease of notation, we will in the following again write t and V instead of $\tilde{t}$ and $\tilde{V}$. Next, we perform a Cole-Hopf transformation; this procedure is described for example by Evans in [Eva10][5]. We define

$$\nu(t,x) = \mathrm{e}^{-\frac{V(t,x)}{c\,\sigma^2}}.$$

Then $V(t,x) = -c\,\sigma^2 \ln(\nu(t,x))$ and we have

$$\begin{aligned}V_t &= -c\,\sigma^2 \frac{1}{\nu}\,\nu_t\\ V_x &= -c\,\sigma^2 \frac{1}{\nu}\,\nu_x\\ V_{xx} &= -c\,\sigma^2 \frac{1}{\nu}\,\nu_{xx} + c\,\sigma^2 \frac{1}{\nu^2}\,\nu_x^2.\end{aligned}$$

Substitution in the PDE results in

$$-c\,\sigma^2 \frac{1}{\nu}\,\nu_t = \frac{1}{2c}\,c^2\,\sigma^4 \frac{1}{\nu^2}\,\nu_x^2 + \frac{1}{2}\,\sigma^2\,c\,\sigma^2 \frac{1}{\nu}\,\nu_{xx} - \frac{1}{2}\,\sigma^2\,c\,\sigma^2 \frac{1}{\nu^2}\,\nu_x^2,$$

which simplifies to

$$\nu_t = \frac{1}{2}\,\sigma^2\,\nu_{xx}$$

with initial condition

$$\nu(0,x) = \mathrm{e}^{-\frac{V(0,x)}{c\sigma^2}} = \mathrm{e}^{-\frac{P(x)}{c\sigma^2}}.$$

Thus, we have arrived at the standard heat equation with conductivity $1/2\,\sigma^2$. It is well known (as given for instance also by Evans [Eva10]) that for a given continuous and bounded initial value function g and conductivity a the standard heat equation is solved by

$$\nu(t,x) = \frac{1}{\sqrt{4\pi a t}} \int_{-\infty}^{\infty} \mathrm{e}^{-\frac{(x-y)^2}{4at}}\, g(y)\mathrm{d}y.$$

Remark 2.5. In Theorem 2.3.1 of Evans[6], which provides the expression of the solution given above, two further results on the solution ν are given:

(i) The solution ν is infinitely differentiable on $(0,\infty)\times\mathbb{R}$.

(ii) For any $\xi_0 \in \mathbb{R}$, the solution ν converges to the initial value function g as $(t,x) \to (0,\xi_0)$, i.e. for $t > 0$ we have

$$\lim_{(t,x)\to(0,\xi_0)} \nu(t,x) = g(\xi_0),$$

which ensures that ν can be continuously extended to satisfy the initial value condition.

[5] This is presented in section 4.4.1 on pages 206-207 in [Eva10].

[6] The theorem can be found on page 47 in [Eva10]; to be precise, it delivers the solution of the standard heat equation with conductivity 1.

In our case, we have $\nu(0,x) = g(x) = \mathrm{e}^{-\frac{P(x)}{c\sigma^2}}$, which is continuous and bounded since the exponent is always non-positive. Therefore

$$\begin{aligned}\nu(t,x) &= \frac{1}{\sqrt{2\pi\sigma^2 t}} \int_{-\infty}^{\infty} \mathrm{e}^{-\frac{(x-y)^2}{2\sigma^2 t}} \mathrm{e}^{-\frac{P(y)}{c\sigma^2}} \mathrm{d}y \\ &= \frac{1}{\sqrt{2\pi\sigma^2 t}} \int_{-\infty}^{e_0} \mathrm{e}^{-\frac{(x-y)^2}{2\sigma^2 t}} \mathrm{d}y + \frac{1}{\sqrt{2\pi\sigma^2 t}} \int_{e_0}^{\infty} \mathrm{e}^{-\frac{(x-y)^2}{2\sigma^2 t}} \mathrm{e}^{-\frac{p(y-e_0)}{c\sigma^2}} \mathrm{d}y. \end{aligned} \tag{2.1}$$

In order to rewrite these integrals, we introduce the error function defined by

$$\operatorname{erf}(x) = \frac{2}{\sqrt{\pi}} \int_0^x \mathrm{e}^{-z^2} \mathrm{d}z$$

and state some of its properties, which will become important in the following.

Proposition 2.6. *For the error function* erf *the following holds:*

(i) The error function is odd, i.e. $\operatorname{erf}(-x) = -\operatorname{erf}(x)$.

(ii) We have

$$\begin{aligned} \operatorname{erf}(x) > 0 \quad &\text{if and only if} \quad x > 0, \\ \operatorname{erf}(x) < 0 \quad &\text{if and only if} \quad x < 0, \\ \operatorname{erf}(x) = 0 \quad &\text{if and only if} \quad x = 0. \end{aligned}$$

(iii) The limits are given by $\lim_{x\to-\infty} \operatorname{erf}(x) = -1$ *and* $\lim_{x\to\infty} \operatorname{erf}(x) = 1$.

(iv) The range of the error function is $(-1,1)$, *i.e.* $-1 < \operatorname{erf}(x) < 1$ *for any* $x \in \mathbb{R}$.

Proof. (i) By substituting $y = -z$, we have for $x \in \mathbb{R}$

$$\operatorname{erf}(-x) = \frac{2}{\sqrt{\pi}} \int_0^{-x} \mathrm{e}^{-z^2} \mathrm{d}z = -\frac{2}{\sqrt{\pi}} \int_0^x \mathrm{e}^{-y^2} \mathrm{d}y = -\operatorname{erf}(x).$$

(ii) By computing the derivative $\operatorname{erf}'(x) = \frac{2}{\sqrt{\pi}} \mathrm{e}^{-x^2} > 0$, we obtain that the error function is strictly increasing. Moreover, we have by definition that $\operatorname{erf}(0) = 0$, so the claim follows.

(iii) The property $\lim_{x\to\infty} \operatorname{erf}(x) = 1$ is for example given in the Handbook of Mathematical Functions [AS72]. Alternatively, we may observe that with the symmetry of the integrand

$$\lim_{x\to\infty} \operatorname{erf}(x) = \frac{2}{\sqrt{\pi}} \int_0^{\infty} \mathrm{e}^{-z^2} \mathrm{d}z = \frac{1}{2} \frac{2}{\sqrt{\pi}} \int_{-\infty}^{\infty} \mathrm{e}^{-z^2} \mathrm{d}z = \frac{1}{\sqrt{\pi}} \int_{-\infty}^{\infty} \mathrm{e}^{-z^2} \mathrm{d}z = 1$$

since $\frac{1}{\sqrt{\pi}} \mathrm{e}^{-z^2}$ is the density of the normal distribution with expectation 0 and variance $\frac{1}{2}$. The property $\lim_{x\to-\infty} \operatorname{erf}(x) = -1$ follows directly with property (i), i.e. that the error function is odd.

(iv) We have seen that $\lim_{x\to-\infty} \operatorname{erf}(x) = -1$ and $\lim_{x\to\infty} \operatorname{erf}(x) = 1$ and that the error function is strictly increasing, so for any $x \in \mathbb{R}$ it needs to hold that $-1 < \operatorname{erf}(x) < 1$. □

Returning to the derivation of the analytical solution, we aim to rewrite the integrals in expression (2.1), which we do separately. For the first integral, we introduce

$$z(y) = \frac{y-x}{\sqrt{2\sigma^2 t}}$$

with derivative

$$\frac{\mathrm{d}z}{\mathrm{d}y} = \frac{1}{\sqrt{2\sigma^2 t}}.$$

By substituting z in the integral we obtain

$$\begin{aligned}
\frac{1}{\sqrt{2\pi\sigma^2 t}} \int_{-\infty}^{e_0} \mathrm{e}^{-\frac{(x-y)^2}{2\sigma^2 t}} \mathrm{d}y &= \frac{\sqrt{2\sigma^2 t}}{\sqrt{2\pi\sigma^2 t}} \int_{-\infty}^{e_0} \frac{\mathrm{d}z}{\mathrm{d}y} \mathrm{e}^{-z(y)^2} \mathrm{d}y \\
&= \frac{1}{\sqrt{\pi}} \int_{-\infty}^{\frac{e_0-x}{\sqrt{2\sigma^2 t}}} \mathrm{e}^{-z^2} \mathrm{d}z \\
&= \frac{1}{2} \left(\frac{2}{\sqrt{\pi}} \int_{-\infty}^{0} \mathrm{e}^{-z^2} \mathrm{d}z + \frac{2}{\sqrt{\pi}} \int_{0}^{\frac{e_0-x}{\sqrt{2\sigma^2 t}}} \mathrm{e}^{-z^2} \mathrm{d}z \right) \\
&= \frac{1}{2} \left(1 + \operatorname{erf}\left(\frac{e_0-x}{\sqrt{2\sigma^2 t}} \right) \right),
\end{aligned} \tag{2.2}$$

where we have used that

$$\frac{2}{\sqrt{\pi}} \int_{-\infty}^{0} \mathrm{e}^{-z^2} \mathrm{d}z = -\frac{2}{\sqrt{\pi}} \int_{0}^{-\infty} \mathrm{e}^{-z^2} \mathrm{d}z = -\lim_{x \to -\infty} \operatorname{erf}(x) = 1$$

by property (iii) of the error function.

In order to simplify the second integral, we first rearrange the exponent in the integrand by completing the squares for y:

$$\begin{aligned}
&-\frac{(x-y)^2}{2\sigma^2 t} - \frac{p(y-e_0)}{c\sigma^2} = -\frac{c(x-y)^2 + 2tp(y-e_0)}{2c\sigma^2 t} = -\frac{cx^2 - 2cxy + cy^2 + 2tpy - 2tpe_0}{2c\sigma^2 t} \\
&= -\frac{cy^2 + 2cy\left(\frac{pt}{c} - x\right) + c\left(\frac{pt}{c} - x\right)^2 - \frac{p^2t^2}{c} + 2ptx - cx^2 + cx^2 - 2pte_0}{2c\sigma^2 t} \\
&= -\frac{c\left(y + \frac{pt}{c} - x\right)^2}{2c\sigma^2 t} + \frac{2pt(e_0 - x) + \frac{p^2t^2}{c}}{2c\sigma^2 t} = -\frac{\left(y + \frac{pt}{c} - x\right)^2}{2\sigma^2 t} + \frac{2cp(e_0 - x) + p^2 t}{2c^2\sigma^2}.
\end{aligned} \tag{2.3}$$

Then we have

$$\frac{1}{\sqrt{2\pi\sigma^2 t}} \int_{e_0}^{\infty} \mathrm{e}^{-\frac{(x-y)^2}{2\sigma^2 t}} \mathrm{e}^{-\frac{p(y-e_0)}{c\sigma^2}} \mathrm{d}y = \frac{1}{\sqrt{2\pi\sigma^2 t}} \mathrm{e}^{\frac{2cp(e_0-x)+p^2t}{2c^2\sigma^2}} \int_{e_0}^{\infty} \mathrm{e}^{-\frac{\left(y+\frac{pt}{c}-x\right)^2}{2\sigma^2 t}} \mathrm{d}y.$$

We now evaluate the integral by proceeding similarly as before: We define

$$z(y) = \frac{y + \frac{pt}{c} - x}{\sqrt{2\sigma^2 t}}$$

and compute the derivative

$$\frac{\mathrm{d}z}{\mathrm{d}y} = \frac{1}{\sqrt{2\sigma^2 t}}.$$

Then we perform the substitution

$$\begin{aligned}
\frac{1}{\sqrt{2\pi\sigma^2 t}}\int_{e_0}^{\infty} \mathrm{e}^{-\frac{\left(y+\frac{pt}{c}-x\right)^2}{2\sigma^2 t}}\mathrm{d}y &= \frac{\sqrt{2\sigma^2 t}}{\sqrt{2\pi\sigma^2 t}}\int_{e_0}^{\infty}\frac{\mathrm{d}z}{\mathrm{d}y}\,\mathrm{e}^{-z(y)^2}\mathrm{d}y \\
&= \frac{1}{\sqrt{\pi}}\int_{\frac{e_0+\frac{pt}{c}-x}{\sqrt{2\sigma^2 t}}}^{\infty}\mathrm{e}^{-z^2}\mathrm{d}z \\
&= \frac{1}{2}\left(\frac{2}{\sqrt{\pi}}\int_0^{\infty}\mathrm{e}^{-z^2}\mathrm{d}z - \frac{2}{\sqrt{\pi}}\int_0^{\frac{e_0+\frac{pt}{c}-x}{\sqrt{2\sigma^2 t}}}\mathrm{e}^{-z^2}\mathrm{d}z\right) \\
&= \frac{1}{2}\left(1-\operatorname{erf}\left(\frac{e_0+\frac{pt}{c}-x}{\sqrt{2\sigma^2 t}}\right)\right) \\
&= \frac{1}{2}\left(1-\operatorname{erf}\left(\frac{c(e_0-x)+pt}{\sqrt{2}c\sigma\sqrt{t}}\right)\right),
\end{aligned}$$

using that $\lim_{x\to\infty}\operatorname{erf}(x)=1$. Combining these results, we obtain

$$\nu(t,x)=\frac{\left(1+\operatorname{erf}\left(\frac{e_0-x}{\sqrt{2}\sigma\sqrt{t}}\right)\right)+\left(1-\operatorname{erf}\left(\frac{c(e_0-x)+pt}{\sqrt{2}c\sigma\sqrt{t}}\right)\right)\mathrm{e}^{\frac{2cp(e_0-x)+p^2t}{2c^2\sigma^2}}}{2}.$$

We now apply the back transformation $V(t,x)=-c\sigma^2\ln(\nu(t,x))$ and revert time again by replacing t by $T-t$. This delivers

$$V(t,x)=-c\sigma^2\ln\left(\frac{\left(1+\operatorname{erf}\left(\frac{e_0-x}{\sqrt{2}\sigma\sqrt{T-t}}\right)\right)+\left(1-\operatorname{erf}\left(\frac{c(e_0-x)+p(T-t)}{\sqrt{2}c\sigma\sqrt{T-t}}\right)\right)\mathrm{e}^{\frac{2cp(e_0-x)+p^2(T-t)}{2c^2\sigma^2}}}{2}\right). \tag{2.4}$$

By computing the derivative with respect to x, we obtain

$$V_x(t,x)=\frac{p}{1+\frac{e^{-\frac{2cp(e_0-x)+p^2(T-t)}{2c^2\sigma^2}}\left(1+\operatorname{erf}\left(\frac{e_0-x}{\sqrt{2}\sigma\sqrt{T-t}}\right)\right)}{1-\operatorname{erf}\left(\frac{c(e_0-x)+p(T-t)}{\sqrt{2}c\sigma\sqrt{T-t}}\right)}}, \tag{2.5}$$

the detailed computation can be found in section A.1.1 in the appendix[7].

2.3.2 Properties of the Analytical Solution

From the explicit expressions for V and V_x derived in the previous section, we may derive some useful properties, which will help us to verify the requirements of the verification theorem for the HJB equation further below in this section. In addition, we will refer back to these results in section 2.5 in order to show that the SDE in the simple model variant satisfies the requirements of the theorems we will prove below.

Proposition 2.7. *For the function V and its derivative V_x as given by equations (2.4) and (2.5) and the derivatives V_{xx} and V_{xt} derived from these we have the following properties:*

(i) V is infinitely differentiable on $(-\infty,T)\times\mathbb{R}$, i.e. $V\in C^{\infty}((-\infty,T)\times\mathbb{R})$.

[7] All these computations, starting with the reformulation of the integrals, were also conducted and thus validated by using the symbolic mathematics Python package `Sympy`.

(ii) $0 \leq V_x(t,x) \leq p$ *for any* $(t,x) \in [0,T] \times \mathbb{R} \backslash \{(T, e_0)\}$.

(iii) For all $t \in [0,T]$ *the limits of* V_x *are given by*

$$\lim_{x \to \infty} V_x(t,x) = p \quad \textit{and} \quad \lim_{x \to -\infty} V_x(t,x) = 0.$$

(iv) For any $\varepsilon > 0$ *the derivatives* V_{xx} *and* V_{xt} *are bounded on* $[0, T-\varepsilon] \times \mathbb{R}$.

Proof. To simplify the formulation of the proof, we first introduce some auxiliary functions given by

$$\begin{aligned}
F_1(t,x) &= 1 - \operatorname{erf}\left(\frac{ce_0 - cx + p(T-t)}{\sqrt{2}c\sigma\sqrt{T-t}}\right) \\
F_2(t,x) &= 1 + \operatorname{erf}\left(\frac{e_0 - x}{\sqrt{2}\sigma\sqrt{T-t}}\right) \\
E_1(t,x) &= \mathrm{e}^{\frac{(c(e_0-x)+p(T-t))^2}{2c^2\sigma^2(T-t)}} \\
E_2(t,x) &= \mathrm{e}^{\frac{(e_0-x)^2}{2\sigma^2(T-t)}} \\
E_3(t,x) &= \mathrm{e}^{\frac{2cp(e_0-x)+p^2(T-t)}{2c^2\sigma^2}}.
\end{aligned}$$

By Proposition 2.6 (iv), we know that the range of the error function is $(-1,1)$. Therefore we have

$$F_1(t,x) > 0 \quad \text{and} \quad F_2(t,x) > 0,$$

and since the exponential function is always positive,

$$E_1(t,x) > 0, \quad E_2(t,x) > 0 \quad \text{and} \quad E_3(t,x) > 0.$$

Additionally, we remark that all auxiliary functions are well defined as long as $t \in (-\infty, T)$.

(i) As stated above in Remark 2.5, ν is infinitely differentiable on $(0,\infty) \times \mathbb{R}$. We now perform the time reversion on ν by replacing t with $T-t$. Then

$$\tilde{\nu}(t,x) = \frac{\left(1 + \operatorname{erf}\left(\frac{e_0-x}{\sqrt{2}\sigma\sqrt{T-t}}\right)\right) + \left(1 - \operatorname{erf}\left(\frac{c(e_0-x)+p(T-t)}{\sqrt{2}c\sigma\sqrt{T-t}}\right)\right) \mathrm{e}^{\frac{2cp(e_0-x)+p^2(T-t)}{2c^2\sigma^2}}}{2}$$

and we have that $\tilde{\nu}$ is infinitely differentiable on $(-\infty, T) \times \mathbb{R}$. Furthermore, if we write $\tilde{\nu}$ in terms of the auxiliary functions, we obtain

$$\tilde{\nu}(t,x) = \frac{F_2(t,x) + E_3(t,x)\, F_1(t,x)}{2}.$$

Since all auxiliary functions are positive, we directly have that $\tilde{\nu} > 0$ for all $t \in (-\infty, T)$ and all $x \in \mathbb{R}$. From the time-reversed function $\tilde{\nu}$, we can compute the function V as

$$V(t,x) = -c\sigma^2 \ln(\tilde{\nu}(t,x)).$$

Thus V is essentially given as the composition of $\tilde{\nu}$ and the natural logarithm. But $\tilde{\nu}$ is infinitely differentiable on $(-\infty, T) \times \mathbb{R}$ and its range on this set is $(0,\infty)$. Furthermore, the natural logarithm is infinitely differentiable on $(0,\infty)$. Hence it follows that V is infinitely differentiable on $(-\infty, T) \times \mathbb{R}$.

(ii) We first let $t \in [0,T)$, $x \in \mathbb{R}$ arbitrary and consider V_x as given in equation (2.5). With the help of the auxiliary functions, we may rewrite V_x as

$$V_x(t,x) = \frac{p}{1 + \frac{F_2(t,x)}{E_3(t,x)\,F_1(t,x)}}.$$

Since all auxiliary functions are positive, we have that

$$\frac{F_2(t,x)}{E_3(t,x)\,F_1(t,x)} > 0,$$

which implies

$$1 + \frac{F_2(t,x)}{E_3(t,x)\,F_1(t,x)} > 1,$$

so it follows that $V_x(t,x) < p$. In particular, we have for the denominator

$$1 + \frac{F_2(t,x)}{E_3(t,x)F_1(t,x)} > 0;$$

with the assumption that $p > 0$, this delivers the lower bound $V_x(t,x) > 0$.

For $t = T$ and $x \in \mathbb{R}\backslash\{e_0\}$ arbitrary, V_x is given by the terminal condition of the PDE with

$$V_x(T,x) = \begin{cases} p & \text{if} \quad x > e_0 \\ 0 & \text{if} \quad x < e_0, \end{cases}$$

which clearly satisfies the bounds in the claim.

(iii) For $t = T$, this can be seen directly from the expression for $V_x(T,x)$ given above, so we assume that $t \in [0,T)$. We first consider the limit $x \to \infty$. We have that

$$\lim_{x\to\infty} \operatorname{erf}\left(\frac{e_0 - x}{\sqrt{2}\sigma\sqrt{T-t}}\right) = -1$$

since $\lim_{z\to-\infty} \operatorname{erf}(z) = -1$ by Proposition 2.6 (iii), and therefore

$$\lim_{x\to\infty} F_2(t,x) = \lim_{x\to\infty} \left(1 + \operatorname{erf}\left(\frac{e_0 - x}{\sqrt{2}\sigma\sqrt{T-t}}\right)\right) = 0.$$

Furthermore,

$$\lim_{x\to\infty} E_3(t,x) = \lim_{x\to\infty} \mathrm{e}^{\frac{2cp(e_0-x)+p^2(T-t)}{2c^2\sigma^2}} = 0.$$

Therefore we may apply l'Hôpital's rule to determine

$$\begin{aligned}
\lim_{x\to\infty} \frac{F_2(t,x)}{E_3(t,x)} &= \lim_{x\to\infty} \frac{1 + \operatorname{erf}\left(\frac{e_0-x}{\sqrt{2}\sigma\sqrt{T-t}}\right)}{\mathrm{e}^{\frac{2cp(e_0-x)+p^2(T-t)}{2c^2\sigma^2}}} = \lim_{x\to\infty} \frac{\frac{\mathrm{d}}{\mathrm{d}x}\left(1 + \operatorname{erf}\left(\frac{e_0-x}{\sqrt{2}\sigma\sqrt{T-t}}\right)\right)}{\frac{\mathrm{d}}{\mathrm{d}x}\,\mathrm{e}^{\frac{2cp(e_0-x)+p^2(T-t)}{2c^2\sigma^2}}} \\
&= \lim_{x\to\infty} \frac{-\frac{2}{\sqrt{2\pi}\sigma\sqrt{T-t}}\,\mathrm{e}^{-\frac{(e_0-x)^2}{2\sigma^2(T-t)}}}{-\frac{p}{c\sigma^2}\,\mathrm{e}^{\frac{2cp(e_0-x)+p^2(T-t)}{2c^2\sigma^2}}} \\
&= \lim_{x\to\infty} \frac{\sqrt{2}c\sigma}{\sqrt{\pi}p\sqrt{T-t}}\,\mathrm{e}^{-\frac{c^2(e_0-x)^2+2cp(e_0-x)(T-t)+p^2(T-t)^2}{2c^2\sigma^2(T-t)}} = 0,
\end{aligned}$$

since the coefficient of the term with the highest order in the polynomial in the exponential function is negative. With

$$\lim_{x\to\infty} F_1(t,x) = \lim_{x\to\infty}\left(1-\operatorname{erf}\left(\frac{c(e_0-x)+p(T-t)}{\sqrt{2}c\sigma\sqrt{T-t}}\right)\right) = 2,$$

we obtain that

$$\lim_{x\to\infty}\frac{F_2(t,x)}{E_3(t,x)\,F_1(t,x)} = 0$$

and therefore

$$\lim_{x\to\infty} V_x(t,x) = \lim_{x\to\infty}\frac{p}{1+\frac{F_2(t,x)}{E_3(t,x)\,F_1(t,x)}} = \frac{p}{1+0} = p.$$

We proceed similarly for $x\to-\infty$. Here we observe that

$$\lim_{x\to-\infty}\operatorname{erf}\left(\frac{c(e_0-x)+p(T-t)}{\sqrt{2}c\sigma\sqrt{T-t}}\right) = 1$$

and thus

$$\lim_{x\to-\infty} F_1(t,x) = \lim_{x\to-\infty}\left(1-\operatorname{erf}\left(\frac{c(e_0-x)+p(T-t)}{\sqrt{2}c\sigma\sqrt{T-t}}\right)\right) = 0.$$

In addition, we have

$$\lim_{x\to-\infty}\frac{1}{E_3(t,x)} = \lim_{x\to-\infty}\mathrm{e}^{-\frac{2cp(e_0-x)+p^2(T-t)}{2c^2\sigma^2}} = 0.$$

Again we may apply l'Hôpital's rule to compute

$$\begin{aligned}
\lim_{x\to-\infty}\frac{1}{E_3(t,x)F_1(t,x)} &= \lim_{x\to-\infty}\frac{\mathrm{e}^{-\frac{2cp(e_0-x)+p^2(T-t)}{2c^2\sigma^2}}}{1-\operatorname{erf}\left(\frac{c(e_0-x)+p(T-t)}{\sqrt{2}c\sigma\sqrt{T-t}}\right)}\\
&= \lim_{x\to-\infty}\frac{\frac{\mathrm{d}}{\mathrm{d}x}\mathrm{e}^{-\frac{2cp(e_0-x)+p^2(T-t)}{2c^2\sigma^2}}}{\frac{\mathrm{d}}{\mathrm{d}x}\left(1-\operatorname{erf}\left(\frac{c(e_0-x)+p(T-t)}{\sqrt{2}c\sigma\sqrt{T-t}}\right)\right)}\\
&= \lim_{x\to-\infty}\frac{\frac{p}{c\sigma^2}\mathrm{e}^{-\frac{2cp(e_0-x)+p^2(T-t)}{2c^2\sigma^2}}}{\frac{2}{\sqrt{2\pi}\sigma\sqrt{T-t}}\mathrm{e}^{-\frac{(c(e_0-x)+p(T-t))^2}{2c^2\sigma^2(T-t)}}}\\
&= \lim_{x\to-\infty}\frac{p\sqrt{\pi(T-t)}}{\sqrt{2}c\sigma}\mathrm{e}^{\frac{(c(e_0-x)+p(T-t))^2-2cp(e_0-x)(T-t)-p^2(T-t)^2}{2c^2\sigma^2(T-t)}}\\
&= \infty
\end{aligned}$$

because in this case the coefficient of the term with highest order in the polynomial in the exponential function is positive and additionally the corresponding exponent is even. Since

$$\lim_{x\to-\infty} F_2(t,x) = \lim_{x\to-\infty}\left(1+\operatorname{erf}\left(\frac{e_0-x}{\sqrt{2}\sigma\sqrt{T-t}}\right)\right) = 2,$$

we have

$$\lim_{x\to\infty}\frac{F_2(t,x)}{E_3(t,x)\,F_1(t,x)} = \infty,$$

so the denominator in the expression for V_x tends to infinity and therefore we may conclude that

$$\lim_{x\to-\infty} V_x(t,x) = \lim_{x\to-\infty} \frac{p}{1+\frac{F_2(t,x)}{E_3(t,x)\,F_1(t,x)}} = 0.$$

(iv) Let $\varepsilon > 0$ arbitrary and let $t \in [0, T-\varepsilon]$. We first consider the derivative V_{xx}. In section A.1.2 in the appendix, we derive V_{xx} expressed in terms of the auxiliary functions as

$$\begin{aligned} V_{xx}(t,x) &= \frac{p\sqrt{2}}{\sqrt{\pi}\sigma\sqrt{T-t}\,(E_2(t,x)\,F_2(t,x)+E_1(t,x)\,F_1(t,x))} \\ &\quad - \frac{p^2}{c\sigma^2\left(\frac{F_2(t,x)}{E_3(t,x)\,F_1(t,x)}+2+\frac{E_3(t,x)\,F_1(t,x)}{F_2(t,x)}\right)} \\ &=: A^{xx} + B^{xx}. \end{aligned}$$

We look at the two terms A^{xx} and B^{xx} separately. For the second term B^{xx}, we use that all auxiliary functions are positive and therefore

$$\frac{F_2(t,x)}{E_3(t,x)\,F_1(t,x)} + 2 + \frac{E_3(t,x)\,F_1(t,x)}{F_2(t,x)} > 2.$$

Thus we have a lower bound given by

$$B^{xx} = -\frac{p^2}{c\sigma^2\left(\frac{F_2(t,x)}{E_3(t,x)\,F_1(t,x)}+2+\frac{E_3(t,x)\,F_1(t,x)}{F_2(t,x)}\right)} \geq -\frac{p^2}{2c\sigma^2}.$$

In particular, we have

$$\frac{F_2(t,x)}{E_3(t,x)\,F_1(t,x)} + 2 + \frac{E_3(t,x)\,F_1(t,x)}{F_2(t,x)} > 0,$$

which delivers the upper bound as

$$B^{xx} = -\frac{p^2}{c\sigma^2\left(\frac{F_2(t,x)}{E_3(t,x)\,F_1(t,x)}+2+\frac{E_3(t,x)\,F_1(t,x)}{F_2(t,x)}\right)} < 0.$$

For the first term A^{xx}, we have by the positivity of the auxiliary functions that

$$E_2(t,x)\,F_2(t,x) + E_1(t,x)\,F_1(t,x) > 0$$

and obtain the lower bound

$$A^{xx} = \frac{p\sqrt{2}}{\sqrt{\pi}\sigma\sqrt{T-t}\,(E_2(t,x)\,F_2(t,x)+E_1(t,x)\,F_1(t,x))} > 0.$$

For the upper bound, we observe that

$$E_1(t,x) = \mathrm{e}^{\frac{(c(e_0-x)+p(T-t))^2}{2c^2\sigma^2(T-t)}} \geq 1 \quad \text{and} \quad E_2(t,x) = \mathrm{e}^{\frac{(e_0-x)^2}{2\sigma^2(T-t)}} \geq 1$$

since with $t < T$ both exponents are non-negative. We now perform a case distinction. Let us first assume that $x \leq e_0$. Then we have

$$\frac{e_0 - x}{\sqrt{2}\sigma\sqrt{T-t}} \geq 0$$

and by property (ii) of the error function, we obtain the bound

$$\operatorname{erf}\left(\frac{e_0 - x}{\sqrt{2}\sigma\sqrt{T-t}}\right) \geq 0,$$

which implies that

$$F_2(t,x) = 1 + \operatorname{erf}\left(\frac{e_0 - x}{\sqrt{2}\sigma\sqrt{T-t}}\right) \geq 1.$$

Then $E_2(t,x)\,F_2(t,x) \geq 1$ and since all auxiliary functions are positive, we obtain

$$E_2(t,x)\,F_2(t,x) + E_1(t,x)\,F_1(t,x) > 1.$$

Now we consider the case that $x \geq e_0 + {}^{pT}/_{c}$. Then we have

$$ce_0 - cx + p(T-t) \leq ce_0 - c\left(e_0 + \frac{pT}{c}\right) + p(T-t) = -pt \leq 0$$

and therefore

$$\operatorname{erf}\left(\frac{ce_0 - cx + p(T-t)}{\sqrt{2}c\sigma\sqrt{T-t}}\right) \leq 0.$$

This implies

$$F_1(t,x) = 1 - \operatorname{erf}\left(\frac{ce_0 - cx + p(T-t)}{\sqrt{2}c\sigma\sqrt{T-t}}\right) \geq 1,$$

so $E_1(t,x)\,F_1(t,x) \geq 1$ and we obtain

$$E_2(t,x)\,F_2(t,x) + E_1(t,x)\,F_1(t,x) > 1$$

as in the first case. We now combine these results: If $x \leq e_0$ or $x \geq e_0 + {}^{pT}/_{c}$, we have

$$A^{xx} = \frac{p\sqrt{2}}{\sqrt{\pi}\sigma\sqrt{T-t}\,(E_2(t,x)\,F_2(t,x) + E_1(t,x)\,F_1(t,x))} \leq \frac{p\sqrt{2}}{\sqrt{\pi}\sigma\sqrt{T-t}}.$$

This bound is increasing in t, thus we obtain a global bound if we insert the maximum value for t given by $t = T - \varepsilon$, which delivers

$$A^{xx} = \frac{p\sqrt{2}}{\sqrt{\pi}\sigma\sqrt{T-t}\,(F_2(t,x)E_2(t,x) + F_1(t,x)E_1(t,x))} \leq \frac{p\sqrt{2}}{\sqrt{\pi}\sigma\sqrt{\varepsilon}}.$$

By taking the sum of the bounds of the two terms A^{xx} and B^{xx}, we obtain an upper bound for any x with $x \leq e_0$ or $x \geq e_0 + {}^{pT}/_{c}$ and a lower bound for any $x \in \mathbb{R}$.

It remains to show[8] that there is also an upper bound for $x \in [e_0, e_0 + {}^{pT}/_{c}]$. With part (i) of this proposition, we know that V_{xx} is continuous. We then apply the extreme value theorem (or the boundedness theorem) to V_{xx} on the bounded and closed set $[0, T-\varepsilon] \times$

[8] More precisely, we only still need the upper bound for the first term A^{xx} if $x \in (e_0, e_0 + {}^{pT}/_{c})$ but in this case it is easier to show boundedness on the closed interval for the complete function V_{xx}.

$[e_0, e_0 + {}^{pT}/_c]$ and obtain that V_{xx} is indeed bounded on this set. By taking the maximum of the thus obtained upper bound and the upper bound determined in the computations above, we can conclude that V_{xx} is bounded on $[0, T-\varepsilon] \times \mathbb{R}$.

We now consider the mixed derivative V_{xt}. This is computed in section A.1.3 in the appendix; in terms of the auxiliary functions it can be expressed as

$$\begin{aligned} V_{xt}(t,x) = & \frac{p^2}{\sqrt{2\pi} c\sigma\sqrt{T-t}\,(E_2(t,x)\,F_2(t,x) + E_1(t,x)\,F_1(t,x))} \\ & - \frac{p^3}{2c^2\sigma^2\left(\frac{F_2(t,x)}{E_3(t,x)\,F_1(t,x)} + 2 + \frac{E_3(t,x)\,F_1(t,x)}{F_2(t,x)}\right)} \\ & - \frac{p^2}{\sqrt{2\pi} c\sigma\sqrt{T-t}\left(\frac{E_2(t,x)\,F_2(t,x)^2}{E_3(t,x)\,F_1(t,x)} + 2E_2(t,x)\,F_2(t,x) + E_1(t,x)\,F_1(t,x)\right)} \\ & - \frac{p(e_0-x)}{\sqrt{2\pi}\sigma(T-t)^{\frac{3}{2}}\,(E_2(t,x)\,F_2(t,x) + E_1(t,x)\,F_1(t,x))} \\ =: & A^{xt} + B^{xt} + C^{xt} + D^{xt}. \end{aligned}$$

We first note that the first and the second fraction, A^{xt} and B^{xt}, strongly resemble the terms A^{xx} and B^{xx} in the expression of V_{xx}. Indeed, we have that $A^{xt} = \frac{p}{2}\,A^{xx}$ and $B^{xt} = \frac{p}{2}\,B^{xx}$ and therefore

$$\begin{aligned} V_{xt}(t,x) = & \frac{p}{2}\,V_{xx}(t,x) \\ & - \frac{p^2}{\sqrt{2\pi} c\sigma\sqrt{T-t}\left(\frac{E_2(t,x)\,F_2(t,x)^2}{E_3(t,x)\,F_1(t,x)} + 2E_2(t,x)\,F_2(t,x) + E_1(t,x)\,F_1(t,x)\right)} \\ & - \frac{p(e_0-x)}{\sqrt{2\pi} c\sigma(T-t)^{\frac{3}{2}}\,(E_2(t,x)\,F_2(t,x) + E_1(t,x)\,F_1(t,x))}. \end{aligned}$$

Since we have already shown that $V_{xx}(t,x)$ is bounded, we only need to consider the remaining two terms. We start with C^{xt}. As all auxiliary functions are positive, we have

$$\frac{E_2(t,x)\,F_2(t,x)^2}{E_3(t,x)\,F_1(t,x)} + 2E_2(t,x)\,F_2(t,x) + E_1(t,x)\,F_1(t,x) > 0$$

and obtain the upper bound as

$$C^{xt} = -\frac{p^2}{\sqrt{2\pi} c\sigma\sqrt{T-t}\left(\frac{E_2(t,x)\,F_2(t,x)^2}{E_3(t,x)\,F_1(t,x)} + 2E_2(t,x)\,F_2(t,x) + E_1(t,x)\,F_1(t,x)\right)} < 0.$$

With the auxiliary functions being positive, we also have

$$\frac{E_2(t,x)\,F_2(t,x)^2}{E_3(t,x)\,F_1(t,x)} + 2E_2(t,x)\,F_2(t,x) + E_1(t,x)\,F_1(t,x) > E_2(t,x)\,F_2(t,x) + E_1(t,x)\,F_1(t,x)$$

which implies that

$$\begin{aligned} C^{xt} &= -\frac{p^2}{\sqrt{2\pi} c\sigma\sqrt{T-t}\left(\frac{E_2(t,x)\,F_2(t,x)^2}{E_3(t,x)\,F_1(t,x)} + 2E_2(t,x)\,F_2(t,x) + E_1(t,x)\,F_1(t,x)\right)} \\ &> -\frac{p^2}{\sqrt{2\pi} c\sigma\sqrt{T-t}\,(E_2(t,x)\,F_2(t,x) + E_1(t,x)\,F_1(t,x))} = -A^{xt} = -\frac{p}{2}\,A^{xx}. \end{aligned}$$

Thus the upper bound of A^{xx} provides a lower bound for C^{xt}.

It remains to consider the term D^{xt}. As in our considerations for V_{xx}, we will perform a case distinction. We first assume that $x < e_0$; in contrast to the above, we now require strict inequality. Then $p(e_0 - x) > 0$ and as we already know that the denominator is positive, we have

$$D^{xt} = -\frac{p(e_0 - x)}{\sqrt{2\pi}\sigma(T-t)^{\frac{3}{2}}\left(E_2(t,x)\,F_2(t,x) + E_1(t,x)\,F_1(t,x)\right)} < 0.$$

For the lower bound, we first observe that

$$\frac{e_0 - x}{\sqrt{2}\sigma\sqrt{T-t}} > 0$$

and thus by Proposition 2.6 (ii)

$$F_2(t,x) = 1 + \operatorname{erf}\left(\frac{e_0 - x}{\sqrt{2}\sigma\sqrt{T-t}}\right) > 1.$$

By recalling that $E_1(t,x)\,F_1(t,x) > 0$, we have

$$\begin{aligned} D^{xt} &= -\frac{p(e_0 - x)}{\sqrt{2\pi}\sigma(T-t)^{\frac{3}{2}}\left(E_2(t,x)\,F_2(t,x) + E_1(t,x)\,F_1(t,x)\right)} \\ &> -\frac{p(e_0 - x)}{\sqrt{2\pi}\sigma(T-t)^{\frac{3}{2}}E_2(t,x)} =: g(t,x). \end{aligned}$$

We aim to determine the limit of $g(t,x)$ for $x \to -\infty$ and show that this delivers a bound which is uniform in t. We have that

$$\lim_{x\to-\infty} p(e_0 - x) = \infty$$

and

$$\lim_{x\to-\infty} \sqrt{2\pi}\sigma(T-t)^{\frac{3}{2}}\,E_2(t,x) = \lim_{x\to-\infty} \sqrt{2\pi}\sigma(T-t)^{\frac{3}{2}}\,\mathrm{e}^{\frac{(e_0-x)^2}{2\sigma^2(T-t)}} = \infty.$$

Therefore we may apply l'Hôpital's rule. We first compute the partial derivative of E_2 with respect to x as

$$\frac{\partial E_2(t,x)}{\partial x} = \mathrm{e}^{\frac{(e_0-x)^2}{2\sigma^2(T-t)}}\,\frac{2(e_0-x)}{2\sigma^2(T-t)}\cdot(-1) = -\mathrm{e}^{\frac{(e_0-x)^2}{2\sigma^2(T-t)}}\,\frac{e_0-x}{\sigma^2(T-t)} = -\frac{e_0-x}{\sigma^2(T-t)}\,E_2(t,x).$$

Then we can compute the limit of g as

$$\begin{aligned} \lim_{x\to-\infty} g(t,x) &= -\lim_{x\to-\infty} \frac{p(e_0-x)}{\sqrt{2\pi}\sigma(T-t)^{\frac{3}{2}}\,E_2(t,x)} \\ &= -\lim_{x\to-\infty} \frac{\frac{\partial}{\partial x}\left(p(e_0-x)\right)}{\frac{\partial}{\partial x}\left(\sqrt{2\pi}\sigma(T-t)^{\frac{3}{2}}\,E_2(t,x)\right)} \\ &= -\lim_{x\to-\infty} \frac{-p}{-\sqrt{2\pi}\sigma(T-t)^{\frac{3}{2}}\,\frac{e_0-x}{\sigma^2(T-t)}\,E_2(t,x)} \\ &= -\lim_{x\to-\infty} \frac{p}{\frac{\sqrt{2\pi}}{\sigma}\sqrt{T-t}\,(e_0-x)\,E_2(t,x)} \\ &= 0 \end{aligned}$$

since the denominator tends to infinity. Next we determine t such that g is minimized for all sufficiently small x. We compute the partial derivative of E_2 with respect to t given by

$$\begin{aligned}\frac{\partial E_2(t,x)}{\partial t} &= \mathrm{e}^{\frac{(e_0-x)^2}{2\sigma^2(T-t)}}\,\frac{(e_0-x)^2}{2\sigma^2}\cdot(-1)\cdot(T-t)^{-2}\cdot(-1)\\ &= \mathrm{e}^{\frac{(e_0-x)^2}{2\sigma^2(T-t)}}\,\frac{(e_0-x)^2}{2\sigma^2(T-t)^2} = \frac{(e_0-x)^2}{2\sigma^2(T-t)^2}\,E_2(t,x)\end{aligned}$$

and with this we have

$$\begin{aligned}\frac{\partial g(t,x)}{\partial t} &= -\frac{-p(e_0-x)\sqrt{2\pi}\sigma\left(\frac{3}{2}(T-t)^{\frac{1}{2}}\cdot(-1)\cdot E_2(t,x)+(T-t)^{\frac{3}{2}}\frac{(e_0-x)^2}{2\sigma^2(T-t)^2}\,E_2(t,x)\right)}{2\pi\sigma^2(T-t)^3\,E_2(t,x)^2}\\ &= \frac{p(e_0-x)\left(-\frac{3}{2}\sqrt{T-t}+\frac{(e_0-x)^2}{2\sigma^2\sqrt{T-t}}\right)}{\sqrt{2\pi}\sigma(T-t)^3\,E_2(t,x)}.\end{aligned}$$

With $e_0 - x > 0$ and $E_2(t,x) > 0$, this is positive as long as

$$\frac{(e_0-x)^2}{2\sigma^2\sqrt{T-t}} > \frac{3}{2}\sqrt{T-t},$$

which is equivalent to

$$(e_0-x)^2 > 3\sigma^2(T-t)$$

and this holds if

$$x < e_0 - \sqrt{3}\sigma\sqrt{T-t}.$$

In other words, for $x < e_0 - \sqrt{3}\sigma\sqrt{T}$, which ensures that $x < e_0 - \sqrt{3}\sigma\sqrt{T-t}$ for any $t \in [0, T-\varepsilon]$, we have that $\frac{\partial}{\partial t}g(t,x) > 0$, so g is strictly increasing in t. By inserting the minimum value for t, we obtain a lower bound independent of t as

$$g(t,x) \geq g(0,x) = -\frac{p(e_0-x)}{\sqrt{2\pi}\sigma T^{\frac{3}{2}}\,E_2(0,x)}.$$

As shown above, we have that $\lim_{x\to-\infty} g(0,x) = 0$. In addition, $g(0,\cdot)$ is clearly continuous. Then we apply Lemma 2.8, which is stated and proven below this proof: It allows us to choose $K > 0$ and delivers that there exists $\tilde{x}_1$ such that $|g(0,x)| < K$ for all $x \leq \tilde{x}_1$. We now set

$$x_1 = \min\left\{\tilde{x}_1, e_0 - \sqrt{3}\sigma\sqrt{T}\right\}.$$

Then we have for all $x < x_1$ and for any $t \in [0, T-\varepsilon]$ that $g(t,x) \geq g(0,x) > -K$ and have thus obtained a lower bound of the term D^{xt} on $[0, T-\varepsilon] \times (-\infty, x_1)$ since

$$D^{xt} > g(t,x) > -K.$$

Next we consider the case that $x > e_0 + {}^{pT}/_{c}$. Then we have $p(e_0 - x) < -{}^{p^2T}/_{c} < 0$ and therefore we obtain the lower bound as

$$D^{xt} = -\frac{p(e_0-x)}{\sqrt{2\pi}\sigma(T-t)^{\frac{3}{2}}\,(E_2(t,x)F_2(t,x)+E_1(t,x)F_1(t,x))} > 0.$$

For the upper bound, we proceed similarly as in the first case. As seen in our considerations on V_{xx}, we know that since $c(e_0 - x) + pT < 0$, we now have $F_1(t,x) > 1$ by property (ii) of the error function. With $E_2(t,x)\,F_2(t,x) > 0$, we then have

$$\begin{aligned} D^{xt} &= -\frac{p(e_0 - x)}{\sqrt{2\pi}\sigma(T-t)^{\frac{3}{2}}\left(E_2(t,x)\,F_2(t,x) + E_1(t,x)\,F_1(t,x)\right)} \\ &< -\frac{p(e_0 - x)}{\sqrt{2\pi}\sigma(T-t)^{\frac{3}{2}}E_1(t,x)} =: h(t,x). \end{aligned}$$

For this case, we need to determine the limit of $h(t,x)$ for $x \to \infty$ and again we show that this delivers a bound which is uniform in t. We clearly have

$$\lim_{x\to\infty}\left(-p(e_0 - x)\right) = \infty$$

and

$$\lim_{x\to\infty}\sqrt{2\pi}\sigma(T-t)^{\frac{3}{2}}\,E_1(t,x) = \lim_{x\to\infty}\sqrt{2\pi}\sigma(T-t)^{\frac{3}{2}}\,\mathrm{e}^{\frac{(c(e_0-x)+p(T-t))^2}{2c^2\sigma^2(T-t)}} = \infty,$$

so we may apply l'Hôpital's rule. We compute the partial derivative of E_1 with respect to x as

$$\begin{aligned} \frac{\partial E_1(t,x)}{\partial x} &= \mathrm{e}^{\frac{(c(e_0-x)+p(T-t))^2}{2c^2\sigma^2(T-t)}}\,\frac{2(c(e_0-x)+p(T-t))}{2c^2\sigma^2(T-t)}\cdot(-c) \\ &= -\mathrm{e}^{\frac{(c(e_0-x)+p(T-t))^2}{2c^2\sigma^2(T-t)}}\,\frac{c(e_0-x)+p(T-t)}{c\sigma^2(T-t)} = -\frac{c(e_0-x)+p(T-t)}{c\sigma^2(T-t)}\,E_1(t,x) \end{aligned}$$

and then determine the limit

$$\begin{aligned} \lim_{x\to\infty} h(t,x) &= \lim_{x\to\infty}\frac{-p(e_0-x)}{\sqrt{2\pi}c\sigma(T-t)^{\frac{3}{2}}\,E_1(t,x)} \\ &= \lim_{x\to\infty}\frac{\frac{\partial}{\partial x}\left(-p(e_0-x)\right)}{\frac{\partial}{\partial x}\left(\sqrt{2\pi}\sigma(T-t)^{\frac{3}{2}}\,E_1(t,x)\right)} \\ &= \lim_{x\to\infty}\frac{p}{\sqrt{2\pi}\sigma(T-t)^{\frac{3}{2}}\left(-\frac{c(e_0-x)+p(T-t)}{c\sigma^2(T-t)}\right)E_1(t,x)} \\ &= 0 \end{aligned}$$

since $\lim_{x\to\infty} E_1(t,x) = \infty$ and with $c(e_0 - x) + p(T-t) < 0$, we have

$$\lim_{x\to\infty}\left(-\frac{c(e_0-x)+p(T-t)}{c\sigma^2(T-t)}\right) = \infty.$$

Next, we aim to find t which minimizes $h(t,x)$ for sufficiently large x. We compute the partial derivative of E_1 with respect to t as

$$\begin{aligned} \frac{\partial E_1(t,x)}{\partial t} &= \mathrm{e}^{\frac{(c(e_0-x)+p(T-t))^2}{2c^2\sigma^2(T-t)}}\left(\frac{2\big(c(e_0-x)+p(T-t)\big)\cdot(-p)\cdot 2c^2\sigma^2(T-t)}{4c^4\sigma^4(T-t)^2}\right. \\ &\qquad \left.-\frac{\big(c(e_0-x)+p(T-t)\big)^2\cdot(-2c^2\sigma^2)}{4c^4\sigma^4(T-t)^2}\right) \\ &= E_1(t,x)\,\frac{\big(c(e_0-x)+p(T-t)\big)\big(-2p(T-t)+c(e_0-x)+p(T-t)\big)}{2c^2\sigma^2(T-t)^2} \\ &= \frac{\big(c(e_0-x)+p(T-t)\big)\big(c(e_0-x)-p(T-t)\big)}{2c^2\sigma^2(T-t)^2}\,E_1(t,x). \end{aligned}$$

Then we have for the partial derivative of h

$$\begin{aligned}\frac{\partial h(t,x)}{\partial t} &= -\frac{-p(e_0-x)\sqrt{2\pi}\sigma}{2\pi\sigma^2(T-t)^3\,E_1(t,x)^2}\left(\frac{3}{2}(T-t)^{\frac{1}{2}}\cdot(-1)\cdot E_1(t,x)\right.\\ &\qquad\left.+\,(T-t)^{\frac{3}{2}}\,E_1(t,x)\frac{\big(c(e_0-x)+p(T-t)\big)\big(c(e_0-x)-p(T-t)\big)}{2c^2\sigma^2(T-t)^2}\right)\\ &= \frac{p(e_0-x)}{\sqrt{2\pi}\sigma(T-t)^3E_1(t,x)}\left(-\frac{3}{2}\sqrt{T-t}+\frac{c^2(e_0-x)^2-p^2(T-t)^2}{2c^2\sigma^2\sqrt{T-t}}\right).\end{aligned}$$

Since $e_0 - x < 0$, this expression is strictly negative if

$$\frac{c^2(e_0-x)^2-p^2(T-t)^2}{2c^2\sigma^2\sqrt{T-t}} > \frac{3}{2}\sqrt{T-t}$$

or, equivalently, if

$$c^2(e_0-x)^2 > 3c^2\sigma^2(T-t)+p^2(T-t)^2.$$

As $e_0 - x < 0$, we consider the negative of the term under the square and therefore require

$$-(e_0-x) > \sqrt{3\sigma^2(T-t)+\frac{p^2}{c^2}(T-t)^2},$$

which is equivalent to

$$x > e_0+\sqrt{3\sigma^2(T-t)+\frac{p^2}{c^2}(T-t)^2}.$$

For $t \in [0, T-\varepsilon]$, this is decreasing in t, so if

$$x > e_0+\sqrt{3\sigma^2\,T+\frac{p^2}{c^2}\,T^2},$$

the inequality above is satisfied for any $t \in [0, T-\varepsilon]$. Hence we then have $\frac{\partial}{\partial t}h(t,x) < 0$ for any $t \in [0, T-\varepsilon]$ and therefore h is decreasing in t. Thus it attains its maximum value on $[0, T-\varepsilon]$ for $t = 0$, implying that

$$h(t,x) \le h(0,x) = -\frac{p(e_0-x)}{\sqrt{2\pi}\sigma T^{\frac{3}{2}}E_1(0,x)} \quad \text{for all} \quad t \in [0, T-\varepsilon].$$

We have shown above that $\lim_{x\to\infty} h(0,x) = 0$ and furthermore $h(0,\cdot)$ is continuous. Therefore we again apply Lemma 2.8: We choose $K > 0$. Then there exists $\tilde{x}_2$ such that $|h(0,x)| < K$ and in particular $h(0,x) < K$ for all $x \ge \tilde{x}_2$. Now we set

$$x_2 = \max\left\{\tilde{x}_2, e_0+\sqrt{3\sigma^2\,T+\frac{p^2}{c^2}\,T^2}\right\}.$$

Then for any $x > x_2$ and for all $t \in [0, T-\varepsilon]$ we have that $h(t,x) \le h(0,x) < K$ and therefore

$$D^{xt} < h(t,x) < K.$$

Thus we have found an upper bound for the term D^{xt} on $[0, T-\varepsilon] \times (x_2, \infty)$.

With the results from above, we now have that V_{xt} is bounded on

$$[0, T-\varepsilon] \times \big((-\infty, x_1) \cup (x_2, \infty)\big).$$

It remains to consider the set $[0, T-\varepsilon] \times [x_1, x_2]$. But this is again bounded and closed. Since in addition V_{xt} is continuous, we may apply the extreme value theorem and obtain that V_{xt} is bounded on $[0, T-\varepsilon] \times [x_1, x_2]$. By combining this bound with the ones determined above, we may conclude that V_{xt} is bounded on $[0, T-\varepsilon] \times \mathbb{R}$. □

To complete the proof of Proposition 2.7 (iv), it remains to prove the following Lemma.

Lemma 2.8. *Let $g : \mathbb{R} \to \mathbb{R}$ be a continuous function.*

(i) If $\lim_{x\to\infty} g(x) = 0$, then for any $\kappa > 0$ there exists $x_0 \in \mathbb{R}$ such that $|g(x)| < \kappa$ for all $x \geq x_0$.

(ii) If $\lim_{x\to-\infty} g(x) = 0$, then for any $\kappa > 0$ there exists $x_0 \in \mathbb{R}$ such that $|g(x)| < \kappa$ for all $x \leq x_0$.

Proof. We only show part (i); part (ii) can be shown analogously. From $\lim_{x\to\infty} g(x) = 0$, we know that for any sequence $(y_n)_{n\in\mathbb{N}}$ with $\lim_{n\to\infty} y_n = \infty$ we have $\lim_{n\to\infty} g(y_n) = 0$. Since g is continuous, we have by the extreme value theorem that it attains its maximum on any closed and bounded subset. Thus we may define

$$y_n \coloneqq \underset{x\in[n,n+1]}{\arg\max} \{|g(x)|\}.$$

Then clearly $\lim_{n\to\infty} y_n = \infty$ and therefore $\lim_{n\to\infty} g(y_n) = 0$. This implies for $\kappa > 0$ arbitrary that there exists $N_0 \in \mathbb{N}$ such that

$$|g(y_n)| < \kappa$$

for all $n > N_0$. We define $x_0 \coloneqq y_{N_0}$ and observe that $x_0 \geq N_0$. For any $x \geq x_0$, we then know that there exists $n \geq N_0$ such that $x \in [n, n+1]$. By definition of $(y_n)_{n\in\mathbb{N}}$, we have

$$|g(x)| \leq |g(y_n)| < \kappa$$

as desired. □

These results will now help us to verify the requirements of the verification theorem for the HJB equation.

Proposition 2.9. *The function V as given by equation (2.4) for $t \in [0, T)$ and by the terminal condition of the PDE for $t = T$ satisfies the requirements of the verification theorem for the HJB equation, i.e. it holds that*

(i) V is continuously differentiable in t and twice continuously differentiable in x on $[0, T) \times \mathbb{R}$, i.e. $V \in C^{1,2}([0, T), \mathbb{R})$,

(ii) V is continuous on $[0, T] \times \mathbb{R}$, i.e. $V \in C([0, T], \mathbb{R})$,

(iii) V satisfies a quadratic growth condition, uniformly in t, i.e. there exists a constant $K > 0$ such that

$$|V(t, x)| \leq K(1 + |x|^2) \qquad \text{for all} \quad t \in [0, T].$$

Proof. (i) This follows directly from part (i) of Proposition 2.7.

(ii) First we note that the terminal condition given by the penalty function P is continuous in x and that V is continuous on $[0,T)\times\mathbb{R}$ by Proposition 2.7 (i). In Remark 2.5 (ii), we have stated the result from Evans that ν converges to the initial value function as $(t,x)\to(0,\xi_0)$, i.e.

$$\lim_{(t,x)\to(0,\xi_0)}\nu(t,x)=\mathrm{e}^{-\frac{P(\xi_0)}{c\sigma^2}}.$$

We perform the time reversion and define the time reversed solution $\tilde{\nu}$ as in the proof of Proposition 2.7 (i). For any $\xi_T\in\mathbb{R}$, we then have

$$\lim_{(t,x)\to(T,\xi_T)}\tilde{\nu}(t,x)=\mathrm{e}^{-\frac{P(\xi_T)}{c\sigma^2}}.$$

In addition, we have seen in the proof of Proposition 2.7 (i) that the transformation function $-c\sigma^2\ln(\cdot)$ is continuous on the image of $(0,\infty)\times\mathbb{R}$ under $\tilde{\nu}$, therefore also the transformed function V converges, i.e.

$$\lim_{(t,x)\to(T,\xi_T)}V(t,x)=P(\xi_T)$$

for any $\xi_T\in\mathbb{R}$. As V is continuous on $[0,T)\times\mathbb{R}$ and P is continuous on $\mathbb{R}$, it follows that continuity holds on $[0,T]\times\mathbb{R}$.

(iii) We first consider the case that $t\in[0,T)$. By Proposition 2.7 (ii), we then have for any $x\in\mathbb{R}$ that $0\le V_x(t,x)\le p$. For fixed t and arbitrary $x_0\in\mathbb{R}$, we apply the fundamental theorem of calculus to obtain a linear growth bound for V as

$$|V(t,x)|=\left|\int_{x_0}^{x}V_x(t,y)\mathrm{d}y+V(t,x_0)\right|\le\int_{x_0}^{x}|V_x(t,x)|\mathrm{d}y+|V(t,x_0)|\le p|x-x_0|+|V(t,x_0)|.$$

It remains to show that this bound is uniform in t. As we may choose x_0 arbitrarily, we set $x_0=e_0$. For $t\in[0,T)$, we then have

$$V(t,e_0)=-c\sigma^2\ln\left(\frac{1+\left(1-\operatorname{erf}\left(\frac{p\sqrt{T-t}}{\sqrt{2}c\sigma}\right)\right)\mathrm{e}^{\frac{p^2(T-t)}{2c^2\sigma^2}}}{2}\right).$$

Since the argument of the error function is non-negative and the range of the error function is $(-1,1)$, we have

$$1>\operatorname{erf}\left(\frac{p\sqrt{T-t}}{\sqrt{2}c\sigma}\right)\ge 0$$

and therefore

$$0<1-\operatorname{erf}\left(\frac{p\sqrt{T-t}}{\sqrt{2}c\sigma}\right)\le 1.$$

By using that the exponential function is positive, this implies

$$\frac{1}{2}\le\frac{1+\left(1-\operatorname{erf}\left(\frac{p\sqrt{T-t}}{\sqrt{2}c\sigma}\right)\right)\mathrm{e}^{\frac{p^2(T-t)}{2c^2\sigma^2}}}{2}\le\frac{1+\mathrm{e}^{\frac{p^2T}{2c^2\sigma^2}}}{2}.$$

But as the logarithm is monotone, we have

$$-c\sigma^2\ln\left(\frac{1}{2}\right)\ge-c\sigma^2\ln\left(\frac{1+\left(1-\operatorname{erf}\left(\frac{p\sqrt{T-t}}{\sqrt{2}c\sigma}\right)\right)e^{\frac{p^2(T-t)}{2c^2\sigma^2}}}{2}\right)\ge-c\sigma^2\ln\left(\frac{1+\mathrm{e}^{\frac{p^2T}{2c^2\sigma^2}}}{2}\right),$$

so $V(t, e_0)$ is bounded by the constant

$$K \coloneqq \max\left\{\left|c\sigma^2 \ln\left(\frac{1}{2}\right)\right|, \left|c\sigma^2 \ln\left(\frac{1+\mathrm{e}^{\frac{p^2 T}{2c^2\sigma^2}}}{2}\right)\right|\right\}.$$

Together with the above, we therefore obtain a linear bound of V in x, uniformly for all $t \in [0, T)$. Now we consider $V(T, x)$, which is given by the terminal condition of the PDE. By the definition of the penalty function, this is linear for $x \geq e_0$ and constant for $x \leq e_0$ and therefore in particular linearly bounded in x. Hence by choosing the maximum slope and the maximum constant of the two bounds, we have a linear bound of V in x, which is uniform for all $t \in [0, T]$. □

Proposition 2.10. *Let X be a continuous stochastic process which is adapted to $\mathcal{F}$. Then for any $t \in [0, T]$, the control process given by $u = (u_s)_{s\in[t,T]} = (u(s, X_s))_{s\in[t,T]}$ where*

$$u(s, x) = \frac{V_x(s, x)}{c}$$

satisfies $u \in \mathcal{A}(t)$.

Proof. For $s \in [t, T)$, u is continuous as a function in x by Proposition 2.7 (i). Since X is adapted to $\mathcal{F}$, it follows that the composition $u_s = u(s, X_s)$ is $\mathcal{F}_s$-measurable. For $s = T$, the function $u(T, \cdot)$ is piecewise constant and thus measurable, so again the composition $u(T, X_T)$ is measurable with respect to $\mathcal{F}_T$. Therefore u is $\mathcal{F}$-adapted; furthermore, X is continuous and u is right-continuous as a function in t by Proposition 2.7 (i). Hence u is progressively measurable.

From Proposition 2.7 (ii), we have that V_x is bounded and in particular $V_x \geq 0$. Then also $u \geq 0$, so the image of u lies in $\mathcal{U}$. Moreover, u is also bounded, i.e. for some constant K we have $|u(s, x)| \leq K$ for any $s \in [t, T]$ and any $x \in \mathbb{R}$. Thus

$$\mathrm{E}\left[\int_t^T |u_s|^2 \mathrm{d}s\right] = \mathrm{E}\left[\int_t^T |u(s, X_s)|^2 \mathrm{d}s\right] \leq T\,K^2 < \infty$$

and therefore $u \in \mathcal{A}(t)$. □

For the simple model variant, we may conclude that the verification theorem holds and the characteristic PDE indeed delivers the minimum costs and an optimal abatement rate, as long as the SDE

$$\mathrm{d}X_t = -u(t, X_t)\mathrm{d}t + G(t)\mathrm{d}W_t$$

has a unique solution which is continuous and adapted.

Remark 2.11. In the motivational heuristic derivation of the HJB equation above, we have also assumed that $G(s)V_x(s, X_s)$ is integrable with respect to Brownian motion such that the integral is a martingale. This follows directly from boundedness of V_x as we have

$$\mathrm{E}\left[\int_0^T \left(G(s)\,V_x(s, X_s)\right)^2 \mathrm{d}\,[W]_s\right] = \mathrm{E}\left[\int_0^T G(s)^2\,V_x(s, X_s)^2 \mathrm{d}s\right] \leq p^2 \int_0^T G(s)^2 \mathrm{d}s < \infty,$$

by observing that G is continuous on $[0, T]$ for all model variants and thus Lebesgue integrable.

2.3.3 Time Reversion in the Brownian and Ornstein-Uhlenbeck Variant

In the Brownian model variant, we need to solve

$$\begin{aligned} V_t &= \frac{1}{2c}\,\mathrm{e}^{rt}\,(V_x)^2 - \frac{1}{2}\,\sigma^2\,(T-t)^2\,V_{xx} \\ V(T,x) &= \mathrm{e}^{-rT}\,P(x). \end{aligned}$$

Again we perform a time reversion to turn the terminal condition into an initial condition. We proceed as for the simple model variant: We set $t = T - \tilde{t}$ and define $\tilde{V}(\tilde{t},x) = V(T-\tilde{t},x)$. Then we have

$$V_t(t,x) = V_t(T-\tilde{t},x) = -V_{\tilde{t}}(T-\tilde{t},x) = -\tilde{V}_{\tilde{t}}(\tilde{t},x)$$

and $V_{xx}(T-\tilde{t},x) = \tilde{V}_{xx}(\tilde{t},x)$ and $V_x(T-\tilde{t},x) = \tilde{V}_x(\tilde{t},x)$. The PDE therefore becomes

$$\begin{aligned} \tilde{V}_{\tilde{t}} &= -\frac{1}{2c}\,\mathrm{e}^{r(T-\tilde{t})}\,\left(\tilde{V}_x\right)^2 + \frac{1}{2}\,\sigma^2\,\tilde{t}^2\,\tilde{V}_{xx} \\ V(T,x) &= \tilde{V}(0,x) = \mathrm{e}^{-rT}\,P(x). \end{aligned}$$

We proceed similarly for the Ornstein-Uhlenbeck model: The characteristic PDE takes the form

$$\begin{aligned} V_t &= \frac{1}{2c}\,\mathrm{e}^{rt}\,(V_x)^2 - \frac{1}{2}\,\sigma^2\,\frac{\left(1-\mathrm{e}^{-\theta(T-t)}\right)^2}{\theta^2}V_{xx} \\ V(T,x) &= \mathrm{e}^{-rT}\,P(x), \end{aligned}$$

which after time reversion becomes

$$\begin{aligned} \tilde{V}_{\tilde{t}} &= -\frac{1}{2c}\,\mathrm{e}^{r(T-\tilde{t})}\,\left(\tilde{V}_x\right)^2 + \frac{1}{2}\,\sigma^2\,\frac{\left(1-\mathrm{e}^{-\theta\tilde{t}}\right)^2}{\theta^2}\,\tilde{V}_{xx} \\ V(T,x) &= \tilde{V}(0,x) = \mathrm{e}^{-rT}\,P(x). \end{aligned}$$

Since in both cases we have time-dependent coefficients, we cannot apply the Cole-Hopf transformation and therefore have to solve the PDE numerically. The method used for this and the challenges arising are described in section 5.1.

With no analytical solution available, it is not possible to rigorously verify the requirements of the verification theorem for the HJB equation. Instead, we will study the numerical solution in section 6.1.

Summary

At the beginning of this section, we derived an analytical solution to the characteristic PDE for the simple model variant. For this solution, we showed that some useful properties hold, which we will apply below. Moreover, we showed that the analytical PDE solution and the candidate optimal abatement rate derived from it satisfy the requirements of the verification theorem for the HJB equation. It therefore only remains to show that the SDE describing X has a unique continuous and adapted solution.

In case of the Brownian and Ornstein-Uhlenbeck model variants, it was not possible to determine an analytical solution to the characteristic PDE; to prepare the PDE for a numerical solution, we already performed a time reversion.

2.4 Solution of the SDE

We are interested in the behavior of the emission trading system, in particular in the resulting emissions and the development of allowance prices. By solving the SDE

$$\mathrm{d}X_t = -u(t, X_t)\mathrm{d}t + G(t)\mathrm{d}W_t$$

we are able to simulate the process X and thus obtain the resulting emissions X_T. Furthermore we may then compute the allowance prices $S(t, X_t) = c\,u(t, X_t)$. Additionally, to verify the HJB equation by applying the verification theorem in Proposition 2.3, we require that a unique solution to the SDE exists, as mentioned above. In this section we will therefore derive results on existence and uniqueness of a solution to the SDE as well as on the convergence of a simple numerical solution method.

2.4.1 Existence and Uniqueness of a Solution

We will restrict our considerations to the notion of a strong solution: This will allow us to obtain a process X solving the SDE for a given Brownian motion W such that X is adapted to the corresponding filtration $\mathcal{F}$. In contrast to this, the existence of a weak solution only guarantees that there exist processes $(\tilde{X}, \tilde{W})$ and a filtration $\tilde{\mathcal{F}}$ such that $\tilde{X}$ is adapted to $\tilde{\mathcal{F}}$, $\tilde{W}$ is a Brownian motion with respect to $\tilde{\mathcal{F}}$ and $(\tilde{X}, \tilde{W})$ solves the SDE. Furthermore, we will work with the concept of strong uniqueness, meaning that any two solutions of the SDE are indistinguishable.

For the remainder of this section we will consider an SDE of the form

$$\mathrm{d}X_t = b(t, X_t)\mathrm{d}t + \sigma(t, X_t)\mathrm{d}W_t,$$

where W denotes a standard Brownian motion. The standard result on strong existence and uniqueness of a solution to an SDE requires the following assumption:

Assumption 2.12. Let $T > 0$ and let $b : [0, T] \times \mathbb{R}^d \to \mathbb{R}^d$ and $\sigma : [0, T] \times \mathbb{R}^d \to \mathbb{R}^d$ be measurable functions. We assume that

$$\|b(t, x)\|^2 + \|\sigma(t, x)\|^2 \leq C^2 \left(1 + \|x\|^2\right) \quad \text{for } x \in \mathbb{R}^d, t \in [0, T]$$

for some constant C and

$$\|b(t, x) - b(t, y)\| + \|\sigma(t, x) - \sigma(t, y)\| \leq D\|x - y\| \quad \text{for all } t \in [0, T]$$

for a constant D.

The statement we give here is provided for instance by Øksendal [Øks98] and by Karatzas and Shreve [KS98][9]:

Theorem 2.13. *Suppose that b and σ satisfy Assumption 2.12 and let Z be an $\mathbb{R}^d$-valued random variable, independent of W, with*

$$\mathrm{E}\left[\|Z\|^2\right] < \infty.$$

Then the stochastic differential equation

$$\mathrm{d}X_t = b(t, X_t)\mathrm{d}t + \sigma(t, X_t)\mathrm{d}W_t, \quad 0 \leq t \leq T, \quad X_0 = Z$$

[9] This can be found in Theorem 5.2.1 on page 66 in [Øks98] and in Theorem 2.9 on page 289 in [KS98].

has a unique t-continuous solution $X = (X_t)_{t\in[0,T]}$ *which is adapted to the filtration* $\mathcal{F}^{Z,W}$ *generated by* Z *and* W*. Furthermore there exists a constant* K *such that*

$$\mathrm{E}\left[\|X_t\|^2\right] \leq K(1 + \mathrm{E}\left[\|Z\|^2\right])\,\mathrm{e}^{Kt} \quad \textit{for } 0 \leq t \leq T. \tag{2.6}$$

and in particular we have

$$\mathrm{E}\left[\int_0^T \|X_t\|^2 \mathrm{d}t\right] < \infty.$$

Note on the Proof. For the proof we mainly refer to Øksendal [Øks98]. Since the relation (2.6) is not given by Øksendal and its proof is only sketched by Karatzas and Shreve, we will give a detailed proof of this further below in Lemma 2.24, where we will require this part of the result.

As can be seen in Assumption 2.12, the above theorem on existence and uniqueness requires Lipschitz continuity both for the drift and volatility term. In our case this is not satisfied: The drift is not even continuous everywhere. More precisely, u is not continuous in x for $t = T$. We may see this by looking at the final condition of the PDE given by

$$V(T,x) = \begin{cases} p\,(x - e_0) & \text{if} \quad x > e_0 \\ 0 & \text{if} \quad x \leq e_0 \end{cases}$$

with derivative

$$V_x(T,x) = \begin{cases} p & \text{if} \quad x > e_0 \\ 0 & \text{if} \quad x \leq e_0 \end{cases}$$

and we obtain that

$$u(T,x) = \begin{cases} \frac{p}{c}\,\mathrm{e}^{rT} & \text{if} \quad x > e_0 \\ 0 & \text{if} \quad x \leq e_0. \end{cases}$$

As long as $p > 0$, this is clearly not continuous in $x = e_0$.

Various authors have studied the existence and uniqueness of strong solutions under weaker assumptions. Zvonkin [Zvo74] introduces a transformation that removes the drift coefficient and thus shows that in one dimension, it suffices for the drift to be measurable and bounded to obtain a unique strong solution. For this, he imposes stronger requirements on the volatility, in particular, the volatility needs to be bounded away from zero uniformly in both its arguments.

The approach of Zvonkin has been extended to multiple dimensions for example by Veretennikov [Ver81] and Zhang [Zha05]. Both only make weak assumptions on the drift, but stronger assumptions on the volatility, one of which is the requirement that the volatility is uniformly non-degenerate, i.e. they impose that there exists a constant $C > 0$ such that

$$\sigma(t,x)\,\sigma(t,x)^T \geq C\,I_d \qquad \text{for any} \quad t \in \mathbb{R}_+ \quad \text{and any} \quad x \in \mathbb{R}^d,$$

where σ denotes the volatility and I_d is the identity matrix in d dimensions. Veretennikov extends his results further by loosening the non-degeneracy condition [Ver84]: He splits the SDE into two possibly multi-dimensional SDEs, where the volatility is allowed to be degenerate for one of these SDEs as long as the corresponding drift is Lipschitz continuous and all coefficient functions are Lipschitz continuous in the corresponding variables.

A similar approach is presented by Leobacher, Szölgyenyi and Thonhauser [LST15]. They allow the drift to be discontinuous in the first variable on the hyperplane $\{x_1 = 0\}$

and impose a differentiability condition elsewhere. The non-degeneracy condition for the volatility then reduces to the requirement that $\left(\sigma\,\sigma^T\right)_{11}$ needs to be bounded away from zero uniformly. Under some further assumptions Leobacher et al. show that a unique strong solution exists by following a similar transformation approach as Zvonkin. Notably, they only allow for time-homogeneous SDEs of the form

$$\mathrm{d}X_t = b(X_t)\mathrm{d}t + \sigma(X_t)\mathrm{d}W_t.$$

They further extend this result by allowing the discontinuity to occur on a hypersurface. In that case the non-degeneracy condition is replaced by the requirement that in each point the volatility is not parallel to the discontinuity surface. Shardin and Szölgyenyi [SS16] transfer this result to time-inhomogeneous SDEs by introducing a transformation method that allows them to transform a time-inhomogeneous SDE to a time-homogeneous SDE.

Halidias and Kloeden [HK06] also study time-homogeneous SDEs, but take an entirely different approach: They introduce the notion of an upper and a lower solution of the SDE and show that if such solutions exist and if furthermore the drift is increasing, the volatility is Lipschitz continuous and both satisfy a linear growth bound, then a strong solution exists. They do not prove uniqueness.

For the SDE we consider here, the drift is bounded and measurable, which allows us to apply the result of Zvonkin [Zvo74] in case of the simple model but not for the Brownian and the Ornstein-Uhlenbeck variant since $\sigma(t,x) \to 0$ for $t \to T$ in both these model variants. The extensions to multiple dimensions and in particular the result of Zhang [Zha05] might be of interest in section 3.2, where we will encounter a volatility with $\sigma : \mathbb{R}_+ \times \mathbb{R}^2 \to \mathbb{R}^2$: In contrast to Vetennikov [Ver81], Zhang allows the volatility matrix to be non-quadratic. Again, this will only work for the simple model. The results of Leobacher et al. [LST15] and Shardin and Szölgyenyi [SS16] also cannot easily be applied to the Brownian and Ornstein-Uhlenbeck model variant, as a straightforward choice to describe the discontinuity surface violated the non-parallelity requirement. The approach of Halidias and Kloeden [HK06] clearly cannot be applied here, as it only allows for time-homogeneous SDEs. In addition, the requirement that an upper and a lower solution exists at first glance seems to be challenging to verify. Interestingly, the example they consider, the Heaviside function as the drift, is very similar to the drift of our SDE at final time, where the discontinuity occurs. Thus if the drift was constant in time and given by the drift at final time, we could easily find an upper and lower solution as Halidias and Kloeden do for their example.

Notably, the discontinuity that prevents us from using standard results only occurs at final time. In our approach, we therefore exploit this specific structure and thus are able to obtain an existence and uniqueness results that may apply to all model variants. We refer back to the standard result as e.g. presented by Øksendal [Øks98] and formulate a slightly modified assumption that requires Lipschitz-continuity only on $[0,T)$; at the same time we require boundedness by a constant instead of a linear growth bound as present in the standard result. Since we will formulate our result in a multi-dimensional setting, we will work with the Euclidean norm, which in the following will be denoted by $\|\cdot\|$.

Assumption 2.14. Let $T > 0$ and let $b : [0,T] \times \mathbb{R}^d \to \mathbb{R}^d$ and $\sigma : [0,T] \times \mathbb{R}^d \to \mathbb{R}^d$ be measurable functions. We assume that

$$\|b(t,x)\| + \|\sigma(t,x)\| \leq C \quad \text{for } x \in \mathbb{R}^d, t \in [0,T] \tag{2.7}$$

for some constant C. Furthermore we require: For all $\varepsilon > 0$ there exists a constant D_ε such that

$$\|b(t,x) - b(t,y)\| + \|\sigma(t,x) - \sigma(t,y)\| \leq D_\varepsilon \|x - y\| \quad \text{for all } t \in [0, T-\varepsilon]. \tag{2.8}$$

Under these assumptions we may show that the SDE

$$\mathrm{d}X_t = b(t, X_t)\mathrm{d}t + \sigma(t, X_t)\mathrm{d}W_t$$

has a unique solution. Note that although b and σ are d-dimensional, W is still assumed to be one-dimensional. The SDE above is therefore an equation of $\mathbb{R}^d$-valued vectors, which we could rewrite as a system of SDEs as

$$\begin{aligned}
\mathrm{d}X_{t,1} &= b_1(t, X_{t,1}, X_{t,2}, \ldots, X_{t,d})\mathrm{d}t + \sigma_1(t, X_{t,1}, X_{t,2}, \ldots, X_{t,d})\mathrm{d}W_t \\
\mathrm{d}X_{t,2} &= b_2(t, X_{t,1}, X_{t,2}, \ldots, X_{t,d})\mathrm{d}t + \sigma_2(t, X_{t,1}, X_{t,2}, \ldots, X_{t,d})\mathrm{d}W_t \\
&\vdots \qquad\qquad \vdots \qquad\qquad\qquad \vdots \\
\mathrm{d}X_{t,d} &= b_d(t, X_{t,1}, X_{t,2}, \ldots, X_{t,d})\mathrm{d}t + \sigma_d(t, X_{t,1}, X_{t,2}, \ldots, X_{t,d})\mathrm{d}W_t.
\end{aligned}$$

To simplify notation, in the following we will only use the vector equation and work with the $\mathbb{R}^d$-valued functions b, σ and with the $\mathbb{R}^d$-valued process X.

Theorem 2.15. *Suppose that b and σ satisfy Assumption 2.14 and let Z be an $\mathbb{R}^d$-valued random variable, independent of W, such that*

$$\mathrm{E}\left[\|Z\|^2\right] < \infty.$$

Then the stochastic differential equation

$$\mathrm{d}X_t = b(t, X_t)\mathrm{d}t + \sigma(t, X_t)\mathrm{d}W_t, \quad 0 \leq t \leq T, \quad X_0 = Z \tag{2.9}$$

has a unique t-continuous solution $X = (X_t)_{t\in[0,T]}$ which is adapted to the filtration $\mathcal{F}^{Z,W}$ generated by Z and W and we have

$$\mathrm{E}\left[\int_0^T \|X_t\|^2 \mathrm{d}t\right] < \infty. \tag{2.10}$$

Before we may prove this, we state two lemmata, which we will apply in this proof as well as in the proofs of section 2.4.2.

Lemma 2.16. *For $N \in \mathbb{N}$ and $x_i \in \mathbb{R}^d$ with $i = 1, \ldots, N$ we have that*

$$\Big\| \sum_{i=1}^N x_i \Big\|^2 \leq N \sum_{i=1}^N \|x_i\|^2.$$

Proof. We first show the claim in the one-dimensional case, i.e. we assume that $x_i \in \mathbb{R}$. From $0 \leq (x_i - x_j)^2 = x_i^2 - 2x_i x_j + x_j^2$ we have $2x_i x_j \leq x_i^2 + x_j^2$ for any i and j and

therefore

$$\begin{aligned}\left(\sum_{i=1}^N x_i\right)^2 &= \sum_{i=1}^N x_i^2 + \sum_{i=1}^{N-1}\sum_{j=i+1}^N 2x_i x_j \\ &\le \sum_{i=1}^N x_i^2 + \sum_{i=1}^{N-1}\sum_{j=i+1}^N \left(x_i^2 + x_j^2\right) = \sum_{i=1}^N x_i^2 + \sum_{i=1}^{N-1}\sum_{j=i+1}^N x_i^2 + \sum_{j=2}^N\sum_{i=1}^{j-1} x_j^2 \\ &= \sum_{i=1}^N x_i^2 + \sum_{i=1}^{N-1}(N-i)\,x_i^2 + \sum_{j=2}^N (j-1)\,x_j^2 \\ &= \sum_{i=1}^N x_i^2 + \sum_{i=2}^{N-1}(N-i)\,x_i^2 + \sum_{i=2}^{N-1}(i-1)\,x_i^2 + (N-1)\,x_1^2 + (N-1)\,x_N^2 \\ &= N\sum_{i=1}^N x_i^2.\end{aligned}$$

Then for $x_i \in \mathbb{R}^d$ we directly obtain

$$\left\|\sum_{i=1}^N x_i\right\|^2 = \sum_{j=1}^d \left(\sum_{i=1}^N x_{i,j}\right)^2 \le \sum_{j=1}^d N\sum_{i=1}^N x_{i,j}^2 = N\sum_{i=1}^N\sum_{j=1}^d x_{i,j}^2 = N\sum_{i=1}^N \|x_i\|^2. \qquad \square$$

Lemma 2.17. *Let $f : \mathbb{R} \to \mathbb{R}$ be an integrable function. Then*

$$\left(\int_s^t f(r)\mathrm{d}r\right)^2 \le (t-s)\int_s^t f(r)^2\mathrm{d}r.$$

Furthermore, for an integrable function $g : \mathbb{R} \to \mathbb{R}^d$ we have

$$\left\|\int_s^t g(r)\mathrm{d}r\right\| \le (t-s)\int_s^t \|g(r)\|^2\mathrm{d}r.$$

Proof. By applying Jensen's inequality on the probability space $([s,t], \mathcal{B}([s,t]), \frac{1}{t-s}\lambda)$ to the function f we have

$$\left(\frac{1}{t-s}\int_s^t f(r)\mathrm{d}r\right)^2 \le \frac{1}{t-s}\int_s^t \big(f(r)\big)^2\mathrm{d}r.$$

Therefore it follows that

$$\begin{aligned}\left(\int_s^t f(r)\mathrm{d}r\right)^2 &= \left(\frac{1}{t-s}\int_s^t (t-s)\cdot f(r)\mathrm{d}r\right)^2 \\ &\le \frac{1}{t-s}\int_s^t (t-s)^2\cdot f(r)^2\mathrm{d}r = (t-s)\int_s^t f(r)^2\mathrm{d}r.\end{aligned}$$

We apply this to show the second part of the claim:

$$\begin{aligned}\left\|\int_s^t g(r)\mathrm{d}r\right\|^2 &= \sum_{j=1}^d \left(\int_s^t g_j(r)\mathrm{d}r\right)^2 \\ &\le \sum_{j=1}^d (t-s)\int_s^t g_j(r)^2\mathrm{d}r = (t-s)\int_s^t \sum_{j=1}^d g_j(r)^2\mathrm{d}r \\ &= (t-s)\int_s^t \|g(r)\|^2\mathrm{d}r. \qquad \square\end{aligned}$$

Remark 2.18. In a similar manner we show that the Itô-Isometry also can be applied to the square of the Euclidean norm:

$$\begin{aligned}\mathrm{E}\left[\left\|\int_s^t g(r)\mathrm{d}W_r\right\|^2\right] &= \mathrm{E}\left[\sum_{j=1}^d\left(\int_s^t g_j(r)\mathrm{d}W_r\right)^2\right] = \sum_{j=1}^d \mathrm{E}\left[\left(\int_s^t g_j(r)\mathrm{d}W_r\right)^2\right] \\ &= \sum_{j=1}^d \mathrm{E}\left[\int_s^t g_j(r)^2\mathrm{d}r\right] = \mathrm{E}\left[\int_s^t \sum_{j=1}^d g_j(r)^2\mathrm{d}r\right] = \mathrm{E}\left[\int_s^t \|g(r)\|^2\mathrm{d}r\right].\end{aligned}$$

We will mainly use this formulation of the Itô-Isometry in the proofs below.

In the proof of the theorem we apply the standard result for existence and uniqueness of a solution to an SDE as stated in Theorem 2.13. Some arguments in this proof are closely aligned to the proof by Øksendal in [Øks98][10] and we will therefore also make use of some results contained in his proof.

Proof of Theorem 2.15. Let $\varepsilon > 0$ and fix $T' = T - \varepsilon$. Then due to the boundedness and Lipschitz continuity of b and σ on $[0, T']$ as given by Assumption 2.14, we obtain a unique solution X_t on $[0, T']$ by applying the standard result in Theorem 2.13. This solution does not depend on D_ε and therefore not on the choice of ε, hence if we consider $\varepsilon > \tilde{\varepsilon}$ and the corresponding solutions X_t^ε and $X_t^{\tilde{\varepsilon}}$, we have with uniqueness of the solution that $X_t^\varepsilon = X_t^{\tilde{\varepsilon}}$ almost surely for all $t \in [0, T - \varepsilon]$. We then let $\varepsilon \to 0$ and obtain a unique solution X_t on $[0, T)$. It remains to consider $t = T$.

We apply the iterative formula as in Øksendal, i.e. we define $Y_t^{(0)} = X_0$ and

$$Y_t^{(k+1)} = X_0 + \int_0^t b\left(s, Y_s^{(k)}\right)\mathrm{d}s + \int_0^t \sigma\left(s, Y_s^{(k)}\right)\mathrm{d}W_s. \tag{2.11}$$

By the proof of Øksendal, we know that on any interval of the form $[0, T - \delta]$, the process $Y^{(k+1)}$ converges uniformly and in L^2 to a process X which satisfies the SDE in equation (2.9). We aim to show that also for $t = T$ we have convergence of $Y_T^{(k+1)}$ in L^2 such that the limit satisfies the SDE. Furthermore, we will show that the resulting process $X = (X_t)_{t\in[0,T]}$ is continuous in T and that this solution is unique.

(i) Show convergence in L^2: Let $\delta > 0$. Then by applying Lemma 2.17, the Itô-Isometry and the relation $\|a + b\|^2 \leq 2\|a\|^2 + 2\|b\|^2$ given by Lemma 2.16, we have:

$$\begin{aligned}\mathrm{E}\left[\left\|Y_T^{(n)} - Y_{T-\delta}^{(n)}\right\|^2\right] &= \mathrm{E}\left[\left\|\int_{T-\delta}^T b\left(s, Y_s^{(n-1)}\right)\mathrm{d}s + \int_{T-\delta}^T \sigma\left(s, Y_s^{(n-1)}\right)\mathrm{d}W_s\right\|^2\right] \\ &\leq 2\,\delta\,\mathrm{E}\left[\int_{T-\delta}^T \left\|b\left(s, Y_s^{(n-1)}\right)\right\|^2\mathrm{d}s\right] + 2\,\mathrm{E}\left[\int_{T-\delta}^T \left\|\sigma\left(s, Y_s^{(n-1)}\right)\right\|^2\mathrm{d}s\right] \\ &\leq 2\,\delta\,\mathrm{E}\left[\int_{T-\delta}^T C^2\mathrm{d}s\right] + 2\,\mathrm{E}\left[\int_{T-\delta}^T C^2\mathrm{d}s\right] \\ &= 2\,\delta^2\,C^2 + 2\,\delta\,C^2 = 2\,\delta\,C^2\,(1+\delta) < 4\,C^2\,\delta\end{aligned}$$

by using the boundedness as given by equation (2.7) in Assumption 2.14 and assuming $\delta < 1$.

[10] This can be found on pages 67–70 of [Øks98].

Now let $\varepsilon > 0$ arbitrary and set $\delta = \varepsilon/36C^2$. Since $Y_{T-\delta}^{(n)}$ converges in L^2, we know that it is also a Cauchy sequence in L^2. Therefore there exists an $N \in \mathbb{N}$ such that

$$\mathrm{E}\left[\left\|Y_{T-\delta}^{(m)} - Y_{T-\delta}^{(n)}\right\|^2\right] < \frac{\varepsilon}{9} \quad \forall\, m, n > N.$$

Thus with $\|a+b+c\|^2 \leq 3\|a\|^2 + 3\|b\|^2 + 3\|c\|^2$ as given by Lemma 2.16 and the results from above we obtain

$$\begin{aligned}
\mathrm{E}\left[\left\|Y_T^{(m)} - Y_T^{(n)}\right\|^2\right] &= \mathrm{E}\left[\left\|Y_T^{(m)} - Y_{T-\delta}^{(m)} + Y_{T-\delta}^{(m)} - Y_{T-\delta}^{(n)} + Y_{T-\delta}^{(n)} - Y_T^{(n)}\right\|^2\right] \\
&\leq 3\,\mathrm{E}\left[\left\|Y_T^{(m)} - Y_{T-\delta}^{(m)}\right\|^2\right] + 3\,\mathrm{E}\left[\left\|Y_{T-\delta}^{(m)} - Y_{T-\delta}^{(n)}\right\|^2\right] \\
&\quad + 3\,\mathrm{E}\left[\left\|Y_{T-\delta}^{(n)} - Y_T^{(n)}\right\|^2\right] \\
&< 12\,C^2\,\delta + \frac{\varepsilon}{3} + 12\,C^2\,\delta \\
&= \frac{\varepsilon}{3} + \frac{\varepsilon}{3} + \frac{\varepsilon}{3} = \varepsilon.
\end{aligned}$$

Hence $Y_T^{(n)}$ also is a Cauchy sequence in L^2 and thus converges in L^2 to a limit X_T. From L^2-convergence, we obtain convergence in probability and therefore the existence of a subsequence $Y_T^{(n_k)}$ that converges $\mathcal{P}$-a.s. to X_T. As we know that $Y_T^{(n)}$ is $\mathcal{F}_T^{Z,W}$-measurable, this implies that also X_T is $\mathcal{F}_T^{Z,W}$-measurable since the a.s.-limit of a sequence of measurable random variables is again measurable.

(ii) We proceed to show that X satisfies the SDE as given by equation (2.9) on $[0,T]$ and again we only need to consider $t = T$. First we look at the integral of the drift term b. Let $\varepsilon > 0$ arbitrary. We set $\delta = \sqrt{\varepsilon}/3C$ and again apply the inequalities in Lemma 2.16 and Lemma 2.17. Furthermore, we use the boundedness and Lipschitz continuity of b on $[0, T-\delta]$ given by Assumption 2.14 to compute

$$\begin{aligned}
&\mathrm{E}\left[\left\|\int_0^T b\left(s, Y_s^{(n)}\right)\mathrm{d}s - \int_0^T b\left(s, X_s\right)\mathrm{d}s\right\|^2\right] \\
&= \mathrm{E}\left[\left\|\int_0^{T-\delta}\left(b\left(s, Y_s^{(n)}\right) - b\left(s, X_s\right)\right)\mathrm{d}s + \int_{T-\delta}^T b\left(s, Y_s^{(n)}\right)\mathrm{d}s - \int_{T-\delta}^T b\left(s, X_s\right)\mathrm{d}s\right\|^2\right] \\
&\leq 3\,\mathrm{E}\left[\left\|\int_0^{T-\delta}\left(b\left(s, Y_s^{(n)}\right) - b\left(s, X_s\right)\right)\mathrm{d}s\right\|^2\right] \\
&\quad + 3\,\mathrm{E}\left[\left\|\int_{T-\delta}^T b\left(s, Y_s^{(n)}\right)\mathrm{d}s\right\|^2\right] + 3\,\mathrm{E}\left[\left\|\int_{T-\delta}^T b\left(s, X_s\right)\mathrm{d}s\right\|^2\right] \\
&\leq 3\,\mathrm{E}\left[(T-\delta)\int_0^{T-\delta}\left\|b\left(s, Y_s^{(n)}\right) - b\left(s, X_s\right)\right\|^2\mathrm{d}s\right] \\
&\quad + 3\,\mathrm{E}\left[\delta\int_{T-\delta}^T\left\|b\left(s, Y_s^{(n)}\right)\right\|^2\mathrm{d}s\right] + 3\,\mathrm{E}\left[\delta\int_{T-\delta}^T\left\|b\left(s, X_s\right)\right\|^2\mathrm{d}s\right] \\
&\leq 3\,(T-\delta)\,D_\delta^2\,\mathrm{E}\left[\int_0^{T-\delta}\left\|Y_s^{(n)} - X_s\right\|^2\mathrm{d}s\right] + 3\,\delta^2\,C^2 + 3\,\delta^2\,C^2.
\end{aligned}$$

From L^2-convergence of $Y_s^{(n)}$ on $[0, T-\delta]$, we know that we have $\mathrm{E}\big[\|Y_s^{(n)} - X_s\|^2\big] \to 0$ as $n \to \infty$. Furthermore, by definition of $Y_t^{(n)}$ (see equation 2.11) and with boundedness

of b and σ we have

$$\begin{aligned}
\mathrm{E}\left[\left\|Y_t^{(n)}\right\|^2\right] &\leq 3\,\mathrm{E}\left[\|X_0\|^2\right] + 3\,\mathrm{E}\left[\left\|\int_0^t b\left(s, Y_s^{(n-1)}\right)\mathrm{d}s\right\|^2\right] \\
&\quad + 3\,\mathrm{E}\left[\left\|\int_0^t \sigma\left(s, Y_s^{(n-1)}\right)\mathrm{d}W_s\right\|^2\right] \\
&\leq 3\,\mathrm{E}\left[\|X_0\|^2\right] + 3\,t\,\mathrm{E}\left[\int_0^t \left\|b\left(s, Y_s^{(n-1)}\right)\right\|^2\mathrm{d}s\right] \\
&\quad + 3\,\mathrm{E}\left[\int_0^t \left\|\sigma\left(s, Y_s^{(n-1)}\right)\right\|^2\mathrm{d}s\right] \\
&\leq 3\,\mathrm{E}\left[\|X_0\|^2\right] + 3\,t^2\,C^2 + 3\,t\,C^2 \qquad (2.12)
\end{aligned}$$

and therefore

$$\begin{aligned}
\mathrm{E}\left[\left\|Y_t^{(n)} - X_t\right\|^2\right] &\leq 2\,\mathrm{E}\left[\left\|Y_t^{(n)}\right\|^2\right] + 2\,\mathrm{E}\left[\left\|X_t\right\|^2\right] \\
&\leq 6\,\mathrm{E}\left[\|X_0\|^2\right] + 6\,t^2\,C^2 + 6\,t\,C^2 + 2\,\mathrm{E}\left[\|X_t\|^2\right].
\end{aligned}$$

The right hand-side is integrable with respect to the Lebesgue measure on $[0, T-\delta]$: By assumption, $\mathrm{E}\left[\|X_0\|^2\right] < \infty$ and since this is constant in t, also $\int_0^{T-\delta} \mathrm{E}\left[\|X_0\|^2\right]\mathrm{d}t < \infty$. Moreover, with Tonelli's theorem

$$\int_0^{T-\delta} \mathrm{E}\left[\|X_t\|^2\right]\mathrm{d}t = \mathrm{E}\left[\int_0^{T-\delta} \|X_t\|^2\mathrm{d}t\right] < \infty$$

by the existence and uniqueness result of Theorem 2.13. Thus we have found a dominating function and apply the dominated convergence theorem to obtain

$$\begin{aligned}
\lim_{n\to\infty} \mathrm{E}\left[\int_0^{T-\delta} \left\|Y_s^{(n)} - X_s\right\|^2\mathrm{d}s\right] &= \lim_{n\to\infty} \int_0^{T-\delta} \mathrm{E}\left[\left\|Y_s^{(n)} - X_s\right\|^2\right]\mathrm{d}s \\
&= \int_0^{T-\delta} \lim_{n\to\infty} \mathrm{E}\left[\left\|Y_s^{(n)} - X_s\right\|^2\right]\mathrm{d}s = 0.
\end{aligned}$$

Hence there exists $N \in \mathbb{N}$ such that

$$\mathrm{E}\left[\int_0^{T-\delta} \left\|Y_s^{(n)} - X_s\right\|^2\mathrm{d}s\right] < \frac{\varepsilon}{9\,D_\delta^2\,(T-\delta)} \qquad \text{for all } n > N.$$

This delivers

$$\mathrm{E}\left[\left\|\int_0^T b\left(s, Y_s^{(n)}\right)\mathrm{d}s - \int_0^T b\left(s, X_s\right)\mathrm{d}s\right\|^2\right] \leq \frac{\varepsilon}{3} + \frac{\varepsilon}{3} + \frac{\varepsilon}{3} = \varepsilon \qquad \text{for all } n > N.$$

We now turn to the stochastic integral of the SDE. Again we choose $\varepsilon > 0$ arbitrary and this time we set $\delta = \varepsilon/9C^2$. Then again with Lemma 2.16 as well as boundedness and

Lipschitz continuity of σ given by Assumption 2.14

$$\begin{aligned}
&\mathrm{E}\left[\left\| \int_0^T \sigma\left(s, Y_s^{(n)}\right) \mathrm{d}W_s - \int_0^T \sigma\left(s, X_s\right) \mathrm{d}W_s \right\|^2\right] \\
&= \mathrm{E}\left[\left\| \int_0^{T-\delta} \left(\sigma\left(s, Y_s^{(n)}\right) - \sigma\left(s, X_s\right)\right) \mathrm{d}W_s \right.\right. \\
&\quad \left.\left. + \int_{T-\delta}^T \sigma\left(s, Y_s^{(n)}\right) \mathrm{d}W_s - \int_{T-\delta}^T \sigma\left(s, X_s\right) \mathrm{d}W_s \right\|^2\right] \\
&\leq 3\,\mathrm{E}\left[\left\| \int_0^{T-\delta} \left(\sigma\left(s, Y_s^{(n)}\right) - \sigma\left(s, X_s\right)\right) \mathrm{d}W_s \right\|^2\right] \\
&\quad + 3\,\mathrm{E}\left[\left\| \int_{T-\delta}^T \sigma\left(s, Y_s^{(n)}\right) \mathrm{d}W_s \right\|^2\right] + 3\,\mathrm{E}\left[\left\| \int_{T-\delta}^T \sigma\left(s, X_s\right) \mathrm{d}W_s \right\|^2\right] \\
&= 3\,\mathrm{E}\left[\int_0^{T-\delta} \left\|\sigma\left(s, Y_s^{(n)}\right) - \sigma\left(s, X_s\right)\right\|^2 \mathrm{d}s\right] \\
&\quad + 3\,\mathrm{E}\left[\int_{T-\delta}^T \left\|\sigma\left(s, Y_s^{(n)}\right)\right\|^2 \mathrm{d}s\right] + 3\,\mathrm{E}\left[\int_{T-\delta}^T \left\|\sigma\left(s, X_s\right)\right\|^2 \mathrm{d}s\right] \\
&\leq 3\,D_\delta^2\,\mathrm{E}\left[\int_0^{T-\delta} \left\|Y_s^{(n)} - X_s\right\|^2 \mathrm{d}s\right] + 3\,\delta\,C^2 + 3\,\delta\,C^2.
\end{aligned}$$

We choose $N \in \mathbb{N}$ such that we have

$$\mathrm{E}\left[\int_0^{T-\delta} \left\|Y_s^{(n)} - X_s\right\|^2 \mathrm{d}s\right] < \frac{\varepsilon}{9\,D_\delta^2} \qquad \text{for all } n > N$$

and obtain

$$\mathrm{E}\left[\left\| \int_0^T \sigma\left(s, Y_s^{(n)}\right) \mathrm{d}W_s - \int_0^T \sigma\left(s, X_s\right) \mathrm{d}W_s \right\|^2\right] < \frac{\varepsilon}{3} + \frac{\varepsilon}{3} + \frac{\varepsilon}{3} = \varepsilon \qquad \text{for all } n > N.$$

Thus we have shown that

$$X_0 + \int_0^T b\left(s, Y_s^{(n)}\right) \mathrm{d}s + \int_0^T \sigma\left(s, Y_s^{(n)}\right) \mathrm{d}W_s \longrightarrow X_0 + \int_0^T b\left(s, X_s\right) \mathrm{d}s + \int_0^T \sigma\left(s, X_s\right) \mathrm{d}W_s$$

in L^2. As we also have $Y_T^{(n)} \longrightarrow X_T$ in L^2, it follows from the iterative formula (2.11) and the uniqueness of the L^2-limit that

$$X_T = X_0 + \int_0^T b(s, X_s)\mathrm{d}s + \int_0^T \sigma(s, X_s)\mathrm{d}W_s$$

and therefore X_T satisfies the SDE in equation (2.9).

(iii) It still remains to show that X_t is continuous on $[0, T]$. We have that

$$\int_0^t \sigma(s, X_s)\mathrm{d}W_s$$

has continuous paths by definition of the stochastic integral. To obtain continuity of the drift term we view the integrator s as a continuous process of finite variation; then the continuity of the integral follows from the corresponding property of the Lebesgue-Stieltjes integral. As the right-hand side of the integral equation for X is continuous, continuity of X on $[0, T]$ follows.

(iv) We now derive the uniqueness of the solution from continuity: As argued at the beginning of this proof, the solution X_t on $[0,T)$ is unique. We now fix $\omega \in \Omega$. As $X_t(\omega)$ is continuous in $[0,T]$, we have

$$X_T(\omega) = \lim_{t \to T} X_t(\omega)$$

and since X_t on $[0,T)$ is a unique solution, X_T also needs to be unique.

(v) Finally, we show that X is square integrable, i.e. that

$$\mathrm{E}\left[\int_0^T \left\|X_t\right\|^2 \mathrm{d}t\right] < \infty.$$

From equation (2.12), we know that $Y_t^{(n)}$ is bounded uniformly in t on $[0,T]$ since

$$\mathrm{E}\left[\left\|Y_t^{(n)}\right\|^2\right] \leq 3\,\mathrm{E}\left[\|X_0\|^2\right] + 3\,T^2\,C^2 + 3\,T\,C^2 =: K,$$

where we have by assumption that $\mathrm{E}\left[\|X_0\|^2\right] < \infty$. Furthermore, we know that a subsequence $\left(Y_t^{(n_k)}\right)_{k\in\mathbb{N}}$ converges almost surely to X_t. Then by Fatou's Lemma

$$\mathrm{E}\left[\left\|X_t\right\|^2\right] = \mathrm{E}\left[\lim_{k\to\infty} \left\|Y_t^{(n_k)}\right\|^2\right] \leq \liminf_{k\to\infty} \mathrm{E}\left[\left\|Y_t^{(n_k)}\right\|^2\right] \leq K.$$

Thus $\mathrm{E}\left[\|X_t\|^2\right]$ is bounded uniformly in t, so with Tonelli's Theorem, in particular we have

$$\mathrm{E}\left[\int_0^T \|X_t\|^2 \mathrm{d}t\right] = \int_0^T \mathrm{E}\left[\|X_t\|^2\right] \mathrm{d}t < \infty. \qquad \square$$

2.4.2 Convergence of the Euler-Maruyama-Scheme

The complex dependency of the SDE on X, which is in particular not linear, does not allow for the application of common analytical solution approaches. Hence, we will need to apply a numerical method to solve the SDE. To this end, we introduce the Euler-Maruyama scheme, named after Gisiro Maruyama, who was one of the first to analyze this method [Mar55]. It provides an extension to SDEs of the well-known Euler scheme for ordinary differential equations and is explained in detail e.g. by Kloeden and Platen [KP92].

Definition 2.19. We consider a process $X = (X_t)_{t\in[0,T]}$ satisfying the SDE

$$\mathrm{d}X_t = b(t, X_t)\mathrm{d}t + \sigma(t, X_t)\mathrm{d}W_t$$

and a partition $0 = t_0 < t_1 < \ldots < t_N = T$ of the interval $[0,T]$. Then the Euler-Maruyama scheme is given by

$$Y_0 = X_0 \quad \text{and} \quad Y_{n+1} = Y_n + b(t_n, Y_n)\Delta_n + \sigma(t_n, Y_n)\Delta W_n, \tag{2.13}$$

where $\Delta_n = t_{n+1} - t_n$ denotes the size of the n-th time step and $\Delta W_n = W_{t_{n+1}} - W_{t_n}$ the corresponding increment of Brownian motion.

In order to judge how well the Euler-Maruyama scheme approximates the solution of an SDE, we use the notion of strong convergence.

Definition 2.20. For a given partition, let $\delta = \max_n \Delta_n$ be its maximum step size and let $Y^\delta(T)$ denote the approximation result of the Euler-Maruyama scheme at time T . Then we say that the Euler-Maruyama scheme converges strongly to X at time T if

$$\lim_{\delta \to 0} \mathrm{E}\left[\left\|X_T - Y^\delta(T)\right\|\right] = 0.$$

Under the same assumptions as for the standard results on existence and uniqueness of a solution, it is well known that the Euler-Maruyama scheme converges strongly, as can be seen for example in [KP92] by Kloeden and Platen for time-homogeneous SDEs. Again the discontinuity of the drift in the SDE we consider prevents us from applying this result. As in the case of existence and uniqueness of a solution, more general results are available, which relax the requirement of the drift being Lipschitz continuous. Gyöngy and Krylov [GK96] assume that either the drift and the volatility are continuous or the volatility is non-degenerate and locally Hölder continuous: A function f is Hölder continuous if there exists a constant C and $\alpha \in (0, 1]$ such that

$$\|f(x) - f(y)\| \leq C\|x - y\|^\alpha \quad \text{for all} \quad x, y \in \mathbb{R}^d.$$

Under some further assumptions, Gyöngy and Krylov show that the Euler-Maruyama scheme then converges in probability. Gyöngy [Gyö98] extends this result: He additionally assumes that the drift b locally satisfies a one-sided Lipschitz condition, as given by

$$\langle x - y, b(t, x) - b(t, y)\rangle \leq K\|x - y\|^2 \qquad \text{for any} \quad t \in \mathbb{R}_+ \quad \text{and any} \quad x, y \in \mathbb{R}^d,$$

and shows that under otherwise similar assumptions the Euler-Maruyama scheme also converges almost surely. However, neither of these modes of convergence, in probability or almost surely, suffices to guarantee strong convergence in the sense of Definition 2.20.

Marion, Mao and Renshaw [MMR02] obtain a similar result for time-homogeneous SDEs. They assume that both the drift and the volatility are locally Lipschitz continuous and make a further assumption similar to that of Gyöngy and Krylov to show convergence in probability. Higham, Mao and Stuart [HMS03] also assume that the drift and the volatility are locally Lipschitz continuous and furthermore assume that both are p-integrable for some $p > 2$. In this setting, they prove that the Euler-Maruyama scheme converges strongly.

Ngo and Taguchi [NT16] assume that the drift is one-sided Lipschitz in space and that each component belongs to a class of bounded functions satisfying quite technical assumptions. Furthermore, they assume that the volatility is non-degenerate and that both coefficient functions are Hölder continuous in time. These assumptions allow them to derive the strong convergence rate, separately for one dimension and for multiple dimensions, thus in particular proving strong convergence. In a subsequent work [NT17] they focus on one-dimensional time-homogeneous SDEs, which allows them to drop the requirement of one-sided Lipschitz continuity.

Similar to their result on existence of a solution, Halidias and Kloeden [HK08] again assume that the SDE has an upper and a lower solution. Furthermore, they still assume that the drift is increasing, the volatility is Lipschitz continuous and both satisfy a linear growth bound. Additionally, they now require the drift to be continuous from below. Under these assumptions, they prove strong convergence of the Euler-Maruyama scheme to the solution of a time-homogeneous SDE.

Leobacher and Szölgyenyi [LS18] also consider a time-homogeneous SDE and as for their existence and uniqueness result, they aim to relax the requirement of non-degeneracy.

They introduce the notion of a piecewise Lipschitz function in multiple dimensions and require the drift only to be piecewise Lipschitz and bounded. The volatility needs to be Lipschitz continuous and bounded. Under some further very technical assumptions, they show that the SDE has a unique strong solution and that the Euler-Maruyama scheme converges strongly.

In the case of the SDE considered here, many of these results are not applicable, as they only apply to time-homogeneous SDEs (Marion et al. [MMR02], Higham et al. [HMS03], Halidias and Kloeden [HK08] and Leobacher and Szölgyenyi [LS18]). Also for several results, the drift of our SDE is still not regular enough, as it is not even locally Lipschitz continuous, as required in the work by Marion et al. and Higham et al., and in particular not continuous, as needed for some results by Gyöngy [Gyö98] and Gyöngy and Krylov [GK96]. However, the drift satisfies the one-sided Lipschitz condition, since this requires the drift to be Lipschitz continuous only where it is increasing, but the discontinuity is in fact a downward jump. Therefore, if we manage to verify the other conditions of Gyöngy and Ngo and Taguchi, we may apply their results to the simple model variant of our SDE. Again in case of the Brownian and Ornstein-Uhlenbeck model variant, this is no longer possible.

In order to show convergence under the conditions of our model variants, we will again make use of the fact that the discontinuity only occurs at final time. We will refer back to the standard result by Kloeden and Platen [KP92] and adapt it to our setting. However, their proof only covers the case of a time-homogeneous SDE. Therefore we will first modify their approach slightly to show that their result also holds for time-inhomogeneous SDEs. To this end we need to introduce the assumption that both coefficient functions are Hölder continuous in time with $\alpha = \frac{1}{2}$ in addition to the standard assumptions, namely a linear growth condition and Lipschitz continuity in x.

Assumption 2.21. Let $T > 0$ and let $b : [0,T] \times \mathbb{R}^d \to \mathbb{R}^d$ and $\sigma : [0,T] \times \mathbb{R}^d \to \mathbb{R}^d$ be measurable functions. We assume that

$$\|b(t,x)\|^2 + \|\sigma(t,x)\|^2 \leq C^2 \left(1 + \|x\|^2\right) \quad \text{for } x \in \mathbb{R}^d, t \in [0,T] \tag{2.14}$$

for some constant C. Furthermore, we require

$$\|b(t,x) - b(t,y)\| + \|\sigma(t,x) - \sigma(t,y)\| \leq D_1 \|x - y\| \quad \text{for all } t \in [0,T] \tag{2.15}$$

and

$$\|b(t,x) - b(s,x)\| + \|\sigma(t,x) - \sigma(s,x)\| \leq D_2 |t - s|^{\frac{1}{2}} \qquad \text{for all } x \in \mathbb{R}^d \tag{2.16}$$

for constants D_1 and D_2.

Based on these assumptions we now show that strong convergence holds for the Euler-Maruyama scheme as defined above; this result is well-known but rarely proven for a time-inhomogeneous SDE.

Theorem 2.22. *Let $T > 0$ and suppose that b and σ satisfy Assumption 2.21. Let $(X_t)_{t\in[0,T]}$ denote the solution of*

$$\mathrm{d}X_t = b(t, X_t)\mathrm{d}t + \sigma(t, X_t)\mathrm{d}W_t, \qquad 0 \leq t \leq T, \tag{2.17}$$

where X_0 is $\mathcal{F}_0$-measurable and integrable. Then the Euler-Maruyama scheme converges strongly to X.

For the proof we require a specific version of Grönwall's inequality, for which we will also provide a proof, since a detailed proof of similar variants is to the best of our knowledge rarely given.

Lemma 2.23. *Let Z be a Borel-measurable function which is bounded on bounded intervals and let $a, b \in \mathbb{R}_+$ be positive constants. If the integral inequality*

$$Z(t) \leq a + b \int_0^t Z(s)\mathrm{d}s$$

is satisfied for any $t \geq 0$, then it holds that

$$Z(t) \leq a\, \mathrm{e}^{bt}.$$

Proof. This proof is motivated by the proof given by Ethier and Kurtz [EK86] but provides more details and includes a rigorous treatment of the remainder R_n introduced below. We define $s_0 = t$ and claim that we have

$$Z(t) \leq a + a \sum_{k=0}^{n-1} b^{k+1} \int_0^{s_0} \cdots \int_0^{s_k} \mathrm{d}s_{k+1} \cdots \mathrm{d}s_1 + R_n, \tag{2.18}$$

where we define the remainder R_n as

$$R_n \coloneqq b^{n+1} \int_0^{s_0} \cdots \int_0^{s_n} Z(s_{n+1})\mathrm{d}s_{n+1} \cdots \mathrm{d}s_1.$$

We show this by induction: For $n = 0$, we obtain

$$Z(t) \leq a + b \int_0^{s_0} Z(s_1)\mathrm{d}s_1,$$

which is simply the assumed integral inequality since $t = s_0$. We now pass from n to $n+1$. We apply the integral inequality to R_n:

$$\begin{aligned}
R_n &= b^{n+1} \int_0^{s_0} \cdots \int_0^{s_n} Z(s_{n+1})\mathrm{d}s_{n+1} \cdots \mathrm{d}s_1 \\
&\leq b^{n+1} \int_0^{s_0} \cdots \int_0^{s_n} \left(a + b \int_0^{s_{n+1}} Z(s_{n+2})\mathrm{d}s_{n+2} \right) \mathrm{d}s_{n+1} \cdots \mathrm{d}s_1 \\
&= a\, b^{n+1} \int_0^{s_0} \cdots \int_0^{s_n} \mathrm{d}s_{n+1} \cdots \mathrm{d}s_1 + b^{n+2} \int_0^{s_0} \cdots \int_0^{s_{n+1}} Z(s_{n+2})\mathrm{d}s_{n+2} \cdots \mathrm{d}s_1 \\
&= a\, b^{n+1} \int_0^{s_0} \cdots \int_0^{s_n} \mathrm{d}s_{n+1} \cdots \mathrm{d}s_1 + R_{n+1}.
\end{aligned}$$

With the induction hypothesis we have

$$\begin{aligned}
Z(t) &\leq a + a \sum_{k=0}^{n-1} b^{k+1} \int_0^{s_0} \cdots \int_0^{s_k} \mathrm{d}s_{k+1} \cdots \mathrm{d}s_1 + R_n \\
&\leq a + a \sum_{k=0}^{n-1} b^{k+1} \int_0^{s_0} \cdots \int_0^{s_k} \mathrm{d}s_{k+1} \cdots \mathrm{d}s_1 + a\, b^{n+1} \int_0^{s_0} \cdots \int_0^{s_n} \mathrm{d}s_{n+1} \cdots \mathrm{d}s_1 + R_{n+1} \\
&= a + a \sum_{k=0}^{n} b^{k+1} \int_0^{s_0} \cdots \int_0^{s_k} \mathrm{d}s_{k+1} \cdots \mathrm{d}s_1 + R_{n+1},
\end{aligned}$$

which proves that the inequality (2.18) holds.

Next, we aim to evaluate the multiple integral in the inequality above and claim that

$$\int_0^{s_0} \cdots \int_0^{s_k} \mathrm{d}s_{k+1} \cdots \mathrm{d}s_1 = \frac{1}{(k+1)!}\, s_0^{k+1}. \tag{2.19}$$

Again we show this by induction, this time over the number of integrals K (thus $K = k+1$). For $K = 1$, we have

$$\int_0^{s_0} \mathrm{d}s_1 = s_0,$$

which clearly holds. To pass from K to $K+1$, we consider

$$\int_0^{s_0} \cdots \int_0^{s_{k+1}} \mathrm{d}s_{k+2} \cdots \mathrm{d}s_1 = \int_0^{s_0} \left(\int_0^{s_1} \cdots \int_0^{s_{k+1}} \mathrm{d}s_{k+2} \cdots \mathrm{d}s_2 \right) \mathrm{d}s_1.$$

The term

$$\int_0^{s_1} \cdots \int_0^{s_{k+1}} \mathrm{d}s_{k+2} \cdots \mathrm{d}s_2$$

consists of K integrals, therefore we may apply the induction hypothesis and obtain

$$\begin{aligned} \int_0^{s_0} \cdots \int_0^{s_{k+1}} \mathrm{d}s_{k+2} \cdots \mathrm{d}s_1 &= \int_0^{s_0} \frac{1}{(k+1)!}\, \mathrm{d}s_1^{k+1} \\ &= \left[\frac{1}{(k+2)(k+1)!}\, s_1^{k+2} \right]_0^{s_0} = \frac{1}{(k+2)!}\, s_0^{k+2}, \end{aligned}$$

which proves the claim. Then we have

$$a \sum_{k=0}^{n-1} b^{k+1} \int_0^{s_0} \cdots \int_0^{s_k} \mathrm{d}s_{k+1} \mathrm{d}s_1 = a \sum_{k=0}^{n-1} b^{k+1} \frac{1}{(k+1)!}\, s_0^{k+1} = a \sum_{k=1}^{n} b^k \frac{1}{k!}\, s_0^k.$$

Furthermore, note that by boundedness of Z on the interval $[0, t]$, we have

$$\begin{aligned} R_n(t) &= b^{n+1} \int_0^{s_0} \cdots \int_0^{s_n} Z(s_{n+1}) \mathrm{d}s_{n+1} \cdots \mathrm{d}s_1 \\ &\leq C\, b^{n+1} \int_0^{s_0} \cdots \int_0^{s_n} \mathrm{d}s_{n+1} \cdots \mathrm{d}s_1 = C\, b^{n+1}\, \frac{1}{(n+1)!}\, s_0^{n+1} \end{aligned}$$

for some constant C, where we used the result in equation (2.19).

Combining our results so far yields

$$\begin{aligned} Z(t) &\leq a + a \sum_{k=1}^{n} b^k \frac{1}{k!}\, s_0^k + R_n \\ &\leq a \sum_{k=0}^{n} b^k \frac{1}{k!}\, t^k + C\, b^{n+1} \frac{1}{(n+1)!}\, t^{n+1} \longrightarrow a\, \mathrm{e}^{bt} \quad \text{as} \quad n \to \infty \end{aligned}$$

by the series representation of the exponential function and since $b^{n+1} \frac{1}{(n+1)!}\, t^{n+1}$ converges to zero. □

Furthermore, we will now require the square integrability of the SDE solution as stated already in the standard result on existence and uniqueness in Theorem 2.13.

Lemma 2.24. *Let X be the solution of the SDE as given by Theorem 2.13 and $X_0 = Z$ with $\mathrm{E}\left[\|Z\|^2\right] < \infty$. Then there exists a constant $\tilde{K}$ depending only on the constants D and T such that*

$$\mathrm{E}\left[\|X_t\|^2\right] \leq K(1 + \mathrm{E}\left[\|Z\|^2\right])\,\mathrm{e}^{Kt} \quad \textit{for } 0 \leq t \leq T.$$

Proof. As in the proof of Theorem 2.15, we apply the iterative formula defined by $Y_t^{(0)} = X_0$ and

$$Y_t^{(k+1)} = X_0 + \int_0^t b\left(s, Y_s^{(k)}\right) \mathrm{d}s + \int_0^t \sigma\left(s, Y_s^{(k)}\right) \mathrm{d}W_s.$$

Then with the Lemmata 2.16, 2.17 and the Itô-Isometry and by applying the growth bound in Assumption 2.12, we compute

$$\begin{aligned}
\mathrm{E}\left[\left\|Y_t^{(k+1)}\right\|\right] &\leq 3\left(\mathrm{E}\left[\|Z\|^2\right] + t\,\mathrm{E}\left[\int_0^t \left\|b\left(s, Y_s^{(k)}\right)\right\|^2 \mathrm{d}s\right] + \mathrm{E}\left[\int_0^t \left\|\sigma\left(s, Y_s^{(k)}\right)\right\|^2 \mathrm{d}s\right]\right) \\
&\leq 3\left(\mathrm{E}\left[\|Z\|^2\right] + t\,D^2\,\mathrm{E}\left[\int_0^t \left(1 + \left\|Y_s^{(k)}\right\|^2\right) \mathrm{d}s\right]\right. \\
&\quad \left. + D^2\,\mathrm{E}\left[\int_0^t \left(1 + \left\|Y_s^{(k)}\right\|^2\right) \mathrm{d}s\right]\right) \\
&= 3\left(\mathrm{E}\left[\|Z\|^2\right] + D^2(t+1)\int_0^t \mathrm{d}s + D^2(t+1)\int_0^t \mathrm{E}\left[\left\|Y_s^{(k)}\right\|^2\right] \mathrm{d}s\right) \\
&\leq \tilde{K}\left(\mathrm{E}\left[\|Z\|^2\right] + D^2\int_0^t \mathrm{d}s + D^2\int_0^t \mathrm{E}\left[\left\|Y_s^{(k)}\right\|^2\right] \mathrm{d}s\right), \qquad (2.20)
\end{aligned}$$

where $\tilde{K}$ is chosen so that $\tilde{K} \geq 3(1+T)$. In particular, we then have

$$\mathrm{E}\left[\|Y_t^{(1)}\|\right] \leq \tilde{K}\left(\mathrm{E}\left[\|Z\|^2\right] + D^2\int_0^t \mathrm{d}s + D^2\int_0^t \mathrm{E}\left[\|Z\|^2\right] \mathrm{d}s\right).$$

We set $s_0 \coloneqq t$ and claim that for $k \geq 1$, it holds that

$$\mathrm{E}\left[\left\|Y_t^{(k)}\right\|^2\right] \leq \tilde{K}\,\mathrm{E}\left[\|Z\|^2\right] + \sum_{j=0}^{k-1} \tilde{K}^{j+1}\,D^{2(j+1)} \int_0^{s_0} \cdots \int_0^{s_j} \left(1 + \tilde{K}\,\mathrm{E}\left[\|Z\|^2\right]\right) \mathrm{d}s_{j+1} \cdots \mathrm{d}s_1.$$

We show this by induction. With the result from above, we have for $k = 1$

$$\mathrm{E}\left[\left\|Y_t^{(1)}\right\|^2\right] \leq \tilde{K}\left[\|Z\|^2\right] + \tilde{K}\,D^2 \int_0^{s_0} \left(1 + \tilde{K}\,\mathrm{E}\left[\|Z\|^2\right]\right) \mathrm{d}s_1$$

since $\tilde{K} > 1$. In order to pass from k to $k+1$, we reformulate the induction hypothesis by an index shift and by renaming the integration variables as

$$\mathrm{E}\left[\left\|Y_{s_1}^{(k)}\right\|^2\right] \leq \tilde{K}\,\mathrm{E}\left[\|Z\|^2\right] + \sum_{j=1}^{k} \tilde{K}^{j}\,D^{2j} \int_0^{s_1} \cdots \int_0^{s_j} \left(1 + \tilde{K}\,\mathrm{E}\left[\|Z\|^2\right]\right) \mathrm{d}s_{j+1} \cdots \mathrm{d}s_2$$

and apply this to the relation (2.20) from above to obtain

$$\begin{aligned}
\mathrm{E}\left[\|Y_t^{(k+1)}\|\right] &\leq \tilde{K}\left(\mathrm{E}\left[\|Z\|^2\right] + D^2\int_0^{s_0}\mathrm{d}s_1 + D^2\int_0^{s_0}\mathrm{E}\left[\left\|Y_{s_1}^{(k)}\right\|^2\right]\mathrm{d}s_1\right)\\
&\leq \tilde{K}\left(\mathrm{E}\left[\|Z\|^2\right] + D^2\int_0^{s_0}\mathrm{d}s_1 + D^2\int_0^{s_0}\tilde{K}\,\mathrm{E}\left[\|Z\|^2\right]\mathrm{d}s_1\right.\\
&\quad \left. + D^2\int_0^{s_0}\sum_{j=1}^{k}\tilde{K}^j\,D^{2j}\int_0^{s_1}\cdots\int_0^{s_j}\left(1+\tilde{K}\,\mathrm{E}\left[\|Z\|^2\right]\right)\mathrm{d}s_{j+1}\cdots\mathrm{d}s_2\mathrm{d}s_1\right)\\
&\leq \tilde{K}\,\mathrm{E}\left[\|Z\|^2\right] + \tilde{K}\,D^2\int_0^{s_0}\left(1+\mathrm{E}\left[\|Z\|^2\right]\right)\mathrm{d}s_1\\
&\quad + \sum_{j=1}^{k}\tilde{K}^{j+1}\,D^{2(j+1)}\int_0^{s_0}\cdots\int_0^{s_j}\left(1+\tilde{K}\,\mathrm{E}\left[\|Z\|^2\right]\right)\mathrm{d}s_{j+1}\cdots\mathrm{d}s_1\\
&\leq \tilde{K}\,\mathrm{E}\left[\|Z\|^2\right] + \sum_{j=0}^{k}\tilde{K}^{j+1}\,D^{2(j+1)}\int_0^{s_0}\cdots\left(1+\tilde{K}\,\mathrm{E}\left[\|Z\|^2\right]\right)\mathrm{d}s_{j+1}\cdots\mathrm{d}s_1,
\end{aligned}$$

which concludes the induction. With the result (2.19) from the proof of the previous Lemma 2.23 we have

$$\begin{aligned}
\mathrm{E}\left[\left\|Y_t^{(k)}\right\|^2\right] &\leq \tilde{K}\,\mathrm{E}\left[\|Z\|^2\right] + \left(1+\tilde{K}\,\mathrm{E}\left[\|Z\|^2\right]\right)\sum_{j=0}^{k-1}\tilde{K}^{j+1}\,D^{2(j+1)}\int_0^{s_0}\cdots\int_0^{s_j}\mathrm{d}s_{j+1}\cdots\mathrm{d}s_1\\
&= \tilde{K}\,\mathrm{E}\left[\|Z\|^2\right] + \left(1+\tilde{K}\,\mathrm{E}\left[\|Z\|^2\right]\right)\sum_{j=0}^{k-1}\frac{\left(\tilde{K}\,D^2\,s_0\right)^{j+1}}{(j+1)!}\\
&\leq \tilde{K}\left(1+\mathrm{E}\left[\|Z\|^2\right]\right) + \tilde{K}\left(1+\mathrm{E}\left[\|Z\|^2\right]\right)\sum_{j=1}^{k}\frac{\left(\tilde{K}\,D^2\,t\right)^{j}}{j!}\\
&\leq \tilde{K}\left(1+\mathrm{E}\left[\|Z\|^2\right]\right)\sum_{j=0}^{k}\frac{\left(\tilde{K}\,D^2\,t\right)^{j}}{j!}.
\end{aligned}$$

Then we have for the limit that

$$\lim_{k\to\infty}\mathrm{E}\left[\left\|Y_t^{(k)}\right\|^2\right] \leq \lim_{k\to\infty}\tilde{K}\left(1+\mathrm{E}\left[\|Z\|^2\right]\right)\sum_{j=0}^{k}\frac{\left(\tilde{K}\,D^2\,t\right)^{j}}{j!} = \tilde{K}\left(1+\mathrm{E}\left[\|Z\|^2\right]\right)\mathrm{e}^{\tilde{K}D^2t}.$$

From the proof of Øksendal for the existence and uniqueness result in Theorem 2.13, we know that there exists a subsequence $(n_k)_{k\in\mathbb{N}}$ such that $Y^{(n_k)}$ converges to X almost surely. Therefore we have with Fatou's Lemma

$$\begin{aligned}
\mathrm{E}\left[\|X_t\|^2\right] &= \mathrm{E}\left[\lim_{k\to\infty}\|Y_t^{(n_k)}\|^2\right]\\
&\leq \liminf_{k\to\infty}\mathrm{E}\left[\|Y_t^{(n_k)}\|^2\right] \leq \lim_{k\to\infty}\mathrm{E}\left[\left\|Y_t^{(n_k)}\right\|^2\right] \leq \tilde{K}\left(1+\mathrm{E}\left[\|Z\|^2\right]\right)\mathrm{e}^{\tilde{K}D^2t}.
\end{aligned}$$

Choosing $K = \max\{\tilde{K}, \tilde{K}\,D^2\}$ concludes the proof. □

Proof of Theorem 2.22. We proceed similarly as Kloeden and Platen[11]. We fix a partition of $[0,T]$ with N steps of maximum size δ, denoted by $0 = t_0 < t_1 < \ldots < t_N = T$. We define

$$Z(t) = \sup_{0\leq s\leq t} \mathrm{E}\left[\|Y_{n_s} - X_s\|^2\right],$$

where n_s denotes the iteration index corresponding to time s, i.e. $n_s = \max\{n|t_n \leq s\}$.

(i) We first show that Z satisfies an integral equality as required for the application of Grönwall's inequality. With the SDE in (2.17) and the definition of the Euler-Maruyama scheme in (2.13), we have

$$\begin{aligned} Z(t) &= \sup_{0\leq s\leq t} \mathrm{E}\left[\left\| \sum_{n=0}^{n_s-1} (Y_{n+1} - Y_n) - \int_0^s b(r, X_r)\mathrm{d}r - \int_0^s \sigma(r, X_r)\mathrm{d}W_r \right\|^2\right] \\ &= \sup_{0\leq s\leq t} \mathrm{E}\left[\left\| \sum_{n=0}^{n_s-1} b(t_n, Y_n)\Delta_n + \sum_{n=0}^{n_s-1} \sigma(t_n, Y_n)\Delta W_n \right.\right. \\ &\quad \left.\left. - \int_0^s b(r, X_r)\mathrm{d}r - \int_0^s \sigma(r, X_r)\mathrm{d}W_r \right\|^2\right]. \end{aligned}$$

Next, we aim to write the sums as integrals. We let $r \in [0, t_{n_s})$. Then similar to the above, we have that $n_r = \max\{n|t_n \leq r\}$, so in particular $r \in [t_{n_r}, t_{n_r+1})$ and furthermore $n_r \in \{0, 1, \ldots, n_s - 1\}$. We can therefore write

$$b(t_{n_r}, Y_{n_r}) = \sum_{n=0}^{n_s-1} b(t_n, Y_n)\, \mathbf{1}_{[t_n, t_{n+1})}(r)$$

and we then have

$$\begin{aligned} \int_0^{t_{n_s}} b(t_{n_r}, Y_{n_r})\mathrm{d}r &= \int_0^{t_{n_s}} \sum_{n=0}^{n_s-1} b(t_n, Y_n)\, \mathbf{1}_{[t_n, t_{n+1})}(r)\mathrm{d}r \\ &= \sum_{n=0}^{n_s-1} b(t_n, Y_n) \int_{t_n}^{t_{n+1}} \mathrm{d}r = \sum_{n=0}^{n_s-1} b(t_n, Y_n)\Delta_n, \end{aligned}$$

which delivers an integral to replace the sum in the expression above. Furthermore, we write

$$\sigma(t_{n_r}, Y_{n_r}) = \sum_{n=0}^{n_s-1} \sigma(t_n, Y_n)\, \mathbf{1}_{[t_n, t_{n+1})}(r)$$

and by definition of the stochastic integral, we then have

$$\int_0^{t_{n_s}} \sigma(t_{n_r}, Y_{n_r})\mathrm{d}W_r = \sum_{n=0}^{n_s-1} \sigma(t_n, Y_n)\left(W_{t_{n+1}} - W_{t_n}\right) = \sum_{n=0}^{n_s-1} \sigma(t_n, Y_n)\Delta W_n,$$

so we can now rewrite Z as

$$\begin{aligned} Z(t) = \sup_{0\leq s\leq t} \mathrm{E}\left[\left\| \int_0^{t_{n_s}} b(t_{n_r}, Y_{n_r})\mathrm{d}r + \int_0^{t_{n_s}} \sigma(t_{n_r}, Y_{n_r})\mathrm{d}W_r \right.\right. \\ \left.\left. - \int_0^s b(r, X_r)\mathrm{d}r - \int_0^s \sigma(r, X_r)\mathrm{d}W_r \right\|^2\right]. \end{aligned}$$

[11] Proof of Theorem 9.6.2, pp. 324 in [KP92].

We then add zero, rearrange and separate the expectation operator by using the inequality relation in Lemma 2.16 for $N = 6$, resulting in

$$\begin{aligned}
Z(t) = \sup_{0\le s\le t} \mathrm{E}\Bigg[\Big\| &\int_0^{t_{n_s}} b(t_{n_r}, Y_{n_r})\mathrm{d}r + \int_0^{t_{n_s}} \sigma(t_{n_r}, Y_{n_r})\mathrm{d}W_r \\
&- \int_0^{t_{n_s}} b(r, Y_{n_r})\mathrm{d}r - \int_0^{t_{n_s}} \sigma(r, Y_{n_r})\mathrm{d}W_r + \int_0^{t_{n_s}} b(r, Y_{n_r})\mathrm{d}r + \int_0^{t_{n_s}} \sigma(r, Y_{n_r})\mathrm{d}W_r \\
&- \int_0^{s} b(r, X_r)\mathrm{d}r - \int_0^{s} \sigma(r, X_r)\mathrm{d}W_r\Big\|^2\Bigg] \\
\le 6 \sup_{0\le s\le t} \Bigg\{ &\mathrm{E}\left[\Big\| \int_0^{t_{n_s}} \big(b(t_{n_r}, Y_{n_r}) - b(r, Y_{n_r})\big)\mathrm{d}r\Big\|^2\right] \\
&+ \mathrm{E}\left[\Big\| \int_0^{t_{n_s}} \big(\sigma(t_{n_r}, Y_{n_r}) - \sigma(r, Y_{n_r})\big)\mathrm{d}W_r\Big\|^2\right] \\
&+ \mathrm{E}\left[\Big\| \int_0^{t_{n_s}} \big(b(r, Y_{n_r}) - b(r, X_r)\big)\mathrm{d}r\Big\|^2\right] + \mathrm{E}\left[\Big\| \int_0^{t_{n_s}} \big(\sigma(r, Y_{n_r}) - \sigma(r, X_r)\big)\mathrm{d}W_r\Big\|^2\right] \\
&+ \mathrm{E}\left[\Big\| \int_{t_{n_s}}^{s} b(r, X_r)\mathrm{d}r\Big\|^2\right] + \mathrm{E}\left[\Big\| \int_{t_{n_s}}^{s} \sigma(r, X_r)\mathrm{d}W_r\Big\|^2\right]\Bigg\}.
\end{aligned}$$

We apply Lemma 2.17 and the Itô-Isometry to obtain

$$\begin{aligned}
Z(t) \le 6 \sup_{0\le s\le t} \Bigg\{ &T\,\mathrm{E}\left[\int_0^{t_{n_s}} \|b(t_{n_r}, Y_{n_r}) - b(r, Y_{n_r})\|^2\mathrm{d}r\right] \\
&+ \mathrm{E}\left[\int_0^{t_{n_s}} \|\sigma(t_{n_r}, Y_{n_r}) - \sigma(r, Y_{n_r})\|^2\mathrm{d}r\right] \\
&+ T\,\mathrm{E}\left[\int_0^{t_{n_s}} \|b(r, Y_{n_r}) - b(r, X_r)\|^2\mathrm{d}r\right] + \mathrm{E}\left[\int_0^{t_{n_s}} \|\sigma(r, Y_{n_r}) - \sigma(r, X_r)\|^2\mathrm{d}r\right] \\
&+ T\,\mathrm{E}\left[\int_{t_{n_s}}^{s} \|b(r, X_r)\|^2\mathrm{d}r\right] + \mathrm{E}\left[\int_{t_{n_s}}^{s} \|\sigma(r, X_r)\|^2\mathrm{d}r\right]\Bigg\}.
\end{aligned}$$

By the Hölder condition in time given by (2.16) in Assumption 2.21 and with $|t_{n_r} - r| \le \Delta_{n_r} \le \delta$, we have

$$\int_0^{t_{n_s}} \|b(t_{n_r}, Y_{n_r}) - b(r, Y_{n_r})\|^2\mathrm{d}r \le \int_0^{t_{n_s}} D_2^2\,|t_{n_r} - r|\mathrm{d}r \le \int_0^{t_{n_s}} D_2^2\,\delta\mathrm{d}r \le D_2^2\,t_{n_s}\,\delta$$

and by the Lipschitz condition in x as given by (2.15) in Assumption 2.21

$$\int_0^{t_{n_s}} \|b(r, Y_{n_r}) - b(r, X_r)\|^2\mathrm{d}r \le D_1^2 \int_0^{t_{n_s}} \|Y_{n_r} - X_r\|^2\mathrm{d}r.$$

In the standard existence and uniqueness result for SDEs in Theorem 2.13, we have stated and in Lemma 2.24 we have shown that there exists a constant K such that

$$\mathrm{E}\left[\|X_t\|^2\right] \le K(1 + \mathrm{E}\left[\|Z\|^2\right])\,\mathrm{e}^{Kt} \quad \text{for } 0 \le t \le T.$$

So in particular there exists a constant K_2 such that

$$\mathrm{E}\left[\|X_t\|^2\right] \le K_2 \quad \text{for any } t \in [0, T].$$

With the linear growth condition in (2.14) in Assumption 2.21 and Tonelli's theorem, this yields

$$\begin{aligned}
\mathrm{E}\left[\int_{t_{n_s}}^{s} \|b(r,X_r)\|^2 \mathrm{d}r\right] &\leq \mathrm{E}\left[\int_{t_{n_s}}^{s} C^2\,\left(1+\|X_r\|^2\right)\,\mathrm{d}r\right] \\
&\leq C^2\left((s-t_{n_s}) + \mathrm{E}\left[\int_{t_{n_s}}^{s}\|X_r\|^2\mathrm{d}r\right]\right) \\
&\leq C^2\left(\delta + \int_{t_{n_s}}^{s}\mathrm{E}\left[\|X_r\|^2\right]\mathrm{d}r\right) \\
&\leq C^2\,\delta\,(1+K_2).
\end{aligned}$$

We proceed similarly for the terms with the volatility σ and apply these estimates to our considerations on $Z(t)$ above:

$$\begin{aligned}
Z(t) \leq 6 \sup_{0\leq s\leq t}\Bigg\{&(T+1)\,T\,D_2^2\,\delta + (T+1)\,D_1^2\,\mathrm{E}\left[\int_0^{t_{n_s}}\|Y_{n_r}-X_r\|^2\mathrm{d}r\right] \\
&+\,(T+1)\,C^2\,\delta(1+K_2)\Bigg\}.
\end{aligned}$$

To simplify notation, we introduce constants K_3 and K_4 such that

$$\begin{aligned}
K_3 &\geq 6\,D_1^2\,(T+1) \\
K_4 &\geq 6\left((T+1)\,T\,D_2^2 + C^2(T+1)(1+K_2)\right).
\end{aligned}$$

Then by using again Tonelli's theorem and the definition of Z we have

$$\begin{aligned}
Z(t) &\leq K_3 \sup_{0\leq s\leq t}\mathrm{E}\left[\int_0^{t_{n_s}}\|Y_{n_r}-X_r\|^2\mathrm{d}r\right] + K_4\,\delta \\
&\leq K_3 \sup_{0\leq s\leq t}\int_0^{t_{n_s}}\mathrm{E}\left[\|Y_{n_r}-X_r\|^2\right]\mathrm{d}r + K_4\,\delta \\
&\leq K_3\int_0^t \sup_{0\leq v\leq r}\mathrm{E}\left[\|Y_{n_v}-X_v\|^2\right]\mathrm{d}r + K_4\,\delta \\
&\leq K_3\int_0^t Z(r)\mathrm{d}r + K_4\,\delta.
\end{aligned}$$

(ii) Next we aim to apply Grönwall's inequality as given in Lemma 2.23 and therefore we need to show that Z is bounded on the interval $[0,T]$. We recall that

$$Z(t) = \sup_{0\leq s\leq t}\mathrm{E}\left[\|Y_{n_s}-X_s\|^2\right]$$

and note that if $\mathrm{E}\left[\|Y_{n_s}-X_s\|^2\right]$ is bounded on $[0,T]$ uniformly in s, then this also holds for the supremum. Further, we have

$$\mathrm{E}\left[\|Y_{n_s}-X_s\|^2\right] \leq 2\left(\mathrm{E}\left[\|Y_{n_s}\|^2\right] + \mathrm{E}\left[\|X_s\|^2\right]\right).$$

We have already shown above that $\mathrm{E}\left[\|X_s\|^2\right]$ is bounded, therefore it remains to consider $\mathrm{E}\left[\|Y_{n_s}\|^2\right]$. First, by applying the iteration procedure of the Euler-Maruyama scheme and with Lemma 2.16, we compute

$$\begin{aligned}\mathrm{E}\left[\|Y_{n+1}\|^2\right] &= \mathrm{E}\left[\|Y_n + b(t_n, Y_n)\,\Delta_n + \sigma(t_n, Y_n)\,\Delta W_n\|^2\right] \\ &\leq 3\left(\mathrm{E}\left[\|Y_n\|^2\right] + \Delta_n^2\,\mathrm{E}\left[\|b(t_n, Y_n)\|^2\right] + \mathrm{E}\left[\|\sigma(t_n, Y_n)\|^2 \cdot |\Delta W_n|^2\right]\right).\end{aligned}$$

By definition of Brownian motion, the increment ΔW_n and Y_n are independent and thus also ΔW_n and $\|\sigma(t_n, Y_n)\|^2$. In addition, we have $\mathrm{E}\left[|\Delta W_n|^2\right] = \Delta_n$, therefore

$$\mathrm{E}\left[\|\sigma(t_n, Y_n)\|^2 \cdot |\Delta W_n|^2\right] = \mathrm{E}\left[\|\sigma(t_n, Y_n)\|^2\right] \cdot \mathrm{E}\left[|\Delta W_n|^2\right] = \Delta_n\,\mathrm{E}\left[\|\sigma(t_n, Y_n)\|^2\right].$$

We use this and apply the linear growth condition (2.14) in Assumption 2.21 to result in

$$\begin{aligned}\mathrm{E}\left[\|Y_{n+1}\|^2\right] &\leq 3\left(\mathrm{E}\left[\|Y_n\|^2\right] + \Delta_n^2\,\mathrm{E}\left[\|b(t_n, Y_n)\|^2\right] + \Delta_n\,\mathrm{E}\left[\|\sigma(t_n, Y_n)\|^2\right]\right) \\ &\leq 3\left(\mathrm{E}\left[\|Y_n\|^2\right] + \delta^2\,\mathrm{E}\left[C^2\left(1 + \|Y_n\|^2\right)\right] + \delta\,\mathrm{E}\left[C^2\left(1 + \|Y_n\|^2\right)\right]\right) \\ &\leq 3\left(\mathrm{E}\left[\|Y_n\|^2\right] + \delta\,(1+\delta)\,C^2\,\left(1 + \mathrm{E}\left[\|Y_n\|^2\right]\right)\right) \\ &= 3\left(\delta\,(1+\delta)\,C^2 + \left(1 + \delta\,(1+\delta)\,C^2\right)\,\mathrm{E}\left[\|Y_n\|^2\right]\right) \\ &= 3\left(\tilde{K}_1 + \tilde{K}_2\,\mathrm{E}\left[\|Y_n\|^2\right]\right), \qquad (2.21)\end{aligned}$$

where we define $\tilde{K}_1 \coloneqq \delta(1+\delta)C^2$ and $\tilde{K}_2 \coloneqq 1 + \delta(1+\delta)C^2$. Now we show by induction that for any $n \in \mathbb{N}$, we have

$$\mathrm{E}\left[\|Y_n\|^2\right] \leq 3\,\tilde{K}_1 + \sum_{i=1}^{n-1} 3^{i+1}\,\tilde{K}_1\,\tilde{K}_2^i + 3^n\,\tilde{K}_2^n\,\mathrm{E}\left[\|Y_0\|^2\right]. \qquad (2.22)$$

For $n = 1$, this follows directly from the inequality above in equation (2.21). We now assume that the claim in equation (2.22) holds for n and pass to $n+1$. With the relation (2.21) we have

$$\begin{aligned}\mathrm{E}\left[\|Y_{n+1}\|^2\right] &\leq 3\left(\tilde{K}_1 + \tilde{K}_2\,\mathrm{E}\left[\|Y_n\|^2\right]\right) \\ &\leq 3\left(\tilde{K}_1 + \tilde{K}_2\left(3\,\tilde{K}_1 + \sum_{i=1}^{n-1} 3^{i+1}\,\tilde{K}_1\,\tilde{K}_2^i + 3^n\,\tilde{K}_2^n\,\mathrm{E}\left[\|Y_0\|^2\right]\right)\right) \\ &= 3\,\tilde{K}_1 + 3^2\,\tilde{K}_1\,\tilde{K}_2 + \sum_{i=1}^{n-1} 3^{i+2}\,\tilde{K}_1\,\tilde{K}_2^{i+1} + 3^{n+1}\,\tilde{K}_2^{n+1}\,\mathrm{E}\left[\|Y_0\|^2\right] \\ &= 3\,\tilde{K}_1 + 3^2\,\tilde{K}_1\,\tilde{K}_2 + \sum_{i=2}^{n} 3^{i+1}\,\tilde{K}_1\,\tilde{K}_2^{i} + 3^{n+1}\,\tilde{K}_2^{n+1}\,\mathrm{E}\left[\|Y_0\|^2\right] \\ &= 3\,\tilde{K}_1 + \sum_{i=1}^{n} 3^{i+1}\,\tilde{K}_1\,\tilde{K}_2^{i} + 3^{n+1}\,\tilde{K}_2^{n+1}\,\mathrm{E}\left[\|Y_0\|^2\right]\end{aligned}$$

and thus we have shown the claim (2.22). By definition of the Euler-Maruyama scheme and the assumption that $X_0 \in L_2$, we have $\mathrm{E}\left[\|Y_0\|^2\right] = \mathrm{E}\left[\|X_0\|^2\right] < \infty$. Hence the inequality (2.22) provides us with a bound of $\mathrm{E}\left[\|Y_n\|^2\right]$ for each n. Since this bound is increasing in n, we obtain a global bound of $\mathrm{E}\left[\|Y_{n_s}\|^2\right]$ for any s in the interval $[0, T]$ by inserting the number of steps N of the partition we consider.

(iii) Finally, we now apply Grönwall's inequality and obtain

$$Z(t) \leq \delta\, K_4\, \mathrm{e}^{K_3\, t} \leq \delta\, K_4\, \mathrm{e}^{K_3\, T}.$$

We choose K_5 such that $K_5 \geq K_4\, e^{K_3\, T}$. Then by the Hölder inequality, we arrive at

$$\mathrm{E}\left[\left\|Y^\delta(T) - X_T\right\|\right] \leq \left(\mathrm{E}\left[\left\|Y^\delta(T) - X_T\right\|^2\right]\right)^{\frac{1}{2}} \leq \sqrt{Z(T)} \leq \sqrt{K_5\, \delta} \longrightarrow 0 \quad \text{as } \delta \to 0$$

which delivers the convergence of the Euler-Maruyama scheme. □

This theorem cannot be applied to the SDE we consider, as we again face the challenge that the drift coefficient does not satisfy Assumption 2.21. Therefore, we can only impose Assumption 2.14 and in addition, we formulate a similar requirement regarding Hölder continuity in time:

Assumption 2.25. Let $T > 0$ and $b : [0,T] \times \mathbb{R}^d \to \mathbb{R}^d$ and $\sigma : [0,T] \times \mathbb{R}^d \to \mathbb{R}^d$ be measurable functions. We assume that for all $\varepsilon > 0$ there exists $D_{\varepsilon,2}$ such that

$$\|b(t,x) - b(s,x)\| + \|\sigma(t,x) - \sigma(s,x)\| \leq D_{\varepsilon,2}\, |t-s|^{\frac{1}{2}} \quad \text{for } t,s \in [0, T-\varepsilon] \text{ and for } x \in \mathbb{R}^d.$$

By using Theorem 2.22 we now can show that the Euler-Maruyama scheme converges also if we only have the Assumptions 2.14 and 2.25.

Theorem 2.26. *Let $T > 0$ and suppose that b and σ satisfy Assumptions 2.14 and 2.25. Let $X = (X_t)_{t\in[0,T]}$ denote the solution of*

$$\mathrm{d}X_t = b(t, X_t)\mathrm{d}t + \sigma(t, X_t)\mathrm{d}W_t \quad \textit{for } 0 \leq t \leq T, \tag{2.23}$$

where X_0 is a $\mathcal{F}_0$-measurable and integrable $\mathbb{R}^d$-valued random variable. Then the Euler-Maruyama scheme converges strongly to X.

Proof. We let $\kappa \in [0,T]$ arbitrary and define $T^\kappa = T - \kappa$. Then by Theorem 2.22, we have that the Euler-Maruyama scheme converges strongly on $[0, T^\kappa]$ and therefore

$$\lim_{\delta \to 0} \mathrm{E}\left[\left\|X_{T^\kappa} - Y^\delta(T^\kappa)\right\|\right] = 0. \tag{2.24}$$

We fix $\delta > 0$ arbitrary and write

$$\mathrm{E}\left[\left\|X_T - Y^\delta(T)\right\|\right] \leq \mathrm{E}\left[\left\|X_{T^\kappa} - Y^\delta(T^\kappa)\right\|\right] + \mathrm{E}\left[\left\|Y^\delta(T) - Y^\delta(T^\kappa)\right\|\right] + \mathrm{E}\Big[\left\|X_T - X_{T^\kappa}\right\|\Big].$$

For notational purposes, we choose an arbitrary partition with maximum step size δ and we choose $n \in \mathbb{N}$ such that $t_n = T^\kappa$. Further, we choose $k \in \mathbb{N}$ such that $t_{n+k} = T$. Then by applying the Euler-Maruyama scheme in (2.13) we have

$$\begin{aligned}
\mathrm{E}\left[\left\|Y^\delta(T) - Y^\delta(T^\kappa)\right\|\right] &= \mathrm{E}\Big[\left\|Y_{n+k} - Y_n\right\|\Big] = \mathrm{E}\left[\Big\| \sum_{i=0}^{k-1} (Y_{n+i+1} - Y_{n+i}) \Big\|\right] \\
&= \mathrm{E}\left[\Big\| \sum_{i=0}^{k-1} \big(b(t_{n+i}, Y_{n+i})\, \Delta_{n+i} + \sigma(t_{n+i}, Y_{n+i})\, \Delta W_{n+i}\big) \Big\|\right] \\
&\leq \mathrm{E}\left[\Big\| \sum_{i=0}^{k-1} b(t_{n+i}, Y_{n+i})\, \Delta_{n+i} \Big\|\right] + \mathrm{E}\left[\Big\| \sum_{i=0}^{k-1} \sigma(t_{n+i}, Y_{n+i})\, \Delta W_{n+i} \Big\|\right]
\end{aligned}$$

and we use boundedness as given in (2.7) of Assumption 2.14 to yield

$$\begin{aligned}\mathrm{E}\left[\Big\|\sum_{i=0}^{k-1} b(t_{n+i}, Y_{n+i})\,\Delta_{n+i}\Big\|\right] &\le \mathrm{E}\left[\sum_{i=0}^{k-1}\big\|b(t_{n+i}, Y_{n+i})\big\|(t_{n+i+1}-t_{n+i})\right]\\ &\le \mathrm{E}\left[C\,(t_{n+k}-t_n)\right]\\ &= C\,(T-T^\kappa)\\ &= C\,\kappa.\end{aligned}$$

We set $\xi_i = \sigma(t_{n+i}, Y_{n+i})$. Then $\tilde\sigma(t) \coloneqq \xi_0 \mathbf{1}_{\{0\}}(t) + \sum_{i=0}^{k-1}\xi_i \mathbf{1}_{(t_i, t_{i+1}]}$ is an $\mathbb{R}^d$-valued simple process with $\|\tilde\sigma(t)\| < C$ by the boundedness condition (2.7). By the definition of stochastic integrals for simple processes, we have

$$\mathrm{E}\left[\Big\|\sum_{i=0}^{k-1}\sigma(t_{n+i}, Y_{n+i})(W_{t_{n+i+1}} - W_{t_{n+i}})\Big\|\right] = \mathrm{E}\left[\Big\|\int_{T^\kappa}^{T}\tilde\sigma(t)\,\mathrm{d}W_t\Big\|\right].$$

We apply Hölder's inequality and the Itô-Isometry and use that σ is bounded to obtain

$$\begin{aligned}\mathrm{E}\left[\Big\|\int_{T^\kappa}^{T}\tilde\sigma(t)\,\mathrm{d}W_t\Big\|\right] = \mathrm{E}\left[\Big\|\int_{T^\kappa}^{T}\tilde\sigma(t)\,\mathrm{d}W_t\Big\|\right]^{2\cdot\frac12} &\le \mathrm{E}\left[\Big\|\int_{T^\kappa}^{T}\tilde\sigma(t)\,\mathrm{d}W_t\Big\|^2\right]^{\frac12}\\ \le \mathrm{E}\left[\int_{T^\kappa}^{T}\|\tilde\sigma(t)\|^2\,\mathrm{d}t\right]^{\frac12} &\le C\,\mathrm{E}\left[T-T^\kappa\right]^{\frac12} \le C\,\sqrt{\kappa}.\end{aligned}$$

Thus we have

$$E\left[\Big\|Y^\delta(T) - Y^\delta(T^\kappa)\Big\|\right] \le C\,\kappa + C\,\sqrt{\kappa}.$$

On the other hand, we apply the integral form of the SDE in (2.23) and again Hölder's inequality to compute

$$\begin{aligned}\mathrm{E}\left[\big\|X_T - X_{T^\kappa}\big\|\right] &\le \mathrm{E}\left[\Big\|\int_{T^\kappa}^{T} b(t, X_t)\,\mathrm{d}t\Big\|\right] + E\left[\Big\|\int_{T^\kappa}^{T}\sigma(t, X_t)\,\mathrm{d}W_t\Big\|\right]\\ &\le \mathrm{E}\left[\Big\|\int_{T^\kappa}^{T} b(t, X_t)\,\mathrm{d}t\Big\|^2\right]^{\frac12} + \mathrm{E}\left[\Big\|\int_{T^\kappa}^{T}\sigma(t, X_t)\,\mathrm{d}W_t\Big\|^2\right]^{\frac12}\\ &\le \mathrm{E}\left[\kappa\int_{T^\kappa}^{T}\|b(t, X_t)\|^2\mathrm{d}t\right]^{\frac12} + \mathrm{E}\left[\int_{T^\kappa}^{T}\|\sigma(t, X_t)\|^2\mathrm{d}t\right]^{\frac12}\\ &\le C\,\mathrm{E}\left[\kappa\,(T-T^\kappa)\right]^{\frac12} + C\,\mathrm{E}\left[T-T^\kappa\right]^{\frac12}\\ &= C\,\kappa + C\,\sqrt{\kappa}\end{aligned}$$

by applying again Lemma 2.17 and the Itô-Isometry. Taking everything together we have

$$\mathrm{E}\left[\big\|X_T - Y^\delta(T)\big\|\right] \le \mathrm{E}\left[\big\|X_{T^\kappa} - Y^\delta(T^\kappa)\big\|\right] + 2\,C\,(\kappa + \sqrt{\kappa}).$$

Now we let $\varepsilon > 0$ arbitrary. Then there exists $\kappa > 0$ such that

$$2\,C\,(\kappa + \sqrt{\kappa}) < \frac{\varepsilon}{2}.$$

Since the Euler-Maruyama scheme converges strongly on $[0, T^\kappa]$, as stated in (2.24), we have that there exists $\delta_0(\kappa)$ such that

$$\mathrm{E}\left[\big\|X_{T^\kappa} - Y^\delta(T^\kappa)\big\|\right] < \frac{\varepsilon}{2}$$

for any $\delta \leq \delta_0$. Hence we have

$$\mathrm{E}\left[\left\|X_T - Y^{\delta}(T)\right\|\right] < \varepsilon$$

for all $\delta \leq \delta_0$, i.e. the Euler-Maruyama scheme converges strongly on $[0, T]$. □

Summary

This section served to provide the theoretical foundation of the SDE solution: Under assumptions adapted to the SDE in our model, we showed that a unique solution to the SDE exists. Moreover, we first provided a proof on convergence of the Euler-Maruyama scheme for a time-inhomogeneous SDE with standard assumptions. We then used this result to show that the Euler-Maruyama scheme also converges under assumptions suitable to our setting.

2.5 Application of Results to the SDE in the ETS Model

It now remains to verify that the assumptions of Theorems 2.15 and 2.26 hold in case of the SDE in our model. For the simple model variant presented in Section 2.1.1, we may do this rigorously; for the Brownian and Ornstein-Uhlenbeck model, this is not possible due to the lack of a closed-form expression of the drift term. Existence and uniqueness of the SDE solution then enable us to fully confirm the requirements of the verification theorem for the HJB equation.

Corollary 2.27. *The SDE of the simple model variant given by*

$$\mathrm{d}X_t = -u(t, X_t)\mathrm{d}t + \sigma \mathrm{d}W_t$$

with $u(t,x) = \frac{V_x(t,x)}{c}$ *and* V_x *as given in equation (2.5) has a unique strong solution which is continuous and adapted to the filtration* $\mathcal{F}$*.*

Proof. We need to verify the conditions of Assumption 2.14.

(i) Show boundedness: The volatility σ is constant and therefore clearly bounded. In Proposition 2.7 (ii), we have seen that V_x is bounded with $0 \leq V_x(t,x) \leq p$ for any t and x, which directly implies that the drift $-u$ is also bounded.

(ii) Show Lipschitz continuity on intervals of the form $[0, T-\varepsilon]$: The constant volatility σ is trivially Lipschitz continuous on $[0, T]$ and therefore in particular on any interval of the form $[0, T-\varepsilon]$. It remains to consider the drift term $-u$: Let $\varepsilon > 0$ be arbitrary. Then we know from Proposition 2.7 (iv) that V_{xx} is bounded on $[0, T-\varepsilon] \times \mathbb{R}$, which implies that V_x and therefore $-u$ is Lipschitz continuous in x on $[0, T-\varepsilon] \times \mathbb{R}$.

With Theorem 2.15 we then obtain the desired result. In particular, we also obtain that the solution X is adapted to the filtration $\mathcal{F}$: Theorem 2.15 delivers that X is adapted to $\mathcal{F}^{Z,W}$, where Z is the initial value of the process X. But since we have that $X_0 = x_0$ is a constant, it follows that $\mathcal{F}^{Z,W} = \mathcal{F}^W$. Furthermore, we defined $\mathcal{F}$ as the filtration generated by Brownian motion and augmented with the null sets. Therefore $\mathcal{F}_t^W \subseteq \mathcal{F}_t$ for any $t \in [0, T]$ and thus X is also adapted to $\mathcal{F}$. □

Corollary 2.28. *Let X be the solution of the SDE of the simple model variant. Then the Euler-Marayma scheme converges strongly to X.*

Proof. We have already shown boundedness and Lipschitz continuity in x on $[0, T-\varepsilon] \times \mathbb{R}$ in the preceding proof. Thus it only remains to show $\frac{1}{2}$-Hölder continuity in time on $[0, T-\varepsilon] \times \mathbb{R}$. For the constant volatility σ, this is again trivial. Furthermore, for $\varepsilon > 0$ arbitrary, we have with Proposition 2.7 (iv) that V_{xt} is bounded on $[0, T-\varepsilon] \times \mathbb{R}$. Therefore it follows that V_x is Lipschitz continuous in t on $[0, T-\varepsilon] \times \mathbb{R}$, which implies that this also holds for the drift $-u$. Since Lipschitz continuity implies Hölder continuity for $\alpha \in (0, 1]$, Theorem 2.26 then delivers the strong convergence of the Euler-Maruyama scheme. □

Corollary 2.29. *The function V as given by equation (2.4) delivers the minimum costs and the abatement rate $u_t = u(t, X_t)$ given by*

$$u(t, x) = \frac{V_x(t, x)}{c},$$

with V_x as given in equation (2.5), is optimal.

Proof. By Proposition 2.9 and by construction, we know that V satisfies the requirements of the verification theorem in Proposition 2.3 and solves the HJB equation when the control is given by u. With Corollary 2.27, we now have that the SDE

$$\mathrm{d}X_s = -u(s, X_s)\mathrm{d}s + G(s)\mathrm{d}W_s$$

has a unique solution for any given initial condition $X_t = x$. Furthermore, since the solution X is continuous and $\mathcal{F}$-adapted, we know that $u = (u(s, X_s))_{s \in [t,T]} \in \mathcal{A}(t)$ by Proposition 2.10. Thus we apply the verification theorem and obtain that V represents the minimum costs and u is an optimal control. □

For the Brownian and Ornstein-Uhlenbeck model variant we may verify the requirements of Theorems 2.15 and 2.26 only for the volatility.

Lemma 2.30. *The volatility functions of*

(i) the Brownian model variant given by $G_B(t) = \sigma(T - t)$ and

(ii) the Ornstein-Uhlenbeck model variant given by $G_{OU}(t) = \sigma \frac{1-\mathrm{e}^{\theta(t-T)}}{\theta}$

satisfy the requirements of Assumptions 2.14 and 2.25.

Proof. (i) On $[0, T]$, the function $G_{\mathrm{B}}(t) = \sigma(T - t)$ is bounded from above by σT and from below by 0. In addition, since it is constant in x, it is clearly Lipschitz continuous in x. Thus Assumption 2.14 is satisfied. Furthermore, the function is linear in t and therefore Lipschitz continuous in t (with constant σ), so Assumption 2.25 also holds.

(ii) We can see directly for $t \in [0, T]$ that

$$0 \leq \sigma \frac{1 - \mathrm{e}^{-\theta(T-t)}}{\theta} \leq \sigma \frac{1 - \mathrm{e}^{-\theta T}}{\theta}$$

and $G_{\mathrm{OU}}(t) = \sigma \frac{1-\mathrm{e}^{\theta(t-T)}}{\theta}$ is constant in x, thus Lipschitz continuous in x. Therefore Assumption 2.14 holds. We now compute the derivative $G'_{\mathrm{OU}}(t) = -\sigma \mathrm{e}^{-\theta(T-t)}$ and observe that this is also bounded on $[0, T]$, so G_{OU} is Lipschitz continuous in t on $[0, T]$ and Assumption 2.25 is thus satisfied. □

Remark 2.31. As mentioned above, we cannot provide any rigorous arguments to show that the drift term in the Brownian and Ornstein-Uhlenbeck model variant satisfies the assumptions of the theorems in the preceding sections. We may only study the numerical PDE solution, which is presented in Section 6.1.1.

Summary

This section assures that the simple variant of our ETS model has a solution as desired: By using the theorems of the previous section and the properties of the PDE solution, we showed that the SDE has a unique solution and that the Euler-Maruyama scheme converges to this solution. Moreover, we showed that the PDE solution indeed delivers the minimum costs and the optimal abatement rate. Such an extensive theoretical result could not be obtained for the Brownian and Ornstein-Uhlenbeck model variant.

Chapter 3

Multi-Period Model

In the one-period model of Chapter 2, we implicitly assumed that all allowances which are not needed to account for emissions become invalid at the end of the respective time period. However, already since 2008 it is possible in the EU ETS to exchange such allowances for valid ones; by now, the allowances do not expire anymore. Hence they can freely be transferred to later time periods, i.e. unrestricted banking is possible. Banking – and partly also borrowing – of allowances was studied already in early models for instance by Rubin [Rub96] or Schennach [Sch00]. Also the models of Kollenberg and Taschini in [KT16] and [KT19] allow for banking; here the bank of allowances plays a major role in the model formulation. Liang and Huang [LH20]/[LH22] provide an extension to the approach of Seifert et al. that combines banking and borrowing with the auctioning of allowances. In order to incorporate the transfer of allowances to the subsequent time period in an ETS model, we need to determine the value of an unused allowance at the end of the time period. Since such an allowance can be used or sold in the next time period, its value is given by its price at the beginning of the next period. Liang and Huang essentially assume that this price is exogeneously given; in contrast, our strategy is to model several subsequent time periods to be able to compute this price from the results of later time periods.

There are two different approaches to proceed: On the one hand, we may assume that the price of an allowance in the next period enters the optimization procedure as an exogenous parameter, which remains unchanged during the time period considered. This allows for a rather simple extension of the previous model, which will be explored in Section 3.1. In the following we will refer to this model as multi-period model I. The price of an allowance at the beginning of the next time period can be determined from the initial value of the total expected emissions X_0^i of that time period. As we will see below, this value depends on the development of the emission rate, which we may observe in the course of the time period. Therefore, it is more realistic that the price of an allowance we anticipate for the next period changes as we proceed in time in the current time period. To capture this effect, a second approach introducing an additional dimension to the value function is presented in Section 3.2; we will refer to this model by multi-period model II.

3.1 Multi-Period Model with Constant Price Parameter

In this section, we assume that the allowance price that we expect in period i for the beginning of the next time period is given by the constant parameter s^i. We will elaborate

on how to determine this parameter in Section 3.1.5. To construct the model, we will proceed similarly as we did for the one-period model in Chapter 2; this model will be referred to as multi-period model I.

3.1.1 Derivation of the SDE

We consider a time interval $[0, T]$ partitioned into $0 = T_0 < T_1 < \ldots < T_i < \ldots < T_N = T$, i.e. we split the interval into N smaller time periods $0, 1, \ldots, N-1$. We assume that the emission rate develops continuously over the whole time horizon $[0, T]$, whereas the representative agent only takes into account the sub-period for her cost minimization problem.

As before, let $(Y_t)_{t\in[0,T]}$ denote the emission rate and assume that the dynamics are given as

$$\mathrm{d}Y_t = \mu(t, Y_t)\mathrm{d}t + \sigma(t, Y_t)\mathrm{d}W_t,$$

where again μ and σ are real-valued functions and W is a Brownian motion. We now introduce the total expected emissions X by defining it piecewise on each time period $(T_i, T_{i+1}]$.

Definition 3.1. The total expected emissions for the time period $[0, T]$ are given by the process $X = (X_t)_{t\in[0,T]}$ defined as

$$\begin{aligned} X_0 &= \mathrm{E}\left[\int_0^{T_1} Y_s \mathrm{d}s\right] \qquad \text{and} \\ X_t &= -\int_{T_i}^{t} u_s \mathrm{d}s + \mathrm{E}\left[\int_{T_i}^{T_{i+1}} Y_s \mathrm{d}s \,\middle|\, \mathcal{F}_t\right] \qquad \text{for } t \in (T_i, T_{i+1}]. \end{aligned}$$

Note that X is not continuous in T_i for any i. As in the one-period model we now rewrite the process X as an SDE; however, we have to specify the SDEs separately for each time period $(T_i, T_{i+1}]$. As a result, we obtain an SDE of the form

$$\mathrm{d}X_t^i = -u_t^i \mathrm{d}t + G^i(t)\mathrm{d}W_t^i,$$

where we define the processes X^i, u^i and W^i by shifting the original processes as will be detailed further below for each of the model variants.

Brownian Model Variant

In the Brownian model variant we have that μ and σ are constant, therefore we can rewrite Y_t as

$$Y_t = y_0 + \mu t + \sigma W_t.$$

We consider $t \in (T_i, T_{i+1}]$ and define $\Delta T_i \coloneqq T_{i+1} - T_i$. In accordance with Definition 3.1, we need to compute

$$\begin{aligned}
\mathrm{E}\left[\int_{T_i}^{T_{i+1}} Y_s \mathrm{d}s \,\middle|\, \mathcal{F}_t\right] &= \int_{T_i}^{T_{i+1}} (y_0 + \mu s)\,\mathrm{d}s + \mathrm{E}\left[\int_{T_i}^{T_{i+1}} \sigma W_s \mathrm{d}s \,\middle|\, \mathcal{F}_t\right] \\
&= y_0\,(T_{i+1} - T_i) + \frac{T_{i+1}^2 - T_i^2}{2}\,\mu + \sigma\,\mathrm{E}\left[\int_0^{T_{i+1}} W_s \mathrm{d}s - \int_0^{T_i} W_s \mathrm{d}s \,\middle|\, \mathcal{F}_t\right] \\
&= y_0\,\Delta T_i + \frac{T_{i+1}^2 - T_i^2}{2}\,\mu \\
&\quad + \sigma\,\mathrm{E}\left[W_{T_{i+1}}\,T_{i+1} - \int_0^{T_{i+1}} s \mathrm{d}W_s - W_{T_i}\,T_i + \int_0^{T_i} s \mathrm{d}W_s \,\middle|\, \mathcal{F}_t\right] \\
&= y_0\,\Delta T_i + \frac{T_{i+1}^2 - T_i^2}{2}\,\mu + \sigma\,T_{i+1}\,\mathrm{E}\left[W_{T_{i+1}} \,\middle|\, \mathcal{F}_t\right] - \sigma\,T_i\,\mathrm{E}\left[W_{T_i} \,\middle|\, \mathcal{F}_t\right] \\
&\quad - \sigma\,\mathrm{E}\left[\int_0^{T_{i+1}} s \mathrm{d}W_s \,\middle|\, \mathcal{F}_t\right] + \sigma\,\mathrm{E}\left[\int_0^{T_i} s \mathrm{d}W_s \,\middle|\, \mathcal{F}_t\right],
\end{aligned}$$

where we have applied the product rule to both integrals. We then use the martingale property and adaptedness of Brownian motion and the stochastic integral:

$$\begin{aligned}
\mathrm{E}\left[\int_{T_i}^{T_{i+1}} Y_s \mathrm{d}s \,\middle|\, \mathcal{F}_t\right] &= y_0\,\Delta T_i + \frac{T_{i+1}^2 - T_i^2}{2}\,\mu + \sigma\,T_{i+1}\,W_t - \sigma\,T_i\,W_{T_i} \\
&\quad - \sigma\int_0^t s \mathrm{d}W_s + \sigma\int_0^{T_i} s \mathrm{d}W_s + \sigma\,T_{i+1}\,W_{T_i} - \sigma\,T_{i+1}\,W_{T_i} \\
&= y_0\,\Delta T_i + \frac{T_{i+1}^2 - T_i^2}{2}\,\mu + \sigma\int_0^t T_{i+1} \mathrm{d}W_s - \sigma\int_0^{T_i} T_{i+1} \mathrm{d}W_s \\
&\quad + \sigma\,\Delta T_i\,W_{T_i} - \sigma\int_{T_i}^t s \mathrm{d}W_s \\
&= y_0\,\Delta T_i + \frac{T_{i+1}^2 - T_i^2}{2}\,\mu + \sigma\,\Delta T_i\,W_{T_i} + \sigma\int_{T_i}^t (T_{i+1} - s) \mathrm{d}W_s.
\end{aligned}$$

By setting $t = T_i$, we obtain the right-sided limit, i.e. the limit of X for $t \downarrow T_i$, as

$$X_{T_i}^+ = \mathrm{E}\left[\int_{T_i}^{T_{i+1}} Y_s \mathrm{d}s \,\middle|\, \mathcal{F}_{T_i}\right] = y_0\,\Delta T_i + \frac{T_{i+1}^2 - T_i^2}{2}\,\mu + \sigma\,\Delta T_i\,W_{T_i} = x_0^i + \sigma\,\Delta T_i\,W_{T_i},$$

where $x_0^i \coloneqq y_0\,\Delta T_i + \frac{T_{i+1}^2 - T_i^2}{2}\,\mu$ similar to the definition of x_0 in the one-period model. If the partition of $[0, T]$ is equidistant, i.e. if $\Delta T_i = \Delta T_j$ for any i and j, we set $\Delta T = \Delta T_i$ and with $T_i = i\,\Delta T$ rewrite

$$\begin{aligned}
x_0^i &= y_0\,\Delta T + \frac{(T_{i+1} - T_i)\,(T_{i+1} + T_i)}{2}\,\mu = y_0\,\Delta T + \frac{\Delta T\,((i+1)\,\Delta T + i\,\Delta T)}{2}\,\mu \\
&= y_0\,\Delta T + \frac{1}{2}\,\Delta T^2\,\mu + i\,\Delta T^2\,\mu = x_0^0 + i\,\Delta T^2\,\mu.
\end{aligned}$$

Returning to the more general case, we use the result for $X_{T_i}^+$ to write

$$X_t = X_{T_i}^+ - \int_{T_i}^t u_s \mathrm{d}s + \sigma\int_{T_i}^t (T_{i+1} - s) \mathrm{d}W_s.$$

Hence we have an expression for X_t, where t is a time point on $[0, T]$. In order to rewrite this in differential form and also to be able to perform the optimization on the smaller time period, we will now transform our expression for X_t to the sub-period $(T_i, T_{i+1}]$.

To that end, we define $\hat{t} = t - T_i$ as the time relative to the corresponding sub-period $(T_i, T_{i+1}]$. For $\hat{t} \in (0, \Delta T_i]$, we define $u^i_{\hat{t}} = u_{T_i+\hat{t}}$, $X^i_{\hat{t}} = X_{T_i+\hat{t}}$ and $W^i_{\hat{t}} = W_{T_i+\hat{t}}$. Furthermore, we set $X^i_0 = X^+_{T_i}$ and $W^i_0 = W_{T_i}$. By substituting $\hat{s} = s - T_i$, we obtain

$$\begin{aligned} X^i_{\hat{t}} &= X^i_0 - \int_0^{\hat{t}} u_{T_i+\hat{s}}\, \mathrm{d}\hat{s} + \sigma \int_0^{\hat{t}} (T_{i+1} - T_i - \hat{s}) \mathrm{d}W_{T_i+\hat{s}} \\ &= X^i_0 - \int_0^{\hat{t}} u^i_{\hat{s}} \mathrm{d}\hat{s} + \sigma \int_0^{\hat{t}} (\Delta T_i - \hat{s}) \mathrm{d}W^i_{\hat{s}}. \end{aligned}$$

We rewrite this in differential form as

$$\mathrm{d}X^i_{\hat{t}} = -u^i_{\hat{t}} \mathrm{d}\hat{t} + \sigma(\Delta T_i - \hat{t}) \mathrm{d}W^i_{\hat{t}}$$

with $X^i_0 = x^i_0 + \sigma\, \Delta T_i\, W_{T_i}$.

Ornstein-Uhlenbeck Model Variant

Here we have that the emission rate Y is modeled by

$$\mathrm{d}Y_t = \theta\,(\mu - Y_t) + \sigma \mathrm{d}W_t.$$

As in Section 2.1.3, we rewrite this as

$$Y_t = y_0\, \mathrm{e}^{-\theta t} + \mu\, \left(1 - \mathrm{e}^{-\theta t}\right) + \sigma \int_0^t \mathrm{e}^{-\theta(t-s)} \mathrm{d}W_s.$$

We now proceed as we did for the Brownian model. We consider $t \in (T_i, T_{i+1}]$ and recall the definition $\Delta T_i \coloneqq T_{i+1} - T_i$. In order to obtain the total expected emissions as defined by Definition 3.1, we aim to compute

$$\begin{aligned} \mathrm{E}\left[\int_{T_i}^{T_{i+1}} Y_s \mathrm{d}s \,\middle|\, \mathcal{F}_t\right] &= \int_{T_i}^{T_{i+1}} \left[y_0\, \mathrm{e}^{-\theta v} + \mu\, \left(1 - \mathrm{e}^{-\theta v}\right)\right] \mathrm{d}v \\ &\quad + \mathrm{E}\left[\int_{T_i}^{T_{i+1}} \int_0^v \mathrm{e}^{-\theta(v-s)} \mathrm{d}W_s \mathrm{d}v \,\middle|\, \mathcal{F}_t\right]. \end{aligned}$$

We directly compute the integral in the first term to result in

$$\begin{aligned} \int_{T_i}^{T_{i+1}} \left[y_0\, \mathrm{e}^{-\theta v} + \mu\, \left(1 - \mathrm{e}^{-\theta v}\right)\right] \mathrm{d}v &= \left[-\frac{y_0}{\theta}\, \mathrm{e}^{-\theta v} + \mu\, \left(v + \frac{1}{\theta}\, \mathrm{e}^{-\theta v}\right)\right]_{T_i}^{T_{i+1}} \\ &= \frac{1}{\theta}\, (\mu - y_0) \left(\mathrm{e}^{-\theta T_{i+1}} - \mathrm{e}^{-\theta T_i}\right) + \mu\, (T_{i+1} - T_i) \\ &= \frac{1}{\theta}\, (\mu - y_0) \left(\mathrm{e}^{-\theta T_{i+1}} - \mathrm{e}^{-\theta T_i}\right) + \mu\, \Delta T_i. \end{aligned} \tag{3.1}$$

For the second term, we again define $Z_v = \int_0^v \mathrm{e}^{\theta s} \mathrm{d}W_s$ and $\tilde{Z}_v = \mathrm{e}^{-\theta v}$. With our computations in Section 2.1.3, we then know that

$$\begin{aligned} \int_0^{T_{i+1}} Z_v \mathrm{d}\tilde{Z}_v - \int_0^{T_i} Z_v \mathrm{d}\tilde{Z}_v &= -\theta \int_0^{T_{i+1}} \int_0^v \mathrm{e}^{-\theta(v-s)} \mathrm{d}W_s \mathrm{d}v + \theta \int_0^{T_i} \int_0^v \mathrm{e}^{-\theta(v-s)} \mathrm{d}W_s \mathrm{d}v \\ &= -\theta \int_{T_i}^{T_{i+1}} \int_0^v \mathrm{e}^{-\theta(v-s)} \mathrm{d}W_s \mathrm{d}v \end{aligned}$$

and again with results from Section 2.1.3, we have

$$\begin{aligned}\int_{T_i}^{T_{i+1}} \int_0^v \mathrm{e}^{-\theta(v-s)} \mathrm{d}W_s \mathrm{d}v &= -\frac{1}{\theta}\left(\int_0^{T_{i+1}} Z_v \mathrm{d}\tilde{Z}_v - \int_0^{T_i} Z_v \mathrm{d}\tilde{Z}_v\right) \\ &= -\frac{1}{\theta}\left(\mathrm{e}^{-\theta T_{i+1}} \int_0^{T_{i+1}} \mathrm{e}^{\theta s} \mathrm{d}W_s - \int_0^{T_{i+1}} \mathrm{d}W_s \right. \\ &\quad \left. - \mathrm{e}^{-\theta T_i} \int_0^{T_i} \mathrm{e}^{\theta s} \mathrm{d}W_s + \int_0^{T_i} \mathrm{d}W_s\right).\end{aligned}$$

Now we compute

$$\begin{aligned}&\mathrm{E}\left[\int_{T_i}^{T_{i+1}} \int_0^v \mathrm{e}^{-\theta(v-s)} \mathrm{d}W_s \,\middle|\, \mathcal{F}_t\right] \\ &= \mathrm{E}\left[-\frac{1}{\theta}\left(\mathrm{e}^{-\theta T_{i+1}} \int_0^{T_{i+1}} \mathrm{e}^{\theta s} \mathrm{d}W_s - \int_0^{T_{i+1}} \mathrm{d}W_s - \mathrm{e}^{-\theta T_i} \int_0^{T_i} \mathrm{e}^{\theta s} \mathrm{d}W_s + \int_0^{T_i} \mathrm{d}W_s\right) \,\middle|\, \mathcal{F}_t\right] \\ &= -\frac{1}{\theta}\left(\mathrm{e}^{-\theta T_{i+1}} \mathrm{E}\left[\int_0^{T_{i+1}} \mathrm{e}^{\theta s} \mathrm{d}W_s \,\middle|\, \mathcal{F}_t\right] - \mathrm{E}\left[\int_0^{T_{i+1}} \mathrm{d}W_s \,\middle|\, \mathcal{F}_t\right]\right. \\ &\quad \left. - \mathrm{e}^{-\theta T_i} \mathrm{E}\left[\int_0^{T_i} \mathrm{e}^{\theta s} \mathrm{d}W_s \,\middle|\, \mathcal{F}_t\right] + \mathrm{E}\left[\int_0^{T_i} \mathrm{d}W_s \,\middle|\, \mathcal{F}_t\right]\right).\end{aligned}$$

We make use of the martingale property of the stochastic integral and the measurability with respect to $\mathcal{F}_t$ and add zero to obtain

$$\begin{aligned}&\mathrm{E}\left[\int_{T_i}^{T_{i+1}} \int_0^v \mathrm{e}^{-\theta(v-s)} \mathrm{d}W_s \,\middle|\, \mathcal{F}_t\right] \\ &= -\frac{1}{\theta}\left(\mathrm{e}^{-\theta T_{i+1}} \int_0^t \mathrm{e}^{\theta s} \mathrm{d}W_s - \int_0^t \mathrm{d}W_s - \mathrm{e}^{-\theta T_i} \int_0^{T_i} \mathrm{e}^{\theta s} \mathrm{d}W_s + \int_0^{T_i} \mathrm{d}W_s\right) \\ &= -\frac{1}{\theta}\left(\mathrm{e}^{-\theta T_{i+1}} \int_0^t \mathrm{e}^{\theta s} \mathrm{d}W_s - \mathrm{e}^{-\theta T_{i+1}} \int_0^{T_i} \mathrm{e}^{\theta s} \mathrm{d}W_s + \mathrm{e}^{-\theta T_{i+1}} \int_0^{T_i} \mathrm{e}^{\theta s} \mathrm{d}W_s\right. \\ &\quad \left. - \mathrm{e}^{-\theta T_i} \int_0^{T_i} \mathrm{e}^{\theta s} \mathrm{d}W_s - \int_{T_i}^t \mathrm{d}W_s\right) \\ &= -\frac{1}{\theta}\left(\mathrm{e}^{-\theta T_{i+1}} \int_{T_i}^t \mathrm{e}^{\theta s} \mathrm{d}W_s - \int_{T_i}^t \mathrm{d}W_s + \left(\mathrm{e}^{-\theta T_{i+1}} - \mathrm{e}^{-\theta T_i}\right) \int_0^{T_i} \mathrm{e}^{\theta s} \mathrm{d}W_s\right) \\ &= \int_{T_i}^t \frac{1 - \mathrm{e}^{-\theta(T_{i+1}-s)}}{\theta} \mathrm{d}W_s - \frac{\mathrm{e}^{-\theta T_{i+1}} - \mathrm{e}^{-\theta T_i}}{\theta} \int_0^{T_i} \mathrm{e}^{\theta s} \mathrm{d}W_s. \qquad (3.2)\end{aligned}$$

Next we aim to determine the right-sided limit $X_{T_i}^+$ of X on the interval $(T_i, T_{i+1}]$. By the definition of the total expected emissions, i.e. Definition 3.1, we insert $t = T_i$ in the previous computations of equations (3.1), (3.2) and obtain

$$\begin{aligned}X_{T_i}^+ &= \mathrm{E}\left[\int_{T_i}^{T_{i+1}} Y_s \mathrm{d}s \,\middle|\, \mathcal{F}_{T_i}\right] \\ &= \frac{1}{\theta}\left(\mu - y_0\right)\left(\mathrm{e}^{-\theta T_{i+1}} - \mathrm{e}^{-\theta T_i}\right) + \mu\,\Delta T_i - \sigma \frac{\mathrm{e}^{-\theta T_{i+1}} - \mathrm{e}^{-\theta T_i}}{\theta} \int_0^{T_i} \mathrm{e}^{\theta s} \mathrm{d}W_s \\ &= x_0^i - \sigma \frac{\mathrm{e}^{-\theta T_{i+1}} - \mathrm{e}^{-\theta T_i}}{\theta} \int_0^{T_i} \mathrm{e}^{\theta s} \mathrm{d}W_s,\end{aligned}$$

where we have collected all constants by defining

$$x_0^i \coloneqq \frac{1}{\theta}\,(\mu - y_0)\left(\mathrm{e}^{-\theta T_{i+1}} - \mathrm{e}^{-\theta T_i}\right) + \mu\,\Delta T_i.$$

If we have an equidistant partition, i.e. with $\Delta T_i = \Delta T$ for all i, then $T_i = i\,\Delta T$ and with

$$x_0^0 = \frac{1}{\theta}\,(\mu - y_0)\left(\mathrm{e}^{-\theta \Delta T} - 1\right) + \mu\,\Delta T$$

we rewrite

$$\begin{aligned} x_0^i &= \frac{1}{\theta}\,(\mu - y_0)\left(\mathrm{e}^{-\theta (i+1)\Delta T} - \mathrm{e}^{-\theta i \Delta T}\right) + \mu\,\Delta T \\ &= \mathrm{e}^{-\theta i \Delta T}\left(x_0^0 - \mu\,\Delta T\right) + \mu\,\Delta T = \mathrm{e}^{-\theta i \Delta T}\,x_0^0 + \left(1 - \mathrm{e}^{-\theta i \Delta T}\right)\mu\,\Delta T. \end{aligned}$$

Furthermore, for an equidistant partition, we have

$$X_{T_i}^+ = x_0^i - \sigma\,\mathrm{e}^{-\theta i \Delta T}\,\frac{\mathrm{e}^{-\theta \Delta T} - 1}{\theta}\int_0^{T_i} \mathrm{e}^{\theta s}\mathrm{d}W_s.$$

We return to the more general case. For the total expected emissions, we combine the results in equations (3.1) and (3.2) and arrive at the integral equation

$$\begin{aligned} X_t &= -\int_{T_i}^t u_s \mathrm{d}s + x_0^i - \sigma\,\frac{\mathrm{e}^{-\theta T_{i+1}} - \mathrm{e}^{-\theta T_i}}{\theta}\int_0^{T_i} \mathrm{e}^{\theta s}\mathrm{d}W_s + \sigma\int_{T_i}^t \frac{1 - \mathrm{e}^{-\theta(T_{i+1} - s)}}{\theta}\,\mathrm{d}W_s \\ &= X_{T_i}^+ - \int_{T_i}^t u_s \mathrm{d}s + \sigma\int_{T_i}^t \frac{1 - \mathrm{e}^{-\theta(T_{i+1} - s)}}{\theta}\,\mathrm{d}W_s. \end{aligned}$$

As for the Brownian model, we now perform a shift in time. We again define $\hat{t} = t - T_i$ to obtain time relative to the sub-period $(T_i, T_{i+1}]$. Further, for $\hat{t} \in (0, \Delta T_i]$ we define as above $u_{\hat{t}}^i = u_{T_i + \hat{t}}$, $X_{\hat{t}}^i = X_{T_i+\hat{t}}$ and $W_{\hat{t}}^i = W_{T_i+\hat{t}}$, additionally we set $X_0^i = X_{T_i}^+$ and $W_0^i = W_{T_i}$. Again we substitute $\hat{s} = s - T_i$, which gives us

$$\begin{aligned} X_{\hat{t}}^i &= X_0^i - \int_0^{\hat{t}} u_{T_i+\hat{s}}\mathrm{d}\hat{s} + \sigma\int_0^{\hat{t}} \frac{1 - \mathrm{e}^{-\theta(T_{i+1} - \hat{s} - T_i)}}{\theta}\,\mathrm{d}W_{T_i+\hat{s}} \\ &= X_0^i - \int_0^{\hat{t}} u_{\hat{s}}^i \mathrm{d}\hat{s} + \sigma\int_0^{\hat{t}} \frac{1 - \mathrm{e}^{-\theta(\Delta T_i - \hat{s})}}{\theta}\,\mathrm{d}W_{\hat{s}}^i. \end{aligned}$$

We may rewrite this in differential form and arrive at the desired SDE

$$\mathrm{d}X_{\hat{t}}^i = -u_{\hat{t}}^i \mathrm{d}\hat{t} + \sigma\,\frac{1 - \mathrm{e}^{-\theta(\Delta T_i - \hat{t})}}{\theta}\,\mathrm{d}W_{\hat{t}}^i,$$

where we have

$$X_0^i = x_0^i - \sigma\,\frac{\mathrm{e}^{-\theta T_{i+1}} - \mathrm{e}^{-\theta T_i}}{\theta}\int_0^{T_i} \mathrm{e}^{\theta s}\mathrm{d}W_s.$$

Simple Model Variant

In the simple model variant, we do not have an explicit understanding of the emission rate Y itself. Therefore, in the one-period model, we modeled the total expected emissions directly as

$$X_t = x_0 - \int_0^t u_s \mathrm{d}s + \sigma \int_0^t \mathrm{d}W_s,$$

which translates to

$$X_t = X_{T_i}^+ - \int_{T_i}^t u_s \mathrm{d}s + \sigma \int_{T_i}^t \mathrm{d}W_s$$

in the multi-period model. We define $\hat{t} = t - T_i$ and $u_{\hat{t}}^i$, $X_{\hat{t}}^i$ and $W_{\hat{t}}^i$ as for the previous model variants and apply the substitution $\hat{s} = s - T_i$ to result in

$$X_{\hat{t}}^i = X_0^i - \int_0^{\hat{t}} u_{\hat{s}}^i \mathrm{d}\hat{s} + \sigma \int_0^{\hat{t}} \mathrm{d}W_{\hat{s}}^i.$$

In this case, we cannot compute the right-sided limit $X_{T_i}^+ = X_0^i$. Therefore, we define $X_{T_i}^+ = X_0^i = x_0^i + \sigma W_{T_i}$ for $x_0^i \in \mathbb{R}$, which is consistent with the one-period model. Note that we now may freely assign a value to x_0^i for all i; it cannot be computed from other parameters as in the Brownian or Ornstein-Uhlenbeck model. In differential form, we then have

$$\mathrm{d}X_{\hat{t}}^i = -u_{\hat{t}}^i \mathrm{d}\hat{t} + \sigma \mathrm{d}W_{\hat{t}}^i.$$

Summary

In this section, we defined the total expected emissions X in a multi-period setting. For each of the model variants, we derived an SDE to describe the total expected emissions X^i in every time period i.

3.1.2 Cost Minimization

The next step is to solve the cost minimization problem of the representative agent. We consider this optimization separately for each time period. Let s^i be the price parameter in the i-th time period. This parameter represents the price of an allowance at the beginning of the next time period; we assume that it is exogenous to the optimization, so we will assume that this parameter is given. Note that we cannot compute the actual allowance price of the next time period as we will explain in Section 3.1.5.

The key idea to incorporate the value of an unused allowance at the end of the time period is now to modify the penalty function as follows:

$$P^i\left(X_{T_{i+1}}\right) = \begin{cases} \left(p + s^i\right)\left(X_{T_{i+1}} - e_0^i\right) & \text{if} \quad X_{T_{i+1}} > e_0^i, \\ s^i\left(X_{T_{i+1}} - e_0^i\right) & \text{else.} \end{cases}$$

Here the second case reflects that any surplus allowances have value s^i at the end of the current time period. In the first case we incorporate the following mechanism of the EU ETS: In addition to a penalty payment, emissions exceeding the number of allowances also have to be balanced out by the corresponding number of allowances in the next time period. Hence each additional ton of emissions incurs costs of $p + s^i$. Furthermore, we allow the cap e_0^i to change for each time period.

As before, we assume the cost of abatement to be given as

$$C^i(u) = \frac{1}{2}\, c^i\, u^2,$$

where the control takes on values in $\mathcal{U} = [0, \infty)$; the cost coefficient c^i may differ for different time periods. Similarly to before, we define the admissibility set for $t \in [T_i, T_{i+1}]$ as

$$\mathcal{A}_1^i(t) = \Bigg\{ u = (u_s)_{s\in[t,T_{i+1}]} \text{ an } \mathcal{F}\text{-progressively measurable process into } \mathcal{U} \\ \text{with } \mathrm{E}\left[\int_t^{T_{i+1}} |u_s|^2 \mathrm{d}s\right] < \infty \Bigg\}.$$

Now we derive the HJB equation based on the dynamics of X^i as obtained in the previous section. We define the value function for the i-th time period as

$$V^i(t,x) = \inf_{u\in\mathcal{A}_1^i(t)} \mathrm{E}^{t,x}\left[\mathrm{e}^{-rT_{i+1}}\, P^i\left(X_{T_{i+1}}\right) + \int_t^{T_{i+1}} C^i\left(u_s\right)\mathrm{e}^{-rs}\mathrm{d}s\right].$$

In order to apply the SDE describing X^i, we need to shift time again, i.e. we consider the time $\hat{t} = t - T_i$ relative to the current time period i. In analogy to the shifted processes defined above, we introduce the shifted filtration $\mathcal{F}^i$ as

$$\mathcal{F}_{\hat{t}}^i = \mathcal{F}_{T_i+\hat{t}}.$$

For any $\hat{t} \in [0, \Delta T_i]$, we define the admissibility set of the shifted control u^i as

$$\mathcal{A}^i(\hat{t}) = \Bigg\{ u^i = \left(u_s^i\right)_{s\in[\hat{t},\Delta T_i]} \text{ an } \mathcal{F}^i\text{-progressively measurable process into } \mathcal{U} \\ \text{with } \mathrm{E}\left[\int_{\hat{t}}^{\Delta T_i} |u_s^i|^2 \mathrm{d}s\right] < \infty \Bigg\}.$$

Note that we have $(u_s)_{s\in[t,T_{i+1}]} \in \mathcal{A}_1^i(t)$ if and only if $u^i = \left(u_{\hat{s}}^i\right)_{\hat{s}\in[\hat{t},\Delta T_i]} \in \mathcal{A}^i(\hat{t})$ by definition of u^i. Then we apply the substitution $\hat{s} = s - T_i$ to the value function, delivering

$$V^i(\hat{t},x) = \inf_{u^i\in\mathcal{A}^i(\hat{t})} \mathrm{E}^{t,x}\left[\mathrm{e}^{-rT_{i+1}}\, P^i\left(X_{\Delta T_i}^i\right) + \int_{\hat{t}}^{\Delta T_i} C^i\left(u_{\hat{s}}^i\right)\mathrm{e}^{-r(T_i+\hat{s})}\mathrm{d}\hat{s}\right].$$

We motivate the HJB equation by applying the Bellman principle; for ease of notation we again write s and t instead of $\hat{s}$ and $\hat{t}$. Then for $\tau \in \mathbb{R}$ with $\tau > t$ we have

$$V^i(t,x) = \inf_{u^i\in\mathcal{A}^i(t)} \mathrm{E}^{t,x}\left[\int_t^{\tau} C^i\left(u_s^i\right)\mathrm{e}^{-r(T_i+s)}\mathrm{d}s + V^i\left(\tau, X_\tau^i\right)\right].$$

We apply the Itô-formula and use that $\mathrm{d}X_t^i = -u_t^i\mathrm{d}t + G^i(t)\mathrm{d}W_t^i$; we note that since $W_0^i = W_{T_i} \neq 0$, the process W^i is not a Brownian motion according to the usual definition. However, we can still show for the quadratic covariation that $[W^i]_t = t$ and therefore

$[X^i]_t = \int_0^t G^i(s)^2 \mathrm{d}s$ as before (see Section A.4.1 in the appendix), so we have

$$\begin{aligned} V^i(t,x) &= \inf_{u^i \in \mathcal{A}^i(t)} \mathrm{E}^{t,x} \left[\int_t^\tau C^i\left(u_s^i\right) \mathrm{e}^{-r(T_i+s)} \mathrm{d}s + V^i\left(t, X_t^i\right) + \int_t^\tau V_t^i\left(x, X_s^i\right) \mathrm{d}s \right. \\ &\quad \left. - \int_t^\tau u_s^i V_x^i\left(s, X_s^i\right) \mathrm{d}s + \int_t^\tau G^i(s) V_x^i(s, X_s) \mathrm{d}W_s^i + \frac{1}{2} \int_t^\tau G^i(s)^2 \, V_{xx}^i\left(s, X_s^i\right) \mathrm{d}s \right] \\ &= \inf_{u^i \in \mathcal{A}^i(t)} \mathrm{E}^{t,x} \left[\int_t^\tau C^i\left(u_s^i\right) \mathrm{e}^{-r(T_i+s)} \mathrm{d}s + V^i\left(t, X_t^i\right) \right. \\ &\quad \left. + \int_t^\tau \left(V_t^i\left(s, X_s^i\right) - u_s^i \, V_x^i\left(s, X_s^i\right) + \frac{1}{2} \, G^i(s)^2 \, V_{xx}^i\left(s, X_s^i\right) \right) \mathrm{d}s \right], \end{aligned}$$

by assuming that the integral of $G^i(s)\, V_x^i(s, X_s)$ with respect to W^i exists and is a martingale. We then subtract $V^i(t, X_t^i)$, divide by $\tau - t$ and let $\tau \to t$ to obtain

$$\begin{aligned} 0 &= \inf_{u^i \in \mathcal{A}^i(t)} \mathrm{E}^{t,x} \left[\lim_{\tau \downarrow t} \frac{1}{\tau - t} \int_t^\tau \left(C^i\left(u_s^i\right) \mathrm{e}^{-r(T_i+s)} \mathrm{d}s \right. \right. \\ &\quad \left. \left. + \; V_t^i\left(s, X_s^i\right) - u_s^i \, V_x^i\left(s, X_s^i\right) + \frac{1}{2} \, G^i(s)^2 \, V_{xx}^i\left(s, X_s^i\right) \right) \mathrm{d}s \right] \\ &= \inf_{u^i \in \mathcal{A}^i(t)} \mathrm{E}^{t,x} \left[C^i\left(u_t^i\right) \mathrm{e}^{-r(T_i+t)} + V_t^i\left(t, X_t^i\right) - u_t^i \, V_x^i\left(t, X_t^i\right) + \frac{1}{2} \, G^i(s)^2 \, V_{xx}^i\left(t, X_t^i\right) \right]. \end{aligned}$$

By setting $X_t^i = x$ and omitting the conditional expectation, we arrive at the HJB equation

$$0 = \inf_{u^i \in \mathcal{U}} \left\{ C^i(u^i) \, \mathrm{e}^{-r(T_i+t)} + V_t^i(t,x) - u^i \, V_x^i(t,x) + \frac{1}{2} \, G^i(t)^2 \, V_{xx}^i(t,x) \right\}.$$

Minimization with respect to u^i yields

$$u^i(t,x) = \frac{V_x^i(t,x)}{c^i} \, \mathrm{e}^{r(T_i+t)}$$

and we obtain the characteristic PDE as

$$V_t^i = \frac{1}{2} \, \frac{\left(V_x^i(t,x)\right)^2}{c^i} \mathrm{e}^{r(T_i+t)} - \frac{1}{2} \, G^i(t)^2 \, V_{xx}^i(t,x)$$

with final condition

$$V^i(\Delta T_i, x) = \mathrm{e}^{-rT_{i+1}} P^i(x).$$

Recall that $G^i(t)$ is given by the following functions for the different model variants:

- Simple model: $G^i(t) = \sigma$
- Brownian model: $G^i(t) = \sigma(\Delta T_i - t)$
- Ornstein-Uhlenbeck model: $G^i(t) = \sigma \, \frac{1 - \mathrm{e}^{-\theta(\Delta T_i - t)}}{\theta}$.

Summary

This section discussed the cost minimization problem of the agent in a multi-period setting: We defined the value function and formulated the corresponding HJB equation, from which we derived the characteristic PDE.

3.1.3 Solution of the PDE

In this section, we aim to solve the characteristic PDE in order to obtain a solution for the value function and thus for the abatement rate u^i; for notational convenience, we assume that both c^i and e_0^i do not depend on the corresponding time period and therefore write c and e_0 instead. Again we may find an analytical solution in a special case of the simple model variant. We will study its properties and show that it satisfies the requirements of the verification theorem of the HJB equation. For the Brownian and Ornstein-Uhlenbeck model variants, we need to solve the PDE numerically.

Analytical Solution in the Simple Model

We take the PDE derived in the previous section and as for the one-period model, we perform a time reversion. We substitute $t = \Delta T_i - \tilde{t}$ and define $\tilde{V}^i(\tilde{t}, x) = V^i(\Delta T_i - \tilde{t}, x)$. Then

$$V_t^i(t,x) = V_t^i(\Delta T_i - \tilde{t}, x) = -V_{\tilde{t}}^i(\Delta T_i - \tilde{t}, x) = -\tilde{V}_{\tilde{t}}^i(\tilde{t}, x)$$

and we obtain

$$\tilde{V}_{\tilde{t}}^i = -\frac{\left(\tilde{V}_x^i\right)^2}{2c}\,\mathrm{e}^{r(T_{i+1}-\tilde{t})} + \frac{1}{2}\,\sigma^2\,\tilde{V}_{xx}^i$$

with initial condition $\tilde{V}^i(0,x) = \mathrm{e}^{-r(T_{i+1})}\,P^i(x)$. In the following we will again write V and t instead of $\tilde{V}$ and $\tilde{t}$.

The analytical solution is only available for the case $r = 0$, i.e. we consider the PDE

$$V_t^i = -\frac{\left(V_x^i\right)^2}{2c} + \frac{1}{2}\,\sigma^2\,V_{xx}^i$$

with initial condition

$$V^i(0,x) = P^i(x) = \begin{cases} \left(p + s^i\right)(x - e_0) & \text{if} \quad x > e_0, \\ s^i(x - e_0) & \text{else.} \end{cases}$$

We again apply the Cole-Hopf transformation $V^i(t,x) = -c\,\sigma^2\,\ln\left(\nu^i(t,x)\right)$. Since the PDE is identical to the one-period case, we directly obtain the transformed PDE

$$\nu_t^i = \frac{1}{2}\,\sigma^2\,\nu_{xx}^i,$$

which is the standard heat equation. The initial condition is transformed as follows:

$$g(x) \coloneqq \nu^i(0,x) = \mathrm{e}^{-\frac{V^i(0,x)}{c\sigma^2}} = \mathrm{e}^{-\frac{P^i(x)}{c\sigma^2}} = \begin{cases} \mathrm{e}^{-\frac{(p+s^i)(x-e_0)}{c\sigma^2}} & \text{if} \quad x > e_0, \\ \mathrm{e}^{-\frac{s^i(x-e_0)}{c\sigma^2}} & \text{else.} \end{cases} \tag{3.3}$$

This function is continuous, but in contrast to the one-period case no longer bounded as the exponent may now take on positive values. Nevertheless we again refer to Evans [Eva10]: As can be seen from the proof of Theorem 2.3.1[1], we still obtain an analytical solution of the PDE as

$$\nu^i(t,x) = \frac{1}{\sqrt{2\pi\sigma^2 t}} \int_{-\infty}^{\infty} \nu^i(0,y)\,\mathrm{e}^{-\frac{(x-y)^2}{2\sigma^2 t}}\,\mathrm{d}y.$$

[1] The theorem and the proof can be found on pages 47-48 in [Eva10].

We also again have the property that ν^i is infinitely differentiable on $(0,\infty)\times\mathbb{R}$. However, we do not get directly that the solution ν^i converges to the initial value, i.e. the property that $\nu^i(t,x)\to g(x_0)$ as $(t,x)\to(0,x_0)$ for arbitrary $x_0\in\mathbb{R}$. We will therefore need to prove this explicitly further below.

We rewrite the expression for the solution ν^i as

$$\nu^i(t,x)=\frac{1}{\sqrt{2\pi\sigma^2 t}}\int_{-\infty}^{e_0}\mathrm{e}^{-\frac{s^i(y-e_0)}{c\sigma^2}}\,\mathrm{e}^{-\frac{(x-y)^2}{2\sigma^2 t}}\,\mathrm{d}y+\frac{1}{\sqrt{2\pi\sigma^2 t}}\int_{e_0}^{\infty}\mathrm{e}^{-\frac{\left(p+s^i\right)(y-e_0)}{c\sigma^2}}\,\mathrm{e}^{-\frac{(x-y)^2}{2\sigma^2 t}}\,\mathrm{d}y.$$

In Section 2.3.1 in equation (2.2), we have seen that

$$\begin{aligned}\frac{1}{\sqrt{2\pi\sigma^2 t}}\int_{e_0}^{\infty}\mathrm{e}^{-\frac{(x-y)^2}{2\sigma^2 t}}\,\mathrm{e}^{-\frac{p(y-e_0)}{c\sigma^2}}\,\mathrm{d}y&=\frac{1}{\sqrt{2\pi\sigma^2 t}}\,\mathrm{e}^{\frac{2cp(e_0-x)+p^2t}{2c^2\sigma^2}}\int_{e_0}^{\infty}\mathrm{e}^{-\frac{\left(y+\frac{pt}{c}-x\right)^2}{2\sigma^2 t}}\,\mathrm{d}y\\&=\frac{1}{2}\,\mathrm{e}^{\frac{2cp(e_0-x)+p^2t}{2c^2\sigma^2}}\left(1-\operatorname{erf}\left(\frac{c(e_0-x)+pt}{c\sigma\sqrt{2t}}\right)\right).\end{aligned}$$

In this expression, p can be replaced by any other constant; thus we directly obtain the second integral of ν^i as

$$\begin{aligned}&\frac{1}{\sqrt{2\pi\sigma^2\,t}}\int_{e_0}^{\infty}\mathrm{e}^{-\frac{\left(p+s^i\right)(y-e_0)}{c\sigma^2}}\mathrm{e}^{-\frac{(x-y)^2}{2\sigma^2 t}}\,\mathrm{d}y\\&\quad=\frac{1}{2}\,\mathrm{e}^{\frac{2c\left(p+s^i\right)(e_0-x)+\left(p+s^i\right)^2t}{2c^2\sigma^2}}\left(1-\operatorname{erf}\left(\frac{c(e_0-x)+\left(p+s^i\right)t}{c\sigma\sqrt{2t}}\right)\right).\end{aligned}$$

Furthermore, we know from Section 2.3.1 in equation (2.3) that

$$-\frac{(x-y)^2}{2\sigma^2 t}-\frac{s^i(y-e_0)}{c\sigma^2}=-\frac{\left(y+\frac{s^it}{c}-x\right)^2}{2\sigma^2 t}+\frac{2cs^i(e_0-x)+\left(s^i\right)^2t}{2c^2\sigma^2}.$$

For the first integral, we therefore need to compute

$$\frac{1}{\sqrt{2\pi\sigma^2 t}}\int_{-\infty}^{e_0}\mathrm{e}^{-\frac{s^i(y-e_0)}{c\sigma^2}}\,\mathrm{e}^{-\frac{(x-y)^2}{2\sigma^2 t}}\,\mathrm{d}y=\frac{1}{\sqrt{2\pi\sigma^2 t}}\,\mathrm{e}^{\frac{2cs^i(e_0-x)+\left(s^i\right)^2t}{2c^2\sigma^2}}\int_{-\infty}^{e_0}\mathrm{e}^{-\frac{\left(y+\frac{s^it}{c}-x\right)^2}{2\sigma^2 t}}\,\mathrm{d}y.$$

We set

$$z(y)=\frac{y+\frac{s^it}{c}-x}{\sqrt{2\sigma^2 t}}$$

with derivative

$$\frac{\mathrm{d}z}{\mathrm{d}y}=\frac{1}{\sqrt{2\sigma^2 t}}$$

and substitute this in the integral, as we did in Section 2.3.1, to compute

$$\begin{aligned}\frac{1}{\sqrt{2\pi\sigma^2 t}}\int_{-\infty}^{e_0} \mathrm{e}^{-\frac{\left(y+\frac{s^i t}{c}-x\right)^2}{2\sigma^2 t}}\mathrm{d}y &= \frac{\sqrt{2\sigma^2 t}}{\sqrt{2\pi\sigma^2 t}}\int_{-\infty}^{e_0}\frac{\mathrm{d}z}{\mathrm{d}y}\,\mathrm{e}^{-z(y)^2}\mathrm{d}y \\ &= \frac{1}{\sqrt{\pi}}\int_{-\infty}^{\frac{e_0+\frac{s^i t}{c}-x}{\sqrt{2\sigma^2 t}}} \mathrm{e}^{-z^2}\mathrm{d}z \\ &= \frac{1}{2}\left(\frac{2}{\sqrt{\pi}}\int_{-\infty}^{0}\mathrm{e}^{-z^2}\mathrm{d}z + \frac{2}{\sqrt{\pi}}\int_{0}^{\frac{e_0+\frac{s^i t}{c}-x}{\sqrt{2\sigma^2 t}}}\mathrm{e}^{-z^2}\mathrm{d}z\right) \\ &= \frac{1}{2}\left(1+\operatorname{erf}\left(\frac{e_0+\frac{s^i t}{c}-x}{\sqrt{2\sigma^2 t}}\right)\right)\end{aligned}$$

by using that $\lim_{z\to-\infty}\operatorname{erf}(z) = -1$ as given in Proposition 2.6 (iii). Thus we obtain the solution as

$$\begin{aligned}v^i(t,x) = &\frac{1}{2}\left(1+\operatorname{erf}\left(\frac{c(e_0-x)+s^i t}{\sqrt{2}c\sigma\sqrt{t}}\right)\right)\mathrm{e}^{\frac{2cs^i(e_0-x)+\left(s^i\right)^2 t}{2c^2\sigma^2}} \\ &+\frac{1}{2}\left(1-\operatorname{erf}\left(\frac{c(e_0-x)+\left(p+s^i\right)t}{\sqrt{2}c\sigma\sqrt{t}}\right)\right)\mathrm{e}^{\frac{2c\left(p+s^i\right)(e_0-x)+\left(p+s^i\right)^2 t}{2c^2\sigma^2}}.\end{aligned} \tag{3.4}$$

By applying the transformation function, we may compute $\tilde{V}^i$ as

$$\begin{aligned}\tilde{V}^i(t,x) = -c\sigma^2\ln\Bigg[&\frac{1}{2}\left(1+\operatorname{erf}\left(\frac{c(e_0-x)+s^i t}{\sqrt{2}c\sigma\sqrt{t}}\right)\right)\mathrm{e}^{\frac{2cs^i(e_0-x)+\left(s^i\right)^2 t}{2c^2\sigma^2}} \\ &+\frac{1}{2}\left(1-\operatorname{erf}\left(\frac{c(e_0-x)+\left(p+s^i\right)t}{\sqrt{2}c\sigma\sqrt{t}}\right)\right)\mathrm{e}^{\frac{2c\left(p+s^i\right)(e_0-x)+\left(p+s^i\right)^2 t}{2c^2\sigma^2}}\Bigg].\end{aligned}$$

We still need to revert back time by substituting $\Delta T_i - t$ for t. Then we have

$$\begin{aligned}V^i(t,x) = -c\sigma^2\ln\Bigg[&\frac{1}{2}\left(1+\operatorname{erf}\left(\frac{c(e_0-x)+s^i(\Delta T_i-t)}{\sqrt{2}c\sigma\sqrt{\Delta T_i-t}}\right)\right)\mathrm{e}^{\frac{2cs^i(e_0-x)+\left(s^i\right)^2(\Delta T_i-t)}{2c^2\sigma^2}} \\ &+\frac{1}{2}\left(1-\operatorname{erf}\left(\frac{c(e_0-x)+\left(p+s^i\right)(\Delta T_i-t)}{\sqrt{2}c\sigma\sqrt{\Delta T_i-t}}\right)\right)\mathrm{e}^{\frac{2c\left(p+s^i\right)(e_0-x)+\left(p+s^i\right)^2(\Delta T_i-t)}{2c^2\sigma^2}}\Bigg].\end{aligned} \tag{3.5}$$

In Section A.2.1 in the appendix, we compute the derivative of this expression, resulting in

$$V_x^i(t,x) = s^i + \frac{p}{1+\frac{\mathrm{e}^{-\frac{2cp(e_0-x)+p(p+2s^i)(\Delta T_i-t)}{2c^2\sigma^2}}\left(1+\operatorname{erf}\left(\frac{c(e_0-x)+s^i(\Delta T_i-t)}{\sqrt{2}c\sigma\sqrt{\Delta T_i-t}}\right)\right)}{1-\operatorname{erf}\left(\frac{c(e_0-x)+\left(p+s^i\right)(\Delta T_i-t)}{\sqrt{2}c\sigma\sqrt{\Delta T_i-t}}\right)}}. \tag{3.6}$$

This is consistent with the analytical solution for the one-period model: If we set $s = 0$ and $\Delta T_i = T$, we obtain the same result as we had in equation (2.5) for the one-period model.

Properties of the Analytical Solution

It remains to show that the solution ν^i of the transformed PDE converges to the initial value function as time tends to zero. Furthermore, we again need to show that the solution V^i of the characteristic PDE satisfies the requirements of the verification theorem for the HJB equation. We will also prove some properties of V^i and its derivatives, which will be useful further below. The two latter proofs work similarly to the one-period case discussed in Section 2.3.2 and are therefore not repeated here (these proofs can be found in Section B.1 of the appendix). We first consider the convergence of the PDE solution to the initial value function.

Proposition 3.2. *For the solution ν^i of the transformed PDE as given in equation (3.4) and the initial value function g as defined in equation (3.3), we have for any $\xi_0 \in \mathbb{R}$ that*

$$\lim_{(t,x)\to(0,\xi_0)} \nu^i(t,x) = g(\xi_0).$$

Proof. We again make use of auxiliary functions to simplify notation. These are defined in a similar way as in the one-period model; but since in this case we consider the time-reversed PDE, we introduce auxiliary functions in reversed time as

$$\begin{aligned}
\tilde{F}_1^i(t,x) &= 1 - \operatorname{erf}\left(\frac{c(e_0-x) + \left(p+s^i\right)t}{\sqrt{2}c\sigma\sqrt{t}}\right) \\
\tilde{F}_2^i(t,x) &= 1 + \operatorname{erf}\left(\frac{c(e_0-x) + s^i t}{\sqrt{2}c\sigma\sqrt{t}}\right) \\
\tilde{E}_3^i(t,x) &= \mathrm{e}^{\frac{2c\left(p+s^i\right)(e_0-x)+\left(p+s^i\right)^2 t}{2c^2\sigma^2}} \\
\tilde{E}_4^i(t,x) &= \mathrm{e}^{\frac{2cs^i(e_0-x)+\left(s^i\right)^2 t}{2c^2\sigma^2}}.
\end{aligned}$$

By the properties of the error function and the exponential function, these auxiliary functions are well-defined and positive on $\mathbb{R} \times (0,\infty)$. With the help of these functions, we write ν^i as

$$\nu^i(t,x) = \frac{1}{2}\,\tilde{F}_2^i(t,x)\,\tilde{E}_4^i(t,x) + \frac{1}{2}\,\tilde{F}_1^i(t,x)\,\tilde{E}_3^i(t,x).$$

We perform a case distinction and analyze the auxiliary functions separately.

(i) We first consider $\xi_0 < e_0$. Let (t_n, x_n) be an arbitrary sequence with $(t_n, x_n) \to (0, \xi_0)$ for $n \to \infty$. We now define

$$y_n \coloneqq \frac{c(e_0 - x_n) + (p + s^i)t_n}{\sqrt{2}c\sigma\sqrt{t_n}}.$$

Since $\xi_0 < e_0$ and in particular $\lim_{n\to\infty} x_n = \xi_0$, there exists $\kappa > 0$ and $N \in \mathbb{N}$ such that $e_0 - x_n > \kappa$ for all $n \geq N$. But then we have

$$\begin{aligned}
y_n &= \frac{c(e_0 - x_n) + (p + s^i)t_n}{\sqrt{2}c\sigma\sqrt{t_n}} \\
&= \frac{e_0 - x_n}{\sqrt{2}\sigma\sqrt{t_n}} + \frac{p + s^i}{\sqrt{2}c\sigma}\sqrt{t_n} \\
&> \frac{\kappa}{\sqrt{2}\sigma\sqrt{t_n}} + \frac{p + s^i}{\sqrt{2}c\sigma}\sqrt{t_n} \longrightarrow \infty \quad \text{as} \quad t_n \to 0,
\end{aligned}$$

which implies that $\lim_{n\to\infty} y_n = \infty$. By definition, we have $\tilde{F}_1^i(t_n, x_n) = 1 + \operatorname{erf}(y_n)$. Since the limit of the error function is $\lim_{x\to\infty} \operatorname{erf}(x) = 1$ by Proposition 2.6 (iii), we then have

$$\lim_{n\to\infty} \tilde{F}_1^i(t_n, x_n) = \lim_{n\to\infty} (1 + \operatorname{erf}(y_n)) = 1 + \lim_{n\to\infty} \operatorname{erf}(y_n) = 1 + 1 = 2.$$

By defining z_n as

$$z_n \coloneqq \frac{c(e_0 - x) + s^i t_n}{\sqrt{2} c\sigma\sqrt{t_n}},$$

we proceed in the same way to again show that $\lim_{n\to\infty} z_n = \infty$. By definition, we have $\tilde{F}_2^i(t_n, x_n) = 1 - \operatorname{erf}(z_n)$ and therefore

$$\lim_{n\to\infty} \tilde{F}_2^i(t_n, x_n) = \lim_{n\to\infty} (1 - \operatorname{erf}(z_n)) = 1 - \lim_{n\to\infty} \operatorname{erf}(z_n) = 1 - 1 = 0.$$

The exponential functions $\tilde{E}_3^i$ and $\tilde{E}_4^i$ are continuous in t and x on $[0, \infty) \times \mathbb{R}$ and we obtain directly

$$\lim_{n\to\infty} \tilde{E}_3^i(t_n, x_n) = \tilde{E}_3^i(0, \xi_0) = \mathrm{e}^{\frac{2c\left(p+s^i\right)(e_0-\xi_0)}{2c^2\sigma^2}} = \mathrm{e}^{-\frac{\left(p+s^i\right)(\xi_0-e_0)}{c\sigma^2}}$$

$$\lim_{n\to\infty} \tilde{E}_4^i(t_n, x_n) = \tilde{E}_4^i(0, \xi_0) = \mathrm{e}^{\frac{2cs^i(e_0-\xi_0)}{2c^2\sigma^2}} = \mathrm{e}^{-\frac{s^i(\xi_0-e_0)}{c\sigma^2}}.$$

Combining these results delivers

$$\begin{aligned}\lim_{n\to\infty} \nu^i(t_n, x_n) &= \lim_{n\to\infty} \left(\frac{1}{2} \tilde{F}_2^i(t_n, x_n)\, \tilde{E}_4^i(t_n, x_n) + \frac{1}{2} \tilde{F}_1^i(t_n, x_n)\, \tilde{E}_3^i(t_n, x_n) \right) \\ &= \frac{1}{2} \cdot 2 \cdot \mathrm{e}^{-\frac{s^i(\xi_0-e_0)}{c\sigma^2}} + \frac{1}{2} \cdot 0 \cdot \mathrm{e}^{-\frac{\left(p+s^i\right)(\xi_0-e_0)}{c\sigma^2}} = \mathrm{e}^{-\frac{s^i(\xi_0-e_0)}{c\sigma^2}} = g(\xi_0).\end{aligned}$$

(ii) Next, we consider the case that $\xi_0 > e_0$. We first determine the limit for $\tilde{F}_1^i$. Since $\xi_0 - e_0 > 0$, we may find $\kappa > 0$ such that

$$\left(2 + \frac{p + s^i}{c}\right) \kappa = \xi_0 - e_0.$$

Again let (t_n, x_n) be an arbitrary sequence with $(t_n, x_n) \to (0, \xi_0)$ as $n \to \infty$. Then there exists $N \in \mathbb{N}$ such that $\|(t_n, x_n) - (0, \xi_0)\| < \kappa$ for all $n \geq N$ and in particular we have $|t_n| < \kappa$ and $|x_n - \xi_0| < \kappa$. We therefore compute

$$\begin{aligned}e_0 - x_n + \frac{p + s^i}{c} t_n &= e_0 - \xi_0 + \xi_0 - x_n + \frac{p + s^i}{c} t_n \\ &\leq -\left(2 + \frac{p + s^i}{c}\right) \kappa + |\xi_0 - x_n| + \frac{p + s^i}{c} |t_n| \\ &< -\left(2 + \frac{p + s^i}{c}\right) \kappa + \kappa + \frac{p + s^i}{c} \kappa = -\kappa.\end{aligned}$$

We again define y_n as above and we then have for all $n > N$

$$\begin{aligned}y_n &= \frac{c(e_0 - x_n) + (p + s^i)t_n}{\sqrt{2} c\sigma\sqrt{t_n}} \\ &= \frac{e_0 - x_n + \frac{p+s^i}{c} t_n}{\sqrt{2}\sigma\sqrt{t_n}} \\ &< -\frac{\kappa}{\sqrt{2}\sigma\sqrt{t_n}} \to -\infty \quad \text{as} \quad t_n \to 0,\end{aligned}$$

which shows that $\lim_{n\to\infty} y_n = -\infty$. As $\lim_{x\to-\infty} \operatorname{erf}(x) = -1$ and we know by definition that $\tilde{F}_1^i(t_n, x_n) = 1 + \operatorname{erf}(y_n)$, we obtain

$$\lim_{n\to\infty} \tilde{F}_1^i(t_n, x_n) = \lim_{n\to\infty} (1 + \operatorname{erf}(y_n)) = 1 + \lim_{n\to\infty} \operatorname{erf}(y_n) = 1 - 1 = 0.$$

In the same way we show for z_n defined as

$$z_n \coloneqq \frac{c(e_0 - x) + s^i t_n}{\sqrt{2}c\sigma\sqrt{t_n}}$$

that $\lim_{n\to\infty} z_n = -\infty$. With $\tilde{F}_2^i(t_n, x_n) = 1 - \operatorname{erf}(z_n)$, we have

$$\lim_{n\to\infty} \tilde{F}_2^i(t_n, x_n) = \lim_{n\to\infty} (1 - \operatorname{erf}(z_n)) = 1 - \lim_{n\to\infty} \operatorname{erf}(z_n) = 1 + 1 = 2.$$

We now use the results from above for $\tilde{E}_3^i$ and $\tilde{E}_4^i$ to result in

$$\begin{aligned}\lim_{n\to\infty} \nu^i(t_n, x_n) &= \lim_{n\to\infty} \left(\frac{1}{2} \tilde{F}_2^i(t_n, x_n)\, \tilde{E}_4^i(t_n, x_n) + \frac{1}{2} \tilde{F}_1^i(t_n, x_n)\, \tilde{E}_3^i(t_n, x_n) \right) \\ &= \frac{1}{2} \cdot 0 \cdot \mathrm{e}^{-\frac{s^i(\xi_0 - e_0)}{c\sigma^2}} + \frac{1}{2} \cdot 2 \cdot \mathrm{e}^{-\frac{\left(p + s^i\right)(\xi_0 - e_0)}{c\sigma^2}} = \mathrm{e}^{-\frac{\left(p + s^i\right)(\xi_0 - e_0)}{c\sigma^2}} = g(\xi_0).\end{aligned}$$

(iii) The only case we have left is when $\xi_0 = e_0$. Let (t_n, x_n) be an arbitrary sequence with $(t_n, x_n) \to (0, e_0)$ as $n \to \infty$. We again define

$$y_n \coloneqq \frac{c(e_0 - x_n) + (p + s^i)t_n}{\sqrt{2}c\sigma\sqrt{t_n}}$$

and

$$z_n \coloneqq \frac{c(e_0 - x_n) + s^i t_n}{\sqrt{2}c\sigma\sqrt{t_n}}.$$

Then we have

$$\begin{aligned}\lim_{n\to\infty} |y_n - z_n| &= \lim_{n\to\infty} \left| \frac{c(e_0 - x_n) + (p + s^i)t_n}{\sqrt{2}c\sigma\sqrt{t_n}} - \frac{c(e_0 - x_n) + s^i t_n}{\sqrt{2}c\sigma\sqrt{t_n}} \right| \\ &= \lim_{n\to\infty} \left| \frac{pt_n + s^i t_n - s^i t_n}{\sqrt{2}c\sigma\sqrt{t_n}} \right| = \lim_{n\to\infty} \left| \frac{p}{\sqrt{2}c\sigma} \sqrt{t_n} \right| = 0.\end{aligned}$$

Since the derivative of the error function given by $\operatorname{erf}(x)' = {}^2/_{\sqrt{\pi}}\, \mathrm{e}^{-x^2}$ is clearly bounded, the error function is Lipschitz continuous and we have

$$|\operatorname{erf}(y_n) - \operatorname{erf}(z_n)| \leq L|y_n - z_n|$$

for some constant $L > 0$. Then it follows that

$$\lim_{n\to\infty} |\operatorname{erf}(y_n) - \operatorname{erf}(z_n)| = 0.$$

We again use the continuity of the functions $\tilde{E}_3^i$ and $\tilde{E}_4^i$ to compute

$$\begin{aligned}\lim_{n\to\infty} \tilde{E}_3^i(t_n, x_n) &= \mathrm{e}^{\frac{2c\left(p + s^i\right)(e_0 - e_0) + \left(p + s^i\right) \cdot 0}{2c^2\sigma^2}} = 1 \\ \lim_{n\to\infty} \tilde{E}_4^i(t_n, x_n) &= \mathrm{e}^{\frac{2cs^i(e_0 - e_0) + \left(s^i\right)^2 \cdot 0}{2c^2\sigma^2}} = 1.\end{aligned}$$

From this we obtain

$$\lim_{n\to\infty} \left|\tilde{E}_3^i(t_n, x_n) - \tilde{E}_4^i(t_n, x_n)\right| = |1-1| = 0$$

which implies that

$$\begin{aligned}
&\left|\tilde{E}_3^i(t_n, x_n)\ \mathrm{erf}(y_n) - \tilde{E}_4^i(t_n, x_n)\ \mathrm{erf}(z_n)\right| \\
&\quad = \left|\tilde{E}_3^i(t_n, x_n)\ \mathrm{erf}(y_n) - \tilde{E}_3^i(t_n, x_n)\ \mathrm{erf}(z_n) + \tilde{E}_3^i(t_n, x_n)\ \mathrm{erf}(z_n) - \tilde{E}_4^i(t_n, x_n)\ \mathrm{erf}(z_n)\right| \\
&\quad \le \tilde{E}_3^i(t_n, x_n)\,|\,\mathrm{erf}(y_n) - \mathrm{erf}(z_n)| + \left|\tilde{E}_3^i(t_n, x_n) - \tilde{E}_4^i(t_n, x_n)\right|\ |\,\mathrm{erf}(z_n)| \\
&\quad \le \tilde{E}_3^i(t_n, x_n)\,|\,\mathrm{erf}(y_n) - \mathrm{erf}(z_n)| + \left|\tilde{E}_3^i(t_n, x_n) - \tilde{E}_4^i(t_n, x_n)\right| \to 0 \quad \text{as} \quad n \to \infty
\end{aligned}$$

since $|\,\mathrm{erf}(z_n)| \le 1$. Then also

$$\lim_{n\to\infty} \Big(\tilde{E}_3^i(t_n, x_n)\ \mathrm{erf}(y_n) - \tilde{E}_4^i(t_n, x_n)\ \mathrm{erf}(z_n)\Big) = 0.$$

We now use this and obtain

$$\begin{aligned}
\lim_{n\to\infty} \nu^i(t_n, x_n) &= \lim_{n\to\infty} \left(\frac{1}{2}\,\tilde{F}_2^i(t_n, x_n)\,\tilde{E}_4^i(t_n, x_n) + \frac{1}{2}\,\tilde{F}_1^i(t_n, x_n)\,\tilde{E}_3^i(t_n, x_n)\right) \\
&= \lim_{n\to\infty} \left(\frac{1}{2}\ (1 - \mathrm{erf}(z_n))\ \tilde{E}_4^i(t_n, x_n) + \frac{1}{2}\ (1 + \mathrm{erf}(y_n))\ \tilde{E}_3^i(t_n, x_n)\right) \\
&= \lim_{n\to\infty} \left(\frac{1}{2}\left(\tilde{E}_4^i(t_n, x_n) + \tilde{E}_3^i(t_n, x_n)\right)\right. \\
&\quad \left. + \frac{1}{2}\left(\tilde{E}_3^i(t_n, x_n)\ \mathrm{erf}(y_n) - \tilde{E}_4^i(t_n, x_n)\ \mathrm{erf}(z_n)\right)\right) \\
&= \frac{1}{2}\cdot(1+1) + \frac{1}{2}\cdot 0 = 1 = g(\xi_0).
\end{aligned}$$

Thus we have shown that the solution ν^i converges to the initial value function g as required. □

In the following, we will proceed as we did for the one-period model: We first establish some properties of the solution V^i and use these to show that it indeed satisfies the requirements of the verification theorem for the HJB equation.

Proposition 3.3. *The function V^i as given by (3.5) and its derivative V_x^i given by (3.6) satisfy the following properties:*

(i) V^i is infinitely differentiable on $(-\infty, \Delta T_i) \times \mathbb{R}$, i.e. $V^i \in C^\infty\left((-\infty, \Delta T_i) \times \mathbb{R}\right)$.

(ii) V_x^i satisfies $s^i \le V_x^i(t,x) \le p + s^i$ for all $(t,x) \in [0, \Delta T_i] \times \mathbb{R}\backslash\{(\Delta T_i, e_0)\}$, i.e. V_x^i is bounded.

(iii) For any $t \in [0, \Delta T_i]$ we have

$$\lim_{x\to\infty} V_x^i(t,x) = p + s^i \quad \text{and} \quad \lim_{x\to-\infty} V_x^i(t,x) = s^i.$$

(iv) Let $\varepsilon > 0$ arbitrary. Then the derivatives V_{xx}^i and V_{xt}^i are bounded on $[0, \Delta T_i - \varepsilon] \times \mathbb{R}$.

Proof. The proof is very similar to the proof of the corresponding result in the one-period model in Proposition 2.7; therefore it is omitted here and instead provided in Section B.1 in the appendix.

These results now help us to establish the requirements of the verification theorem for the HJB equation and to show that the corresponding control is admissible.

Proposition 3.4. *The functions V^i given by equation (3.5) for $t \in [0, \Delta T_i)$ and by the terminal condition of the PDE for $t = \Delta T_i$ satisfy the requirements of the verification theorem for the HJB equation, i.e. we have*

(i) V^i is continuously differentiable in t and twice continuously differentiable in x on $[0, \Delta T_i) \times \mathbb{R}$,

(ii) V^i is continuous on $[0, \Delta T_i] \times \mathbb{R}$,

(iii) V^i satisfies a quadratic growth condition, uniformly in t, i.e. there exists $K > 0$ such that

$$|V^i(t,x)| \leq K\left(1 + |x|^2\right) \quad \text{for all} \quad t \in [0, \Delta T_i].$$

Proof. The proof is again along the same lines as the corresponding result in the one-period model given by Proposition 2.9; the proof can be found in Section B.1 of the appendix.

Proposition 3.5. *Fix a time period i and let X be a continuous $\mathbb{R}$-valued stochastic process on $[0, \Delta T_i]$ which is $\mathcal{F}^i$-adapted. Then for any $t \in [0, \Delta T_i]$ the control process u^i given by*

$$u^i = \left(u^i_s\right)_{s\in[t,\Delta T_i]} = \left(u^i(s, X_s)\right)_{s\in[t,\Delta T_i]} \quad \text{where} \quad u^i(s,x) = \frac{V^i_x(s,x)}{c}$$

lies in $\mathcal{A}^i(t)$.

Proof. Since the function u^i has similar properties as u in the one-period model, the proof is analogous to the one of Proposition 2.10 and can be found in Section B.1 of the appendix.

In conclusion, we see that also for the multi-period model I, we obtain an analytical solution of the characteristic PDE in the simple model variant. By the verification theorem of the HJB equation in Proposition 2.3, this solution allows us to determine an optimal abatement rate as long as the SDE has a unique solution which is continuous and adapted.

Time Reversion in the Brownian and Ornstein-Uhlenbeck Model Variant

For the Brownian model variant, we have the PDE

$$V^i_t(t,x) = \frac{1}{2}\,\frac{\left(V^i_x(t,x)\right)^2}{c}\,\mathrm{e}^{r(T_i+t)} - \frac{1}{2}\,\sigma^2\left(\Delta T_i - t\right)^2 V^i_{xx}(t,x)$$

with final condition

$$V^i(\Delta T_i, x) = e^{-rT_{i+1}} P^i(x).$$

We reverse time by substituting $t = \Delta T_i - \tilde{t}$ and defining $\tilde{V}^i(\tilde{t}, x) = V^i(\Delta T_i - \tilde{t}, x)$ as before. Then

$$V^i_t(t,x) = V^i_t(\Delta T_i - \tilde{t}, x) = -V^i_{\tilde{t}}(\Delta T_i - \tilde{t}, x) = -\tilde{V}^i_{\tilde{t}}(\tilde{t}, x)$$

and we obtain

$$\begin{aligned}\tilde{V}^i_{\tilde{t}} &= -\frac{1}{2}\,\frac{\left(\tilde{V}^i_x\right)^2}{c}\,\mathrm{e}^{r(T_i+\Delta T_i-\tilde{t})} + \frac{1}{2}\,\sigma^2\,(\Delta T_i - \Delta T_i + \tilde{t})^2\tilde{V}^i_{xx} \\ &= -\frac{1}{2}\,\frac{\left(\tilde{V}^i_x\right)^2}{c}\,\mathrm{e}^{r(T_{i+1}-\tilde{t})} + \frac{1}{2}\,\sigma^2\,\tilde{t}^2\,\tilde{V}^i_{xx}.\end{aligned}$$

The final condition is turned into an initial condition given by

$$\tilde{V}^i(0,x) = \mathrm{e}^{-rT_{i+1}}\,P^i(x).$$

The PDE of the Ornstein-Uhlenbeck model variant is given by

$$V^i_t(t,x) = \frac{1}{2}\,\frac{\left(V^i_x(t,x)\right)^2}{c}\,\mathrm{e}^{r(T_i+t)} - \frac{1}{2}\,\sigma^2\,\frac{\left(1-\mathrm{e}^{-\theta(\Delta T_i-t)}\right)^2}{\theta^2}\,V^i_{xx}(t,x)$$

with final condition

$$V^i(\Delta T_i, x) = \mathrm{e}^{-rT_{i+1}}P^i(x).$$

After time reversion this becomes

$$\begin{aligned}\tilde{V}^i_{\tilde{t}} &= -\frac{1}{2}\,\frac{\left(\tilde{V}^i_x\right)^2}{c}\,\mathrm{e}^{r(T_i+\Delta T_i-\tilde{t})} + \frac{1}{2}\,\sigma^2\,\frac{(1-\mathrm{e}^{-\theta(\Delta T_i-\Delta T_i+\tilde{t})})^2}{\theta^2}\,\tilde{V}^i_{xx} \\ &= -\frac{1}{2}\,\frac{\left(\tilde{V}^i_x\right)^2}{c}\,\mathrm{e}^{r(T_{i+1}-\tilde{t})} + \frac{1}{2}\,\sigma^2\,\frac{\left(1-\mathrm{e}^{-\theta\tilde{t}}\right)^2}{\theta^2}\,\tilde{V}^i_{xx}\end{aligned}$$

and the final condition becomes the initial condition

$$V^i(\Delta T_i, x) = \mathrm{e}^{-rT_{i+1}}P^i(x),$$

identical to the one in the Brownian model variant. Again for both of these model variants an analytical solution is not available, hence we will have to solve the PDE numerically, as explained in Section 5.1. Thus we cannot show that the verification theorem for the HJB equation holds in case of these model variants.

Summary

In this section, we derived an analytical solution of the characteristic PDE in the simple model variant of multi-period model I; in contrast to the one-period model we needed to show explicitly that this solution converges to the initial value function. For the remainder of the section, we proceeded as in the one-period model: We derived useful properties of the PDE solution and showed that it satisfies the requirements of the verification theorem for the HJB equation. Furthermore, we showed that the corresponding control is admissible. To apply the verification theorem, it only remains to show that the SDE describing X has a unique solution which is continuous and adapted.

As in the one-period model, the analytical solution is only available in the simple model variant; in the Brownian and Ornstein-Uhlenbeck model variant, we prepared the numerical solution by conducting the necessary time reversion.

3.1.4 Solution of the SDE

Again the motivation to analyze the solution of the SDE is two-fold: Firstly, we are interested in the quantities that such a solution may deliver, namely the process of total expected emissions X and the allowance prices we may compute from it. And secondly, we again require the existence of a unique solution to be able to apply the verification theorem of the HJB equation in Proposition 2.3. In this section, we will refer to our results in Sections 2.4.1 and 2.4.2 and discuss how they apply to multi-period model I.

Remark 3.6. We have to keep in mind that $W_0^i \neq 0$ and thus W^i is not a standard Brownian motion. By definition of W^i we can view it as a shifted Brownian motion, so all other properties of Brownian motion are preserved. Moreover, W^i enters the statements below only as an increment, i.e. as $W_t^i - W_s^i$ for some $s < t$, or as the integrator of a stochastic integral, i.e. as $\int_0^t Z_s \mathrm{d}W_s^i$ for some process Z. Therefore the shift does not impact any of the results and the theorems of Section 2.4 still apply.

Corollary 3.7. *Let i be an arbitrary time period of multi-period model I and furthermore let $u^i(t,x) = \frac{V_x^i(t,x)}{c}$ with V_x^i as given in equation (3.6). Then the SDE of the simple model variant given by*

$$\mathrm{d}X_t^i = -u^i(t, X_t^i)\mathrm{d}t + \sigma \mathrm{d}W_t^i,$$

has a unique strong solution which is continuous in t. In addition, the solution X^i is adapted to the shifted filtration $\mathcal{F}^i$ and the process X defined by

$$X_t = \sum_{i=1}^{N} X_{t-T_i}^i \mathbf{1}_{(T_i, T_{i+1}]}(t) \quad \text{for } t \in [0,T]$$

is adapted to the filtration $\mathcal{F}$.

Proof. As for Corollary 2.27, we need to verify Assumption 2.14 and may then apply Theorem 2.15. As the volatility σ is constant, it is clearly bounded and Lipschitz continuous and thus satisfies the assumption. The drift term is bounded, since by Proposition 3.3 (ii) the derivative of the value function V_x^i is bounded. Moreover, in Proposition 3.3 (iv) we have seen for any $\varepsilon > 0$ that V_{xx}^i is bounded on $[0, T-\varepsilon] \times \mathbb{R}$, which implies that V_x^i is Lipschitz continuous in x on $[0, T-\varepsilon] \times \mathbb{R}$. Hence Lipschitz continuity of u^i follows and thus the drift also satisfies Assumption 2.14.

Theorem 2.15 then delivers the existence of a unique t-continuous solution, which is adapted to $\mathcal{F}^{X_0^i, W^i}$. By definition we know that X_0^i is $\mathcal{F}_{T_i}$-measurable. Furthermore, W^i is defined as $W_t^i = W_{T_i+t}$ and therefore W_t^i is $\mathcal{F}_{T_i+t}$-measurable. Thus

$$\mathcal{F}_t^{X_0^i, W^i} \subseteq \mathcal{F}_{T_i+t} = \mathcal{F}_t^i$$

and the claim follows. □

Corollary 3.8. *For an arbitrary time period i of multi-period model I with $u^i(t,x) = \frac{V_x^i(t,x)}{c}$ and V_x^i as given in equation (3.6) let X^i denote the solution of the SDE*

$$\mathrm{d}X_t^i = -u^i(t, X_t^i)\mathrm{d}t + \sigma \mathrm{d}W_t^i.$$

Then the Euler-Maruyama scheme as given in Definition 2.19 converges strongly to X^i.

Proof. Assumption 2.14 holds as seen above, thus it remains to show $\frac{1}{2}$-Hölder continuity on $[0, \Delta T_i - \varepsilon]$ with respect to t as required in Assumption 2.25. For the constant volatility this is again trivial. We now let $\varepsilon > 0$ arbitrary. Then we know from Proposition 3.3 (iv) that V^i_{xt} is bounded on $[0, T - \varepsilon] \times \mathbb{R}$, thus V^i_x and therefore also u^i is Lipschitz continuous in t on $[0, T - \varepsilon] \times \mathbb{R}$, which in particular implies $\frac{1}{2}$-Hölder continuity. With Theorem 2.26 convergence of the Euler-Maruyama scheme follows. □

Corollary 3.9. *Let i be an arbitrary time period in multi-period model I. Further, let V^i be given by equation (3.5) and let the abatement rate be given by $u^i_t = u^i(t, X^i_t)$, where $u^i(t,x) = \frac{V^i_x(t,x)}{c}$ and V^i_x is given by equation (3.6). Then, for the simple model variant, V^i delivers the minimum costs and the abatement rate u^i is optimal.*

Proof. Since the drift and the volatility of the SDE are essentially unchanged in comparison to the one-period model, they satisfy the assumptions stated in the prequel of the verification theorem. Also the cost function still satisfies a quadratic growth bound. The terminal condition is still piecewise linear, but no longer partly constant. This suffices for a quadratic growth condition to hold. Thus the verification theorem in Proposition 2.3 can be applied also to multi-period model I.

With Proposition 3.4, we know that $V^i \in C^{1,2}([0, \Delta T_i) \times \mathbb{R})$ and $V^i \in C([0, \Delta T_i] \times \mathbb{R})$ as well as that V^i grows at most quadratically. By construction, V^i solves the HJB equation with u^i as the control. Furthermore, with Corollary 3.7, we know that the SDE

$$\mathrm{d}X^i_t = -u^i(t, X^i_t)\mathrm{d}t + \sigma \mathrm{d}W^i_t$$

has a unique solution and by Proposition 3.5 we have $u^i \in \mathcal{A}(t)$ since the solution of the SDE X^i is continuous and $\mathcal{F}^i$-adapted. Then, with the verification theorem in Proposition 2.3, the claim follows. □

As in the one-period model, we cannot rigorously analyze the drift term of the Brownian and Ornstein-Uhlenbeck model variant due to the lack of a closed-form expression. Thus we may only provide a theoretical result concerning the volatility term.

Lemma 3.10. *The volatility functions in multi-period model I of*

(i) the Brownian model variant given by $G^i_B(t) = \sigma(\Delta T_i - t)$ and

(ii) the Ornstein-Uhlenbeck model variant given by $G^i_{OU}(t) = \sigma \frac{1 - \mathrm{e}^{-\theta(\Delta T_i - t)}}{\theta}$

satisfy Assumptions 2.14 and 2.25.

Proof. (i) The volatility of the Brownian model variant G^i_B is linear in t and constant in x and thus clearly Lipschitz continuous in t and x and in particular $\frac{1}{2}$-Hölder continuous in t. Furthermore it also directly follows that G^i_B is bounded on the bounded interval $[0, \Delta T_i]$.

(ii) The volatility of the Ornstein-Uhlenbeck model variant is also constant in x and therefore in particular Lipschitz continuous in x. In addition it is continuous in t, so boundedness on $[0, \Delta T_i]$ follows. We now compute the derivative $G^i_{OU}(t)' = -\sigma \mathrm{e}^{-\theta(\Delta T_i - t)}$. This is clearly bounded for $t \leq \Delta T_i$, hence G^i_{OU} is Lipschitz continuous in t and therefore $\frac{1}{2}$-Hölder continuous in t on $[0, \Delta T_i]$. □

Remark 3.11. Since in the Brownian and in the Ornstein-Uhlenbeck model variant we cannot study the drift term analytically, we will analyze the numerical solution in Section 6.2.1.

Summary

With the help of the theorems of Section 2.4 and the results of Section 3.1.3, we showed that the SDE in the simple variant of our model has a unique solution, which can be approximated by the Euler-Maruyama scheme. Furthermore, we concluded that the solution of the characteristic PDE delivers the minimum costs and that the corresponding control is optimal. In the Brownian and Ornstein-Uhlenbeck model variant, comparable results could not be obtained.

3.1.5 Procedure to Combine the Time Periods

So far we have derived SDEs and solved the minimization problem for each time period separately. Now we need to combine these results. As in the one-period model, our aim is to determine the price path and the path of total expected emissions and in particular the resulting emissions as given by X_{T_i}. Therefore, we need to solve the SDE for all time periods. To determine the drift functions u^i, we first need to solve the PDE for the corresponding time period i. Here we require the price of an allowance at the beginning of the subsequent period since this enters the penalty function. In the approach presented in this section, we assume this price to be exogenous to the optimization procedure, i.e. the price as given by s^i enters the PDE as a constant parameter.

The price function in the model is given by $S^i(t,x) = c\,u^i(t,x)$, so it depends on the drift u^i. Therefore, the PDE solutions are computed in reversed order: We first determine the drift of the last time period u^{N-1}, then u^{N-2} and so forth until we reach u^0. For the last time period $N-1$, the parameter s^{N-1} needs to be given in advance. For all remaining time periods, we compute the input parameter s^i from the price function of the next time period S^{i+1} by using the previously computed function u^{i+1}. The actual price of an allowance at the beginning of time period $i+1$ is given by $S^{i+1}(0, X_0^{i+1})$. However, since X_0^{i+1} is not available, we need to estimate this value. Two approaches are possible: Firstly, we may use the expectation of the price given by

$$s^i = \mathrm{E}\left[S^{i+1}(0, X_0^{i+1})\right] = \mathrm{E}\left[c\,u^{i+1}\left(0, X_0^{i+1}\right)\right].$$

In Section 3.1.1, we determined $X_0^{i+1} = X^+_{T_{i+1}}$ for each model. In the simple model variant, we then have

$$s^i = \mathrm{E}\left[c\,u^{i+1}\left(0, x_0^{i+1} + \sigma\, W_{T_{i+1}}\right)\right]$$

and similarly in the Brownian model variant

$$s^i = \mathrm{E}\left[c\,u^{i+1}\left(0, x_0^{i+1} + \sigma\,\Delta T_{i+1}\, W_{T_{i+1}}\right)\right].$$

In the Ornstein-Uhlenbeck model variant, this becomes

$$s^i = \mathrm{E}\left[c\,u^{i+1}\left(0, x_0^{i+1} - \sigma\,\frac{\mathrm{e}^{-\theta T_{i+2}} - \mathrm{e}^{-\theta T_{i+1}}}{\theta}\int_0^{T_{i+1}} \mathrm{e}^{\theta s}\mathrm{d}W_s\right)\right].$$

Since we know the distribution of $W_{T_{i+1}}$ as well as of $\int_0^{T_{i+1}} \mathrm{e}^{\theta s}\mathrm{d}W_s$, we can compute these expressions by Monte Carlo methods.

We may simplify these computations if we instead estimate the price by applying the price function to the expectation of X_0^{i+1}. We then obtain

$$s^i = S^{i+1}\left(0, \mathrm{E}\left[X_0^{i+1}\right]\right) = S^{i+1}\left(0, x_0^{i+1}\right),$$

since in the simple model variant we have

$$\mathrm{E}\left[X_0^{i+1}\right] = \mathrm{E}\left[x_0^{i+1} + \sigma W_{T_{i+1}}\right] = x_0^{i+1}$$

and in the Brownian model variant

$$\mathrm{E}\left[X_0^{i+1}\right] = \mathrm{E}\left[x_0^{i+1} + \sigma\,\Delta T_{i+1}\,W_{T_{i+1}}\right] = x_0^{i+1}.$$

In the Ornstein-Uhlenbeck model variant, we use that $\int_0^{T_{i+1}} \mathrm{e}^{\theta s}\mathrm{d}W_s \sim \mathcal{N}\left(0, \int_0^{T_{i+1}} \mathrm{e}^{2\theta s}\mathrm{d}s\right)$ and therefore

$$\mathrm{E}\left[X_0^{T_{i+1}}\right] = \mathrm{E}\left[x_0^{i+1} - \sigma\,\frac{\mathrm{e}^{-\theta T_{i+2}} - \mathrm{e}^{-\theta T_{i+1}}}{\theta}\int_0^{T_{i+1}} \mathrm{e}^{\theta s}\mathrm{d}W_s\right] = x_0^{i+1}.$$

We already remark that we will use this more simple approach to compute s^i in numerical simulations.

When we have solved the PDEs, we can start to solve the SDEs. This is done forward in time: We first solve the SDE on $[0, T_1]$ which also delivers the path of W on $[0, T_1]$ and in particular a realization of W_{T_1}. Therefore, we can compute[2] $X_0^1 = X_{T_1}^+$ and solve the SDE on $[T_1, T_2]$. We continue in this way until we reach T_N. In summary, the procedure works as follows:

1. Choose a constant s^{N-1} as input for the last time period.

2. Solve the PDEs in reversed order

$$u^{N-1} \to u^{N-2} \to \ldots \to u^{i+1} \to u^i \to \ldots \to u^1 \to u^0.$$

   In each time period we compute s^i from the subsequent time period $i+1$ as $s^i = c\,u^{i+1}(0, x_0^{i+1})$ or $s^i = c\,u^{i+1}\left(0, \mathrm{E}\left[X_0^{i+1}\right]\right)$.

3. Solve the SDEs forward in time

$$X^0 \to X^1 \to \ldots \to X^i \to X^{i+1} \to \ldots \to X^{N-2} \to X^{N-1}$$

   by computing X_0^i from $(W_t)_{t\in[0,T_i]}$.

Remark 3.12. We argued above that X_0^{i+1} is not available when solving the PDEs. This is due to the fact that X_0^{i+1} depends on $W_{T_{i+1}}$ in case of the simple and Brownian model variants and on the entire path $(W_t)_{t\in[0,T_{i+1}]}$ in case of the Ornstein-Uhlenbeck model. The Brownian motion W is usually simulated when solving the SDEs and therefore after solving the PDEs as explained above. Of course, it would be possible to simulate the Brownian motion in advance. Then we would have to compute the solution of the PDE separately for each run, which would entail a very high computational effort. More importantly, this approach is questionable with regards to its interpretation: The results of the PDE solution for the period $[T_i, T_{i+1}]$ are applied from the beginning of this period on; therefore all the information required to compute the PDE solution should be available at time T_i. This certainly does not hold for the realization of the Brownian motion $W_{T_{i+1}}$ at time T_{i+1} which is required to compute X_0^{i+1} and hence $S^{i+1}(0, X_0^{i+1})$. Moreover, for the computation of u^{i+1} we require $W_{T_{i+2}}$ and so on. Hence both in theory and in practice X_0^{i+1} is not available when computing the PDE solution.

[2] For the simple and Brownian model we only require W_{T_1}, for the Ornstein-Uhlenbeck model we need the entire path.

Remark 3.13. From a theoretical point of view, the estimates given above may correspond to the situation that we perform the optimization for all time periods before the beginning of the first time period: By simply computing the expectation, we do not include any further information we might acquire in the course of time. Possibly it is more realistic to assume that the cost optimization is in each case done right before the corresponding time period, so for solving the PDE on $[T_i, T_{i+1}]$ the information of time T_i is available. Then the expression for the parameter s^i is given by

$$s^i = \mathrm{E}\left[S^{i+1}\left(0, X_0^{i+1}\right) \,\middle|\, \mathcal{F}_{T_i}\right].$$

However, as mentioned above, the function u^{i+1} and thus also S^{i+1} is dependent on s^{i+1}. We therefore consider $S^{i+1}(0, x, s)$ as a function of x and the price parameter s^i. For the last period, s^{N-1} has to be given in advance. We then have

$$s^{N-2} = \mathrm{E}\left[S^{N-1}\left(0, X_0^{N-1}, s^{N-1}\right) \,\middle|\, \mathcal{F}_{T_{N-2}}\right]$$

as input price parameter for the second last period. For the period before that, we obtain

$$s^{N-3} = \mathrm{E}\left[S^{N-2}\left(0, X_0^{N-2}, \mathrm{E}\left[S^{N-1}\left(0, X_0^{N-1}, s^{N-1}\right) \,\middle|\, \mathcal{F}_{T_{N-2}}\right]\right) \,\middle|\, \mathcal{F}_{T_{N-3}}\right],$$

which continues in a similar manner for the remaining time periods. Already this expression is complicated to handle both in theory and in numerical computations. More importantly, the parameter s^{N-3} (and s^{N-2}, s^{N-4}, ...) is now a random variable. This contradicts our assumption of a constant parameter and such a random variable cannot be processed by the optimization procedure described in Section 3.1.2.

If we again take the price function of the expectation of X_0^i, we have

$$s^{N-2} = S^{N-1}\left(0, \mathrm{E}\left[X_0^{N-1} \,\middle|\, \mathcal{F}_{T_{N-2}}\right], s^{N-1}\right).$$

As an example, we compute in the Brownian model

$$\begin{aligned} s^{N-2} &= S^{N-1}\left(0, \mathrm{E}\left[x_0^{N-1} + \sigma\,\Delta T_{N-1}\, W_{T_{N-1}} \,\middle|\, \mathcal{F}_{T_{N-2}}\right], s^{N-1}\right) \\ &= S^{N-1}\left(0, x_0^{N-1} + \sigma\,\Delta T_{N-1}\, W_{T_{N-2}}, s^{N-1}\right) \end{aligned}$$

and similarly

$$\begin{aligned} s^{N-3} &= S^{N-2}\left(0, \mathrm{E}\left[X_0^{N-2} \,\middle|\, \mathcal{F}_{T_{N-3}}\right], s^{N-2}\right) \\ &= S^{N-2}\left(0, x_0^{N-2} + \sigma\,\Delta T_{N-2}\, W_{T_{N-3}}, s^{N-2}\right). \end{aligned}$$

However, s^{N-2} still depends on $W_{T_{N-2}}$ which is not available at time $W_{T_{N-3}}$. Hence we would have to consider the conditional expectation $\mathrm{E}\left[s^{N-2} \,\middle|\, \mathcal{F}_{T_{N-3}}\right]$, imposing the same complications as above. Moreover, $s^{N-2}, s^{N-3}, s^{N-4}\ldots$ are again random variables and therefore cannot be used in this model.

A more realistic but also more complex approach to the multi-period model, which evades the difficulties explored here, will be described in Section 3.2.

Summary

We described how we proceed to combine the PDE and SDE solutions of the different time periods: We solve the PDEs of all time periods in reversed order and use the solution of the subsequent time period to estimate the price parameter s^i. Then we solve the SDEs forward in time by using the simulated realization of Brownian motion to determine the initial value of the SDE in each time period.

3.1.6 Multi-Period Model with Expiring Allowances

In order to evaluate the impact of allowing for the transfer of allowances, we need to compare the results we obtain in the multi-period model with a setting where allowances expire after one time period. However, the multi-period model presented above should not directly be compared to the one-period model. One important reason is that we also use the parameter s^i to account for the costs of the missing allowances in the case of non-compliance in addition to the penalty payment, which we could not do in the one-period model. In addition, constructing a multi-period model with expiring allowances also enables us to compare more than the first time period. To obtain such a model we only need to apply one simple change in the penalty function.

The SDE is derived directly from the emission rate process, which is not influenced by the validity of the allowances. Therefore, also in this case we model the total expected emissions as

$$\mathrm{d}X_t^i = -u_t^i \mathrm{d}t + G^i(t)\mathrm{d}W_t^i.$$

For the cost minimization, we modify the penalty function to

$$P^i\left(X_{T_{i+1}}\right) = \begin{cases} \left(p + s^i\right)\left(X_{T_{i+1}} - e_0\right) & \text{if} \quad X_{T_{i+1}} > e_0, \\ 0 & \text{else.} \end{cases}$$

In case of surpassing the emission threshold, we still account for both the penalty payment and the requirement to hand over the missing allowances in the next period. But in case of compliance with the emission goal, surplus allowances now have a value of 0, since they expire and cannot be transferred to the next period.

The remainder of the optimization procedure can be applied as before, so that we obtain the same PDE, only with a modified final condition as given by the penalty function above:

$$V_t^i(t,x) = \frac{1}{2}\frac{\left(V_x^i(t,x)\right)^2}{c}\,\mathrm{e}^{r(T_i+t)} - \frac{1}{2}\,G^i(t)^2\,V_{xx}^i(t,x)$$

with final condition

$$V^i(\Delta T_i, x) = \begin{cases} \mathrm{e}^{-rT_{i+1}}\left(p + s^i\right)(x - e_0) & \text{if} \quad x > e_0, \\ 0 & \text{else.} \end{cases}$$

Hence for all model variants, we may proceed similarly as in the multi-period model I presented above to solve the PDE; we only need to adapt the final condition.

Analytical Solution of the PDE in the Simple Model Variant

We may also in this setting derive an analytical solution in the simple model variant if we set $r = 0$. We consider the PDE

$$V_t^i = \frac{\left(V_x^i\right)^2}{2c} - \frac{1}{2}\,\sigma^2\,V_{xx}^i$$

with final condition

$$V^i(\Delta T_i, x) = P^i(x) = \begin{cases} \left(p + s^i\right)(x - e_0) & \text{if} \quad x > e_0, \\ 0 & \text{else.} \end{cases}$$

This is identical to the one-period model with p replaced by $p + s^i$ and T replaced by ΔT_i. Therefore, we obtain the solution directly from the one-period model as

$$V_x^i(t,x) = \frac{p + s^i}{1 + \frac{e^{-\frac{2c(p+s^i)(e_0-x)+(p+s^i)^2(\Delta T_i - t)}{2c^2\sigma^2}\left(1+\operatorname{erf}\left(\frac{e_0-x}{\sqrt{2}\sigma\sqrt{\Delta T_i - t}}\right)\right)}}{1-\operatorname{erf}\left(\frac{c(e_0-x)+(p+s^i)(\Delta T_i - t)}{\sqrt{2}c\sigma\sqrt{\Delta T_i - t}}\right)}}.$$

3.2 Multi-Period Model with Varying Price Parameter

In this section, we introduce a more realistic approach to the multi-period model, as we now allow the price parameter to vary throughout the sub-period considered. This means that during the optimization procedure, the agent takes into account the changes in her expectation of the initial allowance price for the next time period. To this end, we need to introduce an additional process Z driven solely by Brownian motion that simulates the initial value of X in the next time period. From this process, we may therefore compute the anticipated price. Based on this approach, we will construct the multi-period model II.

3.2.1 Derivation of the SDE

As before in Section 3.1, we consider a time period $[0, T]$ partitioned into $0 = T_0 < T_1 < \ldots < T_i < \ldots < T_N = T$. We define the emission rate $(Y_t)_{t\in[0,T]}$ for the three different model variants as before and the total expected emissions $(X_t)_{t\in[T_i,T_{i+1}]}$ are still defined as given in Definition 3.1. For each model we now present the derivation of the SDEs and the definition of the newly introduced process Z separately. In each case we will obtain SDEs of the form

$$\begin{aligned} \mathrm{d}X_t^i &= -u_t^i \mathrm{d}t + G^i(t)\mathrm{d}W_t^i \\ \mathrm{d}Z_t^i &= H^i(t)\mathrm{d}W_t^i. \end{aligned}$$

Brownian Model Variant

In the Brownian model variant with Y given by

$$\mathrm{d}Y_t = \mu \mathrm{d}t + \sigma \mathrm{d}W_t$$

we compute X as in Section 3.1 and obtain

$$X_t = X_{T_i}^+ - \int_{T_i}^t u_s \mathrm{d}s + \sigma \int_{T_i}^t (T_{i+1} - s)\mathrm{d}W_s$$

where $X_{T_i}^+$ is again

$$X_{T_i}^+ = \mathrm{E}\left[\int_{T_i}^{T_{i+1}} Y_s \mathrm{d}s \,\middle|\, \mathcal{F}_{T_i}\right] = y_0\,\Delta T_i + \frac{T_{i+1}^2 - T_i^2}{2}\,\mu + \sigma\,\Delta T_i\,W_{T_i} = x_0^i + \sigma\,\Delta T_i\,W_{T_i}$$

with ΔT_i defined as $\Delta T_i = T_{i+1} - T_i$. Note that we then have

$$X^+_{T_{i+1}} = y_0\,\Delta T_{i+1} + \frac{T^2_{i+2} - T^2_{i+1}}{2}\,\mu + \sigma\,\Delta T_{i+1}\,W_{T_i+1}.$$

Now we assume that the partition considered here is equidistant, i.e. $\Delta T_i = \Delta T_j$ for any i and j, and define $\Delta T \coloneqq \Delta T_i$. By noting that $T_i = i\Delta T$, we rewrite the expression as

$$\begin{aligned}
X^+_{T_{i+1}} &= y_0\,\Delta T_{i+1} + \frac{(T_{i+2} - T_{i+1})\,(T_{i+2} + T_{i+1})}{2}\,\mu + \sigma\,\Delta T_{i+1}\,W_{T_{i+1}} \\
&= y_0\,\Delta T + \frac{\Delta T\,((i+2)\Delta T + (i+1)\Delta T)}{2}\,\mu + \sigma\,\Delta T\,W_{T_{i+1}} \\
&= y_0\,\Delta T + \frac{\Delta T\,((i+1)\Delta T + i\Delta T)}{2}\,\mu + \frac{\Delta T\,(\Delta T + \Delta T)}{2}\,\mu + \sigma\,\Delta T\,W_{T_{i+1}} \\
&= y_0\,\Delta T + \frac{(T_{i+1} - T_i)\,(T_{i+1} + T_i)}{2}\,\mu + \Delta T^2\,\mu + \sigma\,\Delta T\,\left(W_{T_{i+1}} - W_{T_i} + W_{T_i}\right) \\
&= y_0\,\Delta T + \frac{T^2_{i+1} - T^2_i}{2}\,\mu + \sigma\,\Delta T\,W_{T_i} + \Delta T^2\,\mu + \sigma\,\Delta T\,\left(W_{T_{i+1}} - W_{T_i}\right) \\
&= X^+_{T_i} + \Delta T^2\,\mu + \sigma\,\Delta T\,\left(W_{T_{i+1}} - W_{T_i}\right).
\end{aligned}$$

We therefore define another stochastic process $Z = (Z_t)_{t\in[0,T]}$ as $Z_0 = X_0 + \Delta T^2\,\mu$ and

$$Z_t = Z^+_{T_i} + \sigma\,\Delta T\int_{T_i}^{t} \mathrm{d}W_s \quad \text{for } t \in (T_i, T_{i+1}],$$

with $Z^+_{T_i} = X^+_{T_i} + \Delta T^2\,\mu$. Then it follows that

$$Z_{T_{i+1}} = Z^+_{T_i} + \sigma\,\Delta T\int_{T_i}^{T_{i+1}} \mathrm{d}W_s = X^+_{T_i} + \Delta T^2\,\mu + \sigma\,\Delta T\,\left(W_{T_{i+1}} - W_{T_i}\right) = X^+_{T_{i+1}}.$$

Therefore, we may use the process Z to predict the initial value of the total expected emissions X in the next time period. Furthermore, by definition, Z satisfies the martingale property within each time period, i.e. for $s, t \in (T_i, T_{i+1}]$ and $s < t$ it holds that $Z_s = \mathrm{E}\left[Z_t \,|\, \mathcal{F}_s\right]$. In particular, we have $Z_t = \mathrm{E}\left[Z_{T_{i+1}} | \mathcal{F}_t\right]$ for $t \in (T_i, T_{i+1}]$. Hence for each $t \in (T_i, T_{i+1}]$, we have that Z_t indeed represents the agents expectation at time t on the total expected emissions at the beginning of time period $i+1$ given by $X^+_{T_{i+1}}$.

Remark 3.14. Alternatively, we could define Z as

$$Z_t = Z^+_{T_i} + \mu\,\Delta T\int_{T_i}^{t} \mathrm{d}s + \sigma\,\Delta T\int_{T_i}^{t} \mathrm{d}W_s$$

with $Z^+_{T_i} = X^+_{T_i}$. In this case $Z_{T_{i+1}} = X^+_{T_{i+1}}$ still holds but Z would no longer be a martingale.

We now proceed similarly to Section 3.1.1: We transform our time horizon from $[0, T]$ to the respective sub-period $(T_i, T_{i+1}]$ by setting $\hat{t} = t - T_i$. We define $u^i_{\hat{t}} = u_{T_i+\hat{t}}$, $X^i_{\hat{t}} = X_{T_i+\hat{t}}$, $Z^i_{\hat{t}} = Z_{T_i+\hat{t}}$ and $W^i_{\hat{t}} = W_{T_i+\hat{t}}$. Furthermore, we set $X^i_0 = X^+_{T_i}$, $Z^i_0 = Z^+_{T_i}$ and $W^i_0 = W_{T_i}$. By substituting $\hat{s} = s - T_i$ in the integral equations for X and Z, we obtain

$$\begin{aligned}
X^i_{\hat{t}} &= X^i_0 - \int_0^{\hat{t}} u^i_{\hat{s}}\mathrm{d}\hat{s} + \sigma\int_0^{\hat{t}} (\Delta T - \hat{s})\mathrm{d}W^i_{\hat{s}} \\
Z^i_{\hat{t}} &= Z^i_0 + \sigma\,\Delta T\int_0^{\hat{t}} \mathrm{d}W^i_{\hat{s}},
\end{aligned}$$

from which we derive the stochastic differential equations

$$\begin{aligned} \mathrm{d}X^i_{\hat{t}} &= -u^i_{\hat{t}}\mathrm{d}\hat{t} + \sigma\left(\Delta T - \hat{t}\right)\mathrm{d}W^i_{\hat{t}}, \qquad X^i_0 = x^i_0 + \sigma\,\Delta T\,W_{T_i} \\ \mathrm{d}Z^i_{\hat{t}} &= \sigma\,\Delta T\,\mathrm{d}W^i_{\hat{t}}, \qquad Z^i_0 = x^i_0 + \sigma\,\Delta T\,W_{T_i} + \Delta T^2\,\mu. \end{aligned}$$

These deliver the functions G^i and H^i as $G^i(t) = \sigma\,(\Delta T - t)$ and $H^i(t) = \sigma\,\Delta T$.

Ornstein-Uhlenbeck Model Variant

We now have Y given as

$$\mathrm{d}Y_t = \theta\,(\mu - Y_t) + \sigma\mathrm{d}W_t,$$

which implies as shown in Section 3.1.1 that for X we have

$$X_t = X^+_{T_i} - \int_{T_i}^t u_s\mathrm{d}s + \sigma\int_{T_i}^t \frac{1-\mathrm{e}^{-\theta(T_{i+1}-s)}}{\theta}\,\mathrm{d}W_s$$

for $t \in (T_i, T_{i+1}]$. Furthermore, we have seen that $X^+_{T_i}$ can be expressed as

$$X^+_{T_i} = x^i_0 - \sigma\,\frac{\mathrm{e}^{-\theta T_{i+1}} - \mathrm{e}^{-\theta T_i}}{\theta}\int_0^{T_i}\mathrm{e}^{\theta s}\mathrm{d}W_s,$$

where

$$x^i_0 = (\mu - y_0)\,\frac{\mathrm{e}^{-\theta T_{i+1}} - \mathrm{e}^{-\theta T_i}}{\theta} + \mu\,\Delta T_i.$$

Then clearly we have

$$X^+_{T_{i+1}} = x^{i+1}_0 - \sigma\,\frac{\mathrm{e}^{-\theta T_{i+2}} - \mathrm{e}^{-\theta T_{i+1}}}{\theta}\int_0^{T_{i+1}}\mathrm{e}^{\theta s}\mathrm{d}W_s$$

with

$$x^{i+1}_0 = (\mu - y_0)\,\frac{\mathrm{e}^{-\theta T_{i+2}} - \mathrm{e}^{-\theta T_{i+1}}}{\theta} + \mu\,\Delta T_{i+1}.$$

We now again assume that all time periods are equidistant, i.e. we assume that $\Delta T_i = \Delta T_j$ for any $i \neq j$. We define $\Delta T \coloneqq \Delta T_i$, thus we have $T_i = i\Delta T$ and rewrite

$$\mathrm{e}^{-\theta T_{i+1}} - \mathrm{e}^{-\theta T_i} = \mathrm{e}^{-\theta(i+1)\Delta T} - \mathrm{e}^{-\theta i\Delta T} = \mathrm{e}^{-\theta i\Delta T}\left(\mathrm{e}^{-\theta\Delta T} - 1\right).$$

With this we have

$$\begin{aligned} X^+_{T_i} &= (\mu - y_0)\,\frac{\mathrm{e}^{-\theta T_{i+1}} - \mathrm{e}^{-\theta T_i}}{\theta} + \mu\,\Delta T_i - \sigma\,\frac{\mathrm{e}^{-\theta T_{i+1}} - \mathrm{e}^{-\theta T_i}}{\theta}\int_0^{T_i}\mathrm{e}^{\theta s}\mathrm{d}W_s \\ &= (\mu - y_0)\,\mathrm{e}^{-\theta i\Delta T}\,\frac{\mathrm{e}^{-\theta\Delta T} - 1}{\theta} + \mu\,\Delta T - \sigma\,\mathrm{e}^{-\theta i\Delta T}\,\frac{\mathrm{e}^{-\theta\Delta T} - 1}{\theta}\int_0^{T_i}\mathrm{e}^{\theta s}\mathrm{d}W_s \end{aligned}$$

and compute

$$\begin{aligned} X^+_{T_{i+1}} &= (\mu - y_0)\,\mathrm{e}^{-\theta(i+1)\Delta T}\,\frac{\mathrm{e}^{-\theta\Delta T} - 1}{\theta} + \mu\,\Delta T - \sigma\,\mathrm{e}^{-\theta(i+1)\Delta T}\,\frac{\mathrm{e}^{-\theta\Delta T} - 1}{\theta}\int_0^{T_{i+1}}\mathrm{e}^{\theta s}\mathrm{d}W_s \\ &= \mathrm{e}^{-\theta\Delta T}\left((\mu - y_0)\,\mathrm{e}^{-\theta i\Delta T}\,\frac{\mathrm{e}^{-\theta\Delta T} - 1}{\theta} + \mu\,\Delta T - \sigma\,\mathrm{e}^{-\theta i\Delta T}\,\frac{\mathrm{e}^{-\theta\Delta T} - 1}{\theta}\int_0^{T_i}\mathrm{e}^{\theta s}\mathrm{d}W_s\right) \\ &\quad - \mathrm{e}^{-\theta\Delta T}\,\mu\,\Delta T + \mu\,\Delta T - \sigma\,\mathrm{e}^{-\theta(i+1)\Delta T}\,\frac{\mathrm{e}^{-\theta\Delta T} - 1}{\theta}\int_{T_i}^{T_{i+1}}\mathrm{e}^{\theta s}\mathrm{d}W_s \\ &= \mathrm{e}^{-\theta\Delta T}X^+_{T_i} + \mu\,\Delta T\left(1 - \mathrm{e}^{-\theta\Delta T}\right) + \sigma\,\mathrm{e}^{-\theta(i+1)\Delta T}\,\frac{1-\mathrm{e}^{-\theta\Delta T}}{\theta}\int_{T_i}^{T_{i+1}}\mathrm{e}^{\theta s}\mathrm{d}W_s. \end{aligned}$$

We therefore define the process Z on $(T_i, T_{i+1}]$ as

$$Z_t = Z^+_{T_i} + \sigma\, \mathrm{e}^{-\theta(i+1)\Delta T}\, \frac{1-\mathrm{e}^{-\theta\Delta T}}{\theta} \int_{T_i}^{t} \mathrm{e}^{\theta s} \mathrm{d}W_s,$$

where $Z^+_{T_i}$ is defined as

$$Z^+_{T_i} = \mathrm{e}^{-\theta\Delta T} X^+_{T_i} + \mu\, \Delta T \left(1 - \mathrm{e}^{-\theta\Delta T}\right).$$

Then we have again

$$Z_{T_{i+1}} = Z^+_{T_i} + \sigma\, \mathrm{e}^{-\theta(i+1)\Delta T}\, \frac{1-\mathrm{e}^{-\theta\Delta T}}{\theta} \int_{T_i}^{T_{i+1}} \mathrm{e}^{\theta s} \mathrm{d}W_s = X^+_{T_{i+1}}.$$

So again we have defined Z in such a way that it can be used to predict the initial value of the total expected emissions of the next time period as given by $X^+_{T_{i+1}}$; in particular, also here Z satisfies the martingale property within each time period $(T_i, T_{i+1}]$.

As for the Brownian model, the next step is to perform the shift in time: We set $\hat{t} = t - T_i$ and define $u^i_{\hat{t}} = u_{T_i+\hat{t}}$, $X^i_{\hat{t}} = X_{T_i+\hat{t}}$, $Z^i_{\hat{t}} = Z_{T_i+\hat{t}}$ and $W^i_{\hat{t}} = W_{T_i+\hat{t}}$. In addition, we define $X^i_0 = X^+_{T_i}$, $Z^i_0 = Z^+_{T_i}$ and $W^i_0 = W_{T_i}$. In order to derive the corresponding SDEs, we substitute $\hat{s} = s - T_i$ in the integral equations as

$$\begin{aligned}
X^i_{\hat{t}} &= X^i_0 - \int_0^{\hat{t}} u^i_{\hat{s}} \mathrm{d}\hat{s} + \sigma \int_0^{\hat{t}} \frac{1-\mathrm{e}^{-\theta(\Delta T-\hat{s})}}{\theta} \mathrm{d}W^i_{\hat{s}} \\
Z^i_{\hat{t}} &= Z^i_0 + \sigma\, \mathrm{e}^{-\theta(i+1)\Delta T}\, \frac{1-\mathrm{e}^{-\theta\Delta T}}{\theta} \int_0^{\hat{t}} \mathrm{e}^{\theta(T_i+\hat{s})} \mathrm{d}W^i_{\hat{s}} \\
&= Z^i_0 + \sigma\, \mathrm{e}^{-\theta(i+1)\Delta T}\, \frac{1-\mathrm{e}^{-\theta\Delta T}}{\theta} \int_0^{\hat{t}} \mathrm{e}^{\theta(i\Delta T+\hat{s})} \mathrm{d}W^i_{\hat{s}} \\
&= Z^i_0 + \sigma\, \mathrm{e}^{-\theta\Delta T}\, \frac{1-\mathrm{e}^{-\theta\Delta T}}{\theta} \int_0^{\hat{t}} \mathrm{e}^{\theta\hat{s}} \mathrm{d}W^i_{\hat{s}} \\
&= Z^i_0 + \sigma\, \frac{1-\mathrm{e}^{-\theta\Delta T}}{\theta} \int_0^{\hat{t}} \mathrm{e}^{-\theta(\Delta T-\hat{s})} \mathrm{d}W^i_{\hat{s}}
\end{aligned}$$

and obtain

$$\begin{aligned}
\mathrm{d}X^i_{\hat{t}} &= -u^i_{\hat{t}} \mathrm{d}\hat{t} + \sigma\, \frac{1-\mathrm{e}^{-\theta(\Delta T-\hat{t})}}{\theta} \mathrm{d}W^i_{\hat{t}} \qquad X^i_0 = x^i_0 + \sigma\, \mathrm{e}^{-\theta i\Delta T}\, \frac{1-\mathrm{e}^{-\theta\Delta T}}{\theta} \int_0^{T_i} \mathrm{e}^{\theta s} \mathrm{d}W_s \\
\mathrm{d}Z^i_{\hat{t}} &= \sigma\, \frac{1-\mathrm{e}^{-\theta\Delta T}}{\theta}\, \mathrm{e}^{-\theta(\Delta T-\hat{t})}\, \mathrm{d}W^i_{\hat{t}} \qquad Z^i_0 = \mathrm{e}^{-\theta\Delta T} X^i_0 + \mu\, \Delta T \left(1 - \mathrm{e}^{-\theta\Delta T}\right).
\end{aligned}$$

Thus for the Ornstein-Uhlenbeck model, G^i and H^i are given by

$$\begin{aligned}
G^i(t) &= \sigma\, \frac{1-\mathrm{e}^{-\theta(\Delta T-t)}}{\theta}, \\
H^i(t) &= \sigma\, \frac{1-\mathrm{e}^{-\theta\Delta T}}{\theta}\, \mathrm{e}^{-\theta(\Delta T-t)}.
\end{aligned}$$

Simple Model Variant

In analogy to Section 3.1.1, we have

$$X_t = X_{T_i}^+ - \int_{T_i}^t u_s \mathrm{d}s + \sigma \int_{T_i}^t \mathrm{d}W_s.$$

Since we cannot compute $X_{T_i}^+$ in this case, we define it as

$$X_{T_i}^+ = x_0^i + \sigma\, W_{T_i},$$

where $x_0^i \in \mathbb{R}$. In the following we assume that $x_0^i = x_0^j =: x_0$, so we can simplify to

$$X_{T_i}^+ = x_0 + \sigma\, W_{T_i}.$$

Then it holds that

$$\begin{aligned} X_{T_{i+1}}^+ &= x_0 + \sigma\, W_{T_{i+1}} \\ &= x_0 + \sigma\, W_{T_i} + \sigma(W_{T_{i+1}} - W_{T_i}) \\ &= X_{T_i}^+ + \sigma(W_{T_{i+1}} - W_{T_i}). \end{aligned}$$

Therefore, we define Z as $Z_0 = X_0$ and

$$Z_t = Z_{T_i}^+ + \sigma \int_{T_i}^t \mathrm{d}W_s \quad \text{for } t \in (T_i, T_{i+1}]$$

with $Z_{T_i}^+ = X_{T_i}^+$. Then it follows that $Z_{T_{i+1}} = X_{T_{i+1}}^+$ and Z satisfies the martingale property on $(T_i, T_{i+1}]$. Moreover, this implies $Z_{T_{i+1}} = Z_{T_{i+1}}^+$, thus Z is continuous. We define $\hat{t} = t - T_i$ and substitute $\hat{s} = s - T_i$ as above to result in

$$\begin{aligned} X_{\hat{t}}^i &= X_0^i - \int_0^{\hat{t}} u_{\hat{s}}^i \mathrm{d}\hat{s} + \sigma \int_0^{\hat{t}} \mathrm{d}W_{\hat{s}}^i \\ Z_{\hat{t}}^i &= Z_0^i + \sigma \int_0^{\hat{t}} \mathrm{d}W_{\hat{s}}^i \end{aligned}$$

and obtain the differential equations

$$\begin{aligned} \mathrm{d}X_{\hat{t}}^i &= -u_{\hat{t}}^i \mathrm{d}\hat{t} + \sigma \mathrm{d}W_{\hat{t}}^i, \quad X_0^i = x_0 + \sigma\, \Delta T\, W_{T_i} \\ \mathrm{d}Z_{\hat{t}}^i &= \sigma \mathrm{d}W_{\hat{t}}^i, \quad Z_0^i = x_0 + \sigma\, \Delta T\, W_{T_i}. \end{aligned}$$

Thus we have for the functions G^i and H^i that $G^i(t) = H^i(t) = \sigma$.

Summary

For each of the model variants, we defined a process Z which represents the agent's expectation on $X_{T_{i+1}}^+$ in the course of time period i. This is useful since the initially expected BAU emissions of the next time period $X_{T_{i+1}}^+$ are needed to compute the allowance price at the beginning of the next time period; the thus computed price in turn is required to assess the value of an unused allowance. We then derived an SDE to describe Z^i in each time period.

3.2.2 Cost Minimization

We consider the minimization of costs on the time period i given by the interval $[T_i, T_{i+1}]$. In the previous model we have seen that there exists a function $S^i : [0, \Delta T_i] \times \mathbb{R} \to \mathbb{R}$ which allows us to compute the price of an allowance in time period i for a given time and a given value of x. We now assume that also in this model there exists a function $\tilde{S}_0^i : \mathbb{R} \to \mathbb{R}$ representing the price of an allowance at the beginning of time period i for a given value of x; we will ascertain that this holds in Section 3.2.5 below. Then $\tilde{S}_0^{i+1}$ is the function describing the price at the beginning of the subsequent period and we may compute the price as $\tilde{S}_0^{i+1}\big(X^+_{T_{i+1}}\big)$. Therefore we formulate the penalty function as

$$P^i\left(X_{T_{i+1}}, X^+_{T_{i+1}}\right) = \begin{cases} \left(p + \tilde{S}_0^{i+1}\left(X^+_{T_{i+1}}\right)\right)\left(X_{T_{i+1}} - e_0^i\right) & \text{if} \quad X_{T_{i+1}} > e_0^i, \\ \tilde{S}_0^{i+1}\left(X^+_{T_{i+1}}\right)\left(X_{T_{i+1}} - e_0^i\right) & \text{else.} \end{cases}$$

In comparison to multi-period model I, the price parameter s^i has now been replaced by $\tilde{S}_0^{i+1}\big(X^+_{T_{i+1}}\big)$. Since $Z_{T_{i+1}} = X^+_{T_{i+1}}$, we rewrite this as

$$P^i\left(X_{T_{i+1}}, Z_{T_{i+1}}\right) = \begin{cases} \left(p + \tilde{S}_0^{i+1}\left(Z_{T_{i+1}}\right)\right)\left(X_{T_{i+1}} - e_0^i\right) & \text{if} \quad X_{T_{i+1}} > e_0^i, \\ \tilde{S}_0^{i+1}\left(Z_{T_{i+1}}\right)\left(X_{T_{i+1}} - e_0^i\right) & \text{else.} \end{cases}$$

Hence Z enters the penalty function as a second variable and is therefore also a variable of the value function, which is now defined by

$$V^i(t,x,z) = \inf_{u \in \mathcal{A}_1^i(t)} \mathrm{E}^{t,x,z}\left[\mathrm{e}^{-rT_{i+1}} P^i\left(X_{T_{i+1}}, Z_{T_{i+1}}\right) + \int_t^{T_{i+1}} C(u_s)\,\mathrm{e}^{-rs}\mathrm{d}s\right].$$

In this expression, the admissibility set is defined as in the previous model as

$$\mathcal{A}_1^i(t) = \Bigg\{ u = (u_s)_{s\in[t,T_{i+1}]} \text{ an } \mathcal{F}\text{-progressively measurable process into } \mathcal{U} \\ \text{with } \mathrm{E}\left[\int_t^{T_{i+1}} |u_s|^2 \mathrm{d}s\right] < \infty \Bigg\}$$

with $\mathcal{U} = [0, \infty)$, and the costs are modeled by the cost function

$$C^i(u) = \frac{1}{2}\, c^i\, u^2.$$

We perform the shift in time $\hat{t} = t - T_i$ again and substitute $\hat{s} = s - T_i$ to result in

$$V^i(\hat{t},x,z) = \inf_{u^i \in \mathcal{A}^i(\hat{t})} \mathrm{E}^{\hat{t},x,z}\left[\mathrm{e}^{-rT_{i+1}} P^i\left(X^i_{\Delta T}, Z^i_{\Delta T}\right) + \int_{\hat{t}}^{\Delta T} C^i(u^i_{\hat{s}})\,\mathrm{e}^{-r(T_i+\hat{s})}\mathrm{d}\hat{s}\right],$$

where again

$$\mathcal{A}^i(t) = \Bigg\{ u^i = \left(u^i_s\right)_{s\in[0,\Delta T_i]} \text{ an } \mathcal{F}^i\text{-progressively measurable process into } \mathcal{U} \\ \text{with } \mathrm{E}\left[\int_0^{\Delta T_i} |u^i_s|^2 \mathrm{d}s\right] < \infty \Bigg\}.$$

As before, we apply the Bellman principle to heuristically derive the HJB equation (for ease of notation we write s and t instead of $\hat{s}$ and $\hat{t}$ in the following). For $\tau \in \mathbb{R}$ with $\tau > t$ we compute

$$\begin{aligned}
V^i(t,x,z) &= \inf_{u^i \in \mathcal{A}^i(t)} \mathrm{E}^{t,x,z}\left[\int_t^\tau C^i(u_s^i)\,\mathrm{e}^{-r(T_i+s)}\mathrm{d}s + V^i\left(\tau, X_\tau^i, Z_\tau^i\right)\right] \\
&= \inf_{u^i \in \mathcal{A}^i(t)} \mathrm{E}^{t,x,z}\left[\int_t^\tau C^i(u_s^i)\,\mathrm{e}^{-r(T_i+s)}\mathrm{d}s + V^i\left(t, X_t^i, Z_t^i\right) + \int_t^\tau V_t^i\left(s, X_s^i, Z_s^i\right)\mathrm{d}s\right. \\
&\quad + \int_t^\tau V_x^i\left(s, X_s^i, Z_s^i\right)\mathrm{d}X_s^i + \int_t^\tau V_z^i\left(s, X_s^i, Z_s^i\right)\mathrm{d}Z_s^i \\
&\quad + \frac{1}{2}\int_t^\tau V_{xx}^i\left(s, X_s^i, Z_s^i\right)\mathrm{d}[X^i]_s + \frac{1}{2}\int_t^\tau V_{xz}^i\left(s, X_s^i, Z_s^i\right)\mathrm{d}[X^i, Z^i]_s \\
&\quad \left. + \frac{1}{2}\int_t^\tau V_{zx}^i\left(s, X_s^i, Z_s^i\right)\mathrm{d}[Z^i, X^i]_s + \frac{1}{2}\int_t^\tau V_{zz}^i\left(s, X_s^i, Z_s^i\right)\mathrm{d}[Z^i]_s\right].
\end{aligned}$$

We note that although $W_0^i \neq 0$, we still have $[W^i]_t = t$, as can be seen in appendix A.4.1, and therefore

$$\begin{aligned}
[X^i]_t &= \int_0^t G^i(s)^2\mathrm{d}s, \\
[X^i, Z^i]_t = [Z^i, X^i]_t &= \int_0^t G^i(s)\,H^i(s)\mathrm{d}s, \\
[Z^i]_t &= \int_0^t H^i(s)^2\mathrm{d}s.
\end{aligned}$$

Furthermore, we assume that $V_{xz} = V_{zx}$. Then, by assuming that the stochastic integral is a martingale, we rewrite

$$\begin{aligned}
V^i(t,x,z) &= \inf_{u^i \in \mathcal{A}^i(t)} \mathrm{E}^{t,x,z}\left[\int_t^\tau C^i(u_s^i)\,\mathrm{e}^{-r(T_i+s)}\mathrm{d}s + V^i(t, X_t^i, Z_t^i) + \int_t^\tau V_t^i\left(s, X_s^i, Z_s^i\right)\mathrm{d}s\right. \\
&\quad - \int_t^\tau V_x^i\left(s, X_s^i, Z_s^i\right)\,u_s^i\mathrm{d}s + \int_t^\tau V_x^i\left(s, X_s^i, Z_s^i\right)\,G^i(s)\mathrm{d}W_s^i \\
&\quad + \int_t^\tau V_z^i\left(s, X_s^i, Z_s^i\right)H^i(s)\mathrm{d}W_s^i + \frac{1}{2}\int_t^\tau V_{xx}^i\left(s, X_s^i, Z_s^i\right)\,G^i(s)^2\mathrm{d}s \\
&\quad \left. + \int_t^\tau V_{xz}^i\left(s, X_s^i, Z_s^i\right)G^i(s)\,H^i(s)\mathrm{d}s + \frac{1}{2}\int_t^\tau V_{zz}^i\left(s, X_s^i, Z_s^i\right)\,H^i(s)^2\mathrm{d}s\right] \\
&= \inf_{u^i \in \mathcal{A}^i(t)} \mathrm{E}^{t,x,z}\left[V^i\left(t, X_t^i, Z_t^i\right) + \int_t^\tau \left(C^i(u_s^i)\,\mathrm{e}^{-r(T_i+s)} + V_t\left(s, X_s^i, Z_s^i\right)\right.\right. \\
&\quad - u_s^i\,V_x^i\left(s, X_s^i, Z_s^i\right) + \frac{1}{2}\,G^i(s)^2\,V_{xx}^i\left(s, X_s^i, Z_s^i\right) \\
&\quad \left.\left. + \;G^i(s)\,H^i(s)\,V_{xz}^i\left(s, X_s^i, Z_s^i\right) + \frac{1}{2}\,H^i(s)^2\,V_{zz}^i\left(s, X_s^i, Z_s^i\right)\right)\mathrm{d}s\right].
\end{aligned}$$

Again we eliminate $V^i(t,x,z)$ on both sides, divide by $\tau - t$ and let $\tau \to t$:

$$\begin{aligned}
0 = \inf_{u^i \in \mathcal{A}^i(t)} \mathrm{E}^{t,x,z} \Bigg[\lim_{\tau \downarrow t} \frac{1}{\tau - t} \int_t^\tau \Big(& C^i(u_s^i)\, \mathrm{e}^{-r(T_i+s)} + V_t\left(s, X_s^i, Z_s^i\right) \\
& - u_s^i\, V_x^i\left(s, X_s^i, Z_s^i\right) + \frac{1}{2}\, G^i(s)^2\, V_{xx}^i\left(s, X_s^i, Z_s^i\right) \\
& + G^i(s)\, H^i(s)\, V_{xz}^i\left(s, X_s^i, Z_s^i\right) + \frac{1}{2}\, H^i(s)^2\, V_{zz}^i\left(s, X_s^i, Z_s^i\right) \mathrm{d}s \Big) \Bigg] \\
= \inf_{u^i \in \mathcal{A}^i(t)} \mathrm{E}^{t,x,z} \Big[& C^i(u_t^i)\, \mathrm{e}^{-r(T_i+t)} + V_t^i\left(t, X_t^i, Z_t^i\right) - u_t^i\, V_x^i\left(t, X_t^i, Z_t^i\right) \\
& + \frac{1}{2}\, G^i(t)^2\, V_{xx}^i\left(t, X_t^i, Z_t^i\right) + G^i(t)\, H^i(t)\, V_{xz}^i\left(t, X_t^i, Z_t^i\right) \\
& + \frac{1}{2} H^i(t)^2\, V_{zz}^i\left(t, X_t^i, Z_t^i\right) \Big] \\
= \inf_{u^i \in \mathcal{U}} \Big\{ & C^i(u^i)\, \mathrm{e}^{-r(T_i+t)} + V_t^i(t,x,z) - u^i\, V_x^i(t,x,z) + \frac{1}{2}\, G^i(t)^2\, V_{xx}^i(t,x,z) \\
& + G^i(t)\, H^i(t)\, V_{xz}^i(t,x,z) + \frac{1}{2}\, H^i(t)^2\, V_{zz}^i(t,x,z) \Big\}.
\end{aligned}$$

Thus we have arrived at the HJB equation. Minimizing with respect to u^i yields as before

$$u^i(t,x,z) = \frac{V_x^i(t,x,z)}{c^i}\, \mathrm{e}^{r(T_i+t)}.$$

We insert this in the HJB equation above and obtain the characteristic PDE

$$V_t^i = \frac{1}{2}\, \frac{\left(V_x^i\right)^2}{c^i}\, \mathrm{e}^{r(T_i+\hat{t})} - \frac{1}{2}\, G^i(t)^2\, V_{xx}^i - G^i(t)\, H^i(t)\, V_{xz}^i - \frac{1}{2}\, H^i(t)^2\, V_{zz}^i.$$

This differs from the PDE of multi-period model I in Section 3.1.2 by the two final terms only; the remainder of the PDE remains unchanged. We compute the final condition by inserting $t = \Delta T$ in the value function as follows:

$$\begin{aligned}
V^i(\Delta T, x, z) &= \inf_{u_{\Delta T}} \mathrm{E}\left[\mathrm{e}^{-rT_{i+1}}\, P^i\left(X_{\Delta T}^i, Z_{\Delta T}^i\right) \,\middle|\, X_{\Delta T}^i = x, Z_{\Delta T}^i = z \right] \\
&= \mathrm{e}^{-rT_{i+1}} P^i(x,z) \\
&= \begin{cases} \mathrm{e}^{-rT_{i+1}} \left(p + \tilde{S}_0^{i+1}(z) \right)(x - e_0^i) & \text{if} \quad x > e_0^i, \\ \mathrm{e}^{-rT_{i+1}} \tilde{S}_0^{i+1}(z)(x - e_0^i) & \text{else.} \end{cases}
\end{aligned}$$

Again the solution of the PDE allows us to compute the allowance price by introducing the price function S^i for each period i, which is given as

$$S^i(t,x,z) = c^i\, u^i(t,x,z).$$

Note that in contrast to the price function $\tilde{S}_0^i$ we assumed to exist above, this depends also on z. We will explain how this can be handled in Section 3.2.5.

Summary

We formulated the cost minimization problem of the agent and derived the corresponding HJB equation, from which we obtained the characteristic PDE. Due to the additional stochastic process Z in this model, both the value function and the PDE depend on a second spatial variable; the same holds for the allowance price function.

3.2.3 Solution of the PDE

The next step is again to solve the characteristic PDE; to simplify notation, we again write c and e_0 instead of c^i and e_0^i. In the present model, we will need to solve the PDE numerically for each of the model variants; we will argue why also for the simple model variant no analytical solution is available. Hence we cannot apply the verification theorem in Proposition 2.3 to show that u^i as obtained from the numerical PDE solution is indeed the optimal abatement rate.

Simple Model Variant

Since in the simple model we have $G^i(t) = H^i(t) = \sigma$, we need to consider the PDE

$$V_t^i = \frac{1}{2}\frac{\left(V_x^i\right)^2}{c}\,\mathrm{e}^{r(T_i+t)} - \frac{1}{2}\,\sigma^2\,V_{xx}^i - \sigma^2\,V_{xz}^i - \frac{1}{2}\,\sigma^2\,V_{zz}^i$$

with final condition

$$V^i(\Delta T, x, z) = \mathrm{e}^{-rT_{i+1}}P^i(x, z).$$

We again perform a time reversion by substituting $t = \Delta T - \tilde{t}$ and defining $\tilde{V}^i(t, x, z) = V^i(\Delta T - \tilde{t}, x, z)$. As before, $V_t^i(t, x, z) = -\tilde{V}_{\tilde{t}}^i(\tilde{t}, x, z)$ and therefore

$$\tilde{V}_t^i = -\frac{1}{2}\frac{\left(\tilde{V}_x^i\right)^2}{c}\,\mathrm{e}^{r(T_{i+1}-\tilde{t})} + \frac{1}{2}\,\sigma^2\,\tilde{V}_{xx}^i + \sigma^2\,\tilde{V}_{xz}^i + \frac{1}{2}\,\sigma^2\,\tilde{V}_{zz}^i$$

with initial value

$$\tilde{V}^i(0, x, z) = \mathrm{e}^{-rT_{i+1}}P^i(x, z).$$

If we now set $r = 0$ as we did in the simple variant of previous models, we need to consider

$$\tilde{V}_t^i = -\frac{1}{2}\frac{\left(\tilde{V}_x^i\right)^2}{c} + \frac{1}{2}\,\sigma^2\,\tilde{V}_{xx}^i + \sigma^2\,\tilde{V}_{xz}^i + \frac{1}{2}\,\sigma^2\,\tilde{V}_{zz}^i$$

with

$$\tilde{V}^i(0, x, z) = P^i(x, z),$$

where we again have time-independent coefficient functions. The Cole-Hopf transform is also available for multi-dimensional PDEs; as explored by Evans [Eva10], it can be applied to PDEs of the form

$$\begin{aligned} v_t - a\Delta v + b|Dv|^2 = 0 \quad &\text{in} \quad (0,\infty)\times\mathbb{R}^d \\ v = g \quad &\text{on} \quad \{0\}\times\mathbb{R}^d, \end{aligned} \tag{3.7}$$

where Δ is the Laplace operator, D the differential operator, g is a function on $\mathbb{R}^d$ and $a > 0$, b are constants. Let us assume that we have a smooth solution v of this PDE. Evans then shows that if v solves the PDE above, then

$$w = \mathrm{e}^{\frac{-bv}{a}}$$

solves the PDE

$$\begin{aligned} w_t - a\Delta w = 0 \quad &\text{in} \quad (0,\infty)\times\mathbb{R}^d \\ w = \mathrm{e}^{\frac{-bg}{a}} \quad &\text{on} \quad \{0\}\times\mathbb{R}^d. \end{aligned}$$

Thus we see that $w = e^{\frac{-bv}{a}}$ is the Cole-Hopf transformation in d dimensions.

However, this does not apply in our particular case: The PDE in equation (3.7) does not contain any mixed derivatives, whereas in our PDE we have the term V_{xz}. Furthermore, we have different coefficients for the terms V_{xx} and V_{zz} as well as for the terms V_x^2 and V_z^2 (with the latter being zero). In the PDE given by equation (3.7), these are identically a and b, respectively. Thus the approach via the Cole-Hopf transformation cannot trivially be extended to the PDE in our model, so we will need to compute the solution of the PDE numerically also for the simple model variant.

Brownian Model Variant

By combining our results for G^i and H^i and the PDE derived above, we obtain as the PDE for the Brownian model variant

$$V_t^i = \frac{1}{2}\,\frac{\left(V_x^i\right)^2}{c}\,\mathrm{e}^{r(T_i+t)} - \frac{1}{2}\,\sigma^2\,(\Delta T - t)^2\;V_{xx}^i - \sigma^2\,(\Delta T - t)\,\Delta T\,V_{xz}^i - \frac{1}{2}\,\sigma^2\,\Delta T^2\,V_{zz}^i$$

with final condition

$$V^i(\Delta T, x, z) = \mathrm{e}^{-rT_{i+1}}P^i(x, z).$$

Time reversion then yields

$$\begin{aligned}\tilde{V}_t^i &= -\frac{\left(\tilde{V}_x^i\right)^2}{2c}\,\mathrm{e}^{r(T_i+\Delta T-\tilde{t})} + \frac{1}{2}\,\sigma^2\,\left(\Delta T - \Delta T + \tilde{t}\right)^2\,\tilde{V}_{xx}^i \\ &\quad + \sigma^2\,\left(\Delta T - \Delta T + \tilde{t}\right)\,\Delta T\,\tilde{V}_{xz}^i + \frac{1}{2}\,\sigma^2\,\Delta T^2\,\tilde{V}_{zz}^i \\ &= -\frac{\left(\tilde{V}_x^i\right)^2}{2c}\,\mathrm{e}^{r(T_{i+1}-\tilde{t})} + \frac{1}{2}\,\sigma^2\,\tilde{t}^2\,\tilde{V}_{xx}^i + \sigma^2\,\tilde{t}\,\Delta T\,\tilde{V}_{xz}^i + \frac{1}{2}\,\sigma^2\,\Delta T^2\,\tilde{V}_{zz}^i.\end{aligned}$$

As initial condition we obtain

$$\tilde{V}^i(0, x, z) = \mathrm{e}^{-rT_{i+1}}P^i(x, z).$$

Ornstein-Uhlenbeck Model Variant

With the results from above, the PDE in the Ornstein-Uhlenbeck model variant is given as

$$\begin{aligned}V_t^i &= \frac{1}{2}\,\frac{\left(V_x^i\right)^2}{c}\,\mathrm{e}^{r(T_i+t)} - \frac{1}{2}\,\sigma^2\,\frac{\left(1-\mathrm{e}^{-\theta(\Delta T-t)}\right)^2}{\theta^2}\,V_{xx}^i \\ &\quad - \sigma^2\,\frac{\left(1-\mathrm{e}^{-\theta(\Delta T-t)}\right)\left(1-\mathrm{e}^{-\theta\Delta T}\right)}{\theta^2}\,\mathrm{e}^{-\theta(\Delta T-t)}\,V_{xz}^i - \frac{1}{2}\,\sigma^2\,\frac{\left(1-\mathrm{e}^{-\theta\Delta T}\right)^2}{\theta^2}\,\mathrm{e}^{-2\theta(\Delta T-t)}\,V_{zz}^i\end{aligned}$$

with terminal condition

$$V^i(\Delta T, x, z) = \mathrm{e}^{-rT_{i+1}}P^i(x, z).$$

By performing the time reversion as above, we obtain

$$\begin{aligned}
\tilde{V}_t^i &= -\frac{1}{2}\frac{\left(\tilde{V}_x^i\right)^2}{c}\,\mathrm{e}^{r(T_i+\Delta T-\tilde{t})} + \frac{1}{2}\,\sigma^2\,\frac{\left(1-\mathrm{e}^{-\theta(\Delta T-\Delta T+\tilde{t})}\right)^2}{\theta^2}\,\tilde{V}_{xx}^i \\
&\quad + \sigma^2\,\frac{\left(1-\mathrm{e}^{-\theta(\Delta T-\Delta T+\tilde{t})}\right)\left(1-\mathrm{e}^{-\theta\Delta T}\right)}{\theta^2}\,\mathrm{e}^{-\theta(\Delta T-\Delta T+\tilde{t})}\,\tilde{V}_{xz}^i \\
&\quad + \frac{1}{2}\,\sigma^2\,\frac{\left(1-\mathrm{e}^{-\theta\Delta T}\right)^2}{\theta^2}\,\mathrm{e}^{-2\theta(\Delta T-\Delta T+\tilde{t})}\,\tilde{V}_{zz}^i \\
&= -\frac{1}{2}\frac{\left(\tilde{V}_x^i\right)^2}{c}\,\mathrm{e}^{r(T_{i+1}-\tilde{t})} + \frac{1}{2}\,\sigma^2\,\frac{\left(1-\mathrm{e}^{-\theta\tilde{t}}\right)^2}{\theta^2}\,\tilde{V}_{xx}^i \\
&\quad + \sigma^2\,\frac{\left(1-\mathrm{e}^{-\theta\tilde{t}}\right)\left(1-\mathrm{e}^{-\theta\Delta T}\right)}{\theta^2}\,\mathrm{e}^{-\theta\tilde{t}}\,\tilde{V}_{xz}^i + \frac{1}{2}\,\sigma^2\,\frac{\left(1-\mathrm{e}^{-\theta\Delta T}\right)^2}{\theta^2}\,\mathrm{e}^{-2\theta\tilde{t}}\,\tilde{V}_{zz}^i
\end{aligned}$$

with initial condition

$$\tilde{V}^i(0,x,z) = \mathrm{e}^{-rT_{i+1}}P^i(x,z).$$

Summary

We discussed why the Cole-Hopf transformation cannot be applied in multi-period model II, so that the PDE needs to be solved numerically in all model variants. In preparation of the numerical PDE solution, we performed the time reversion for all model variants.

3.2.4 Solution of the SDE

For each time period i, we aim to study the resulting emissions $X^i_{\Delta T_i}$ and the price process given by $S^i(t, X^i_t, Z^i_t)$. Thus, we need to solve the system of SDEs describing X^i and Z^i. Furthermore, we again require a unique solution for the verification of the HJB equation to work. We therefore again aim to apply the results in Section 2.4 to the current model; note that in this case we have a two-dimensional SDE, so we need to make use of the multi-dimensional formulation of the results.

However, in the present model we do not have an explicit solution of the characteristic PDE for any of our model variants and in turn we also do not know the drift function $-u^i$ explicitly. Therefore we may only study the volatility functions of all model variants analytically.

Lemma 3.15. *In multi-period model II the volatility functions of*

(i) the simple model variant given by

$$\begin{pmatrix} G_S^i(t) \\ H_S^i(t) \end{pmatrix} = \begin{pmatrix} \sigma \\ \sigma \end{pmatrix},$$

(ii) the Brownian model variant given by

$$\begin{pmatrix} G_B^i(t) \\ H_B^i(t) \end{pmatrix} = \begin{pmatrix} \sigma(\Delta T - t) \\ \sigma\Delta T \end{pmatrix},$$

(iii) and the Ornstein-Uhlenbeck model variant given by

$$\begin{pmatrix} G^i_{OU}(t) \\ H^i_{OU}(t) \end{pmatrix} = \begin{pmatrix} \sigma \frac{1-\mathrm{e}^{-\theta(\Delta T-t)}}{\theta} \\ \sigma \frac{1-\mathrm{e}^{-\theta\Delta T}}{\theta} \mathrm{e}^{-\theta(\Delta T-t)} \end{pmatrix}$$

satisfy Assumptions 2.14 and 2.25.

Proof. We first note that the volatility functions for all model variants are constant in (x, z) and therefore also clearly Lipschitz continuous in (x, z).

(i) In the simple model variant, the volatility function is constant and thus bounded and $\frac{1}{2}$-Hölder continuous in t.

(ii) In the Brownian model variant, both components are bounded on $[0, \Delta T]$, therefore also the norm is bounded. For Lipschitz continuity in t, we use that the second component does not depend on t, and for arbitrary $s, t \in [0, \Delta T]$ we compute

$$\left\| \begin{pmatrix} \sigma(\Delta T - t) - \sigma(\Delta T - s) \\ \sigma\Delta T - \sigma\Delta T \end{pmatrix} \right\| = \left\| \begin{pmatrix} -\sigma(t-s) \\ 0 \end{pmatrix} \right\| = \sigma|t-s|.$$

Thus the volatility is Lipschitz continuous in t, which implies $\frac{1}{2}$-Hölder continuity.

(iii) In the Ornstein-Uhlenbeck model variant, both components are continuous in t. Then also

$$\left(\sigma \frac{1-\mathrm{e}^{-\theta(\Delta T-t)}}{\theta} \right)^2 \quad \text{and} \quad \left(\sigma \frac{1-\mathrm{e}^{-\theta\Delta T}}{\theta} \mathrm{e}^{-\theta(\Delta T-t)} \right)^2$$

are continuous and by the maximum value theorem bounded on $[0, \Delta T]$. Thus for some suitable constants C_1 and C_2, we have

$$\begin{aligned} \left\| \begin{pmatrix} \sigma \frac{1-\mathrm{e}^{-\theta(\Delta T-t)}}{\theta} \\ \sigma \frac{1-\mathrm{e}^{-\theta\Delta T}}{\theta} \mathrm{e}^{-\theta(\Delta T-t)} \end{pmatrix} \right\| &= \sqrt{\left(\sigma \frac{1-\mathrm{e}^{-\theta(\Delta T-t)}}{\theta} \right)^2 + \left(\sigma \frac{1-\mathrm{e}^{-\theta\Delta T}}{\theta} \mathrm{e}^{-\theta(\Delta T-t)} \right)^2} \\ &\leq \sqrt{C_1 + C_2}, \end{aligned}$$

which provides the desired bound of the norm. To show Lipschitz continuity, we again look at both components separately. For the derivative of the first component, we have

$$G^i_{OU}(t)' = -\sigma \mathrm{e}^{-\theta(\Delta T-t)}.$$

Since this is continuous, we again obtain a bound on $[0, \Delta T]$, which implies that G^i_{OU} is Lipschitz continuous, i.e. there exists a constant K_G such that

$$|G^i_{OU}(t) - G^i_{OU}(s)| \leq K_G |t-s| \qquad \text{for all } s, t \in [0, \Delta T].$$

The derivative of the second component is given by

$$H^i_{OU}(t)' = \sigma (1 - \mathrm{e}^{-\theta\Delta T}) \mathrm{e}^{-\theta(\Delta T-t)},$$

which is also continuous and therefore bounded on $[0, \Delta T]$, so there exists a constant K_H such that

$$|H^i_{OU}(t) - H^i_{OU}(t)| \leq K_H |t-s| \qquad \text{for all } s, t \in [0, \Delta T].$$

Then we have

$$\left\| \begin{pmatrix} G^i_{OU}(t) - G^i_{OU}(s) \\ H^i_{OU}(t) - H^i_{OU}(s) \end{pmatrix} \right\| = \sqrt{\left(G^i_{OU}(t) - G^i_{OU}(s)\right)^2 + \left(H^i_{OU}(t) - H^i_{OU}(s)\right)^2}$$
$$\leq \sqrt{K_G^2 \left|t-s\right|^2 + K_H^2 \left|t-s\right|^2} = \sqrt{K_G^2 + K_H^2}\left|t-s\right|,$$

which delivers Lipschitz continuity in t, and $\frac{1}{2}$-Hölder continuity follows. □

Remark 3.16. As we cannot study the drift functions analytically, we will analyze the numerical solutions of the characteristic PDE and the drift derived from this in Section 6.3.1. We will aim to find an indication that also the drift does not violate Assumptions 2.14 and 2.25.

Remark 3.17. Since we do not have an explicit expression for the solution of the HJB equation, we cannot apply the verification theorem as given by Proposition 2.3. However, we may still try to check if the theorem applies to the setting of the present model by verifying the assumptions in the prequel of the theorem. The drift b as a function of t, x and u given by

$$b(t,x,u) = \begin{pmatrix} -u \\ 0 \end{pmatrix}$$

is clearly Lipschitz continuous in x, and $\|b\| = |u|$, thus also the linear growth bound is satisfied. As argued in the proof above, both of these properties also hold for any of the volatility functions of the model variants. The cost function remains unchanged in comparison to multi-period model I; thus it remains to consider the terminal condition given by

$$g\left((x,z)^\top\right) \coloneqq \mathrm{e}^{rT} P^i(x,z) = \begin{cases} \mathrm{e}^{rT}\left(p + \tilde{S}_0^{i+1}(z)\right)(x-e_0) & \text{if } x > e_0 \\ \mathrm{e}^{rT}\,\tilde{S}_0^{i+1}(z)(x-e_0) & \text{else.} \end{cases}$$

Under the assumption that the price function $\tilde{S}_0^{i+1}$ is bounded, the terminal condition again satisfies a linear growth bound and therefore in particular a quadratic growth bound. In Section 3.2.5 we will see that we obtain $\tilde{S}_0^{i+1}$ from u^{i+1}; therefore, since we do not know u^{i+1} explicitly, we cannot verify whether $\tilde{S}_0^{i+1}$ is bounded or satisfies some suitable growth condition. Hence we do not know if the terminal condition satisfies a quadratic growth bound and thus cannot ensure that the verification theorem applies to the general setting of the model.

Summary

In this section, we showed that the volatility of all model variants satisfies the assumptions of the theorems of Section 2.4. As a closed-form expression for the drift is not available in any of the model variants, it was not possible to verify these assumptions for the drift. Thus in multi-period model II, we cannot show that the SDE has a unique solution and that the Euler-Maruyama scheme converges; also a verification of the HJB equation cannot be given.

3.2.5 Procedure to Combine the Time Periods

Again we need to combine the results from solving the PDEs and SDEs of the separate time periods in order to simulate the process X. The procedure is similar as in multi-period model I of Section 3.1. We start by specifying a price function $\tilde{S}_0^N$ and use this to solve the PDE for the last time period $N-1$. Then we solve the PDEs backwards in time. In each time period i, we need to determine the corresponding initial price function $\tilde{S}_0^{i+1}$. From the PDE solution of the subsequent time period, we obtain the price function $S^{i+1} : [T_{i+1}, T_{i+2}] \times \mathbb{R} \times \mathbb{R} \to \mathbb{R}$, which depends both on x and z. But in all model variants the initial value of Z is a linear function of X; i.e. we have $Z_0^i = a\, X_0^i + b$ for some constants a and b. More specifically, in the simple model variant we have $Z_0^i = X_0^i$ and therefore

$$\tilde{S}_0^{i+1}(x) = S^{i+1}(0, x, x),$$

in the Brownian model variant we have $Z_0^i = X_0^i + \Delta T^2\, \mu$, thus

$$\tilde{S}_0^{i+1}(x) = S^{i+1}(0, x, x + \Delta T^2\, \mu) = c\, u^{i+1}(0, x, x + \Delta T^2\, \mu),$$

and in the Ornstein-Uhlenbeck model we have $Z_0^i = \mathrm{e}^{-\theta \Delta T}\, X_0^i + \mu\, \Delta T \left(1 - \mathrm{e}^{-\theta \Delta T}\right)$, delivering

$$\begin{aligned}\tilde{S}_0^{i+1}(x) &= S^{i+1}\left(0, x, e^{-\theta \Delta T}\, x + \mu\, \Delta T \left(1 - \mathrm{e}^{-\theta \Delta T}\right)\right) \\ &= c\, u^{i+1}\left(0, x, e^{-\theta \Delta T}\, x + \mu\, \Delta T \left(1 - \mathrm{e}^{-\theta \Delta T}\right)\right).\end{aligned}$$

We recall that the abatement function u^{i+1} can be computed from the PDE solution of period $i+1$ as

$$u^{i+1}(t, x, z) = \frac{V_x^{i+1}(t, x, z)}{c}\, \mathrm{e}^{r T_{i+1} + t}.$$

The price function then enters the penalty function and thus allows us to solve the PDE for time period i. We proceed in this way until we reach time period 0.

Then we start solving the SDEs forward in time. For each time period i, we compute the initial values of X and Z from the realization of the Brownian motion W up to time T_i. As shown in the derivation of the respective SDEs, we need to compute for the simple model variant

$$X_0^i = x_0^i + \sigma\, \Delta T\, W_{T_i}, \quad Z_0^i = x_0^i + \sigma\, \Delta T\, W_{T_i},$$

for the Brownian model variant we have

$$X_0^i = x_0^i + \sigma\, \Delta T\, W_{T_i}, \quad Z_0^i = x_0^i + \sigma\, \Delta T\, W_{T_i} + \Delta T^2\, \mu,$$

and for the Ornstein-Uhlenbeck model we compute

$$X_0^i = x_0^i + \sigma\, \mathrm{e}^{-\theta i \Delta T}\, \frac{1 - \mathrm{e}^{-\theta \Delta T}}{\theta} \int_0^{T_i} \mathrm{e}^{-\theta s} \mathrm{d}W_s, \quad Z_0^i = \mathrm{e}^{-\theta \Delta T} X_0^i + \mu \Delta T \left(1 - \mathrm{e}^{-\theta \Delta T}\right).$$

The procedure can again be summarized as follows:

1. Choose a function $\tilde{S}_0^N(x)$ as input for the last time period.
2. Solve the PDEs in reversed order

$$u^{N-1} \to u^{N-2} \to \ldots \to u^{i+1} \to u^i \to \ldots \to u^1 \to u^0.$$

In each time period, we apply the price function $\tilde{S}_0^{i+1}(x) = c\, u^{i+1}(0, x, ax + b)$.

3. Solve the SDEs forward in time

$$X^0 \to X^1 \to \ldots \to X^i \to X^{i+1} \to \ldots \to X^{N-2} \to X^{N-1}$$
$$Z^0 \to Z^1 \to \ldots \to Z^i \to Z^{i+1} \to \ldots \to Z^{N-2} \to Z^{N-1}$$

by computing X_0^i and Z_0^i from $(W_t)_{t\in[0,T_i]}$.

Summary

We demonstrated that the approach to combine the PDE and SDE solutions of all time periods is the same as in multi-period model I: We first solve the PDEs backwards in time. For each time period, we obtain the function to describe the initial price $\tilde{S}_0^i$ from the price function S^i by using the linear relation between the initial values of X^i and Z^i. The SDEs are then again solved forward in time.

3.2.6 Multi-Period Model with Allowances Becoming Invalid

If we want to analyze the effect of being able to transfer allowances to the subsequent period, we again need to formulate a multi-period model where this is not possible. Again this leaves the SDEs unchanged. We only need to modify the penalty function to

$$P^i\left(X_{T_{i+1}}, Z_{T_{i+1}}\right) = \begin{cases} \left(p + \tilde{S}_0^{i+1}\left(Z_{T_{i+1}}\right)\right)\left(X_{T_{i+1}} - e_0\right) & \text{if} \quad X_{T_{i+1}} > e_0, \\ 0 & \text{else.} \end{cases}$$

Then we obtain the PDE of time period i as

$$V_t^i = \frac{1}{2}\frac{\left(V_x^i\right)^2}{c}\,\mathrm{e}^{r(T_i+t)} - \frac{1}{2}\,G^i(t)^2\,V_{xx}^i - G^i(t)\,H^i(t)\,V_{xz}^i - \frac{1}{2}\,H^i(t)^2\,V_{zz}^i$$

with terminal condition

$$\begin{aligned} V^i(\Delta T, x, z) &= \mathrm{e}^{-rT_{i+1}}\,P^i(x,z) \\ &= \begin{cases} \mathrm{e}^{-rT_{i+1}}\,\left(p + \tilde{S}_0^{i+1}(z)\right)(x - e_0) & \text{if} \quad x > e_0 \\ 0 & \text{else.} \end{cases} \end{aligned}$$

Also this PDE needs to be solved numerically in all model variants; we may proceed to solve the PDEs and SDEs of all time periods as presented above.

Chapter 4

Auctioning

In contrast to the free allocation of allowances during the early phases of the EU ETS, since 2013 an increasingly large share of allowances has been auctioned. Therefore, in this chapter we will present an approach to model an ETS, where allowances are auctioned. We still allow for free allocation of allowances in addition. If allowances are auctioned, the costs of purchasing allowances at the auction enter the cost function as an additional term. Moreover, also at the auction an optimization problem needs to be solved, as the agent aims to choose her demand so that her total costs are minimized. This raises the question in which order the two optimization problems should be solved. We follow the approach taken in the work by Haita [Hai14]: In her static two-step model, she first solves the minimization problem of determining optimal abatement and trading strategies and then solves the optimization problem at the auction. We adapt this procedure to our dynamic continuous-time setting. Liang and Huang proceed in a similar way in [LH20] and [LH22]; in the latter they also work with the opposite order.

4.1 Model Formulation

As in the one-period model introduced in Chapter 2, we assume that the emission rate Y is described by

$$\mathrm{d}Y_t = \mu(t, Y_t)\mathrm{d}t + \sigma(t, Y_t)\mathrm{d}W_t.$$

We again define the total expected emissions X as

$$X_t = -\int_0^t u_s \mathrm{d}s + \mathrm{E}^t\left[\int_0^T Y_s \mathrm{d}s\right]$$

and derive the corresponding SDE

$$\mathrm{d}X_t = -u_t\mathrm{d}t + G(t)\mathrm{d}W_t,$$

where G differs between the model variants as presented in the previous chapters.

In the EU ETS, allowances are auctioned in a uniform price sealed-bid auction, as established in [EU10], therefore all allowances are given out for the same price. Let S_A be this uniform price. Further, let e_A be the total amount of allowances distributed by auctioning and let D_A be the demand for allowances at the auction. We first consider the optimization problem during the trading period, i.e. the time period $[0, T]$, in which allowances are traded and emissions occur. Since this happens after the auction was

completed, we assume that the parameters S_A, e_A and D_A are fixed. Afterwards we will consider the optimization problem at the auction. The reasoning behind this is that the companies involved in the system will have already made some considerations on what they expect to happen during the trading period in order to place their bids at the auction. Thus it is plausible to model these beforehand-considerations by solving the optimization problem of the trading period first.

4.1.1 Cost Minimization in the Trading Period

The allowances obtained at the auction given by D_A can be used to cover emissions and thus avoid paying the penalty. If we let e_F denote the number of allowances allocated to the agent for free, the penalty function therefore needs to be modified to

$$P^A(x) = \max(0, p(x - e_F - D_A)) = P(x; e_F + D_A),$$

i.e. in the definition of the penalty function for the one-period model, we set the amount of allowances available to the agent e_0 to $e_F + D_A$. Note that in numerical computations we will set $e_F = 0$.

We again assume that the abatement costs are given by

$$C(u) = \frac{1}{2}\, c\, u^2,$$

where the abatement rate u takes values in $\mathcal{U} = [0, \infty)$. Additionally, the auction induces costs of $S_A\, D_A$, so the overall costs in the system are given by

$$\mathrm{e}^{-rT}\, P^A(X_T) + \int_0^T \mathrm{e}^{-rs}\, C(u_s)\mathrm{d}s + S_A\, D_A.$$

We assume that the admissible abatement rates are given by the set

$$\mathcal{A}(t) = \Bigg\{ u = (u_s)_{s\in[t,T]} \text{ a progressively measurable } \mathcal{U}\text{-valued process with } \mathrm{E}\left[\int_t^T |u_s|^2 \mathrm{d}s\right] < \infty \Bigg\}.$$

The optimization problem we aim to solve is therefore

$$\inf_{u\in\mathcal{A}(0)} \mathrm{E}\left[\mathrm{e}^{-rT}\, P^A(X_T) + \int_0^T \mathrm{e}^{-rs}\, C(u_s)\mathrm{d}s + S_A\, D_A\right].$$

We write the corresponding value function as

$$\begin{aligned} V^A(t,x) &= \inf_{u\in\mathcal{A}(t)} \mathrm{E}^{t,x}\left[\mathrm{e}^{-rT}\, P^A(X_T) + \int_t^T \mathrm{e}^{-rs}\, C(u_s)\mathrm{d}s + S_A\, D_A\right] \\ &= \inf_{u\in\mathcal{A}(t)} \mathrm{E}^{t,x}\left[\mathrm{e}^{-rT}\, P(X_T; e_F + D_A) + \int_t^T \mathrm{e}^{-rs}\, C(u_s)\mathrm{d}s\right] + S_A\, D_A. \end{aligned}$$

The first term in this expression is almost identical to the value function of the one-period model defined in Section 2.2; we only have $P(X_T; e_F + D_A)$ instead of $P(X_T)$. We therefore define

$$V(t,x; e_F + D_A) = \inf_{u\in\mathcal{A}(t)} \mathrm{E}^{t,x}\left[\mathrm{e}^{-rT}\, P(X_T; e_F + D_A) + \int_t^T \mathrm{e}^{-rs}\, C(u_s)\mathrm{d}s\right]$$

as the value function in the one-period model with e_0 replaced by $e_F + D_A$. Then the value function with auctioning can be written as

$$V^A(t,x) = V(t,x;e_F + D_A) + S_A\, D_A.$$

Thus we obtain the corresponding HJB equation and its solution directly from the results in the one-period model. In particular, we have

$$V_x^A(t,x) = V_x(t,x;e_F + D_A);$$

this implies that the function describing the abatement rate u given as

$$u(t,x;e_F + D_A) = \mathrm{e}^{-rt}\,\frac{V_x(t,x;e_F + D_A)}{c}$$

is independent of S_A. As we can compute the allowance price as

$$S(t,x;e_F + D_A) = c\,u(t,x;e_F + D_A) = \mathrm{e}^{-rt}\,V_x(t,x;e_F + D_A),$$

also the price function in the trading period is independent of the price at the auction. In particular, both the abatement rate u and the price function S can be obtained from the results in the one-period model by replacing e_0 with $e_F + D_A$.

Summary

We formulated the cost minimization problem of the trading period, i.e. the problem to choose the optimal abatement in order to minimize expected costs. We observed that this problem is almost identical to the one considered in the one-period model, therefore we obtain the HJB equation and its solution directly from the results of the one-period model given in Chapter 2.

4.1.2 Cost Minimization Problem at the Auction

We assume that the representative agent is a price-taker of the auction. She therefore chooses her demand for a given price to minimize her overall costs as expected at the time of the auction. We assume that the PDE was already solved and we have a solution u^{D_A} as a function of t and x. Importantly, as can be seen above, the solution depends on the constant – yet unknown – parameter D_A. Furthermore, we assume that the solution u^{D_A} is indeed an optimal control for the minimization problem of the trading period. Note that we need to apply the verification theorem of Proposition 2.3 to make sure that this holds[1]. Having an optimal control u^{D_A} greatly simplifies the formulation of this problem; the idea of the strategy we adopt below was taken from Liang and Huang [LH22].

We now write down the optimization problem at the auction as

$$\inf_{D_A} \mathrm{E}\left[\mathrm{e}^{-rT}P(X_T) + \int_0^T \mathrm{e}^{-rs}\,C\left(u^{D_A}(s,X_s)\right)\mathrm{d}s + S_A D_A\right].$$

[1] As can be seen in the one-period model, the verification of the HJB equation can only be conducted in the simple model variant.

Since we have assumed above that $\left(u_t^{D_A}\right)_{t\in[0,T]}$ given by $u_t^{D_A} = u^{D_A}(t, X_t)$ is a minimizer for the optimization problem of the trading period, we have

$$\begin{aligned} V(0,x;e_F+D_A) &= \inf_{u\in\mathcal{A}(1)} \mathrm{E}\left[\mathrm{e}^{-rT}P(X_T) + \int_0^T \mathrm{e}^{-rs}\,C(u_s)\mathrm{d}s\right] \\ &= \mathrm{E}\left[\mathrm{e}^{-rT}P(X_T) + \int_0^T \mathrm{e}^{-rs}\,C\left(u_s^{D_A}\right)\mathrm{d}s\right]. \end{aligned}$$

As D_A and S_A are deterministic, we rewrite the optimization problem as

$$\begin{aligned} &\inf_{D_A} \mathrm{E}\left[\mathrm{e}^{-rT}P(X_T) + \int_0^T \mathrm{e}^{-rs}\,C\left(u_s^{D_A}\right)\mathrm{d}s + S_A D_A\right] \\ &\quad= \inf_{D_A}\left\{\mathrm{E}\left[\mathrm{e}^{-rT}P(X_T) + \int_0^T \mathrm{e}^{-rs}\,C\left(u_s^{D_A}\right)\mathrm{d}s\right] + S_A\,D_A\right\} \\ &\quad= \inf_{D_A}\left\{V(0,x;e_F+D_A) + S_A\,D_A\right\}. \end{aligned}$$

Now we can formulate the first order condition

$$V_d(0,x;e_F+D_A) + S_A \overset{!}{=} 0.$$

Thus any solution for the optimal allowance demand at the auction D_A^* needs to satisfy this equation. Furthermore, such a solution will be dependent on S_A and we may write this as $D_A^*(S_A)$, representing the demand schedule of the representative agent. We assume that the market at the auction clears, so we have $e_A = D_A^*(S_A)$. By solving this for S_A, we therefore obtain the price at the auction. Indeed, since $V(0,x;e_F+D_A)$ and thus $V_d(0,x;e_F+D_A)$ do not depend on S_A, we directly have

$$S_A = -V_d(0,x;e_F+e_A).$$

The second order condition to ensure that D_A^* is a minimum is given by

$$V_{dd}(0,x;e_F+D_A) > 0;$$

the validity of this condition cannot be established in general.

Summary

In this section, we formulated the optimization problem at the auction. We derived the first and second order condition. Under the assumption that the market at the auction clears, we obtained an expression for the allowance price at the auction.

4.1.3 Computation of the Auction Price

We now aim to compute $V_d(0,x;e_F+e_A)$ in order to obtain the auction price S_A. Strikingly, the variable x enters the cost minimization problem of the trading period only in the expression $x - e_F - D_A$. We will exploit this structure to derive a relation between the derivatives V_d and V_x.

Proposition 4.1. *Let $V(\cdot,\cdot;e_F+d)$ be the value function of the one-period model, i.e.*

$$V(t,x;e_F+d)=\inf_{u\in\mathcal{A}(t)}\mathrm{E}^{t,x}\left[\mathrm{e}^{-rT}\,P(X_T;e_f+d)+\int_t^T C(u_s)\mathrm{d}s\right].$$

Then there exists a function $U:[0,T]\times\mathbb{R}\to\mathbb{R}$ such that

$$V(t,x;e_F+d)=U(t,x-e_F-d)$$

for any $t\in[0,T]$ and any $x,d\in\mathbb{R}$.

Proof. We define a process Z as $Z_t=X_t-e_F-d$. Then we have

$$Z_t=X_0-\int_0^t u_s\mathrm{d}s+\int_0^t G(s)\mathrm{d}W_s-e_F-d=Z_0-\int_0^t u_s\mathrm{d}s+\int_0^t G(s)\mathrm{d}W_s$$

with $Z_0=X_0-e_F-d$. Furthermore, we define a penalty function

$$P^Z(z)=\begin{cases}p\,z & \text{if}\quad z>0,\\ 0 & \text{else.}\end{cases}$$

Thus we obtain a transformed minimization problem with value function

$$U(t,z)=\inf_{u\in\mathcal{A}(t)}\mathrm{E}^{t,z}\left[\mathrm{e}^{-rT}\,P^Z(Z_T)+\int_t^T \mathrm{e}^{-rs}\,C(u_s)\mathrm{d}s\right].$$

We now consider $U(t,x-e_F-d)$. We have

$$\begin{aligned}Z_T&=Z_t-\int_t^T u_s\mathrm{d}s+\int_0^t G(s)\mathrm{d}W_s\\&=X_t-e_F-d-\int_t^T u_s\mathrm{d}s+\int_0^t G(s)\mathrm{d}W_s=X_T-e_F-d\end{aligned}$$

and

$$\begin{aligned}P^Z(x-e_F-d)&=\begin{cases}p(x-e_F-d) & \text{if}\quad x-e_F-d>0\\ 0 & \text{else}\end{cases}\\&=P(x;e_F+d).\end{aligned}$$

Therefore we rewrite

$$\begin{aligned}U(t,x-e_F-d)&=\inf_{u\in\mathcal{A}(t)}\mathrm{E}\left[\mathrm{e}^{-rT}\,P^Z(Z_T)+\int_t^T C(u_s)\mathrm{d}s\,\middle|\,Z_t=x-e_F-d\right]\\&=\inf_{u\in\mathcal{A}(t)}\mathrm{E}\left[\mathrm{e}^{-rT}\,P^Z(X_T-e_F-d)+\int_t^T C(u_s)\mathrm{d}s\,\middle|\,X_t=x\right]\\&=\inf_{u\in\mathcal{A}(t)}\mathrm{E}^{t,x}\left[\mathrm{e}^{-rT}\,P(X_T;e_F+d)+\int_t^T C(u_s)\mathrm{d}s\right]\\&=V(t,x;e_F+d)\end{aligned}$$

and thus U is the desired function. □

With this Proposition at hand, we compute the derivative V_d as

$$\begin{aligned} V_d(t,x;e_F+d) &= U_d(t,x-e_F-d) = -U_z(t,x-e_F-d) = -U_x(t,x-e_F-d) \\ &= -V_x(t,x;e_F+d) \end{aligned}$$

and obtain for the auction price that

$$S_A = -V_d(0,x;e_F+e_A) = V_x(0,x;e_F+e_A) = S(0,x;e_F+e_A).$$

Thus the auction price is equal to the price at the beginning of the trading period as long as the assumptions made above hold. More specifically, we need that there exists an optimal control u and that V is sufficiently differentiable. Both of these requirements can only be proven in the simple model variant.

Summary

Under the assumption that an optimal abatement rate exists, we showed that the auction price is equal to the allowance price on the market at the beginning of the trading period.

4.1.4 Relation to the One-Period Model

With the results from Section 4.1.1, we will now show that we do not need to consider the case of auctioned allowances separately in our model, as this does not change the quantities of interest.

Proposition 4.2. *We assume that the market at the auction clears, i.e. $e_A = D_A$ and fix the total number of distributed allowances $e_{tot} = e_F + e_A$. Furthermore, we assume that u as computed above indeed is an optimal abatement rate. Then in the present model the number of allowances which are auctioned e_A and the auction price S_A do not have an impact on the resulting emissions and the allowance price.*

Proof. From the computations above we have that the optimal abatement rate is given by $u(t,x;e_F+D_A)$, i.e. by the optimal abatement rate obtained in the one-period model with e_0 replaced by $e_F + D_A$. Under the assumption that the market at the auction clears, we have

$$u(t,x;e_F+D_A) = u(t,x;e_F+e_A) = u(t,x;e_{\text{tot}}).$$

Therefore the SDE describing the total expected emissions

$$\mathrm{d}X_t = -u(t,X_t;e_{\text{tot}})\mathrm{d}t + G(t)\mathrm{d}W_t$$

remains unchanged regardless how many of the total allowances e_{tot} are auctioned, i.e. how large e_A is. Hence with e_{tot} fixed, X is not impacted by e_A. The same holds for the path of the allowance price since this is given by

$$S(t,X_t;e_{\text{tot}}) = \mathrm{e}^{-rT}\, V_x(t,X_t;e_{\text{tot}}),$$

which is again independent of e_A as long as e_{tot} remains constant.

Furthermore we have seen above that S_A does not enter the abatement rate u, therefore the SDE and thus the process X as well as the price process S do not depend on S_A. □

Remark 4.3. The total costs arising in the system of course do depend on both the fraction of auctioned allowances and the auction price. If we assume that V indeed represents the minimum costs from abatement and penalty payments, and that the market at the auction clears, we have from the results above

$$V^A(0,x_0) = V(0,x_0;e_{\text{tot}}) + S_A\, e_A$$

for the total costs.

Summary

In this section, we showed that the introduction of the auctioning of allowances does not impact the process of total expected emissions X and the allowance price process S, which are the quantities we mainly study in this thesis. On the other hand, the auctioning of allowances does have an impact on the total costs.

4.2 The Auction Model in the Simple Model Variant

We have seen in Section 4.1.1 that the value function in the auction model is given as

$$V^A(t,x) = V(t,x;e_F + D_A) + S_A\, D_A.$$

Then with the results in the one-period model of equation (2.4), we obtain

$$\begin{aligned} V^A(t,x) = -c\sigma^2 \ln\Bigg(&\frac{1}{2}\left(1+\operatorname{erf}\left(\frac{e_F+D_A-x}{\sqrt{2}\sigma\sqrt{T-t}}\right)\right) \\ &+\frac{1}{2}\left(1-\operatorname{erf}\left(\frac{c(e_F+D_A-x)+p(T-t)}{\sqrt{2}c\sigma\sqrt{T-t}}\right)\right)\mathrm{e}^{\frac{2cp(e_F+D_A-x)+p^2(T-t)}{2c^2\sigma^2}}\Bigg) + S_A\, D_A. \end{aligned}$$

Furthermore, we have seen for the first derivative that $V_x^A(t,x) = V_x(t,x;e_F+D_A)$ and therefore again with the result in the one-period model, given in equation (2.5), we have

$$V_x^A(t,x) = \frac{p}{1+\dfrac{e^{-\frac{2cp(e_F+D_A-x)+p^2(T-t)}{2c^2\sigma^2}}\left(1+\operatorname{erf}\left(\frac{e_F+D_A-x}{(\sqrt{2}\sigma\sqrt{T-t})}\right)\right)}{1-\operatorname{erf}\left(\frac{c(e_F+D_A-x)+p(T-t)}{\sqrt{2}c\sigma\sqrt{T-t}}\right)}}.$$

Since the results in the auction model are directly derived from the one-period model, also the verification results carry over.

Proposition 4.4. *The value function V^A of the auction model in the simple model variant satisfies the requirements of the verification theorem in Proposition 2.3. Furthermore, the SDE*

$$\mathrm{d}X_t = -u(t,X_t;e_F+D_A)\mathrm{d}t + \sigma \mathrm{d}W_t,$$

where $u(t,x;e_F+D_A) = \frac{V_x^A(t,x)}{c}\,\mathrm{e}^{rt}$, has a unique solution and $(u(s,X_s))_{s\in[t,T]} \in \mathcal{A}(t)$ for any $t\in[0,T]$. In particular, V^A delivers the minimum costs and u is an optimal control.

Proof. From Proposition 2.9, we know that $V(\cdot,\cdot;e_F+D_A)$ satisfies the requirements on the (candidate) value function of the verification theorem in Proposition 2.3, i.e. we have that $V(\cdot,\cdot;e_F+D_A)$ is continuously differentiable in t, twice continuously differentiable in

x on $[0,T)\times\mathbb{R}$, continuous on $[0,T]\times\mathbb{R}$ and quadratically bounded. But since V^A differs from $V(\cdot,\cdot;e_F+D_A)$ only by a constant, these properties directly follow for V^A.

Furthermore, with $V^A_x(t,x)=V_x(t,x;e_F+D_A)$ we have that the result of Corollary 2.27 also holds in the auction model: In the drift term, we only replace e_0 by e_F+D_A, which does not affect the proof of the Corollary or any of the preceding propositions; the volatility remains unchanged in comparison to the one-period model. Thus the requirements of Assumption 2.14 are satisfied and the existence of a unique solution for SDE follows by Theorem 2.15.

With Proposition 2.10, we have that $(u(s,Z_s;e_F+D_A))_{s\in[t,T]}\in\mathcal{A}(t)$ for any continuous and adapted process Z and any $t\in[0,T]$. In particular, this also holds for the solution of the SDE given by X since X is continuous and adapted by Theorem 2.15. By the verification theorem in Proposition 2.3, we obtain that $V(\cdot,\cdot;e_F+D_A)$ delivers the minimum costs if we neglect the costs of the auction, and that $u(\cdot,\cdot;e_F+D_A)$ is an optimal control. But since the costs of the auction do not depend on the control u, we only need to add them to the costs $V(\cdot,\cdot;e_F+D_A)$ and therefore V^A represents the minimum costs of the trading period, including auction costs. □

Next we aim to compute the price at the auction. With Proposition 4.1, we obtain

$$V_d(t,x;e_F+D_A)=-V_x(t,x;e_F+D_A)=-\frac{p}{1+\frac{e^{-\frac{2cp(e_F+D_A-x)+p^2(T-t)}{2c^2\sigma^2}}\left(1+\operatorname{erf}\left(\frac{e_F+D_A-x}{(\sqrt{2}\sigma\sqrt{T-t})}\right)\right)}{1-\operatorname{erf}\left(\frac{c(e_F+D_A-x)+p(T-t)}{\sqrt{2}c\sigma\sqrt{T-t}}\right)}}.$$

In the particular case of the simple model variant, we may alternatively also compute the derivative V_d directly; this was done in Section A.3.2 in the appendix to deliver

$$V_d(t,x;e_F+D_A)=-\frac{p}{1+\frac{\mathrm{e}^{-\frac{2cp(e_F+D_A-x)+p^2(T-t)}{2c^2\sigma^2}}\left(1+\operatorname{erf}\left(\frac{e_F+D_A-x}{\sqrt{2}\sigma\sqrt{T-t}}\right)\right)}{1-\operatorname{erf}\left(\frac{c(e_F+D_A)-cx+p(T-t)}{\sqrt{2}c\sigma\sqrt{T-t}}\right)}}=-V_x(t,x;e_F+D_A).$$

We now compute the second derivative with the aim to validate the second order condition. By Proposition 4.1, we have

$$\begin{aligned}V_{dd}(t,x;e_F+D_A)&=-V_{xd}(t,x;e_F+D_A)=-U_{xd}(t,x-e_F-D_A)\\&=U_{xz}(t,x-e_F-D_A)=U_{xx}(t,x-e_F-D_A)=V_{xx}(t,x;e_F+D_A),\end{aligned}$$

so we obtain V_{dd} from the expression for V_{xx} of the one-period model, as given in A.3.3 in the appendix. This expression does not easily allow to determine its sign for $D_A=e_A$ as would be required for verifying the second order condition. Therefore, a detailed verification of the second order condition is omitted.

With the results from above, the auction price is then given as

$$S_A=S(0,x;e_F+D_A)=V_x(0,x;e_F+D_A)=\frac{p}{1+\frac{e^{-\frac{2cp(e_F+D_A-x)+p^2T}{2c^2\sigma^2}}\left(1+\operatorname{erf}\left(\frac{e_F+D_A-x}{(\sqrt{2}\sigma\sqrt{T})}\right)\right)}{1-\operatorname{erf}\left(\frac{c(e_F+D_A-x)+pT}{\sqrt{2}c\sigma\sqrt{T}}\right)}}.$$

Finally, we consider the model with fixed total number of distributed allowances $\mathrm{e_{tot}}=e_A+e_F$ but possibly varying number of auctioned allowances e_A, meaning that the number of freely allocated allowances e_F needs to change accordingly. Under the assumption that

the market at the auction clears so that we have $D_A = e_A$, we may rewrite the results for V^A and V_x^A as

$$V^A(t,x) = -c\sigma^2 \ln\left(\frac{1}{2}\left(1+\operatorname{erf}\left(\frac{e_{\text{tot}}-x}{\sqrt{2}\sigma\sqrt{T-t}}\right)\right)\right.$$
$$\left. + \frac{1}{2}\left(1-\operatorname{erf}\left(\frac{c(e_{\text{tot}}-x)+p(T-t)}{\sqrt{2}c\sigma\sqrt{T-t}}\right)\right)\mathrm{e}^{\frac{2cp(e_{\text{tot}}-x)+p^2(T-t)}{2c^2\sigma^2}}\right) + S_A\, e_A$$

and

$$V_x^A(t,x) = \frac{p}{1+\frac{e^{-\frac{2cp(e_{\text{tot}}-x)+p^2(T-t)}{2c^2\sigma^2}}\left(1+\operatorname{erf}\left(\frac{e_{\text{tot}}-x}{(\sqrt{2}\sigma\sqrt{T-t})}\right)\right)}{1-\operatorname{erf}\left(\frac{c(e_{\text{tot}}-x)+p(T-t)}{\sqrt{2}c\sigma\sqrt{T-t}}\right)}}.$$

Then clearly V^A still depends on e_A, whereas V_x^A does not. Thus as long as we keep e_{tot} fixed, varying e_A does not affect V_x^A. Therefore, also X and the price process S are not impacted, which is in line with the results of Proposition 4.2.

Summary

This section serves to apply the general results obtained for the model with auctioning to the particular case of the simple model variant. We provided the verification of the HJB equation and showed that the SDE has a unique solution. Furthermore, we computed the auction price explicitly and obtained that it indeed equals the allowance price on the market at the beginning of the trading period. However, the verification of the second order condition to ensure that the optimum characterizing the auction price is a minimum was omitted. Finally, we verified explicitly that the derivative of the value function V_x^A and therefore the abatement rate u do not depend on the number of auctioned allowances e_A as long as the total number of allowances distributed e_{tot} is fixed.

Chapter 5

Implementation of the Models

To find a solution to the model, we need numerical methods both for solving the PDE in all model variants, except for the simple model variant, and for solving the SDE. In this chapter we describe the methods and strategies we apply and the challenges arising. The implementation of these methods was done in `Python`, with frequent use of the packages `NumPy` [Har+20], `SciPy` [Vir+20] and `Matplotlib` [Hun07]; we do not discuss the details of the implementation.

Furthermore, the model heavily depends on numerous parameters describing the ETS and the economy it regulates. Therefore, this chapter concludes with an explanation of our parameter choices.

5.1 Numerical Solution of the PDE

We consider the time-reversed PDE as obtained in Sections 2.3.3, 3.1.3 and 3.2.3 since we need to have an initial condition instead of a terminal condition. The numerical solution of the PDE requires its reformulation in a way that can be handled by a computer. A straightforward idea is to evaluate the functions and derivatives involved only at discrete points both on the t-axis and the x-axis and replace all derivatives by difference quotients; then we could proceed to solve the resulting equation. We follow a slightly different approach which is known as the method of lines, explained for example by Schiesser [Sch91]: In a first step, we fix discrete points on the x-axis and approximate all derivatives with respect to x by suitable difference quotients. As a result, we obtain an ordinary differential equation (ODE), which we solve in a second step by using a well-known ODE solving method.

While leading in general to decent results, this procedure introduced several numerical errors and therefore required adaptations in the choice of grid points to improve numerical results. Furthermore, in multi-period model II the PDE we need to solve has an additional dimension. As a consequence, some further adjustments need to be made to solve this PDE as well.

5.1.1 Discretization of the PDE

We consider the PDE

$$V_t(t,x) = -\tilde{R}(t)\,\frac{V_x^2(t,x)}{2c} + \frac{1}{2}\,\tilde{G}^2(t)\,V_{xx}(t,x) \tag{5.1}$$

with initial value

$$V(0,x) = \tilde{R}(0)^{-1}\,P(x).$$

Here we let $\tilde{G}(t)$ denote the time-reversed volatility of the process X and P the penalty function. Furthermore, by $\tilde{R}(t)$ we denote the (time-reversed) discount factor for the corresponding model. With $\tilde{R}(t) = \mathrm{e}^{r(T-t)}$, we obtain the PDE in the one-period model, whereas with $\tilde{R}(t) = \mathrm{e}^{r(T_{i+1}-t)}$, this is the PDE of multi-period I (i.e. with constant price parameter, as described in Section 3.1) for period i. In Section 5.1.4 we will explain how we can handle the PDE of multi-period model II, i.e. with varying price parameter as presented in Section 3.2.

The first step is to turn the PDE into an ODE. For this purpose, we define a grid covering a given interval $[a, b]$, which represents the range of possible values for x. For the time being, we assume that the grid is equidistant. We let h denote the step size and N the number of grid points. Then we denote the grid by $x^h \in \mathbb{R}^N$, and we have

$$x^h = [a, a+h, \ldots, a+ih, \ldots, a+(N-1)h].$$

Each grid point is therefore given as $x_i^h = a + ih$. Now we can approximate the derivatives with respect to x in equation (5.1) by corresponding difference quotients, where we use the centered difference quotient for the first derivative, i.e.

$$\begin{aligned} V_x(t, x_i^h) &\approx \frac{V(t, x_{i+1}^h) - V(t, x_{i-1}^h)}{2h} =: V_x^h(t, x_i^h) \\ V_{xx}(t, x_i^h) &\approx \frac{V(t, x_{i-1}^h) - 2V(t, x_i^h) + V(t, x_{i+1}^h)}{h^2} =: V_{xx}^h(t, x_i^h). \end{aligned}$$

Then we obtain an ODE

$$\begin{aligned} V_t(t, x_i^h) = &-\frac{1}{2c}\,\tilde{R}(t)\,\left(\frac{V(t, x_{i+1}^h) - V(t, x_{i-1}^h)}{2h}\right)^2 \\ &+ \frac{1}{2}\,\tilde{G}(t)^2\,\frac{V(t, x_{i-1}^h) - 2V(t, x_i^h) + V(t, x_{i+1}^h)}{h^2} \end{aligned}$$

with initial value $V(0, x_i^h) = \tilde{R}(0)^{-1}\,P(x_i^h)$.

The setting of our problem does not deliver any natural boundary conditions for the boundaries on the x-axis; hence we cannot yet compute the difference quotients for x_0^h and x_{N-1}^h. Since boundary conditions have a strong impact on the resulting solution, we aim to avoid the need for them by applying modified difference quotients at the boundary: If we use a left-sided difference quotient instead of the centered difference quotient above, we have

$$V_x(t, x_{N-1}^h) \approx \frac{V(t, x_{N-1}^h) - V(t, x_{N-2}^h)}{h} =: V_x^{h,l}(t, x_{N-1}^h).$$

By again applying a left-sided difference quotient to the thus approximated first derivative we obtain for the second derivative

$$V_{xx}(t, x_{N-1}^h) \approx \frac{V_x^{h,l}(t, x_{N-1}^h) - V_x^{h,l}(t, x_{N-2}^h)}{h} = \frac{V(t, x_{N-1}^h) - 2V(t, x_{N-2}^h) + V(t, x_{N-3}^h)}{h^2}.$$

Note that in this way we obtain the difference quotient of the grid point before; so implicitly we assume that near the boundary V_{xx} is constant[1]. For the simple model variant, we

[1] In contrast to setting an explicit boundary condition, by this construction we do not need to know the constant value of V_{xx} at the boundary.

have seen in Propositions 2.7 (iii) and 3.3 (iii) that V_x converges for $x \to \infty$ and $x \to -\infty$. Thus if we choose the grid large enough, we might expect that even V_x is constant, thus approximating the second derivative at the boundary as indicated above should not impact the solution much. At the right-hand side boundary, we therefore have

$$V_t(t, x^h_{N-1}) = -\frac{1}{2c}\,\tilde{R}(t)\,\left(\frac{V(t, x^h_{N-1}) - V(t, x^h_{N-2})}{h}\right)^2 + \frac{1}{2}\,\tilde{G}(t)^2\,\frac{V(t, x^h_{N-1}) - 2V(t, x^h_{N-2}) + V(t, x^h_{N-3})}{h^2}$$

and thus do not require a boundary condition. In analogy, on the left-hand side boundary we use a right-sided difference quotient

$$V_x(t, x^h_0) \approx \frac{V(t, x^h_1) - V(t, x^h_0)}{h}$$

and for the second derivative

$$V_{xx}(t, x^h_0) \approx \frac{V(t, x^h_2) - 2V(t, x^h_1) + V(t, x^h_0)}{h^2}$$

to obtain the ODE

$$V_t(t, x^h_0) = -\frac{1}{2c}\,\tilde{R}(t)\,\left(\frac{V(t, x^h_1) - V(t, x^h_0)}{h}\right)^2 + \frac{1}{2}\,\tilde{G}(t)^2\,\frac{V(t, x^h_2) - 2V(t, x^h_1) + V(t, x^h_0)}{h^2}.$$

The resulting system of ODEs can now be solved for instance by an implicit Runge-Kutta method, as described in Section 5.1.3.

5.1.2 Adaptation of the Grid in x-Direction

It remains to choose an appropriate grid. First computations were conducted on a grid with step size $h = 10$ ranging from 2000 to 10 000. This range was chosen since the endowment of allowances e_0 was set to $e_0 = 6000$, with initially expected emissions $x_0 = 6240$. We discuss the parameter choices for e_0 and x_0 in detail in Section 5.3. With these choices, the total expected emissions X would reasonably take values in $[2000, 10\,000]$. Furthermore, from analytical results in the simple model, as shown in Figure 5.1, we observe that the PDE solution is of interest mostly on the interval $[4000, 8000]$ since it is almost constant elsewhere. We also obtain from the numerical SDE solution that X indeed remains in $[2000, 10\,000]$ in most runs.

However, first numerical PDE results, conducted in the Brownian model variant, show an interesting phenomenon occurring close to time zero (i.e. close to the initial condition since we are considering the time-reversed PDE): For small values of t, the first derivative V_x of the PDE solution takes negative values for certain values of x, as can be seen in Figure 5.2. This results in a negative abatement rate u and thus leads to negative allowance prices S; both is not plausible from a practical point of view. Moreover, we have shown in Proposition 2.7 (ii) that V_x is non-negative in the simple model variant, so we might expect a similar behavior also in the Brownian variant. As the volatility $\tilde{G}(t) = \sigma\, t$ of the Brownian model variant (in its time reversed form) is small at the beginning of the time period, the PDE is mostly driven by the term $-\frac{1}{2c}\,\tilde{R}(t)\,V_x^2(t, x)$, i.e. by the first derivative of V. From the initial condition, we have for $x > e_0$ that V_x is strictly positive and almost

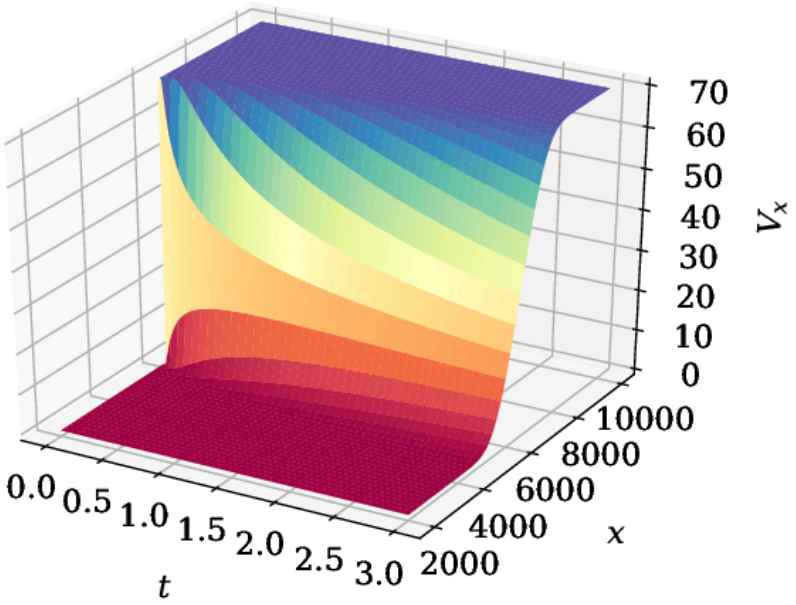

Figure 5.1: Analytical solution V_x of the time-reversed PDE in the simple model variant.

constant. On the other hand we know that V is zero for $x < e_0$ and continuous at time $t = 0$, so if we assume that V is continuous also for $t > 0$, it will be small for $x > e_0$ and x close to e_0. This means that even close to an x-value of e_0 we still get a large value for V_x, whereas V is already very small. Hence as we proceed in time, V will decrease. However, if we move even closer to e_0 on the x-axis, at some point V_x will decrease fast if we assume that V_x is continuous for $t > 0$. This might prevent that we obtain negative values in the analytical solution. On the other hand, when approximating this solution numerically, depending on the step size used for discretizing the x-axis, we might fail to capture the decrease in V_x and therefore V might move to negative values for some $\tilde{x}$ close to e_0. But since for $x < e_0$ and x small enough, V is zero and thus larger than for $\tilde{x}$, we

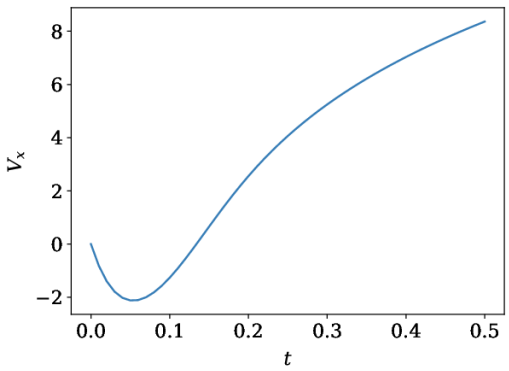

Figure 5.2: Trajectory of V_x for $x = 5990$ and $t \in [0, 0.5]$ in the Brownian model variant. V_x clearly takes negative values for t close to 0.

also obtain negative values for V_x.

We aim to avoid this numerical error by using a smaller step size. Furthermore, this will in general reduce the error of the numerical solution as can be observed when comparing the analytical solution in the simple model variant with the numerical solution: This can be seen in Figure 5.3, which shows the error of the numerical solution as the absolute value of the difference to the analytical solution for two different step sizes. A smaller step

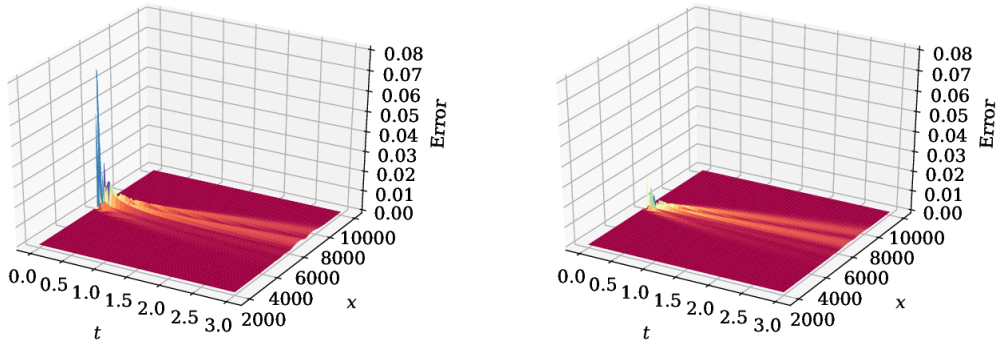

(a) $h = 10$ **(b)** $h = 5$

Figure 5.3: Comparison between the numerical and the analytical solution in the simple model variant on two different grids.

size entails a higher computational effort, which we attempt to limit by using the small step size only where we need it: The undesired negative values only occur close to e_0 and in Figure 5.3 we can see that the error in general is largest for x around e_0. Therefore, we apply a grid which is not equidistant. We denote such a grid by two vectors h and k, where h contains all step sizes and k the number of steps taken with the respective step size. We then construct the grid in the following way: We start in e_0 and then use the smallest step size h_1 for k_1 steps in both directions. Then we change the step size to h_2, which we now apply for k_2 steps and so on. In this way we obtain a grid with the following structure:

$$[\ldots, e_0 - k_1\, h_1 - h_2, e_0 - k_1\, h_1, \ldots, e_0 - h_1, e_0, e_0 + h_1, \ldots, e_0 + k_1\, h_1, e_0 + k_1\, h_1 + h_2, \ldots].$$

Furthermore, we need to introduce modified difference quotients to approximate the derivatives at the points where the step sizes change. Let x_i^h be such a grid point, i.e. with step size h_m on the left-hand side and step size h_n on the right-hand side, where $m \neq n$. We then have $x_i^h - x_{i-1}^h = h_m$ and $x_{i+1}^h - x_i^h = h_n$. The centered difference quotient introduced above can be derived by taking the average of the left- and right-sided difference quotient. In analogy to this procedure, we approximate the first derivative at the points of step size change as

$$V_x(t, x_i^h) \approx \frac{1}{2}\left(\frac{V(t, x_i^h) - V(t, x_{i-1}^h)}{h_m} + \frac{V(t, x_{i+1}^h) - V(t, x_i^h)}{h_n}\right).$$

We derive the difference quotient for the second derivative again in analogy to the derivation of the difference quotient given above. First we approximate the first derivative by a one-sided difference quotient, e.g. a left-sided difference quotient given by

$$V_x^{h,l}(t, x_i^h) := \frac{V(t, x_i^h) - V(t, x_{i-1}^h)}{h_m} \quad \text{and} \quad V_x^{h,l}(t, x_{i+1}^h) := \frac{V(t, x_{i+1}^h) - V(t, x_i^h)}{h_n}.$$

Then we apply the right-sided quotient on these approximations, where we need to use the average of the two step sizes as the denominator, to obtain an approximation for the second derivative as

$$V_{xx}(t, x_i^h) \approx \frac{V_x^{h,l}(t, x_{i+1}^h) - V_x^{h,l}(t, x_i^h)}{\frac{h_m + h_n}{2}} = \frac{\frac{V(t,x_{i+1}^h) - V(t,x_i^h)}{h_n} - \frac{V(t,x_i^h) - V(t,x_{i-1}^h)}{h_m}}{\frac{h_m + h_n}{2}}.$$

Both of these expressions were shown to produce good results; nevertheless, this approach still introduces an additional error, as we show by conduction several trial runs with varying grids. We tested grids where the step size changes by a factor 10, e.g. with step sizes varying between $100, 10, 1, \ldots$, or by a factor 2, e.g. with steps sizes of $64, 32, 16, 8, \ldots$. To reduce this error, the area covering the finest grid was enlarged. Furthermore, we observe

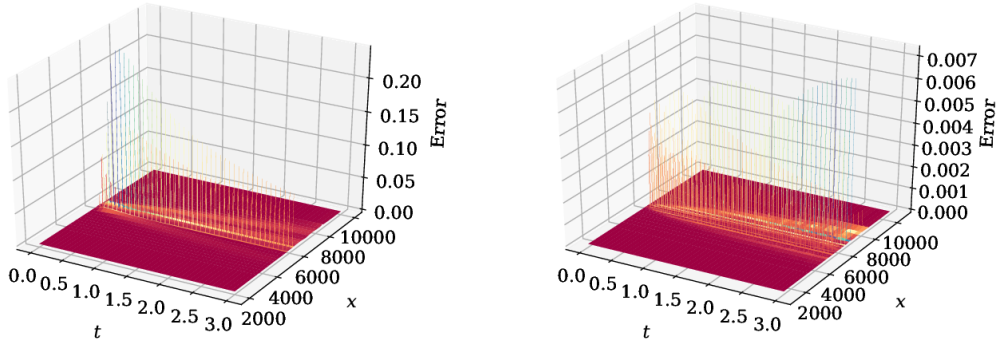

(a) $h = (0.1, 1, 10, 100)$ **(b)** $h = (0.0625, 0.125, 0.25, 0.5, 1, 2, 4, 8, 16)$

Figure 5.4: Comparison between the numerical and the analytical solution in the simple model variant on two different grids with varying step size.

that the error is smaller when changing step sizes only with factor 2, which spreads the error over several steps; thus the maximum error is reduced. The error as computed in the simple model variant by comparing the numerical solution with the analytical solution for two different grids of varying step size - one with factor 10, the other with factor 2 - can be seen in Figure 5.4, showing that the maximum error is smaller in the latter case. For our simulations we therefore choose the grid

$$h = (0.0625, 0.125, 0.25, 0.5, 1, 2, 4, 8, 16)$$
$$k = (1024, 512, 512, 512, 512, 512, 128, 64, 96)\,,$$

which spans the range $[1392, 10\,608]$ and delivers a maximum error of 0.0073.

Whereas this grid indeed reduces the negative values in the PDE solution to a tolerable extent, in particular the very fine grids seem to impact the stability of the PDE solution, as illustrated by Figure 5.5. We observe large fluctuations which change in position and amplitude for different grids. Moreover, they are no longer present on coarse grids. Therefore, these fluctuations are most likely numerical artifacts. It should be noted that such instabilities of large amplitudes as seen in Figure 5.5 strongly affect the results of the SDE solution. The core problem seems to be the computation of difference quotients: This

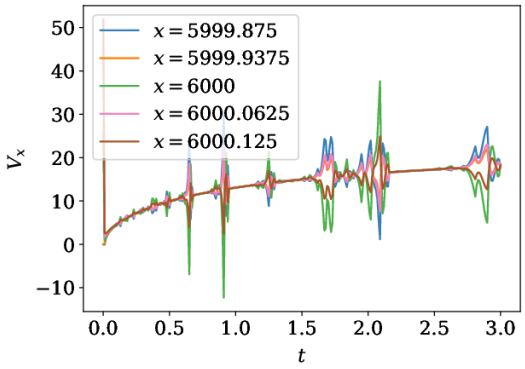

Figure 5.5: Trajectories of V_x for fixed values of x close to e_0 in the Brownian model variant. The solution was computed on a grid with step sizes $h = (0.0625, 0.125, 0.25, 0.5, 1, 2, 4, 8, 16)$.

is an ill-conditioned problem since it involves taking the difference of two similar values, which results in cancellation effects. Remarkably, the problem of instability occurs most notably at the end of the time period and is not present at the very beginning. In contrast to the discussion above, we now have the second derivative term as the main driver of the PDE for time range, which leads to the assumption that this term introduces the instability. This assumption can be supported by solving the PDE for smaller values of σ, thus reducing the impact of the second derivative term; for small σ the instabilities are no longer observed (this result is not shown).

So there are two computational problems arising in computing a solution to the PDE: At the beginning of the time period, unwanted negative values occur if the step size of the grid is too large. Towards the end of the time period, the solution becomes unstable if the step size is too small. Therefore, to tackle both of these problems, it is a natural approach to change the step size at some point in time.

We introduce the following procedure: We start with the grid chosen above, i.e.

$$\begin{aligned} h &= (0.0625, 0.125, 0.25, 0.5, 1, 2, 4, 8, 16) \\ k &= (1024, 512, 512, 512, 512, 512, 128, 64, 96)\,, \end{aligned}$$

and recall that the smallest step size is used around e_0, and that the step size gets larger as we proceed in both directions along the x-axis. We then solve the PDE on this grid by applying the usual initial condition. As soon as the first instability occurs, we construct a new grid: We omit the smallest step size and use the second smallest (0.125 in the grid given above) instead. In case of the grid given above, we then have

$$\begin{aligned} h &= (0.125, 0.25, 0.5, 1, 2, 4, 8, 16) \\ k &= (1024, 512, 512, 512, 512, 128, 64, 96)\,. \end{aligned}$$

Note that we now take 1024 steps of size 0.125 in both directions, as 512 of these are required to cover the range where we formerly applied the step size 0.0625. The rest of the grid remains unchanged. We take the result of the previous calculations on the finer grid as initial value and again proceed to solve the PDE. This pattern is repeated until we reach the grid that only uses the largest step size of the grid we started with (16 in this case). On this grid we complete the computation until final time.

Crucial in this approach is the detection of instabilities in the PDE solution. It is difficult to observe the occurrence of instabilities during the computation: Firstly because a pre-implemented ODE-solver is used but also since the behavior of the solution at several time points needs to be analyzed to find an instability. Therefore, we examine the computation results: On each grid, the solution of the PDE is computed up to a previously fixed time point. Then we test for instabilities and determine which part of these results is saved for later use. In choosing the time point, we try to make sure that the time interval on which computations are done is significantly longer than necessary, while we do not want to cover the entire time axis to avoid unnecessary computational effort.

Instabilities are then identified in the following way: We consider the PDE solution along the time axis for all grid points around e_0 up to a certain point and analyze all these trajectories separately. We assume that after a short irregular period in the beginning they are increasing, as long as no instabilities occur. For each point in time we proceed as follows:

1. If so far the trajectory has not been increasing, check if in the next step it increases. If so, save this.

2. If the trajectory has been increasing before, check if in the next step it is decreasing and surpasses a given threshold. This might be caused by an instability.

3. To verify if we indeed found an instability, check if for one of the following three steps we obtain a peak-like structure, which is typical for an instability. This is characterized as two consecutive steps, where the trajectory moves in opposite directions with similar amplitude. If a peak-like structure is found, return the index of the detected decreasing step as the beginning of an instability.

4. If such a peak is not found, reset the status of being increasing. This means that before a new peak can be identified, we first need to find a decreasing step.

This procedure may seem rather complicated and a definite downside is that upward peaks in single trajectories cannot be identified. As usually an instability affects multiple trajectories, in practice we can assume that we will still find the corresponding instability. In fact, by this approach, peaks are identified quite reliably and continuous movements are not falsely declared an instability; this is illustrated in Figure 5.6.

This approach was tested on several grids of the structure $h = (\ldots, 2, 4, 8, 16)$ with differing smallest step size. By using the simple model again and comparing with the analytical solution, it was found that the error on the final grid is in all cases of similar size whereas the error on the finest grid for the beginning of the time interval is smallest for the grid with smallest step size. In this case, the overall maximum error was approximately 0.007, which is of similar order of magnitude as the threshold used for peak detection at 0.01. Moreover, negative values only occur at one time point, reaching no more than 0.23 for V_x. Hence this grid was chosen to solve the PDE in computations of the SDE solution.

In multi-period model I (the multi-period model with constant price parameter, i.e. as described in Section 3.1), we can apply the same technique to solve the PDE. The main difference lies in the more complex overall procedure presented in Section 3.1.5. Importantly, in all simulations we compute s^i by the formula $s^i = S^{i+1}(0, x_0^{i+1})$, which is the more simple approach introduced in Section 3.1.5.

However, when applying the peak detection method described above to multi-period model I, it failed to find some irregularities in the PDE solution. This is shown in Figure 5.7a, where it can clearly be seen that although the solution fluctuates, the peak

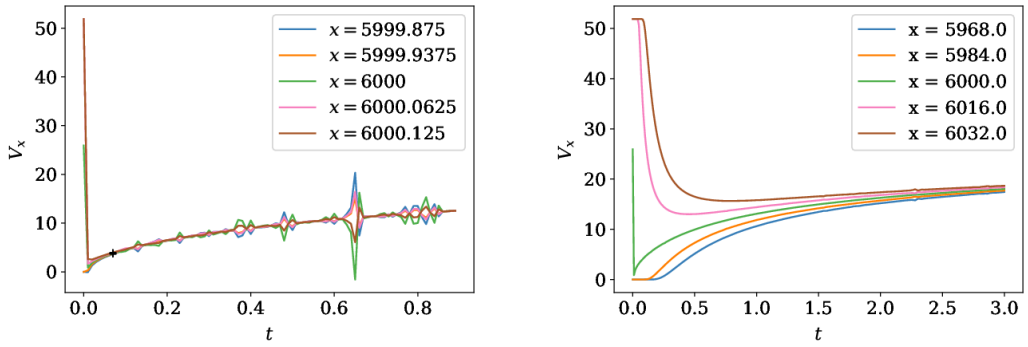

(a) On the sub-grid with smallest minimum step size.

(b) On all sub-grids, only trajectories of common grid points are considered.

Figure 5.6: Trajectories of V_x in the Brownian model variant for fixed values of x close to e_0. V_x was computed numerically on a grid with varying step size, starting with step sizes $h = (0.0625, 0.125, 0.25, 0.5, 1, 2, 4, 8, 16)$.

detection method does not initiate a grid change. Therefore, an additional peak detection method searching for irregular behavior on the x-axis was introduced. For each time point of the given solution, this method studies the x-trajectory on a certain interval around e_0 and aims to classify each step on the trajectory as increasing, decreasing or approximately constant. If this classification changes too often on a short interval, this is interpreted as unstable behavior. In detail, the method proceeds in the following way:

1. By comparing with a tolerance level, check if the first step on the given trajectory is increasing, decreasing or approximately constant; if the difference between the first values is greater than the tolerance, the trajectory at this point is classified as being increasing, if it is smaller than the negative tolerance, it is classified as decreasing, and else it is classified as approximately constant.

2. Proceed along the trajectory, i.e. study the PDE solution at the given time point for increasing values of x. In each step:

   (a) Compare with the tolerance level and conduct the classification as described above.

   (b) If the classification changes, save the index of the current point on the x-axis.

   (c) Delete saved indices if they are further away from the current point than some given value `limit`.

   (d) Check if the currently saved indices amount to more than a given maximum value denoted by `max_val`. If so, return the currently studied time point as an instability.

Several values for `limit` and `max_val` were tested; the most coherent results were obtained by setting `limit` $= 2$ and `max_val` $= 2$, i.e. by requiring two consecutive changes in the classification. Furthermore, some limitations on the search for instabilities were introduced to make sure that the grid does not get coarser too quickly, which would again lead to false negative values and additionally cause errors in the peak detection methods. The resulting behavior of the trajectories of V_x can be found in Figure 5.7b; we now observe

that although the peak detection method still misses some smaller fluctuations, it does react when they get larger.

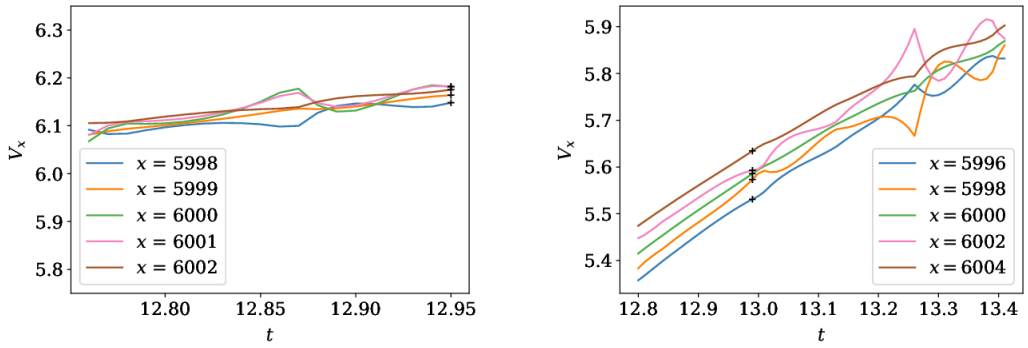

(a) Peak detection only in t-direction.

(b) Peak detection in t- and in x-direction.

Figure 5.7: Trajectories of V_x for fixed values of x close to e_0 on one sub-grid of the fourth time period computed numerically in the Brownian variant of multi-period model I. The point in time chosen by the peak detection method for the grid point change is indicated by the "+".

With regard to both peak detection methods, it should be noted that these approaches are strongly heuristic; a priori it is impossible to know which elements of the numerical solution are correct and which are corrupted by numerical errors. As argued above, we are fairly confident that the instabilities observed for instance in Figure 5.5 are not features of a correct solution. However, it is debatable which structures we aim to exclude. But since the measure we take to avoid unwanted features is to merely change the grid, we expect that this strategy does not introduce further errors to the solution. Additionally, we remark that, whereas the instabilities observed without any peak detection may have a strong impact on the quality of the overall solution, the second peak detection method probably is not strictly necessary. The fluctuations we observed in multi-period model I with the first peak detection method applied are by far not as severe and probably do not impact the solution much.

5.1.3 Implicit Runge-Kutta Method to Solve the ODE

By discretizing the x-axis as discussed above, we have obtained a system of ODEs, which we solve by applying an implicit Runge-Kutta method. To illustrate how such a method works, we consider a general initial value problem of an ODE given as

$$y' = f(t, y) \qquad y(0) = y_0$$

where $f : [0, T] \times \mathbb{R}^d \to \mathbb{R}^d$ and $y : [0, T] \to \mathbb{R}^d$. A simple method to solve such a problem is the explicit Euler method given by

$$y_{n+1} = y_n + h\, f(t_n, y_n)$$

for a given partition $0 = t_0 < t_1 < \ldots < t_n < \ldots < t_N = T$. As explained by Hairer and Wanner in [HNW93], this method only converges slowly, therefore further methods were studied. The Runge-Kutta methods, which were first introduced by Runge [Run95]

and formulated more generally by Kutta [Kut01], apply numerical integration schemes to differential equations: From the ODE given above, we know that

$$y(t_1) = y_0 + \int_{t_0}^{t_1} y'(t)\mathrm{d}t.$$

The idea is now to apply a quadrature rule given by nodes $c_1, \ldots, c_s$ and weights $b_1, \ldots, b_s$ to the integral resulting in the approximation

$$y(t_1) \approx y_0 + \sum_{i=1}^{s} b_i\, y'(t_0 + c_i\, h)$$

where we know that

$$y'(t_0 + c_i\, h) = f(t_0 + c_i\, h, y(t_0 + c_i\, h)).$$

In this expression we still need to compute $y(t_0 + c_i\, h)$. We do this by again applying a quadrature rule, with the same nodes but potentially different weights $a_{i1}, \ldots, a_{is}$, delivering

$$y(t_0 + c_i\, h) = y_0 + \int_{t_0}^{t_n + c_i\, h} y'(t)\mathrm{d}t \approx y_0 + h \sum_{j=1}^{s} a_{ij}\, y'(t_0 + c_j\, h).$$

We denote the approximated value of $y'(t_0 + c_i\, h)$ by z_i. Then this procedure can by summarized in the general formulation of an s-staged Runge-Kutta method given by

$$z_i = f\Big(x_0 + c_i\, h, y_0 + h \sum_{j=1}^{s} a_{ij}\, z_j\Big) \quad \text{for} \quad i = 1, \ldots, s,$$

$$y_1 = y_0 + h \sum_{i=1}^{s} b_i\, z_i.$$

Such a scheme can be computed directly as long as $a_{ij} = 0$ for all $j \geq i$, making it an explicit Runge-Kutta method. We work with an implicit Runge-Kutta method, where this does not hold. Therefore, Newton's method needs to be applied to solve the non-linear equations arising in the scheme.

In our setting, the dimension of the ODE corresponds to the number of grid points and y is the discretization of the function V evaluated on all grid points, which we denote by V^h. Then the function $f : [0, T] \times \mathbb{R}^N \to \mathbb{R}^N$ is given by

$$f_i(t, V^h) = -\frac{1}{2c}\, \tilde{R}(t) \left(\frac{V^h_{i+1} - V^h_{i-1}}{2h}\right)^2 + \frac{1}{2}\, \tilde{G}(t)^2\, \frac{V^h_{i-1} - 2V^h_i + V^h_{i+1}}{h^2}$$

for $i = 1, \ldots, N-1$ and by

$$f_0(t, V^h) = -\frac{1}{2c}\, \tilde{R}(t) \left(\frac{V^h_1 - V^h_0}{h}\right)^2 + \frac{1}{2}\, \tilde{G}(t)^2\, \frac{V^h_2 - 2V^h_1 + V^h_0}{h^2}$$

$$f_{N-1}(t, V^h) = -\frac{1}{2c}\, \tilde{R}(t) \left(\frac{V^h_{N-1} - V^h_{N-2}}{h}\right)^2 + \frac{1}{2}\, \tilde{G}(t)^2\, \frac{V^h_{N-1} - 2V^h_{N-2} + V^h_{N-3}}{h^2}.$$

For grids with varying step sizes, the former expression needs to be modified accordingly at the points where the step size changes. To facilitate the application of Newton's method, we also compute the Jacobian J of f as

$$\begin{aligned} J_{i,i-1} &= \frac{\partial f_i}{\partial V_{i-1}^h} = \frac{\tilde{R}(t)}{2c}\,\frac{V_{i+1}^h - V_i^h}{2h^2} + \frac{\tilde{G}(t)^2}{2h^2} \\ J_{i,i} &= \frac{\partial f_i}{\partial V_i^h} = -\frac{\tilde{G}(t)^2}{h^2} \\ J_{i,i+1} &= \frac{\partial f_i}{\partial V_{i+1}^h} = -\frac{\tilde{R}(t)}{2c}\,\frac{V_{i+1}^h - V_i^h}{2h^2} + \frac{\tilde{G}(t)^2}{2h^2} \end{aligned}$$

for $i = 1, \ldots, N-1$, with $J_{ij} = 0$ if $j < i-1$ or $j > i+1$. We again need to treat the boundary cases $J_{0,j}$ and $J_{N-1,j}$ separately, which for the sake of brevity we do not do explicitly here.

The Runge-Kutta method we apply is the so-called Radau IIA method, which was first introduced by Ehle [Ehl69] and independently by Axelsson [Axe69]. In the implementation, we make use of the `scipy` method `solve_ivp` in the `integrate` package [Com], where we set the integration method to 'Radau'. The implementation of this method including an adaptive step size selection (on the t-axis) to control the error is described in detail by Hairer and Wanner in Section IV.8 of [HW96].

5.1.4 Modifications for Multi-Period Model II

Whereas the procedure described above works in the same way for multi-period model I, i.e. with constant price parameter, we need to introduce some adjustments when we turn to multi-period model II, where the price parameter is allowed to vary (i.e. the model presented in Section 3.2). We now consider the PDE

$$V_t = -\tilde{R}(t)\,\frac{(V_x)^2}{2c} + \frac{1}{2}\,\tilde{G}(t)^2\,V_{xx} + \tilde{G}(t)\,\tilde{H}(t)\,V_{xz} + \frac{1}{2}\,\tilde{H}(t)^2\,V_{zz}$$

with initial value

$$V(0, x, z) = \tilde{R}(0)^{-1}\,P(x, z),$$

where $\tilde{R}(t) = \mathrm{e}^{r(T_{i+1}-t)}$ is the discount factor, P the penalty function and $\tilde{G}$ and $\tilde{H}$ denote the time-reversed volatility functions of X and Z, respectively. We only consider one fixed time period, therefore in contrast to the notation of Section 3.2, we omit the index i. To solve this PDE numerically, we introduce two equidistant grids $x^h \in \mathbb{R}^N$ and $z^h \in \mathbb{R}^M$, each on a given interval $[a_x, b_x]$ and $[a_z, b_z]$. If we let h_x denote the step size of the grid for x and h_z the step size of the grid for z, we have $x_i^h = a_x + ih_x$ and $z_j^h = a_z + jh_z$. In practice we always use the same step size for both grids, therefore we assume that $h := h_x = h_z$.

Then we approximate the derivatives V_x and V_{xx} as described above, where the additional variable z is fixed at $z = z_j^h$. Similarly to the difference quotient for V_{xx} we introduce

$$V_{zz}(t, x_i^h, z_j^h) \approx \frac{V(t, x_i^h, z_{j-1}^h) - 2V(t, x_i^h, z_j^h) + V(t, x_i^h, z_{j+1}^h)}{h^2}.$$

For the mixed derivative, we approximate the derivative V_x by the centered difference quotient, i.e. we compute

$$V_x^h(t, x_i^h, z_j^h) = \frac{V(t, x_{i+1}^h, z_j^h) - V(t, x_{i-1}^h, z_j^h)}{2h}.$$

Then we approximate the derivative with respect to z of V_x^h also by the centered difference quotient and obtain

$$\begin{aligned} V_{xz}(t, x_i^h, z_j^h) &\approx \frac{V_x^h(t, x_i^h, z_{j+1}^h) - V_x^h(t, x_i^h, z_{j-1}^h)}{2h} \\ &= \frac{V(t, x_{i+1}^h, z_{j+1}^h) - V(t, x_{i-1}^h, z_{j+1}^h) - V(t, x_{i+1}^h, z_{j-1}^h) + V(t, x_{i-1}^h, z_{j-1}^h)}{4h^2}. \end{aligned}$$

This only works for $i = 1, \dots, N-2$ and $j = 1, \dots, M-2$; as in Section 5.1.1, we need to treat the cases at the boundary separately. Again we use left-sided or right-sided difference quotients as necessary. As an example, we consider the case that $j = 0$. For V_{zz} we then have by twice applying a right-sided difference quotient

$$V(t, x_i^h, z_0^h) \approx \frac{V(t, x_i^h, z_2^h) - 2V(t, x_i^h, z_1^h) + V(t, x_i^h, z_0^h)}{h^2}.$$

For the mixed derivative we still apply the centered difference quotient to approximate the derivative V_x as long as x_i^h does not also lie at the boundary. Then we use the right-sided difference quotient in z resulting in

$$V_{xz}(t, x_i^h, z_0^h) \approx \frac{V(t, x_{i+1}^h, z_1^h) - V(t, x_{i-1}^h, z_1^h) - V(t, x_{i+1}^h, z_0^h) + V(t, x_{i-1}^h, z_0^h)}{2h^2}.$$

Since we have to consider the cases where x_i^h or z_j^h lie at one of the boundaries, as well as the cases at the corners where $(i, j) \in \{(0,0), (N-1,0), (0,M-1), (N-1,M-1)\}$, many other special cases arise, which we omit here for brevity.

Thus we have again transformed the PDE into an ODE, which now has dimension $N \times M$, i.e. takes the form of a matrix, where

$$\begin{aligned} V_t(t, x_i^h, z_j^h) = &-\frac{\tilde{R}(t)}{2c} \left(\frac{V(t, x_{i+1}^h, z_j^h) - V(t, x_{i-1}^h, z_j^h)}{2h} \right)^2 \\ &+ \frac{\tilde{G}(t)^2}{2} \frac{V(t, x_{i-1}^h, z_j^h) - 2V(t, x_i^h, z_j^h) + V(t, x_{i+1}^h, z_j^h)}{h^2} \\ &+ \tilde{G}(t)\, \tilde{H}(t) \frac{V(t, x_{i+1}^h, z_{j+1}^h) - V(t, x_{i-1}^h, z_{j+1}^h) - V(t, x_{i+1}^h, z_{j-1}^h) + V(t, x_{i-1}^h, z_{j-1}^h)}{4h^2} \\ &+ \frac{\tilde{H}(t)^2}{2} \frac{V(t, x_i^h, z_{j-1}^h) - 2V(t, x_i^h, z_j^h) + V(t, x_i^h, z_{j+1}^h)}{h^2}. \end{aligned}$$

for $(i, j) \in \{1, \dots, N-2\} \times \{1, \dots, M-2\}$; otherwise we need to apply the modified difference quotients as indicated above. By introducing again the function V^h as the discretization of the function V, where now $V^h : [0, T] \to \mathbb{R}^{N \times M}$, we reformulate the ODE as

$$\begin{aligned} \frac{\mathrm{d}V_{i,j}^h}{\mathrm{d}t} = &-\frac{\tilde{R}(t)}{2c} \left(\frac{V_{i+1,j}^h - V_{i-1,j}^h}{2h} \right)^2 + \frac{\tilde{G}(t)^2}{2} \frac{V_{i-1,j}^h - 2V_{i,j}^h + V_{i+1,j}^h}{h^2} \\ &+ \tilde{G}(t)\, \tilde{H}(t) \frac{V_{i+1,j+1}^h - V_{i-1,j+1}^h - V_{i+1,j-1}^h + V_{i-1,j-1}^h}{4h^2} \\ &+ \frac{\tilde{H}(t)^2}{2} \frac{V_{i,j-1}^h - 2V_{i,j}^h + V_{i,j+1}^h}{h^2}. \end{aligned}$$

This ODE is again solved numerically by the Radau IIA Runge-Kutta method as described above. Also in this case we provide the Jacobian, which now takes the form of a four-dimensional tensor where

$$J_{ijkl} = \frac{\partial f_{ij}}{\partial V^h_{kl}}.$$

For $(i,j) \in \{1,\dots,N-2\} \times \{1,\dots,M-2\}$ we then have

$$(J_{ijkl})_{k=i-1,i,i+1;l=j-1,j,j+1} = \begin{pmatrix} \frac{\tilde{G}(t)\,\tilde{H}(t)}{4h^2} & \frac{\tilde{R}(t)}{2c}\,\frac{V^h_{i+1,j}-V_{i-1,j}}{2h^2} + \frac{\tilde{G}(t)^2}{2h^2} & -\frac{\tilde{G}(t)\,\tilde{H}(t)}{4h^2} \\ \frac{\tilde{H}(t)^2}{2h^2} & -\frac{\tilde{G}(t)^2}{h^2} - \frac{\tilde{H}(t)^2}{h^2} & \frac{\tilde{H}(t)^2}{2h^2} \\ -\frac{\tilde{G}(t)\,\tilde{H}(t)}{4h^2} & -\frac{\tilde{R}(t)}{2c}\,\frac{V^h_{i+1,j}-V^h_{i-1,j}}{2h^2} + \frac{\tilde{G}(t)^2}{2h^2} & \frac{\tilde{G}(t)\,\tilde{H}(t)}{4h^2} \end{pmatrix}$$

and $J_{ijkl} = 0$ for any other k and l. The boundary cases again need to be considered separately and are omitted here. Since the solver `solve_ivp` cannot handle matrix ODEs, we first flatten the matrix valued function V^h to an $\mathbb{R}^{NM}$-valued function. Then we obtain an ODE of the form

$$y' = f(t,y)$$

where $f : [0,T] \times \mathbb{R}^{NM} \to \mathbb{R}^{NM}$. For the corresponding Jacobian J_f we have $J_f : [0,T] \times \mathbb{R}^{NM} \to \mathbb{R}^{NM \times NM}$. Both the function f as the right-hand side of the ODE and the Jacobian J_f are passed to the ODE solver and treated as described in the previous section.

As can be seen from the dimensions of f and J_f, the second variable in multi-period model II greatly increases computational effort and storage requirements. Additionally, using non-equidistant grids would again entail further modifications on the difference quotients and the implementation thereof. Thus only coarser equidistant grids with step sizes 10, 20 and 50 were tested; these tests were done in the simple model variant. As shown in

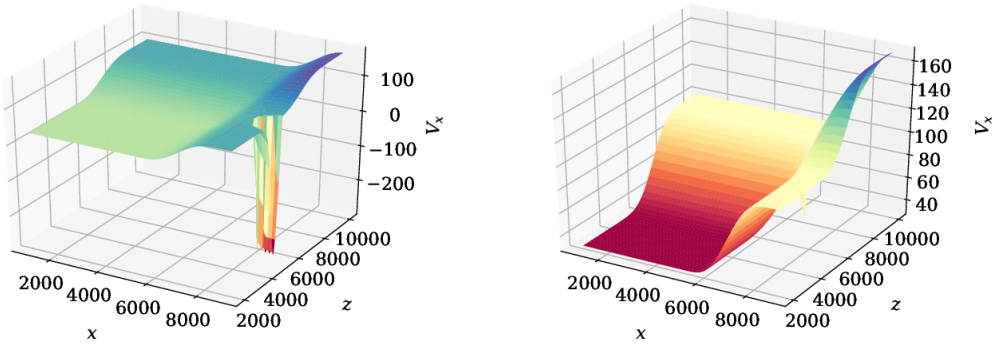

(a) $h = 10$ **(b)** $h = 20$

Figure 5.8: PDE solution V_x of the last time period in the simple model variant of multi-period model II. The solution is shown at the fixed time point $t = 1.5$ for two different step sizes h.

Figure 5.8, the result with a step size of 10 shows a strong anomaly for large values of x and rather small values of z; this also appears to greatly increase the run time of solving the PDE. Since the anomaly lies at a position that the SDE system rarely reaches, because X and Z are strongly correlated, the high run time is the more problematic issue. On a grid with step size $h = 20$ the anomaly is still present, but by far not as severe; moreover, the run time in this case is acceptable. The grid with step size $h = 50$ is already quite

coarse and might lead to less accurate results; although the above mentioned anomaly is not present on this grid, there seems to be an error for large values of z. Therefore, an equidistant grid with $h = 20$ was chosen for numerical computations in the simple model variant. In the Brownian and Ornstein-Uhlenbeck model variants, the solution algorithm fails for a step size of $h = 20$ or $h = 50$. Thus simulations had to be conducted with the very coarse step size of $h = 100$.

As explained in Section 3.2.5, we need to specify the price function for the last time period $\tilde{S}_0^N$ in advance. One straight-forward approach to this is to set $\tilde{S}_0^N(z) = s$ for some constant s, similar to the case of multi-period model I. To be able to let the price parameter vary also for the last time period, we make use of multi-period model I: For a given constant s, we solve the PDE of this model on a time period after the actual final time point T and use the resulting price function as input for multi-period model II. More precisely, we compute a solution V_x^{fin} of the PDE derived in Section 3.1.2 on $[T, T + \Delta T]$, which delivers the price function as $\tilde{S}_0^N(z) = V_x^{\text{fin}}(0, z)\,\mathrm{e}^{rT}$.

Summary

We first introduced the discretization of our PDE along the x-axis, which transforms the PDE into an ODE. Then we discussed the choice of an appropriate grid for the discretization: To reduce numerical errors, we use a grid with varying step sizes, which becomes coarser in time. Since we apply an implicit Runge-Kutta method to solve the ODE, we provided an introduction to this class of ODE solution methods. Additionally, we described how we obtain the functions required for the Runge-Kutta method from the discretized PDE. Finally, we commented on the adjustments that need to be made to apply this procedure to multi-period model II.

5.2 Numerical Solution of the SDE

We aim to solve the SDE

$$\mathrm{d}X_t = -u(t, X_t)\mathrm{d}t + G(t)\mathrm{d}W_t.$$

To compute a numerical solution, we will apply the Euler-Maruyama scheme as already introduced in Section 2.4.2 in Definition 2.19. Again this involves a discretization of a particular input variable, in this case the time variable t. We choose an equidistant partition $0 = t_0 < t_1 < \ldots < t_N = T$ with step size $\Delta t = 0.01$, so we have $t_n = n\,\Delta t$. Then we set $X_0 = x_0$ (we will discuss in Section 5.3.3 how we choose the constant x_0) and apply the scheme

$$X_{t_{n+1}} = X_{t_n} - u(t_n, X_{t_n})\,\Delta t + G(t_n)\Delta W_n.$$

For each time step n, we have to simulate a Brownian increment as $\Delta W_n \sim \mathcal{N}(0, \Delta t)$. Furthermore, we need to evaluate the drift function u at given points t_n and X_n. If we have an analytical solution of the PDE, this can easily be implemented by writing the analytical solution as a function in the code. If on the other hand we only have a numerical PDE solution, this gives us the function values at the corresponding grid points, but not in-between. The output of the PDE solution is chosen in such a way that the time points match the partition used in the Euler-Maruyama scheme. Along the x-axis we then need to perform linear interpolation to obtain an approximation of the PDE solution $V_x(t_n, x)$ at any given point x. From the PDE solution, we can directly compute the drift $u(t_n, x)$.

In the rare case that the process X leaves the grid on which the PDE was solved, linear extrapolation is applied to compute $V_x(t_n, x)$. At the same time the occurrence of this is documented.

By applying the scheme as described, we obtain one realization of the process X. Since we are interested in the distribution of X, we repeat this procedure many times; we choose to do 10 000 repetitions. From the thus obtained realizations of X we compute quantities such as the expectation $\mathrm{E}[X_t]$, the variance $\mathrm{Var}(X_t)$ for any $t \in \{t_0, \ldots, t_N\}$, but also visualize for example the distribution of X_T.

If we are aiming to solve the SDE in multi-period model I, i.e. with constant price parameter, we have to introduce some minor modifications. We now define a partition for each time period $[0, \Delta T_i]$ with N steps and again step size $\Delta t = 0.01$, i.e. we have $0 = t_0 < t_1 < \ldots < t_{N-1} < t_N = \Delta T_i$ with $t_n = n\,\Delta t$. In each time period i - except for the first - we need to compute the initial value given by X_0^i from the realization of the Brownian motion W until time T_i, as shown in Section 3.1.1. More precisely, in the simple model variant we have

$$X_0^i = x_0^i + \sigma W_{T_i}$$

and in the Brownian variant

$$X_0^i = x_0^i + \sigma\,\Delta T_i\, W_{T_i},$$

therefore in these two model variants we require the realized value of W_{T_i}. In the Ornstein-Uhlenbeck variant we have

$$X_0^i = x_0^i - \sigma\,\frac{\mathrm{e}^{-\theta T_{i+1}} - \mathrm{e}^{-\theta T_i}}{\theta} \int_0^{T_i} \mathrm{e}^{\theta s}\mathrm{d}W_s,$$

so we need to approximate the realization of the stochastic integral $\int_0^{T_i} \mathrm{e}^{\theta s}\mathrm{d}W_s$. We compute W_{T_i} from the simulated Brownian increments as

$$W_{T_i} = \sum_{n=0}^{iN-1} \Delta W_n = \sum_{n=0}^{iN-1} (W_{t_{n+1}} - W_{t_n}) = W_{t_{iN}}$$

and approximate the stochastic integral by its discretization

$$\int_0^{T_i} \mathrm{e}^{\theta s}\mathrm{d}W_s \approx \sum_{n=0}^{iN-1} \mathrm{e}^{\theta t_n}\,\Delta W_n.$$

Note that if we are in time period i, the increments ΔW_n for $n = 0, \ldots, iN-1$ are available since we solve the SDEs forward in time and have thus simulated these increments when solving the SDE for time period $0, \ldots, i-1$.

In the case of multi-period model II, where the price parameter is allowed to vary, we need to make some further modifications. Firstly, we now also need to solve the SDE describing the process Z given by

$$\mathrm{d}Z_t^i = H^i(t)\mathrm{d}W_t^i.$$

This can be done by applying the Euler-Maruyama scheme as for the process X, delivering

$$Z_{t_{n+1}}^i = Z_{t_n}^i + H^i(t_n)\,\Delta W_n,$$

where in each time period Z_0^i is computed from X_0^i.

Furthermore, the evaluation of u becomes more challenging: The drift u is now a function of t, x and z, where both x and z usually do not lie on the grid for which we have computed the PDE solution. For $x \in [x_i^h, x_{i+1}^h]$ and $z \in [z_j^h, z_{j+1}^h]$ and a grid point t_n we therefore need to perform a bilinear interpolation between the four points (x_i^h, z_j^h), (x_{i+1}^h, z_j^h), (x_i^h, z_{j+1}^h) and (x_{i+1}^h, z_{j+1}^h). We first interpolate between (x_i^h, z_j^h) and (x_{i+1}^h, z_j^h) to obtain an approximation for $u(t_n, x, z_j^h)$ and between (x_i^h, z_{j+1}^h) and (x_{i+1}^h, z_{j+1}^h) to approximate $u(t_n, x, z_{j+1}^h)$. By then interpolating between (x, z_j^h) and (x, z_{j+1}^h), we obtain the desired approximation for $u(t_n, x, z)$. Also in this model we use linear extrapolation if the processes X or Z leave their respective grid. Since they might do so independently, we also need to allow for mixed cases. If for example X leaves its grid, but Z is still on its grid, we perform extrapolation in the direction of x and interpolation in the direction of z.

Summary

In this section, we described how we apply the Euler-Maruyama scheme to the SDEs for X, and in case of multi-period model II also for Z. We discussed the evaluation of the drift u away from the grid points of the PDE solution and explained the computation of the initial values of later time periods, given by X_0^i and Z_0^i, in the multi-period models.

5.3 Parameter Choices

For the purpose of consistency parameters were largely chosen as in the work by Seifert et al. [SUW08]; the default value of each parameter can be found in Table 5.1. We will discuss the choice of these parameters below. Since many parameters are hard to estimate, we also conduct numerical simulations with varying parameters to cover a wider range for the parameters in question. It should be noted that the choice of units is a bit unusual:

Table 5.1: Default parameter choices for numerical simulations.

Parameter	Value	Unit
T	3	years
e_0	6000	Mt CO_2 equivalents
p	70	Euro per ton
r	0.10	
c	0.24	Euro times years per $10^6\,t^2$
x_0	6240	Mt CO_2 equivalents
P	6	
s^{N-1}	0	Euro per ton

The emissions and also the emission threshold are measured in mega tons (Mt) to avoid the use of large numbers. At the same time, the penalty is given in Euro per ton for the same reason. Thus the unit of the costs in the system given by V is 10^6 Euro; the unit of the abatement rate is Mt per year. Since the price of an allowance should be given in Euro per ton, the resulting unit for the cost coefficient c is Euro times years per $10^6\,t^2$, which is also consistent with the unit of the abatement cost function given as 10^6 Euro per year. In this way, the cost coefficient balances out the mismatch of units for emission data and price data.

5.3.1 Regulatory Parameters

Several parameters appearing in our model are regulatory parameters which are set by the respective regulatory institution; in case of the EU ETS, this is the European Union or its member states. The regulatory framework of the EU ETS was established in 2003 by the Directive 2003/87/EC of the European Parliament and the Council [EU03]; major adjustments were made in 2018 by the Directive 2018/410 [EU18]. The figures quoted below mainly can be found in these documents.

One parameter to be set by the regulator is the length of the trading period T or the length of one sub-period ΔT. The first phase of the EU ETS was three years long (from 2005 until 2007). Later phases were increasingly longer with Phase 2 lasting 5 years (from 2008 until 2012), Phase 3 of 8 years (from 2013 until 2020) and the current Phase 4 spanning 10 years (from 2021 until 2030). Since in the one-period model allowances become invalid at the end of the time period and no auctioning is possible, this is closest to the regulatory framework of the EU ETS in its earliest phase. Thus we choose $T = 3$. Also in multi-period models we set $\Delta T = 3$ so that any differences to the one-period model can be attributed to the multi-period setting rather than a change in the length of one time period. We study the effect of such a change separately.

A key choice by the regulator concerns the initial endowment of allowances to the system given by the parameter e_0. In the initial phase of the EU ETS, the allocation of allowances was done by each country separately via so-called national allocations plans. The total allocations of each country can be found in the European Union Transaction Log [ECb] and were formerly stored in its predecessor, the Community Independent Transaction Log (CITL). In their analysis on abatement in Phase 1, Anderson and Di Maria [AD11] use this data and obtain an amount of 6246.6 Mt CO_2 from the sum of all national allocation plans. In line with Seifert et al. we choose $e_0 = 6000$, although this is considerably lower than the actual amount. As we will see below, the expected emissions without abatement x_0 can reasonably be set to $x_0 = 6240$, which means that in expectation no abatement would be required. In order to study the impact of the emission trading system, we therefore choose a value slightly below x_0. The allocation of allowances plays a key role in ensuring the efficacy of an ETS: If too many allowances are present, there is no longer an incentive to reduce emissions, whereas if there are too few allowances, costs of abatement may prove to be so large that companies choose to pay the penalty instead. Therefore, we vary the amount of allocated allowances to study how this affects the system. Since the third phase, i.e. since 2013, the allocation of allowances is done centrally on a union-wide level. For the year 2013, the number of allowances was set to 2048 Mt CO_2; this figure decreased yearly by 1.74% until 2020 and by 2.2% from 2021 onward, amounting to 1572 Mt CO_2 for 2021. Therefore, we also study the effect of decreasing the amount of allocated allowances in multi-period model I.

Another important regulatory parameter is the choice of the penalty payment: As can already be seen from theoretical considerations, this strongly impacts the allowance price. Initially, the penalty was set to 40 Euro per ton of surplus emissions. In their work, Seifert et al. set the penalty parameter to $p = 70$ to account for the requirement to surrender the missing allowances in the subsequent time period; they assume that the price of these allowances is approximately 30 Euro. We will therefore also set $p = 70$ in the one-period model. In the multi-period models, we use the price parameter s^i to represent the price of the missing allowances, thus we set $p = 40$. Furthermore, from 2008 on the penalty in the EU ETS was increased to 100 Euro; to account for this and to study the effects of a further

increase in the penalty, we additionally work with $p = 100$ and $p = 160$. Furthermore, we vary the penalty in the one-period model to observe how this impacts the emission trading system.

5.3.2 Descriptory Parameters

Two further parameters are required which are not chosen by the regulator but are also not determined from emission data. The interest rate r needs to be set to $r = 0$ to be able to compute analytical solutions in the simple model variant. For all other variants, the reference interest rate of the European Central Bank (ECB) can be used as orientation; for the years from 2005 to 2007, during phase 1 of the EU ETS, an interest rate between 2% and 4% would be plausible. For later years, a lower interest rate would be more realistic; since 2013 the main refinancing operations rate of the ECB is close to zero, thus $r = 0$ as required for analytical solutions is realistic. Seifert et al. on the contrary choose an artificially high interest rate of 10% to stress the effect of interest. Again for consistency we work with $r = 0.1$ where it is possible.

Furthermore, we need to set the cost coefficient c. In theory, this parameter captures the cost of abatement for each company in the system in an aggregated way, hence it is very difficult to estimate. One way to circumvent this problem is to assume that abatement is undertaken by fuel-switching, as it is done for example by Carmona et al. [CFH09]; then coal and gas prices can be used to obtain the cost of abatement Seifert et al. adopt a different approach: They argue that in a deterministic setting with parameters chosen as given above, the representative agent would need to abate 80 Mt per year, leading to marginal abatement costs and thus an allowance price of $80c$. They choose $c = 0.24$, corresponding to an allowance price of 19.2, which lies in the range of allowance prices of the year 2006 that varied between 10 and 30 Euro. This however can only be a very rough estimate: Any other value between 0.125 and 0.375 would also work in this argumentation; moreover, the value of e_0 and therefore the yearly abatement of 80 Mt is not exact, so possibly it would be more reasonable to work with the estimates in the literature of approximately 60 Mt per year for the first phase of the EU ETS. As default we set $c = 0.24$ but we additionally study the effect that the cost coefficient has on overall results. Due to technological advancement it is plausible that the cost coefficient decreases in time. We analyze the effects of such a decrease in multi-period model I.

5.3.3 Parameters Derived from Emission Data

The remaining parameters, the initially expected emissions x_0 and the parameters characterizing the emission rate Y, are all linked to observable emission data. In this section, we will explain how to obtain x_0 from the so-called historical baseline data collected by governments and derive the parameters to describe Y from data on emissions within the European Union. Emission data is available from the European Union itself but this only dates back to 1990. Therefore, we will use a data set from the World Bank, providing the yearly CO_2 emissions from 1960 until 2016 in the European Union [WBa][2]. We will only use the data until 2004 since we do not want to have the effect of the EU ETS contained in our data. We will denote this data set by $(\tilde{E}_T^{T+1})_{T=0,\dots,N}$, where we let $\tilde{E}_T^{T+1}$ be the emissions in year T. More generally, we denote by $\tilde{E}_{T_1}^{T_2}$ the emissions from the beginning

[2]It should be remarked that this data set is no longer available on the World Bank website; currently only data from 1990 onwards is available.

of year T_1 until the beginning of year T_2. A graphical visualization of the World Bank data set can be found in Figure 5.9. The graph shows a steep increase in yearly emissions between 1960 and 1975 but after that the development of yearly emissions changed drastically; since 1979 emissions have slightly decreased again on average and exhibit a much more irregular behavior. It seems unreasonable that the increase until 1975 contains any information on how yearly emissions would behave from 2005 onwards. We will therefore consider several different ranges for our data set, all starting in 1975 or later.

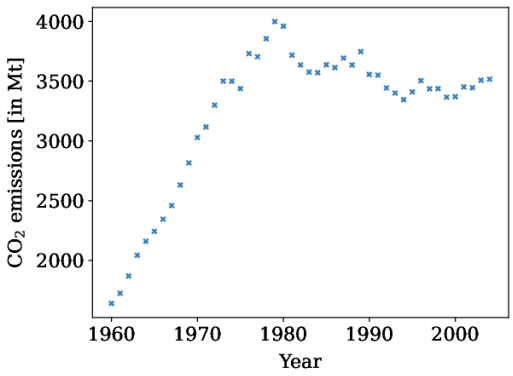

Figure 5.9: CO_2 emissions of the European Union between 1960 and 2004 as given by the World Bank data set [WBa].

Importantly, the EU ETS only covers the greenhouse gas emissions in the European Union partially[3], whereas the World Bank data comprises all CO_2 emissions of the respective year. We thus need to scale the data set by an appropriate scaling factor, denoted by ρ. To obtain this factor, we will make use of the parameter x_0, which represents the initially expected emissions in the EU ETS without abatement and is thus in particular a figure that only takes emissions into account which underlie the EU ETS. We will then denote the scaled emission data as $\left(E_T^{T+1}\right)_{T=0,\dots,N}$. The parameters estimated in this section for the different variants are summarized in Table 5.2.

Table 5.2: Parameters derived from emission data for the three different model variants.

Model variant	Parameter	Value
All	x_0	6240
	σ	115.47 or 288.68
Brownian	μ	-10
Ornstein-Uhlenbeck (one-period model)	θ	0.2
Ornstein-Uhlenbeck (multi-period model)	θ	0.04
	μ	2000

It should be noted that the data available is scarce and may contain biases and flaws. Furthermore, the structure of the process Y does not allow for simple estimation techniques for all parameters required. Thus the description below can only show that the parameters given here are plausible; we cannot provide a precise derivation of these results.

[3]More precisely, it also only covered CO_2 emissions in its first phase from 2005 until 2007, emissions of other greenhouse gases were added in the subsequent phases.

The Initially Expected Emissions x_0

The parameter x_0 represents the emissions we expect initially and without abatement to occur in course of the trading period. Before the start of the EU ETS, it was crucial to know how many emissions were to be expected in the relevant sectors without the emission trading system, therefore the EU member states attempted to estimate a corresponding figure by gathering a historical emission baseline. The results can be found at the German Emissions Trading Authority [Lan+05]; as commented by Ellerman and Buchner in their analysis on abatement or over-allocation in 2005 [EB08], the baseline data may be biased due to the mechanism and the time pressure under which it was collected. Nevertheless we will use this data to obtain the parameter x_0. The historical baseline emissions for the EU, based on data from 2001 until 2003, amount to 2078 Mt CO_2 per year. For a period of three years we would therefore obtain 6234 Mt CO_2, which is approximately the value of $x_0 = 6240$ that Seifert et al. use in their simulations. Ellerman and Buchner continue to adjust this value by taking into account economic growth and the change in carbon intensity, which delivers expected BAU emissions of 2150 Mt CO_2 in 2005. Since we are only interested in a rough estimate and to maintain consistency with the work by Seifert et al., we will use the value of $x_0 = 6240$.

The Drift Parameter μ in the Brownian Model Variant

We aim to use the emission data to estimate the drift parameter μ of the Brownian model variant. Since we only have yearly emission data, we approximate the emission rate Y_T of year T by E_T^{T+1}, thus we have in the Brownian model that

$$E_T^{T+1} \approx Y_T = y_0 + \mu\, T + \sigma\, W_T = y_0 + \mu\, T + \varepsilon$$

with $\varepsilon \sim \mathcal{N}(0, \sigma^2\, T)$. Therefore, we perform simple linear regression on the data pairs (T, E_T^{T+1}). This is done by using the Python package `scikit-learn` [Ped+11]. We first apply linear regression to the unscaled data $(T, \tilde{E}_T^{T+1})$ and obtain the corresponding parameters $\tilde{y}_0$ and $\tilde{\mu}$. We use these estimates to extrapolate the line to the years 2005 until 2007, which corresponds to the first phase of the EU ETS. From this extrapolation, we derive an estimate for the emissions expected from 2005 until 2007 given by

$$\tilde{x}_0 = Y_{2005} + Y_{2006} + Y_{2007} = 3\tilde{y}_0 + (2005 - T_0)\tilde{\mu} + (2006 - T_0)\tilde{\mu} + (2007 - T_0)\tilde{\mu},$$

where we need to subtract the year T_0 that we use as zero in the linear regression. In the data sets we work with below, we have $T_0 = 1974$, $T_0 = 1978$ and $T_0 = 1989$ for the time period starting in 1975, 1979 and 1990, respectively. The linear regression performed on the unscaled data including the extrapolation is shown in Figure 5.10. From $\tilde{x}_0$, we compute the scaling factor to obtain the emissions that underlie the EU ETS as

$$\rho = \frac{\tilde{x}_0}{x_0}.$$

By applying the scaling factor to the parameters estimated from linear regression we arrive at the scaled parameters that can be used in our model. We perform these computations on three different time periods, namely 1975 to 2004, 1979 to 2004 and 1990 to 2004, as these years all mark a changing behavior of the yearly emissions. Moreover, 1990 is also a common reference to judge emission reductions and was for instance the reference year in the Kyoto Protocol. The results are summarized in Table 5.3. The determination

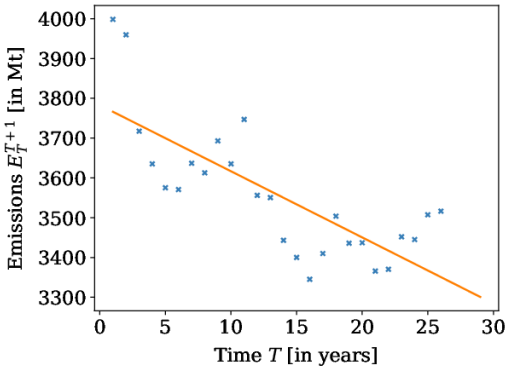

Figure 5.10: Yearly emissions from 1979 to 2004 and corresponding regression line, extrapolated for the years 2005 to 2007.

Table 5.3: Results from linear regression to estimate the parameter μ in the Brownian model

Time period	$\tilde{y}_0$	$\tilde{\mu}$	R^2	$\tilde{x}_0$	ρ	y_0	μ
1975 – 2004	3782.51	−13.39	0.48	10061.69	0.62	2345.16	−8.30
1979 – 2004	3782.87	−16.62	0.58	9952.35	0.63	2383.21	−10.47
1990 – 2004	3460.70	−1.43	0.0094	10309.12	0.61	2111.02	−0.87

coefficients R^2 indicate that the model fits the data fairly well when the data from 1975 to 2004 or from 1979 to 2004 are used (as can be also observed in Figure 5.10 for the years from 1979 to 2004), whereas the data set from 1990 to 2004 does not seem to follow a linear relation as assumed in the Brownian model. We also observe that the drift coefficient μ is negative in all three cases, ranging from -0.87 to -10.47. Since the fit is best for the data from 1979 to 2004 and the result is only slightly different for the data from 1975 to 2004, we will use a drift coefficient of $\mu = -10$ in our simulations. Note that we only require μ in the multi-period model; in the one-period model this parameter is contained in the parameter x_0. The same holds for the parameter y_0 in general, which we therefore do not require at all.

The second parameter we have in the Brownian model variant is the volatility σ. Since this is difficult to estimate in the Brownian model variant and for better comparability with the simple model variant, we will use the volatility estimated in the setting of the simple model variant, as described next.

The Volatility Parameter σ in the Simple Model Variant

In the simple model variant we model the total expected emissions X directly. At final time of a given time period $[0, T]$, we then have

$$X_T = x_0 - \int_0^T u_t \mathrm{d}t + \sigma W_T.$$

By omitting the abatement term, we obtain the realized emissions without abatement, i.e. the Business-As-Usual (BAU) emissions

$$X_T^{\mathrm{BAU}} = x_0^{(T)} + \sigma W_T \sim \mathcal{N}\left(x_0^{(T)}, \sigma^2 T\right),$$

where the initially expected total emissions $\tilde{x}_0^{(T)}$ depend on the length of the time period T, as indicated by the superscript. With the notations introduced above, we have for the unscaled data with unscaled parameters $\tilde{x}_0^{(T)}$ and $\tilde{\sigma}$

$$\tilde{E}_{T_1}^{T_2} \approx X_{T_2-T_1}^{\mathrm{BAU}} = \tilde{x}_0^{(T_2-T_1)} + \tilde{\sigma}\, W_{T_2-T_1}$$

and more specifically for the emissions in year T

$$\tilde{E}_T^{T+1} \approx \tilde{x}_0^{(1)} + \tilde{\sigma}\, W_1 \sim \mathcal{N}\left(\tilde{x}_0^{(1)}, \tilde{\sigma}^2\right).$$

Thus we compute the sample mean and sample standard deviation to estimate $\tilde{x}_0^{(1)}$ and $\tilde{\sigma}$. Since the initially expected emissions x_0 are given for a period of three years, we compute the scaling factor ρ by

$$\rho = \frac{x_0}{3\tilde{x}_0^{(1)}}.$$

To maintain consistency with the estimates from the Brownian model variant, we also apply the scaling factor computed in the Brownian model variant for the respective time period. We then obtain the appropriately scaled result for the volatility as $\sigma = \rho\,\tilde{\sigma}$. The results of all computations are summarized in Table 5.4. For the data from the time

Table 5.4: Estimation of the volatility σ and the initially expected total emissions $x_0^{(1)}$ in the simple model variant. Scaled results were computed both from the scaling factor derived in the Brownian and in the simple model variant.

Time period	$\tilde{x}_0^{(1)}$	$\tilde{\sigma}$	Origin of ρ	ρ	$x_0^{(1)}$	σ
1975 – 2004	3574.90	170.16	Simple model	0.58	2073.44	98.70
			Brownian model	0.62	2216.44	105.50
1979 – 2004	3558.47	166.67	Simple model	0.58	2063.91	96.67
			Brownian model	0.63	2241.84	105.00
1990 – 2004	3449.25	65.94	Simple model	0.60	2069.55	39.56
			Brownian model	0.61	2104.04	40.22

periods from 1975 to 2004 and from 1979 to 2004, we obtain a volatility of approximately 100, whereas the data set from 1990 to 2004 delivers a volatility of only 40. As can be seen from Figure 5.11, both of these results should be treated with caution; the histograms of the underlying data do not provide strong support for the assumption that this data follows a normal distribution.

In their work, Seifert et al. work with a volatility that depends on the length T of the time period considered and is given by $\sigma = \frac{500}{\sqrt{T}}$; thus the variance of the BAU emissions X_T^{BAU} is constant in the length of the time period. For a time period of three years, this corresponds to a volatility of $\sigma = 288.68$. They argue that this should lead to a volatility of the price of about 50% as observed in market prices. This value deviates considerably from the estimation results above; additionally we will observe below that the volatility strongly impacts the system as a whole. In early simulations, we studied the impact of a small volatility by setting $\sigma = \frac{200}{\sqrt{T}} = 115.47$ for $T = 3$, in line with the approach by Seifert et al. Since this is close to the volatility of approximately 100 derived above, we will use the value of 115.47 instead. In summary, we mainly work with a volatility of 288.68 and provide additional results with a smaller volatility of 115.47 in the appendix.

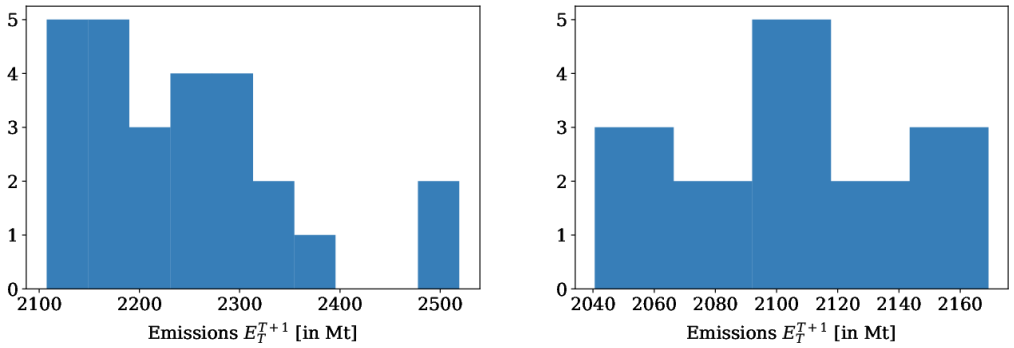

(a) 1979 to 2004

(b) 1990 to 2004

Figure 5.11: Histogram of the yearly emissions E_T^{T+1} for two different time periods.

Additionally, we vary the volatility further to analyze its impact on simulation results. However, in contrast to the approach by Seifert et al., we do not let the volatility vary with the length of the time period; also for varying T we will use a fixed value for the volatility.

The Mean Reversion Speed θ in the Ornstein-Uhlenbeck Model Variant

The Ornstein-Uhlenbeck model variant of the emission rate can be written as

$$Y_T = y_0 \, \mathrm{e}^{-\theta T} + \mu(1 - \mathrm{e}^{-\theta T}) + \sigma \int_0^T \mathrm{e}^{-\theta(t-s)} \mathrm{d}W_s.$$

As in the Brownian model variant, we approximate the emission rate by the yearly emissions E_T^{T+1}. Then we have

$$E_T^{T+1} \approx Y_T = y_0 \, \mathrm{e}^{-\theta T} + \mu(1 - \mathrm{e}^{-\theta T}) + \varepsilon = (y_0 - \mu)\mathrm{e}^{-\theta T} + \mu + \varepsilon,$$

where ε follows a normal distribution with mean zero, i.e. $\varepsilon \sim \mathcal{N}\left(0, \bar{\sigma}^2(T)\right)$ for some T-dependent variance $\bar{\sigma}^2(T)$. We thus have a non-linear function involving four different parameters, which makes it very challenging to find proper estimates. We therefore again use the same volatility parameter σ as for the other two model variants. Furthermore, we can obtain y_0 from the Brownian model variant since this parameter serves a similar purpose in both model variants. However it is not plausible to also take μ from the Brownian model variant; while in the Brownian variant μ denotes the drift, in the Ornstein-Uhlenbeck variant it represents the long term mean. In particular, we have

$$\lim_{T \to \infty} \mathrm{E}\left[Y_T\right] = \mu,$$

whereas in the Brownian variant

$$\lim_{T \to \infty} \mathrm{E}\left[Y_T^B\right] = \begin{cases} \infty & \text{if } \mu > 0 \\ 0 & \text{if } \mu = 0 \\ -\infty & \text{if } \mu < 0. \end{cases}$$

In a first approach, we therefore use the parameter $x_0^{(1)}$ computed in the simple model variant, as this represents the mean emissions of one year, so it may serve as the long term mean of the yearly emission rate.

It remains to determine θ. We have seen that

$$Y_T = (y_0 - \mu)\mathrm{e}^{-\theta T} + \mu + \varepsilon$$

with $\varepsilon \sim \mathcal{N}\left(0, \bar{\sigma}^2(T)\right)$. For varying θ in a given interval $[a, b]$, we compute

$$Y_T(\theta) = (y_0 - \mu)\mathrm{e}^{-\theta T} + \mu$$

and aim to find θ solving

$$\min_{\theta \in [a,b]} \sum_{T=1}^{N} \left(E_T^{T+1} - Y_T(\theta)\right)^2,$$

i.e. as in linear regression, we minimize the sum of the squared residuals. We perform this minimization simply by discretizing the considered interval $[a, b]$, where we choose $[a, b] = [0, 2]$. The results computed from the different time periods can be found in Table 5.5. For each data set we also compute the determination coefficient R^2 as

$$R^2 = \frac{S_N^2\left(E_T^{T+1}\right) - \mathrm{RES}\left(E_T^{T+1}, \theta\right)}{S_N^2\left(E_T^{T+1}\right)}$$

where $S_N^2\left(E_T^{T+1}\right)$ denotes the sample variance of $\left(E_T^{T+1}\right)_{T=0,\ldots,N}$ and $\mathrm{RES}\left(E_T^{T+1}, \theta\right)$ denotes the sum of the squared residuals as given above, i.e.

$$\mathrm{RES}\left(E_T^{T+1}, \theta\right) = \sum_{T=1}^{N} \left(E_T^{T+1} - Y_T(\theta)\right)^2.$$

We again obtain the best fit for the data from the time period 1979 to 2004; but also for

Table 5.5: Estimation of the parameter θ in the Ornstein-Uhlenbeck model variant. The scaling factor computed in the Brownian model variant is applied, parameters μ and y_0 are taken from estimations in the simple and in the Brownian model variant, respectively.

Time period	ρ	y_0	μ	θ	R^2
1975 – 2004	0.62	2345.16	2216.44	0.14	0.20
1979 – 2004	0.63	2383.21	2241.84	0.2	0.39
1990 – 2004	0.61	2111.02	2104.04	0.39	0.096

this data set, the determination coefficient only reaches $R^2 = 0.39$. The fitted line and the underlying data as well as the sum of the squared residuals for this time period are shown in Figure 5.12. In the one-period model, we will use the value $\theta = 0.2$ computed for the time period from 1979 to 2004 in our simulations. As in the Brownian model variant, the parameter y_0 does not appear explicitly in computations, whereas the parameter μ is only required in the multi-period model.

With $\mu = 2240$ as estimated in the simple model variant for the years 1979 to 2004, we obtain expected emissions of 6720 Mt for a time period of three years; this figure is considerably higher than the emissions we expect for the first time period as given by the parameter $x_0 = 6240$. Thus by choosing $\mu = 2240$, we implicitly assume that BAU emissions increase between time period 0 and time period 1; this is not supported by the downward tendency of the data. By repeating the procedure described above for different

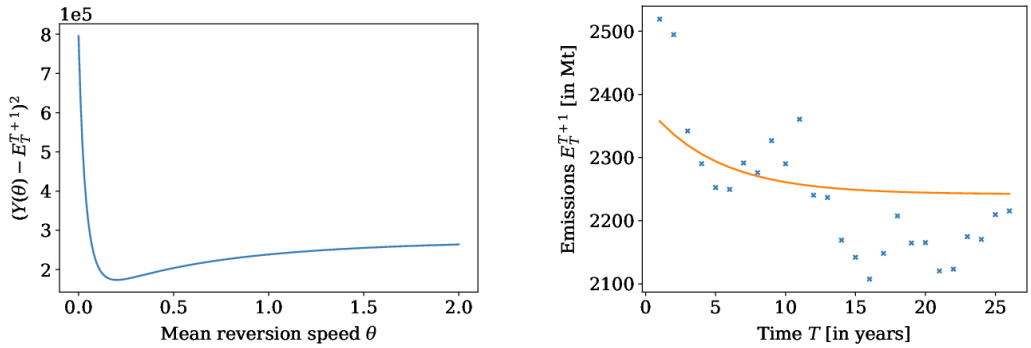

(a) Sum of the squared residuals for varying values of θ.

(b) Yearly emissions and corresponding regression curve.

Figure 5.12: Regression results to determine θ for the time period from 1979 to 2004.

values of μ, we find that we obtain the best fit for $\mu = 2090$; but this still corresponds to emissions within three years that slightly surpass the value of $x_0 = 6240$. Instead we choose $\mu = 2000$; in this way, we assume that the emissions of three years in the long-term are equal to the emission cap e_0. The parameters obtained under this assumption are shown in Table 5.6. We observe that the fit is much better for the two larger data sets;

Table 5.6: Estimation of the parameter θ in the Ornstein-Uhlenbeck model variant. The scaling factor computed in the Brownian model variant is applied, the parameter y_0 is taken from estimations in the Brownian model variant and we assume $\mu = 2000$.

Time period	ρ	y_0	μ	θ	R^2
1975 – 2004	0.62	2345.16	2000	0.03	0.47
1979 – 2004	0.63	2383.21	2000	0.04	0.64
1990 – 2004	0.61	2111.02	2000	0.01	0.077

with the data from 1979 to 2004, we obtain a higher determination coefficient as we did in the estimation of μ in the Brownian model variant. This is underlined by Figure 5.13, showing a distinctive minimum of the squared residuals and a fitted curve that visibly fits the data points. At the same time, the estimates for θ are very small; the highest value, obtained from the 1979 to 2004 data set, only reaches 0.04. As we will see in Sections 6.1.1 and 6.1.5, this implies for the one-period setting that both the PDE solution and the SDE solution are very similar to the respective results in the Brownian model variant. As a consequence, we will use the value of $\theta = 0.2$ in the one-period model to be able to see some effects from the changed model variant. In the multi-period model, the parameter θ also influences the amount of emissions we expect initially for each time period i as given by the parameter x_0^i. Since this differs considerably between the Brownian and Ornstein-Uhlenbeck variant, also for $\theta = 0.04$, we will use the parameters $\theta = 0.04$ and $\mu = 2000$ in the multi-period model.

5.3.4 Additional Model Parameters in the Multi-Period Model

In the multi-period model we additionally need to set the number of time periods P and the price parameter for the last time period s^{N-1}. These parameters can neither be estimated from data nor can they be taken from the regulatory regime in the EU ETS:

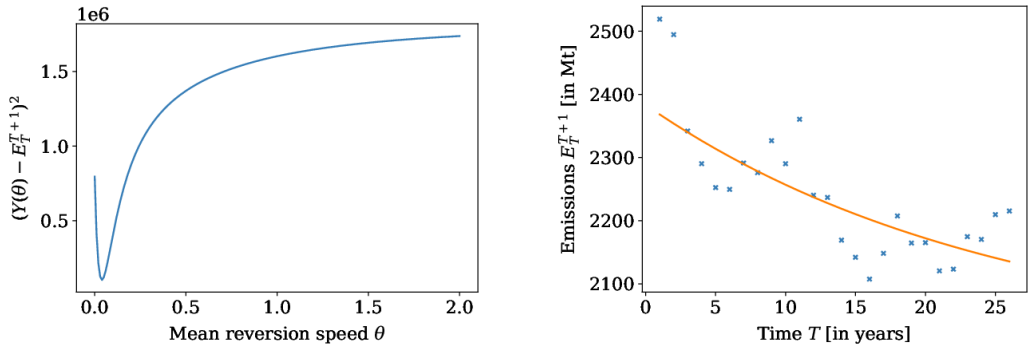

(a) Sum of the squared residuals for varying values of θ.

(b) Yearly emissions and corresponding regression curve.

Figure 5.13: Regression results to determine θ for the time period from 1979 to 2004 under the assumption that $\mu = 2000$.

Actual emission trading systems usually do not have a fixed end point, thus both P and s^{N-1} can be viewed as artificial auxiliary parameters. We choose to work with six time periods. In this way we have sufficiently many time periods to be able to observe the effects of a multi-period setting, while the required computational effort can still be handled.

To avoid arbitrariness, we set the price parameter of the last time period s^{N-1} to zero in multi-period model I, which means that allowances become invalid at the end of the last time period. In multi-period model II, we compute the price function $\tilde{S}_0^N$ for the last time period from the PDE solution in multi-period model I, as explained in Section 5.1.4. For this we again require a price parameter s, which we set to zero.

Summary

This section served to justify our parameter choices: The parameters p, e_0 and T (or ΔT) were obtained from the regulatory framework of the EU ETS. Further parameters, namely r and c, were taken directly from the choice of Seifert et al. [SUW08]; while r alternatively could be retrieved from reference interest rates, the cost coefficient c is very difficult to estimate. The initially expected emissions x_0 were estimated by using the historical emission baseline data. With the help of the estimate for x_0, the parameters required to describe the emission rate, namely μ, σ and θ, could be estimated from data on CO_2 emissions in the EU. The parameters P and s^{N-1}, which we need in the multi-period models, again could not be obtained from data and had to be chosen in a suitable way.

Chapter 6

Numerical Results

The numerical methods presented in Chapter 5 allow us to solve the PDEs and SDEs which are central to the ETS model derived in Chapter 2 and its extensions introduced in Chapters 3 and 4. Thus we obtain realizations of the total expected emissions process X; based on these results, we can assess the impacts of parameter and design choices made by the regulator. We first present the results obtained in the one-period model. Then we continue with the two approaches to the multi-period model; in particular, we aim to analyze the effect of allowing for the transfer of allowances from one time period to the next. Finally, we briefly look into the impact of auctioning on the costs arising in the emission trading system.

6.1 One-Period Model

In this section, we first discuss the PDE solution for the simple, Brownian and Ornstein-Uhlenbeck model variant. Then we study the processes X and S obtained from solving the SDE in each model variant. By varying several model parameters, we analyze their impact on the emission trading system.

6.1.1 Solution to the PDE

For the simple model variant, we have solved the PDE analytically as described in Section 2.3.1. Thus we apply the corresponding formulae to plot the value function V and its derivatives; for the plots, any entries taking the value infinity were set to zero. The plots for V and the first derivative V_x are shown in Figure 6.1. We observe that V is constantly zero for small values of x, i.e. if x lies well below the number of allowances given by $e_0 = 6000$. For high values of x, the value increases almost linearly in x. This is confirmed by the results for V_x: If x is small, then V_x is constantly zero, whereas for large x it is constant and equal to $p = 70$. Around the value of $e_0 = 6000$, the function V_x is increasing in x, with an increasingly steep slope as time t approaches the final time point T, where we have a jump as given by the final condition. Thus we clearly see that V_x is bounded between 0 and p and tends to 0 for x going to $-\infty$ and to p for x going to infinity as shown in Proposition 2.7.

Additionally, we visualize the second derivatives V_{xx} and V_{xt} in Figure 6.2. We directly see that V_{xx} is zero for x away from $e_0 = 6000$; it attains increasingly large values for t approaching T if x is close to e_0. While this indicates that V_{xx} is unbounded on $[0, T]$, the plot is bounded on $[0, T - \varepsilon]$ for any fixed time point $T - \varepsilon < T$, which is in line with

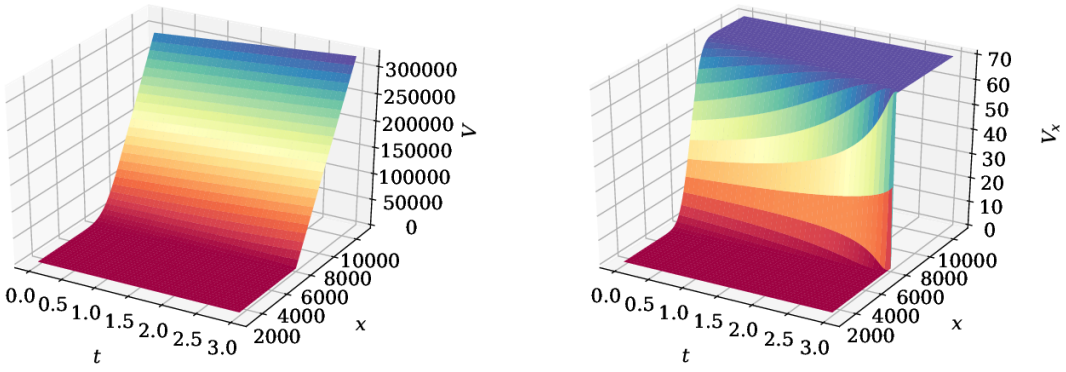

(a) Solution V. **(b)** First derivative V_x.

Figure 6.1: Analytical PDE solution in the simple model variant[1].

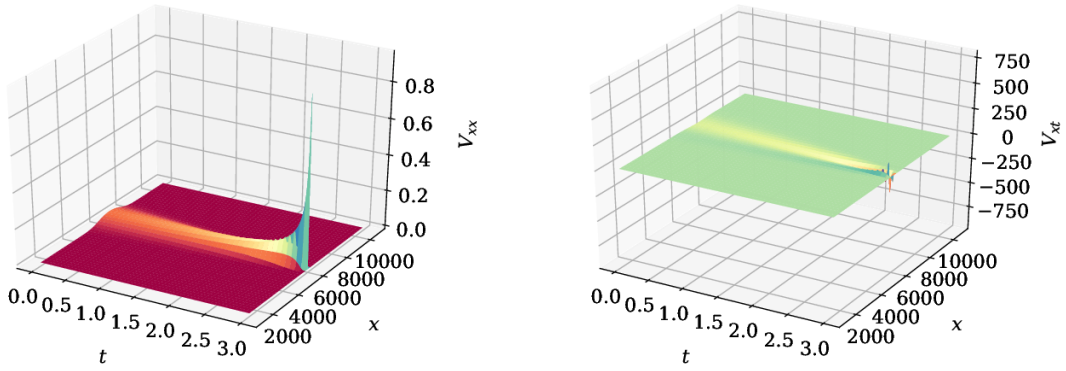

(a) Second derivative V_{xx}. **(b)** Second derivative V_{xt}.

Figure 6.2: Second derivatives of the PDE solution in the simple model variant.

Proposition 2.7 (iv). The derivative V_{xt} also attains its highest value for large values of t; in contrast to all other derivatives, it takes negative values. In this case, it is not as clear to see that boundedness on $[0, T-\varepsilon]$ for any $\varepsilon > 0$ holds.

For the Brownian model variant, the PDE was solved numerically as described in Section 5.1; the derivatives were estimated by difference quotients. The resulting plots for V and V_x are shown in Figure 6.3. The overall structure of the solution is similar to the simple variant, both for V and the derivative V_x, but slight differences are observable: Most notably, the plot is now bounded by 51.85, since we need to take the interest rate into account. Thus the bound corresponds to $p\,\mathrm{e}^{-rT}$. As can be seen in the plot of V_x and more clearly in Figure 6.7 showing the difference between the two model variants, the slope of V_x gets steeper faster: In the Brownian variant, close to time T, V_x is already almost at its upper bound or almost zero also for values of x close to e_0. On the other hand, in the simple variant, V_x still slightly deviates from its bounds at these points. This is also reflected in the second derivatives shown in Figure 6.4: Both V_{xx} and V_{xt} attain higher values than in the simple model variant. Around $x = e_0$, the second derivatives

[1] In interpreting these 3D-plots, note that the tick labels on the x-axis refer to the ticks directly above each number.

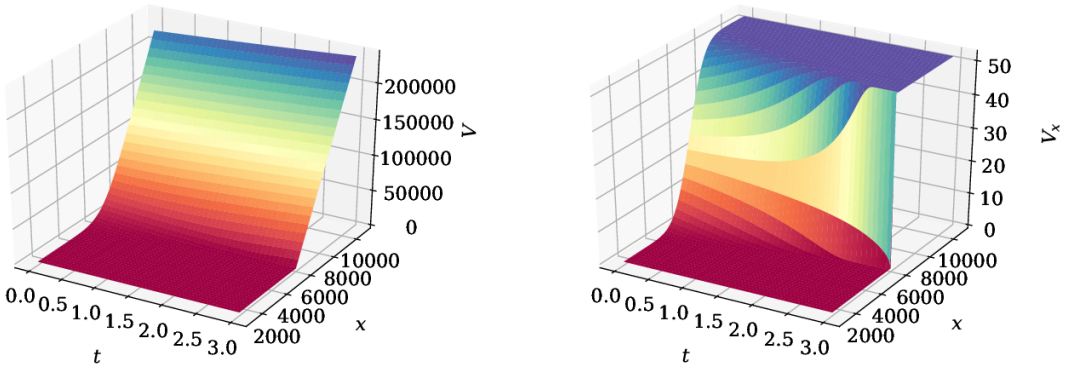

(a) Solution V. **(b)** First derivative V_x.

Figure 6.3: Numerical PDE solution in the Brownian model variant.

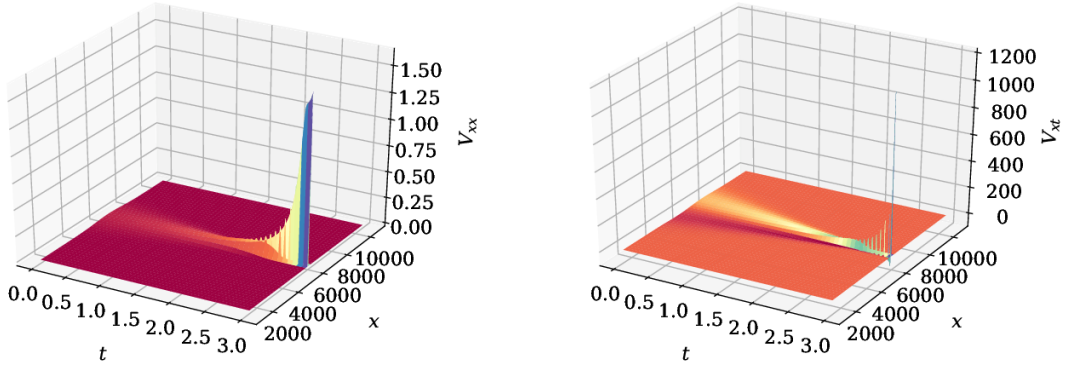

(a) Second derivative V_{xx}. **(b)** Second derivative V_{xt}.

Figure 6.4: Second derivatives of the PDE solution in the Brownian model variant.

appear to tend to infinity for t approaching T. Thus on $[0, T]$ both V_{xx} and V_{xt} can be assumed to be unbounded. But again it is plausible that boundedness can be assured on $[0, T - \varepsilon]$ for any points $T - \varepsilon$ before T.

Also in the Ornstein-Uhlenbeck model variant, the PDE solution needs to be solved numerically; the results for V and V_x are shown in Figure 6.5. These are very similar to those in the Brownian model; the same holds for the second derivatives V_{xx} and V_{xt} shown in Figure 6.6.

The similarity between the Brownian and Ornstein-Uhlenbeck model is underlined by the comparison plot in Figure 6.7b. By considering the PDEs for the two models, this similarity can be easily explained: As shown in Figure 6.8, the coefficients of the second derivative V_{xx} are almost identical for t close to T, where in all models V_{xx} is the largest. Also for small t, the coefficients behave similarly; thus only a small difference between the two model variants can be observed as shown in Figure 6.7. When comparing the Brownian variant to the simple model variant (shown in Figure 6.7a), the resulting difference is in particular also large for t close to T. Thus the deviations between the simple model variant on the one hand and the Brownian and Ornstein-Uhlenbeck model on the other are much more striking. Note that we do not need to compare the coefficients of V_x^2: If we set the

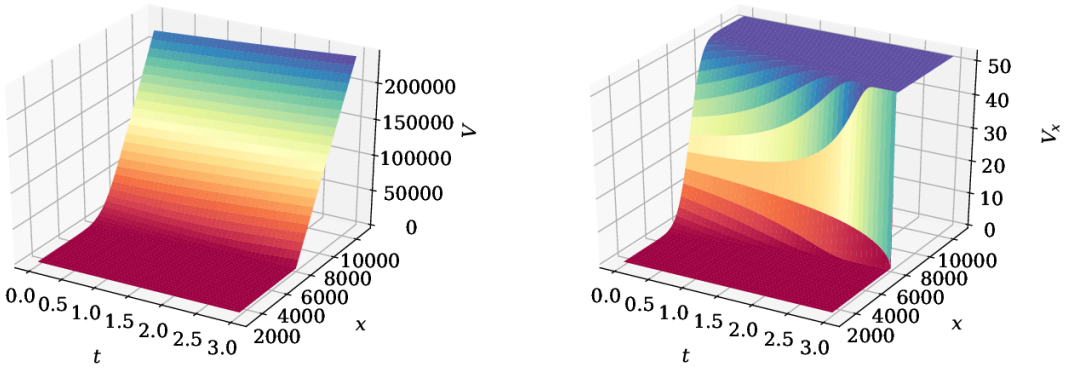

(a) Solution V.

(b) First derivative V_x.

Figure 6.5: Numerical PDE solution in the Ornstein-Uhlenbeck model variant.

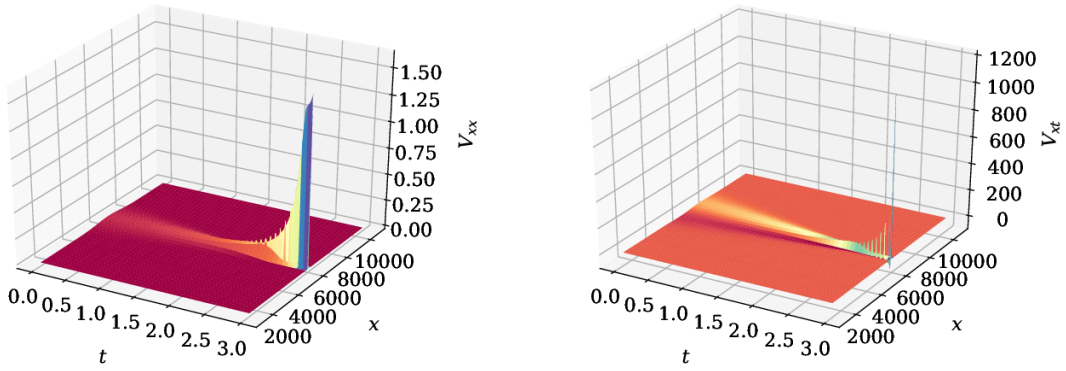

(a) Second derivative V_{xx}.

(b) Second derivative V_{xt}.

Figure 6.6: Second derivatives of the PDE solution in the Ornstein-Uhlenbeck model variant.

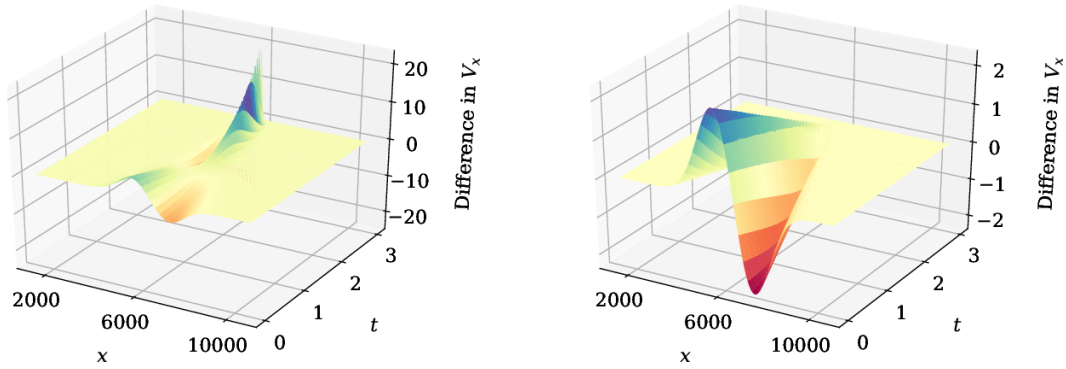

(a) V_x of Brownian variant subtracted by V_x of simple variant (with $r = 0.1$).

(b) V_x of Brownian variant subtracted by V_x of Ornstein-Uhlenbeck variant.

Figure 6.7: Differences of the derivative V_x between the Brownian model variant and the simple or Ornstein-Uhlenbeck model variant.

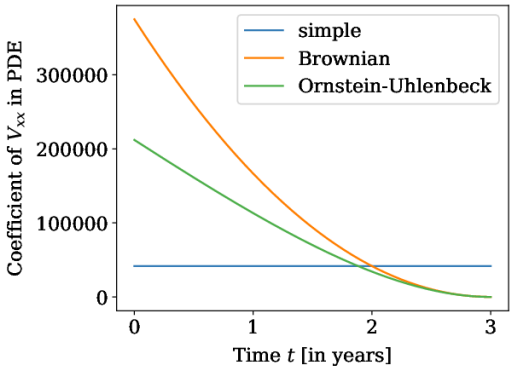

Figure 6.8: Coefficient of the V_{xx}-term in the PDE for the three model variants.

interest rate to $r = 0.1$ also in the simple model variant, as we did in Figure 6.7a for the purpose of comparison, these coefficients are identical in all model variants.

Summary

An understanding of the PDE solution and in particular of its derivative V_x is crucial, as both the abatement rate u, serving as the drift term in the SDE, and the price function S are directly computed from V_x. We observed that V_x is constant for small or large values of x. If x is close to e_0, the function V_x is increasing in x, with a slope that increases in time. This behavior is similar in all model variants; the results obtained in the Ornstein-Uhlenbeck variant are almost identical to those obtained in the Brownian variant.

Moreover, the results shown here suggest that V_x is bounded also in the Brownian and Ornstein-Uhlenbeck model variant. As argued above, the numerical results also support that V_{xx} and V_{xt} are bounded on intervals of the form $[0, T - \varepsilon]$, which would imply Lipschitz continuity of V_x in t and x. These properties together would allow us to apply Theorems 2.15 and 2.26, which provide existence and uniqueness of a solution and convergence of the Euler-Maruyama scheme. While this argumentation cannot replace a rigorous proof of the required properties, it still may serve as a motivation to solve the SDE numerically also in the Brownian and Ornstein-Uhlenbeck model variant.

6.1.2 Solution to the SDE in the Simple Model Variant

With the abatement rate u obtained from the PDE solution, we can solve the SDE describing the process of the total expected emissions X. We first consider the simple model variant. The SDE is solved numerically by applying the Euler-Maruyama method as described in Section 5.2, delivering realizations of the total expected emissions X. From the price function $S(t, X_t) = V_x(t, X_t)$ we compute the corresponding realizations of the price process S.

We first explore three example runs, chosen to represent typical characteristics seen in many simulation results. In Figure 6.9 the trajectories of the total expected emissions X and of the price S for these runs are shown. The first run moves below the emission threshold given by the total number of allowances e_0 early. From time 2 onwards, the fluctuations in X of this run barely influence the price S, as X moves in a region where

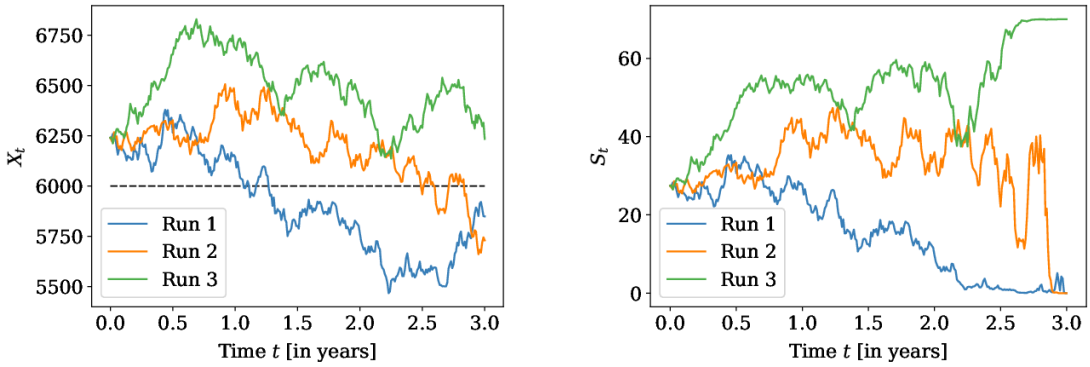

(a) Trajectories of X.

(b) Trajectories of S.

Figure 6.9: Three example trajectories of the total expected emissions X with corresponding trajectories of the price process S. The dashed line represents the emission cap e_0.

V_x and thus S is almost constant and close to zero. As the actual allowance price of the EU ETS towards 2007, the price S is therefore very small. The second run stays slightly above the threshold for a long time. In the earlier part of the time period, fluctuations in X lead to similar fluctuations in S. From time 2 on, small changes in X lead to massive jumps in S due to the increasingly steep slope of V_x. Shortly before the end of the time period, X moves below the threshold, thus prices drop down to zero. The third run remains above the threshold throughout the time period. After an initial increase of both paths, the price S roughly stays constant between time 1 and time 2, whereas X shows a downward tendency. Towards the end, the price jumps to 70 and stays constant despite the fluctuations of X, as the total expected emissions X remain well above the threshold.

In general, changes in X lead to similar changes in S at the beginning, as all runs are still close to e_0 and the range where V_x is increasing almost linearly is broad. As time proceeds, individual runs may move out of this range, while the slope gets steeper. Thus for some runs, changes in price are extreme, whereas for others, the price is almost constant. At the end, the price S either takes the value 0 if the realized emissions X_T are below the threshold, or it takes the value $p = 70$ if they are above. Moreover, the paths of X show a general downward tendency.

This observation is confirmed by the mean trajectory of X shown in Figure 6.10a, which resembles a straight line with negative slope. A downward tendency should be expected from the definition of X: At any time point t, the variable X_t only takes into account abatement until time t. Since the abatement rate is non-negative and positive on average, X is decreasing.

To judge the efficacy of the ETS as an emission reduction instrument, we need to study the emissions which are actually produced in the corresponding time period, given by X_T; in the following, we will refer to this quantity as the realized emissions. The distribution of X_T is visualized as a histogram in Figure 6.10b; the mean is given by 5900.51. We observe that the distribution is slightly asymmetric with a peak at 6000; thus a considerable number of runs leads to realized emissions above the threshold, as for instance run 3 of the runs described above. The relative frequency of having realized emissions above the threshold, which means that the system does not comply with the emission cap, is 39.49%.

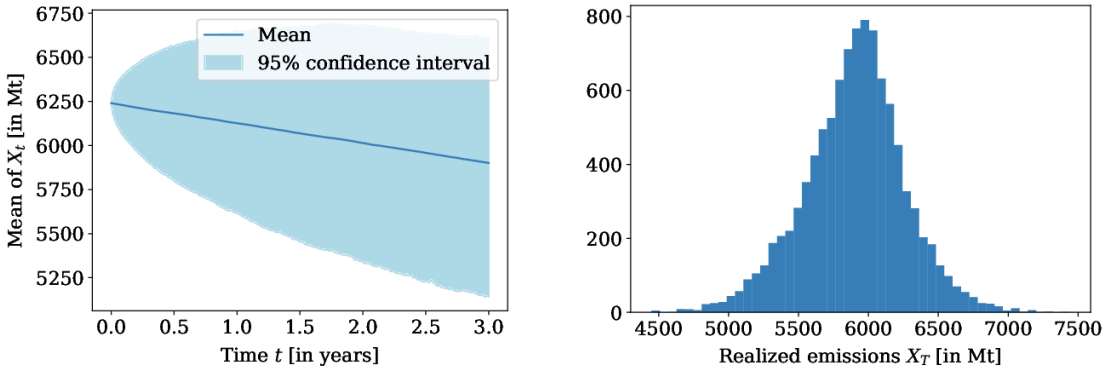

(a) Mean trajectory of X.

(b) Histogram of realized emissions X_T.

Figure 6.10: Mean trajectory of the process X and distribution of the realized emissions X_T in the simple model variant.

The second goal of an ETS is to provide a price signal so that companies have an incentive to reduce emissions and invest in clean and efficient technology. In Figure 6.11a we observe that the mean price trajectory remains almost constant throughout the time period. Additionally, we take the average price of an individual run along the time period and visualize the distribution of this quantity in a histogram, shown in Figure 6.11b. This average varies strongly among the individual runs; while the price is bounded between 0 and 70, we obtain that the average price ranges roughly between 10 and 55. The most frequent average values lie between 10 and 20, which fits the actual allowance prices of the EU ETS in its first phase with an average of 12.38. But on the other hand, prices between 40 and 50 still occur with high frequency.

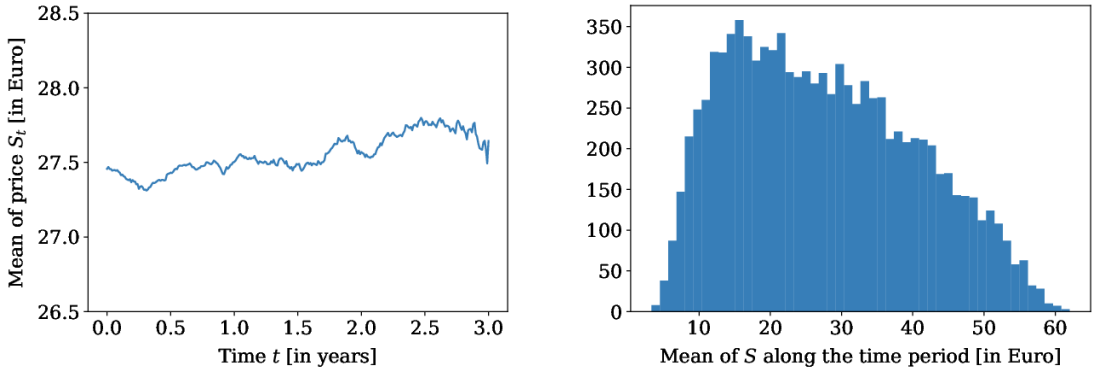

(a) Mean trajectory of S.

(b) Histogram of mean prices within each run.

Figure 6.11: Mean trajectory of the process S and distribution of the mean prices within one run in the simple model variant.

Next to the value of the allowance price, also its variability is relevant to provide an incentive for investment. As shown in Figure 6.12a, the standard deviation of the price process increases in time, which is plausible since all runs start at the same point. More interestingly, this increase has a very steep slope towards the end: At the final time point T, the price is either zero or equal to $p = 70$, so all runs deviate strongly from the mean

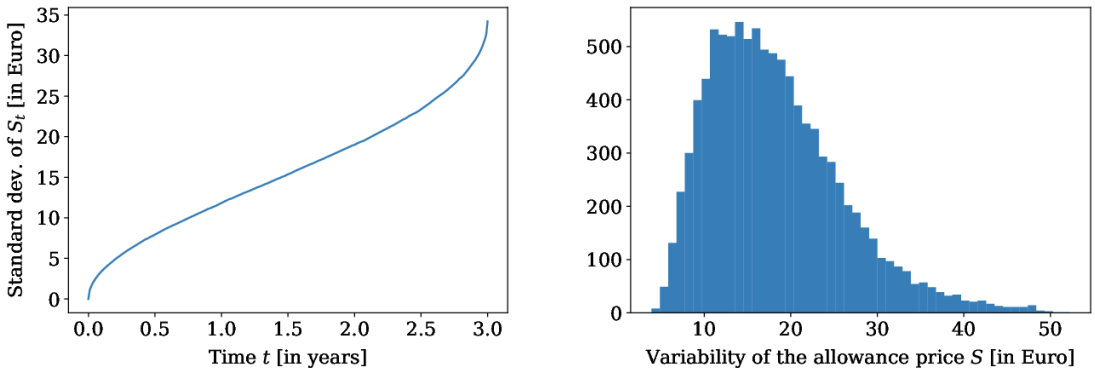

(a) Standard deviation trajectory of S.

(b) Histogram of the standard deviation of absolute daily returns of S, normalized to one year.

Figure 6.12: Trajectory of the standard deviation of the allowance price and distribution of its variability in the simple model variant.

at 27.64. To asses how the price varies within one run in course of the time period, we compute the absolute returns of the price and determine the standard deviation of this quantity, which we normalize to one year. Thus we obtain the standard deviation of the price change for a time step of one year. In the following, we will refer to this quantity as the variability of the allowance price. Its distribution is shown in Figure 6.12b. We observe that most runs lie between 10 and 20, while only few runs reach a value higher than 30. To get a better idea of this quantity, we report the variabilities of the exemplary runs discussed above: The price variabilities of the first and the third run are similar and amount to 11.89 and 14.29, respectively. Possibly due to the large jumps towards the end, the second run has a higher price variability of 25.87.

Summary

We presented example simulation results of the processes X and S and analyzed their behavior in the mean. Moreover, we discussed the distributions of several quantities derived from these processes. From these results, we conclude that the ETS encourages abatement, leading to a decrease in the mean of X and an approximately constant mean allowance price S of about 27.5 Euro. However, in a considerable fraction of simulation runs, the realized emissions X_T violate the cap, and the allowance price varies strongly in many runs.

6.1.3 Solution to the SDE in the Brownian Model Variant

We now study the results in the Brownian model variant in some detail, as there are some relevant differences to the simple model variant. In Figure 6.13 three example trajectories are shown, both for the total expected emission process X and for the price process S. The first run shown here moves downwards at the beginning and stays below the threshold throughout the time period. Thus the corresponding price process decreases and drops down to zero early. The other two runs start by moving upwards and behave rather similarly; nevertheless the corresponding price processes differ massively towards the end: The second run is slightly closer to e_0 than the third, resulting in heavy price fluctuations,

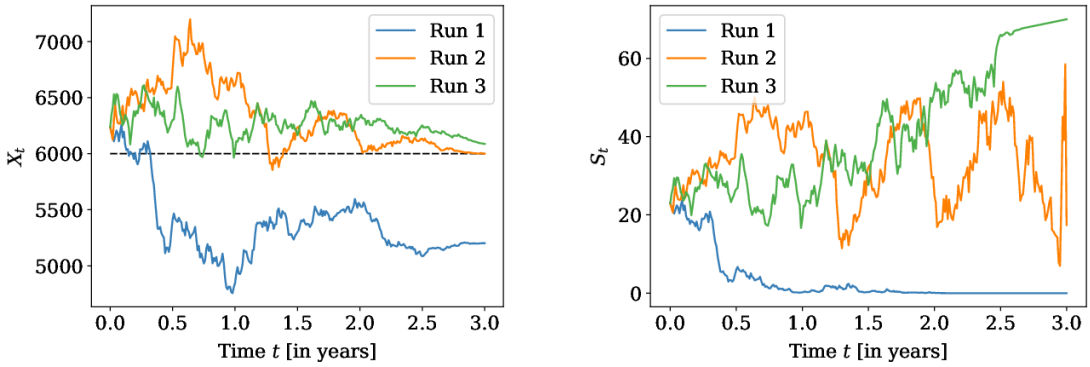

(a) Trajectories of X.

(b) Trajectories of S.

Figure 6.13: Three example trajectories of the total expected emissions X with corresponding trajectories of the price process S in the Brownian model variant.

while the price in the third increases linearly with the interest rate from time 2.5 onwards. Notably, the final price of the second run lies between zero and the upper bound given by $p = 70$. The final value X_T in this case is very close to e_0; since V_x is computed as a finite difference and $V_x(T, X_T)$ is evaluated by linear interpolation of the PDE solution, we obtain a result for S_T between zero and the upper bound.

In general, we observe that the fluctuations in X become less and less as time proceeds; at the same time for some runs which are close to e_0 small variations in X lead to massive fluctuations in the price paths S, as seen for run 2. This is plausible since in the Brownian model the volatility of X approaches zero as time moves towards the final time point T, while V_x and thus the price function is very steep around e_0 towards the end of the time period.

As can be seen in Figure 6.14a, the total expected emissions X follow a linear downward movement in the mean, while the 95% confidence interval is considerably broader than in the simple model variant. For the distribution shown in Figure 6.14b, we observe that it has a very sharp peak at 6000; about 2000 runs – corresponding to 20% of all runs – lead to realized emissions close to 6000 mega tons (Mt). The distribution is only slightly skewed to the left and has long tails; thus a considerable amount of runs violates the threshold e_0 and, due to the long tails, some to a great extent. The relative frequency of compliance with the emission cap is 55.58%.

The mean price trajectory shown in Figure 6.15a is increasing linearly, which is caused by the interest rate. The distribution of the average prices in each run is visualized in Figure 6.15b. Interestingly, this distribution has two peaks: One around 5 Euro and the other around 55 Euro. Thus commonly the price either remains low throughout the time period or it remains high. This may be explained by the fact that in the Brownian model the volatility of X decreases in time as mentioned above, therefore if X either is well below or above e_0, the probability of approaching or crossing the threshold e_0 is small; but this would be required for a drastic change in price behavior. Consequently, for many realizations it is evident on the allowance market fairly early whether it is in over- or in undersupply.

Finally, we consider the variation of the price. In Figure 6.16a we observe that the trajectory of the standard deviation is increasing in time; but in contrast to the case of

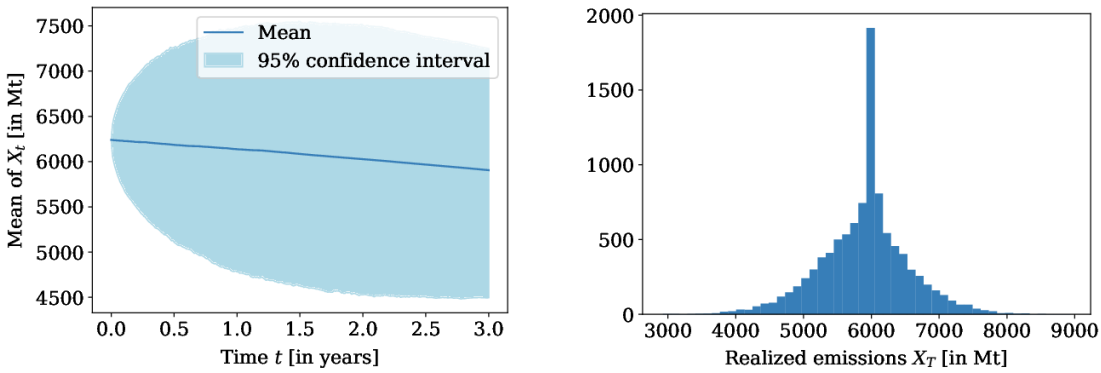

(a) Mean trajectory of X.

(b) Histogram of realized emissions X_T.

Figure 6.14: Mean trajectory of the process X and distribution of the realized emissions X_T in the Brownian model variant.

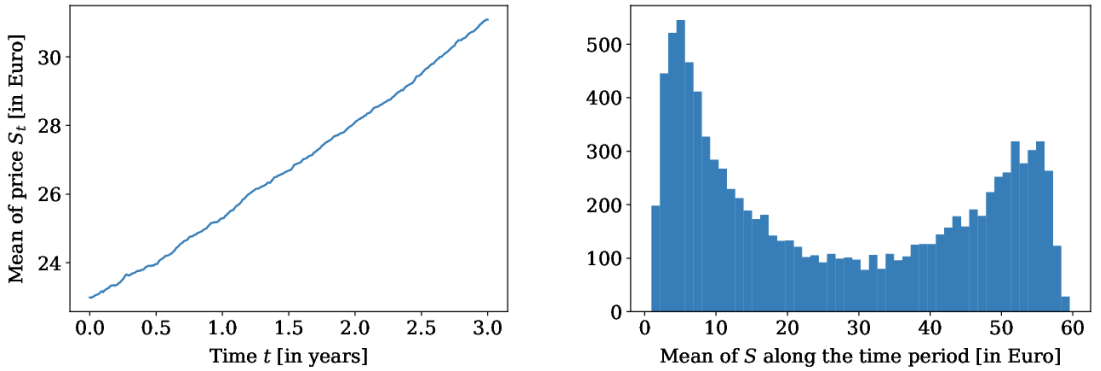

(a) Mean trajectory of S.

(b) Histogram of mean prices within each run.

Figure 6.15: Mean trajectory of the process S and distribution of the mean prices within one run in the Brownian model variant.

the simple model variant, we do not see such a sharp increase towards the end of the time period. The distribution of the price variability shown in Figure 6.16b is strongly skewed to the right with a peak around 12.

Summary

We have seen that the behavior of the total expected emissions X and the allowance price S in the Brownian model variant shows some similarities to the case of the simple variant, especially when considering their characteristics in the mean. As seen both for the realized emissions X_T and the mean price for individual runs, the details of the corresponding distributions display considerable differences.

6.1.4 Solution to the SDE in the Ornstein-Uhlenbeck Model Variant

We may present the results obtained in the Ornstein-Uhlenbeck model variant in more brevity, as we will see that they strongly resemble those from the Brownian model variant.

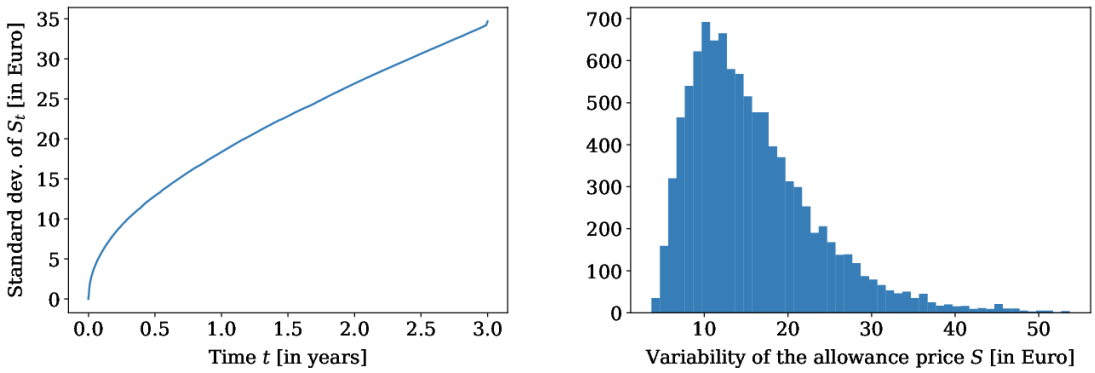

(a) Standard deviation trajectory of S.

(b) Histogram of the standard deviation of absolute daily returns of S, normalized to one year.

Figure 6.16: Trajectory of the standard deviation of the allowance price and distribution of its variability in the Brownian model variant.

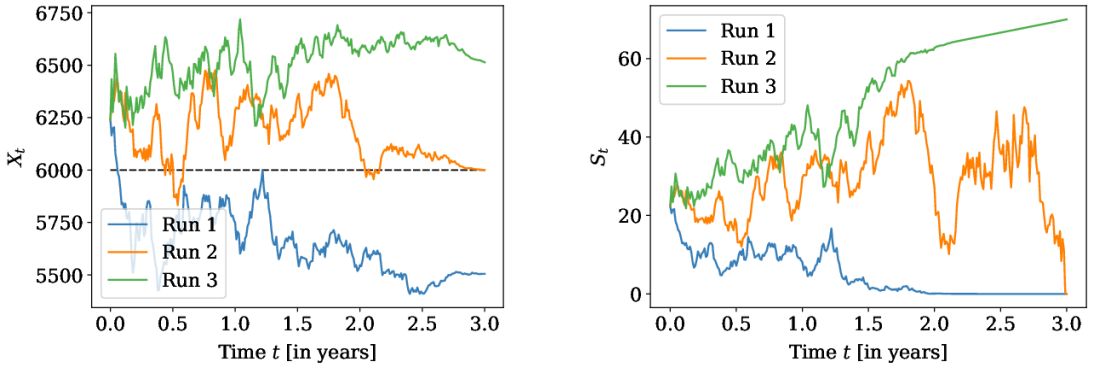

(a) Trajectories of X.

(b) Trajectories of S.

Figure 6.17: Three example trajectories of the total expected emissions X with corresponding trajectories of the price process S in the Ornstein-Uhlenbeck model variant.

In Figure 6.17 again example trajectories of the processes X and S are shown. While the individual processes are of course different to the ones shown for the Brownian variant, they behave in a similar manner; notably the range of fluctuations of the process X is smaller, as can be seen most clearly from the scaling of the axis.

In Figure 6.18a we show the mean trajectory of the total expected emissions X and the distribution of the realized emissions X_T. We observe that the 95% confidence interval of the trajectories is slightly more narrow and the tails of the distribution are shorter than in the Brownian model variant; otherwise these results are very similar.

The same holds for the allowance price: The mean price trajectory shown in Figure 6.19a lies slightly below the price trajectory of the Brownian model variant, while the distribution of the mean price within individual runs is very similar, as can be seen in Figure 6.19b. Also the path of the standard deviation of the price as well as the distribution of the variability shown in Figure 6.20 are almost identical to the results found in the Brownian model variant.

These strong similarities are plausible: As seen in Section 6.1.1, the PDE solutions and

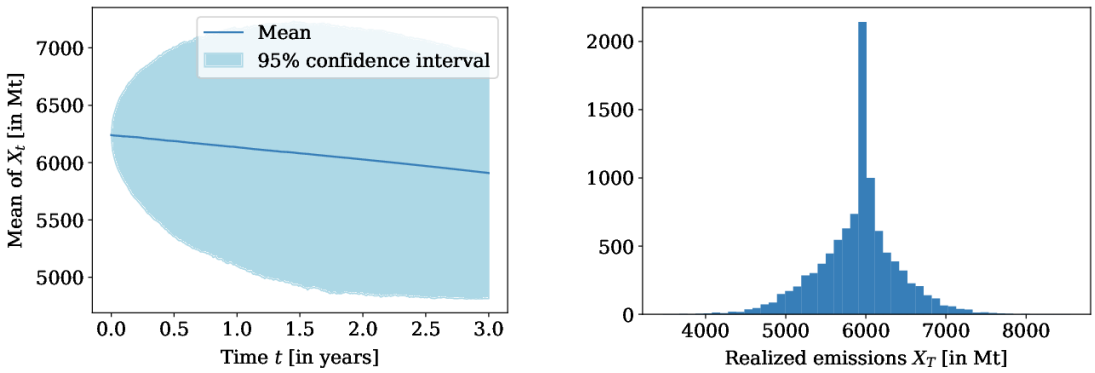

(a) Mean trajectory of X.

(b) Histogram of realized emissions X_T.

Figure 6.18: Mean trajectory of the process X and distribution of the realized emissions X_T in the Ornstein-Uhlenbeck model variant.

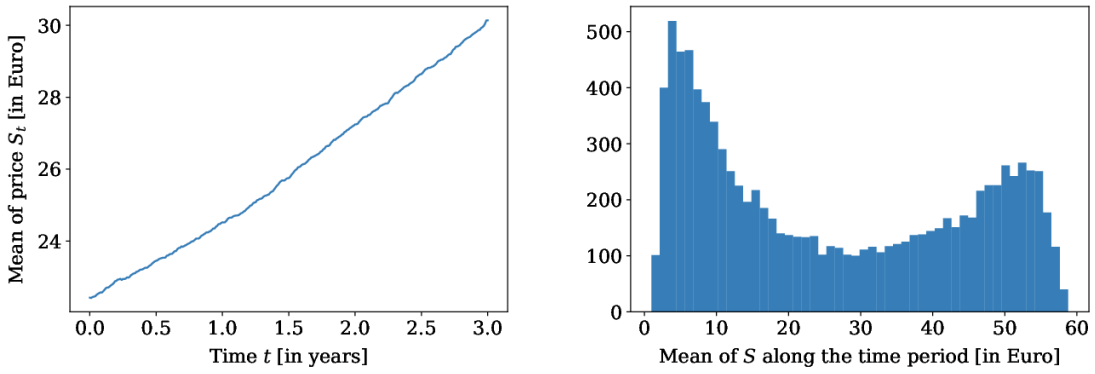

(a) Mean trajectory of S.

(b) Histogram of mean prices within each run.

Figure 6.19: Mean trajectory of the process S and distribution of the mean prices within one run in the Ornstein-Uhlenbeck model variant.

thus the drift functions of the SDE are very similar; moreover, the volatility functions G_B of the Brownian model and G_{OU} of the Ornstein-Uhlenbeck model are similar throughout most of the time period, which is shown in Figure 6.21. The difference is the largest at the beginning of the time period; since this is also when the volatility itself is the largest, the smaller volatility in the Ornstein-Uhlenbeck model appears to lead to a smaller variance of the process X and thus to a more narrow distribution of X_T.

Summary

In this section, we analyzed the results from the Ornstein-Uhlenbeck model variant to find that these are very similar to those obtained in the Brownian variant. Only the process X varies less, meaning that the distribution of X_t at any given time point t is slightly more narrow. Due to this similarity, we focus on the simple and Brownian model variants for the remainder of this chapter.

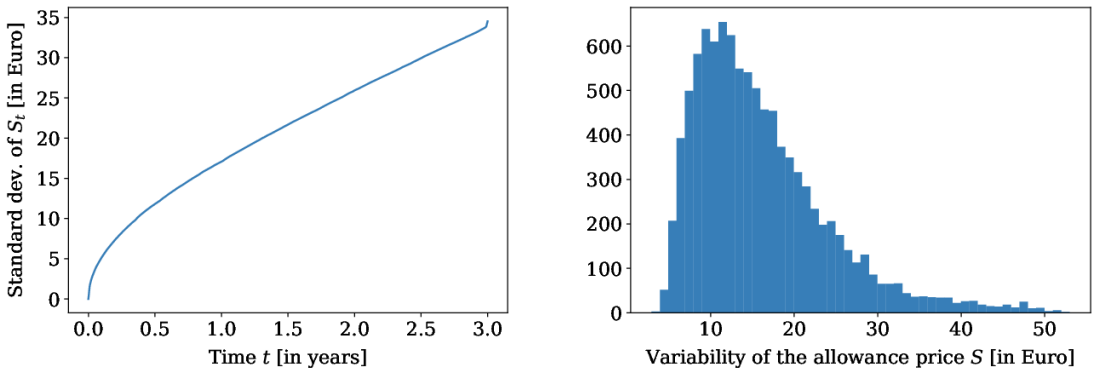

(a) Standard deviation trajectory of S.

(b) Histogram of the standard deviation of absolute daily returns of S, normalized to one year.

Figure 6.20: Trajectory of the standard deviation of the allowance price and distribution of its variability in the Ornstein-Uhlenbeck model variant.

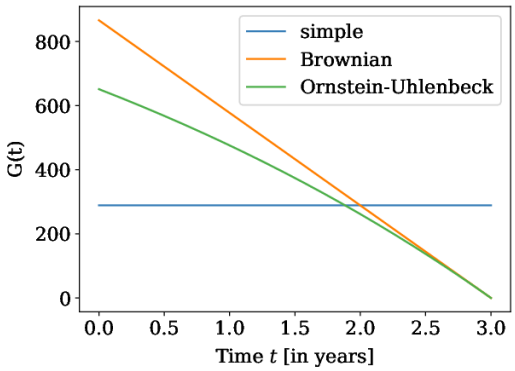

Figure 6.21: Volatility functions $G(t)$ of the simple, Brownian and Ornstein-Uhlenbeck model variants.

6.1.5 Variation of Model Parameters

The model depends on several parameters, which in part may be chosen by the regulator and in part are inherent to the system. In this section, we discuss how varying parameter values affect the SDE solutions presented above.

Variation of Regulatory Parameters

The choice of regulatory parameters affects the behavior of companies underlying the ETS and thus the resulting total expected emissions X as well as the price S. Beside more complex structural changes such as to allow banking or the introduction of a mechanism like the Market Stability Reserve, the regulator chooses the penalty p, the amount of allocated allowances e_0 and the length of one time period T. We will first study the effects of a varying penalty p in detail; then we will cover the impact of varying e_0 or T in a more aggregated manner.

Varying the Penalty in the Simple Model Variant We start by considering the simple model variant and first analyze the results for the total expected emissions X. In Figure 6.22a we observe that the downward slope of the mean trajectory of X becomes steeper for increasing penalties. In particular, as shown in Figure 6.22b, the realized

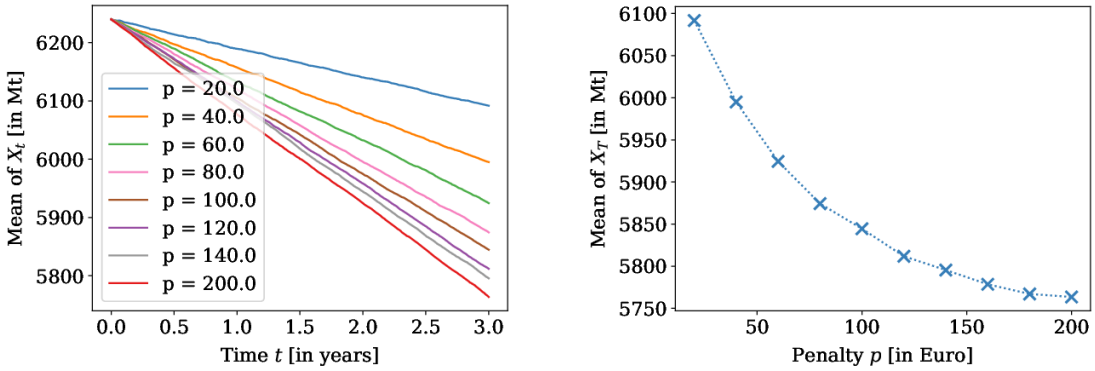

(a) Mean trajectories of X.

(b) Mean realized emissions X_T.

Figure 6.22: Mean results for X in the simple model variant for varying penalties p.

emissions X_T decrease. Notably, this effect becomes smaller for higher penalties. The change in the penalty also affects the distribution of X_T. In Figure 6.23 we visualize this distribution for a very low and a very high penalty. If the penalty is chosen to be only

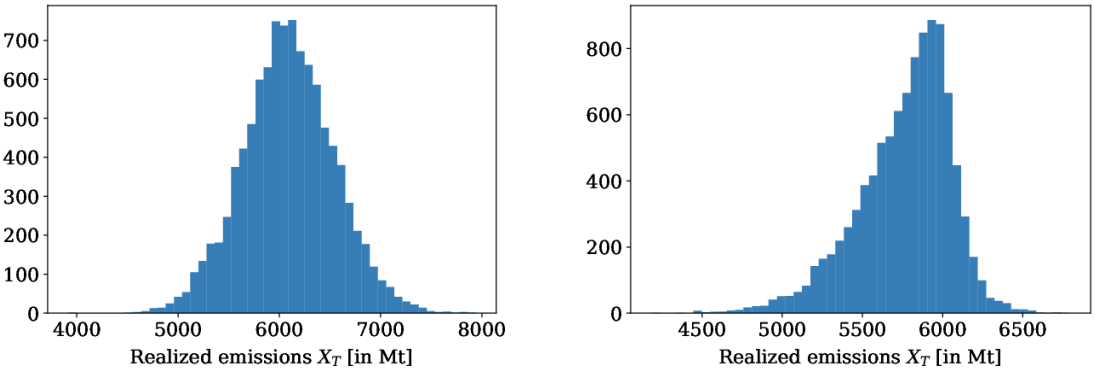

(a) Low penalty of $p = 20$.

(b) High penalty of $p = 200$.

Figure 6.23: Histograms of realized emissions X_T for a very low and a very high penalty in the simple model variant.

$p = 20$, then the ETS hardly seems to affect the realized emissions; their distribution appears to be symmetric with a peak above the threshold $e_0 = 6000$. If on the other hand a very high penalty of $p = 200$ is chosen, the resulting distribution of X_T is strongly skewed to the left and its peak is at or slightly below e_0. In line with this observation, the relative frequency of remaining below the threshold e_0 and thus complying with the emission target increases with an increase of the penalty, as can be seen in Figure 6.24; again this effect weakens with increasing penalties.

A change in the penalty clearly also affects the allowance price as we know that the price is bounded by the penalty. The mean price trajectory is always constant and the

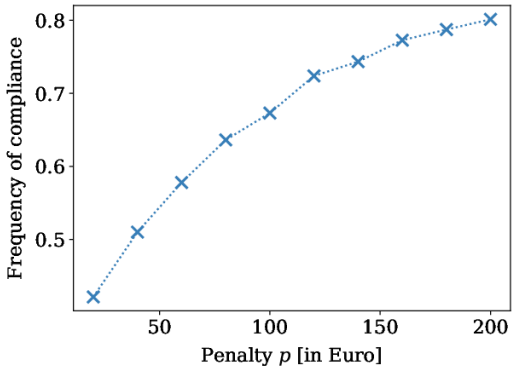

Figure 6.24: Relative frequency of compliance with the emission threshold as given by e_0 in the simple model variant.

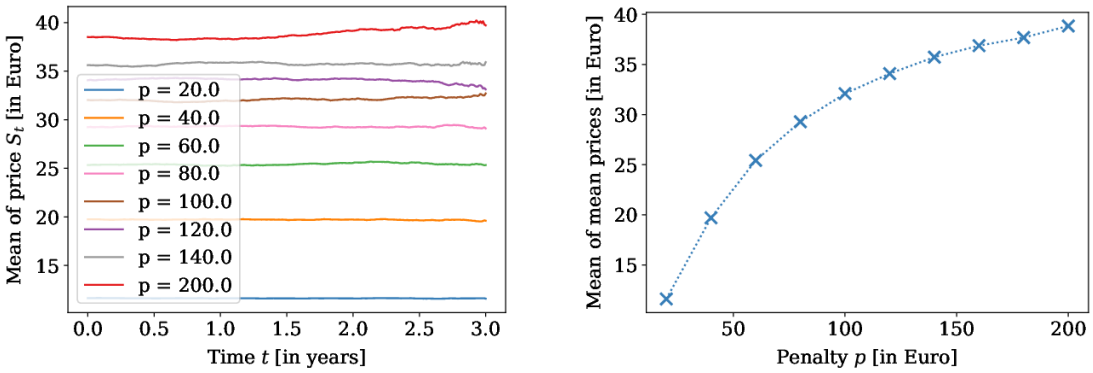

(a) Mean trajectories of the price S.

(b) Mean across all runs of the mean prices within one time period.

Figure 6.25: Mean results for the allowance price S in the simple model variant for varying penalties p.

price increases with the penalty as shown in Figure 6.25a. Again this effect becomes smaller for high penalties. The change in the penalty strongly impacts the distribution of the mean prices of individual runs, visualized in histograms in Figure 6.26: For a low penalty, the distribution is skewed to the left with a peak at approximately 16 Euro, but also very low mean prices of about 5 Euro are fairly frequent. If the penalty is very high on the other hand, the distribution is strongly skewed to the right with mean prices between 20 and 40 Euros being the most frequent.

To be able to assess the price variability, we show the histograms of its distribution in Figure 6.27. We observe that the overall structure is similar; for a high penalty the variability is much higher, which is plausible since the penalty determines the price bound. When considering the variability relative to the penalty, we obtain similar values for both penalties shown here.

Summary An increase of the penalty reduces the expected emissions and increases the probability of compliance with the emission target. It leads to an increase of the allowance price, but also the price variability increases.

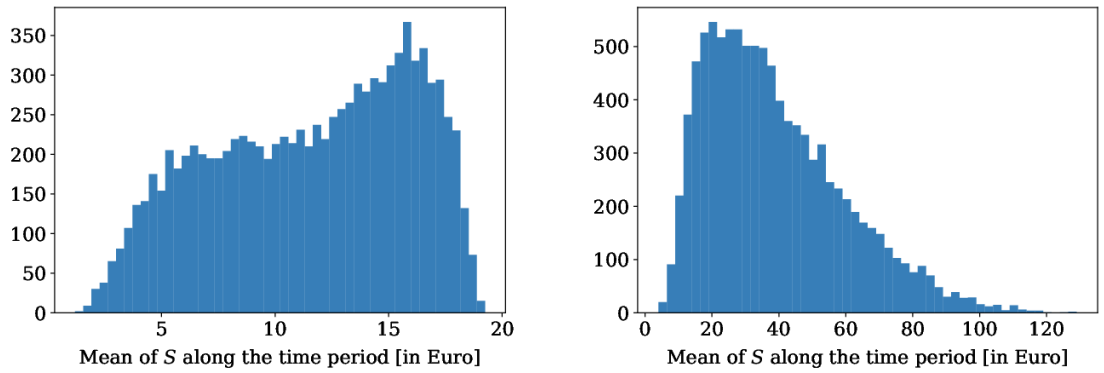

(a) Low penalty of $p = 20$.

(b) High penalty of $p = 200$.

Figure 6.26: Histograms of mean prices along the time period in the simple model variant for a very low and a very high penalty.

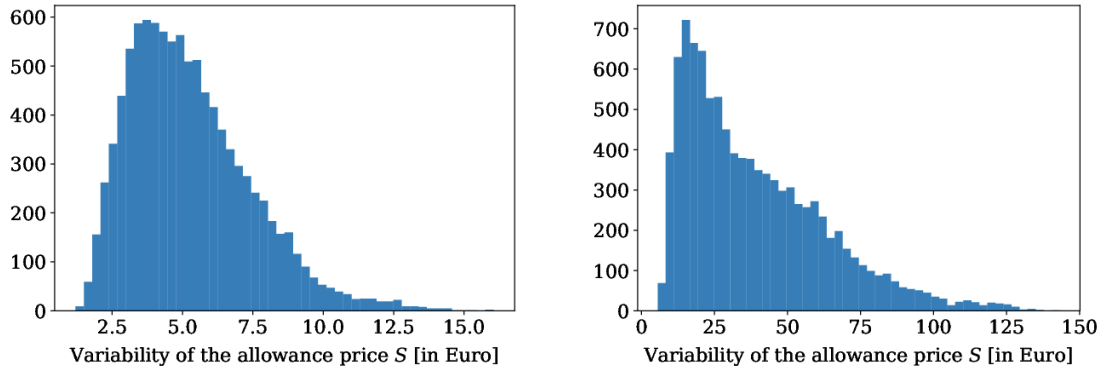

(a) Low penalty of $p = 20$.

(b) High penalty of $p = 200$.

Figure 6.27: Histograms of the variability of the allowance price S normalized to one year for a very low and a very high penalty.

Varying the Penalty in the Brownian Model Variant Next, we study the effect of varying the penalty in the Brownian model variant. In Figure 6.28 the mean trajectory of the total expected emissions X is shown for different penalty values. We observe that an increase of the penalty increases the downward slope of the mean trajectory of X. Consequently, this leads to a decrease of the mean realized emissions from more than 6100 for a penalty of 20 Euro down to approximately 5700 for a penalty of 200 Euro. The change of penalty also has a strong effect on the distribution of the realized emissions, shown in Figure 6.29. For the very low penalty of 20 Euro, the distribution appears to be almost symmetric; however the ETS still has an effect, since there is a clearly visible peak at 6000. This peak becomes higher as the penalty increases; for the very high penalty of 200 Euro, as show in Figure 6.29b, we observe that more than 4000 or 40% of all runs lead to realized emissions close to 6000. Moreover, this distribution has a very long tail on the left and is thus strongly skewed to the left. In accordance with these observations, the relative frequency of compliance with the emission cap e_0, shown in Figure 6.30, increases for an increasing penalty; for a penalty of 200 Euro it reaches 74.75%.

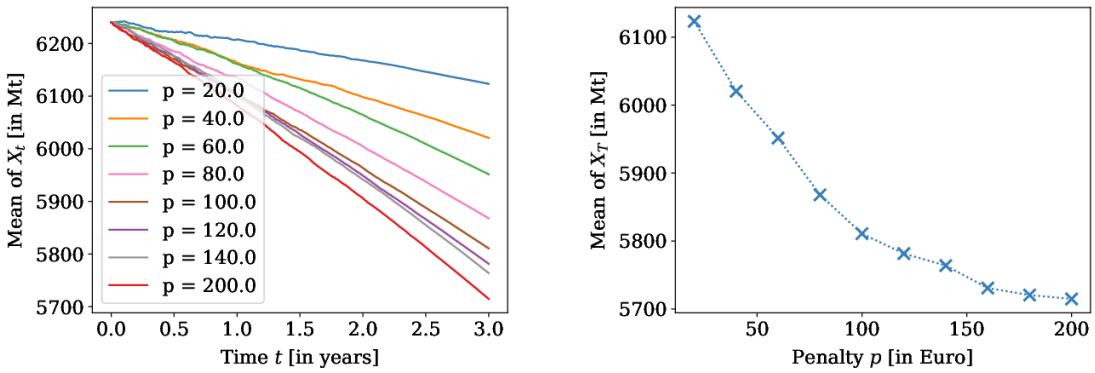

(a) Mean trajectories of X.

(b) Mean realized emissions X_T.

Figure 6.28: Mean results for X in the Brownian model variant for varying penalties p.

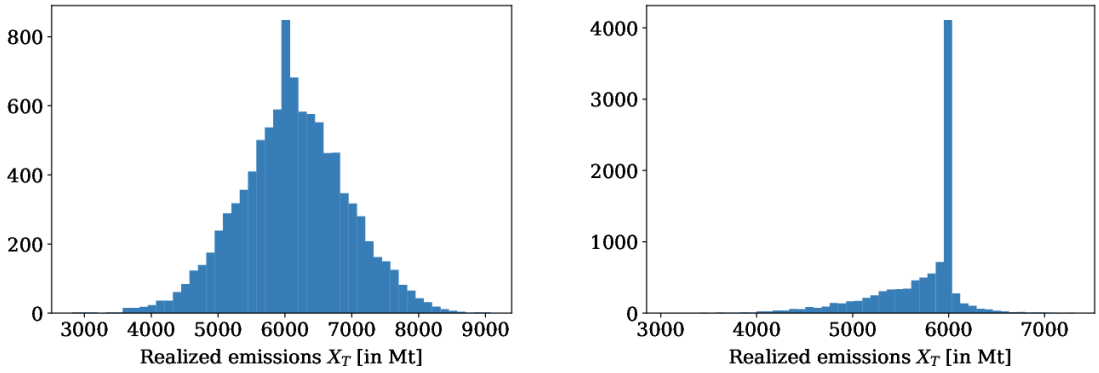

(a) Low penalty of $p = 20$.

(b) High penalty of $p = 200$.

Figure 6.29: Histograms of realized emissions X_T for a very low and a very high penalty in the Brownian model variant.

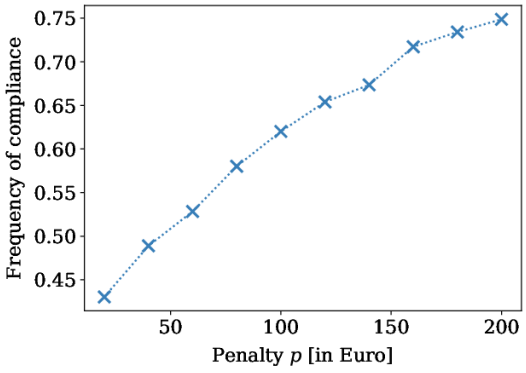

Figure 6.30: Relative frequency of compliance with the emission threshold as given by e_0 in the Brownian model variant.

As can be seen in Figure 6.31a, the mean allowance price increases approximately linearly in time, with a slope that increases with the penalty. Since also at any time point

the mean price is increasing in the penalty, it follows that the mean price across all time points increases if the penalty increases, as can be observed in Figure 6.31b. Moreover, the

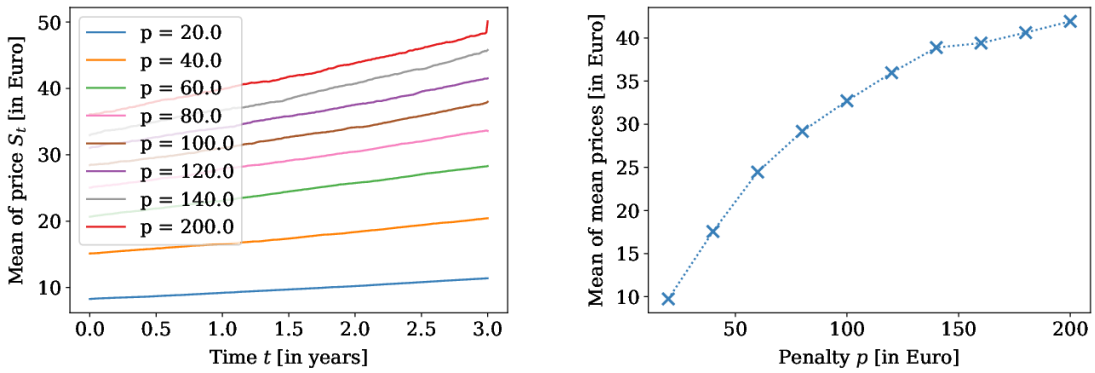

(a) Mean trajectories of the price S.

(b) Mean across all runs of the mean prices within one time period.

Figure 6.31: Mean results for the allowance price S in the Brownian model variant for varying penalties p.

distribution of mean prices within individual runs changes due to the increasing penalty, as shown in Figure 6.32: For a low penalty of $p = 20$, we obtain a distribution with two peaks, where the second peak at approximately 16 Euro is notably higher than the first at 2 Euro. If the penalty is high with $p = 200$, a second peak is no longer visible. Instead the

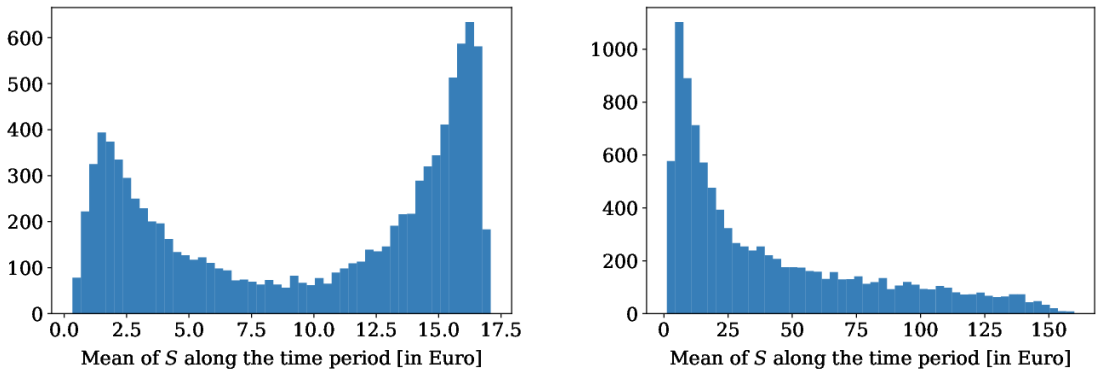

(a) Low penalty of $p = 20$.

(b) High penalty of $p = 200$.

Figure 6.32: Histograms of mean prices along the time period in the Brownian model variant for a very low and a very high penalty.

distribution has a very high peak at approximately 10 Euro and a long tail to the right reaching to about 150 Euro.

Finally, we consider the variability of the allowance price. The distributions shown in Figure 6.33 for a penalty of $p = 20$ and $p = 200$ are similar in structure with a peak at 3 and 20, respectively; the tail of the distribution becomes heavier for the higher penalty. Thus a higher penalty increases the price variability, which can be explained by the larger price bound.

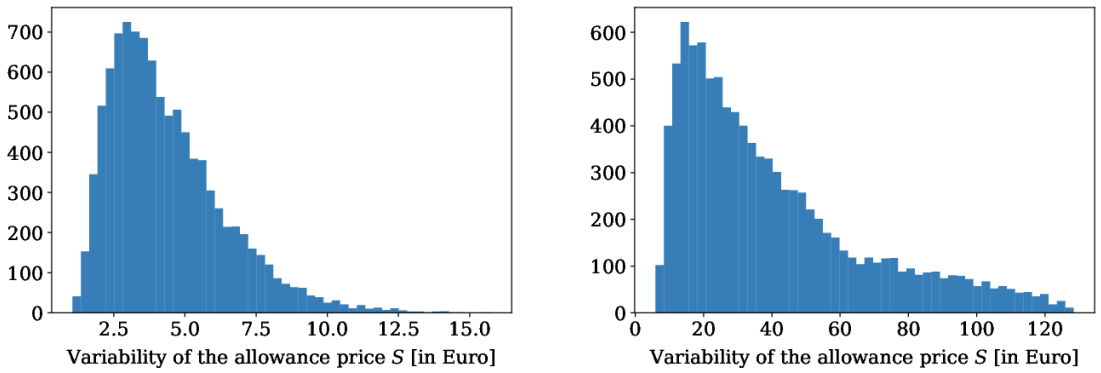

(a) Low penalty of $p = 20$.

(b) High penalty of $p = 200$.

Figure 6.33: Histograms of the variability of the allowance price S normalized to one year in the Brownian model variant for a very low and a very high penalty.

Summary The overall effect is the same as in the simple model variant: An increase of the penalty decreases the mean realized emissions and increases the frequency of compliance as well as the mean allowance price; at the same time, these effects gradually become weaker as the penalty increases. The distributions of the quantities analyzed here behave differently than in the simple model variant: Also for a low penalty, a peak at the emission cap e_0 is visible and the increasing penalty shifts the weight in distribution of mean prices from the second peak to the first.

Varying the Number of Allowances The next parameter we study is the emission cap, given by the number of emission allowances e_0. Again we first analyze the impact of varying this parameter in the simple model variant and then turn to the Brownian model variant. The resulting realized emissions X_T are visualized in Figure 6.34. To

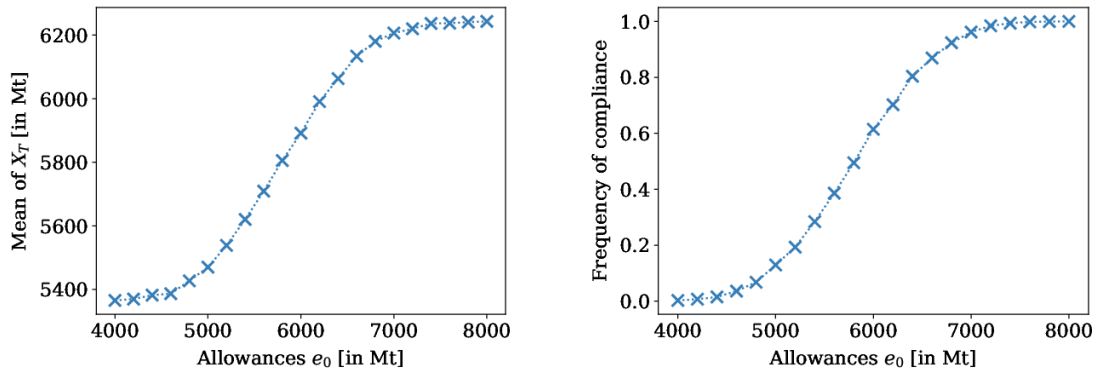

(a) Mean of realized emissions X_T.

(b) Relative frequency of compliance with the emission target e_0.

Figure 6.34: Results on the total expected emissions X for a varying number of allowances in the simple model variant.

interpret these results, we distinguish three different regimes: For small values of e_0, corresponding to a very restrictive cap, we observe that the mean realized emissions are

low and approximately constant in e_0, whereas the relative frequency of compliance with the cap e_0 is zero. In this case, the cap is so strict that in essentially all runs the agent chooses to pay the penalty for some of her emissions since the costs of abatement would be higher. Consequently, as can be seen in Figure 6.35, the allowance price is at its maximum and does not vary. If on the other hand the value of e_0 is high and thus

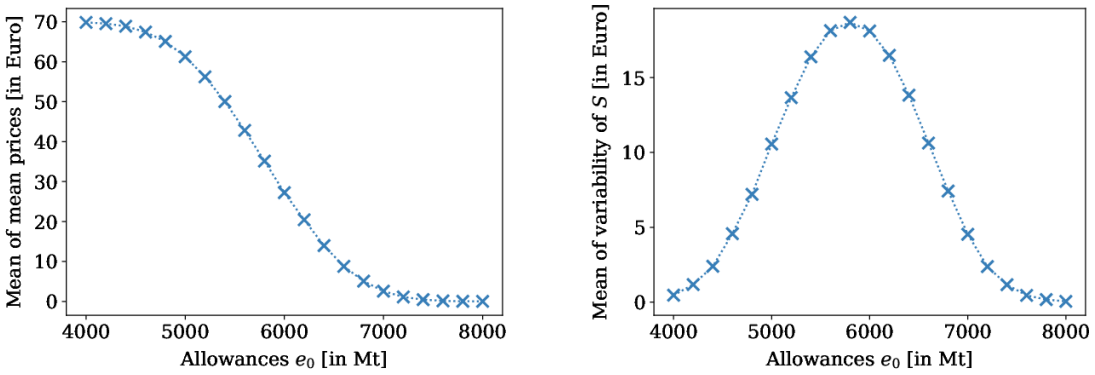

(a) Mean across all runs of the mean prices within one time period.

(b) Mean of the variability of the price S.

Figure 6.35: Results on the allowance price S for a varying number of allowances in the simple model variant.

the cap very loose, we observe the opposite: The mean realized emissions are high and constant, the frequency of compliance is equal to one. In this setting, the cap is well above the initially expected emissions x_0, so no abatement is necessary to ensure that the probability of remaining below the emission threshold e_0 is high. Thus the allowance price is zero with low variability. For a cap that is fairly close to the initially expected emissions e_0, the mean realized emissions and the frequency of compliance increase with e_0, whereas the price decreases; the price variability is the highest. This regime corresponds to the situation that abatement is necessary for compliance and preferable to the penalty payment, at least for part of the simulation runs. Thus an increase in e_0 leads to less abatement but also makes it easier to comply with the threshold. Abatement depends on the development of the total expected emissions X, so the agent reacts to random movements, which leads to more variability of the price.

In the Brownian model, a variation of the emission cap e_0 leads to similar effects. However, in contrast to the simple model variant we observe that also for a very strict or a very loose cap the ETS has en effect: As can be seen in Figure 6.36, changing e_0 among small values of this quantity has an impact on the realized emissions and the frequency of compliance; thus even a very strict cap seems to motivate abatement at least in some cases. This might be due to the heavier tails of the distribution of X_T in the Brownian model variant. For a very loose cap, corresponding to high values for e_0, we do not see an effect on the realized emissions, but the frequency of compliance still increases with increasing e_0. Similarly, as shown in Figure 6.37, the mean of mean allowances prices is affected by a change of e_0 also for small or large e_0, and the price variability is small but does not reach zero. For intermediate values of e_0 we observe the same effects as in the simple model variant: An increase of e_0 leads to increasing realized emissions, an increasing frequency of compliance and decreasing allowance prices.

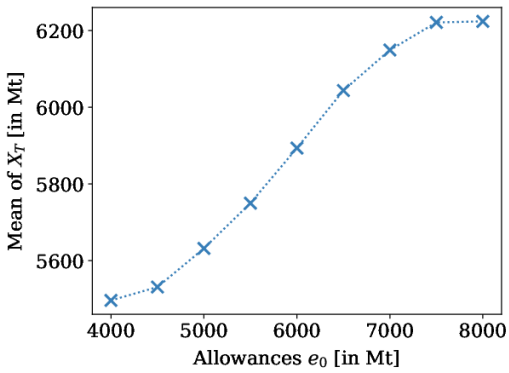

(a) Mean of realized emissions X_T.

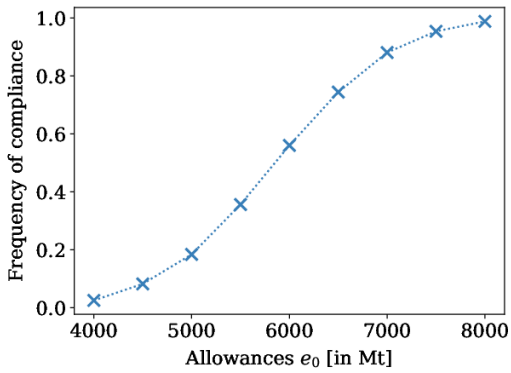

(b) Relative frequency of compliance with the emission target e_0.

Figure 6.36: Results on the total expected emissions X for a varying number of allowances in the Brownian model variant.

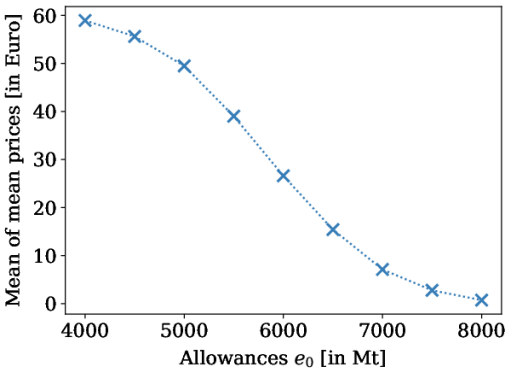

(a) Mean across all runs of the mean prices within one time period.

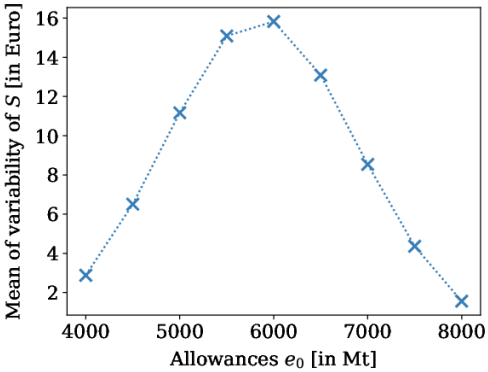

(b) Mean of the variability of the price S.

Figure 6.37: Results on the allowance price S for a varying number of allowances in the Brownian model variant.

Summary If the cap is either very strict or very loose, a small change in the number of allowances has almost no impact. If on the other hand the number of allowances is not too far away from the expected BAU emissions, an increase in the cap leads to higher realized emissions, a higher frequency of compliance and to lower prices. The price variability is the highest if the cap is close to expected BAU emissions. These conclusions can be drawn in a similar way in both the Brownian and the simple model variant.

Varying the Length of the Time Period To study the effects of varying the length of the time period T, we adapt the number of allowances e_0 and the initially expected emissions of the entire time period x_0 proportionally. Figure 6.38 shows the resulting mean realized emissions and the relative frequency of compliance in the simple model variant. As the length of the time period increases, the mean realized emissions increase and approach e_0. Also the frequency of compliance increases, approaching a value of around 68%, while prices decrease towards a value around 22 Euro as shown in Figure 6.39. The

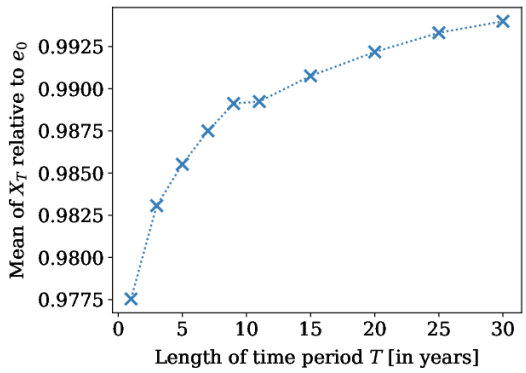

(a) Mean of realized emissions X_T relative to the emission target e_0.

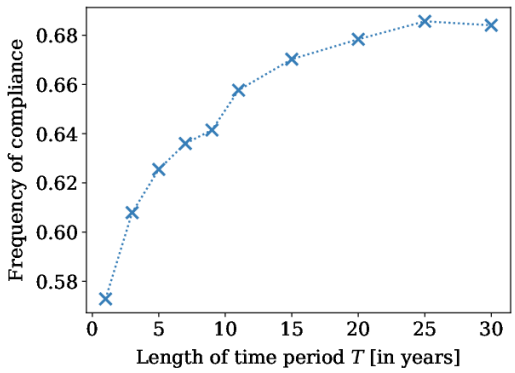

(b) Relative frequency of compliance with the emission target e_0.

Figure 6.38: Results on the total expected emissions X for a varying length of the time period T in the simple model variant.

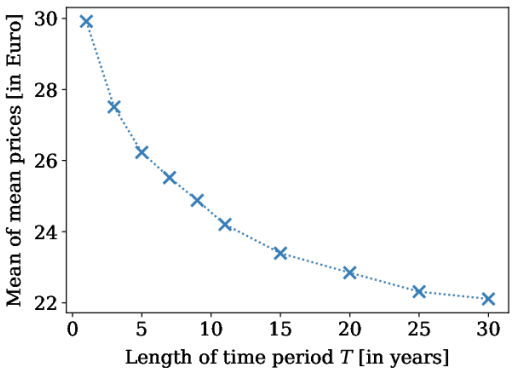

(a) Mean across all runs of the mean prices within one time period.

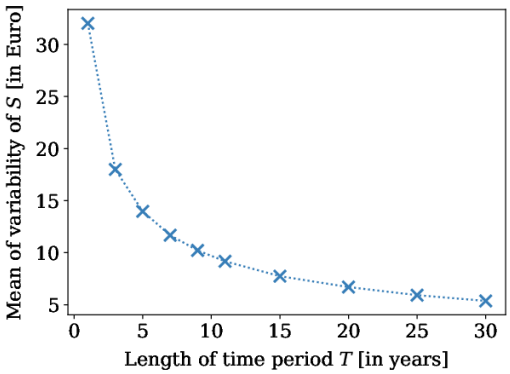

(b) Mean of the variability of the price S.

Figure 6.39: Results on the allowance price S for a varying length of the time period T in the simple model variant.

price variability strongly goes down from more than 30 for a time period of one year to about 10 for a time period lasting 10 years. During a longer time period, the impacts of uncertainty can be smoothed out, therefore the agent aims for realized emissions closer to the threshold e_0. Hence less abatement is necessary, leading to a decrease of the price; at the same time the frequency of compliance is higher. However, it remains far away from one: It is still possible that the emissions move to a level that the required abatement is more expensive than partly paying the penalty; in this case, the emission cap is violated.

In the Brownian model variant, we observe that for longer time periods, realized emissions approach the emission cap e_0, while the frequency of compliance decreases as shown in Figure 6.40. It should be noted that while the last value for $T = 10$ does not seem to confirm this observation, the results of the simulations in this setting need to be interpreted with caution: The path of X left the grid on which the PDE was solved in almost 20% of the simulation runs so that linear extrapolation methods were applied; at the same time the PDE solution (not shown) suggests that extrapolation results are not reliable in

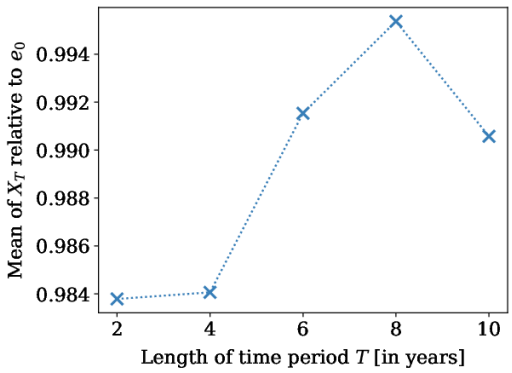

(a) Mean of realized emissions X_T relative to the emission target e_0.

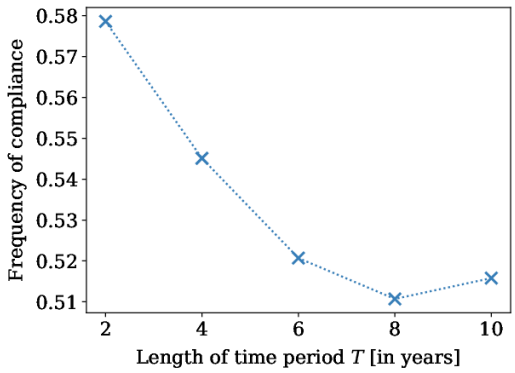

(b) Relative frequency of compliance with the emission target e_0.

Figure 6.40: Results on the total expected emissions X for a varying length of the time period T in the Brownian model variant.

this case. On the other hand, already for a time period of 6 or 8 years the path of X left the grid in a considerable number of runs; in these cases the extrapolation method might yield better results, as the PDE solution is almost constant at the boundary of the grid. Nevertheless, these potential errors need to be kept in mind.

When analyzing the behavior of the allowance price, we observe that as in the simple model variant, prices decrease for longer time periods, and the price variability is drastically reduced, which is shown in Figure 6.41. Notably, the decrease of the mean price has an increasing slope (i.e. the mean price is concave), while the slope of the mean price is decreasing (i.e. convex) in case of the simple model variant. Only the behavior of the mean variability is similar to the one observed in the simple model variant.

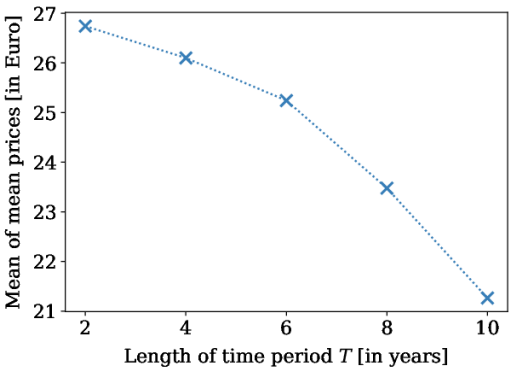

(a) Mean across all runs of the mean prices within one time period.

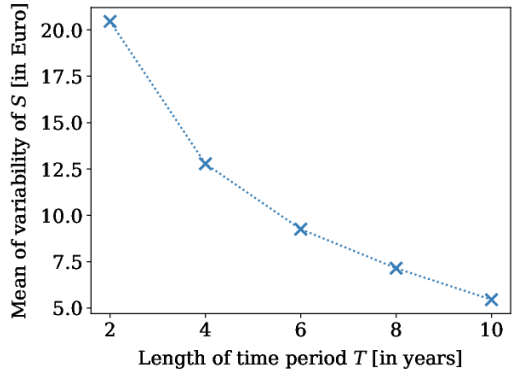

(b) Mean of the variability of the price S.

Figure 6.41: Results on the allowance price S for a varying length of the time period T in the Brownian model variant.

Due to the unreliability of the results obtained in the Brownian model variant, we also present the results from the Ornstein-Uhlenbeck model variant here. These are much less compromised as only a small number of runs left the grid, even for $T = 10$. At the same

time, the PDE solution remains largely constant at the boundary, enabling the extrapolation method to work properly. In Figure 6.42 the mean realized emissions, relative to the cap, and the relative frequency of compliance with the emission cap are shown. These

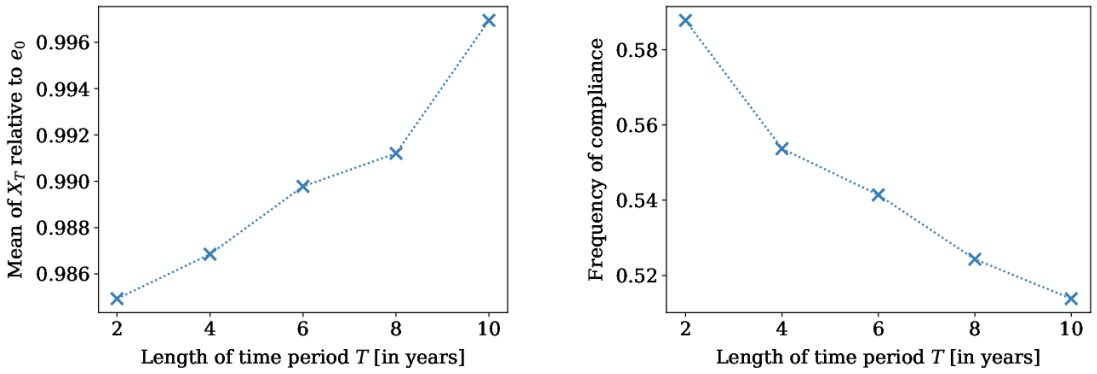

(a) Mean of realized emissions X_T relative to the emission target e_0.

(b) Relative frequency of compliance with the emission target e_0.

Figure 6.42: Results on the total expected emissions X for a varying length of the time period T in the Ornstein-Uhlenbeck model variant.

results confirm the general tendencies observed in the Brownian model variant, namely that mean realized emissions decrease, whereas the frequency of compliance decreases. Interestingly, the latter represents the opposite behavior to the one observed in the simple model variant. Both the increase in the mean realized emissions and the decrease in the compliance frequency are roughly linear, which is not the case in the Brownian variant. In particular, it is not clear how these quantities behave for very large T, as in contrast to the simple model variant they do not appear to approach some constant value. Therefore, simulations with very large T would be of interest to observe whether for instance the mean realized emissions surpass the cap. Due to the computational difficulties already encountered for values of $T = 10$, this might be challenging.

The observations on the allowance price, which can be drawn from Figure 6.43, are similar to what we observed in the Brownian model variant: The mean prices decrease for longer time periods; this decrease accelerates for short time periods but remains constant for later time periods. The variability is also decreasing with longer time periods, but here, as in all other model variants, this decrease becomes weaker for larger values of T.

Summary The results obtained in the simple model variant on the one hand and in the Brownian or Ornstein-Uhlenbeck model variant on the other differ considerably: In the simple model variant, the realized emissions approach e_0 and the frequency of compliance increases, converging to approximately 68%. At the same time, the mean price approaches roughly 22 Euro, while the price variability strongly goes down. In the Brownian and Ornstein-Uhlenbeck model, we obtain a completely different picture: The mean realized emissions might surpass the cap for very large T and the frequency of compliance decreases. At the same time, prices do not seem to converge and thus possibly attain very low values for long time periods. Without further simulations however, these projections cannot be confirmed. The large differences to the simple model variant may be due to the different structure of the volatility function. In case of the simple model

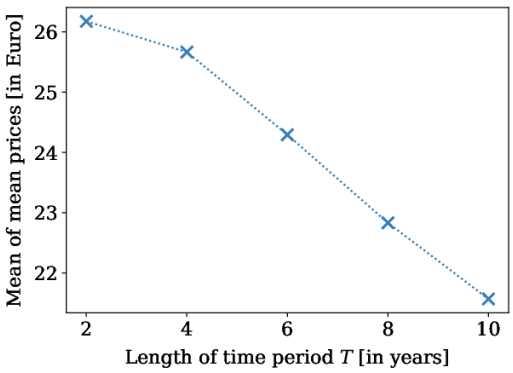

(a) Mean across all runs of the mean prices within one time period.

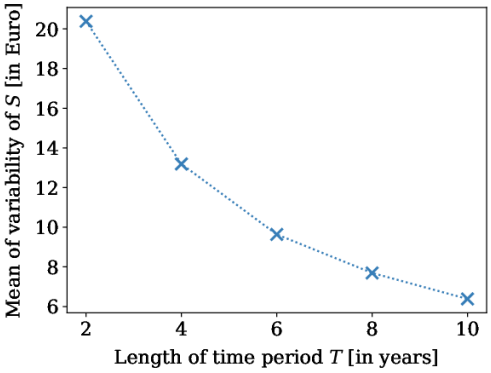

(b) Mean of the variability of the price S.

Figure 6.43: Results on the allowance price S for a varying length of the time period T in the Ornstein-Uhlenbeck model variant.

variant, the volatility of X is not influenced by the length of the time period, while both for the Brownian and the Ornstein-Uhlenbeck model variant, the parameter T enters the volatility function.

Impact of Non-Regulatory Parameters

Several parameters entering the system are not given by the regulator; at the same time, they are difficult to obtain or to estimate. Thus we also assess their impact on simulation results. For the sake of brevity, we restrict this analysis to the simple model variant; only the impact of the parameter θ needs to be studied in the Ornstein-Uhlenbeck model, since it does not appear in the two other model variants.

A variation of the cost coefficient c strongly impacts the mean realized emissions, the frequency of compliance and the allowance price, as shown in Figures 6.44 and 6.45. Increasing c means that abatement becomes more expensive, thus the mean realized emis-

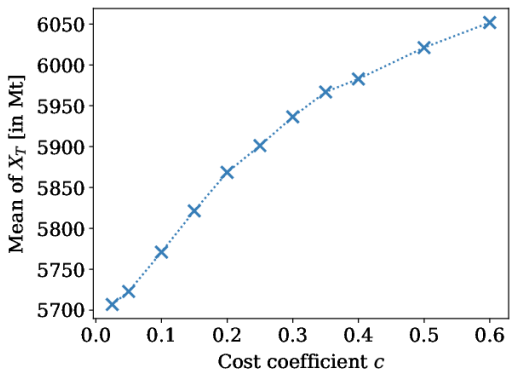

(a) Mean of realized emissions X_T.

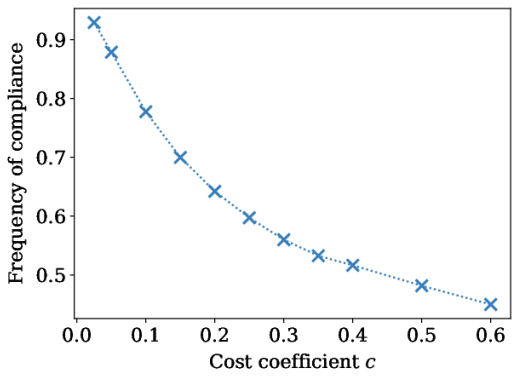

(b) Relative frequency of compliance with the emission target e_0.

Figure 6.44: Results on the total expected emissions X for a varying cost coefficient c in the simple model variant.

sions increase; at the same time the level of abatement at which it becomes cheaper to pay the penalty decreases, leading to a decrease of the frequency of compliance. The allowance price also increases, as it is given by the marginal abatement costs. The impact on the variability of the allowance price however is small.

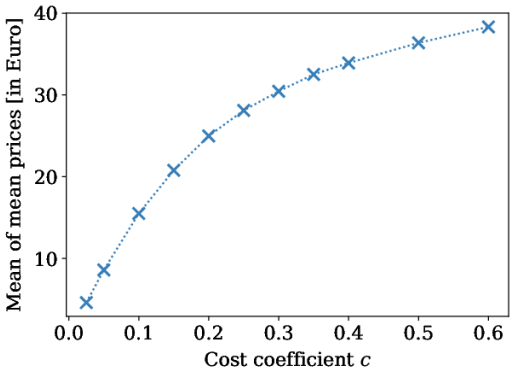

(a) Mean across all runs of the mean prices within one time period.

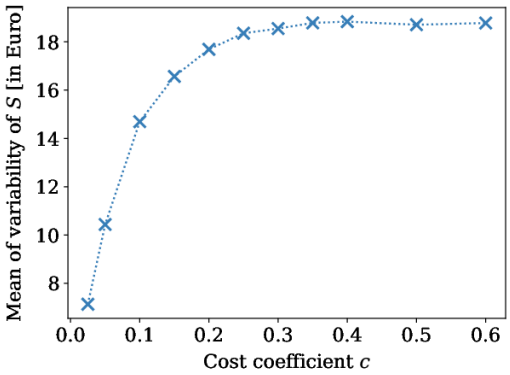

(b) Mean of the variability of the price S.

Figure 6.45: Results on the allowance price S for a varying cost coefficient c in the simple model variant.

Next we vary the volatility parameter σ, which determines the volatility of the process X. In Figure 6.46 we observe that the realized emissions as well as the frequency of compliance decrease. Due to the higher uncertainty, the agent is willing to abate more

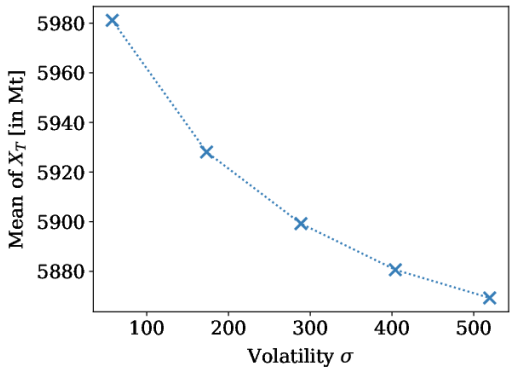

(a) Mean of realized emissions X_T.

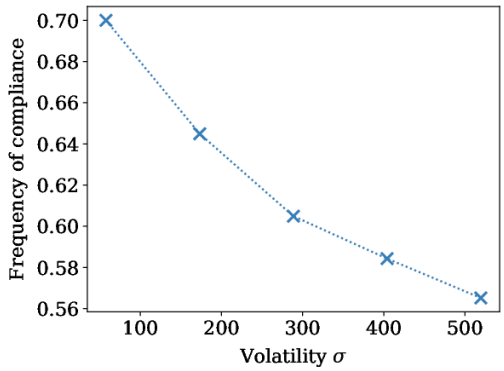

(b) Relative frequency of compliance with the emission target e_0.

Figure 6.46: Results on the total expected emissions X for a varying volatility parameter σ in the simple model variant.

to avoid penalty payments; on the other hand the higher fluctuations more often lead to sufficiently high emissions such that paying the penalty is cheaper than fully abating them. Interestingly, as shown in Figure 6.47, the allowance price does not increase that much with increasing σ, whereas the price variability is barely affected.

Finally we consider the impact of the initially expected emissions x_0. Since this setting is similar to changing the number of allowances, we make similar observations as above.

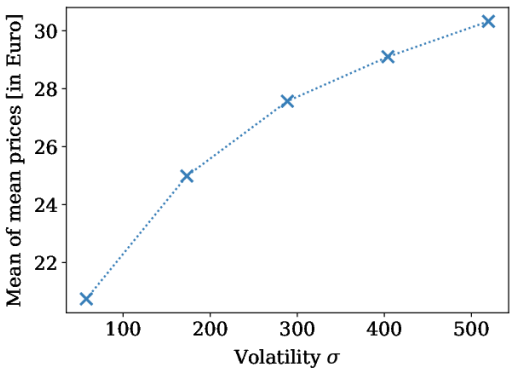

(a) Mean across all runs of the mean prices within one time period.

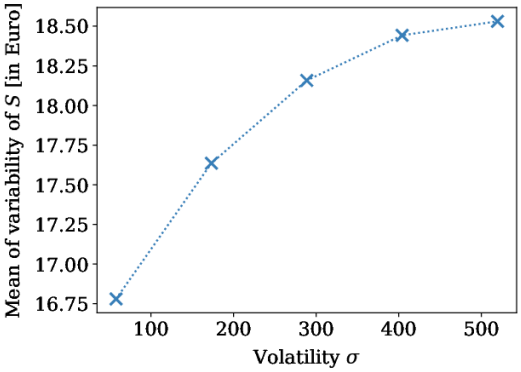

(b) Mean of the variability of the allowance price S.

Figure 6.47: Results on the allowance price S for a varying volatility parameter σ in the simple model variant.

When analyzing the results shown in Figures 6.48 and 6.49, we again notice three different regimes: If only very low emissions are expected initially, the cap is very loose, so that the

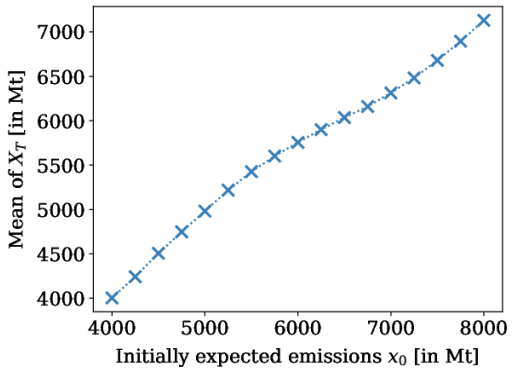

(a) Mean of realized emissions X_T.

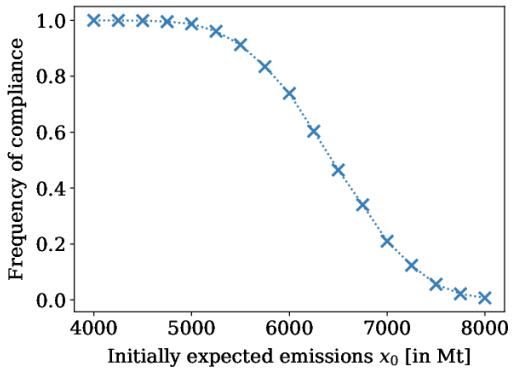

(b) Relative frequency of compliance with the emission target e_0.

Figure 6.48: Results on the total expected emissions X for varying initially expected emissions x_0 in the simple model variant.

presence of the ETS has little impact. Therefore, the realized emissions increase lineary with x_0 and the frequency of compliance is one. Accordingly, the allowance price is zero with zero variability. Conversely, for very high initially expected emissions, the cap is very strict, thus if x_0 increases further, the agent pays the penalty for this increase instead of abating the emissions. As a result, realized emissions again increase linearly with x_0. The frequency of compliance is zero and the allowance price is close to its bound, with small price variability. In the intermediate case, where x_0 is close to the emission cap e_0, higher emissions are at least partly abated. Therefore, an increase in x_0 does not lead to a corresponding increase of the realized emissions X_T. Since for higher x_0 more abatement is necessary, the frequency of compliance decreases and the price increases; the price variability is the highest in this setting.

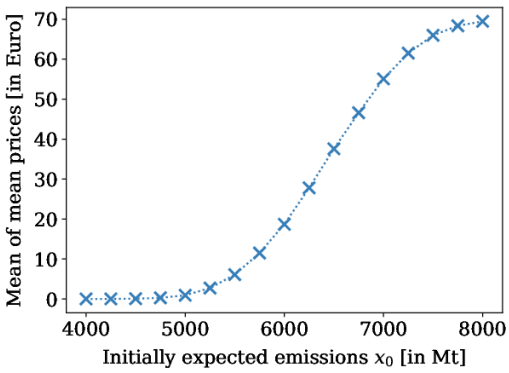

(a) Mean across all runs of the mean prices within one time period.

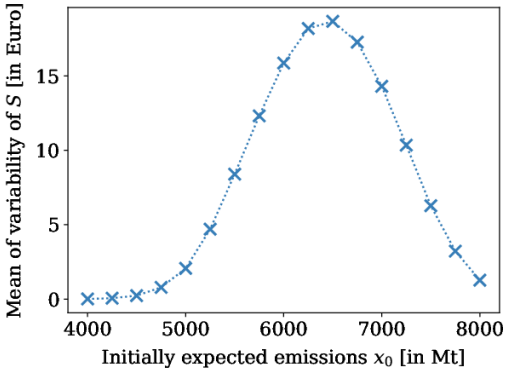

(b) Mean of the variability of the price S.

Figure 6.49: Results on the allowance price S for varying initially expected emissions x_0 in the simple model variant.

In comparison to the simple and the Brownian model variant, the Ornstein-Uhlenbeck model has an additional parameter, namely the mean reversion speed θ. We thus analyze how it affects the SDE solution results if this parameter varies on a range typically used in Ornstein-Uhlenbeck models. From Figure 6.50, we obtain that an increase of θ leads to higher realized emissions and a higher frequency of compliance with the emission cap e_0. An increase of θ implies a smaller volatility of X especially in the beginning of the

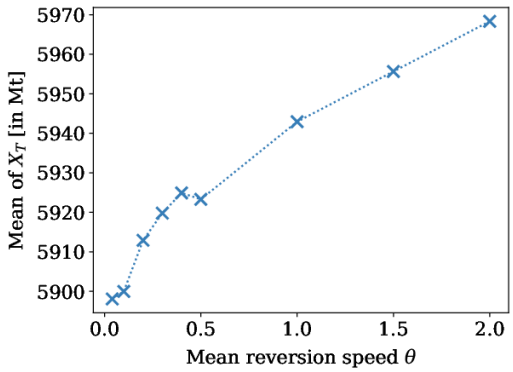

(a) Mean of realized emissions X_T.

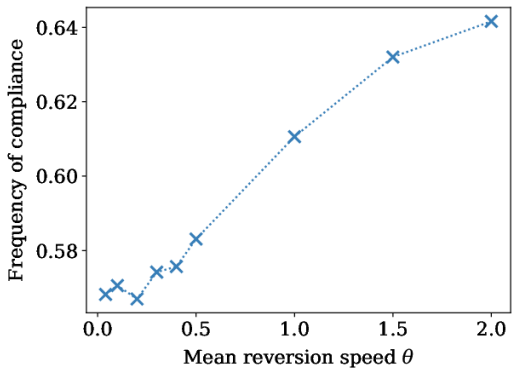

(b) Relative frequency of compliance with the emission target e_0.

Figure 6.50: Results on the total expected emissions X for varying mean reversion speed θ in the Ornstein-Uhlenbeck model variant.

time period, as shown in Figure 6.51. We have already seen above that if the volatility is smaller, the agent does not need to abate as much to avoid penalty payments. So the realized emissions may be higher, while the frequency of compliance also increases since it is less likely that emissions are high enough to make penalty payments cheaper than abatement. This effect causes the mean allowance price to decrease as shown in Figure 6.52a; at the same time, the price variability given in Figure 6.52b increases. Possibly the smaller variance of X causes more runs to remain close to e_0, where the price

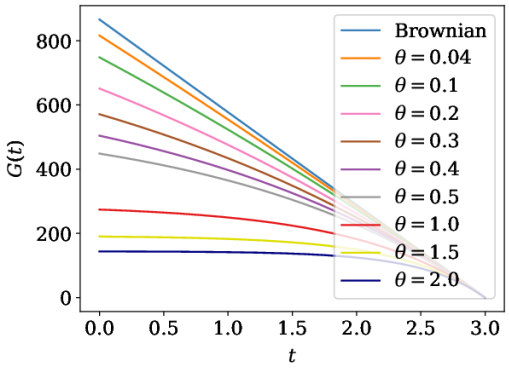

Figure 6.51: Volatility function $G(t)$ of the total expected emissions process X for varying mean reversion speeds θ in the Ornstein-Uhlenbeck model variant and for the Brownian model variant.

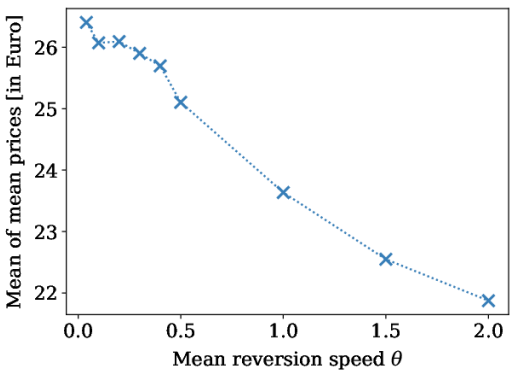

(a) Mean across all runs of the mean prices within one time period.

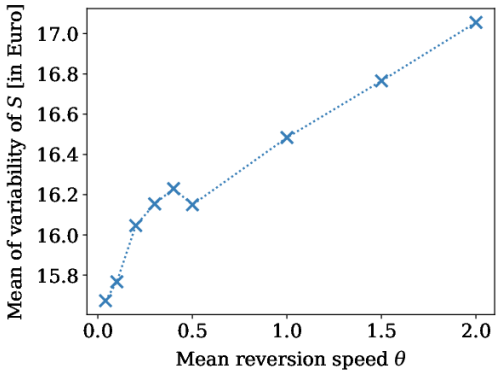

(b) Mean of the variability of the price S.

Figure 6.52: Results on the allowance price S for varying mean reversion speed θ in the Ornstein-Uhlenbeck model variant.

function is the steepest, thus causing higher fluctuations of the price. All these effects however are comparably small. Interestingly, as can be seen in Figure 6.51, an increase of θ also moves the volatility function away from the volatility function of the Brownian model, thus reducing the similarity between the two models. On the other hand, for a value of $\theta = 0.04$ as obtained in the second estimate in Section 5.3.3, we observe that the volatility function is almost identical to the one of the Brownian model variant; thus we do not conduct any simulations with this choice for θ in the one-period model.

Summary We studied the impact of several descriptive parameters that cannot be chosen by the regulator. We find that the cost coefficient has a large impact on the system; only the price variability is not affected much by a varying cost coefficient. The effects of changing the volatility parameter σ are considerably smaller, leaving the price variability almost unchanged. The variation of the initially expected emissions x_0 has similar implications as varying the emission cap e_0. A change in the mean reversion speed θ in the Ornstein-Uhlenbeck model variant only has a small impact on the system. Importantly,

decreasing θ increases the similarity to the Brownian model variant.

6.1.6 Asymptotic Behavior

To gain a more thorough understanding of the model, we analyze the behavior of the model if parameters tend to infinity or to zero by letting them grow large or small in simulation settings.

Firstly, we are interested in the impact of a penalty that tends to infinity. In Figure 6.53 we observe for an increasingly large penalty, that the mean realized emissions X_T appear to converge in all three model variants; notably, for the Ornstein-Uhlenbeck model the limit is about 70 Mt higher. At the same time, the relative frequency of compliance seems to

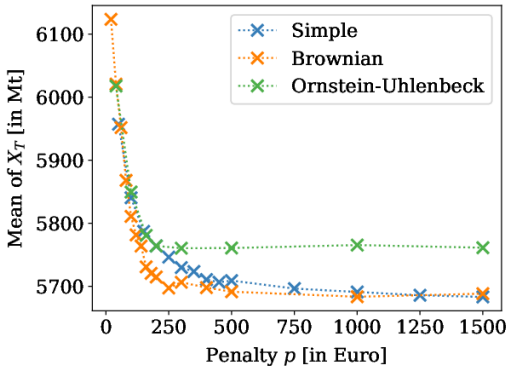

(a) Mean of realized emissions X_T.

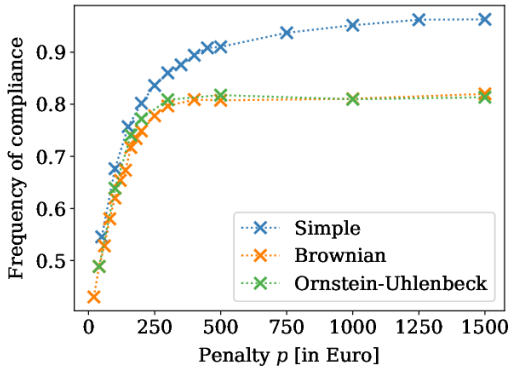

(b) Relative frequency of compliance with the emission cap e_0.

Figure 6.53: Results on the total expected emissions X for a penalty value that becomes large in all model variants.

converge to 1 for increasingly large penalties in case of the simple model variant, but both in the Brownian and the Ornstein-Uhlenbeck variant the limit appears to be around 0.8. Similarly, the mean allowance prices shown in Figure 6.54a converge, with the Brownian and the simple model variant behaving in a similar way, while the asymptotic mean price in the Ornstein-Uhlenbeck model is approximately 5 Euro lower. This is consistent with the observation on the realized emissions: The limit obtained there determines the mean abatement requirement and thus the mean price. The mean price variability, which is shown in Figure 6.54b, appears to diverge in all three models, increasing faster in the Brownian and Ornstein-Uhlenbeck model.

In a further simulation, we let the length of the time period T grow large. Due to the problems encountered already for $T = 10$ in the Brownian and Ornstein-Uhlenbeck model variant, as discussed in the previous section, we only do this in the simple model variant. By using the analytical PDE solution, we increase the length of the time period up to a value of 100 years. Similar to the observations made when varying T among lower values, we see in Figure 6.55 that the mean realized emissions approach the emission cap, while the relative frequency of compliance stabilizes around 70%. Both the mean prices and the mean price variability shown in Figure 6.56 decrease quickly; the price appears to converge to a value slightly below 20 Euro, whereas the price variability becomes very small, reaching a value of 3 Euro for a time period of 100 years. If indeed the mean realized

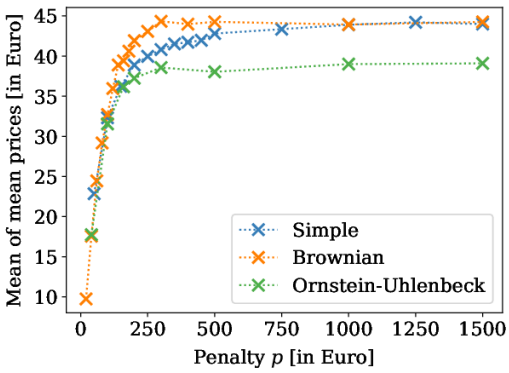

(a) Mean across all runs of the mean prices within one time period.

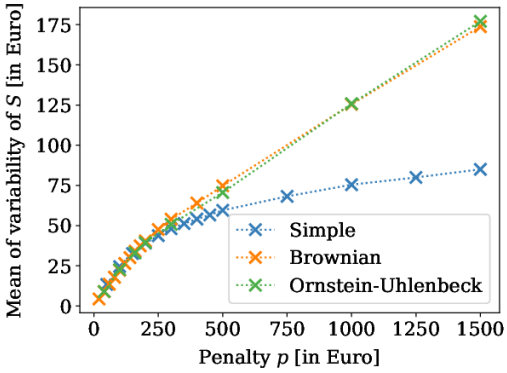

(b) Mean of the variability of the price S.

Figure 6.54: Results on the allowance price S for a penalty value that becomes large in all model variants.

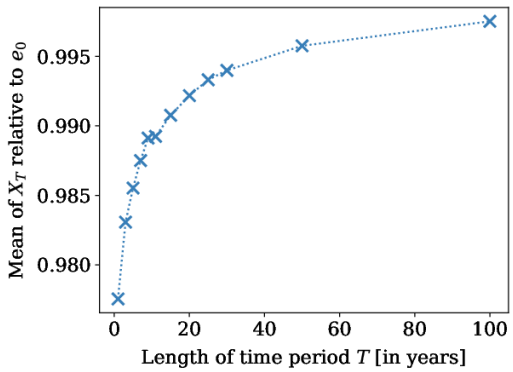

(a) Mean of realized emissions X_T relative to the emission target e_0.

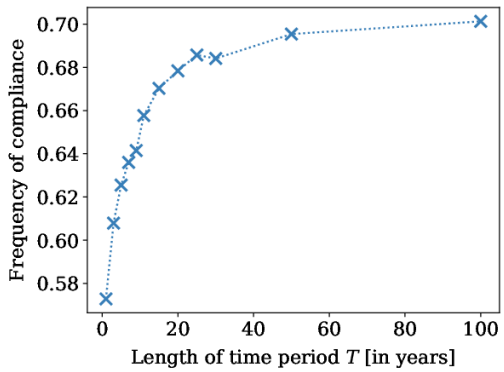

(b) Relative frequency of compliance with the emission target e_0.

Figure 6.55: Results on the total expected emissions X for the length of the time period T becoming large in the simple model variant.

emissions converge to the emission cap, it is plausible that the prices remain positive, since this would still correspond to an abatement of 80 Mt per year.

By letting the volatility parameter σ become small, we approach a deterministic setting. Not surprisingly, Figure 6.57a shows that for small σ the mean realized emissions approach the emission cap e_0. The relative frequency of compliance shown in Figure 6.57b also becomes large, at least in the Brownian and Ornstein-Uhlenbeck model variants. In the simple variant it only reaches 78% for the smallest σ considered here. In contrast to the Brownian and Ornstein-Uhlenbeck model variants the volatility of the process X in the simple variant is not time dependent, thus even in the very last simulation step it is large enough to cross the threshold given by the emission cap e_0; at this time point, it is no longer possible to reduce emissions again by abatement. Accordingly, by analyzing the absolute numbers of the realized emissions (not shown), we can see that for the runs in violation of the emission cap, the realized emissions are only very slightly above the cap. In Figure 6.58a we observe that for small σ the mean price approaches a value

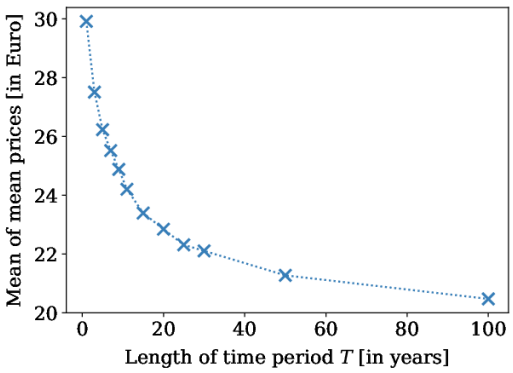

(a) Mean across all runs of the mean prices within one time period.

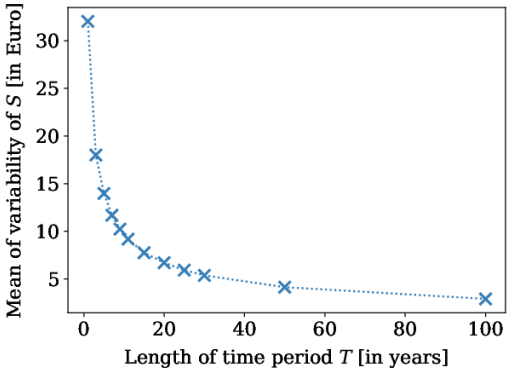

(b) Mean of the variability of the price S.

Figure 6.56: Results on the allowance price S for the length of the time period T becoming large in the simple model variant.

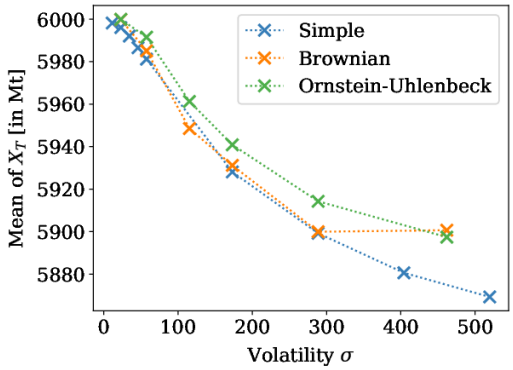

(a) Mean of realized emissions X_T.

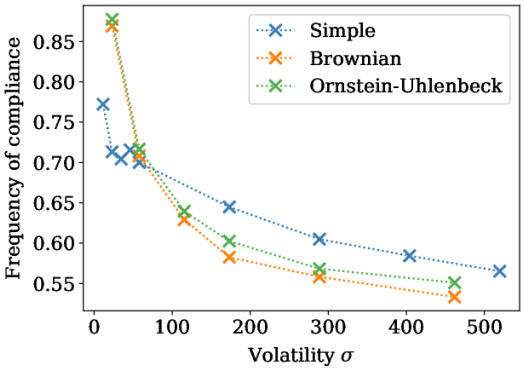

(b) Relative frequency of compliance with the emission target e_0.

Figure 6.57: Results on the total expected emissions X for a volatility σ that becomes small in all model variants.

slightly below 20 Euro. This is again plausible: In deriving the parameter c in Section 5.3.2 we chose c in such a way that the price in a deterministic setting would be 19.2 Euro. The result on the mean price variability shown in Figure 6.58b possibly is more surprising: In all model variants the parameter σ barely influences the price variability for most values of σ. But for very small σ the price variability decreases in case of the Brownian and Ornstein-Uhlenbeck model variants, while it sharply increases in case of the simple model variant. This might be due to the effect mentioned above: Since the price function becomes steeper towards the end of the time period, this is where changes in X have the largest impact on the price variability. In the Brownian and Ornstein-Uhlenbeck model variants the volatility function $G(t)$ of the process X is very small at this time point, which makes it unlikely that relevant jumps in X occur, leading to a small price variability. But in the simple model variant, jumps of relevant size are possible. Moreover, the small volatility parameter σ causes the trajectories to remain close to e_0. Thus jumps crossing the threshold e_0 are likely, resulting in very high price jumps and accordingly in

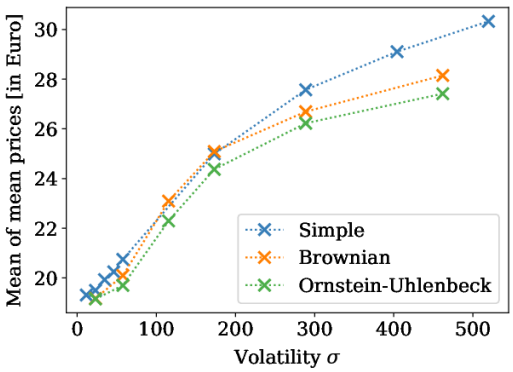

(a) Mean across all runs of the mean prices within one time period.

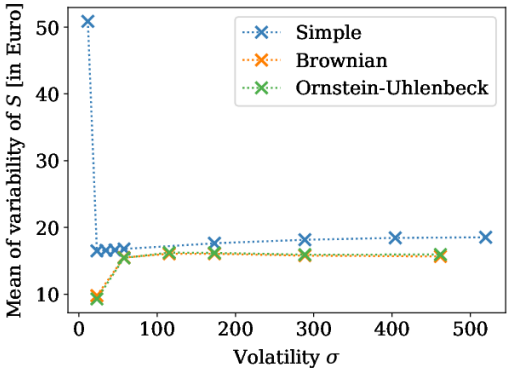

(b) Mean of the variability of the price S.

Figure 6.58: Results on the allowance price S for a volatility σ that becomes small in all model variants.

a high price variability.

Summary

In this section, we studied the asymptotic behavior of the model. For an increasing penalty, we found that most of the characteristic quantities converge; in the Brownian and Ornstein-Uhlenbeck model variant, the frequency of compliance converges to a value of approximately 0.8, well below 1. For increasingly longer time periods, studied only in the simple variant, the trends observed in Section 6.1.5 can be confirmed: The system appears to converge to a state where emissions are equal to the cap, with a frequency of compliance of 0.7 and low price variability. However, we need to be careful to draw conclusions from this result, as the behavior for a varying length of the time period is very different in the Brownian and Ornstein-Uhlenbeck model variant, as seen in Section 6.1.5. Also for a volatility approaching zero, the behavior of the model variants differs: In the simple model variant, the frequency of compliance is smaller and the price variability becomes large for a very small volatility, while the frequency of compliance is large and the price variability is small in the two other model variants. In the Brownian and Ornstein-Uhlenbeck model variant, the results for a decreasing volatility overall approach the results we would expect in a deterministic setting.

6.2 Multi-Period Model I

In this section, we apply multi-period model I as introduced in Section 3.1 to simulate an emission trading system with six time periods. Our main objective is to compare the differences between a system where allowances can be transferred to the case where this is not possible. We discuss the PDE solution obtained with transferable allowances and present the results from solving the SDE for both cases. We then vary several parameter settings and analyze the corresponding effects.

6.2.1 Solution to the PDE

In multi-period model I, we assume that the price parameter s^i, which reflects the anticipated initial allowance price of the next time period, is constant within each time period. As can be seen in Section 3.1.3, we were able to solve the PDE analytically for the simple model variant with interest rate zero. In Figure 6.59 we visualize this solution; here the parameter s^i was chosen to be 30, while the penalty was set to $p = 40$. Since the total

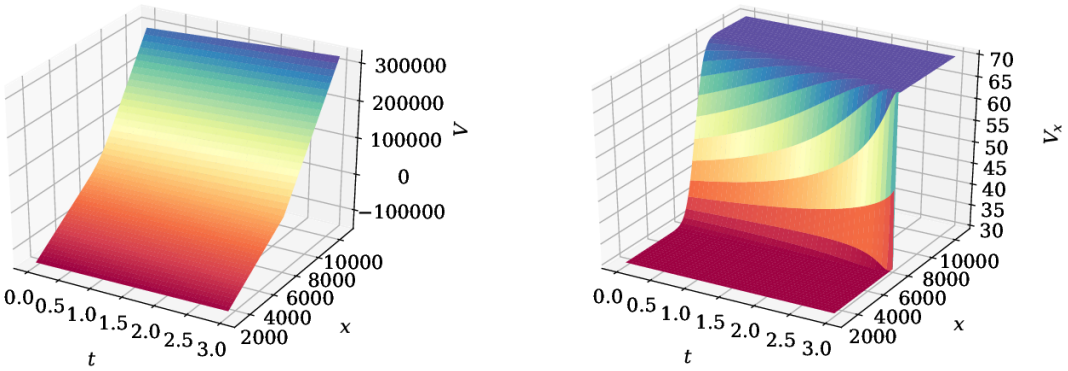

(a) Solution V.

(b) First derivative V_x.

Figure 6.59: Analytical PDE solution in the simple model variant.

payment is given by the sum of these two quantities in case of non-compliance, this situation closely resembles that of Section 6.1.1, while allowing for the transfer of allowances to the subsequent time period. As a result, the cost function V is no longer constant zero for x sufficiently smaller than e_0; in this range, it is instead now negative and approximately linearly increasing in x but with a slope that is smaller than for high values of x. In this way, the benefit obtained from surplus allowances is incorporated in the cost function in the form of negative costs. Around e_0 on the x-axis and zero on the z-axis, there is a visible kink representing the shift from benefits to penalty payments.

The first derivative V_x is similar to the one-period model, but for low values of x, i.e. well below e_0, the derivative is now constant at a value corresponding to the parameter s^i instead of being equal to zero. Thus, as shown in Proposition 3.3, the derivative V_x is bounded between s^i and $s^i + p$. The second derivatives V_{xx} and V_{xt} are shown in Figure 6.60; they are overall similar to the one-period case with small differences in V_{xx} at the beginning of the time period.

In the Brownian model variant, it is again necessary to compute the PDE solution numerically. We consider the setting of six time periods which we will work with throughout this section. To combine these time periods, we proceed as explained in Section 3.1.5: We first solve the PDEs in reversed order and are thus able to compute the price parameter s^i from the PDE of the subsequent time period. Since the price parameter s^{N-1} of the last time period is set to zero, we implicitly assume that after the last time period considered, the allowances become invalid and cannot be transferred to some later time. In this way, we obtain values for s^i as given in Figure 6.61. In particular, the input s^0 of time period 0 is given as $s^0 = 27.31$ in the case of transferable allowances. With this value we can solve the PDE of time period 0; the result for the first derivative V_x is shown in Figure 6.62. The result is similar to the one-period model, except that for small x the derivative is equal to a constant below 25 instead of being zero. In particular, V_x appears

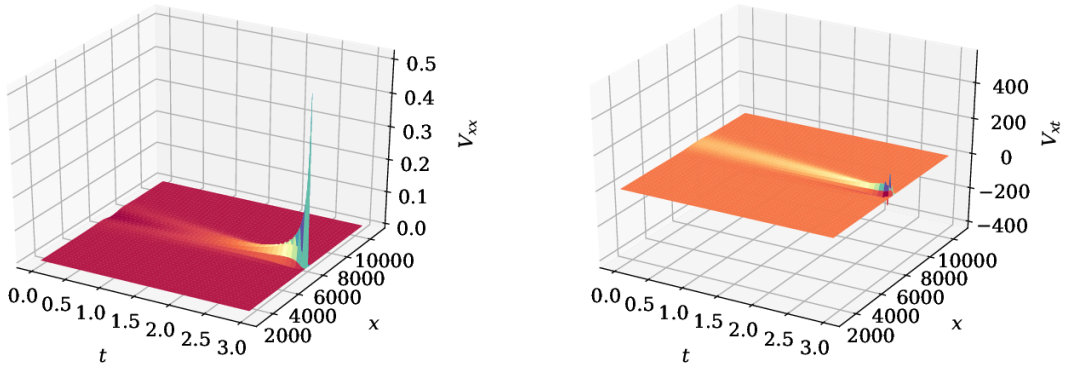

(a) Second derivative V_{xx}. **(b)** Second derivative V_{xt}.

Figure 6.60: Second derivatives of the PDE solution in the simple model variant.

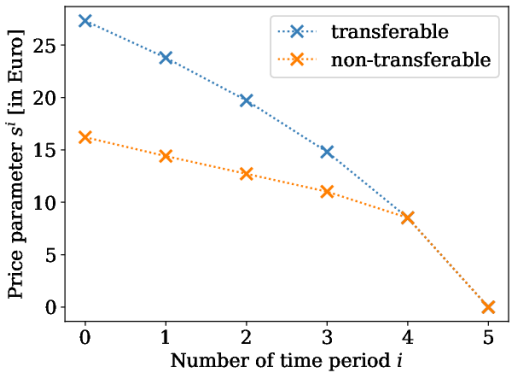

Figure 6.61: Price input parameters s^i computed from the price function of the subsequent time period in the Brownian model variant.

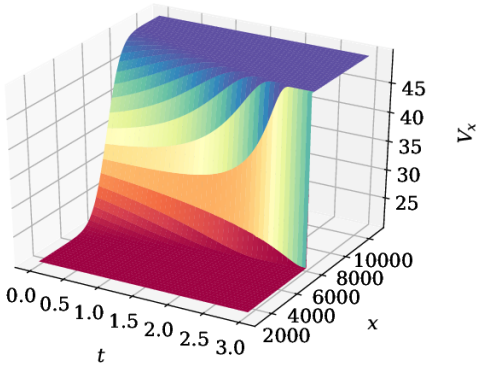

Figure 6.62: Numerical PDE solution in the Brownian model variant.

to be bounded between approximately 25 and 50 Euro; more precisely, these bounds are given by $\mathrm{e}^{-r\Delta T}\, s^0 = 20.23$ and $\mathrm{e}^{-r\Delta T}\,(s^0 + p) = 49.87$.

The second derivatives V_{xx} and V_{xt} are shown in Figure 6.63. Again we observe a high similarity to the results in the one-period model. Thus while both second derivatives

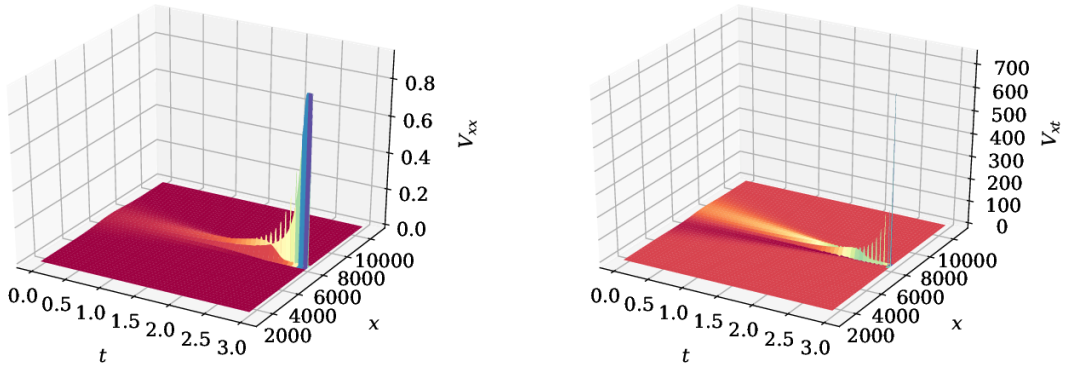

(a) Second derivative V_{xx}.

(b) Second derivative V_{xt}.

Figure 6.63: Second derivatives of the PDE solution in the Brownian model variant.

appear to be unbounded on $[0, T]$, it is plausible to expect that they are bounded on any interval of the form $[0, T-\varepsilon]$ with $\varepsilon > 0$. This observation again motivates the application of the Euler-Maruyama method to compute a numerical SDE solution.

As in the one-period model, the PDE solution in the Ornstein-Uhlenbeck model variant is largely similar to the one in the Brownian model variant. Therefore we omit a detailed discussion here.

Summary

The structure of V_x as obtained from the PDE solution is similar to the results in the one-period model. Importantly, instead of being constant to zero for small x, the function V_x now takes a constant positive value if x is small, reflecting the benefit from surplus allowances. The similarities in V_x imply that also the results for the second derivatives V_{xx} and V_{xt} are similar to the one-period model.

6.2.2 Solution to the SDE in the Simple Model Variant

In order to solve the SDE numerically in the simple model variant, we still require the price parameter s^i for each time period. As described above for the Brownian model variant, we have $s^{N-1} = 0$, thus assuming that all allowances become invalid at the end of the last time period. From s^{N-1}, we proceed in reversed order by computing s^i from the PDE solution that was obtained by using s^{i+1} as price parameter. We do this both for the model where the transfer of allowances, i.e. banking, is possible, and for the model where this is not the case, as introduced in Section 3.1.6. Furthermore, we assume that the penalty is set to $p = 40$. Thus we obtain the price parameters s^i as shown in Figure 6.64. We see that in the case of transferable allowances the price parameter possibly does not converge for an increasing number of time periods, whereas if the transfer of allowances is not possible, the price parameter converges to a value slightly below 30.

To acquire a better understanding of the behavior of the emissions and the allowance price in this model, we study three exemplary trajectories of both processes; we do this both for the case where allowances can be transferred shown in Figure 6.65 and for the opposite case where this is not possible presented in Figure 6.66. In both cases, we observe a discontinuity in the trajectories of X and S at the points where one time period ends.

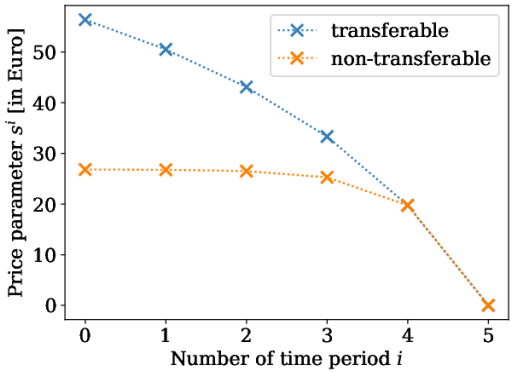

Figure 6.64: Price input parameters s^i computed from the price function of the subsequent time period in the simple model variant.

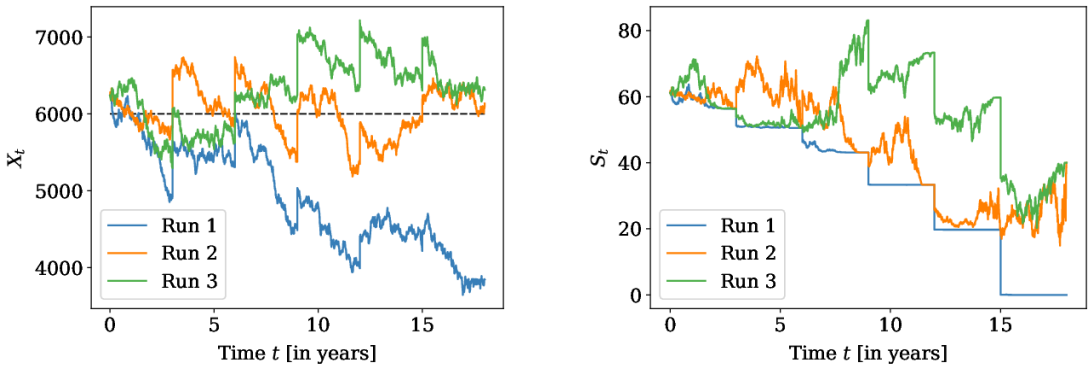

(a) Trajectories of X.

(b) Trajectories of S.

Figure 6.65: Three example trajectories of the total expected emissions X with corresponding trajectories of the price process S when allowances are transferable to subsequent time periods in the simple model variant.

While for the total expected emissions X this is plausible since they are not continuous by construction, the allowance prices observed on the market are continuous across time periods if a transfer of allowances is possible. As already observed in the one-period model, prices fluctuate strongly if the total expected emissions X are close to the emission cap e_0; otherwise they remain close to the minimum or maximum bound. If allowances can be transferred, the minimum price bound is given by s^i and therefore is well above zero for earlier time periods and decreases to zero towards the last time period. If on the other hand allowances cannot be transferred, the minimum price bound is always zero. Furthermore, in the case of transferable allowances, the trajectories of X show a more clear downward tendency; this observation can still be made when considering more examples. Notably, price fluctuations mostly occur during the early time periods, while towards the end in both cases one run has constant prices throughout the time period. This happens since in earlier time periods more runs are still close to e_0 as they all start at the same point. As time proceeds, more and more runs move away from e_0 and thus lead to almost constant prices. This translates to the situation that emissions are sufficiently low or high that in each time period an overall allowance surplus or shortage is expected already from

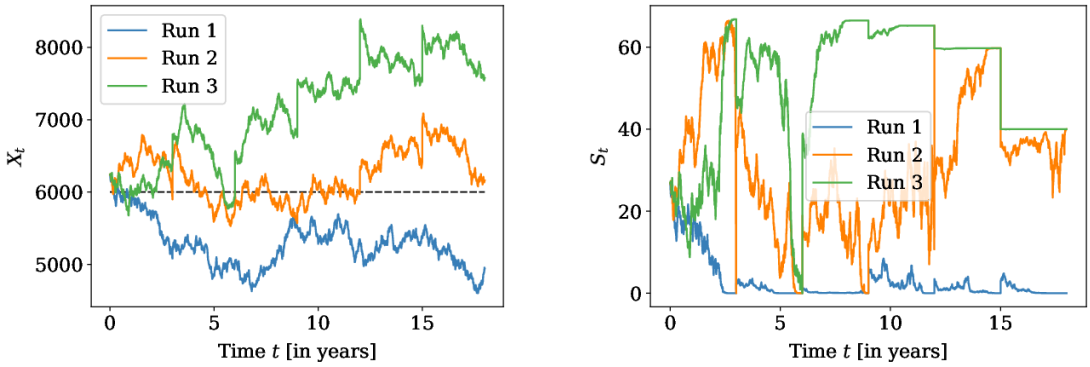

(a) Trajectories of X.

(b) Trajectories of S.

Figure 6.66: Three example trajectories of the total expected emissions X with corresponding trajectories of the price process S when allowances are not transferable to subsequent time periods in the simple model variant.

the start of that particular time period.

When considering the mean trajectories of the process X as shown in Figure 6.67a, we directly see that especially in early time periods, the slope of the trajectory is much steeper in the case of transferable allowances, leading to lower mean realized emissions at the end of each time period. For the last time period the result is identical as was to be expected by the setup of the simulation with $s^{N-1} = 0$. In line with these results, we observe that the distribution of realized emissions in time period 0, which is given in Figure 6.67b, is shifted considerably to the left in the case of transferable allowances. If it is not possible

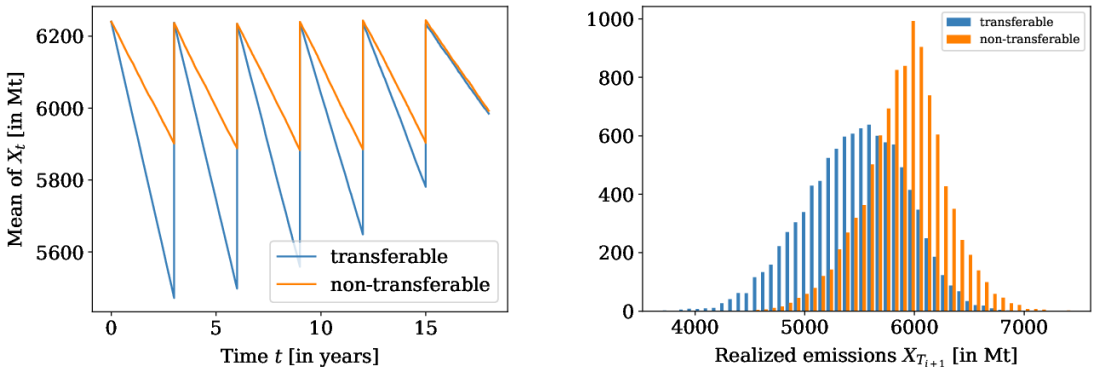

(a) Mean trajectory of X.

(b) Histogram of realized emissions $X_{T_{i+1}}$ in time period 0.

Figure 6.67: Mean trajectory of X and distribution of realized emissions $X_{T_{i+1}}$ in an ETS with transferable and non-transferable allowances, in the simple model variant.

to transfer allowances, the distribution has a high peak at $e_0 = 6000$ and is slightly skewed to the left, as already observed in the one-period model. For later time periods, shown in Figure 6.68, the distributions move closer together until they are identical in the last time period. Allowing for the transfer of allowances substantially increases the relative frequency of compliance as can be seen in Table 6.1; this effect too diminishes for later

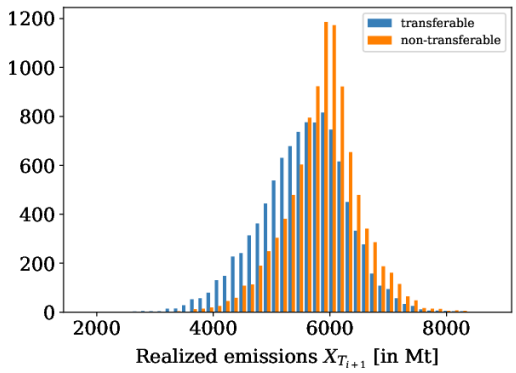

(a) Histogram of realized emissions $X_{T_{i+1}}$ in time period 2.

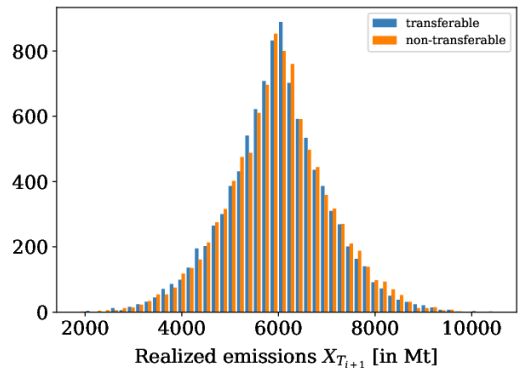

(b) Histogram of realized emissions $X_{T_{i+1}}$ in the last time period.

Figure 6.68: Distribution of realized emissions $X_{T_{i+1}}$ in time periods 2 and 5 in an ETS with transferable or non-transferable allowances in the simple model variant.

time periods.

Table 6.1: Relative frequency of compliance in an ETS with transferable or non-transferable allowances in the simple model variant.

Time period	0	1	2	3	4	5
Transferable	87.98%	79.27%	71.98%	65.94%	59.35%	50.46%
Non-transferable	59.95%	58.13%	57.36%	56.84%	54.85%	50.49%

The mean price trajectories, which we visualize in Figure 6.69a, are constant during each time period. If the transfer of allowances to subsequent time periods is not allowed, the mean prices are almost identical throughout the first five periods; if on the other hand such a transfer is possible, mean prices decrease from one time period to the next. At the same time, they are much higher than in the case when no transfer is allowed. This can be traced back to two effects: Since the price parameters s^i are higher and not convergent if a transfer of allowances is possible, the upper price bound is higher in this case. At the same time, also the lower price bound is higher, leading to higher prices in the mean. Consistently, the mean prices within one simulation run are higher if the transfer of allowances is possibly, as can be seen in the distributions of this quantity for time period 0, shown in Figure 6.69b. If no transfer is allowed, the prices are almost evenly spread between 10 and 50 Euro. If a transfer is possible, mean prices are almost always higher so that the distributions barely overlap. The distribution for transferable allowances shows a high peak around 60 Euro; in rare cases, values up to 80 Euro are reached. Again the distributions move closer to each other for later time periods (not shown here). Moreover, their structure changes: In line with the observations for the price trajectories, we obtain two peaks, each one close to either of the price bounds.

Finally, we consider the variation of the allowance price. The trajectory of the standard deviation given in Figure 6.70a follows a similar pattern as in the one-period model, but the standard deviation is much higher if the transfer of allowances is not possible; this can again be explained by the different price bounds. Accordingly, also the variation within one run measured by the variability of the price is higher for non-transferable allowances. This

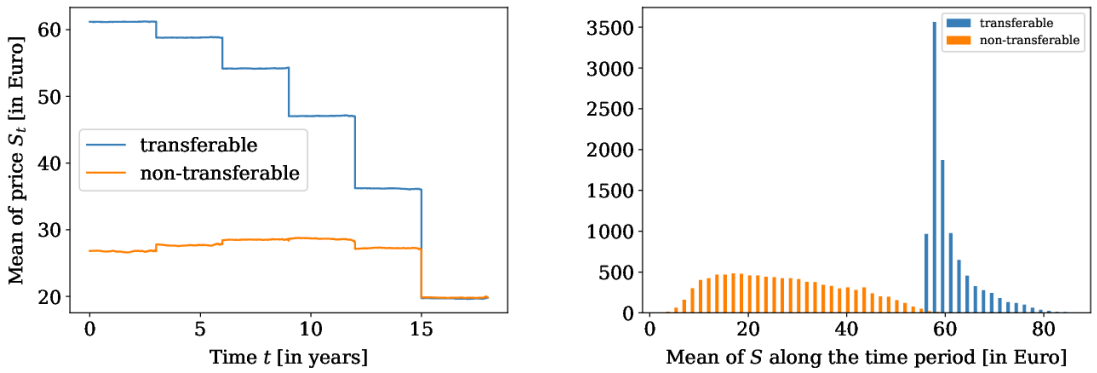

(a) Mean trajectory of S.

(b) Histogram of mean allowance prices within each run for time period 0.

Figure 6.69: Mean price trajectory and distribution of mean allowance prices within each run in an ETS with transferable or non-transferable allowances in the simple model variant.

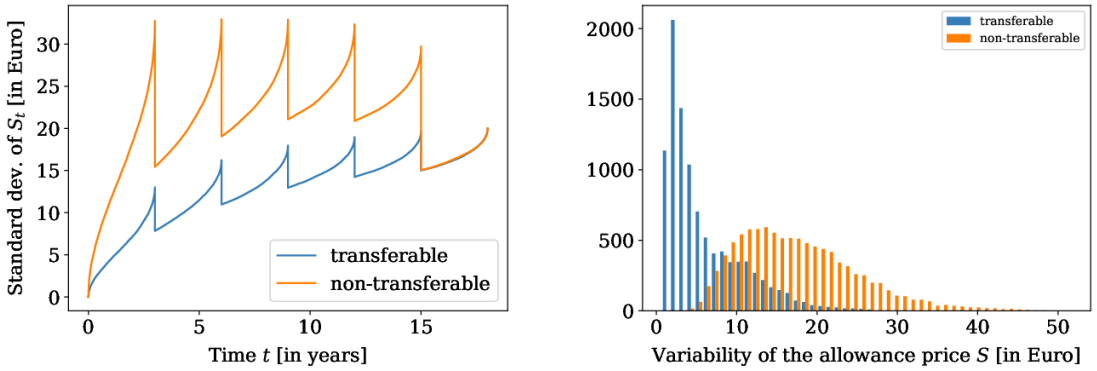

(a) Standard deviation trajectory of S.

(b) Histogram of the standard deviation of absolute daily returns of S in time period 0, normalized to one year.

Figure 6.70: Trajectory of the standard deviation of the allowance price and distribution of its variability in an ETS with transferable or non-transferable allowances.

can be seen in the histogram of the corresponding distribution for time period 0, shown in Figure 6.70b. In the case of non-transferable allowances, most runs show a variability between 10 and 25, whereas if allowances are transferable, the variability mostly is below 10 and barely reaches values of 20 or higher.

Summary

We conclude that the possibility to transfer allowances to the subsequent time period reduces the mean realized emissions and increases the frequency of compliance, while leading to higher prices with reduced variability. These effects become smaller in later time periods as a result of the simulation setup.

It should be noted that the model does not fully capture the consequences of allowing for a transfer of emission allowances: While the value of an unused allowance is taken into

account by the representative agent, the actual allowance is not transferred to the next time period, thus the emission cap e_0 the agent needs to comply with is the same as without the transfer. This is not relevant when considering the time period 0. Additionally, in time period 0, the time point when the allowances eventually do become invalid is still far away. Therefore, time period 0 serves to mimic the situation of transferable allowances that never become invalid.

6.2.3 Solution to the SDE in the Brownian Model Variant

To analyze the simulation results in the Brownian model variant, we first recall the price parameters s^i shown in Figure 6.61. As in the simple model variant, the price parameter diverges if allowances can be transferred; in contrast to the simple model variant it also appears to diverge if no transfer of allowances is possible. The price parameter values are lower than in the simple model variant, which may be due to the effect of the interest rate: Abatement costs and penalty payments in the future are discounted to time zero prices so that an allowance saved for future use loses in value, making the transfer of an allowance less profitable. At the same time, in the Brownian model variant we assume that expected BAU emissions decrease in time, which also leads to a lower price parameter.

The trajectories of the total expected emissions X and the allowance price S shown in Figure 6.71 for transferable allowances and in Figure 6.72 for non-transferable allowances all in all behave similarly as in the simple model variant: While in early time periods most runs are sufficiently close to e_0 that prices fluctuate, they mostly move away from e_0 in later time periods, leading to prices either at the upper or lower price bound. If allowances

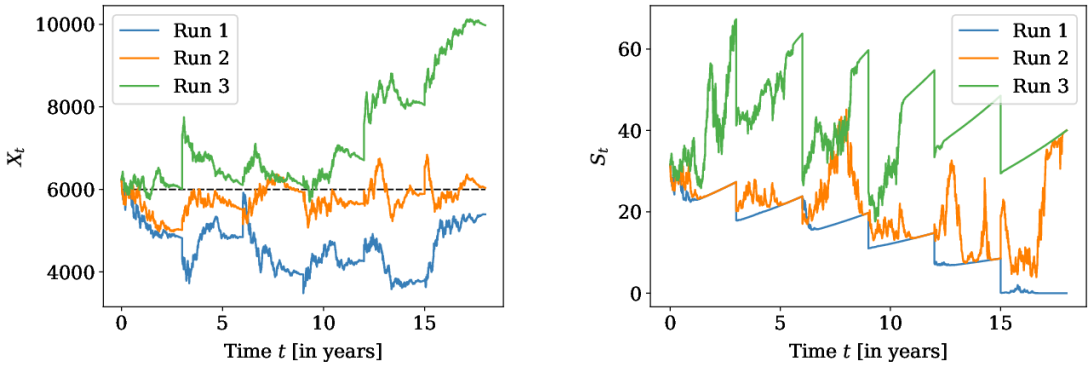

(a) Trajectories of X.

(b) Trajectories of S.

Figure 6.71: Three example trajectories of the total expected emissions X with corresponding trajectories of the price process S when allowances are transferable to subsequent time periods in the Brownian model variant.

cannot be transferred, the lower price bound is always zero, so that prices fluctuate more heavily in early time periods. In contrast to the simple model variant, the price bounds in each time period are increasing approximately linearly due to the positive interest rate.

For the mean trajectories of the total expected emissions X shown in Figure 6.73a, we observe that allowing for the transfer of allowances leads to a steeper slope and lower realized emissions. Moreover, the initially expected emissions for each time period decrease in time since we assume that BAU emissions are decreasing. Strikingly, this effect is stronger if allowances cannot be transferred, and as a result, the trajectories differ also for

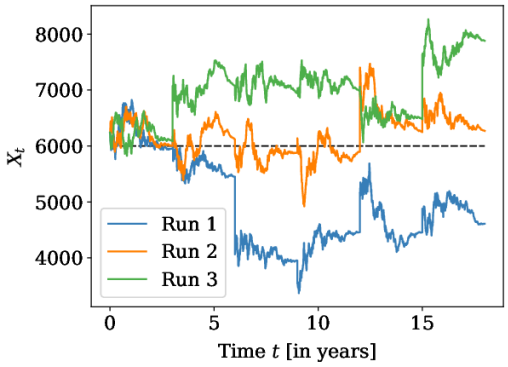

(a) Trajectories of X.

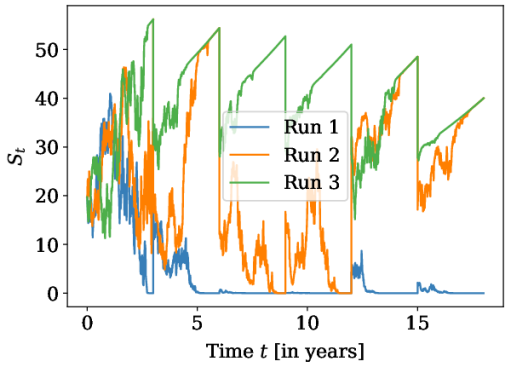

(b) Trajectories of S.

Figure 6.72: Three example trajectories of the total expected emissions X with corresponding trajectories of the price process S when allowances are not transferable to subsequent time periods in the Brownian model variant.

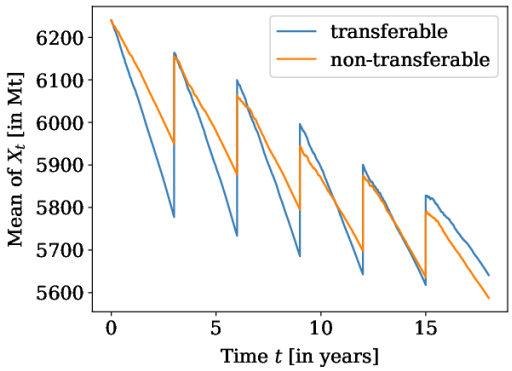

(a) Mean trajectory of X.

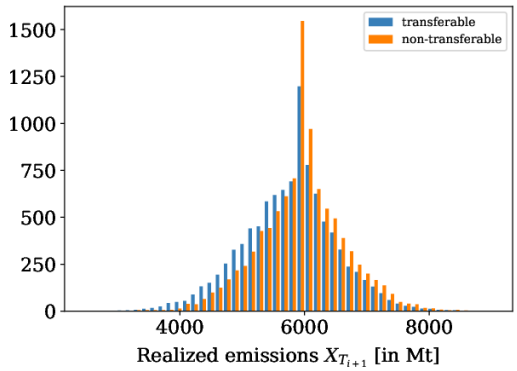

(b) Histogram of realized emissions $X_{T_{i+1}}$ in time period 0.

Figure 6.73: Mean trajectory of X and distribution of realized emissions $X_{T_{i+1}}$ in an ETS with transferable and non-transferable allowances in the Brownian model variant.

the last time period, where emissions are lower in this case. Possibly this is a numerical artifact: The initial value X_0^i depends on W_{T_i}; while the expectation of this random influence is zero, the mean computed from the simulation might not be exact. Especially in later time periods the variance of W_{T_i} is high, favoring such deviations. Moreover, since $W_{T_{i+1}}$ and thus X_0^{i+1} depend on W_{T_i}, these deviations translate to the subsequent time periods.

The distributions of the realized emissions X_T in the time period 0 shown in Figure 6.73b nevertheless are fairly similar. They both have a peak at $e_0 = 6000$, while the distribution for the case of transferable allowances is slightly more skewed to the left. Already for time period 2 this difference is small (Figure 6.74a), while for the last time period (Figure 6.74b) the distributions are essentially identical. At the same time, we observe that the distributions become very broad, even reaching negative values, which is probably due to the higher volatility in the Brownian variant. This is in particular important to note as the grid on which the PDE was solved does not cover this range.

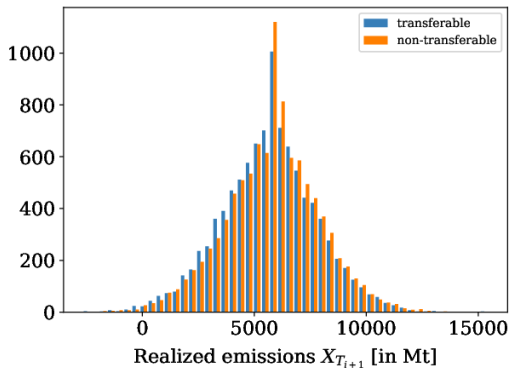

(a) Histogram of realized emissions $X_{T_{i+1}}$ in time period 2.

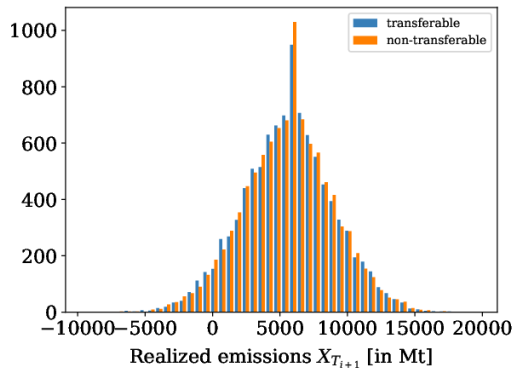

(b) Histogram of realized emissions $X_{T_{i+1}}$ in the last time period

Figure 6.74: Distribution of realized emissions $X_{T_{i+1}}$ in time periods 2 and 5 in an ETS with transferable or non-transferable allowances in the Brownian model variant.

Since the PDE is constant outside the grid, the extrapolation methods used in this case should deliver reasonable results.

The frequency of compliance is increased if the transfer of allowances is possible, as can be seen in Table 6.2. Notably, in comparison to the simple model variant this increase is by far not as large. Interestingly, if allowances cannot be transferred, the frequency of

Table 6.2: Relative frequency of compliance in an ETS with transferable or non-transferable allowances in the Brownian model variant.

Time period	0	1	2	3	4	5
Transferable	61.63%	56.48%	55.96%	55.65%	55.28%	54.1%
Non-transferable	52.93%	53.11%	53.41%	54.77%	54.7%	54.68%

compliance increases towards later time periods; this might be due to the decrease in BAU emissions, making it easier to comply with the emission cap.

The mean price trajectories shown in Figure 6.75a increase with the interest rate in each time period, where the mean prices in the case of transferable allowances are higher, but decrease overall. If allowances cannot be transferred, the price development within each time period does not change much for the first five time periods; prices appear to decrease very slightly, possibly due to the decrease in BAU emissions.

In Figure 6.75b the distribution of the mean prices within each simulation run are shown. As in the one-period model, we obtain distributions with two peaks, one close to the minimum and the other close to the maximum price. If allowances cannot be transferred, the first peak thus lies at approximately 5 Euro and the second around 45 Euro; both peaks are of similar intensity. If the transfer of allowances is possible, the first and much higher peak is positioned at approximately 25 Euro, while the second is found at 55 Euro. In this case the distributions do overlap, with the second peak of the case with non-transferable allowances lying between the two peaks of the case with transferable allowances.

When studying the variation of the allowance price, we find that the standard deviation is higher if allowances cannot be transferred, as shown in Figure 6.76a. Also the variability

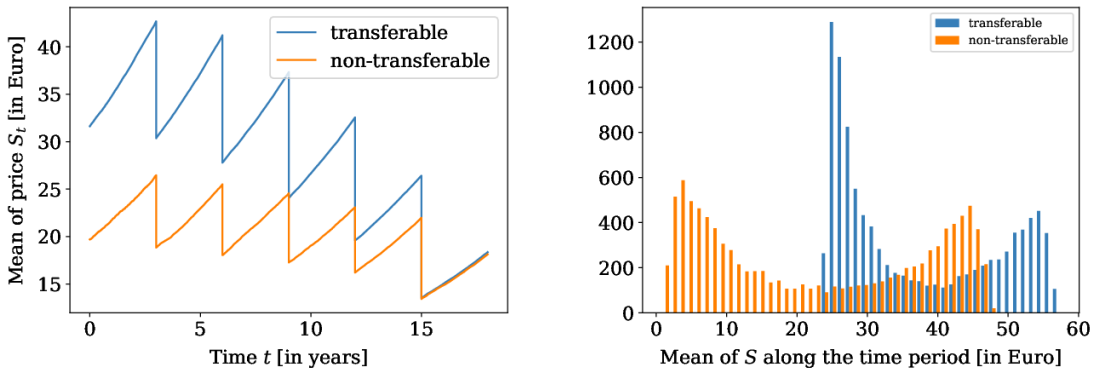

(a) Mean trajectory of S.

(b) Histogram of mean allowance prices within each run for time period 0.

Figure 6.75: Mean price trajectory and distribution of mean allowances prices within each run in an ETS with transferable or non-transferable allowances in the Brownian model variant.

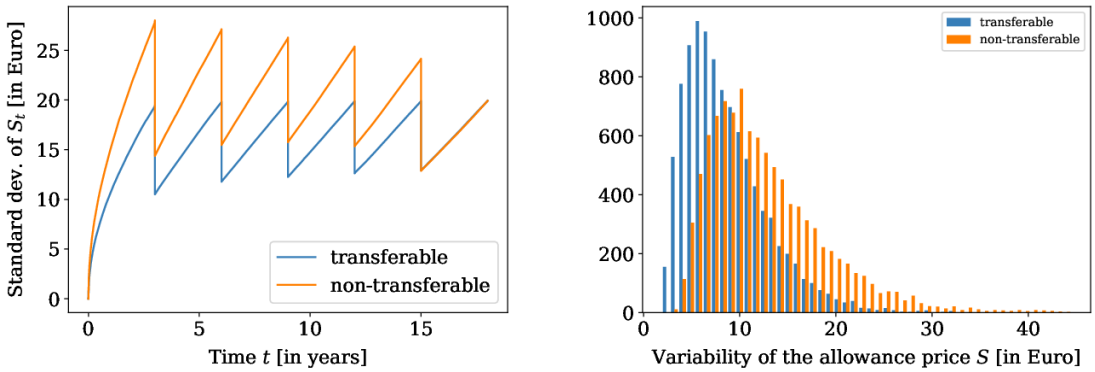

(a) Standard deviation trajectory of S.

(b) Histogram of the standard deviation of absolute daily returns of S in time period 0, normalized to one year

Figure 6.76: Trajectory of the standard deviation of the allowance price and distribution of its variability in an ETS with transferable or non-transferable allowances in the Brownian model variant.

of the allowance price within one run is higher for the case of non-transferable allowances, which can be seen from the distributions of the time period 0 shown in Figure 6.76b. If allowances cannot be transferred, the distribution has its peak at 10 and has a long tail, whereas if such a transfer is possible, the peak is found at 6 or 7. This effect is again probably due to the more tight price bounds present in the case of transferable allowances.

Summary

All in all the results in the Brownian model variant confirm the findings from the simple variant. It should be noted that most effects of allowing for the transfer of allowances are weaker in the Brownian model variant, which is probably caused by the lower values of the price parameter s^i.

Results in the Ornstein-Uhlenbeck model are again very similar. We omit a detailed discussion here; a graphical representation of the corresponding results can be found in Section C.1.2 in the appendix.

6.2.4 Variation of Regulatory Parameters

We vary further regulatory parameters apart from setting the transferability of allowances. In particular, we study the impact of changing the number of allowances e_0 or the cost coefficient c in each time period.

Varying the Penalty

First, we consider varying the penalty in the simple model variant; due to the argumentation above, we focus our analysis on time period 0 in a six-period setting. As can be seen in Figure 6.77, in line with previous results an increase of the penalty decreases the mean realized emissions and increases the relative frequency of compliance. Notably, in

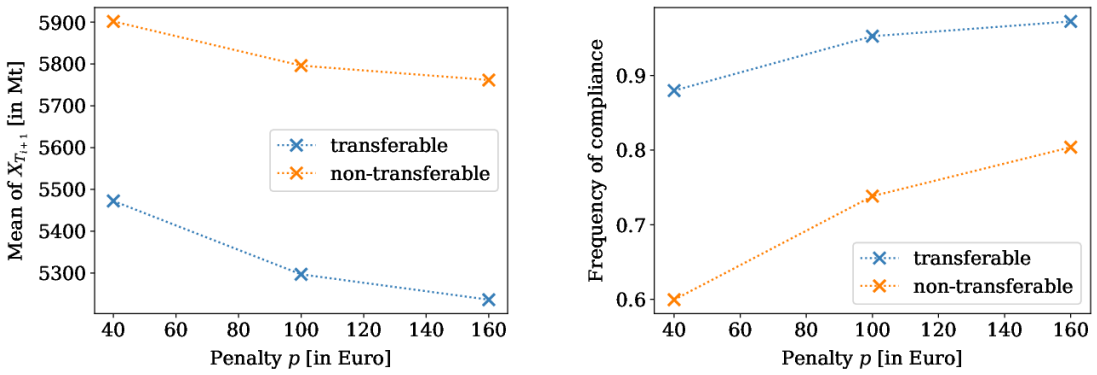

(a) Mean of realized emissions $X_{T_{i+1}}$.

(b) Relative frequency of compliance with the emission target e_0.

Figure 6.77: Results on the total expected emissions X for a varying penalty in the simple model variant in an ETS with transferable or non-transferable allowances.

both cases the effect of allowing for the transfer of allowances is larger than the effect of increasing the penalty. Moreover, if allowances cannot be transferred, the effect of increasing the penalty on the relative frequency of compliance is larger. On the other hand, if the transfer is possible, the compliance reaches almost 100% for penalties of 100 or 160 Euro. Similar observations can be made for the price characteristics shown in Figure 6.78: Increasing the penalty leads to higher prices and to a higher price variability, but the effect of allowing for the transfer of allowances has a much stronger effect. Notably, if allowances can be transferred, the penalty barely has an effect on the price variability.

We also study the effect of varying the penalty in the Brownian variant of the multi-period model. An increase of the penalty leads to lower mean realized emissions and to a higher frequency of compliance, as can be seen in Figure 6.79; especially in case of the frequency of compliance, the effect of increasing the penalty is stronger than the effect of allowing for the transfer of emission allowances. On the other hand, the combination of a high penalty of 160 and the transferability of allowances leads to a frequency of compliance of approximately 85%; this is higher than the limit we observed for very large penalties

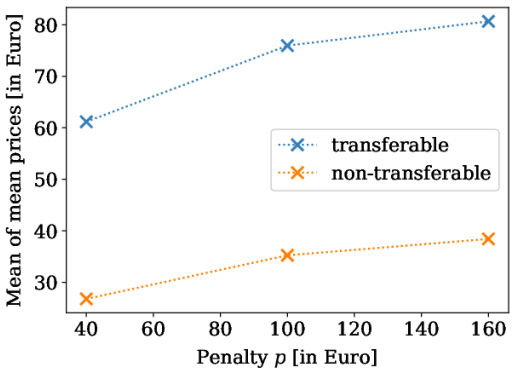

(a) Mean across all runs of the mean prices within one time period.

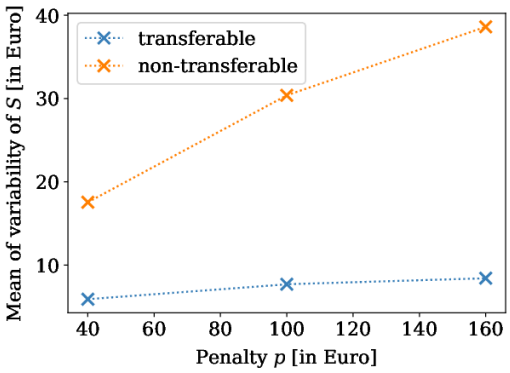

(b) Mean of the variability of the price S.

Figure 6.78: Results on the allowance price S for a varying penalty in the simple model variant in an ETS with transferable or non-transferable allowances.

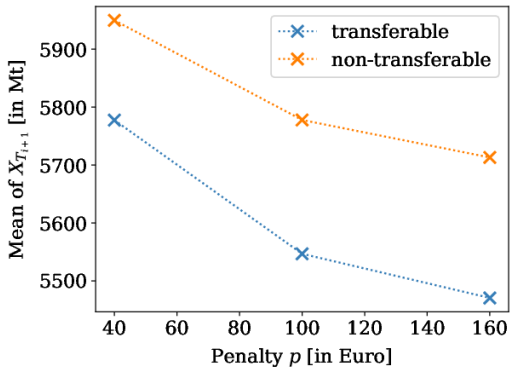

(a) Mean of realized emissions $X_{T_{i+1}}$.

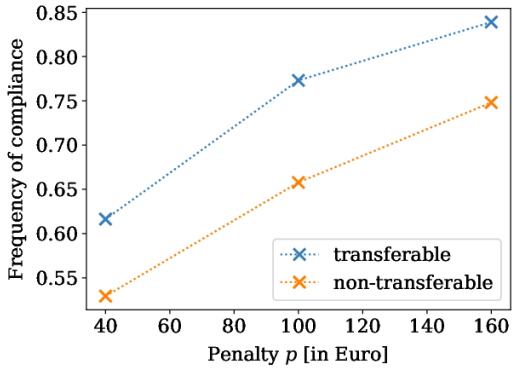

(b) Relative frequency of compliance with the emission target e_0.

Figure 6.79: Results on the total expected emissions X for a varying penalty in the Brownian model variant in an ETS with transferable or non-transferable allowances.

in the one-period model. Furthermore, increasing the penalty leads to higher mean prices and a higher mean variability of the prices, which is shown in Figure 6.80; this effect is also of relevant amplitude if allowances can be transferred.

Summary The increasing penalty decreases the realized emissions and increases the frequency of compliance as well as the allowance price, regardless whether allowances can be transferred or not. Notably, the frequency of compliance reaches almost 100% if the penalty is high and allowances can be transferred. In the simple model variant, the effect of allowing for the transfer outweighs the impact of the penalty. In the Brownian model variant on the other hand, allowing for the transfer of emission allowances has a weaker effect overall, so that the impact of changing the penalty is more relevant in comparison.

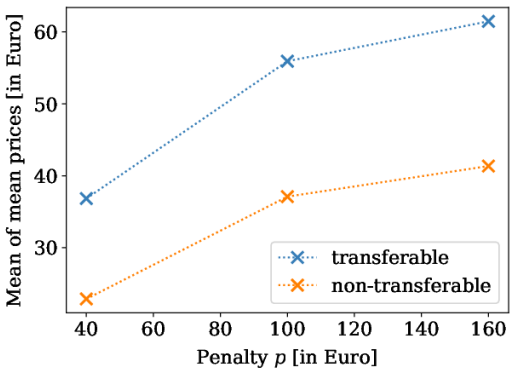

(a) Mean across all runs of the mean prices within one time period.

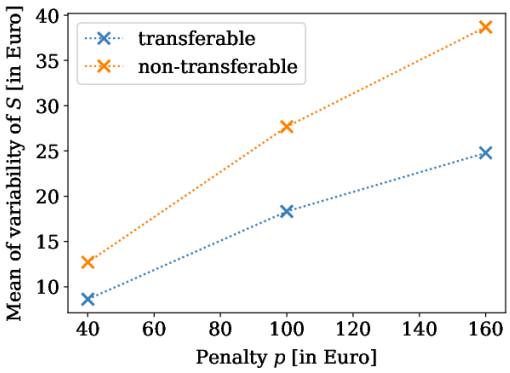

(b) Mean of the variability of the price S.

Figure 6.80: Results on the allowance price S for a varying penalty in the Brownian model variant in an ETS with transferable or non-transferable allowances.

Decreasing the Emission Cap

So far we have assumed that the emission cap e_0 remains constant throughout all time periods. This is neither reasonable in a situation where emissions eventually need to be reduced to net zero, nor does it reflect the situation in the EU ETS. Motivated by the current regulation and the decision adopted by the European Parliament in June 2022 on the recent revision proposal of the Commission, we assume that the emission cap decreases either by 2.2% or by 4.6% each year, while still setting the cap for the first time period to $e_0 = 6000$. To obtain an idea how this influences the system, we analyze the price parameters s^i computed in this setting (with a decrease of 2.2%), which are shown in Figure 6.81; as simulations can be conducted much faster in the simple model variant, we only work with this variant in the current setting. In the case that allowances can be

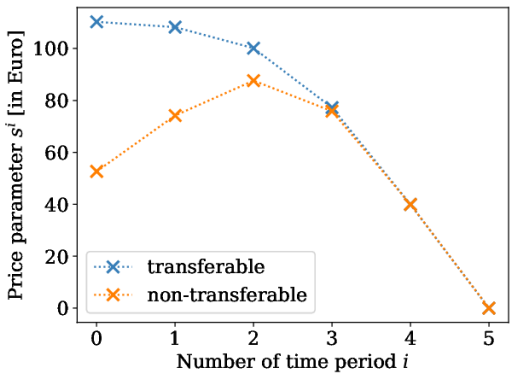

Figure 6.81: Price input parameters s^i computed from the price function of the subsequent time period in an ETS with transferable or non-transferable allowances where the emission cap decreases by 2.2% every year.

transferred, the price parameter is decreasing towards later time periods, attaining higher values than for constant e_0 to account for the tightening cap. If allowances cannot be transferred, two counteracting factors influence the price parameter: The tightening cap

means that in later time periods more abatement is required, which leads to an increase of the price. On the other hand, the costs of non-compliance are the lowest in the last time period, which causes the price parameter to decrease towards the end.

With having these observations in mind, we compare the simulation results for a constant emission cap and for a decreasing cap with a linear reduction factor (LRF) of 2.2% or 4.6%. The corresponding mean realized emissions are shown in Figure 6.82a. If allowances

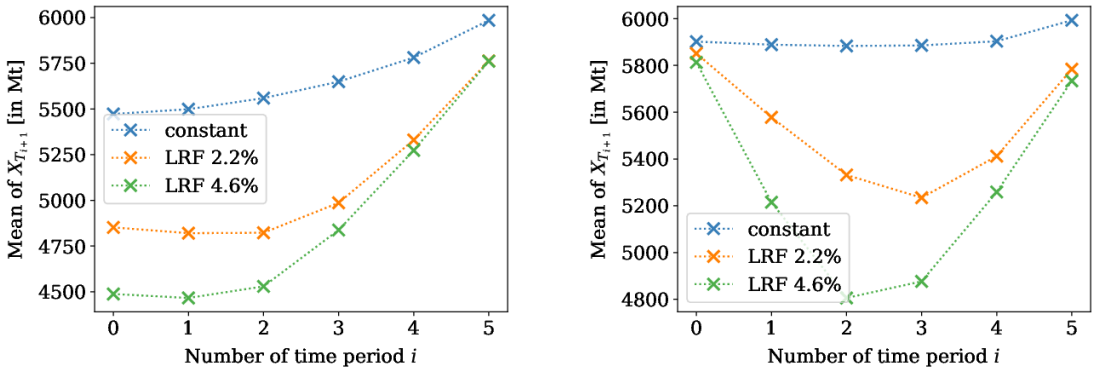

(a) Allowances can be transferred.

(b) Allowances cannot be transferred.

Figure 6.82: Mean of realized emissions $X_{T_{i+1}}$ throughout six time periods in the simple model variant in an ETS with transferable or non-transferable allowances. The emission cap decreases yearly by a linear reduction factor (LRF) as indicated.

can be transferred, mean realized emissions are decreased considerably during the early time periods by decreasing the emission cap; thus the additional abatement occurs in this phase. Towards the end the mean realized emissions are still slightly lower than for a constant cap, but the difference becomes smaller. If it is not possible to transfer allowances, the picture is quite a different one: In line with the behavior of the price parameter, the mean realized emissions are the lowest for time period 2 and 3; in the beginning, they are higher, because the emission cap is not as stringent. Towards the end, mean realized emissions are also higher due to the low costs of cap violations.

In Figure 6.83 we show the frequency of compliance with the emission cap for each time period. In case of a constant cap, this quantity gradually decreases from one time period to the next, arriving at a value of about 50% in the last time period. If allowances can be transferred, the relative frequency of compliance is considerably higher initially, as already observed above. For a decreasing cap we obtain a very high variation: While the frequency of compliance is almost one in the first two time periods as long as allowances are transferable, it drops down to almost zero towards the end, especially if the linear reduction factor is 4.6%. This behavior partly is a result of the model setup, as the allowances saved in early time periods due to additional abatement are not in fact available in later time periods. If allowances cannot be transferred, the general behavior is the same; only the relative frequency of compliance in the first time period is already much lower. Here both effects mentioned above act together: The increasing stringency of the cap makes it more difficult to comply while the cost of non-compliance decreases.

The mean prices shown in Figure 6.84 reflect the results on the realized emissions: If allowances can be transferred, abatement is high in early time periods and even more so for a decreasing cap, thus also the mean allowance price is high. As abatement decreases

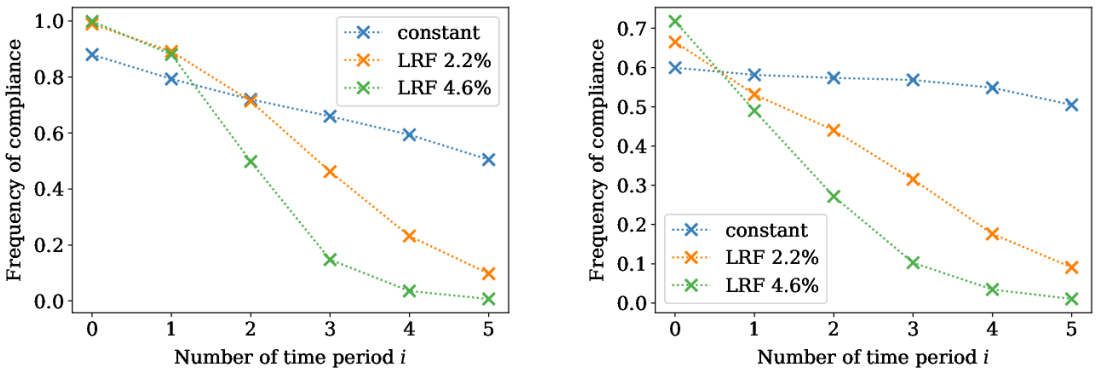

(a) Allowances can be transferred. **(b)** Allowances cannot be transferred.

Figure 6.83: Relative frequency of compliance with the emission target e_0 throughout six time periods in the simple model variant in an ETS with transferable or non-transferable allowances. The emission cap decreases yearly by a linear reduction factor (LRF) as indicated.

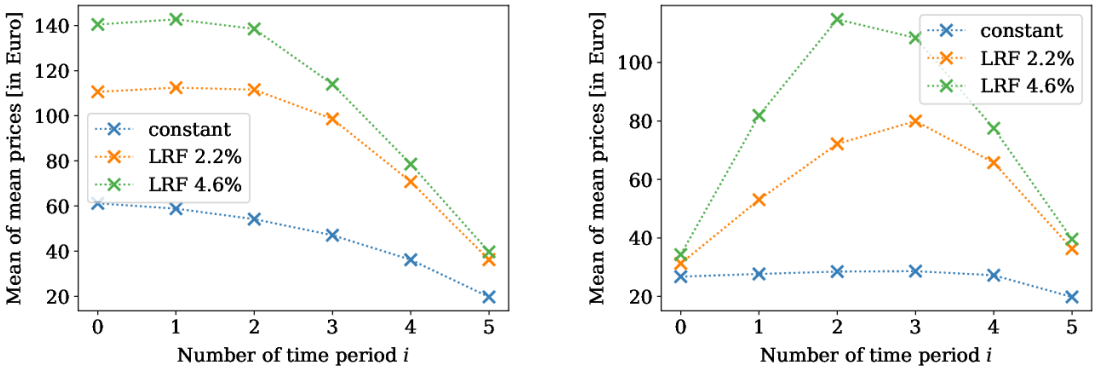

(a) Allowances can be transferred. **(b)** Allowances cannot be transferred.

Figure 6.84: Mean of mean allowance prices throughout six time periods in the simple model variant in an ETS with transferable or non-transferable allowances. The emission cap decreases yearly by a linear reduction factor (LRF) as indicated.

for later time periods so does the price. In the case that allowances cannot be transferred, abatement is highest in time periods 2 and 3, when the cap has already tightened, but non-compliance is still expensive enough to encourage abatement. As a result also the price is highest in these time periods.

Finally, we study the mean variability of the allowance price shown in Figure 6.85. If allowances can be transferred to the next time period, the price variability is lower for a decreasing emission cap in most time periods, reaching almost zero for both the first and the last. This is plausible since in time period 0 full compliance is reached and thus the allowance price is mostly at its minimum value given by the price parameter s^i. For the last time period, almost none of the simulation runs are compliant with the cap and therefore the price is at its maximum given by the penalty $p = 40$. As a result, in both cases the price variability is very low. If a transfer of allowances is not possible, the price variability is in general much higher, especially in the beginning; also in this case it increases at least from time period 0 to 1 if the cap is decreasing. This can be explained

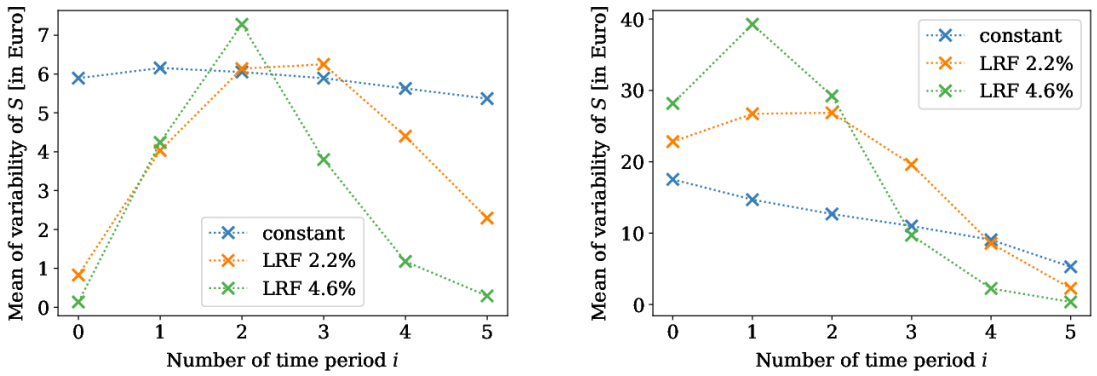

(a) Allowances can be transferred.

(b) Allowances cannot be transferred.

Figure 6.85: Mean of the variability of the allowance price S throughout six time periods in the simple model variant in an ETS with transferable or non-transferable allowances. The emission cap decreases yearly by a linear reduction factor (LRF) as indicated.

by recalling the development of the price parameter and the mean price: Both increase in early time periods, indicating that the range for the allowance price increases. Therefore in increase in the variability is plausible.

While the results for individual time periods provide some valuable insight how the decreasing cap affects the system, they cannot directly reflect the situation in the real-world application, since the model does not capture the actual transfer of allowances. Furthermore, we cannot restrict our considerations to time period 0, as we did in analyses above, since the element of interest, namely the decrease in the cap, takes its effect in later time periods only. Thus in the following, we will consider aggregated quantities of all time periods; we will use these aggregates to analyze the effect of an increase in the penalty.

In Figure 6.86 the sum of the mean realized emissions of all time periods is shown. We observe that a decrease in the emission cap decreases the overall mean realized emissions and it does this much more effectively for higher penalties. Also allowing for the transfer of allowances enhances the effectiveness of the more stringent cap and especially of the increase in the penalty.

By summing up the emission caps of each time period and thus the number of allowances handed out, we obtain the overall cap for the six periods of 18 years in total. In case of a constant cap this simply amounts to 36 000 Mt. If the linear reduction factor is 2.2%, we have an overall cap of 30 666 Mt and if it is 4.6%, we obtain an overall cap of 26 030 Mt. By comparing the overall realized emissions of each run with these thresholds, we compute the aggregate frequency of compliance shown in Figure 6.87. For a low penalty, compliance is low. In case of the more stringent cap, the higher penalties succeed to increase the compliance to similar levels as for the constant (and thus overall less stringent) cap, as long as allowances can be transferred. If the transfer is not possible, the relative frequency of compliance is very low for the decreasing and more stringent emission caps.

To aggregate the mean prices of all time periods, we compute their mean and obtain the overall mean prices, which are shown in Figure 6.88. Their behavior is closely linked to the mean realized emissions: For a more stringent cap and a higher penalty, the prices increase, regardless whether allowances can be transferred or not; but if the transfer is

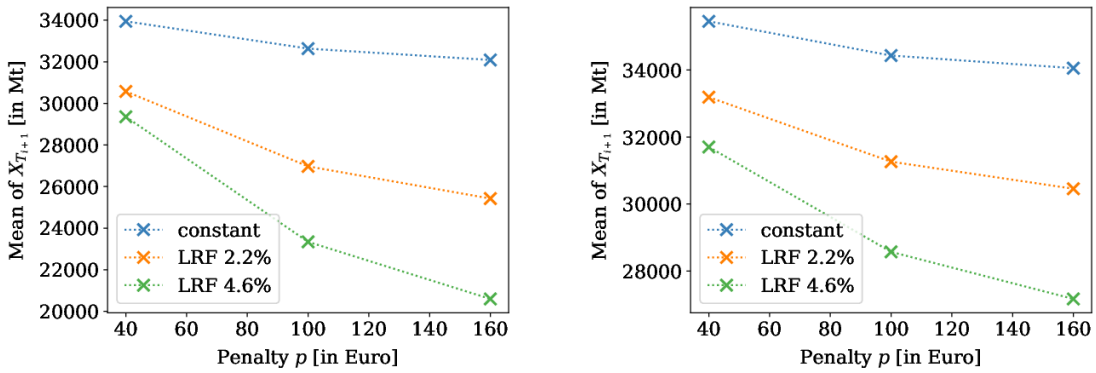

(a) Allowances can be transferred. **(b)** Allowances cannot be transferred.

Figure 6.86: Sum of the mean realized emissions $X_{T_{i+1}}$ for a varying penalty in the simple model variant in an ETS with transferable or non-transferable allowances. The emission cap decreases yearly by a linear reduction factor (LRF) as indicated.

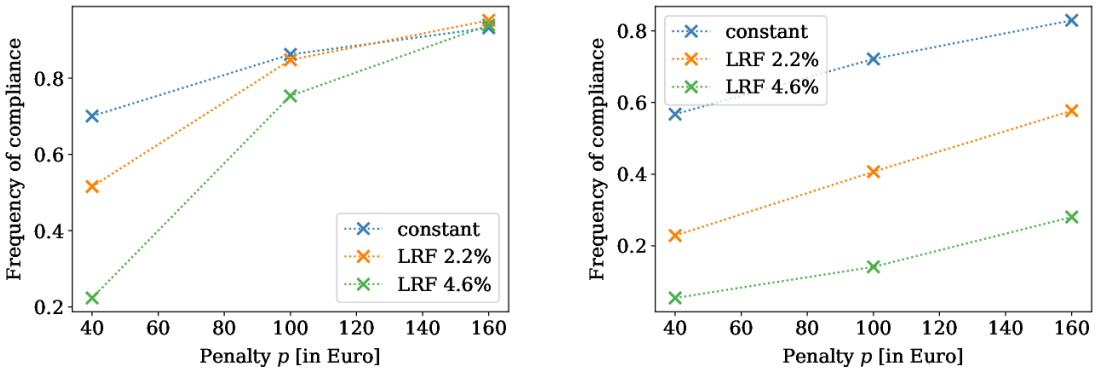

(a) Allowances can be transferred. **(b)** Allowances cannot be transferred.

Figure 6.87: Relative frequency of compliance with the overall cap for a varying penalty in the simple model variant in an ETS with transferable or non-transferable allowances. The emission cap decreases yearly by a linear reduction factor (LRF) as indicated.

possible, prices are in general much higher.

We aggregate the mean price variabilities also by computing their mean; the results are shown in Figure 6.85. Increasing the penalty increases the variability; but while the price variability is smaller for a decreasing cap if allowances can be transferred, they are higher if this is not the case: The decreasing cap leads to a higher value for the price parameter and thus to a broader range for the allowance price if allowances cannot be transferred. If the transfer is possible, the range is only shifted; on the other hand, a more stringent cap moves price paths closer to their maximum value, which leads to less price variability.

Summary If the emission cap decreases in time, the effects strongly depend on whether allowances are transferable or not. If the transfer of allowances is possible, the decreasing cap has a particularly large influence on the early time periods, leading to much lower emissions and a higher allowance price. If allowances cannot be transferred, the impact is highest for the intermediate time periods, when the cap is more stringent but non-

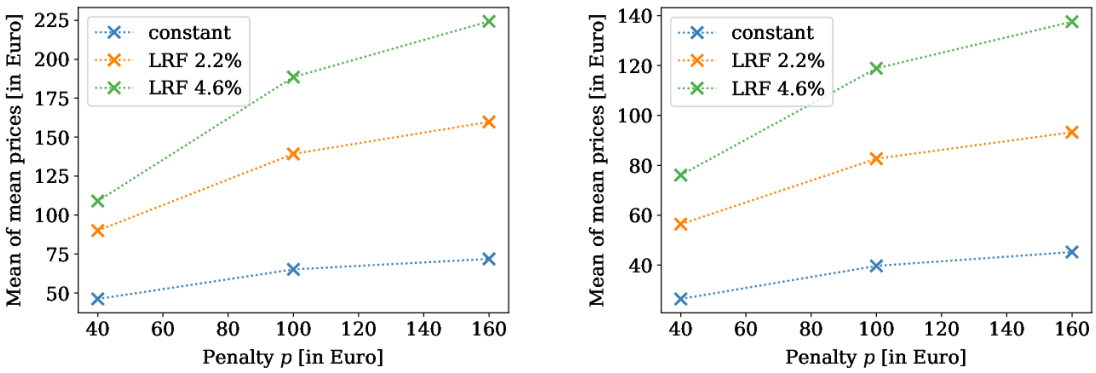

(a) Allowances can be transferred. **(b)** Allowances cannot be transferred.

Figure 6.88: Mean of mean prices for a varying penalty in the simple model variant in an ETS with transferable or non-transferable allowances. The emission cap decreases yearly by a linear reduction factor (LRF) as indicated.

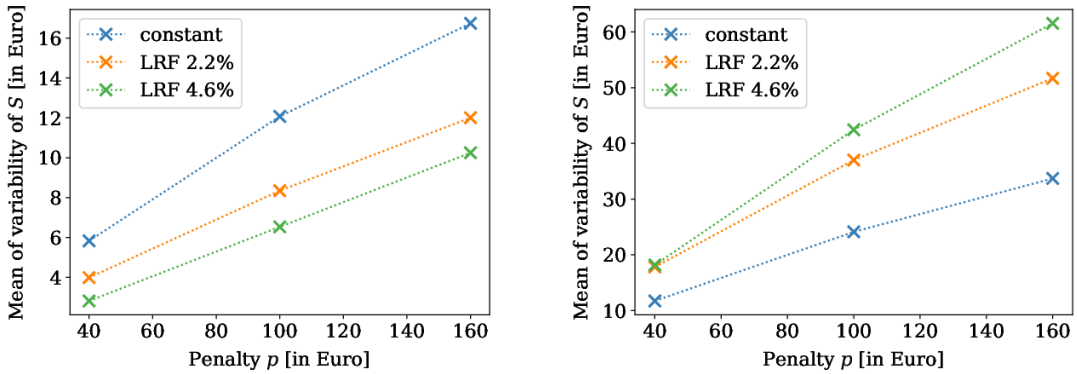

(a) Allowances can be transferred. **(b)** Allowances cannot be transferred.

Figure 6.89: Mean of the variability of the allowance price S for a varying penalty in the simple model variant in an ETS with transferable or non-transferable allowances. The emission cap decreases yearly by a linear reduction factor (LRF) as indicated.

compliance is still expensive.

On aggregate across all time periods, the decreasing and in particular more stringent cap leads to lower emissions and higher prices. The frequency of compliance strongly depends both on the transferability of allowances and the penalty: If the penalty is high and allowances can be transferred, the aggregate compliance is high also for a decreasing emission cap. Otherwise it is very low and in particular much lower than for the constant cap.

Decreasing the Cost Coefficient

As time proceeds, technological progress may cause abatement to become cheaper. Thus we let the cost coefficient c decrease in the course of the six time periods considered. In a model by Beck and Kruse-Andersen [BK20], the technological progress is modeled for a regenerative competitor, whose technology catches up with a fossil-fuel based electricity

generator. They obtain a technological progress of 0.6%. Although their setup does not quite match the situation of our model, we still use this quantity to give us an idea which change in c might be plausible. To simplify calculations and to aggravate the effect of technological progress (TP), we assume that c is reduced by 1% each year. In Figure 6.90 the effect of this on the price parameter s^i is shown for a penalty of 40 Euro both for a setting with transferable and non-transferable allowances. The differences to the case of a constant cost coefficient as shown in Figure 6.64 are almost negligible; the price parameter is only very slightly smaller.

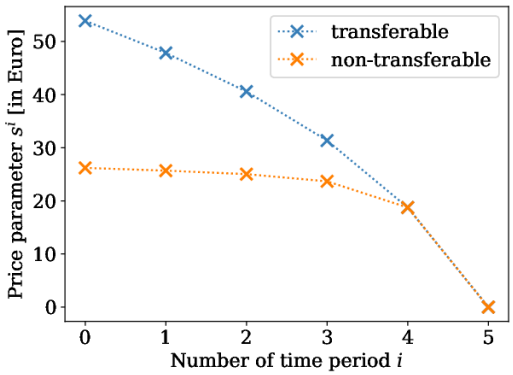

Figure 6.90: Price input parameters s^i computed from the price function of the subsequent time period in an ETS with transferable or non-transferable allowances where the cost coefficient decreases by 1% every year.

Again we study aggregated quantities over all six time periods for varying penalties. In Figure 6.91 we observe that the technological progress barely has an effect on the mean realized emissions; only if allowances cannot be transferred and the stringency of the cap is increasing over time, technological process slightly decreases the mean realized emissions.

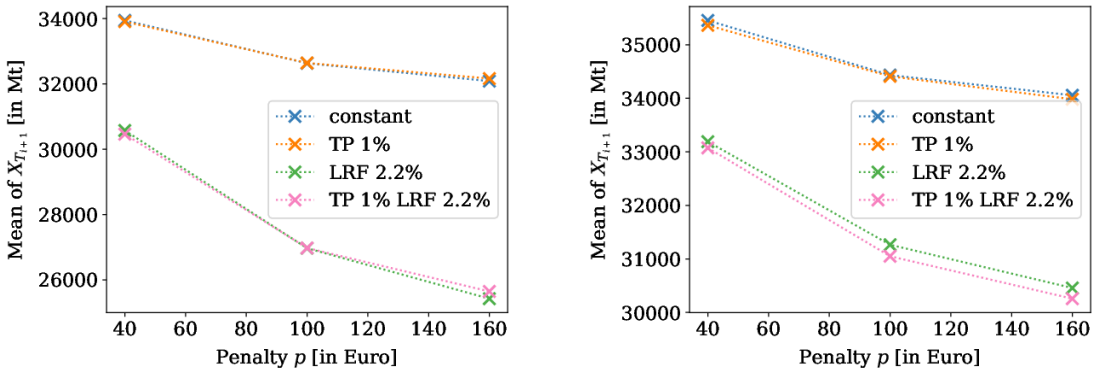

(a) Allowances can be transferred.

(b) Allowances cannot be transferred.

Figure 6.91: Mean of realized emissions $X_{T_{i+1}}$ for a varying penalty in the simple model variant in sum over all time periods. The abatement cost coefficient c decreases yearly due to technological progress (TP) and the emission cap e_0 decreases by a linear reduction factor (LRF) as indicated.

As can be seen in Figure 6.92, the effect on the relative frequency of compliance is slightly more pronounced. Especially if allowances cannot be transferred, the decreas-

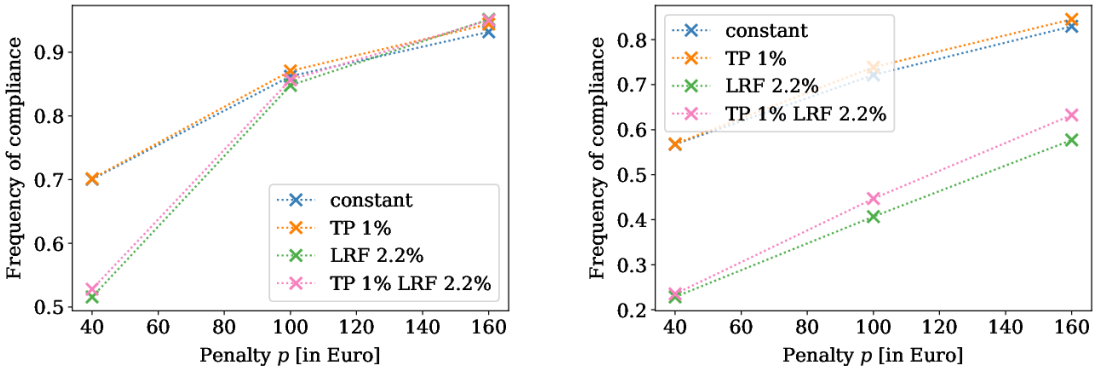

(a) Allowances can be transferred. **(b)** Allowances cannot be transferred.

Figure 6.92: Relative frequency of compliance with the emission target e_0 for a varying penalty in the simple model variant in aggregate over all time periods. The abatement cost coefficient c decreases yearly due to technological progress (TP) and the emission cap e_0 decreases yearly by a linear reduction factor (LRF) as indicated.

ing costs of abatement visibly increase the frequency of compliance; this effect becomes stronger for larger penalties and if the cap is decreasing over time.

The effect on the mean price shown in Figure 6.93 is the most evident which is not surprising, since the price depends directly on the cost coefficient c. Thus the decreasing

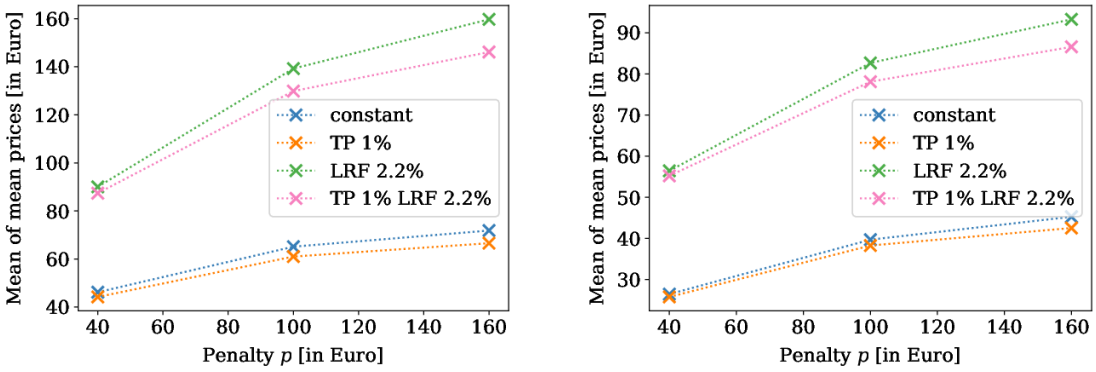

(a) Allowances can be transferred. **(b)** Allowances cannot be transferred.

Figure 6.93: Mean of mean allowance prices for a varying penalty in the simple model variant. The abatement cost coefficient c decreases yearly due to technological progress (TP) and the emission cap e_0 decreases by a linear reduction factor (LRF) as indicated.

cost coefficient leads to lower prices in all cases.

When considering the price variability, the effect of a decreasing cost coefficient differs between the case of transferable allowances and the case where this is not possible, as can be seen in Figure 6.94: If allowances can be transferred, the price variability increases slightly with technological progress, whereas it decreases if a transfer is not possible. In this case, the slightly lower price parameter decreases the range of the allowance price,

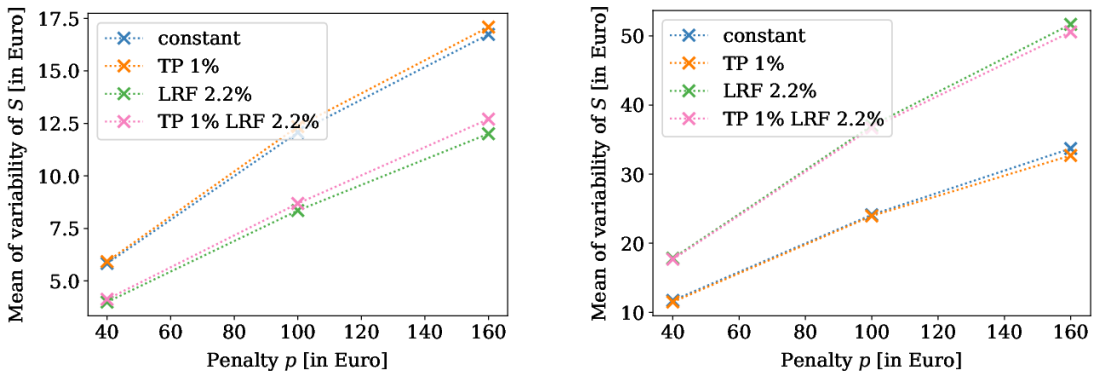

(a) Allowances can be transferred.

(b) Allowances cannot be transferred.

Figure 6.94: Mean of the variability of the allowance price S for a varying penalty in the simple model variant. The abatement cost coefficient c decreases yearly due to technological progress (TP) and the emission cap e_0 decreases by a linear reduction factor (LRF) as indicated.

thus allowing for less variability. In the case that allowances can be transferred, this range is only shifted; the increase of the price variability might be a result of price paths moved away from the maximum price bound by cheaper abatement.

Summary The decreasing cost coefficient only has little effect on the quantities studied here; the highest impact can be observed for the mean allowance price, which directly depends on the cost coefficient. Possibly a higher percentage of technological progress might lead to more distinctive effects.

6.3 Multi-Period Model II

We proceed similarly as in the previous section, applying multi-period model II as introduced in Section 3.2 instead of multi-period model I. Again we simulate a system with six time periods. First we discuss the solution to the PDE in this model, which is more complex and more computationally challenging than in multi-period model I. Then we proceed in the same way as before to discuss the results on the total expected emissions X and on the price process S obtained from solving the SDE. We conclude this section by analyzing the effects of varying the penalty.

6.3.1 Solution to the PDE

We first consider the simple model variant and fix a penalty of 40 Euro to resemble the case studied in multi-period model I. We solve the PDE numerically and restrict our analysis on the first derivative V_x as this is is the function required to determine the allowance price and to describe the total expected emissions process X. Due to the high dimensionality of the solution, a visualization of the results is challenging; we thus need to fix one of the three variables t, x and z. In figures 6.95a and 6.95b we show the resulting plot of V_x in the case of transferable allowances for a small and a high value of z, respectively. If z is small, we obtain a picture that is very similar to the one-period model case, with values ranging between zero and the penalty 40. If on the other hand z is very large, the

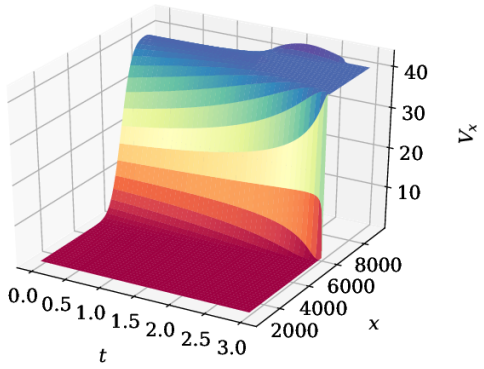

(a) V_x as a function of t and x for $z = 2880$.

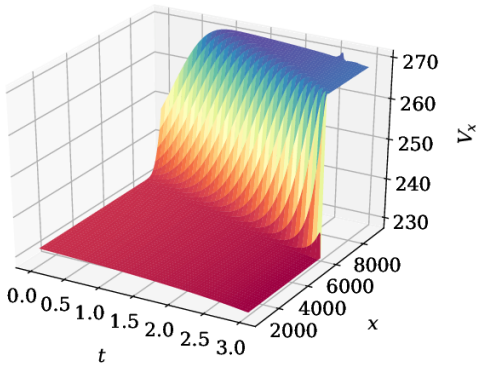

(b) V_x as a function of t and x for $z = 9040$.

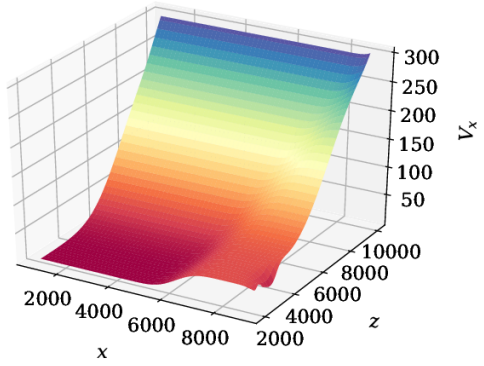

(c) V_x as a function of x and z for $t = 0.33$.

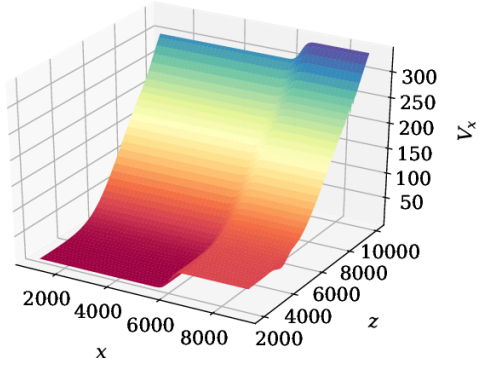

(d) V_x as a function of x and z for $t = 2.64$.

Figure 6.95: Derivative V_x of the PDE solution for the time period 0 in multi-period model II with transferable allowances in the simple model variant.

solution lies in a range between 230 and 270; moreover, at earlier time points, V_x takes on the minimum value 230 for all but the largest values of x. This behavior is confirmed by the plots of V_x in dependence of x and z, where the time point t is fixed, given in figures 6.95c and 6.95d. For small values of both x and z, we obtain a value of zero for V_x. When z reaches a value of about $e_0 = 6000$, the derivative V_x increases approximately linearly with z, since the anticipated allowance price for the next time period computed from z is increasing for sufficiently large z. In the direction of x, we still observe the step-like structure known from the one-period model with an increasingly steep slope as we proceed in time.

If allowances cannot be transferred, the resulting PDE solution shown in Figure 6.96 differs substantially: If x is below e_0, we always obtain a value of approximately zero. For x above e_0, the derivative V_x is approximately constant at a value of 40 as long as z is below e_0, meaning that the anticipated price for the next time period is zero. If z is above e_0, the derivative V_x is again increasing in z; thus for high values of z and varying x, it ranges from zero to values well above 200.

It should be noted that the solutions shown in Figures 6.95 and 6.96 both contain anomalies as was already mentioned in Section 5.1.4; possibly these are caused by the lack of boundary conditions and the use of asymmetric difference quotients as a result. In simulations in the Brownian model, these numerical issues appear to be even more grave:

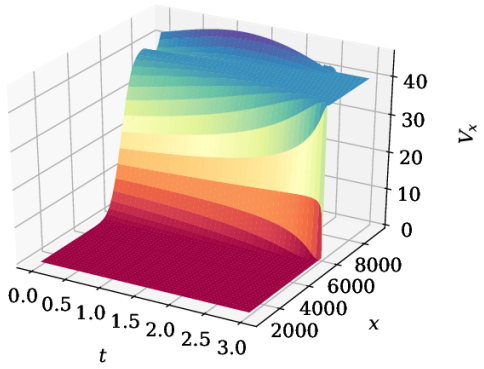

(a) V_x as a function of t and x for $z = 2880$.

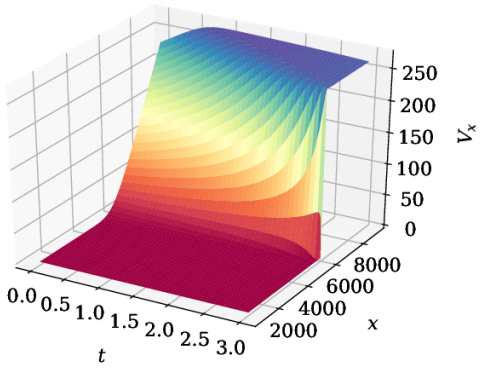

(b) V_x as a function of t and x for $z = 9040$.

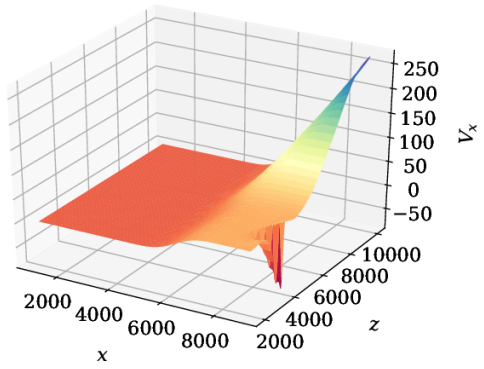

(c) V_x as a function of x and z for $t = 0.33$.

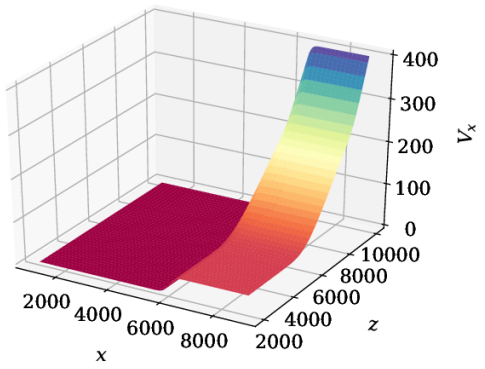

(d) V_x as a function of x and z for $t = 2.64$.

Figure 6.96: Derivative V_x of the PDE solution for the time period 0 in multi-period model II with non-transferable allowances in the simple model variant.

As mentioned in Section 5.1.4, the simulation fails for a step size of 20 or 50. Thus in the Brownian model we apply a step size of 100. Results for V_x in the case of transferable allowances are shown in Figure 6.97. The overall picture for fixed values of z is similar to the one-period model and the previous multi-period model; for large values of z, the lower boundary is well above zero. Strikingly, the formerly constant regions for small or high x are now decreasing in time if z is small and increasing if z is large. Again V_x is almost zero if both x and z are small; as z comes close to e_0, the derivative V_x starts to increase with z. In contrast to the simple model variant, we may observe that for very high values of z the derivative V_x is again almost constant in z. This difference may be due to the larger z-grid applied in the Brownian model variant; for later time periods, the PDE solution in the simple model variant is also constant for large z, so probably the constant region in the time period 0 is cut off by the shorter grid. Moreover, we have that the maximum value of V_x at approximately 90 is much lower than in case of the simple model variant.

If we no longer allow for the transfer of allowances, as shown in Figure 6.98, the picture changes as expected: For x sufficiently below $e_0 = 6000$, the derivative V_x always takes values close to zero; for high values of x it still increases in time. Moreover, if x is well above e_0, the dependence on z is identical to the case of transferable allowances.

Overall, these results can be explained as follows: If allowances can be transferred and we expect that we are in oversupply for the current time period, then the current

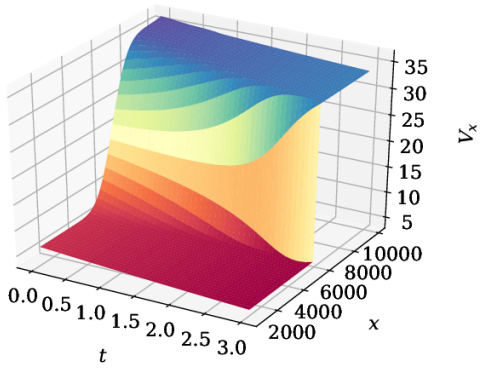

(a) V_x as a function of t and x for $z = 2900$.

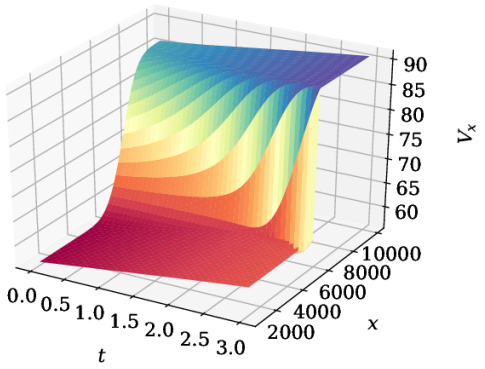

(b) V_x as a function of t and x for $z = 9200$.

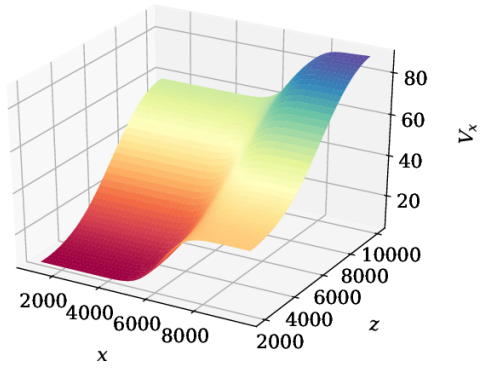

(c) V_x as a function of x and z for $t = 0.33$.

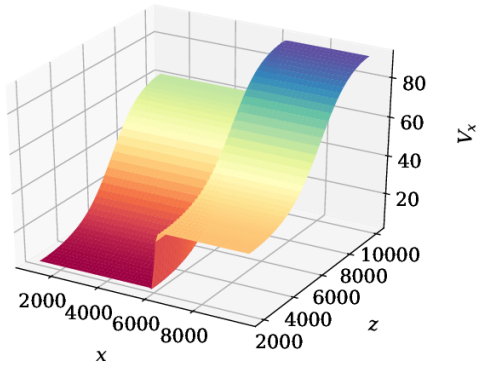

(d) V_x as a function of x and z for $t = 2.64$.

Figure 6.97: Derivative V_x of the PDE solution for time period 0 in multi-period model II with transferable allowances in the Brownian model variant.

allowance price and the abatement rate – and therefore also V_x – mainly depend on the price anticipated for an allowance at the beginning of the next time period since this represents the benefit we get from a surplus allowance. If the total expected emissions of the next time period, which are modeled by z, are small, allowances in the next time period have little or no value, leading to a small value of V_x. On the contrary, if they are high, the anticipated price is also high and thus we obtain a high value of V_x. If in the current time period we do not have sufficiently many allowances corresponding to a value of x well above e_0, we need to account for the additional allowances required from the next time period in addition to the penalty. Thus V_x in principle behaves in a similar way, but is increased by the penalty value. If allowances cannot be transferred, the same arguments apply as long as x is above e_0; for small x we obtain small values of V_x, since in this case we do not receive any benefits from surplus allowances.

Summary

In this section, we discussed the PDE solution in multi-period model II, which is more complex than in previous models due to the additional variable z. For a fixed value of z, the overall structure is still similar to the solutions obtained in the one-period model and in multi-period model I. If allowances can be transferred, the constant values of V_x for

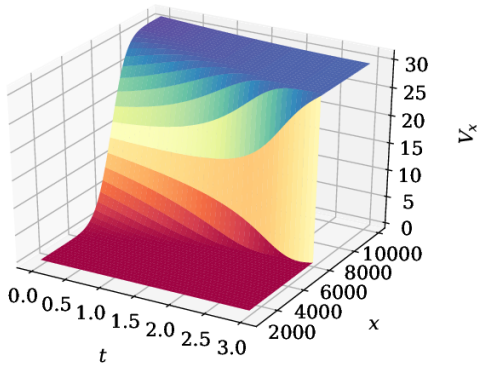

(a) V_x as a function of t and x for $z = 2900$.

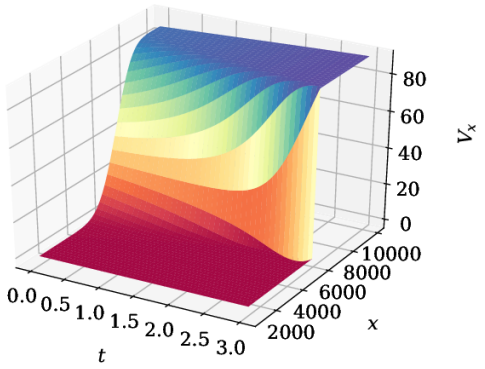

(b) V_x as a function of t and x for $z = 9200$.

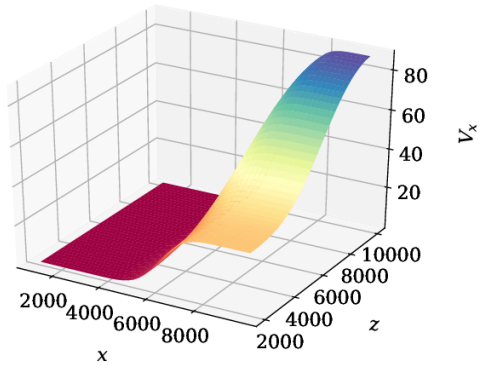

(c) V_x as a function of x and z for $t = 0.33$.

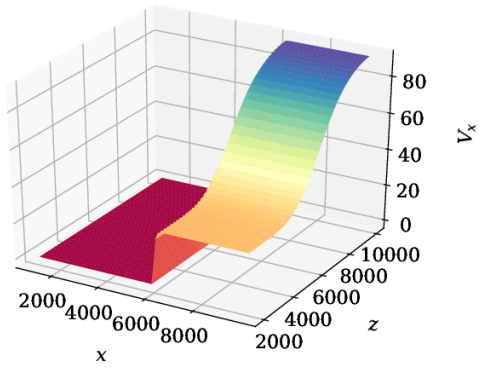

(d) V_x as a function of x and z for $t = 2.64$.

Figure 6.98: Derivative V_x of the PDE solution for time period 0 in multi-period model II with non-transferable allowances in the Brownian model variant.

small or large x are shifted upwards in comparison to the one-period model, depending on the value of z. If the transfer is not possible, this shift only applies for large x.

6.3.2 Solution to the SDE in the Simple Model Variant

We proceed similarly as in previous models to gain an understanding of the results on the processes X, Z and S obtained from the SDE solution. First, we analyze the trajectories of these processes for three example simulation runs shown in Figure 6.99; additionally we show the points on the x-z-plane covered by the trajectories to illustrate the correlation between X and Z.

The X-trajectory of the first run moves to small values rather quickly; while it jumps upwards at the start of most time periods, it remains below the threshold e_0 throughout the six time periods. Accordingly, the allowance price is comparably low, approaching zero in the second to last time period. The trajectory of Z strongly resembles that of X; only the jumps at the start of each time period are smoothened out. Accordingly, in the scatter plot in Figure 6.99d most points lie on the bisecting line.

In case of the second run, the trajectory of X generally moves around the threshold e_0, also jumping upwards at the beginning of each time period; at the end of most time periods it remains below e_0. The price thus fluctuates in an intermediate range. Since in

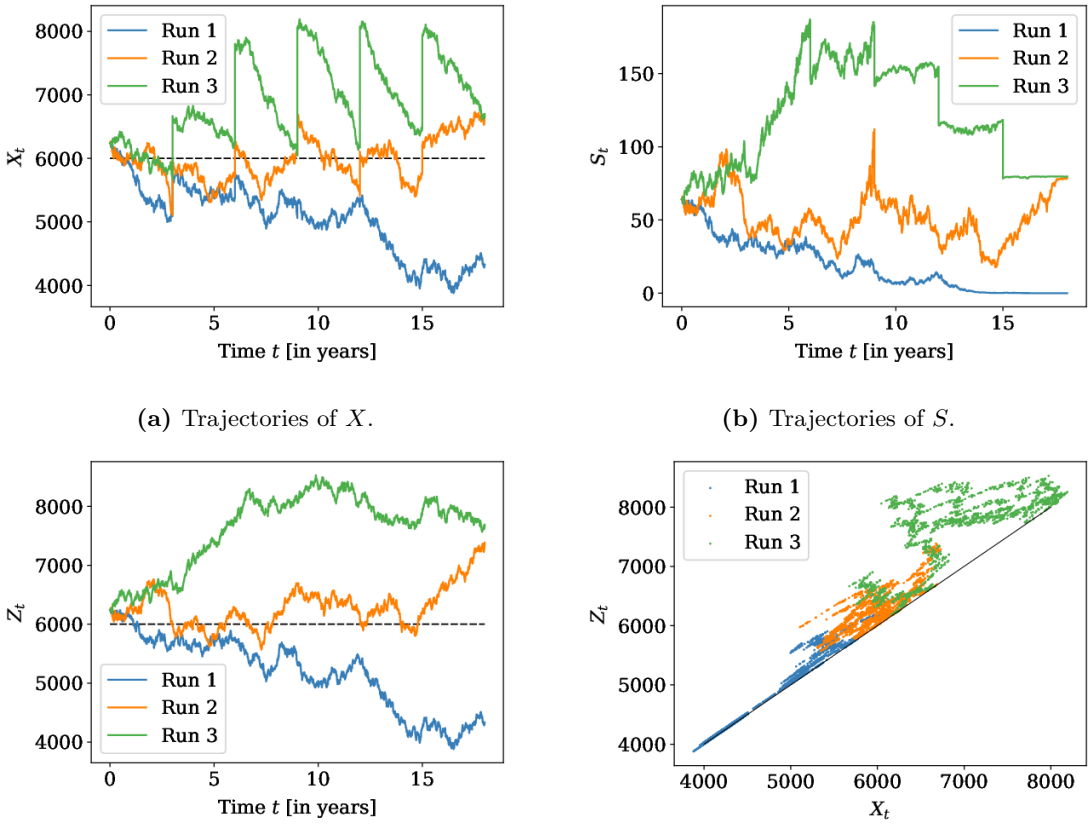

(a) Trajectories of X.

(b) Trajectories of S.

(c) Trajectories of Z.

(d) Scatter plot of X and Z.

Figure 6.99: Three example trajectories of the total expected emissions X with corresponding trajectories of the price process S and the process Z as well as the interdependence between X and Z; allowances are transferable to subsequent time periods.

the last time period, X_T is above e_0, the price reaches a value of about 80 Euro in the end; note that in this setting this value can be higher than the penalty as also for the last time period the anticipated allowance price in the next time period S_0^N depends on Z. As can be seen from the trajectory of Z, this process takes on a fairly large value at the end of the last time period, thus leading to the high allowance price. Throughout the six time periods the trajectory of Z shows similarity to that of X, but all upward movements X lead to stronger upward movements of Z. As a consequence, Z takes higher values than X, remaining above e_0 for most of the time. This in turn leads to the comparably high prices, although the run is in compliance with the cap for most time periods. Figure 6.99d confirms that Z mostly is higher than X.

The third run represents a special case: Especially in the last four time periods, the trajectory of X jumps to large values at the beginning of each time period. Then in course of the time period, X decreases, presumably due to abatement. The trajectory of Z takes considerably large values throughout the six time periods. Thus the BAU emissions remain large, causing the jumps in the trajectory of X at the beginning of each time period. As a result, prices are high, especially in time periods 2 and 3; in contrast to the two other runs shown here and most runs in general, the price process exhibits jumps at the points where time periods change. For later time periods, the derivative V_x is constant in z if z is

very large, thus delivering a maximum price; this constant decreases from one time period to the next. Since the third run reaches this maximum price, it needs to jump down to the maximum price of the subsequent time period. In line with previous observations, the scatter plot in Figure 6.99d shows that Z is much higher than X at most time points.

In general, we mostly obtain price trajectories without clear jumps at the points where the time period changes. This is much more plausible than the trajectories with jumps obtained in multi-period model I. The trajectory of X contains jumps by construction, while Z appears to be continuous as we would expect from its definition. Moreover, Z is never smaller than X: The process Z only contains the random movement of the BAU emissions, while X also contains the effects of abatement. Since abatement is always positive, corresponding to a negative drift term in the SDE of X, the abatement pushes the process X below Z.

We conduct a similar analysis for the case that allowances cannot be transferred, with results shown in Figure 6.100. The first run was again chosen with an X-trajectory

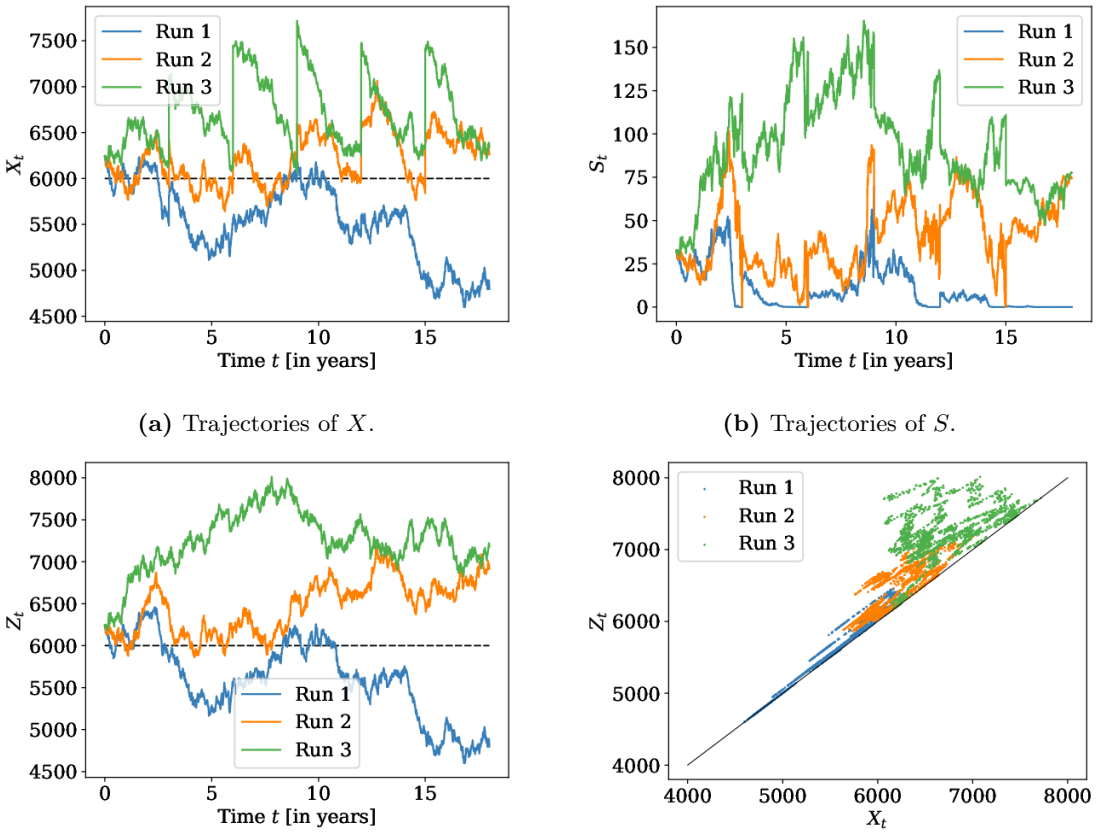

(a) Trajectories of X.

(b) Trajectories of S.

(c) Trajectories of Z.

(d) Scatter plot of X and Z.

Figure 6.100: Three example trajectories of the total expected emissions X with corresponding trajectories of the price process S and the process Z as well as the interdependence between X and Z; allowances are not transferable to subsequent time periods.

remaining below the threshold e_0 for most of the six time periods. Since also the trajectory of Z mostly remains below e_0, abatement only plays a minor role in this run, thus both trajectories are very similar, as can be seen in Figure 6.100d. As a consequence, the trajectory of X barely contains any visible jumps. At the same time the price is low,

reaching zero at the end of most time periods. This partly leads to jumps in the price trajectory: Since the range of X for which the price is not zero is broader at the beginning of a time period, the price jumps to a non-zero value.

The X-trajectory of the second run moves around e_0, thus the price fluctuates strongly. The trajectory of Z is slightly higher than that of X, indicating that some abatement occurs. The third run exhibits large values of X throughout most of the time periods which are caused by large BAU emissions as given by Z, in turn leading to high prices. Notably, in most time periods Z is considerably larger than X towards the end of each time period as abatement efforts push down the values of the process X. The general behavior of the trajectories for the processes X and Z is similar to the case of transferable allowances; but since the price may always take the value zero as long as X is small, more heavy price fluctuations occur.

These trajectories may only serve as examples; to obtain more precise results on how the transfer of allowances influences the system, we turn our analysis to aggregated quantities and distributions across all runs. In Figure 6.101a we show the mean trajectory of X for both the case of transferable allowances and the case where a transfer is not possible. In line with the results of multi-period model I, allowing for the transfer leads to a steeper decreasing slope and thus to lower mean realized emissions. Notably, a small but visible reduction still occurs in the last time period. Moreover, in comparison to the results from multi-period model I, the mean realized emissions in case of non-transferable allowances are lower.

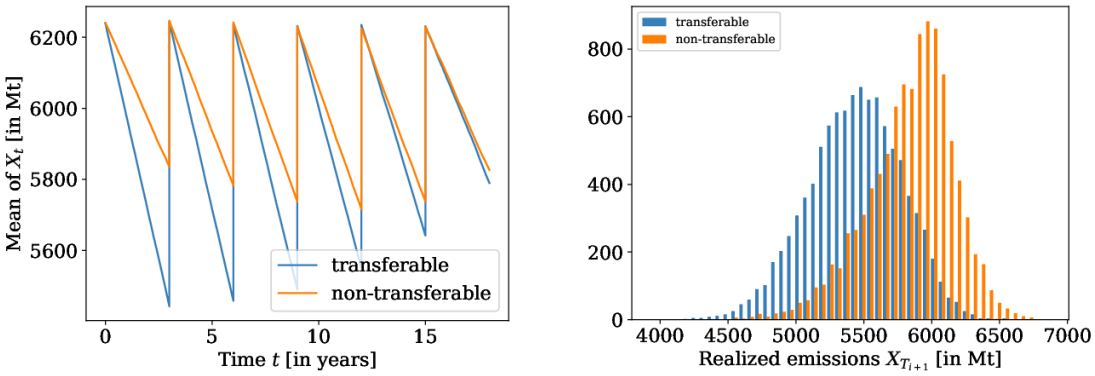

(a) Mean trajectory of X.

(b) Histogram of realized emissions $X_{T_{i+1}}$ in time period 0.

Figure 6.101: Mean trajectory of X and distribution of realized emissions $X_{T_{i+1}}$ in time period 0 in an ETS with transferable and non-transferable allowances in the simple model variant.

The distribution of the realized emissions of time period 0 shown in Figure 6.101b confirms these findings: While the distribution in the case of non-transferable allowances is more skewed, the distribution in a setting with transferable allowances is shifted to the left, thus leading to lower realized emissions. For later time periods, as shown in Figure 6.102 for time periods 2 and 5, these distributions move closer together; for the last time period 5, there is still a slight but visible difference.

The lower realized emissions lead to a higher frequency of compliance as can be seen in Table 6.3; in case of transferable allowances, compliance almost reaches 100% in time period 0, compared to less than 70% if allowances cannot be transferred.

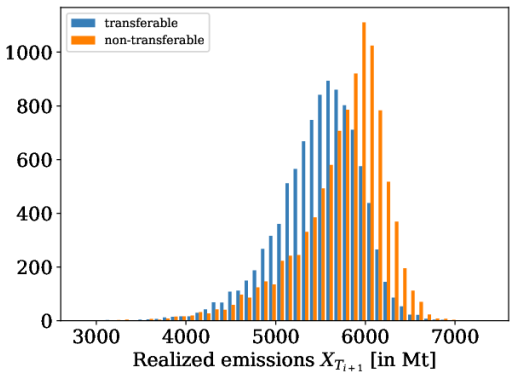

(a) Histogram of realized emissions $X_{T_{i+1}}$ in time period 2.

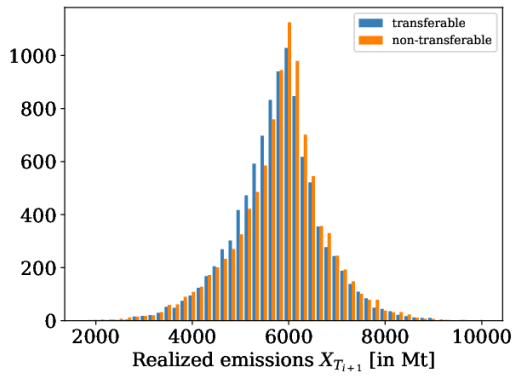

(b) Histogram of realized emissions $X_{T_{i+1}}$ in the last time period.

Figure 6.102: Distribution of realized emissions $X_{T_{i+1}}$ in time periods 2 and 5 in an ETS with transferable or non-transferable allowances in the simple model variant.

Table 6.3: Relative frequency of compliance in an ETS with transferable or non-transferable allowances in the simple model variant.

Time period	0	1	2	3	4	5
Transferable	95.8%	93.59%	88.87%	80.94%	71.54%	60.35%
Non-transferable	68.78%	68.61%	66.7%	64.7%	61.84%	56.3%

The mean prices shown in Figure 6.103a are constant within each time period. If

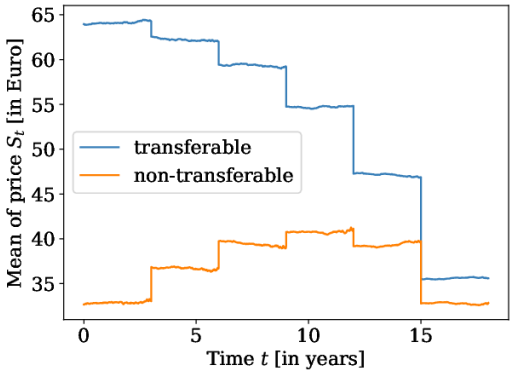

(a) Mean trajectory of S.

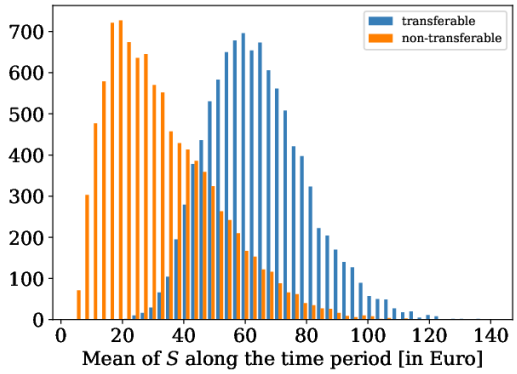

(b) Histogram of mean allowance prices within each run for time period 0.

Figure 6.103: Mean price trajectory and distribution of mean allowance prices within each run in an ETS with transferable or non-transferable allowances in the simple model variant.

allowances can be transferred, the mean price decreases from one time period to the next; it is always higher than in the setting where allowances cannot be transferred. In this case, the mean price increases between early time periods and decreases from one time period to another towards the end. Consequently, the mean of the prices of all time points within one run are higher if allowances can be transferred, in particular in early time periods. In Figure 6.103b we show the distribution of this quantity for time period 0. In case of

non-transferable allowances, the distribution is strongly skewed to the right, with a peak around 20 Euro, while for transferable allowances the distribution is more symmetric, peaking at approximately 60 Euro.

The trajectory of the price standard deviation, which is shown in Figure 6.104a, is similar for both cases early in each time period; but towards the end of each period, the standard deviation sharply increases if allowances cannot be transferred, whereas it continues to increase with almost constant slope if the transfer is possible. To further

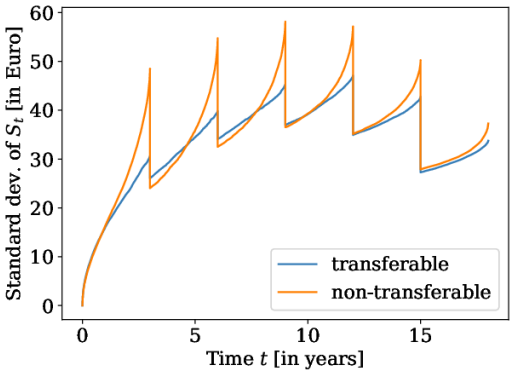

(a) Standard deviation trajectory of S.

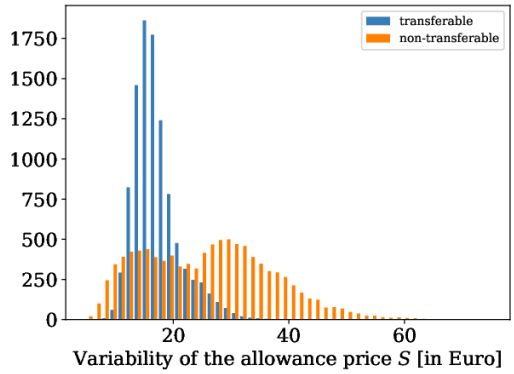

(b) Histogram of the standard deviation of absolute daily returns of S for time period 0, normalized to one year.

Figure 6.104: Trajectory of the standard deviation and the distribution of the variability of the allowance price in an ETS with transferable or non-transferable allowances in the simple model variant.

asses the variation of the price, we show the distribution of its variability within each run in Figure 6.104b for time period 0. If allowances can be transferred, we obtain a slightly right-skewed distribution with a high peak around 18. If the transfer is not allowed, the distribution of the variability has two peaks, one roughly around 10 and the other at 30; additionally, it has a heavy tail to the right. Thus allowing for the transfer leads to a lower variability in the mean, but a similar variability is also likely if the transfer is not allowed.

Summary

As observed in multi-period model I, allowing for the transfer of emission allowances decreases realized emissions and considerably increases the frequency of compliance, while increasing the allowance price and reducing its variability. It should be noted that the results on the total expected emissions X are similar to the results obtained in multi-period model I as described in Section 6.2. The characteristics of the allowance price S on the other hand differ considerably. Also the behavior of individual trajectories is very different between the two approaches to the multi-period model; since in multi-period model II the price process does not jump between two time periods and exhibits more fluctuations, it is more realistic than the price process obtained in multi-period model I.

6.3.3 Solution to the SDE in the Brownian Model Variant

We proceed in the same way for the Brownian model variant. From the SDE solution, we obtain realizations of the processes X, Z and S. Three example trajectories of each process and the relation between X and Z are shown in Figure 6.105. As in multi-period model

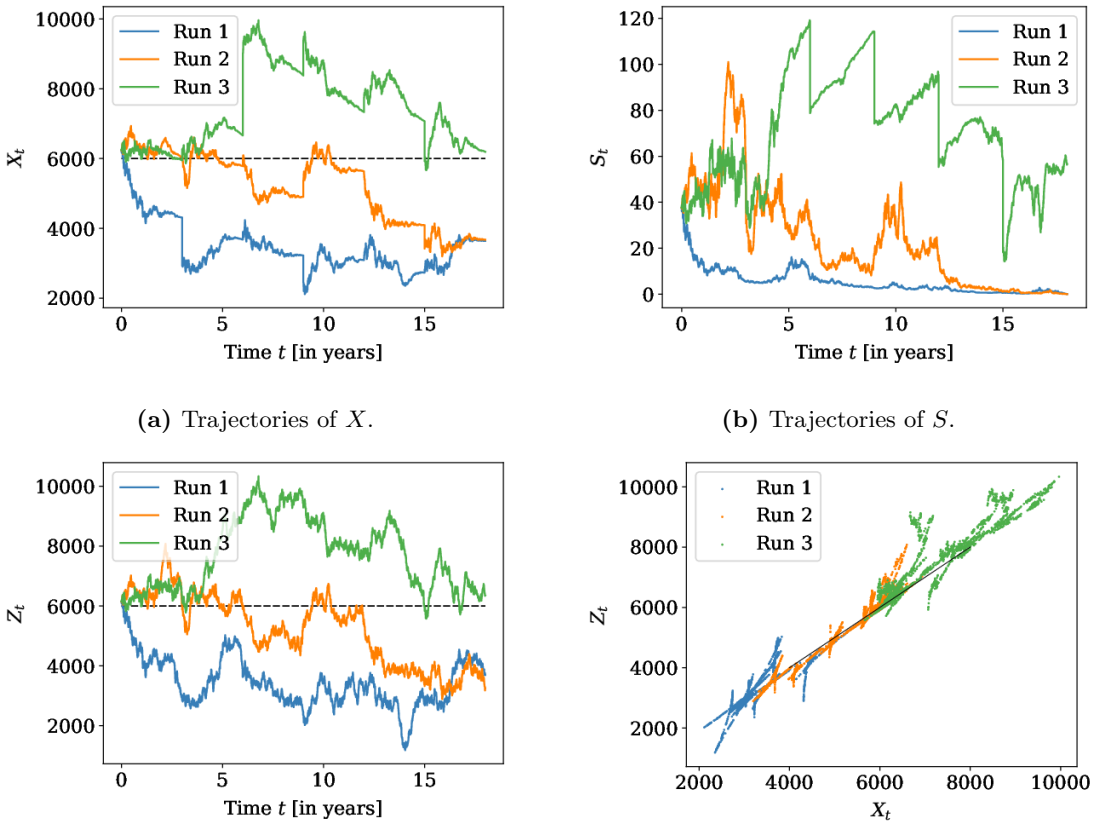

(a) Trajectories of X.

(b) Trajectories of S.

(c) Trajectories of Z.

(d) Scatter plot of X and Z.

Figure 6.105: Three example trajectories of the total expected emissions X with corresponding trajectories of the price process S and the process Z as well as the interdependence between X and Z; allowances are transferable to subsequent time periods, simulations were done in the Brownian model variant.

I, fluctuations in the trajectory of X become weaker towards the end of each time period due to the time-dependent volatility. Moreover, we observe distinctive jumps at each step from one time period to the next; in contrast to the simple model variant, this also occurs if X is well below e_0. The process Z has a constant volatility and does not contain such obvious jumps, although by construction it is not continuous; the difference between $Z^i_{\Delta T}$ and Z^{i+1}_0 amounts to $\Delta T^2\,\mu = -90$ and is thus not visible. Nevertheless, these two effects together may cause Z to be smaller than X: By construction, Z is smaller by $|\Delta T^2\,\mu|$ at the beginning of each time period, while large downward movements in the underlying Brownian motion have a larger effect on Z than on X, explaining the observations in Figure 6.105d. On the other hand, if X is large, the process Z moves to values well above X due to the effects of abatement. For the first run with an X-trajectory remaining below e_0, the price is small and fluctuates only slightly, approaching zero in the course of time

period 4. The two other runs remain close to e_0 in the beginning, leading to notable and in case of the second run heavy price fluctuations. The trajectory of X in the second run then decreases to below e_0 and remains there for most of the time until the end, therefore fluctuations eventually become smaller and the price approaches zero. The third run takes very high values in X and Z, especially in time periods 2 and 3; here again the price appears to move close to its maximum given by the PDE solution, which is increasing in time due to the positive interest rate.

In the case that allowances cannot be transferred, the processes X and Z behave similarly, as can be seen in Figure 6.106; the fluctuations of Z might appear to be slightly stronger, but this possibly is due to the different scaling of the y-axis. The most striking

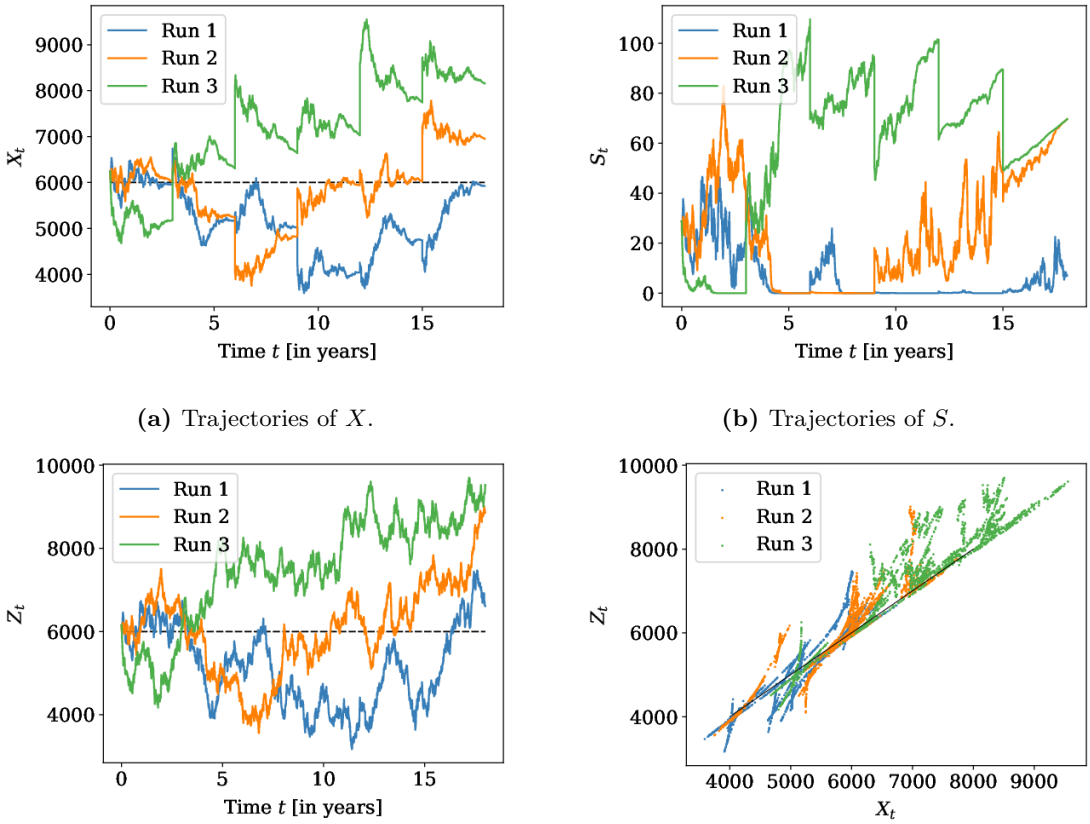

(a) Trajectories of X.

(b) Trajectories of S.

(c) Trajectories of Z.

(d) Scatter plot of X and Z.

Figure 6.106: Three example trajectories of the total expected emissions X with corresponding trajectories of the price process S and the process Z as well as the interdependence between X and Z when allowances are not transferable to subsequent time periods in the Brownian model variant.

differences to the case of transferable allowances can be observed for the price process S. Here, the price trajectories of all three runs are constantly zero in the course of at least one time period. For the first run, this holds for a long time during the six time periods.

The mean trajectories shown in Figure 6.107a have a steeper slope if allowances can be transferred and thus reach lower realized emissions at the end of each time period. Strikingly, also the emissions expected at the beginning of each time period decrease considerably; this effect is much stronger than in multi-period model I. At the same

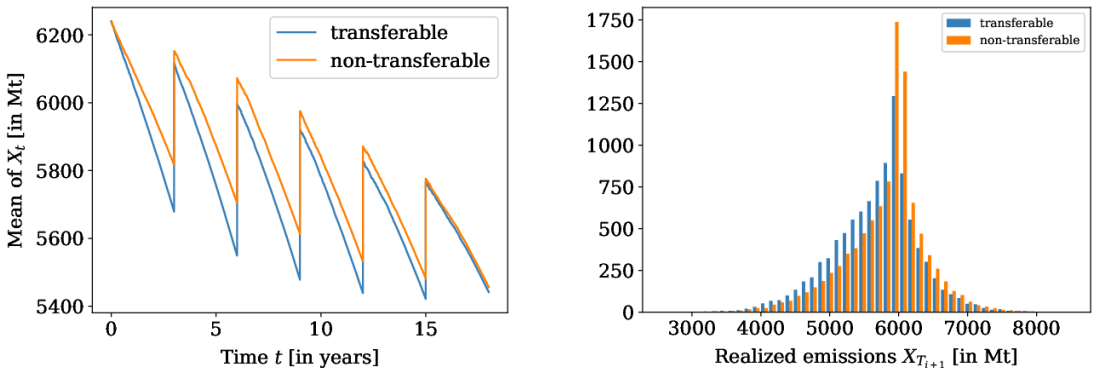

(a) Mean trajectory of X.

(b) Histogram of realized emissions $X_{T_{i+1}}$ in time period 0.

Figure 6.107: Mean trajectory of X and distribution of realized emissions $X_{T_{i+1}}$ in time period 0 in an ETS with transferable and non-transferable allowances in the Brownian model variant.

time the impact of allowing for the transfer is smaller. As in multi-period model I, the distribution of realized emissions in time period 0 shown in Figure 6.107b is slightly more skewed to the left if allowances can be transferred; for time period 2, the difference between the two distributions is already small and for time period 5, they are virtually identical, as can be seen in Figure 6.108.

In accordance with the lower mean realized emissions, the transfer of allowances increases the frequency of compliance as shown in Table 6.4. If allowances can be transferred,

Table 6.4: Relative frequency of compliance in an ETS with transferable or non-transferable allowances in the Brownian model variant.

Time period	0	1	2	3	4	5
Transferable	71.36%	63.09%	60.75%	59.86%	58.26%	57.02%
Non-transferable	60.6%	57.05%	56.8%	56.54%	57.03%	55.73%

this value reaches 71.36% and is thus about 10 percentage points higher than in the case of non-transferable allowances. Notably, this effect is by far not as strong as in the simple model variant.

The differences in the price characteristics between the case of transferable allowances versus non-transferable allowances are also not as large as in multi-period model I: The mean allowance price shown in Figure 6.109a is in both cases increasing within each time period; in time period 0, the price is approximately 10 Euro higher if allowances are transferable. This difference becomes smaller with each time period until both price paths are almost the same. The distribution of the mean price of individual runs in time period 0, which is shown in Figure 6.109b, covers a similar range in both cases. If allowances cannot be transferred, also very low prices are reached and one high peak is found at approximately 7 Euro. If the transfer of allowances is possible, the first peak of the distribution can be observed at about 30 Euro. Both distributions have a second, smaller peak between 70 and 80 Euro.

Also the trajectories of the standard deviation of the price shown in Figure 6.110a are similar for both cases, with only slightly higher values if allowances cannot be transferred.

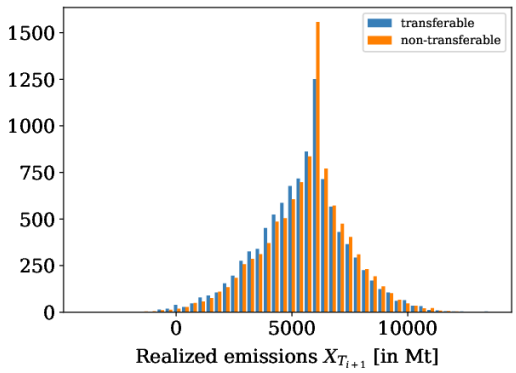

(a) Histogram of realized emissions $X_{T_{i+1}}$ in time period 2.

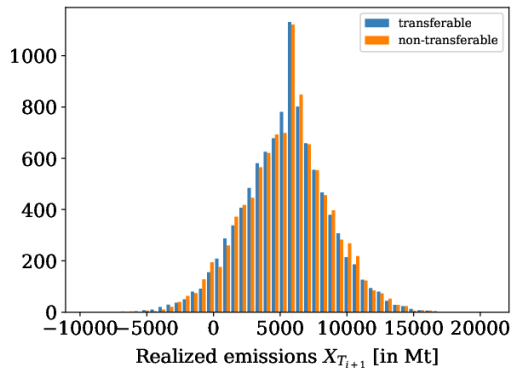

(b) Histogram of realized emissions $X_{T_{i+1}}$ in the last time period.

Figure 6.108: Distribution of realized emissions $X_{T_{i+1}}$ in time periods 2 and 5 in an ETS with transferable or non-transferable allowances in the Brownian model variant.

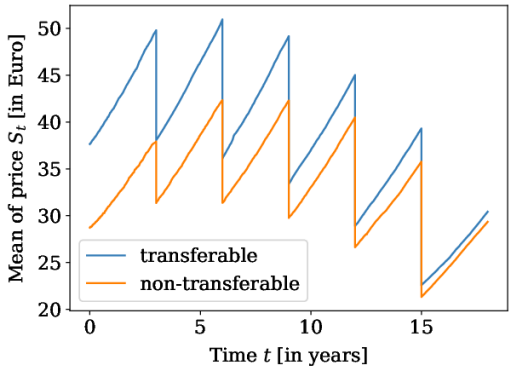

(a) Mean trajectory of S.

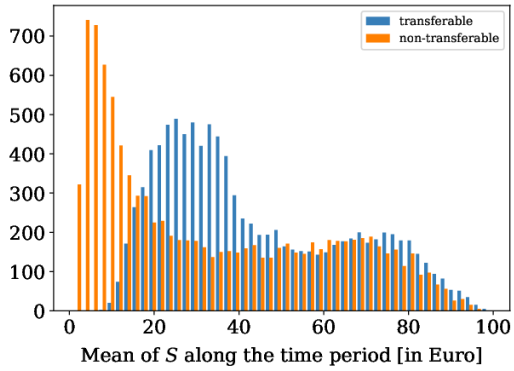

(b) Histogram of mean allowance prices within each run for time period 0.

Figure 6.109: Mean price trajectory and distribution of mean allowance prices within each run in an ETS with transferable or non-transferable allowances in the Brownian model variant.

The distribution of the price variability in time period 0, which is shown in Figure 6.110b, reaches higher values if allowances cannot be transferred and such high values are more likely, but these differences are only small.

Summary

Allowing for the transfer of emission allowances leads to lower realized emissions and a higher frequency of compliance; at the same time, the price increases and the price variability decreases slightly. Qualitatively, the results obtained in the simple model variant can also be confirmed in the Brownian model variant, but the amplitude of these effects is smaller.

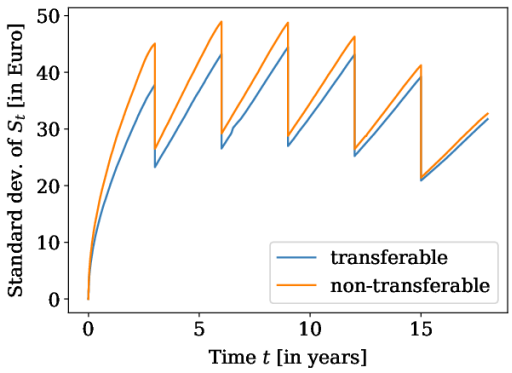

(a) Standard deviation trajectory of S.

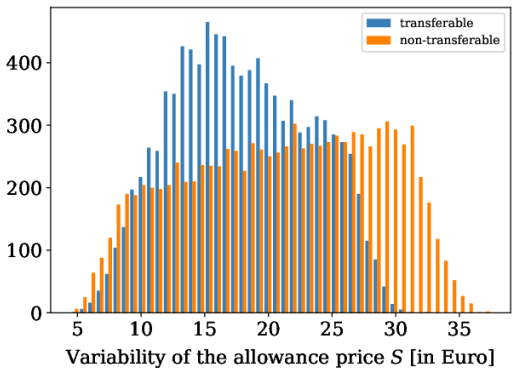

(b) Histogram of the standard deviation of absolute daily returns of S in time period 0, normalized to one year.

Figure 6.110: Trajectory of the standard deviation and the distribution of the variability of the allowance price in an ETS with transferable or non-transferable allowances in the Brownian model variant.

6.3.4 Variation of the Penalty

Similar to previous models, we increase the penalty to observe how this affects the system; for this purpose, we study several characteristic values in each setting for time period 0.

In Figure 6.111a we can see that the effect on the mean realized emissions is small in comparison to the effect of allowing for the transfer of emission allowances. If allowances

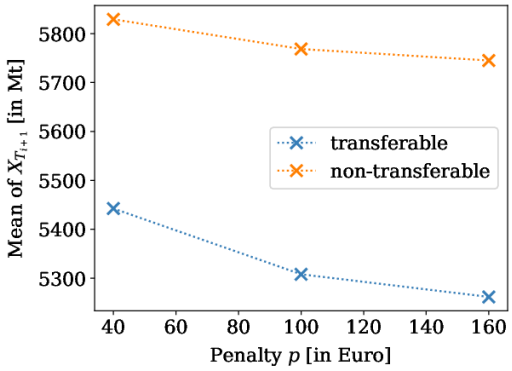

(a) Mean of realized emissions $X_{T_{i+1}}$.

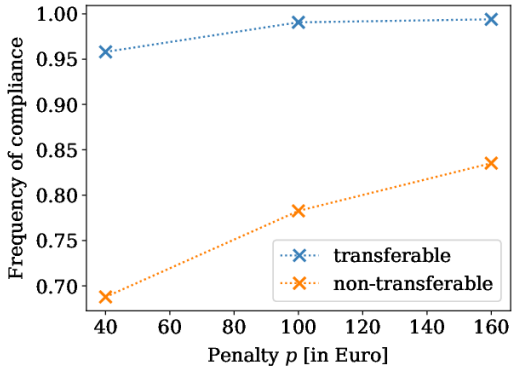

(b) Relative frequency of compliance with the emission target e_0.

Figure 6.111: Results on the total expected emissions X for a varying penalty in the simple model variant in an ETS with transferable or non-transferable allowances.

cannot be transferred, increasing the penalty considerably increases the frequency of compliance, as shown in Figure 6.111b. We have seen above that the frequency of compliance is already high for a penalty of 40 Euro if the transfer of allowances is possible; as the penalty increases, the frequency of compliance approaches 100%.

The mean price increases slightly with an increasing penalty, which is shown in Figure 6.112a; as for the mean realized emissions, the penalty only has a minor effect here,

while the possibility to transfer allowances almost doubles the mean price. The mean price

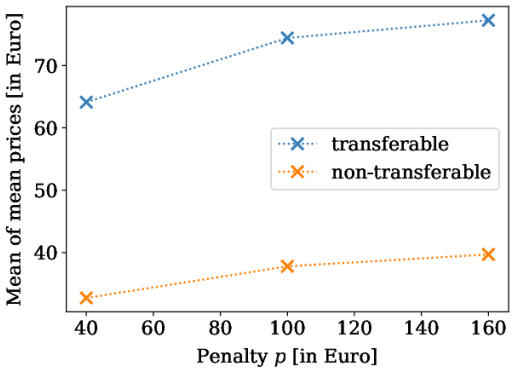

(a) Mean across all runs of the mean prices within one time period.

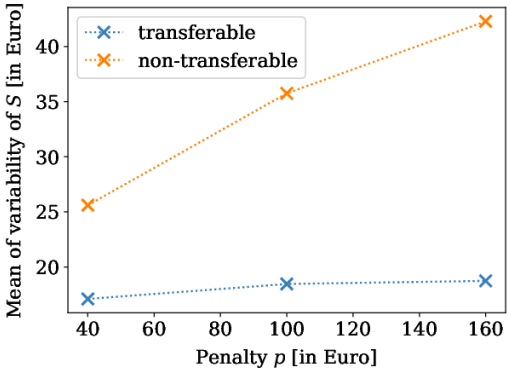

(b) Mean of the variability of the price S.

Figure 6.112: Results on the allowance price S for a varying penalty in the simple model variant in an ETS with transferable or non-transferable allowances.

variability shown in Figure 6.112b increases strongly in the case that allowances cannot be transferred; otherwise the increase of the penalty has almost no effect. These observations strongly resemble those made in multi-period model I; while the exact values of the quantities studied here deviate slightly, the tendencies are very similar.

We proceed in the same way for the Brownian variant. In Figure 6.113 the mean realized emissions and the frequency of compliance are shown. We observe that allowing for the transfer of allowances decreases the mean realized emissions, in particular for a high penalty of $p = 160$. At the same time, it increases the frequency of compliance, but especially for the choice of a high penalty the difference is small; already without the transfer of allowances, the frequency of compliance reaches approximately 95%. If the transfer is allowed, the frequency of compliance is even higher, both if $p = 100$ or if $p = 160$, reaching almost 100%.

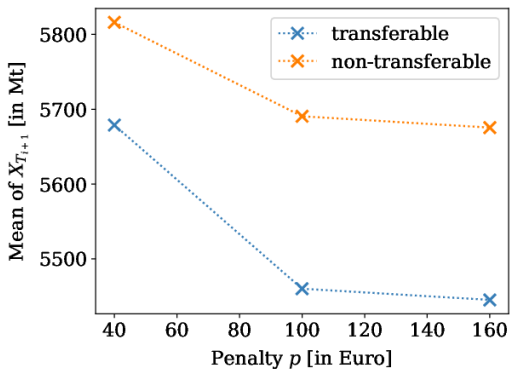

(a) Mean of realized emissions $X_{T_{i+1}}$.

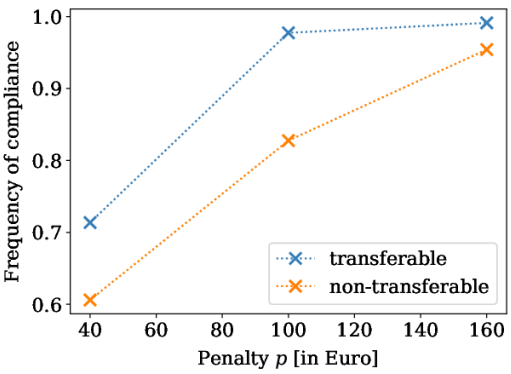

(b) Relative frequency of compliance with the emission target e_0.

Figure 6.113: Results on the total expected emissions X for a varying penalty in the Brownian model variant in an ETS with transferable or non-transferable allowances.

The mean prices shown in Figure 6.114a are higher if the transfer of allowances is possible, and increase further for higher penalties; again the effect of allowing for the transfer is higher for the large penalty of $p = 160$. The mean price variability, which is shown in Figure 6.114b, is slightly smaller in the case of transferable allowances; also here the difference is larger for the high penalty of $p = 160$.

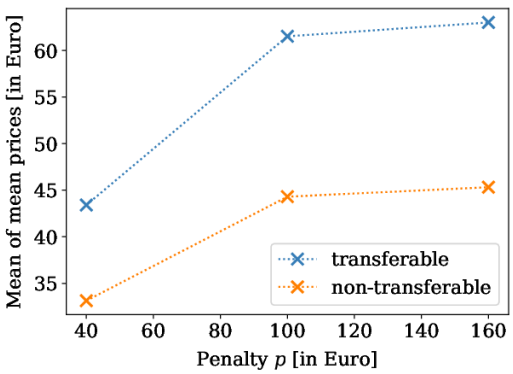

(a) Mean across all runs of the mean prices within one time period.

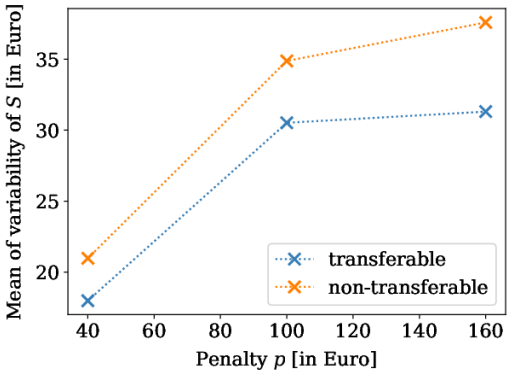

(b) Mean of the variability of the price S.

Figure 6.114: Results on the allowance price S for a varying penalty in the Brownian model variant in an ETS with transferable or non-transferable allowances.

In comparison to the results obtained in multi-period model I, the effect of increasing the penalty to $p = 100$ in the case of transferable allowances is much stronger; all graphs show a notable kink at this position. To a lesser extent and with the exception of the frequency of compliance, this is also notable in the case that allowances cannot be transferred. Apart from this observation, the results discussed here are again similar to those from multi-period model I described in Section 6.2.4.

Summary

As in multi-period model I, increasing the penalty leads to lower realized emissions and higher prices, while increasing the frequency of compliance. Again if the penalty is large and allowances can be transferred, the frequency of compliance reaches very high values of almost 100%.

Since we only consider aggregate quantities, in line with the observations made in the previous sections, the results are very similar to those obtained in multi-period model I.

6.4 Costs in the Auction Model

In Section 4.1.4 we have shown that the introduction of auctioning has no effect on the quantities we have studied so far in this chapter, as long as the total amount of allocated allowances is the same. The value function V only changes by the term $S_A\, D_A$ representing the costs at the auction, which is constant in x so that the derivative V_x remains the same. As a consequence, the process of total expected emissions X and the price process S are not changed. We therefore do not need to discuss the PDE and the SDE solution. Instead, we take a brief look at the impact auctioning has on the total costs arising in the system; we only consider the one-period model.

We first analyze the costs in the simple model variant. Costs arise from penalty payments and abatement costs as given by the solution of the HJB equation V on the one hand, and from purchasing allowances at the auction on the other, in case that allowances are auctioned instead of being distributed for free. These costs as well as the total costs, which we denote as V^A in the auction model, are given in Table 6.5; we assume that a quantity of $e_{\text{tot}} = 6000$ million allowances are either fully auctioned (i.e. $e_F = 0$, $e_A = 6000$) or fully distributed for free ($e_F = 6000$, $e_A = 0$). We observe that the costs

Table 6.5: Costs originating from the ETS as expected initially in the simple model variant with and without auctioning, given in Million Euro. The total costs V^A comprise the costs of abatement and penalty payments V and the costs at the auction given by $S_A\, D_A$. Costs are given in million Euro.

	V	$S_A\, D_A$	V^A
With auctioning	13105.03	164743.28	177848.31
Without auctioning	13105.03	–	13105.03

arising from the auction are by a factor ten higher than those from abatement and penalty payment. This is plausible as the abatement and penalty costs only need to be paid for a fraction of the total emissions, while the auction price of an allowance needs to be paid for any emissions occurring in the system. Moreover, the total costs amount to almost 178 billion Euro for the period of three years considered here, with about 165 billion Euro originating from the auction. Thus the auction generates a relevant revenue for the corresponding regulator.

We proceed in the same way for the Brownian model variant, with results given in Table 6.6. Here the difference between the two sources of costs is even higher, with auction costs

Table 6.6: Costs originating from the ETS as expected initially in the Brownian model variant with and without auctioning. The total costs V^A comprise the costs of abatement and penalty payments V and the costs at the auction given by $S_A\, D_A$. Costs are given in million Euro.

	V	$S_A\, D_A$	V^A
With auctioning	7344.37	137925.42	145269.78
Without auctioning	7344.37	–	7344.37

being almost twenty times as high. They are still slightly lower than in the simple model variant, since the allowance price at the auction is lower in this case. At the same time, the costs arising from abatement and penalty payment are considerably lower than in the simple model variant.

Summary

In the auction model, we only consider the costs arising in the system. We find that the auction costs are by a factor of 10 to 20 higher than costs arising from abatement and penalty payments. Thus, while the introduction of auctioning should not impact the resulting emissions or the allowance price according to our model, it leads to a large shift of revenue from CO_2-emitters to the regulator.

Chapter 7

Discussion and Outlook

In this thesis we present a continuous time stochastic model of an emission trading system. We provide an extension to a multi-period setting and introduce the auctioning of allowances to the model.

One-Period Model

Based on the model of Seifert et al. [SUW08], we construct a one-period model to reflect the first phase of the EU ETS. We follow three different approaches to model the emission rate and thus obtain three model variants, which we call the simple, Brownian and Ornstein-Uhlenbeck model variant. We introduce the total expected emissions X and derive an SDE to describe this process for each of the model variants. A key step in the model is to determine the optimal abatement rate u that minimizes the total costs in the system. To this end we apply a stochastic control approach; thus the problem to find the optimal abatement rate reduces to solving the HJB equation. The optimal abatement rate then enters the SDE describing X. The second central step of the model is to solve the SDE, delivering the process of total expected emissions X. From X, the price process S can be computed. The results on S and X and particularly on the realized emissions X_T allow us to assess the functionality of the ETS and to study the effects of different regulatory parameters.

In the simple model variant, we are able to solve the characteristic PDE derived from the HJB equation analytically, which allows us to show that the solution satisfies the requirements of a standard verification theorem. Moreover, we show that the SDE obtained from the corresponding abatement rate has a unique solution. With the verification theorem, we conclude that the HJB equation delivers an optimal abatement rate and that the PDE solution represents the minimum costs. To prove the existence of a unique solution to the SDE, we formulate a general result on the existence and uniqueness of an SDE solution in the setting of bounded coefficient functions which can be discontinuous at final time. Under similar assumptions, we show that the Euler-Maruyama scheme converges strongly to the unique SDE solution, which implies convergence of the scheme for our model. Both of these general results might be of interest in other applications: The specific structure of a discontinuity that only is present at final time may also more generally arise from a PDE with a final condition that is not continuous or not continuously differentiable. This theoretical foundation to the model provides an extension to the proof that the value function is a viscosity solution of the HJB equation given by Liang and Huang [LH22].

In case of the other model variants, the PDE needs to be solved numerically, which is

done by applying the method of lines. Due to the low regularity of the final condition and the numerical instability of computing difference quotients, finding a proper grid in space for the numerical solution proved to be challenging. Based on the PDE solution results, the SDE is solved numerically by applying the Euler-Maruyama scheme.

Numerical results resembling the settings of the EU ETS in its first phase are plausible when compared to the actual price development: In a large number of simulation runs, the allowance price eventually drops down to zero as it did towards the end of the first phase of the EU ETS. This is not surprising since already the final condition of the PDE delivers that the price is either zero or equal to a positive constant at the end of the time period. Also the mean price observed for the first phase and its variability fit the simulation results; according to the distributions of both quantities derived from simulations, the real-world values are likely. In the mean, realized emissions are slightly below the emission cap e_0. This is in line with results by Seifert et al. [SUW08]: They find that the initial abatement rate is larger than the abatement that would have been expected in the deterministic case, where the latter would correspond to emissions exactly matching the cap (with an abatement rate of 80 Mt per year). The actual abatement in the EU ETS estimated for its first phase is lower, amounting to approximately 60 Mt per year; possibly the BAU emissions in the model were assumed to be too high. Nevertheless, the probability of non-compliance with the emission cap, estimated in the model by the relative frequency of violating the cap, reaches approximately 40%, depending on the model variant considered. Hence the model shows that a violation of the cap is likely. This happens whenever it is cheaper to pay the penalty than to abate: Due to random movements of the process X, the required abatement to keep X_T below the cap may become so high that marginal abatement costs at this level are higher than the penalty, so a violation of the cap is preferred. In many models this case is not taken into account. Deterministic models in particular often introduce the cap as a constraint to the cost minimization problem; in this way, it is assumed a priori that the cap is not violated. Therefore, our results lead to the conclusion that an ETS cannot ensure that emissions remain below a given threshold. It should be noted at this point that the model is imprecise in one aspect: If the cap is violated, in the EU ETS the corresponding number of additional allowances has to be surrendered in the subsequent time period. This is incorporated by assuming a fixed price of 30 Euro for those allowances; it would be more realistic to have a price that varies depending on the developments in the model.

The probability of compliance can be increased by increasing the penalty. Additionally, a higher penalty leads to further reduced realized emissions and higher allowance prices, which is both desirable from the regulator's point of view; on the other hand, as a less favorable effect, the price variability increases. The efficacy of increasing the penalty is reduced if the penalty is already high. In a deterministic setting, we would expect a different behavior: The agent would choose abatement in such a way that marginal abatement costs equal the penalty. Since marginal abatement costs are linear, the resulting abatement is linear in the penalty p. In our model, we observe from the analytical PDE solution in the simple model variant that the abatement rate is non-linear in p. As a result, the mean realized emissions and the allowance price are also non-linear in p, leading to the reduced effect of increasing penalties. Intuitively, this can be explained as follows: A higher penalty provides an incentive to further reduce the probability of having to pay the penalty by increasing the abatement rate. But as this probability becomes smaller, the expected costs of penalty payment have less of an impact on the total expected costs, as the costs of abatement rise with the higher abatement rate. Therefore, the incentive to

increase abatement might become smaller. As penalties increase to large values, we observe that the mean realized emissions and the mean allowance price converge, showing that a larger penalty no longer induces any additional abatement. Possibly, at some point the effects of increasing abatement as a reaction to a higher penalty on the abatement costs on the one hand and the penalty costs on the other balance each other out. This is supported by an observation made by Seifert et al.: They obtain that the allowance price function is bounded for increasing penalties; since the allowance price function is essentially given by the abatement function, this delivers a bound on the abatement rate. The converging realized emissions also have an effect on the probability of compliance: While in the simple model variant this quantity conceivably might converge to one, the probability of compliance appears to converge to approximately 0.8 in both the Brownian and Ornstein-Uhlenbeck model variant. Hence increasing the penalty cannot ensure compliance, even if the penalty rises to unrealistically high values.

A key parameter of the system that needs to be set by the regulator is the emission cap given by the number of allowances allocated to companies. From varying either the emission cap or the BAU emissions expected initially, we observe that an ETS works best if these parameters are sufficiently close together. If there are too many allowances on the market, abatement is no longer necessary and the ETS has no impact on emissions. Importantly, this does not happen if the cap is only slightly higher than the initially expected BAU emissions. Due to the uncertainty about the development of BAU emissions, companies will still reduce their emissions in this case. If on the other hand the cap is too strict with a value far below the initially expected BAU emissions, companies abate their emissions up to a certain point, so that the ETS still has an effect. But as soon as penalty payments become cheaper than abatement, they pay the penalty instead. As a consequence, a further decrease of the cap has no effect on realized emissions; the probability of compliance with the cap is zero. At the same time, allowance prices are high and the price variability is low, providing a strong incentive for investment in low emission technologies. Therefore, in reality, companies would probably reduce their abatement costs, which would allow them to further reduce their emissions; this effect is not captured by the model.

In the course of its existence, the EU ETS has seen an increase in the length of one time period from initially three years to ten years in the current phase. Our results on varying the length of the time period are ambiguous: It is reasonable to expect that a longer time period reduces the effects of uncertainty, as there is more time to react to unfavorable random movements. In the simple model variant, we observe that the realized emissions increase and approach the cap since companies plan for a smaller safety margin between the cap and the realized emissions. At the same time, the probability of compliance with the cap increases but stays well below 1; in accordance with the penalty, it is optimal to allow for non-compliance with a certain probability. The most drastic effect can be observed for the price variability, which is strongly reduced. The largest value used in the numerical study is a time period of 100 years; this clearly undermines the purpose of an ETS, as in this setting a targeted regulation of emissions is no longer possible. Nevertheless, the results from the simple model variant suggest that it might be favorable to choose a time period that is not too short; in accordance with these results, a length of ten years as currently implemented in the EU ETS is probably still reasonable and serves to reduce price variability. This conclusion can no longer be drawn from the results obtained in the Brownian and Ornstein-Uhlenbeck model variant. While also in these variants, the price variability decreases for long time periods, at the same time the probability of

compliance decreases. Moreover, the tendencies observed for the mean realized emissions and the mean prices suggest that for time periods longer than 10 years, the cap might be violated in the mean and prices may become very low; but these projections would need to be confirmed by further simulations. From the Brownian and Ornstein-Uhlenbeck model variant, we therefore conclude that the time period probably should not be longer than 10 years. With regard to the probability of compliance, it might be favorable to choose an even shorter time period of for example 6 years; in this case the price variability is already greatly reduced, while the probability of compliance and the mean price are still high.

Except for the impact of varying the length of the time period, the conclusions drawn from the three different model variants are largely similar. Particularly the Brownian and Ornstein-Uhlenbeck model variant show a high similarity, which can easily be explained by the similarity of their respective volatility functions G. While aggregate quantities computed in the simple model variant are mostly also similar, there are considerable differences in the behavior of individual paths of the processes X and S, and the distributions of quantities computed from these differ. The main structural difference between the simple model on the one hand and the Brownian and Ornstein-Uhlenbeck model on the other lies in the volatility function G of the process X: In the simple model variant, this is a constant, while for the other two variants the volatility converges to zero as time approaches the end of the time period. Both the model derivation and the intuitive understanding are more plausible in the latter case: X_t models the emissions we expect for the entire time period at a given time point t. As we proceed in time, the uncertainty in X should decrease since more is known about the actual development of the emissions. If we derive X from a model of the emission rate, as we did in the Brownian and Ornstein-Uhlenbeck model, this structure arises naturally. In the simple model variant, we model X directly and assume a constant volatility for the sake of simplicity, thus we cannot capture this effect. Hence the Brownian and Ornstein-Uhlenbeck model represent the development of emissions in a more realistic way; on the other hand, the theoretical foundation of the model can only be provided in the simple model variant, and the analytical solution significantly simplifies and accelerates simulations.

Multi-Period Model

Since its earliest phase between 2005 and 2007, the EU ETS has seen numerous changes. An important modification is the possibility to transfer allowances from one time-period to the next, which was enabled in 2008. If such a transfer is possible, an unused allowance has a value at the end of the time period which corresponds to the price of an allowance at the beginning of the next time period. In our model, this value is represented by the price parameter s^i. We model several consecutive time periods and compute the value of an unused allowance, i.e. the price parameter, from the pricing function of the subsequent time period. At the same time, the price parameter allows us to capture the consequences of non-compliance with more precision: The price of the allowances which have to be surrendered in the next time period if the cap is violated can now be modeled by the price parameter.

We introduce two different approaches to a multi-period model. In multi-period model I, we make the simplifying assumption that the price parameter is constant throughout each sub-period. Then we proceed similarly as in the one-period model, with some adaptions to the definition of the process X. The key step to enable the transfer of allowances is done by a modification of the penalty function: In case of non-compliance, the price

parameter is added to the penalty to account for the allowances that need to be handed in in the next time period. If the system is compliant with the cap, the benefit from surplus allowances is represented by a negative penalty equal to the price parameter. If we do not want to allow for the transfer of allowances, the penalty can again be set to zero in the case of compliance. This way to include the value of unused allowances in the model is similar to the approach taken by Liang and Huang in their two-period model [LH20], but they do not include the requirement to hand in the missing allowances in the next time period in the case of non-compliance. Moreover, they compute the price parameter in a different way by modeling it separately as a geometric Brownian motion.

As in the one-period model, we are able to solve the HJB equation analytically in the simple model variant; with the help of the analytical solution, we show that the verification theorem we applied in the one-period model holds, and therefore the solution to the HJB equation delivers an optimal abatement rate and the minimum costs. We again apply the theorems on existence and uniqueness of a solution to the SDE and convergence of the Euler-Maruyama scheme to obtain that a unique solution exists, which can be approximated by the Euler-Maruyama scheme.

Since the price of an allowance at the beginning of the next time period depends on the BAU emissions expected for that time period, it is in fact not realistic to assume that the price parameter is constant: If for instance the BAU emission rate of the current time period is high, then due to the continuity of the emission rate, we might expect that in the next time period, BAU emissions are also high, leading to a high allowance price. In multi-period model II, we therefore introduce a second stochastic process Z to model the BAU emissions anticipated for the next time period from the current state of the system. From this process, we then compute the price anticipated for the beginning of the next time period. Importantly, by construction, the process Z is strongly correlated to X. This approach is in contrast to the one adopted by Liang and Huang: In their model, the auction price S_T serves a similar purpose as the price we compute from Z; but they model the process S as a geometric Brownian motion which is assumed to be uncorrelated to the process X. Both processes X and Z can be described by an SDE in all model variants. From the SDE, we derive the HJB equation of the cost minimization problem and thus obtain the characteristic PDE, which now has two variables in space. This PDE does not allow for an analytical solution, also not in the simple model variant; therefore, it is not possible to provide a verification of the HJB equation and to prove existence of a unique solution to the SDE as well as convergence of the Euler-Maruyama scheme.

The numerical implementation of both multi-period models can be done in a similar way to the one-period model; multi-period model II requires some more profound adaptations due to the additional dimension. Moreover, the solution of the PDE in this case proved to be challenging numerically.

Before we discuss the results obtained in the multi-period models, we need to make the following remark regarding the construction of the model. While the value of an allowance is taken into account, both for the possible transfer of an unused allowance and for the purchase of missing allowances in case of non-compliance, allowances are not in fact added or subtracted from the cap of the subsequent time period. Thus a physical transfer in either direction does not take place. At the same time, the model only works in a finite time horizon, and both multi-period models require us to set the price parameter or the price function for the last time period; in this way we artificially influence the model. As a consequence, we mainly study the first time period of a six-period model; in the first time period, the lack of a physical transfer of allowances has no effect, and at the same

time, it is far away from the artificial price parameter or price function in the last time period. In this way, the first time period might serve as a proxy for a time period in a multi-period setting with infinite time horizon.

All simulations are conducted both in a setting where the transfer of allowances is possible and a setting where this is not the case, so that we can assess the effects of the transferability of allowances. In both multi-period models, results show clearly that allowing for the transfer increases the probability of compliance and reduces the mean realized emissions. In particular, both effects surpass the limits we observed for increasing penalties, at least if the penalty takes a moderate value of 100 Euro or higher, meaning that compliance probabilities close to 1 are reached. This is not surprising: If allowances can be transferred, companies are rewarded for additional abatement efforts, while in the case of no transfer, any abatement below the emission cap induces costs without any benefit and is thus unfavorable. Moreover, if allowances can be transferred, allowance prices are higher and price crashes down to zero are avoided. The policy goals of an ETS therefore strongly benefit from the transferability of allowances.

Interestingly, in multi-period model II, the probability of compliance is higher than in the one-period model or in multi-period model I, even if the transfer is not allowed. The probability of compliance is dependent on the cost of non-compliance; in multi-period model II, this in turn depends on the allowance price at the beginning of the next time period and thus on the process Z. In particular, this implies that the cost of non-compliance is subject to uncertainty. Due to the strong correlation of X and Z, an unfavorable development of the emission rate increases the probability of non-compliance and at the same time also the additional costs in this case. Therefore, the incentive to ensure compliance with the cap is larger, leading to a higher probability of compliance. Another difference between the two multi-period models can be observed for the price variability: While in multi-period model II, the opportunity to transfer allowances on aggregate does not affect the price variability, this quantity is reduced considerably in multi-period model I. However, in this model the paths of the process S are unrealistic in comparison to observed allowance prices, as they are constant or linear in many cases and jump at the end of each time period. In multi-period model II, more realistic price paths are obtained, thus we conclude that allowing for the transfer of allowances does not impact the price variability.

Multi-period model II is more realistic from a theoretical perspective and delivers more plausible results. On the other hand, simulations require a higher computational effort and more storage capacities; the more complex PDE introduces numerical challenges, which lead to crashed simulations. In addition, it is not possible to show that the computations deliver an optimal abatement rate and that the resulting SDE has a unique solution. At the same time, the high similarity between the results of multi-period model I and multi-period model II justify the use of multi-period model I as an approximation to the multi-period setting. For this model, it is possible to derive an analytical solution and provide the theoretical backbone in case of the simple model variant. Simulations are considerably simplified, also in the two other model variants. Moreover, multi-period model I can serve as a model for a governmental buyback program as suggested by Hintermayer in [Hin20] to set a minimum allowance price. By considering only one time-period and letting the regulator fix the price parameter $s = s^1$, we obtain a model of a setting where allowances can be sold back to the regulator for the price s at the end of each time period. At the same time, companies are allowed to buy additional allowances for the price s at the beginning of the next time period to cover emissions exceeding the number of allowances they were holding. In this way, the regulator can set a price corridor with minimum price

s and maximum price $s + p$ by choosing s and p as desired. To obtain a system where the regulator only sets the minimum price, the model would need to be adapted.

We additionally study the effect of changing the allowance cap over time as it is currently implemented in the EU ETS; due to the argumentation above, we conduct this analysis only in the simple variant of multi-period model I. We let the cap decrease yearly by a given percentage and compare this to the case of a constant cap. If allowances are transferable, most of the additional abatement effort for a decreasing cap takes place in early time periods; if on the other hand allowances cannot be transferred, abatement is highest for the sub-periods in the middle of the overall time horizon. In this setting, we obtain that an increasing penalty has a strong impact if allowances can be transferred. Additionally, we study the impact of a cost coefficient that decreases in time due to technological progress; we obtain that the moderate yearly decrease of 1% shows very little effect. It should be noted that the reliability of both these results is limited due to the setup of the model; we set the price parameter for the last time period to zero, causing the violation of the cap to be cheapest for this time period. This probably leads to low abatement and little compliance in the last time period. Moreover, the analysis of a decreasing cap is strongly impaired by the fact that allowances are not actually transferred, as discussed above.

Hence this points to a possible model extension: It is clearly desirable to incorporate the impact of the allowance transfer on the cap in the model. While it is straight-forward to adapt the cap after the preceding time period has been simulated, the question arises how the possibly altered cap affects the cost minimization problem of each time period. Another possible direction of future research is to develop a more elaborate method to evaluate multi-period model II with the goal of avoiding numerical errors and reducing the computational effort. As discussed above, multi-period model II simulates the paths of the processes X and S more accurately, thus it enables a more accurate analysis of regulatory settings. In both multi-period models presented here, we assume that the abatement effort of the previous time period does not affect the BAU emissions of the current time period. As long as abatement measures are assumed to consist of short-term measures such as fuel-switching, this is a reasonable approach since these measures might be reversed if allowance prices are too low. If we aim to take into account investments in clean technology, which have a long-term effect on emissions, we need to allow BAU emissions to react to the abatement of previous time periods.

Auctioning

Another important change that the EU ETS has seen after its initial phase is the introduction of the auctioning of allowances. To include this in our model, we need to add the costs of purchasing allowances at the auction to the value function. Moreover, the auction itself poses an additional optimization problem: The representative agent needs to determine a demand schedule depending on the auction price in such a way that her total costs – including the auction costs – are minimized. In line with the approach by Haita [Hai14] and the second approach of Liang and Huang [LH20], we obtain a two-step optimization problem: We first solve the optimization problem in the course of the trading period; the solution to the problem can be obtained directly from the solution in the model without auctioning. In the second step, we solve the optimization problem at the auction. By using that the abatement rate u minimizes the costs from penalty payment and abatement, we derive a necessary condition for the demand delivering minimum costs. We assume

that the market at the auction clears and thus obtain an expression for the auction price. Under some assumptions, which can only be guaranteed in the simple model variant, we show that the auction price is equal to the allowance price at the beginning of the trading period. This is plausible since the agent does not gain any additional information between the auction and the beginning of the trading period. Moreover, this result is in line with a result by Haita: In her static model, she was able to show that the auction price is equal to the price on the allowance market. We then show that the introduction of auctioning to the model does not affect the processes X and S, as long as the total amount of allocated allowances remains the same. Thus in particular for the results presented above, which solely concern the realized emissions, the compliance probability and the behavior of the allowance price, it is not relevant whether allowances are auctioned or distributed for free. On the other hand, the introduction of auctioning has a large effect on the total costs arising in the system: By simulating an ETS with and without auctioning, we obtain that the costs of purchasing the allowances at an auction by far surpasses the costs arising from emission abatement and penalty payments. The explanation behind this observation is that a price has to be paid for every ton of emissions if allowances are auctioned. On the other hand, costs of abatement and penalty payments only arise for the emissions which are abated or surpass the cap; these usually comprise a fraction of total emissions.

Also in the auction model, further extensions are conceivable. For example, an integration with both multi-period models is of interest to further align the model to the current state of the EU ETS. We expect that this would lead to similar results as in the one-period auction model; still, it would be valuable to verify this projection.

Summary and Concluding Remarks

This thesis provides a thorough analysis of the possible outcomes in an ETS within a stochastic setting, showing that the introduction of uncertainty has a relevant impact on the system. In particular, we obtain that compliance with the emission cap cannot be guaranteed, especially in a one-period framework. Our results stress that allowing for the transfer of allowances (i.e. banking) has a huge positive impact on desirable properties of the development in the ETS. Moreover, we conclude that a sufficiently high penalty is important to increase the probability of compliance, while it is not effective to choose a very large penalty. At the same time, the model suggests that the cap should be chosen in accordance with the expected BAU emissions; in particular, it should not be too large. These results, at least in the one-period setting, are not influenced if allowances are auctioned instead of being allocated for free.

While the multi-period setting and the introduction of auctioning serve to align the model to the framework of the EU ETS, some important features are not included in the model. The multi-period models lack the physical transfer of allowances; and more complex mechanisms of the EU ETS such as the market stability reserve are not included. Since uncertainty has such a notable impact on an ETS, a stochastic model that closely reflects the EU ETS in its current state could provide a valuable tool to assess further policy modifications. However, the model presented here is already complex, so that the integration of an intricate mechanism like the market stability reserve might prove to be challenging.

Appendix A

Derivatives and other Auxiliary Computations

This section serves to provide the derivation of the various derivatives of the PDE solution in the simple model variant as needed in the course of the thesis. As another auxiliary computation, we consider the quadratic covariation of the shifted Brownian motion W^i required in both multi-period models.

A.1 Derivatives in the One-Period Model

In Section 2.3.1 we derived a solution of the characteristic PDE for the simple model variant as

$$V(t,x) = -c\sigma^2 \ln\left(\frac{\left(1+\operatorname{erf}\left(\frac{e_0-x}{\sqrt{2}\sigma\sqrt{T-t}}\right)\right)+\left(1-\operatorname{erf}\left(\frac{c(e_0-x)+p(T-t)}{\sqrt{2}c\sigma\sqrt{T-t}}\right)\right)e^{\frac{2cp(e_0-x)+p^2(T-t)}{2c^2\sigma^2}}}{2}\right).$$

Before we compute the derivative, we first introduce some auxiliary functions[1]

$$\begin{aligned}
F_1(t,x) &= 1-\operatorname{erf}\left(\frac{ce_0-cx+p(T-t)}{\sqrt{2}c\sigma\sqrt{T-t}}\right)\\
F_2(t,x) &= 1+\operatorname{erf}\left(\frac{e_0-x}{\sqrt{2}\sigma\sqrt{T-t}}\right)\\
E_1(t,x) &= \mathrm{e}^{\frac{(c(e_0-x)+p(T-t))^2}{2c^2\sigma^2(T-t)}}\\
E_2(t,x) &= \mathrm{e}^{\frac{(e_0-x)^2}{2\sigma^2(T-t)}}\\
E_3(t,x) &= \mathrm{e}^{\frac{2cp(e_0-x)+p^2(T-t)}{2c^2\sigma^2}}.
\end{aligned}$$

By inserting these functions, we may express V as

$$V(t,x) = -c\sigma^2 \ln\left(\frac{F_2(t,x)+F_1(t,x)\cdot E_3(t,x)}{2}\right).$$

[1] These are identical to the auxiliary functions introduced in Section 2.3.2.

A.1.1 First Derivative V_x

With the expression above for V_x, we compute the derivative with respect to x as

$$V_x(t,x) = -c\sigma^2 \frac{2}{F_2(t,x) + F_1(t,x)\cdot E_3(t,x)} \cdot \frac{1}{2}\left(F_{2,x}(t,x) + F_{1,x}(t,x)\cdot E_3(t,x) + F_1(t,x)\cdot E_{3,x}\right),$$

where $F_{1,x}$, $F_{2,x}$ and $E_{3,x}$ each denote the corresponding partial derivative with respect to x. We have

$$\begin{aligned}
F_{1,x}(t,x) &= -\frac{2}{\sqrt{\pi}}\,\mathrm{e}^{-\frac{(c(e_0-x)+p(T-t))^2}{2c^2\sigma^2(T-t)}}\cdot\left(-\frac{1}{\sqrt{2}\sigma\sqrt{T-t}}\right) = \frac{2}{\sqrt{2\pi}\sigma\sqrt{T-t}}\cdot\frac{1}{E_1(t,x)}\\
F_{2,x}(t,x) &= \frac{2}{\sqrt{\pi}}\,\mathrm{e}^{-\frac{(e_0-x)^2}{2\sigma^2(T-t)}}\cdot\left(-\frac{1}{\sqrt{2}\sigma\sqrt{T-t}}\right) = -\frac{2}{\sqrt{2\pi}\sigma\sqrt{T-t}}\cdot\frac{1}{E_2(t,x)}\\
E_{3,x}(t,x) &= E_3(t,x)\cdot\left(-\frac{2cp}{2c^2\sigma^2}\right) = -\frac{p}{c\sigma^2}\,E_3(t,x).
\end{aligned}$$

Furthermore, we can show that $E_1(t,x) = E_2(t,x)\,E_3(t,x)$ by computing

$$\begin{aligned}
E_1(t,x) &= \mathrm{e}^{\frac{(c(e_0-x)+p(T-t))^2}{2c^2\sigma^2(T-t)}} = \mathrm{e}^{\frac{c^2(e_0-x)^2+2cp(e_0-x)(T-t)+p^2(T-t)^2}{2c^2\sigma^2(T-t)}}\\
&= \mathrm{e}^{\frac{(e_0-x)^2}{2\sigma^2(T-t)}}\cdot\mathrm{e}^{\frac{2cp(e_0-x)+p^2(T-t)}{2c^2\sigma^2}} = E_2(t,x)\,E_3(t,x).
\end{aligned}$$

This also implies that $\frac{E_3(t,x)}{E_1(t,x)} = \frac{1}{E_2(t,x)}$. Thus we have

$$\begin{aligned}
V_x(t,x) &= -c\sigma^2\frac{-\frac{2}{\sqrt{2\pi}\sigma\sqrt{T-t}}\cdot\frac{1}{E_2(t,x)} + \frac{2}{\sqrt{2\pi}\sigma\sqrt{T-t}}\cdot\frac{E_3(t,x)}{E_1(t,x)} - F_1(t,x)\frac{p}{c\sigma^2}E_3(t,x)}{F_2(t,x)+F_1(t,x)E_3(t,x)}\\
&= -c\sigma^2\frac{-\frac{p}{c\sigma^2}F_1(t,x)E_3(t,x)}{F_2(t,x)+F_1(t,x)E_3(t,x)}\\
&= \frac{p}{\frac{F_2(t,x)}{F_1(t,x)E_3(t,x)} + \frac{F_1(t,x)E_3(t,x)}{F_1(t,x)E_3(t,x)}}\\
&= \frac{p}{1+\frac{F_2(t,x)}{F_1(t,x)E_3(t,x)}}.
\end{aligned}$$

By applying the definitions of the auxiliary functions again, we then obtain

$$V_x(t,x) = \frac{p}{1+\frac{\mathrm{e}^{-\frac{2cp(e_0-x)+p^2(T-t)}{2c^2\sigma^2}}\left(1+\mathrm{erf}\left(\frac{e_0-x}{\sqrt{2(T-t)}\sigma}\right)\right)}{1-\mathrm{erf}\left(\frac{ce_0-cx+p(T-t)}{\sqrt{2(T-t)}c\sigma}\right)}}.$$

A.1.2 Second Derivative V_{xx}

We proceed similarly for the second derivatives. We start from V_x given as

$$V_x(t,x) = \frac{p\,F_1(t,x)\,E_3(t,x)}{F_2(t,x)+F_1(t,x)\,E_3(t,x)}.$$

For ease of notation, we will drop the "(t, x)" in the following. We first compute the second derivative with respect to x. This can be expressed as

$$\begin{aligned}
V_{xx} &= \frac{p\,(F_{1,x}\,E_3 + F_1\,E_{3,x})\;(F_2 + F_1\,E_3) - p\,F_1\,E_3\,(F_{2,x} + F_{1,x}\,E_3 + F_1\,E_{3,x})}{(F_2 + F_1\,E_3)^2} \\
&= \frac{pF_{1,x}\,E_3\;(F_2 + F_1\,E_3) + pF_1\,E_{3,x}\;(F_2 + F_1\,E_3) - p\,F_1\,E_3\,(F_{2,x} + F_{1,x}\,E_3 + F_1\,E_{3,x})}{(F_2 + F_1\,E_3)^2} \\
&= \frac{pF_{1,x}\,E_3}{F_2 + F_1\,E_3} + \frac{pF_1\,E_{3,x}\;(F_2 + F_1\,E_3) - p\,F_1\,E_3\,(F_{2,x} + F_{1,x}\,E_3 + F_1\,E_{3,x})}{(F_2 + F_1\,E_3)^2} \\
&=: A^{xx} + B^{xx}.
\end{aligned}$$

We consider the two fractions separately. For the first, we apply the derivatives of the auxiliary functions as given above and recall that $\frac{E_3}{E_1} = \frac{1}{E_2}$ to compute

$$\begin{aligned}
A^{xx} &= \frac{p\,\frac{2}{\sqrt{2\pi}\sigma\sqrt{T-t}} \cdot \frac{1}{E_1} \cdot E_3}{F_2 + F_1\,E_3} \\
&= \frac{p\,\frac{2}{\sqrt{2\pi}\sigma\sqrt{T-t}} \cdot \frac{1}{E_2}}{F_2 + F_1\,E_3} \\
&= \frac{p\sqrt{2}}{\sqrt{\pi}\sigma\sqrt{T-t}\,(F_2\,E_2 + F_1\,E_2\,E_3)} \\
&= \frac{p\sqrt{2}}{\sqrt{\pi}\sigma\sqrt{T-t}\,(F_2\,E_2 + F_1\,E_1)}.
\end{aligned}$$

In the derivation of V_x, we have in particular seen that $F_{2,x} + F_{1,x}\,E_3 = 0$. Then we have for the second fraction

$$\begin{aligned}
B^{xx} &= \frac{p\,F_1\,E_{3,x}\;(F_2 + F_1\,E_3) - p\,F_1\,E_3\,(F_{2,x} + F_{1,x}\,E_3 + F_1\,E_{3,x})}{(F_2 + F_1\,E_3)^2} \\
&= \frac{p\,F_1\,E_{3,x}\;(F_2 + F_1\,E_3) - p\,F_1\,E_3\,F_1\,E_{3,x}}{(F_2 + F_1\,E_3)^2} \\
&= \frac{p\,F_1\,E_{3,x}\;(F_2 + F_1\,E_3 - F_1\,E_3)}{(F_2 + F_1\,E_3)^2} \\
&= \frac{p\,F_1\,F_2\,E_{3,x}}{(F_2 + F_1\,E_3)^2}.
\end{aligned}$$

We apply the derivative of $E_{3,x}$ as computed above and evaluate the square in the denominator, resulting in

$$\begin{aligned}
B^{xx} &= \frac{-p\,\frac{p}{c\sigma^2}\,F_1\,F_2\,E_3}{F_2^2 + 2F_2\,F_1\,E_3 + F_1^2\,E_3^2} \\
&= -\frac{p^2}{c\sigma^2\left(\frac{F_2^2}{F_1\,F_2\,E_3} + 2\frac{F_1\,F_2\,E_3}{F_1\,F_2\,E_3} + \frac{F_1^2\,E_3^2}{F_1\,F_2\,E_3}\right)} \\
&= -\frac{p^2}{c\sigma^2\left(\frac{F_2}{F_1\,E_3} + 2 + \frac{F_1\,E_3}{F_2}\right)}.
\end{aligned}$$

Combining these results, we have

$$V_{xx}(t,x) = \frac{p\sqrt{2}}{\sqrt{\pi}\sigma\sqrt{T-t}\,(F_2\,E_2 + F_1\,E_1)} - \frac{p^2}{c\sigma^2\left(\frac{F_2}{F_1\,E_3} + 2 + \frac{F_1\,E_3}{F_2}\right)}.$$

A.1.3 Second Derivative V_{xt}

For the mixed derivative V_{xt}, we again start from

$$V_x = \frac{p\,F_1\,E_3}{F_2 + F_1\,E_3}.$$

We compute the derivative as

$$V_{xt} = \frac{p\,(F_{1,t}\,E_3 + F_1\,E_{3,t})\;(F_2 + F_1\,E_3) - p\,F_1\,E_3\,(F_{2,t} + F_{1,t}E_3 + F_1E_{3,t})}{(F_2 + F_1\,E_3)^2},$$

where the partial derivatives with respect to t are given by

$$\begin{aligned}
F_{1,t}(t,x) &= -\frac{2}{\sqrt{\pi}}\,\mathrm{e}^{-\frac{(c(e_0-x)+p(T-t))^2}{2c^2\sigma^2(T-t)}} \\
&\qquad \cdot \frac{-p\sqrt{2}c\sigma\sqrt{T-t} - (c(e_0-x)+p(T-t))\,\sqrt{2}c\sigma\cdot\left(-\frac{1}{2\sqrt{T-t}}\right)}{2c^2\sigma^2(T-t)} \\
&= \frac{1}{E_1}\left(\frac{p\sqrt{2}}{\sqrt{\pi}c\sigma\sqrt{T-t}} - \frac{c(e_0-x)+p(T-t)}{\sqrt{2\pi}c\sigma(T-t)^{\frac{3}{2}}}\right) \\
&= \frac{1}{E_1}\left(\frac{2p}{\sqrt{2\pi}c\sigma\sqrt{T-t}} - \frac{e_0-x}{\sqrt{2\pi}\sigma(T-t)^{\frac{3}{2}}} - \frac{p}{\sqrt{2\pi}c\sigma\sqrt{T-t}}\right) \\
&= \frac{1}{E_1}\left(\frac{p}{\sqrt{2\pi}c\sigma\sqrt{T-t}} - \frac{e_0-x}{\sqrt{2\pi}\sigma(T-t)^{\frac{3}{2}}}\right) \\
F_{2,t}(t,x) &= \frac{2}{\sqrt{\pi}}\,\mathrm{e}^{-\frac{(e_0-x)^2}{2\sigma^2(T-t)}}\cdot\left(-\frac{e_0-x}{2\sqrt{2}\sigma(T-t)^{\frac{3}{2}}\cdot(-1)}\right) \\
&= \frac{1}{E_2}\frac{e_0-x}{\sqrt{2\pi}\sigma(T-t)^{\frac{3}{2}}} \\
E_{3,t}(t,x) &= E_3\cdot\left(-\frac{p^2}{2c^2\sigma^2}\right).
\end{aligned}$$

With this, we compute

$$\begin{aligned}
F_{2,t} + F_{1,t}E_3 &= \frac{1}{E_2}\frac{e_0-x}{\sqrt{2\pi}\sigma(T-t)^{\frac{3}{2}}} + \frac{E_3}{E_1}\left(\frac{p}{\sqrt{2\pi}c\sigma\sqrt{T-t}} - \frac{e_0-x}{\sqrt{2\pi}\sigma(T-t)^{\frac{3}{2}}}\right) \\
&= \frac{1}{E_2}\frac{e_0-x}{\sqrt{2\pi}\sigma(T-t)^{\frac{3}{2}}} - \frac{1}{E_2}\frac{c(e_0-x)}{\sqrt{2\pi}c\sigma(T-t)^{\frac{3}{2}}} + \frac{1}{E_2}\frac{p}{\sqrt{2\pi}c\sigma\sqrt{T-t}} \\
&= \frac{1}{E_2}\frac{p}{\sqrt{2\pi}c\sigma\sqrt{T-t}}.
\end{aligned}$$

We again split up the fraction

$$\begin{aligned}
V_{xt} &= \frac{p\,F_{1,t}\,E_3\;(F_2+F_1\,E_3)+p\,F_1\,E_{3,t}\;(F_2+F_1\,E_3)-p\,F_1\,E_3\,(F_{2,t}+F_{1,t}E_3+F_1E_{3,t})}{(F_2+F_1\,E_3)^2}\\
&= \frac{p\,F_{1,t}\,E_3\;(F_2+F_1\,E_3)}{(F_2+F_1\,E_3)^2}\\
&\quad+\frac{p\,F_1\,E_{3,t}\,F_2+p\,F_1\,E_{3,t}\,F_1\,E_3-p\,F_1\,E_3\,F_1\,E_{3,t}-p\,F_1\,E_3\,(F_{2,t}+F_{1,t}E_3)}{(F_2+F_1\,E_3)^2}\\
&= \frac{p\,F_{1,t}\,E_3}{F_2+F_1\,E_3}+\frac{p\,F_1\,E_{3,t}\,F_2-p\,F_1\,E_3\,(F_{2,t}+F_{1,t}E_3)}{(F_2+F_1\,E_3)^2}\\
&= \frac{p\,F_{1,t}\,E_3}{F_2+F_1\,E_3}+\frac{p\,F_1\,E_{3,t}\,F_2}{(F_2+F_1\,E_3)^2}-\frac{p\,F_1\,E_3\,(F_{2,t}+F_{1,t}E_3)}{(F_2+F_1\,E_3)^2}=:A^{xt}+B^{xt}+C^{xt}
\end{aligned}$$

and simplify the three terms separately[2]. For the first, we have with the derivatives of the auxiliary functions computed above and the relation between E_1, E_2 and E_3

$$\begin{aligned}
A^{xt} &= \frac{p\,F_{1,t}\,E_3}{F_2+F_1\,E_3}\\
&= \frac{p\cdot\frac{E_3}{E_1}\cdot\left(\frac{p}{\sqrt{2\pi}c\sigma\sqrt{T-t}}-\frac{e_0-x}{\sqrt{2\pi}\sigma(T-t)^{\frac{3}{2}}}\right)}{F_2+F_1\,E_3}\\
&= \frac{p^2\cdot\frac{1}{E_2}}{\sqrt{2\pi}c\sigma\sqrt{T-t}\,(F_2+F_1\,E_3)}-\frac{p\cdot\frac{1}{E_2}\cdot(e_0-x)}{\sqrt{2\pi}\sigma(T-t)^{\frac{3}{2}}\,(F_2+F_1\,E_3)}\\
&= \frac{p^2}{\sqrt{2\pi}c\sigma\sqrt{T-t}\,(F_2\,E_2+F_1\,E_2\,E_3)}-\frac{p(e_0-x)}{\sqrt{2\pi}\sigma(T-t)^{\frac{3}{2}}\,(F_2\,E_2+F_1\,E_2\,E_3)}\\
&= \frac{p^2}{\sqrt{2\pi}c\sigma\sqrt{T-t}\,(F_2\,E_2+F_1\,E_1)}-\frac{p(e_0-x)}{\sqrt{2\pi}\sigma(T-t)^{\frac{3}{2}}\,(F_2\,E_2+F_1\,E_1)}.
\end{aligned}$$

For the second term, we again apply the derivatives and evaluate the square in the denominator

$$\begin{aligned}
B^{xt} &= \frac{p\,F_1\,E_{3,t}\,F_2}{(F_2+F_1\,E_3)^2}\\
&= \frac{-p\cdot\frac{p^2}{2c^2\sigma^2}\cdot F_1\,E_3\,F_2}{F_2^2+2F_2\,F_1\,E_3+F_1^2\,E_3^2}\\
&= -\frac{p^3}{2c^2\sigma^2\left(\frac{F_2^2}{F_1\,F_2\,E_3}+2\,\frac{F_1\,F_2\,E_3}{F_1\,F_2\,E_3}+\frac{F_1^2\,E_3^2}{F_1\,F_2\,E_3}\right)}\\
&= -\frac{p^3}{2c^2\sigma^2\left(\frac{F_2}{F_1\,E_3}+2+\frac{F_1\,E_3}{F_2}\right)}.
\end{aligned}$$

[2]Note that the term A^{xt} introduced here is split up further into two terms A^{xt} and D^{xt} in the proof of Proposition 2.7 (iv), where this derivative is needed

For the last term, we apply the result computed above and again evaluate the square in the denominator

$$\begin{aligned}
C^{xt} &= -\frac{p\,F_1\,E_3\,(F_{2,t}+F_{1,t}E_3)}{(F_2+F_1\,E_3)^2} \\
&= -\frac{pF_1\cdot\frac{E_3}{E_2}\cdot\frac{p}{\sqrt{2\pi}c\sigma\sqrt{T-t}}}{F_2^2+2F_2\,F_1\,E_3+F_1^2\,E_3^2} \\
&= -\frac{p^2}{\sqrt{2\pi}c\sigma\sqrt{T-t}\left(\frac{F_2^2\,E_2}{F_1E_3}+2\,\frac{F_1\,F_2\,E_2\,E_3}{F_1\,E_3}+\frac{F_1^2\,E_2\,E_3^2}{F_1\,E_3}\right)} \\
&= -\frac{p^2}{\sqrt{2\pi}c\sigma\sqrt{T-t}\left(\frac{F_2^2\,E_2}{F_1E_3}+2F_2\,E_2+F_1\,E_2\,E_3\right)} \\
&= -\frac{p^2}{\sqrt{2\pi}c\sigma\sqrt{T-t}\left(\frac{F_2^2\,E_2}{F_1E_3}+2F_2\,E_2+F_1\,E_1\right)}.
\end{aligned}$$

Finally, we combine these results to obtain

$$\begin{aligned}
V_{xt}(t,x) = &\frac{p^2}{\sqrt{2\pi}c\sigma\sqrt{T-t}\,(F_2\,E_2+F_1\,E_1)}-\frac{p^3}{2c^2\sigma^2\left(\frac{F_2}{F_1\,E_3}+2+\frac{F_1\,E_3}{F_2}\right)} \\
&-\frac{p^2}{\sqrt{2\pi}c\sigma\sqrt{T-t}\left(\frac{F_2^2\,E_2}{F_1E_3}+2F_2\,E_2+F_1\,E_1\right)}-\frac{p(e_0-x)}{\sqrt{2\pi}\sigma(T-t)^{\frac{3}{2}}\,(F_2\,E_2+F_1\,E_1)}.
\end{aligned}$$

A.2 Derivatives in Multi-Period Model I

We have determined a solution of the characteristic PDE V^i in Section 3.1.3 as

$$\begin{aligned}
V^i(t,x) = -c\sigma^2\ln\Bigg[&\frac{1}{2}\left(1+\operatorname{erf}\left(\frac{c(e_0-x)+s^i(\Delta T_i-t)}{\sqrt{2}c\sigma\sqrt{\Delta T_i-t}}\right)\right)\mathrm{e}^{\frac{2cs^i(e_0-x)+\left(s^i\right)^2(\Delta T_i-t)}{2c^2\sigma^2}} \\
&+\frac{1}{2}\left(1-\operatorname{erf}\left(\frac{c(e_0-x)+\left(p+s^i\right)(\Delta T_i-t)}{\sqrt{2}c\sigma\sqrt{\Delta T_i-t}}\right)\right)\mathrm{e}^{\frac{2c\left(p+s^i\right)(e_0-x)+\left(p+s^i\right)^2(\Delta T_i-t)}{2c^2\sigma^2}}\Bigg].
\end{aligned}$$

Again we introduce auxiliary functions similar to the ones for the one-period model of Section A.1 as

$$\begin{aligned}
F_1^i(t,x) &= 1 - \operatorname{erf}\left(\frac{c(e_0-x) + \left(p+s^i\right)(\Delta T_i - t)}{\sqrt{2}c\sigma\sqrt{\Delta T_i - t}}\right) \\
F_2^i(t,x) &= 1 + \operatorname{erf}\left(\frac{c(e_0-x) + s^i(\Delta T_i - t)}{\sqrt{2}c\sigma\sqrt{\Delta T_i - t}}\right) \\
E_1^i(t,x) &= \mathrm{e}^{\frac{\left(c(e_0-x)+\left(p+s^i\right)(\Delta T_i-t)\right)^2}{2c^2\sigma^2(\Delta T_i-t)}} \\
E_2^i(t,x) &= \mathrm{e}^{\frac{\left(c(e_0-x)+s^i(\Delta T_i-t)\right)^2}{2c^2\sigma^2(\Delta T_i-t)}} \\
E_3^i(t,x) &= \mathrm{e}^{\frac{2c\left(p+s^i\right)(e_0-x)+\left(p+s^i\right)^2(\Delta T_i-t)}{2c^2\sigma^2}} \\
E_4^i(t,x) &= \mathrm{e}^{\frac{2cs^i(e_0-x)+\left(s^i\right)^2(\Delta T_i-t)}{2c^2\sigma^2}}.
\end{aligned}$$

Then we write

$$V^i(t,x) = -c\sigma^2 \ln\left(\frac{E_4^i(t,x)\,F_2(t,x) + E_3^i(t,x)\,F_1^i(t,x)}{2}\right).$$

In the following, we will again drop the "(t,x)" where necessary to improve readability.

A.2.1 First Derivative V_x^i

From the expression for V^i, we compute the derivative with respect to x as

$$V_x^i = -c\sigma^2 \frac{2}{E_4^i\,F_2^i + E_3^i\,F_1^i} \cdot \frac{1}{2}\left(E_{4,x}^i\,F_2^i + E_4^i\,F_{2,x}^i + E_{3,x}^i\,F_1^i + E_3^i\,F_{1,x}^i\right)$$

where we compute the partial derivatives as

$$\begin{aligned}
F_{1,x}^i(t,x) &= -\frac{2}{\sqrt{\pi}}\,\mathrm{e}^{-\frac{\left(c(e_0-x)+\left(p+s^i\right)(\Delta T_i-t)\right)^2}{2c^2\sigma^2(\Delta T_i-t)}} \cdot \left(-\frac{c}{\sqrt{2}c\sigma\sqrt{\Delta T - t}}\right) \\
&= \frac{\sqrt{2}}{\sqrt{\pi}\sigma\sqrt{\Delta T - t}}\,\frac{1}{E_1(t,x)} \\
F_{2,x}^i(t,x) &= \frac{2}{\sqrt{\pi}}\,\mathrm{e}^{-\frac{\left(c(e_0-x)+s^i(\Delta T_i-t)\right)^2}{2c^2\sigma^2(\Delta T_i-t)}} \cdot \left(-\frac{c}{\sqrt{2}c\sigma\sqrt{\Delta T_i - t}}\right) \\
&= -\frac{\sqrt{2}}{\sqrt{\pi}\sigma\sqrt{\Delta T_i - t}}\,\frac{1}{E_2(t,x)}
\end{aligned}$$

and for the exponential functions we have

$$\begin{aligned} E^i_{3,x}(t,x) &= \mathrm{e}^{\frac{2c\left(p+s^i\right)(e_0-x)+\left(p+s^i\right)^2(\Delta T_i-t)}{2c^2\sigma^2}} \cdot \left(-\frac{2c\left(p+s^i\right)}{2c^2\sigma^2}\right) \\ &= -\frac{p+s^i}{c\sigma^2}\, E^i_3(t,x) \\ E^i_{4,x}(t,x) &= \mathrm{e}^{\frac{2cs^i(e_0-x)+\left(s^i\right)^2(\Delta T_i-t)}{2c^2\sigma^2}} \left(-\frac{2cs^i}{2c^2\sigma^2}\right) \\ &= -\frac{s^i}{c\sigma^2}\, E^i_4(t,x). \end{aligned}$$

Next we compute

$$\begin{aligned} \frac{E^i_1(t,x)}{E^i_2(t,x)} &= \mathrm{e}^{\frac{\left(c(e_0-x)+\left(p+s^i\right)(\Delta T_i-t)\right)^2}{2c^2\sigma^2(\Delta T_i-t)}}\, \mathrm{e}^{-\frac{\left(c(e_0-x)+s^i(\Delta T_i-t)\right)^2}{2c^2\sigma^2(\Delta T_i-t)}} \\ &= \mathrm{e}^{\frac{c^2(e_0-x)^2+2c(e_0-x)(p+s^i)(\Delta T_i-t)+\left(p+s^i\right)^2(\Delta T_i-t)^2-c^2(e_0-x)^2-2cs^i(e_0-x)(\Delta T_i-t)-\left(s^i\right)^2(\Delta T_i-t)^2}{2c^2\sigma^2(\Delta T_i-t)}} \\ &= \mathrm{e}^{\frac{2c(e_0-x)\left(p+s^i\right)(\Delta T_i-t)+\left(p+s^i\right)^2(\Delta T_i-t)^2}{2c^2\sigma^2(\Delta T_i-t)}}\, \mathrm{e}^{-\frac{2cs^i(e_0-x)(\Delta T_i-t)+\left(s^i\right)^2(\Delta T_i-t)^2}{2c^2\sigma^2(\Delta T_i-t)}} \\ &= \frac{E^i_3(t,x)}{E^i_4(t,x)}. \end{aligned}$$

Then clearly we also have

$$\frac{E^i_4(t,x)}{E^i_2(t,x)} = \frac{E^i_3(t,x)}{E^i_1(t,x)}$$

which implies that

$$\begin{aligned} &E^i_4(t,x)\, F^i_{2,x}(t,x) + E^i_3(t,x)\, F^i_{1,x}(t,x) \\ &\quad = -\frac{\sqrt{2}}{\sqrt{\pi}\sigma\sqrt{\Delta T_i - t}}\, \frac{E^i_4(t,x)}{E^i_2(t,x)} + \frac{\sqrt{2}}{\sqrt{\pi}\sigma\sqrt{\Delta T_i - t}}\, \frac{E^i_3(t,x)}{E_1(t,x)} = 0. \end{aligned}$$

We use this to further evaluate the inner derivative as

$$\begin{aligned} &E^i_{4,x}(t,x)\, F^i_2(t,x) + E^i_4(t,x)\, F^i_{2,x}(t,x) + E^i_{3,x}(t,x)\, F^i_1(t,x) + E^i_3(t,x)\, F^i_{1,x}(t,x) \\ &\quad = -\frac{s^i}{c\sigma^2} E^i_4(t,x)\, F^i_2(t,x) - \frac{\sqrt{2}}{\sqrt{\pi}\sigma\sqrt{\Delta T_i - t}}\, \frac{E^i_4(t,x)}{E^i_2(t,x)} - \frac{p+s^i}{c\sigma^2}\, E^i_3(t,x)\, F^i_1(t,x) \\ &\qquad + \frac{\sqrt{2}}{\sqrt{\pi}\sigma\sqrt{\Delta T_i - t}}\, \frac{E^i_3(t,x)}{E^i_1(t,x)} \\ &\quad = -\frac{s^i}{c\sigma^2} E^i_4(t,x)\, F^i_2(t,x) - \frac{p+s^i}{c\sigma^2}\, E^i_3(t,x)\, F^i_1(t,x) \\ &\quad = -\frac{s^i}{c\sigma^2}\left(E^i_4(t,x)\, F^i_2(t,x) + E^i_3(t,x)\, F^i_1(t,x)\right) - \frac{p}{c\sigma^2}\, E^i_3(t,x)\, F^i_1(t,x). \end{aligned}$$

Then we obtain

$$\begin{aligned} V^i_x &= -\frac{c\sigma^2}{E^i_4\, F^i_2 + E^i_3\, F^i_1} \cdot \left(-\frac{s^i}{c\sigma^2}\left(E^i_4\, F^i_2 + E^i_3\, F^i_1\right)\right) - \frac{c\sigma^2}{E^i_4\, F^i_2 + E^i_3\, F^i_1} \cdot \left(-\frac{p}{c\sigma^2}\, E^i_3\, F^i_1\right) \\ &= s^i + \frac{p\, E^i_3\, F^i_1}{E^i_4\, F^i_2 + E^i_3\, F^i_1} = s^i + \frac{p}{\frac{E^i_4\, F^i_2}{E^i_3\, F^i_1} + \frac{E^i_3\, F^i_1}{E^i_3\, F^i_1}} = s^i + \frac{p}{1 + \frac{E^i_4\, F^i_2}{E^i_3\, F^i_1}}. \end{aligned}$$

Furthermore, we have

$$\begin{aligned}\frac{E_4^i(t,x)}{E_3^i(t,x)} &= \mathrm{e}^{\frac{2cs^i(e_0-x)+\left(s^i\right)^2(\Delta T_i-t)}{2c^2\sigma^2}}\,\mathrm{e}^{-\frac{2c\left(p+s^i\right)(e_0-x)+\left(p+s^i\right)^2(\Delta T_i-t)}{2c^2\sigma^2}}\\ &= \mathrm{e}^{\frac{2cs^i(e_0-x)+\left(s^i\right)^2(\Delta T_i-t)-2cp(e_0-x)-2cs^i(e_0-x)-p^2(\Delta T_i-t)-2ps^i(\Delta T_i-t)-\left(s^i\right)^2(\Delta T_i-t)}{2c^2\sigma^2}}\\ &= \mathrm{e}^{-\frac{2cp(e_0-x)+p(p+2s^i)(\Delta T_i-t)}{2c^2\sigma^2}} =: \frac{1}{E_5^i(t,x)}\end{aligned}$$

which delivers the derivative V_x as

$$V_x^i(t,x) = s^i + \frac{p}{1+\frac{F_2^i(t,x)}{E_5^i(t,x)\,F_1^i(t,x)}}$$

and by substituting the auxiliary functions again, we arrive at

$$V_x^i(t,x) = s^i + \frac{p}{1+\frac{\mathrm{e}^{-\frac{2cp(e_0-x)+p(p+2s^i)(\Delta T_i-t)}{2c^2\sigma^2}}\left(1+\mathrm{erf}\left(\frac{c(e_0-x)+s^i(\Delta T_i-t)}{\sqrt{2}c\sigma\sqrt{\Delta T_i-t}}\right)\right)}{1-\mathrm{erf}\left(\frac{c(e_0-x)+\left(p+s^i\right)(\Delta T_i-t)}{\sqrt{2}c\sigma\sqrt{\Delta T_i-t}}\right)}}.$$

A.2.2 Second Derivative V_{xx}^i

We start with the expression of the first derivative

$$V_x^i = s^i + \frac{p\,E_3^i\,F_1^i}{E_4^i\,F_2^i + E_3^i\,F_1^i}$$

as computed above. Then the second derivative can be written as

$$\begin{aligned}V_{xx}^i = &\frac{p\left(E_{3,x}^i\,F_1^i + E_3^i\,F_{1,x}^i\right)\left(E_4^i\,F_2^i + E_3^i\,F_1^i\right)}{\left(E_4^i\,F_2^i + E_3^i\,F_1^i\right)^2}\\ &- \frac{p\,E_3^i\,F_1^i\left(E_{4,x}^i\,F_2^i + E_4^i\,F_{2,x}^i + E_{3,x}^i\,F_1^i + E_3^i\,F_{1,x}^i\right)}{\left(E_4^i\,F_2^i + E_3^i\,F_1^i\right)^2}.\end{aligned}$$

We now use that we have $E_4^i\,F_{2,x}^i + E_3^i\,F_{1,x}^i = 0$ as computed above and rewrite

$$\begin{aligned}V_{xx}^i &= \frac{p\left(E_{3,x}^i\,F_1^i + E_3^i\,F_{1,x}^i\right)\left(E_4^i\,F_2^i + E_3^i\,F_1^i\right) - p\,E_3^i\,F_1^i\left(E_{4,x}^i\,F_2^i + E_{3,x}^i\,F_1^i\right)}{\left(E_4^i\,F_2^i + E_3^i\,F_1^i\right)^2}\\ &= \frac{p\,E_3^i\,F_{1,x}^i}{E_4^i\,F_2^i + E_3^i\,F_1^i} + \frac{p\left(E_{3,x}^i\,F_1^i\,E_4^i\,F_2^i + E_{3,x}^i\,F_1^i\,E_3^i\,F_1^i - E_3^i\,F_1^i\,E_{4,x}^i\,F_2^i - E_3^i\,F_1^i\,E_{3,x}^i\,F_1^i\right)}{\left(E_4^i\,F_2^i + E_3^i\,F_1^i\right)^2}\\ &= \frac{p\,E_3^i\,F_{1,x}^i}{E_4^i\,F_2^i + E_3^i\,F_1^i} + \frac{p\left(E_{3,x}^i\,F_1^i\,E_4^i\,F_2^i + E_3^i\,F_1^i\,E_{4,x}\,F_2^i\right)}{\left(E_4^i\,F_2^i + E_3^i\,F_1^i\right)^2}\\ &=: A^{xx} + B^{xx}.\end{aligned}$$

To simplify the first term, we apply the relationship $\frac{E_1^i}{E_3^i} = \frac{E_2^i}{E_4^i}$ proven above and insert the partial derivative $F_{1,x}^i$. Then

$$\begin{aligned} A^{xx} &= \frac{p \frac{\sqrt{2}}{\sqrt{\pi}\sigma\sqrt{\Delta T - t}} \frac{E_3^i}{E_1^i}}{E_4^i F_2^i + E_3^i F_1^i} \\ &= \frac{p\sqrt{2}}{\sqrt{\pi}\sigma\sqrt{\Delta T_i - t}\left(\frac{E_4^i F_2^i E_1^i}{E_3^i} + \frac{E_3^i F_1^i E_1^i}{E_3^i}\right)} \\ &= \frac{p\sqrt{2}}{\sqrt{\pi}\sigma\sqrt{\Delta T_i - t}\left(\frac{E_4^i F_2^i E_2^i}{E_4^i} + E_1^i F_1^i\right)} \\ &= \frac{p\sqrt{2}}{\sqrt{\pi}\sigma\sqrt{\Delta T_i - t}\left(E_2^i F_2^i + E_1^i F_1^i\right)}. \end{aligned}$$

For the second, we have with the definition of E_5^i that

$$\begin{aligned} B^{xx} &= \frac{p\left(-\frac{p+s^i}{c\sigma^2} E_3^i F_1^i E_4^i F_2^i - \frac{s^i}{c\sigma^2} E_3^i F_1^i E_4^i F_2^i\right)}{\left(E_4^i F_2^i + E_3^i F_1^i\right)^2} \\ &= \frac{-p\frac{p+2s^i}{c\sigma^2} E_3^i F_1^i E_4^i F_2^i}{(E_4^i)^2 (F_2^i)^2 + 2 E_3^i F_1^i E_4^i F_2^i + (E_3^i)^2 (F_1^i)^2} \\ &= -\frac{p(p+2s^i)}{c\sigma^2\left(\frac{E_4^i F_2^i}{E_3^i F_1^i} + 2 + \frac{E_3^i F_1^i}{E_4^i F_2^i}\right)} \\ &= -\frac{p(p+2s^i)}{c\sigma^2\left(\frac{F_2^i}{E_5^i F_1^i} + 2 + \frac{E_5^i F_1^i}{F_2^i}\right)}. \end{aligned}$$

So by combining these results, we obtain

$$V_{xx}^i = \frac{p\sqrt{2}}{\sqrt{\pi}\sigma\sqrt{\Delta T_i - t}\left(E_2^i F_2^i + E_1^i F_1^i\right)} - \frac{p(p+2s^i)}{c\sigma^2\left(\frac{F_2^i}{E_5^i F_1^i} + 2 + \frac{E_5^i F_1^i}{F_2^i}\right)}.$$

A.2.3 Second Derivative V_{xt}^i

We again start with the expression

$$V_x^i(t,x) = s^i + \frac{p\, E_3^i(t,x)\, F_1^i(t,x)}{E_4^i(t,x)\, F_2^i(t,x) + E_3^i(t,x)\, F_1^i(t,x)}.$$

Then we write the derivative with respect to t as

$$\begin{aligned} V_{xt}^i = &\frac{p\left(E_{3,t}^i F_1^i + E_3^i F_{1,t}^i\right)\left(E_4^i F_2^i + E_3^i F_1^i\right)}{\left(E_4^i F_2^i + E_3^i F_1^i\right)^2} \\ &- \frac{p\, E_3^i F_1^i \left(E_{4,t}^i F_2^i + E_4^i F_{2,t}^i + E_{3,t}^i F_1^i + E_3^i F_{1,t}^i\right)}{\left(E_4^i F_2^i + E_3^i F_1^i\right)^2}. \end{aligned}$$

We compute the partial derivatives with respect to t as

$$\begin{aligned}
F^i_{1,t}(t,x) &= -\frac{2}{\sqrt{\pi}}\,\mathrm{e}^{-\frac{\left(c(e_0-x)+\left(p+s^i\right)(\Delta T_i-t)\right)^2}{2c^2\sigma^2(\Delta T_i-t)}}\cdot\left(\frac{-\left(p+s^i\right)\sqrt{2}c\sigma\sqrt{\Delta T_i-t}}{2c^2\sigma^2(\Delta T_i-t)}\right.\\
&\quad\left.-\frac{\left(c(e_0-x)+\left(p+s^i\right)(\Delta T_i-t)\right)\sqrt{2}c\sigma(\Delta T_i-t)^{-\frac{1}{2}}\cdot\frac{1}{2}\cdot(-1)}{2c^2\sigma^2(\Delta T_i-t)}\right)\\
&= -\frac{1}{E^i_1(t,x)}\left(\frac{-\left(p+s^i\right)\sqrt{2}c\sigma\sqrt{\Delta T_i-t}}{\sqrt{\pi}c^2\sigma^2(\Delta T_i-t)}\right.\\
&\quad\left.+\frac{\sqrt{2}c^2\sigma(e_0-x)\frac{1}{2\sqrt{\Delta T_i-t}}+\frac{1}{2}\left(p+s^i\right)\sqrt{2}c\sigma\sqrt{\Delta T_i-t}}{\sqrt{\pi}c^2\sigma^2(\Delta T_i-t)}\right)\\
&= -\frac{1}{E^i_1(t,x)}\,\frac{-\frac{1}{2}\left(p+s^i\right)\sqrt{2}c\sigma\sqrt{\Delta T_i-t}+\sqrt{2}c^2\sigma(e_0-x)\frac{1}{2\sqrt{\Delta T_i-t}}}{\sqrt{\pi}c^2\sigma^2(\Delta T_i-t)}\\
&= \frac{1}{E^i_1(t,x)}\left(\frac{p+s^i}{\sqrt{2\pi}c\sigma\sqrt{\Delta T_i-t}}-\frac{e_0-x}{\sqrt{2\pi}\sigma\left(\Delta T_i-t\right)^{\frac{3}{2}}}\right)
\end{aligned}$$

and

$$\begin{aligned}
F^i_{2,t}(t,x) &= \frac{2}{\sqrt{\pi}}\,\mathrm{e}^{-\frac{\left(c(e_0-x)+s^i(\Delta T_i-t)\right)^2}{2c^2\sigma^2(\Delta T_i-t)}}\cdot\left(\frac{-s^i\sqrt{2}c\sigma\sqrt{\Delta T_i-t}}{2c^2\sigma^2(\Delta T_i-t)}\right.\\
&\quad\left.-\frac{\left(c(e_0-x)+s^i(\Delta T_i-t)\right)\sqrt{2}c\sigma\frac{1}{2}(\Delta T_i-t)^{-\frac{1}{2}}\cdot(-1)}{2c^2\sigma^2(\Delta T_i-t)}\right)\\
&= \frac{1}{E^i_2(t,x)}\,\frac{-s^i\sqrt{2}c\sigma\sqrt{\Delta T_i-t}+\sqrt{2}c^2\sigma(e_0-x)\frac{1}{2\sqrt{\Delta T_i-t}}+\frac{1}{2}\,s^i\sqrt{2}c\sigma\sqrt{\Delta T_i-t}}{\sqrt{\pi}c^2\sigma^2(\Delta T_i-t)}\\
&= \frac{1}{E^i_2(t,x)}\,\frac{-\frac{1}{2}\,s^i\sqrt{2}c\sigma\sqrt{\Delta T_i-t}+\sqrt{2}c^2\sigma(e_0-x)\frac{1}{2\sqrt{\Delta T_i-t}}}{\sqrt{\pi}c^2\sigma^2(\Delta T_i-t)}\\
&= \frac{1}{E^i_2(t,x)}\left(-\frac{s^i}{\sqrt{2\pi}c\sigma\sqrt{\Delta T_i-t}}+\frac{e_0-x}{\sqrt{2\pi}\sigma(\Delta T_i-t)^{\frac{3}{2}}}\right).
\end{aligned}$$

For the exponential functions, we obtain

$$\begin{aligned}
E^i_{3,t}(t,x) &= \mathrm{e}^{\frac{2c\left(p+s^i\right)(e_0-x)+\left(p+s^i\right)^2(\Delta T_i-t)}{2c^2\sigma^2}}\cdot\left(-\frac{\left(p+s^i\right)^2}{2c^2\sigma^2}\right)\\
&= -\frac{\left(p+s^i\right)^2}{2c^2\sigma^2}\,E^i_3(t,x)\\
E^i_{4,t}(t,x) &= \mathrm{e}^{\frac{2cs^i(e_0-x)+\left(s^i\right)^2(\Delta T_i-t)}{2c^2\sigma^2}}\cdot\left(-\frac{\left(s^i\right)^2}{2c^2\sigma^2}\right)\\
&= -\frac{\left(s^i\right)^2}{2c^2\sigma^2}\,E^i_4(t,x).
\end{aligned}$$

Next, with $\frac{E_4^i}{E_2^i} = \frac{E_3^i}{E_1^i}$ as shown above, we compute

$$\begin{aligned}
E_4^i\, F_{2,t}^i + E_3^i\, F_{1,t}^i &= \frac{E_4^i}{E_2^i}\left(-\frac{s^i}{\sqrt{2\pi}c\sigma\sqrt{\Delta T_i - t}} + \frac{e_0 - x}{\sqrt{2\pi}\sigma(\Delta T_i - t)^{\frac{3}{2}}}\right) \\
&\quad + \frac{E_3^i}{E_1^i}\left(\frac{p + s^i}{\sqrt{2\pi}c\sigma\sqrt{\Delta T_i - t}} - \frac{e_0 - x}{\sqrt{2\pi}\sigma\,(\Delta T_i - t)^{\frac{3}{2}}}\right) \\
&= \frac{E_3^i}{E_1^i}\left(-\frac{s^i}{\sqrt{2\pi}c\sigma\sqrt{\Delta T_i - t}} + \frac{e_0 - x}{\sqrt{2\pi}\sigma(\Delta T_i - t)^{\frac{3}{2}}}\right) \\
&\quad + \frac{E_3^i}{E_1^i}\left(\frac{p + s^i}{\sqrt{2\pi}c\sigma\sqrt{\Delta T_i - t}} - \frac{e_0 - x}{\sqrt{2\pi}\sigma\,(\Delta T_i - t)^{\frac{3}{2}}}\right) \\
&= \frac{E_3^i}{E_1^i}\,\frac{p}{\sqrt{2\pi}c\sigma\sqrt{\Delta T_i - t}}.
\end{aligned}$$

We rewrite the expression for V_{xt}^i by splitting up the fraction as[3]

$$\begin{aligned}
V_{xt}^i &= \frac{p\,\left(E_{3,t}^i\, F_1^i + E_3^i\, F_{1,t}^i\right)\left(E_4^i\, F_2^i + E_3^i\, F_1^i\right)}{\left(E_4^i\, F_2^i + E_3^i\, F_1^i\right)^2} \\
&\quad - \frac{p\, E_3^i\, F_1^i\,\left(E_{4,t}^i\, F_2^i + E_4^i\, F_{2,t}^i + E_{3,t}^i\, F_1^i + E_3^i\, F_{1,t}^i\right)}{\left(E_4^i\, F_2^i + E_3^i\, F_1^i\right)^2} \\
&= \frac{p\, E_3^i\, F_{1,t}^i\,\left(E_4^i\, F_2^i + E_3^i\, F_1^i\right) + p\, E_{3,t}^i\, F_1^i\, E_4^i\, F_2^i}{\left(E_4^i\, F_2^i + E_3^i\, F_1^i\right)^2} \\
&\quad + \frac{p\, E_{3,t}^i\, F_1^i\, E_3^i\, F_1^i - p\, E_3^i\, F_1^i\, E_{4,t}^i\, F_2^i - p\, E_3^i\, F_1^i\, E_{3,t}^i\, F_1^i - p\, E_3^i\, F_1^i\,\left(E_4^i\, F_{2,t}^i + E_3^i\, F_{1,t}^i\right)}{\left(E_4^i\, F_2^i + E_3^i\, F_1^i\right)^2} \\
&= \frac{p\, E_3^i\, F_{1,t}^i}{E_4^i\, F_2^i + E_3^i\, F_1^i} + \frac{p\, F_1^i\, F_2^i\,\left(E_{3,t}^i\, E_4^i - E_3^i\, E_{4,t}^i\right)}{\left(E_4^i\, F_2^i + E_3^i\, F_1^i\right)^2} - \frac{p\, E_3^i\, F_1^i\left(E_4^i\, F_{2,t}^i + E_3^i\, F_{1,t}^i\right)}{\left(E_4^i\, F_2^i + E_3^i\, F_1^i\right)^2} \\
&=: A^{xt} + B^{xt} + C^{xt}.
\end{aligned}$$

[3] As in the one-period model, the term A^{xt} is split up further into two terms A^{xt} and D^{xt} in the proof of Proposition 3.3 (iv), where this derivative is needed.

We first consider the term A^{xt}. By inserting for the partial derivative $F^i_{1,t}$ and using that $\frac{E^i_1}{E^i_3} = \frac{E^i_2}{E^i_4}$, we have

$$\begin{aligned}
A^{xt} &= \frac{p\, E^i_3\, F^i_{1,t}}{E^i_4\, F^i_2 + E^i_3\, F^i_1} \\
&= \frac{p\, \frac{E^i_3}{E^i_1} \left(\frac{p+s^i}{\sqrt{2\pi}c\sigma\sqrt{\Delta T_i - t}} - \frac{e_0 - x}{\sqrt{2\pi}\sigma(\Delta T_i - t)^{\frac{3}{2}}} \right)}{E^i_4\, F^i_2 + E^i_3\, F^i_1} \\
&= \frac{p \left(\frac{p+s^i}{\sqrt{2\pi}c\sigma\sqrt{\Delta T_i - t}} - \frac{e_0 - x}{\sqrt{2\pi}\sigma(\Delta T_i - t)^{\frac{3}{2}}} \right)}{\frac{E^i_1\, E^i_4}{E^i_3}\, F^i_2 + \frac{E^i_1\, E^i_3}{E^i_3}\, F^i_1} \\
&= \frac{p\left(p + s^i\right)}{\sqrt{2\pi}c\sigma\sqrt{\Delta T_i - t}\left(E^i_2\, F^i_2 + E^i_1\, F^i_1\right)} - \frac{p(e_0 - x)}{\sqrt{2\pi}\sigma\left(\Delta T_i - t\right)^{\frac{3}{2}}\left(E^i_2\, F^i_2 + E^i_1\, F^i_1\right)}.
\end{aligned}$$

For the second term, we insert the expressions for $E^i_{3,t}$ and $E^i_{4,t}$ to rewrite

$$\begin{aligned}
B^{xt} &= \frac{p\, F^i_1\, F^i_2\, \left(E^i_{3,t}\, E^i_4 - E^i_3\, E^i_{4,t}\right)}{\left(E^i_4\, F^i_2 + E^i_3\, F^i_1\right)^2} \\
&= \frac{p\, F^i_1\, F^i_2 \left(-\frac{\left(p+s^i\right)^2}{2c^2\sigma^2}\, E^i_3\, E^i_4 + \frac{\left(s^i\right)^2}{2c^2\sigma^2}\, E^i_3\, E^i_4 \right)}{\left(E^i_4\, F^i_2 + E^i_3\, F^i_1\right)^2} \\
&= \frac{p\, E^i_3\, F^i_1\, E^i_4\, F^i_2\, \frac{\left(s^i\right)^2 - p^2 - 2ps^i + \left(s^i\right)^2}{2c^2\sigma^2}}{(E^i_4)^2\,(F^i_2)^2 + 2\, E^i_3\, F^i_1\, E^i_4\, F^i_2 + (E^i_3)^2\,(F^i_1)^2} \\
&= -\frac{p^2\left(p + 2s^i\right)}{2c^2\sigma^2\left(\frac{E^i_4\, F^i_2}{E^i_3\, F^i_1} + 2 + \frac{E^i_3\, F^i_1}{E^i_4\, F^i_2}\right)} \\
&= -\frac{p^2\left(p + 2s^i\right)}{2c^2\sigma^2\left(\frac{F^i_2}{E^i_5\, F^i_1} + 2 + \frac{E^i_5\, F^i_1}{F^i_2}\right)}.
\end{aligned}$$

Finally, with the results from above and with $\frac{E^i_4\, E^i_1}{E^i_3} = E^i_2$, we have for the third term

$$\begin{aligned}
C^{xt} &= -\frac{p\, E^i_3\, F^i_1\left(E^i_4\, F^i_{2,t} + E^i_3\, F^i_{1,t}\right)}{\left(E^i_4\, F^i_2 + E^i_3\, F^i_1\right)^2} \\
&= -\frac{p\, E^i_3\, F^i_1\, \frac{E^i_3}{E^i_1}\, \frac{p}{\sqrt{2\pi}c\sigma\sqrt{\Delta T_i - t}}}{(E^i_4)^2\,(F^i_2)^2 + 2\, E^i_3\, F^i_1\, E^i_4\, F^i_2 + (E^i_3)^2\,(F^i_1)^2} \\
&= -\frac{p^2}{\sqrt{2\pi}c\sigma\sqrt{\Delta T_i - t}\left(\frac{(E^i_4)^2\,(F^i_2)^2\, E^i_1}{(E^i_3)^2\, F^i_1} + 2\,\frac{E^i_1\, E^i_3\, F^i_1\, E^i_4\, F^i_2}{(E^i_3)^2\, F^i_1} + \frac{(E^i_3)^2\,(F^i_1)^2\, E^i_1}{(E^i_3)^2\, F^i_1}\right)} \\
&= -\frac{p^2}{\sqrt{2\pi}c\sigma\sqrt{\Delta T_i - t}\left(\frac{E^i_2\, E^i_4\,(F^i_2)^2}{E^i_3\, F^i_1} + 2\,\frac{E^i_1\, E^i_4\, F^i_2}{E^i_3} + E^i_1\, F^i_1\right)} \\
&= -\frac{p^2}{\sqrt{2\pi}c\sigma\sqrt{\Delta T_i - t}\left(\frac{(E^i_2)^2\,(F^i_2)^2}{E^i_1\, F^i_1} + 2\, E^i_2\, F^i_2 + E^i_1\, F^i_1\right)}.
\end{aligned}$$

Combining all terms delivers

$$V^i_{xt} = \frac{p\left(p+s^i\right)}{\sqrt{2\pi}c\sigma\sqrt{\Delta T_i - t}\left(E^i_2\,F^i_2 + E^i_1\,F^i_1\right)} - \frac{p(e_0-x)}{\sqrt{2\pi}\sigma\left(\Delta T_i - t\right)^{\frac{3}{2}}\left(E^i_2\,F^i_2 + E^i_1\,F^i_1\right)}$$
$$- \frac{p^2\left(p+2s^i\right)}{2c^2\sigma^2\left(\frac{F^i_2}{E^i_5\,F^i_1} + 2 + \frac{E^i_5\,F^i_1}{F^i_2}\right)} - \frac{p^2}{\sqrt{2\pi}c\sigma\sqrt{\Delta T_i - t}\left(\frac{(E^i_2)^2\,(F^i_2)^2}{E^i_1\,F^i_1} + 2\,E^i_2\,F^i_2 + E^i_1\,F^i_1\right)}.$$

A.3 Derivatives in the Auction Model

As argued in Section 4.1.1, we obtain the value function and the solution of the characteristic PDE for the auction model, which is denoted by V^A, from the corresponding results in the one-period model by replacing e_0 with $e_F + D_A$; we denote the corresponding solution from the one-period model as V. Then $V^A = V + S_A\,D_A$ and therefore

$$V^A(t,x) = -c\sigma^2 \ln\left(\frac{1+\operatorname{erf}\left(\frac{e_F+D_A-x}{\sqrt{2\sigma^2(T-t)}}\right)}{2}\right.$$
$$\left. + \frac{\left(1-\operatorname{erf}\left(\frac{c(e_F+D_A-x)+p(T-t)}{c\sigma\sqrt{2(T-t)}}\right)\right)\,\mathrm{e}^{\frac{2cp(e_F+D_A-x)+p^2(T-t)}{2c^2\sigma^2}}}{2}\right) + S_A D_A.$$

Again we introduce auxiliary functions, almost identical to the ones in Section A.1; we only need to replace all occurrences of e_0 with $e_F + D_A$:

$$F_1(t,x) = 1 - \operatorname{erf}\left(\frac{c(e_F+D_A) - cx + p(T-t)}{\sqrt{2}c\sigma\sqrt{T-t}}\right)$$
$$F_2(t,x) = 1 + \operatorname{erf}\left(\frac{e_F+D_A-x}{\sqrt{2}\sigma\sqrt{T-t}}\right)$$
$$E_1(t,x) = \mathrm{e}^{\frac{(c(e_F+D_A-x)+p(T-t))^2}{2c^2\sigma^2(T-t)}}$$
$$E_2(t,x) = \mathrm{e}^{\frac{(e_F+D_A-x)^2}{2\sigma^2(T-t)}}$$
$$E_3(t,x) = \mathrm{e}^{\frac{2cp(e_F+D_A-x)+p^2(T-t)}{2c^2\sigma^2}}.$$

Then we can write

$$V(t,x) = -c\sigma^2 \ln\left(\frac{F_2(t,x) + E_3(t,x)\,F_1(t,x)}{2}\right) + S_A D_A.$$

A.3.1 First Derivative V_x

With the results from Section A.1.1, we directly see that the derivative can be written as

$$V_x(t,x) = \frac{p}{1 + \frac{F_2(t,x)}{F_1(t,x)\cdot E_3(t,x)}}$$

since this differs from the one-period model only by the constant $S_A D_A$ and by having $e_F + D_A$ instead of e_0 in the auxiliary functions. By substituting for the auxiliary functions, we obtain

$$V_x(t,x) = \frac{p}{1 + \frac{\mathrm{e}^{-\frac{2cp(e_F+D_A-x)+p^2(T-t)}{2c^2\sigma^2}} \left(1+\mathrm{erf}\left(\frac{e_F+D_A-x}{\sqrt{2}\sigma\sqrt{T-t}}\right)\right)}{1-\mathrm{erf}\left(\frac{c(e_F+D_A)-cx+p(T-t)}{\sqrt{2}c\sigma\sqrt{T-t}}\right)}}.$$

A.3.2 First Derivative V_d

We now view the value function V as a function of t, x and of the auctioned amount of allowances $d = D_A$. Thus we write

$$V(t,x,d) = -c\sigma^2 \ln\left(\frac{1 + \mathrm{erf}\left(\frac{e_F+d-x}{\sqrt{2\sigma^2 t}}\right) + \left(1 - \mathrm{erf}\left(\frac{c(e_F+d-x)+pt}{c\sigma\sqrt{2t}}\right)\right) \mathrm{e}^{\frac{2cp(e_F+d-x)+p^2 t}{2c^2\sigma^2}}}{2}\right) + S_A\, d.$$

Accordingly, we redefine the auxiliary functions as

$$\begin{aligned}
F_1(t,x,d) &= 1 - \mathrm{erf}\left(\frac{c(e_F+d) - cx + p(T-t)}{\sqrt{2}c\sigma\sqrt{T-t}}\right)\\
F_2(t,x,d) &= 1 + \mathrm{erf}\left(\frac{e_F+d-x}{\sqrt{2}\sigma\sqrt{T-t}}\right)\\
E_1(t,x,d) &= \mathrm{e}^{\frac{(c(e_F+d-x)+p(T-t))^2}{2c^2\sigma^2(T-t)}}\\
E_2(t,x,d) &= \mathrm{e}^{\frac{(e_F+d-x)^2}{2\sigma^2(T-t)}}\\
E_3(t,x,d) &= \mathrm{e}^{\frac{2cp(e_F+d-x)+p^2(T-t)}{2c^2\sigma^2}}
\end{aligned}$$

and write

$$V(t,x,d) = -c\sigma^2 \ln\left(\frac{F_2(t,x,d) + E_3(t,x,d)\, F_1(t,x,d)}{2}\right) + S_A\, d.$$

We therefore have for the derivative with respect to d

$$\begin{aligned}
V_d(t,x,d) &= -c\sigma^2 \frac{2}{F_2(t,x,d) + E_3(t,x,d)\, F_1(t,x,d)}\\
&\quad \cdot \frac{1}{2}\left(F_{2,d}(t,x,d) + E_{3,d}(t,x,d)\, F_1(t,x,d) + E_3(t,x,d)\, F_{1,d}(t,x,d)\right) + S_A\\
&= -\frac{c\sigma^2\left(F_{2,d}(t,x,d) + E_{3,d}(t,x,d)\, F_1(t,x,d) + E_3(t,x,d)\, F_{1,d}(t,x,d)\right)}{F_2(t,x,d) + E_3(t,x,d)\, F_1(t,x,d)} + S_A.
\end{aligned}$$

We compute

$$\begin{aligned}
F_{1,d}(t,x,d) &= -\frac{2}{\sqrt{\pi}}\,\mathrm{e}^{-\frac{\left(c(e_F+d)-cx+p(T-t)\right)^2}{2c^2\sigma^2(T-t)}}\,\frac{c}{\sqrt{2}c\sigma\sqrt{T-t}} \\
&= -\frac{\sqrt{2}}{\sqrt{\pi}\sigma\sqrt{T-t}}\,\frac{1}{E_1(t,x,d)} \\
F_{2,d}(t,x,d) &= \frac{2}{\sqrt{\pi}}\,\mathrm{e}^{-\frac{\left(e_F+d-x\right)^2}{2\sigma^2(T-t)}}\,\frac{1}{\sqrt{2}\sigma\sqrt{T-t}} \\
&= \frac{\sqrt{2}}{\sqrt{\pi}\sigma\sqrt{T-t}}\,\frac{1}{E_2(t,x,d)} \\
E_{3,d}(t,x,d) &= \frac{2cp}{2c^2\sigma^2}\,E_3(t,x,d) = \frac{p}{c\sigma^2}\,E_3(t,x,d).
\end{aligned}$$

Similar to Section A.1.1, it can be shown that $E_1(t,x,d) = E_2(t,x,d)\,E_3(t,x,d)$. Thus we obtain

$$\begin{aligned}
&F_{2,d}(t,x,d) + E_3(t,x,d)\,F_{1,d}(t,x,d) \\
&\quad= \frac{\sqrt{2}}{\sqrt{\pi}\sigma\sqrt{T-t}}\,\frac{1}{E_2(t,x,d)} - \frac{\sqrt{2}}{\sqrt{\pi}\sigma\sqrt{T-t}}\,\frac{E_3(t,x,d)}{E_1(t,x,d)} \\
&\quad= \frac{\sqrt{2}}{\sqrt{\pi}\sigma\sqrt{T-t}}\,\frac{1}{E_2(t,x,d)} - \frac{\sqrt{2}}{\sqrt{\pi}\sigma\sqrt{T-t}}\,\frac{E_3(t,x,d)}{E_2(t,x,d)\,E_3(t,x,d)} = 0.
\end{aligned}$$

Then we have

$$\begin{aligned}
V_d(t,x,d) &= -\frac{c\sigma^2\,\frac{p}{c\sigma^2}\,E_3(t,x,d)\,F_1(t,x,d)}{F_2(t,x,d) + E_3(t,x,d)\,F_1(t,x,d)} + S_A \\
&= -\frac{p}{1+\frac{F_2(t,x,d)}{E_3(t,x,d)\,F_1(t,x,d)}} + S_A.
\end{aligned}$$

A.3.3 Second Derivative V_{xx}

Similar to the case of the first derivative V_x, we obtain the second derivative V_{xx} directly from the one-period model without auctioning by replacing e_0 with $e_F + D_A$ in the auxiliary functions, thus we have

$$V_{xx}(t,x) = \frac{p\sqrt{2}}{\sqrt{\pi}\sigma\sqrt{T-t}\,(F_2\,E_2 + F_1\,E_1)} - \frac{p^2}{c\sigma^2\left(\frac{F_2}{F_1\,E_3} + 2 + \frac{F_1\,E_3}{F_2}\right)}$$

and with Proposition 4.1

$$V_{dd}(t,x) = \frac{p\sqrt{2}}{\sqrt{\pi}\sigma\sqrt{T-t}\,(F_2\,E_2 + F_1\,E_1)} - \frac{p^2}{c\sigma^2\left(\frac{F_2}{F_1\,E_3} + 2 + \frac{F_1\,E_3}{F_2}\right)}.$$

To assess the sign of this expression, another formulation for V_{dd} might be more helpful. From the derivation of V_{xx} in the one-period model without auctioning, we have

$$\begin{aligned}
V_{dd} &= \frac{p\,(F_{1,x}\,E_3 + F_1\,E_{3,x})\;(F_2 + F_1\,E_3) - p\,F_1\,E_3\,(F_{2,x} + F_{1,x}\,E_3 + F_1\,E_{3,x})}{(F_2 + F_1\,E_3)^2} \\
&= \frac{p\,F_2\;(F_{1,x}\,E_3 + F_1\,E_{3,x}) + p\,F_1\,E_3\,(F_{1,x}\,E_3 + F_1\,E_{3,x})}{(F_2 + F_1\,E_3)^2} \\
&\quad - \frac{p\,F_1\,E_3\,F_{2,x} - p\,F_1\,E_3\,(F_{1,x}\,E_3 + F_1\,E_{3,x})}{(F_2 + F_1\,E_3)^2} \\
&= \frac{p\,F_2\,F_{1,x}\,E_3 + p\,F_2\,F_1\,E_{3,x} - p\,F_1\,E_3\,F_{2,x}}{(F_2 + F_1\,E_3)^2} \\
&= \frac{p\,F_2 \cdot \frac{2}{\sqrt{2\pi}\sigma\sqrt{T-t}} \cdot \frac{1}{E_1}\,E_3 + p\,F_2\,F_1 \cdot \left(-\frac{p}{c\sigma^2}\,E_3\right) - p\,F_1\,E_3 \cdot \left(-\frac{2}{\sqrt{2\pi}\sigma\sqrt{T-t}} \cdot \frac{1}{E_2}\right)}{(F_2 + F_1\,E_3)^2} \\
&= \frac{p\,E_3\,\left(\frac{2}{\sqrt{2\pi}\sigma\sqrt{T-t}}\left(\frac{F_2}{E_1} + \frac{F_1}{E_2}\right) - \frac{p}{c\sigma^2}\,F_1\,F_2\right)}{(F_2 + F_1\,E_3)^2}.
\end{aligned}$$

Also in this expression, it is not straight-forward to show that the nominator is positive.

A.4 Auxiliary Computations in the Multi-Period Model

A.4.1 Quadratic Covariation of W^i

The shifted Brownian motion W^i defined in Section 3.1 does not start in zero, as $W_0^i = W_{T_i}$, and is therefore not a standard Brownian motion. By introducing the shifted filtration $\mathcal{F}^i$ given by $\mathcal{F}_t^i = \mathcal{F}_{T_i+t}$, we observe that W^i satisfies all other properties of a Brownian motion with respect to $\mathcal{F}_i$. In particular, W^i is adapted to $\mathcal{F}^i$ and has independent, normally distributed increments. Then for $s < t$, we have as in the standard case

$$\begin{aligned}
\mathrm{E}\left[\left(W_t^i\right)^2 - t \,\middle|\, \mathcal{F}_s^i\right] &= \mathrm{E}\left[\left(W_t^i - W_s^i + W_s^i\right)^2 - t \,\middle|\, \mathcal{F}_s\right] \\
&= \mathrm{E}\left[\left(E_t^i - W_s^i\right)^2\right] + 2\,W_s^i\,\mathrm{E}\left[W_t^i - W_s^i\right] + \left(W_s^i\right)^2 - t \\
&= t - s + \left(W_s^i\right)^2 - t = \left(W_s^i\right)^2 - s
\end{aligned}$$

and therefore the quadratic variation of W^i is given as $\left[W^i\right]_t = t$. With

$$X_t^i = X_0^i - \int_0^t u_s^i \mathrm{d}s + \int_0^t G^i(s)\mathrm{d}W_s^i$$

we obtain that

$$\left[X^i\right]_t = \left[\int G^i(s)\mathrm{d}W_s^i\right]_t = \int_0^t \left(G^i(s)\right)^2 \mathrm{d}s.$$

Similarly, with

$$Z_t^i = Z_0^i + \int_0^t H^i(s)\mathrm{d}W_s^i,$$

we compute the quadratic variation

$$\left[Z^i\right]_t = \left[\int H^i(s)\mathrm{d}W_s^i\right]_t = \int_0^t \left(H^i(s)\right)^2 \mathrm{d}s$$

and the quadratic covariation

$$\left[X^i, Z^i\right] = \left[\int G^i(s)\mathrm{d}W_s^i, \int H^i(s)\mathrm{d}W_s^i\right]_t = \int_0^t G^i(s)\, H^i(s)\mathrm{d}s.$$

Appendix B

Additional Proofs

This section provides additional proofs that were omitted in the main text of the thesis.

B.1 Properties of V^i in Multi-Period Model I

In Section 3.1.3 we formulated the following statement on the properties of the PDE solution V^i in the simple variant of multi-period model I; since the proof is very similar to the one provided for the corresponding statement in the one-period model, we did not include it in the main part of the thesis.

Proposition 3.3. *The function V^i as given by (3.5) and its derivative V^i_x given by (3.6) satisfy the following properties:*

(i) *V^i is infinitely differentiable on $(-\infty, \Delta T_i) \times \mathbb{R}$, i.e. $V^i \in C^\infty\left((-\infty, \Delta T_i) \times \mathbb{R}\right)$.*

(ii) *V^i_x satisfies $s^i \leq V^i_x(t,x) \leq p + s^i$ for all $(t,x) \in [0, \Delta T_i] \times \mathbb{R} \backslash \{(\Delta T_i, e_0)\}$, i.e. V^i_x is bounded.*

(iii) *For any $t \in [0, \Delta T_i]$ we have*

$$\lim_{x \to \infty} V^i_x(t,x) = p + s^i \quad \text{and} \quad \lim_{x \to -\infty} V^i_x(t,x) = s^i.$$

(iv) *Let $\varepsilon > 0$ arbitrary. Then the derivatives V^i_{xx} and V^i_{xt} are bounded on $[0, \Delta T_i - \varepsilon] \times \mathbb{R}$.*

Proof. To simplify notation, we again introduce some auxiliary functions; note that these are similar to the auxiliary functions for the one-period model in Section 2.3.2 and identical

to the ones in Section A.2:

$$
\begin{aligned}
F_1^i(t,x) &= 1 - \operatorname{erf}\left(\frac{c(e_0-x) + \left(p+s^i\right)(\Delta T_i - t)}{\sqrt{2}c\sigma\sqrt{\Delta T_i - t}}\right)\\
F_2^i(t,x) &= 1 + \operatorname{erf}\left(\frac{c(e_0-x) + s^i(\Delta T_i - t)}{\sqrt{2}c\sigma\sqrt{\Delta T_i - t}}\right)\\
E_1^i(t,x) &= \mathrm{e}^{\frac{\left(c(e_0-x)+\left(p+s^i\right)(\Delta T_i-t)\right)^2}{2c^2\sigma^2(\Delta T_i-t)}}\\
E_2^i(t,x) &= \mathrm{e}^{\frac{\left(c(e_0-x)+s^i(\Delta T_i-t)\right)^2}{2c^2\sigma^2(\Delta T_i-t)}}\\
E_3^i(t,x) &= \mathrm{e}^{\frac{2c\left(p+s^i\right)(e_0-x)+\left(p+s^i\right)^2(\Delta T_i-t)}{2c^2\sigma^2}}\\
E_4^i(t,x) &= \mathrm{e}^{\frac{2cs^i(e_0-x)+\left(s^i\right)^2(\Delta T_i-t)}{2c^2\sigma^2}}\\
E_5^i(t,x) &= \mathrm{e}^{\frac{2cp(e_0-x)+p(p+2s^i)(\Delta T_i-t)}{2c^2\sigma^2}}.
\end{aligned}
$$

Due to the similarities to the auxiliary functions used in the one-period model, we directly observe that for any $x \in \mathbb{R}$ and any $t \in (-\infty, \Delta T_i)$, all these functions are well-defined and we have that

$$F_1^i(t,x) > 0 \quad \text{and} \quad F_2^i(t,x) > 0$$

as well as

$$E_1^i(t,x) > 0, \quad E_2^i(t,x) > 0, \quad E_3^i(t,x) > 0, \quad E_4^i(t,x) > 0 \quad \text{and} \quad E_5^i(t,x) > 0.$$

(i) We know that ν^i is infinitely differentiable on $(0,\infty)\times\mathbb{R}$. Then after time reversion

$$\tilde{\nu}^i(t,x) = \frac{E_4^i(t,x)\,F_2^i(t,x) + E_2^i(t,x)\,F_1^i(t,x)}{2}$$

is infinitely differentiable on $(-\infty, \Delta T_i)\times\mathbb{R}$. Again all auxiliary functions are positive, so the range of $\tilde{\nu}^i$ is $(0,\infty)$. Since the back transformation is again essentially the natural logarithm, the function V^i as the composition of $\tilde{\nu}^i$ and the back transformation is also infinitely differentiable on $(-\infty, \Delta T_i)\times\mathbb{R}$.

(ii) For $t \in [0, \Delta T_i)$ and $x \in \mathbb{R}$, we may write

$$V_x^i(t,x) = \frac{p}{1 + \frac{F_2^i(t,x)}{E_5^i(t,x)\,F_1^i(t,x)}} + s^i.$$

Since the auxiliary functions are all positive, we obtain that

$$0 \le \frac{p}{1 + \frac{F_2^i(t,x)}{E_5^i(t,x)\,F_1^i(t,x)}} \le p$$

and thus

$$s^i \le V_x^i(t,x) \le p + s^i$$

follows. For $t = \Delta T_i$ and $x \neq e_0$ we have

$$V_x^i(\Delta T_i, x) = \begin{cases} p + s^i & \text{if} \quad x > e_0, \\ s^i & \text{if} \quad x < e_0 \end{cases}$$

and the claim follows immediately.

(iii) We assume that $t \in [0, \Delta T_i)$ since for $t = \Delta T_i$ this can be seen directly. We start with the limit $x \to \infty$. We have

$$\lim_{x\to\infty} F_2^i(t,x) = 0 \quad \text{and} \quad \lim_{x\to\infty} E_5^i(t,x) = 0$$

and with l'Hôpital's rule we compute

$$\begin{aligned}
\lim_{x\to\infty} \frac{F_2^i(t,x)}{E_5^i(t,x)} &= \lim_{x\to\infty} \frac{1 + \operatorname{erf}\left(\frac{c(e_0-x)+s^i(\Delta T_i - t)}{\sqrt{2}c\sigma\sqrt{\Delta T_i - t}}\right)}{\mathrm{e}^{\frac{2cp(e_0-x)+p(p+2s^i)(\Delta T_i-t)}{2c^2\sigma^2}}} = \lim_{x\to\infty} \frac{\frac{\partial}{\partial x}\left(1 + \operatorname{erf}\left(\frac{c(e_0-x)+s^i(\Delta T_i - t)}{\sqrt{2}c\sigma\sqrt{\Delta T_i - t}}\right)\right)}{\frac{\partial}{\partial x}\mathrm{e}^{\frac{2cp(e_0-x)+p(p+2s^i)(\Delta T_i-t)}{2c^2\sigma^2}}} \\
&= \lim_{x\to\infty} \frac{-\frac{\sqrt{2}}{\sqrt{\pi}\sigma\sqrt{\Delta T_i - t}}\,\mathrm{e}^{-\frac{\left(c(e_0-x)+s^i(\Delta T_i-t)\right)^2}{2c^2\sigma^2(\Delta T_i-t)}}}{-\frac{p}{c\sigma^2}\,\mathrm{e}^{\frac{2cp(e_0-x)+p(p+2s^i)(\Delta T_i-t)}{2c^2\sigma^2}}} \\
&= \lim_{x\to\infty} \frac{\sqrt{2}c\sigma}{\sqrt{\pi}p\sqrt{\Delta T_i - t}}\,\mathrm{e}^{\frac{-\left(c(e_0-x)+s^i(\Delta T_i-t)\right)^2 - 2cp(e_0-x)(\Delta T_i-t) - p(p+2s^i)(\Delta T_i-t)^2}{2c^2\sigma^2(\Delta T_i-t)}} = 0
\end{aligned}$$

since the term of highest order in the polynomial in the exponential function has a negative coefficient. Then with $\lim_{x\to\infty} F_1^i(t,x) = 2$ we obtain

$$\lim_{x\to\infty} V_x^i(t,x) = \lim_{x\to\infty} \left(\frac{p}{1 + \frac{F_2^i(t,x)}{E_5^i(t,x)\,F_1^i(t,x)}} + s^i\right) = \frac{p}{1+0} + s^i = p + s^i.$$

For the limit $x \to -\infty$ we first observe that

$$\lim_{x\to-\infty} F_1^i(t,x) = 0 \quad \text{and} \quad \lim_{x\to-\infty} \frac{1}{E_5^i(t,x)} = 0.$$

We then apply l'Hôpital's rule as

$$\begin{aligned}
&\lim_{x\to-\infty} \frac{\left(E_5^i(t,x)\right)^{-1}}{F_1^i(t,x)} \\
&= \lim_{x\to-\infty} \frac{\mathrm{e}^{-\frac{2cp(e_0-x)+p(p+2s^i)(\Delta T_i-t)}{2c^2\sigma^2}}}{1 - \operatorname{erf}\left(\frac{c(e_0-x)+(p+s^i)(\Delta T_i-t)}{\sqrt{2}c\sigma\sqrt{\Delta T_i - t}}\right)} = \lim_{x\to-\infty} \frac{\frac{\partial}{\partial x}\,\mathrm{e}^{-\frac{2cp(e_0-x)+p(p+2s^i)(\Delta T_i-t)}{2c^2\sigma^2}}}{\frac{\partial}{\partial x}\left(1 - \operatorname{erf}\left(\frac{c(e_0-x)+(p+s^i)(\Delta T_i-t)}{\sqrt{2}c\sigma\sqrt{\Delta T_i - t}}\right)\right)} \\
&= \lim_{x\to-\infty} \frac{\frac{p}{c\sigma^2}\,\mathrm{e}^{-\frac{2cp(e_0-x)+p(p+2s^i)(\Delta T_i-t)}{2c^2\sigma^2}}}{\frac{\sqrt{2}}{\sqrt{\pi}\sigma\sqrt{\Delta T_i - t}}\,\mathrm{e}^{-\frac{\left(c(e_0-x)+(p+s^i)(\Delta T_i-t)\right)^2}{2c^2\sigma^2(\Delta T_i-t)}}} \\
&= \lim_{x\to-\infty} \frac{\sqrt{\pi}p\sqrt{\Delta T_i - t}}{\sqrt{2}c\sigma}\,\mathrm{e}^{\frac{\left(c(e_0-x)+(p+s^i)(\Delta T_i-t)\right)^2 - 2cp(e_0-x)(\Delta T_i-t) - p(p+2s^i)(\Delta T_i-t)^2}{2c^2\sigma^2(\Delta T_i-t)}} = \infty
\end{aligned}$$

because in this case the term of highest order has a positive coefficient. Since we have $\lim_{x\to-\infty} F_2^i(t,x) = 2$, this results in

$$\lim_{x\to-\infty} V_x^i(t,x) = \lim_{x\to-\infty} \left(\frac{p}{1 + \frac{F_2^i(t,x)}{E_5^i(t,x)\,F_1^i(t,x)}} + s^i\right) = 0 + s^i = s^i.$$

(iv) Let $\varepsilon > 0$ be arbitrary and let $t \in [0, \Delta T_i - \varepsilon]$. We first consider the derivative V^i_{xx}. As can be seen in Section A.2.2, we can write this as

$$\begin{aligned} V^i_{xx}(t,x) &= \frac{p\sqrt{2}}{\sqrt{\pi}\sigma\sqrt{\Delta T_i - t}\left(E^i_2(t,x)\,F^i_2(t,x) + E^i_1(t,x)\,F^i_1(t,x)\right)} \\ &\quad - \frac{p(p+2s^i)}{c\sigma^2\left(\frac{F^i_2(t,x)}{E^i_5(t,x)\,F^i_1(t,x)} + 2 + \frac{E^i_5(t,x)\,F^i_1(t,x)}{F^i_2(t,x)}\right)} \\ &=: A^{xx} + B^{xx}. \end{aligned}$$

Since the auxiliary functions are positive, we have for the second term B^{xx}

$$B^{xx} = -\frac{p(p+2s^i)}{c\sigma^2\left(\frac{F^i_2(t,x)}{E^i_5(t,x)\,F^i_1(t,x)} + 2 + \frac{E^i_5(t,x)\,F^i_1(t,x)}{F^i_2(t,x)}\right)} \geq -\frac{p(p+2s^i)}{2c\sigma^2}$$

and

$$B^{xx} = -\frac{p(p+2s^i)}{c\sigma^2\left(\frac{F^i_2(t,x)}{E^i_5(t,x)\,F^i_1(t,x)} + 2 + \frac{E^i_5(t,x)\,F^i_1(t,x)}{F^i_2(t,x)}\right)} < 0,$$

thus B^{xx} is bounded. For the term A^{xx}, we also obtain the lower bound directly as

$$A^{xx} = \frac{p\sqrt{2}}{\sqrt{\pi}\sigma\sqrt{\Delta T_i - t}\left(E^i_2(t,x)\,F^i_2(t,x) + E^i_1(t,x)\,F^i_1(t,x)\right)} > 0$$

with the auxiliary functions being positive. For the upper bound, we have that $E^i_1(t,x) \geq 1$ and $E^i_2(t,x) \geq 1$ as in the one-period model. We again perform a case distinction: First we assume that $x \leq e_0$. We may show that then $F^i_2(t,x) \geq 1$ which implies

$$E^i_2(t,x)\,F^i_2(t,x) + E^i_1(t,x)\,F^i_1(t,x) > 1.$$

Next we assume that $x \geq e_0 + {}^{(p+s^i)\Delta T_i}/_c$. In this case we obtain that $F^i_1(t,x) \geq 1$ and therefore we again have

$$E^i_2(t,x)\,F^i_2(t,x) + E^i_1(t,x)\,F^i_1(t,x) > 1.$$

Together these results imply that if $x \leq e_0$ or $x \geq e_0 + {}^{(p+s^i)\Delta T_i}/_c$, we have

$$A^{xx} = \frac{p\sqrt{2}}{\sqrt{\pi}\sigma\sqrt{\Delta T_i - t}\left(E^i_2(t,x)\,F^i_2(t,x) + E^i_1(t,x)\,F^i_1(t,x)\right)} \leq \frac{p\sqrt{2}}{\sqrt{\pi}\sigma\sqrt{\Delta T_i - t}}.$$

This expression is increasing in t and therefore we obtain an upper bound by setting $t = \Delta T_i - \varepsilon$ as

$$A^{xx} < \frac{p\sqrt{2}}{\sqrt{\pi}\sigma\sqrt{\varepsilon}}.$$

Thus we have shown that V^i_{xx} is bounded on $[0, \Delta T_i - \varepsilon] \times ((-\infty, e_0] \cup [e_0 + {}^{(p+s^i)\Delta T_i}/_c, \infty))$. But since V^i_{xx} is continuous by part (i) of this Proposition, we may apply the extreme value theorem to conclude that V^i_{xx} is also bounded on the bounded and closed set $[0, \Delta T_i - \varepsilon] \times [e_0, e_0 + {}^{(p+s^i)\Delta T_i}/_c]$. By combining these results, the claim follows.

It remains to consider the derivative V^i_{xt}. In Section A.2.3 we derive this as

$$\begin{aligned}
V^i_{xt}(t,x) = &\frac{p\left(p+s^i\right)}{\sqrt{2\pi}c\sigma\sqrt{\Delta T_i - t}\left(E^i_2(t,x)\,F^i_2(t,x) + E^i_1(t,x)\,F^i_1(t,x)\right)} \\
&- \frac{p^2\left(p+2s^i\right)}{2c^2\sigma^2\left(\frac{F^i_2(t,x)}{E^i_5(t,x)\,F^i_1(t,x)} + 2 + \frac{E^i_5(t,x)\,F^i_1(t,x)}{F^i_2(t,x)}\right)} \\
&- \frac{p^2}{\sqrt{2\pi}c\sigma\sqrt{\Delta T_i - t}\left(\frac{(E^i_2(t,x))^2\,(F^i_2(t,x))^2}{E^i_1(t,x)\,F^i_1(t,x)} + 2\,E^i_2(t,x)\,F^i_2(t,x) + E^i_1(t,x)\,F^i_1(t,x)\right)} \\
&- \frac{p(e_0-x)}{\sqrt{2\pi}\sigma\,(\Delta T_i - t)^{\frac{3}{2}}\left(E^i_2(t,x)\,F^i_2(t,x) + E^i_1(t,x)\,F^i_1(t,x)\right)} \\
=:\ &A^{xt} + B^{xt} + C^{xt} + D^{xt}.
\end{aligned}$$

We observe that similar to the one-period model we have $A^{xt} = \frac{p+s^i}{2}\,A^{xx}$ and $B^{xt} = \frac{p}{2}\,B^{xt}$, therefore it remains to consider the terms C^{xt} and D^{xt}. Since the auxiliary functions are positive, we have

$$\begin{aligned}
C^{xt} &= -\frac{p^2}{\sqrt{2\pi}c\sigma\sqrt{\Delta T_i - t}\left(\frac{(E^i_2(t,x))^2\,(F^i_2(t,x))^2}{E^i_1(t,x)\,F^i_1(t,x)} + 2\,E^i_2(t,x)\,F^i_2(t,x) + E^i_1(t,x)\,F^i_1(t,x)\right)} \\
&> -\frac{p^2}{\sqrt{2\pi}c\sigma\sqrt{\Delta T_i - t}\left(E^i_2(t,x)\,F^i_2(t,x) + E^i_1(t,x)\,F^i_1(t,x)\right)} \\
&> -\frac{p^2 + ps^i}{\sqrt{2\pi}c\sigma\sqrt{\Delta T_i - t}\left(E^i_2(t,x)\,F^i_2(t,x) + E^i_1(t,x)\,F^i_1(t,x)\right)} = -A^{xt} = -\frac{p+s^i}{2}A^{xx}
\end{aligned}$$

and A^{xx} is bounded from below as shown above. The upper bound is simply given as

$$C^{xt} = -\frac{p^2}{\sqrt{2\pi}c\sigma\sqrt{\Delta T_i - t}\left(\frac{(E^i_2(t,x))^2\,(F^i_2(t,x))^2}{E^i_1(t,x)\,F^i_1(t,x)} + 2\,E^i_2(t,x)\,F^i_2(t,x) + E^i_1(t,x)\,F^i_1(t,x)\right)} < 0.$$

For the final term D^{xt}, we again perform a case distinction. In the first case, we assume that $x < e_0$, which directly delivers the upper bound as

$$D^{xt} = -\frac{p(e_0-x)}{\sqrt{2\pi}\sigma\,(\Delta T_i - t)^{\frac{3}{2}}\left(E^i_2(t,x)\,F^i_2(t,x) + E^i_1(t,x)\,F^i_1(t,x)\right)} < 0.$$

Furthermore, we may show that $F^i_2(t,x) > 1$ and then we have

$$\begin{aligned}
D^{xt} &= -\frac{p(e_0-x)}{\sqrt{2\pi}\sigma\,(\Delta T_i - t)^{\frac{3}{2}}\left(E^i_2(t,x)\,F^i_2(t,x) + E^i_1(t,x)\,F^i_1(t,x)\right)} \\
&> -\frac{p(e_0-x)}{\sqrt{2\pi}\sigma\,(\Delta T_i - t)^{\frac{3}{2}}\;E^i_2(t,x)} =: g(t,x).
\end{aligned}$$

As in the one-period model we have $\lim_{x\to-\infty} p(e_0-x) = \infty$ and

$$\lim_{x\to-\infty}\sqrt{2\pi}\sigma\,(\Delta T_i - t)^{\frac{3}{2}}\;E^i_2(t,x) = \lim_{x\to-\infty}\sqrt{2\pi}\sigma\,(\Delta T_i - t)^{\frac{3}{2}}\;\mathrm{e}^{\frac{\left(c(e_0-x)+s^i(\Delta T_i - t)\right)^2}{2c^2\sigma^2(\Delta T_i - t)}} = \infty,$$

so we can apply l'Hôpital's rule to compute the limit of g as $x \to \infty$. We have

$$\begin{aligned}\frac{\partial E_2^i(t,x)}{\partial x} &= \mathrm{e}^{\frac{\left(c(e_0-x)+s^i(\Delta T_i-t)\right)^2}{2c^2\sigma^2(\Delta T_i-t)}} \frac{2\left(c(e_0-x)+s^i(\Delta T_i-t)\right)}{2c^2\sigma^2(\Delta T_i-t)} \cdot (-c) \\ &= -\frac{c(e_0-x)+s^i(\Delta T_i-t)}{c\sigma^2(\Delta T_i-t)} E_2^i(t,x)\end{aligned}$$

and therefore

$$\begin{aligned}\lim_{x\to-\infty} g(t,x) &= -\lim_{x\to-\infty} \frac{p(e_0-x)}{\sqrt{2\pi}\sigma\left(\Delta T_i-t\right)^{\frac{3}{2}} E_2^i(t,x)} \\ &= -\lim_{x\to-\infty} \frac{-p}{-\sqrt{2\pi}\sigma\left(\Delta T_i-t\right)^{\frac{3}{2}} \frac{c(e_0-x)+s^i(\Delta T_i-t)}{c\sigma^2(\Delta T_i-t)} E_2^i(t,x)} \\ &= -\lim_{x\to-\infty} \frac{p}{\frac{\sqrt{2\pi}}{c\sigma^2}\sqrt{\Delta T_i-t}\left(c(e_0-x)+s^i(\Delta T_i-t)\right) E_2^i(t,x)} \\ &= 0.\end{aligned}$$

Then we compute

$$\begin{aligned}\frac{\partial E_2^i(t,x)}{\partial t} &= \mathrm{e}^{\frac{\left(c(e_0-x)+s^i(\Delta T_i-t)\right)^2}{2c^2\sigma^2(\Delta T_i-t)}} \left(\frac{2\left(c(e_0-x)+s^i(\Delta T_i-t)\right)\cdot(-s^i)\cdot 2c^2\sigma^2(\Delta T_i-t)}{4c^4\sigma^4(\Delta T_i-t)^2}\right. \\ &\qquad \left. - \frac{\left(c(e_0-x)+s^i(\Delta T_i-t)\right)^2\cdot(-2c^2\sigma^2)}{4c^4\sigma^4(\Delta T_i-t)^2}\right) \\ &= E_2^i(t,x)\frac{\left(c(e_0-x)+s^i(\Delta T_i-t)\right)\left(-2s^i(\Delta T_i-t)+c(e_0-x)+s^i(\Delta T_i-t)\right)}{2c^2\sigma^2(\Delta T_i-t)^2} \\ &= E_2^i(t,x)\frac{c^2(e_0-x)^2-\left(s^i\right)^2(\Delta T_i-t)^2}{2c^2\sigma^2(\Delta T_i-t)^2}\end{aligned}$$

and therefore we have

$$\begin{aligned}\frac{\partial g(t,x)}{\partial t} &= \frac{p(e_0-x)\sqrt{2\pi}\sigma E_2^i(t,x)}{2\pi\sigma^2(\Delta T_i-t)^3 E_2^i(t,x)^2}\left(\frac{3}{2}\left(\Delta T_i-t\right)^{\frac{1}{2}}\cdot(-1)\right. \\ &\qquad \left. + \left(\Delta T_i-t\right)^{\frac{3}{2}}\frac{c^2(e_0-x)^2-\left(s^i\right)^2(\Delta T_i-t)^2}{2c^2\sigma^2(\Delta T_i-t)^2}\right) \\ &= \frac{p(e_0-x)}{\sqrt{2\pi}\sigma(\Delta T_i-t)^3 E_2^i(t,x)}\left(-\frac{3}{2}\sqrt{\Delta T_i-t}+\frac{c^2(e_0-x)^2-\left(s^i\right)^2(\Delta T_i-t)^2}{2c^2\sigma^2\sqrt{\Delta T_i-t}}\right).\end{aligned}$$

Since we assumed $x < e_0$, this is positive if

$$\frac{c^2(e_0-x)^2-\left(s^i\right)^2(\Delta T_i-t)^2}{2c^2\sigma^2\sqrt{\Delta T_i-t}} > \frac{3}{2}\sqrt{\Delta T_i-t}$$

which is equivalent to

$$(e_0-x)^2 > 3\sigma^2(\Delta T_i-t)+\frac{\left(s^i\right)^2}{c^2}(\Delta T_i-t)^2.$$

We know that $e_0 - x > 0$, so we can equivalently require

$$x < e_0 - \sqrt{3\sigma^2(\Delta T_i - t) + \frac{(s^i)^2}{c^2}(\Delta T_i - t)^2}.$$

This expression is increasing in t, implying for any $t \in [0, \Delta T_i - \varepsilon]$ that

$$e_0 - \sqrt{3\sigma^2 \Delta T_i + \frac{(s^i)^2}{c^2}\Delta T_i^2} < e_0 - \sqrt{3\sigma^2(\Delta T_i - t) + \frac{(s^i)^2}{c^2}(\Delta T_i - t)^2}.$$

Thus for any x satisfying

$$x < e_0 - \sqrt{3\sigma^2 \Delta T_i + \frac{(s^i)^2}{c^2}\Delta T_i^2},$$

we have that $\frac{\partial}{\partial t} g(t,x) > 0$, which implies that g is strictly increasing in t. Therefore we may conclude that

$$g(t,x) \geq g(0,x) \quad \text{for any } t \in [0, \Delta T_i - \varepsilon].$$

But since $\lim_{x \to -\infty} g(0,x) = 0$ as shown above, we may now apply Lemma 2.8: We choose $K > 0$ such that there exists $\tilde{x}_1$ so that $|g(0,x)| < K$ for all $x < \tilde{x}_1$. So by setting

$$x_1 = \min \left\{ \tilde{x}_1, e_0 - \sqrt{3\sigma^2 \Delta T_i + \frac{(s^i)^2}{c^2}\Delta T_i^2} \right\},$$

we obtain that

$$g(0,x) > -K \quad \text{for all} \quad x < x_1.$$

Hence we have a lower bound for D^{xt} with

$$D^{xt} > g(t,x) \geq g(0,x) > -K.$$

For the second case, we assume that $x > e_0 + {}^{(p+s^i)\Delta T_i}/_c$. Then in particular we have $x > e_0$ and therefore

$$D^{xt} = -\frac{p(e_0 - x)}{\sqrt{2\pi}\sigma\,(\Delta T_i - t)^{\frac{3}{2}}\left(E_2^i(t,x)\,F_2^i(t,x) + E_1^i(t,x)\,F_1^i(t,x)\right)} > 0.$$

For the lower bound, we recall that $F_1^i(t,x) \geq 1$, so we have

$$\begin{aligned} D^{xt} &= -\frac{p(e_0 - x)}{\sqrt{2\pi}\sigma\,(\Delta T_i - t)^{\frac{3}{2}}\left(E_2^i(t,x)\,F_2^i(t,x) + E_1^i(t,x)\,F_1^i(t,x)\right)} \\ &< -\frac{p(e_0 - x)}{\sqrt{2\pi}\sigma\,(\Delta T_i - t)^{\frac{3}{2}}\;E_1^i(t,x)} =: h(t,x). \end{aligned}$$

By applying l'Hôpital's rule, we obtain that $\lim_{x \to \infty} h(t,x) = 0$, which works in the same way as in the one-period model. We then compute the derivative with respect to t. In analogy to the above, we have

$$\frac{\partial E_1^i(t,x)}{\partial t} = E_1^i(t,x)\,\frac{c^2(e_0 - x)^2 - \left(p + s^i\right)^2(\Delta T_i - t)^2}{2c^2\sigma^2(\Delta T_i - t)^2}$$

and therefore

$$\frac{\partial h(t,x)}{\partial t} = \frac{p(e_0-x)}{\sqrt{2\pi}\sigma(\Delta T_i - t)^3\, E_1^i(t,x)} \left(\frac{c^2(e_0-x)^2 - \left(p+s^i\right)^2 (\Delta T_i - t)^2}{2c^2\sigma^2\sqrt{\Delta T_i - t}} - \frac{3}{2}\sqrt{\Delta T_i - t} \right).$$

Since now $x > e_0$, this expression is negative if

$$\frac{c^2(e_0-x)^2 - \left(p+s^i\right)^2 (\Delta T_i - t)^2}{2c^2\sigma^2\sqrt{\Delta T_i - t}} > \frac{3}{2}\sqrt{\Delta T_i - t},$$

which is equivalent to

$$(e_0-x)^2 > 3\sigma^2(\Delta T_i - t) + \frac{\left(p+s^i\right)^2}{c^2}(\Delta T_i - t)^2.$$

With $e_0 - x < 0$, we rewrite this as

$$-(e_0-x) > \sqrt{3\sigma^2(\Delta T_i - t) + \frac{\left(p+s^i\right)^2}{c^2}(\Delta T_i - t)^2}$$

and, equivalently, as

$$x > e_0 + \sqrt{3\sigma^2(\Delta T_i - t) + \frac{\left(p+s^i\right)^2}{c^2}(\Delta T_i - t)^2}.$$

Here the right-hand side is decreasing in t, so this inequality holds for all $t \in [0, \Delta T_i - \varepsilon]$ if

$$x > e_0 + \sqrt{3\sigma^2\Delta T_i + \frac{\left(p+s^i\right)^2}{c^2}\Delta T_i^2}.$$

Then $\frac{\partial}{\partial t}h(t,x) < 0$ and therefore h is strictly decreasing in t on $[0, \Delta T_i - \varepsilon]$, which implies that

$$h(t,x) \leq h(0,x) \quad \text{for any } t \in [0, \Delta T_i - \varepsilon].$$

We have $\lim_{x\to\infty} h(0,x)$, so we proceed as above by applying Lemma 2.8: We choose $K > 0$, then there exists $\tilde{x}_2$ such that $|h(0,x)| < K$ for all $x > \tilde{x}_2$. Therefore by setting

$$x_2 \coloneqq \max\left\{ \tilde{x}_2, e_0 + \sqrt{3\sigma^2\Delta T_i + \frac{\left(p+s^i\right)^2}{c^2}\Delta T_i^2} \right\},$$

we have that

$$h(t,x) \leq h(0,x) < K \quad \text{for all} \quad t \in [0, \Delta T_i - \varepsilon] \quad \text{and for all} \quad x > x_2,$$

which delivers the upper bound as

$$D^{xt} < h(t,x) \leq h(0,x) < K$$

on $[0, \Delta T_i - \varepsilon] \times (x_2, \infty)$.

Thus we have shown that V_{xt}^i is bounded on $[0, \Delta T_i - \varepsilon] \times ((-\infty, x_1) \cup (x_2, \infty))$. Since V_{xt}^i is continuous on the bounded and closed set $[0, \Delta T_i - \varepsilon] \times [x_1, x_2]$, we apply the extreme value theorem to conclude that V_{xt}^i is bounded on $[0, \Delta T_i - \varepsilon] \times \mathbb{R}$. □

Additionally, in Section 3.1.3, we stated two results on the PDE solution V^i and the corresponding control u^i, which served to ensure applicability of the verification theorem for the HJB equations. The proofs to these statements can be found in the following.

Proposition 3.4. *The functions V^i given by equation (3.5) for $t \in [0, \Delta T_i)$ and by the terminal condition of the PDE for $t = \Delta T_i$ satisfy the requirements of the verification theorem for the HJB equation, i.e. we have*

(i) V^i is continuously differentiable in t and twice continuously differentiable in x on $[0, \Delta T_i) \times \mathbb{R}$,

(ii) V^i is continuous on $[0, \Delta T_i] \times \mathbb{R}$,

(iii) V^i satisfies a quadratic growth condition, uniformly in t, i.e. there exists $K > 0$ such that

$$|V^i(t,x)| \leq K\left(1 + |x|^2\right) \quad \textit{for all} \quad t \in [0, \Delta T_i].$$

Proof. (i) This follows directly with Proposition 3.3 (i).

(ii) In Proposition 3.2 we have shown that the solution ν^i of the transformed PDE converges to the initial value function when $(t,x) \to (0, \xi_0)$. For the solution after time reversion $\tilde{\nu}^i$, we therefore have

$$\lim_{(t,x)\to(\Delta T_i, \xi_{\Delta T_i})} \tilde{\nu}^i(t,x) = \mathrm{e}^{-\frac{P^i\left(\xi_{\Delta T_i}\right)}{c\sigma^2}}$$

for any $\xi_{\Delta T_i} \in \mathbb{R}$. As discussed in the proof of Proposition 3.3 (i), the back transformation function is essentially the natural logarithm and therefore continuous on $(0, \infty)$, which is the image of $[0, \Delta T_i) \times \mathbb{R}$ under $\tilde{\nu}^i$. Thus also the back transformed function V^i converges to the initial value function given by P^i, i.e.

$$\lim_{(t,x)\to(\Delta T_i, \xi_{\Delta T_i})} V^i(t,x) = P^i(\xi_{\Delta T_i}).$$

Since V^i is continuous on $[0, \Delta T_i) \times \mathbb{R}$ and P^i is continuous on $\mathbb{R}$, we conclude that V^i is continuous on $[0, \Delta T_i] \times \mathbb{R}$.

(iii) We first let $t \in [0, \Delta T_i)$ arbitrary. Then we have with Proposition 3.3 that $s^i \leq V^i_x(t,x) \leq p + s^i$ for any $x \in \mathbb{R}$. By applying the fundamental theorem of calculus we obtain

$$\begin{aligned} |V^i(t,x)| &= \left| \int_{e_0}^{x} V^i_x(t,y)\mathrm{d}y + V^i(t,e_0) \right| \\ &\leq \int_{e_0}^{x} |V^i_x(t,y)|\mathrm{d}y + |V^i(t,e_0)| \leq \left(p + s^i\right)|x - e_0| + |V^i(t,e_0)|. \end{aligned}$$

We now consider $V^i(t,e_0)$ given as

$$\begin{aligned} V^i(t,e_0) = -c\sigma^2 \ln \Bigg[&\frac{1}{2}\left(1 + \operatorname{erf}\left(\frac{s^i\sqrt{\Delta T_i - t}}{\sqrt{2}c\sigma}\right)\right) \mathrm{e}^{\frac{\left(s^i\right)^2(\Delta T_i - t)}{2c^2\sigma^2}} \\ &+ \frac{1}{2}\left(1 - \operatorname{erf}\left(\frac{\left(p + s^i\right)\sqrt{\Delta T_i - t}}{\sqrt{2}c\sigma}\right)\right) \mathrm{e}^{\frac{\left(p+s^i\right)^2(\Delta T_i - t)}{2c^2\sigma^2}} \Bigg]. \end{aligned}$$

Since the arguments of the error functions are non-negative, we have

$$1 \leq 1 + \operatorname{erf}\left(\frac{s^i\sqrt{\Delta T_i - t}}{\sqrt{2}c\sigma}\right) \leq 2 \quad \text{and} \quad 0 \leq 1 - \operatorname{erf}\left(\frac{\left(p + s^i\right)\sqrt{\Delta T_i - t}}{\sqrt{2}c\sigma}\right) \leq 1,$$

and as the arguments of the exponential functions are also non-negative, it holds that

$$\mathrm{e}^{\frac{\left(s^i\right)^2(\Delta T_i - t)}{2c^2\sigma^2}} \geq 1 \quad \text{and} \quad \mathrm{e}^{\frac{\left(p+s^i\right)^2(\Delta T_i - t)}{2c^2\sigma^2}} \geq 1.$$

Then we have

$$\begin{aligned}\frac{1}{2} &\leq \frac{1}{2}\left(1 + \operatorname{erf}\left(\frac{s^i\sqrt{\Delta T_i - t}}{\sqrt{2}c\sigma}\right)\right)\mathrm{e}^{\frac{\left(s^i\right)^2(\Delta T_i - t)}{2c^2\sigma^2}} + \frac{1}{2}\left(1 - \operatorname{erf}\left(\frac{\left(p + s^i\right)\sqrt{\Delta T_i - t}}{\sqrt{2}c\sigma}\right)\right)\mathrm{e}^{\frac{\left(p+s^i\right)^2(\Delta T_i - t)}{2c^2\sigma^2}} \\ &\leq \mathrm{e}^{\frac{\left(s^i\right)^2\Delta T_i}{2c^2\sigma^2}} + \frac{1}{2}\mathrm{e}^{\frac{\left(p+s^i\right)^2\Delta T_i}{2c^2\sigma^2}}.\end{aligned}$$

Since the logarithm is monotonically increasing, this is equivalent to

$$-c\sigma^2 \ln\left(\frac{1}{2}\right) \geq V^i(t, e_0) \geq -c\sigma^2 \ln\left(\mathrm{e}^{\frac{\left(s^i\right)^2\Delta T_i}{2c^2\sigma^2}} + \frac{1}{2}\mathrm{e}^{\frac{\left(p+s^i\right)^2\Delta T_i}{2c^2\sigma^2}}\right)$$

and thus $V^i(t, e_0)$ is bounded by a constant. We may conclude that $V^i(t, x)$ is linearly bounded in x, uniformly in t for $t \in [0, \Delta T_i)$. It remains to consider the case that $t = \Delta T_i$. But then V^i is given by the terminal condition of the PDE, which is piecewise linear and therefore linearly bounded. □

Proposition 3.5. *Fix a time period i and let X be a continuous $\mathbb{R}$-valued stochastic process on $[0, \Delta T_i]$ which is $\mathcal{F}^i$-adapted. Then for any $t \in [0, \Delta T_i]$ the control process u^i given by*

$$u^i = \left(u^i_s\right)_{s\in[t,\Delta T_i]} = \left(u^i(s, X_s)\right)_{s\in[t,\Delta T_i]} \quad \textit{where} \quad u^i(s, x) = \frac{V^i_x(s, x)}{c}$$

lies in $\mathcal{A}^i(t)$.

Proof. Since u^i is continuous as a function of x on $[0, \Delta T_i)$ by Proposition 3.3 (i) and piecewise constant for $t = \Delta T_i$, we obtain that u^i is $\mathcal{F}^i$-adapted from $\mathcal{F}^i$-adaptedness of X. By Proposition 3.3 (i), we have that u^i is right-continuous as a function of t; with continuity of X, we conclude that u^i is progressively measurable.

Furthermore, by Proposition 3.3 (iv), we know that V^i_x is bounded and $V^i_x \geq 0$. Therefore $u^i \in \mathcal{U}$ and

$$\mathrm{E}\left[\int_t^{\Delta T_i} |u^i_s|^2 \mathrm{d}s\right] = \mathrm{E}\left[\int_t^{\Delta T_i} \left|\frac{V^i_x(s, X_s)}{c}\right|^2 \mathrm{d}s\right] < \infty,$$

thus $u^i \in \mathcal{A}^i(t)$. □

Appendix C

Additional Numerical Results

In this section we present numerical results that were not discussed in Chapter 6. These include additional results in the Ornstein-Uhlenbeck model variant as well as results obtained in the simple model variant with a lower volatility σ or a modified amount of initially expected BAU emissions x_0.

C.1 Numerical Results in the Ornstein-Uhlenbeck Model

C.1.1 One-Period Model

In the one-period model, we omitted most of the results of varying different regulatory parameters obtained in the Ornstein-Uhlenbeck model variant as these are very similar to the ones presented for the Brownian variant. In Figure C.1 the results for varying the penalty p are shown. Figures C.2 and C.3 show the corresponding graphics obtained when varying the emission cap e_0.

C.1.2 Multi-Period Model I

Due to the high similarity between the Brownian and the Ornstein-Uhlenbeck model variants, in Section 6.2 we did not discuss the results obtained in the Ornstein-Uhlenbeck variant of multi-period model I. As explained in Section 5.3.3, we now have $\theta = 0.04$ and $\mu = 2000$. With the very small value for θ, the results in the one-period model presented in Section 6.1.5 suggest that the difference to the Brownian model variant should be small. However, in the multi-period model, the choice of the model variant also affects the initially expected emissions for each time period, given by x_0^i. In the simple variant, they were chosen to be constant. As shown in Figure C.4a, the value of x_0^i decreases linearly in case of the Brownian model variant. In the Ornstein-Uhlenbeck model variant, it approaches the long term mean of $3\,\mu = 6000$; for the small value of $\theta = 0.04$, this happens very slowly. As a result, x_0^i is much higher than in the Brownian model for all time periods. Since the allowance price at the beginning of each time period is increasing in the initially expected emissions, we observe in Figure C.4b that the price parameter s^i is higher than in the Brownian model variant; at the same time, it decreases only very slowly in the early time periods if allowances cannot be transferred.

The difference in x_0^i leads to a different behavior of the mean trajectory of X and in particular of the mean realized emissions. As can be seen in Figure C.5a, the value reached by the mean trajectory at the end of each time period (i.e. the realized emissions X_{T_i})

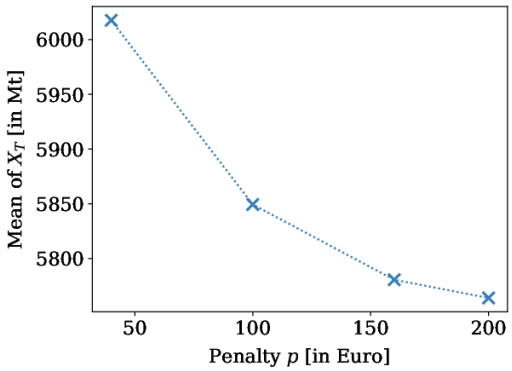

(a) Mean of realized emissions X_T.

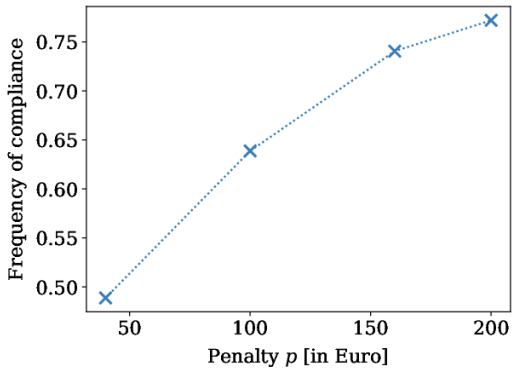

(b) Relative frequency of compliance with the emission target e_0.

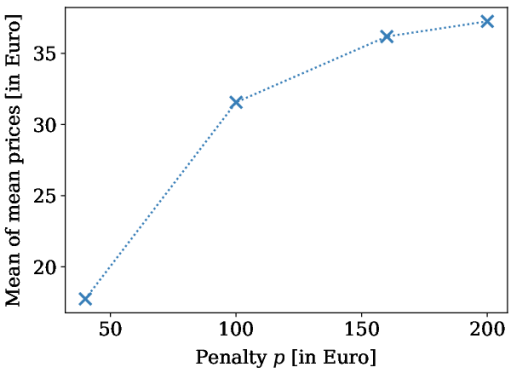

(c) Mean across all runs of the mean prices within one time period.

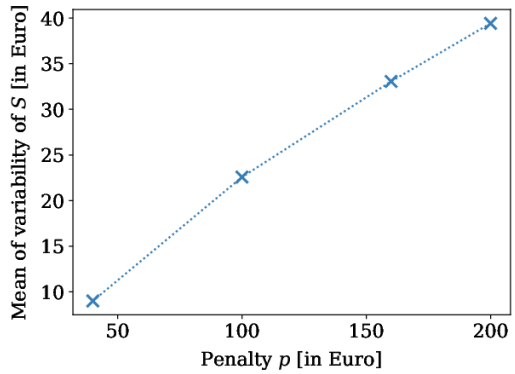

(d) Mean of the variability of the price S.

Figure C.1: Results for varying penalties p in the Ornstein-Uhlenbeck model variant of the one-period model.

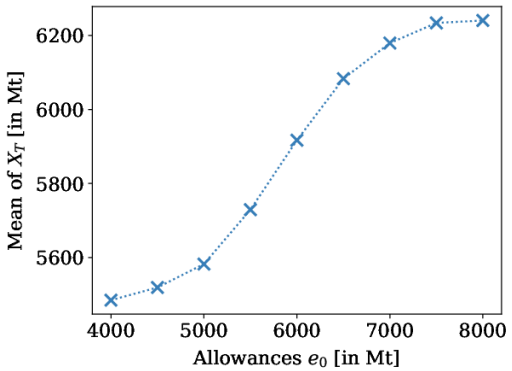

(a) Mean of realized emissions X_T.

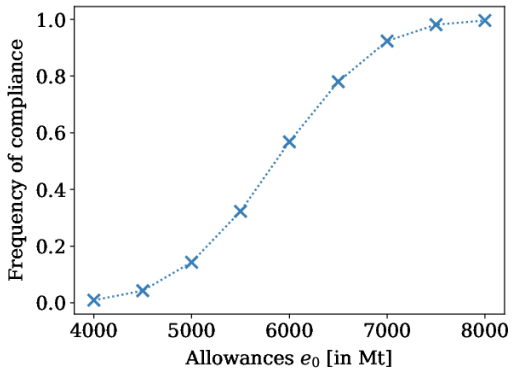

(b) Relative frequency of compliance with the emission target e_0.

Figure C.2: Results on the total expected emissions X for a varying number of allowances in the Ornstein-Uhlenbeck model variant of the one-period model.

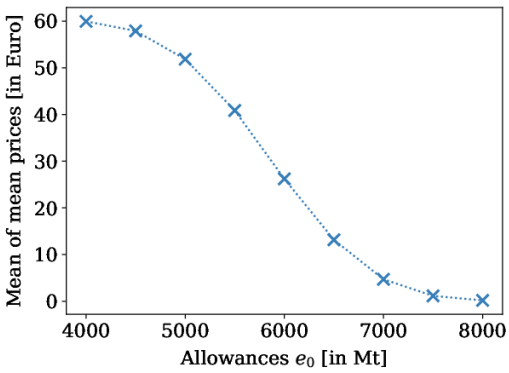

(a) Mean across all runs of the mean prices within one time period

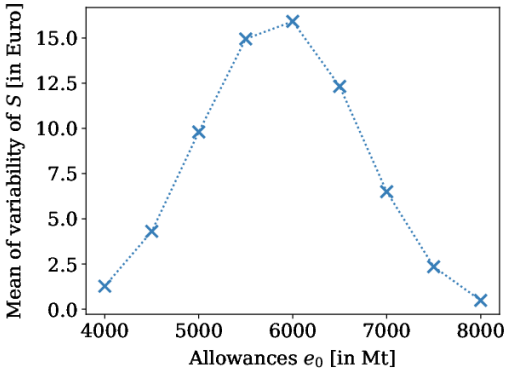

(b) Mean of the variability of the price S.

Figure C.3: Results on the allowance price S for a varying number of allowances in the Ornstein-Uhlenbeck model variant of the one-period model.

decreases for the second time period but increases afterwards. In comparison, in case of the Brownian model variant, this value is decreasing throughout the overall time horizon. In the early time periods, the price parameter s^i in both model variants is high, resulting in high abatement and correspondingly, in low realized emissions. But for later time periods s^i attains lower values, which reduces the incentive for abatement; while in the Brownian variant, the low value of x_0^i still causes low realized emissions, in the Ornstein-Uhlenbeck variant, x_0^i has barely changed so that realized emissions increase again. Although the mean of the realized emissions is different between the two model variants, the structure of its distribution is barely changed, as can be seen in Figures C.5b, C.5c, and C.5d. The resulting frequency of complying with the emission cap is given in Table C.1. We observe that in early time periods, the frequency of compliance is higher than in the Brownian model variant, possibly due to the higher price parameter s^i. For later time periods, compliance is lower, which is probably caused by the differences in x_0^i discussed above.

Table C.1: Relative frequency of compliance in an ETS with transferable or non-transferable allowances in the Ornstein-Uhlenbeck model variant of multi-period model I.

Time period	0	1	2	3	4	5
Transferable	65.09%	57.83%	56.64%	55.79%	54.33%	52.2%
Non-transferable	53.35%	52.39%	52.08%	52.91%	52.36%	51.56%

The characteristics of the allowance price S, visualized in Figure C.6, largely remain unaffected.

In Figure C.7 we show the effect of varying the penalty on the usual characteristics of the system; again the general behavior of the quantities studied is similar as in the Brownian variant, while the absolute numbers differ slightly.

C.1.3 Multi-Period Model II

As in multi-period model I, we omitted the Ornstein-Uhlenbeck variant from the analysis in Section 6.3. In Figure C.8 the mean trajectory of the total expected emissions X and the distributions of the realized emissions X_T for different time periods are shown; in

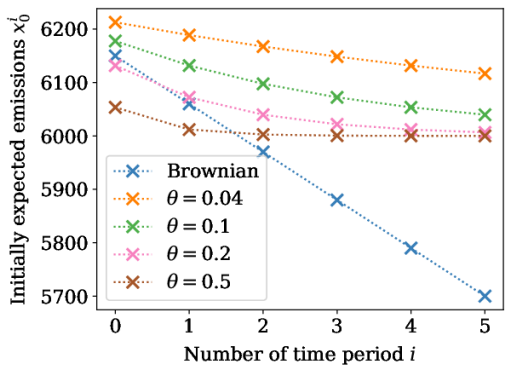

(a) Initially expected emissions x_0^i for each time period in the Brownian variant and for varying θ in the Ornstein-Uhlenbeck variant.

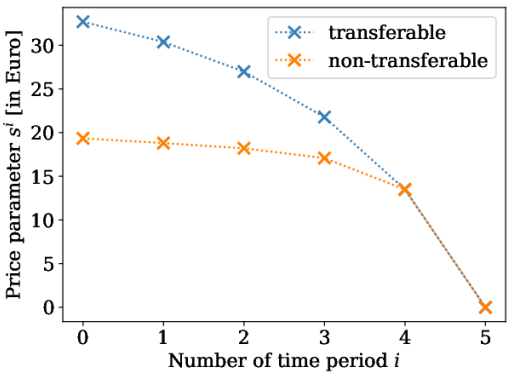

(b) Price input parameters s^i computed from the price function of the subsequent time period in the Ornstein-Uhlenbeck model variant.

Figure C.4: Initially expected emissions x_0^i and price input parameters s^i for all six time periods in multi-period model I.

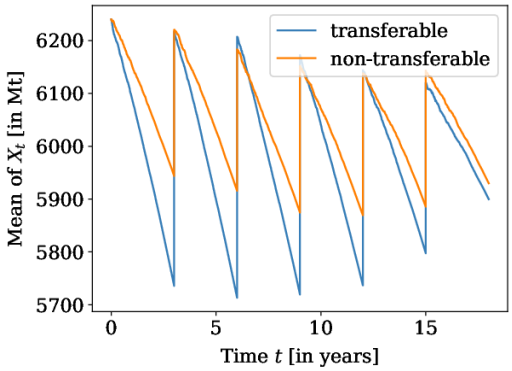

(a) Mean trajectory of X.

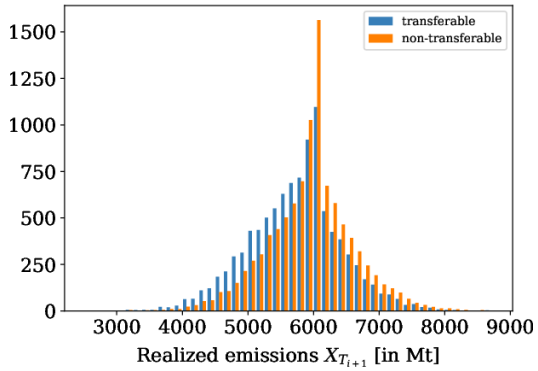

(b) Histogram of realized emissions $X_{T_{i+1}}$ in time period 0.

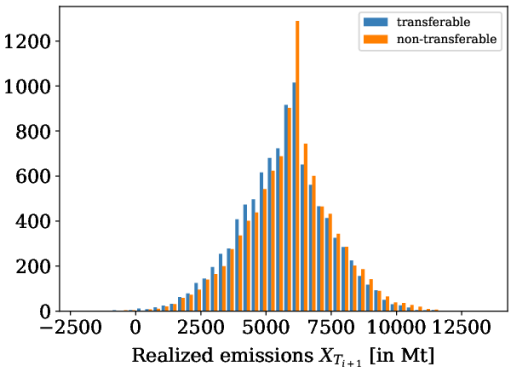

(c) Histogram of realized emissions $X_{T_{i+1}}$ in time period 2.

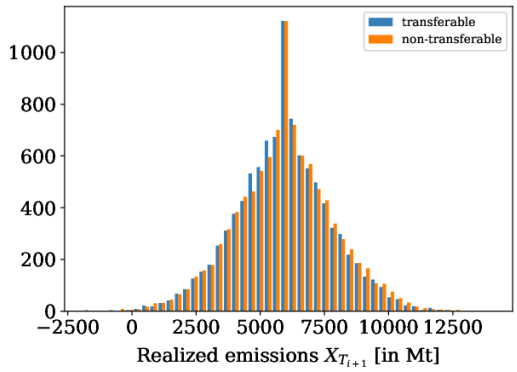

(d) Histogram of realized emissions $X_{T_{i+1}}$ in the last time period.

Figure C.5: Mean trajectory of X and distributions of realized emissions $X_{T_{i+1}}$ in an ETS with transferable or non-transferable allowances in the Ornstein-Uhlenbeck model variant of multi-period model I.

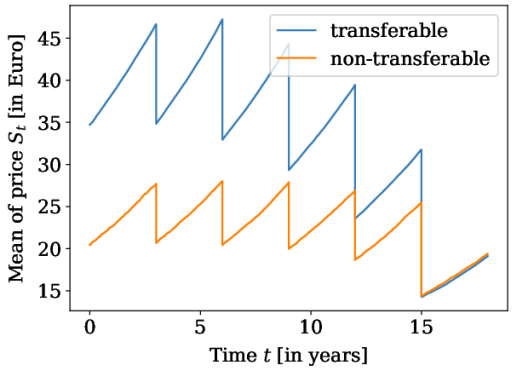

(a) Mean trajectory of S.

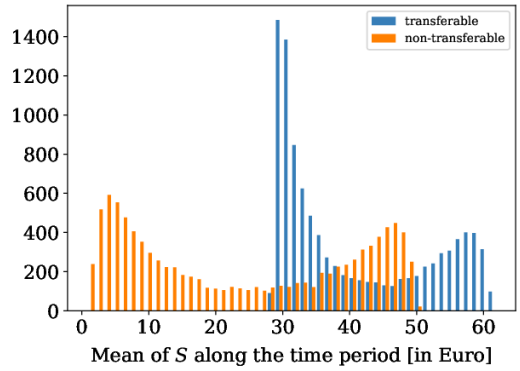

(b) Histogram of mean allowance prices within each run for time period 0.

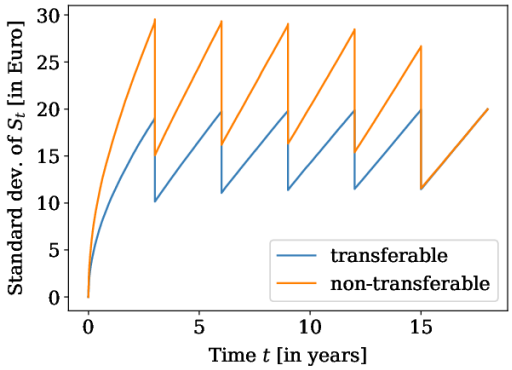

(c) Standard deviation trajectory of S.

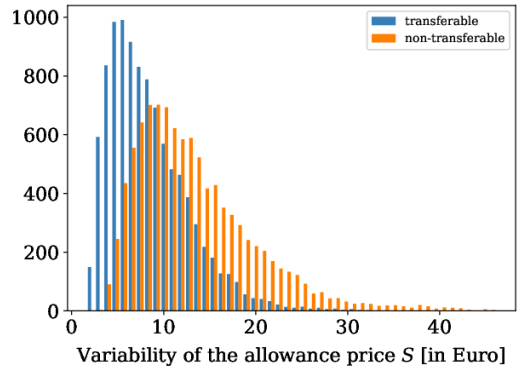

(d) Histogram of the standard deviation of absolute daily returns of S for time period 0, normalized to one year.

Figure C.6: Results on the allowance price S in an ETS with transferable or non-transferable allowances in the Ornstein-Uhlenbeck model variant of multi-period model I.

each case, we visualize the results both for the system where the transfer of allowances is possible and the case where this is not allowed. As the main difference to the Brownian model variant, we observe that the mean realized emissions decrease in the first three time periods but then increase again (this can be most clearly seen in Figure C.8a); in the Brownian model variant, this quantity decreases throughout most of the overall time period. This is in line with the observation made in multi-period model I; the reason for this behavior is again the difference in the development of the initially expected emissions x_0^i, as shown in Figure C.4a.

Table C.2 reports the relative frequency of compliance; these values are only very slightly lower than in case of the Brownian model variant.

Table C.2: Relative frequency of compliance in an ETS with transferable or non-transferable allowances in the Ornstein-Uhlenbeck model variant of multi-period model II.

Time period	0	1	2	3	4	5
Transferable	70.27%	62.01%	59.82%	58.78%	57.5%	55.46%
Non-transferable	61.11%	57.19%	56.69%	55.73%	54.65%	54.18%

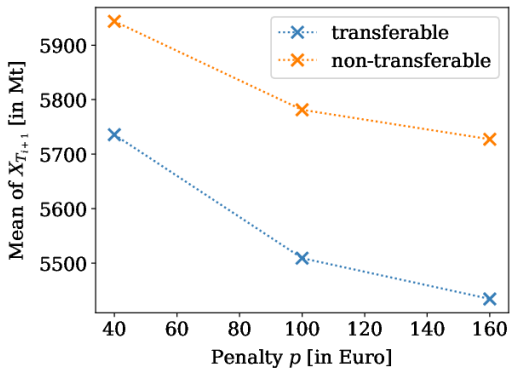

(a) Mean of realized emissions X_T.

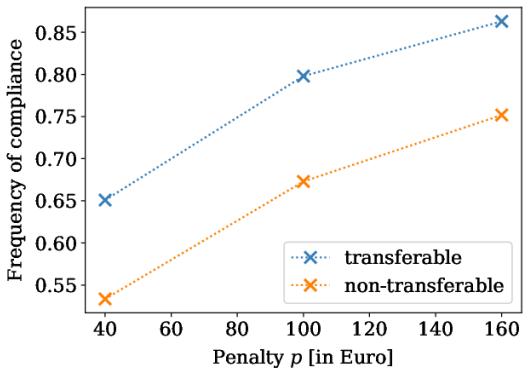

(b) Relative frequency of compliance with the emission target e_0.

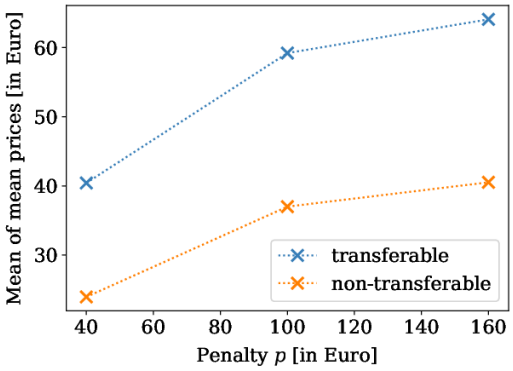

(c) Mean across all runs of the mean prices within one time period.

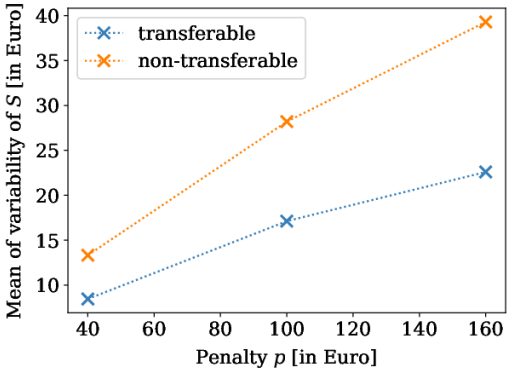

(d) Mean of the variability of the price S.

Figure C.7: Results for a varying penalty in the Ornstein-Uhlenbeck model variant in an ETS with transferable or non-transferable allowances of multi-period model I.

The mean price trajectory and the trajectory of the standard deviation as well as the distributions of the mean price within one run and the price variability are shown in Figures C.9 and C.10; they barely show any difference to the Brownian model variant.

In Figure C.11 the impact of varying the penalty p on resulting emissions and the behavior of the allowance price is visualized; as in the Brownian model variant, we observe a clear kink at a penalty of p, meaning that an increase in the penalty from 40 to 100 has a strong effect on the behavior of the system.

C.2 Numerical Results in the Simple Model Variant with Changed Parameter Settings

As discussed in Section 5.3.3, the value of the volatility parameter σ is particularly difficult to estimate. Therefore, we repeated many simulations with a smaller value of $\sigma = 115.47$; the results are shown in this section.

At the start of the EU ETS, it proved to be challenging to determine the BAU emissions to be expected in the first phase, which are represented by the parameter x_0 in our model.

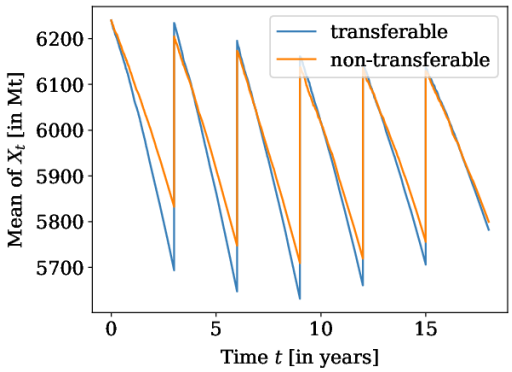

(a) Mean trajectory of X.

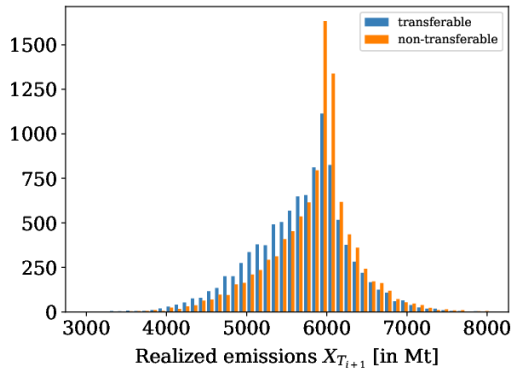

(b) Histogram of realized emissions $X_{T_{i+1}}$ in time period 0.

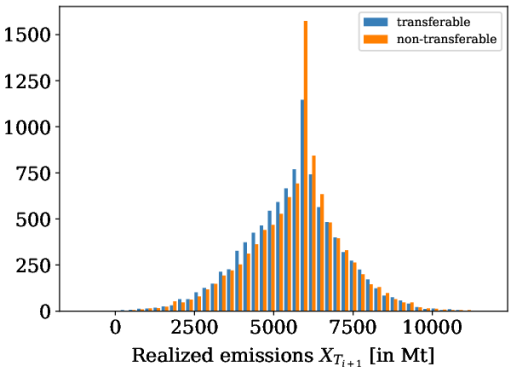

(c) Histogram of realized emissions $X_{T_{i+1}}$ in time period 2.

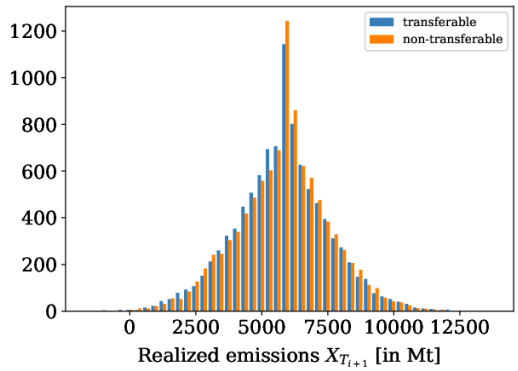

(d) Histogram of realized emissions $X_{T_{i+1}}$ in the last time period.

Figure C.8: Mean trajectory of X and distribution of realized emissions $X_{T_{i+1}}$ in an ETS with transferable or non-transferable allowances in the Ornstein-Uhlenbeck model variant of multi-period model II.

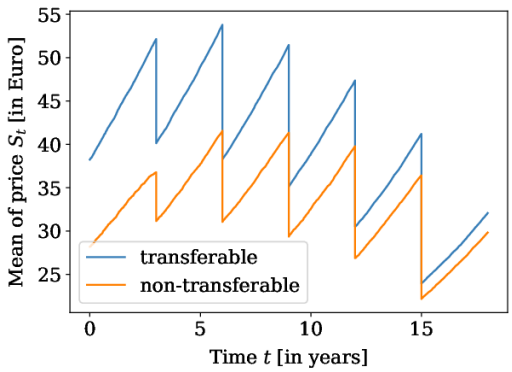

(a) Mean trajectory of S.

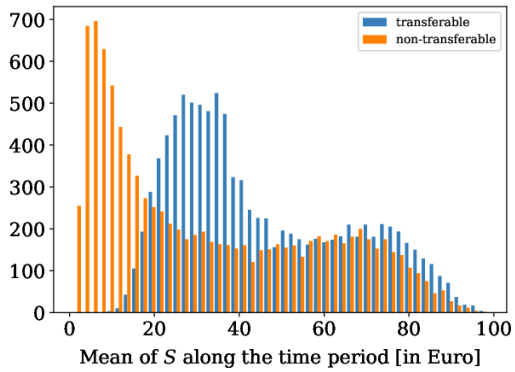

(b) Histogram of mean allowance prices within each run for time period 0.

Figure C.9: Mean price trajectory and distribution of mean allowance prices within each run in an ETS with transferable or non-transferable allowances in the Ornstein-Uhlenbeck variant of multi-period model II.

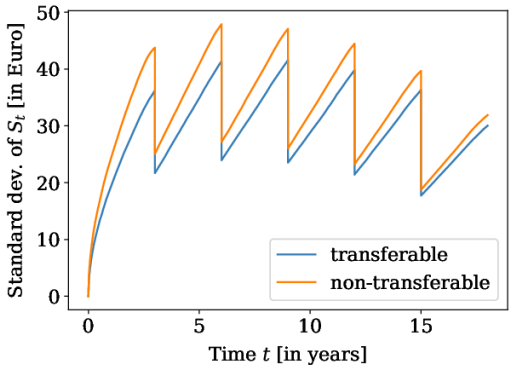

(a) Standard deviation trajectory of S

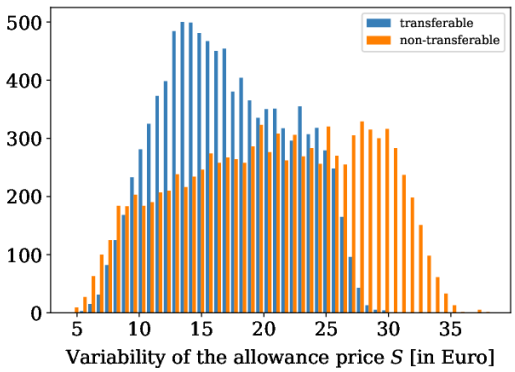

(b) Histogram of the standard deviation of absolute daily returns of S for time period 0, normalized to one year

Figure C.10: Trajectory of the standard deviation and the distribution of the variability of the allowance price in an ETS with transferable or non-transferable allowances in the Ornstein-Uhlenbeck model variant of multi-period model II.

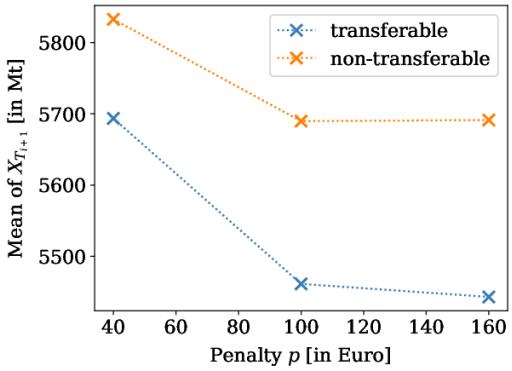

(a) Mean of realized emissions X_T.

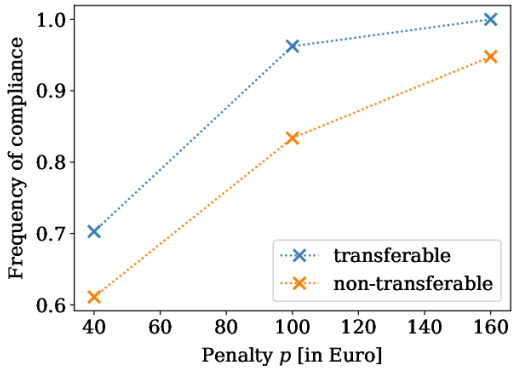

(b) Relative frequency of compliance with the emission target e_0.

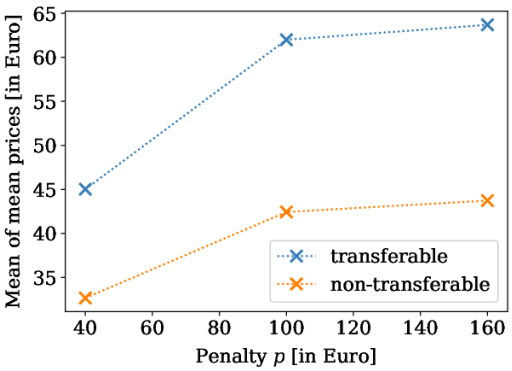

(c) Mean across all runs of the mean prices within one time period.

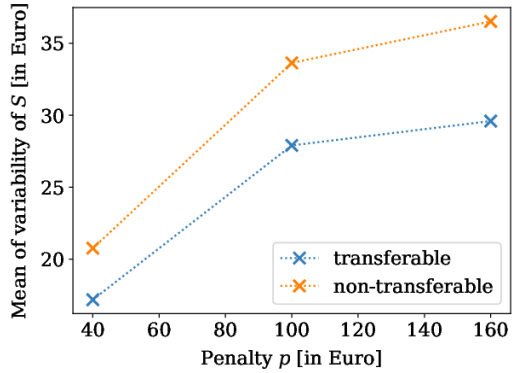

(d) Mean of the variability of the price S.

Figure C.11: Results for a varying penalty in an ETS with transferable or non-transferable allowances in the Ornstein-Uhlenbeck model variant of multi-period model II.

In the one-period model, we analyzed the impact of varying this parameter in Section 6.1.5; to also gain an idea how x_0 affects simulation results in a multi-period setting, we set $x_0 = 5750$ (i.e. lower than the default value) or $x_0 = 6750$ (i.e. higher than the default) in a simulation in the simple variant of multi-period model I.

C.2.1 One-Period Model with Small Volatility

We present the results obtained in the simple model variant with $\sigma = 115.47$. In Figure C.12 three example trajectories of both X and S are shown. The mean trajectory with a 95%-confidence interval as well as the distribution of the mean realized emissions X_T are shown in Figure C.13. The smaller volatility reduces the amplitude of fluctuations in the trajectories and leads to a more narrow confidence interval; the distribution of realized emissions is strongly skewed to the left but the frequency of compliance still only reaches 67.38%.

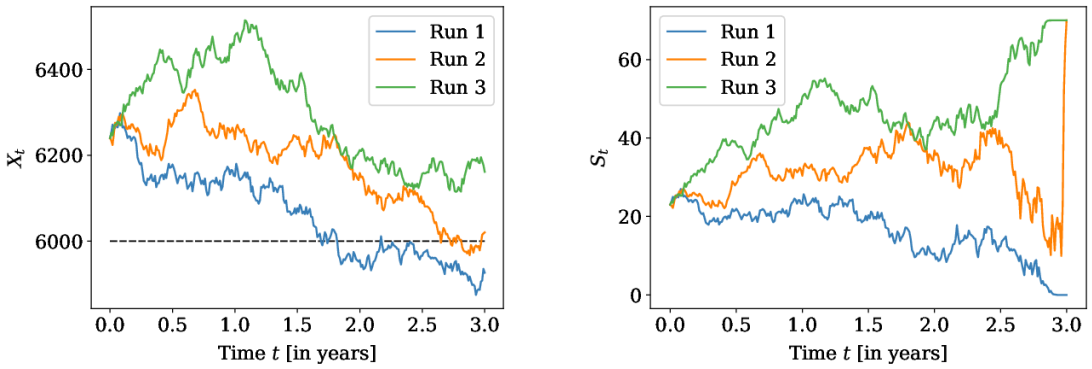

(a) Trajectories of X.

(b) Trajectories of S.

Figure C.12: Three example trajectories of the total expected emissions X with corresponding trajectories of the price process S in the simple model variant of the one-period model. The dashed line represents the threshold e_0. The volatility was set to $\sigma = 115.47$.

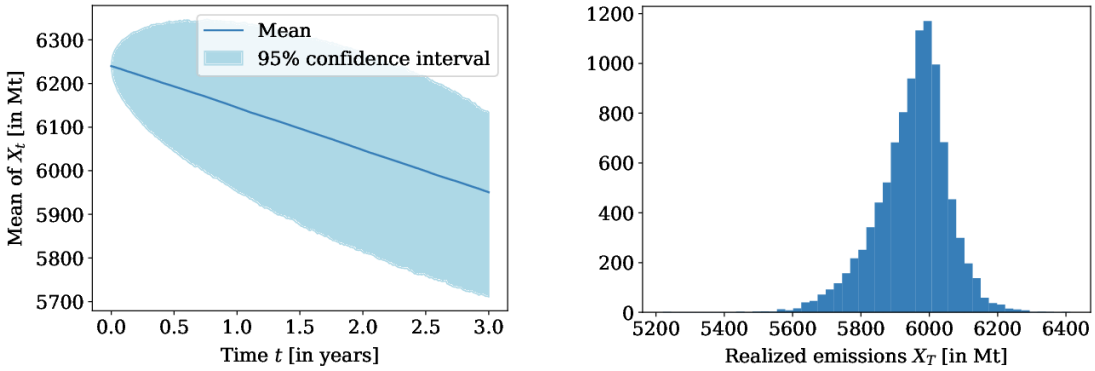

(a) Mean trajectory of X.

(b) Histogram of realized emissions X_T.

Figure C.13: Mean trajectory of the process X and distribution of the realized emissions X_T in the simple model variant of the one-period model. The volatility was set to $\sigma = 115.47$.

In Figure C.14 the corresponding characteristics of the allowance price are shown: The mean price trajectory is again approximately constant but at a lower level than for a higher volatility; the mean prices of each simulation run are more concentrated around lower prices of approximately 20 Euro. Interestingly, both the standard deviation trajectory and the price variability are barely affected by the lower volatility parameter.

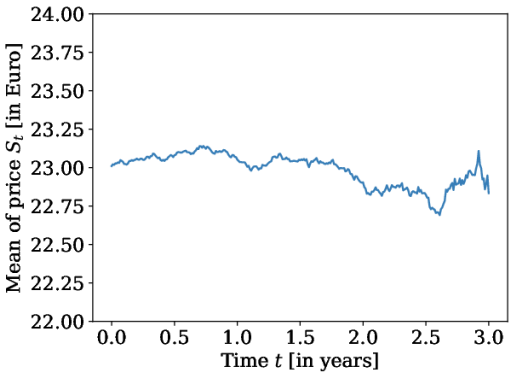

(a) Mean trajectory of S.

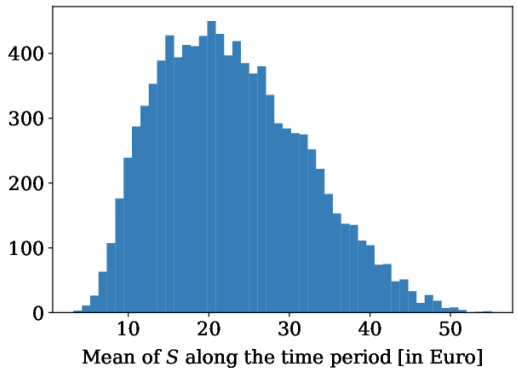

(b) Histogram of mean prices within each run.

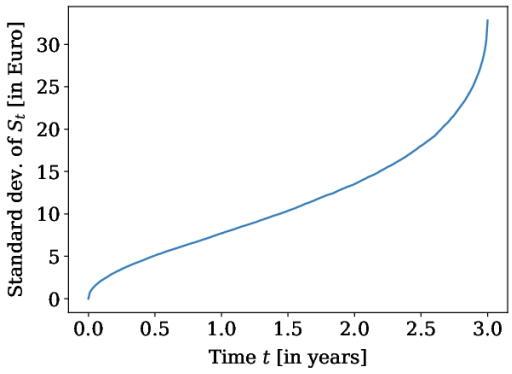

(c) Standard deviation trajectory of S.

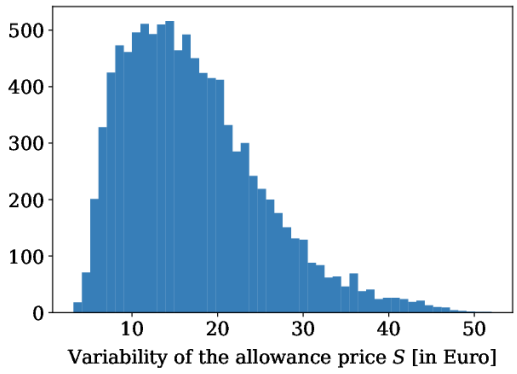

(d) Histogram of the standard deviation of absolute daily returns of S for time period 0, normalized to one year.

Figure C.14: Results on the allowance price S in the simple model variant of the one-period model. The volatility was set to $\sigma = 115.47$.

Varying Parameters

We also study the effect of varying several parameters in the case that $\sigma = 115.47$. In Figure C.15 the results of varying the penalty p are shown. While the numbers attained in parts strongly differ from the results obtained with a higher value of σ, the impact of changing the penalty essentially remains the same.

A similar conclusion can be drawn for varying the emission cap e_0, as visualized in Figures C.16 and C.17: The smaller volatility reduces the range for the emission cap in which the ETS has the largest effect; but the general behavior in reaction to the changing cap is not affected.

Also when varying the length of the time period T, as shown in Figure C.18, the overall

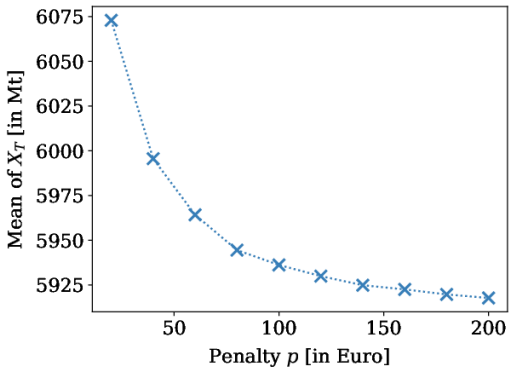

(a) Mean of realized emissions X_T.

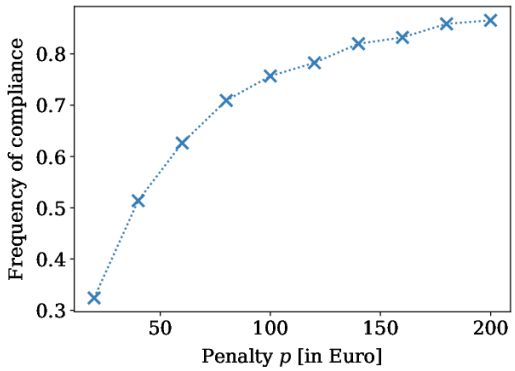

(b) Relative frequency of compliance with the emission target e_0.

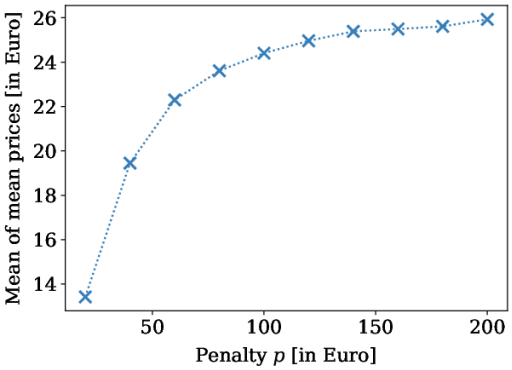

(c) Mean across all runs of the mean prices within one time period.

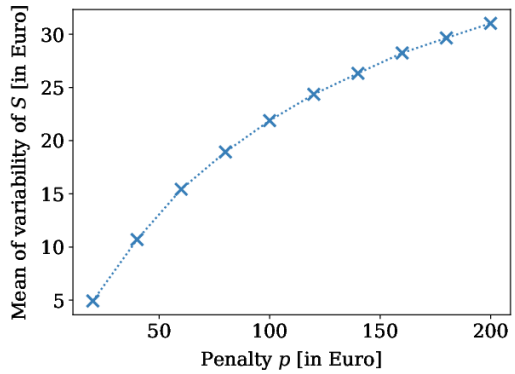

(d) Mean of the variability of the price S.

.

Figure C.15: Results for varying penalties p and volatility $\sigma = 115.47$ in the simple model variant of the one-period model.

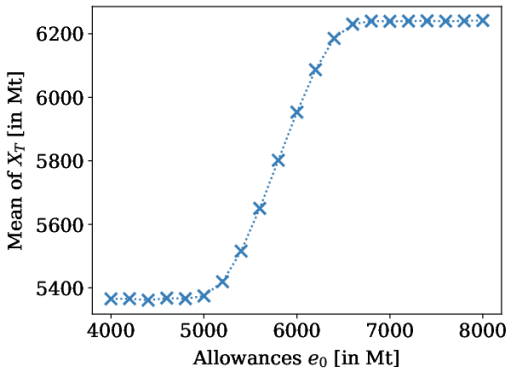

(a) Mean of realized emissions X_T.

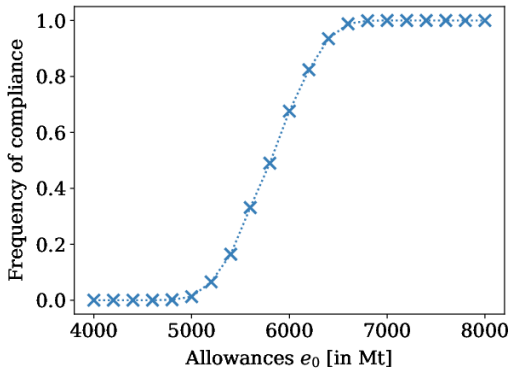

(b) Relative frequency of compliance with the emission target e_0.

Figure C.16: Results on the total expected emissions X for a varying number of allowances and volatility $\sigma = 115.47$ in the simple model variant of the one-period model.

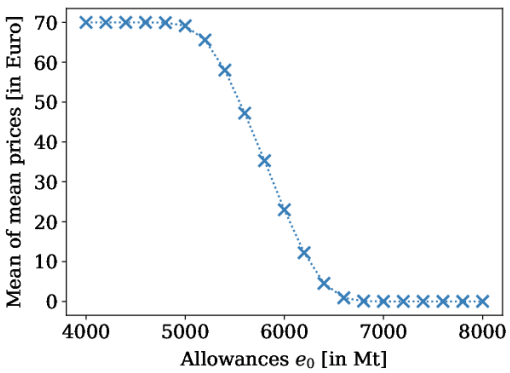

(a) Mean across all runs of the mean prices within one time period.

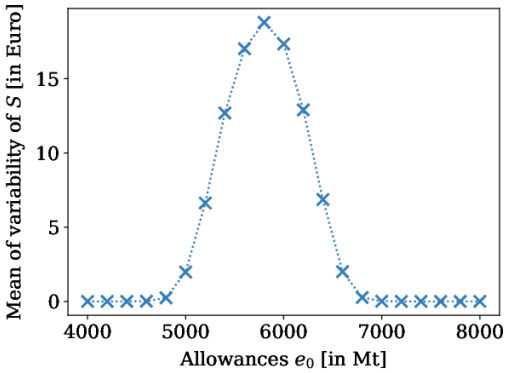

(b) Mean of the variability of the price S.

Figure C.17: Results on the allowance price S for a varying number of allowances and volatility $\sigma = 115.47$ in the simple model variant of the one-period model.

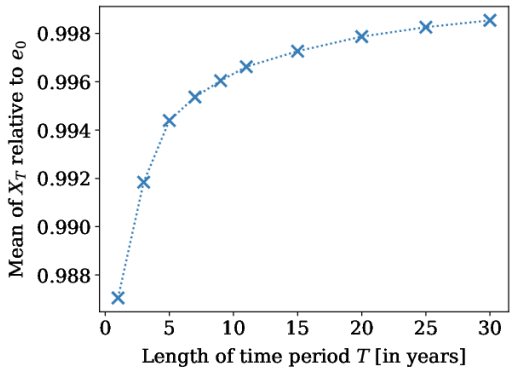

(a) Mean of realized emissions X_T relative to the emission target e_0.

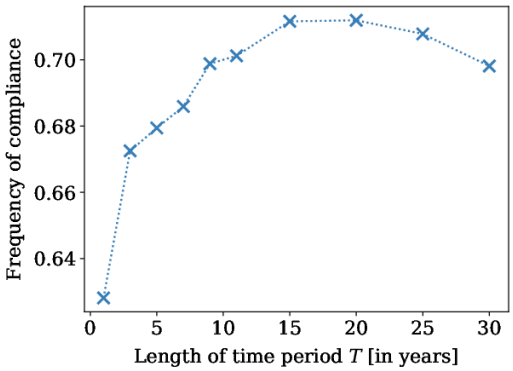

(b) Relative frequency of compliance with the emission target e_0.

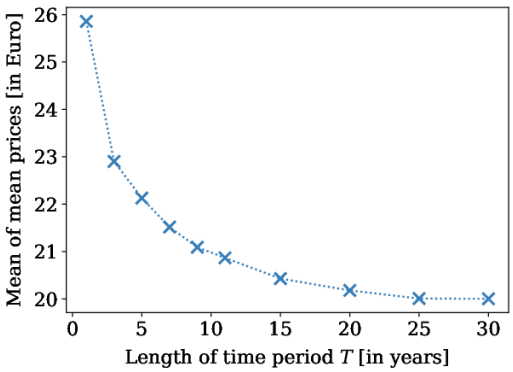

(c) Mean across all runs of the mean prices within one time period.

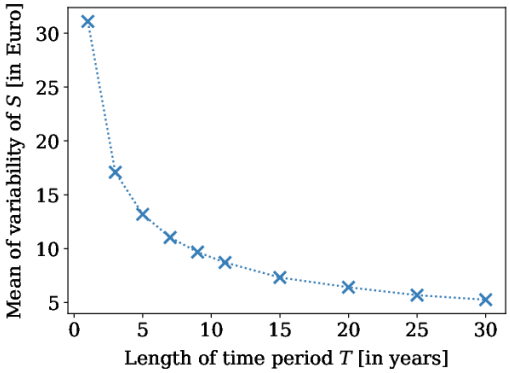

(d) Mean of the variability of the price S.

Figure C.18: Results for a varying length of the time period and volatility $\sigma = 115.47$ in the simple model variant of the one-period model.

results are similar as in the case of a higher volatility. The only striking difference is that the frequency of compliance with the cap appears to decrease again for long time periods; as the analysis for large values of T in Section 6.1.6 shows, this is not the case with a volatility parameter of $\sigma = 288.68$.

C.2.2 Multi-Period Model I with Small Volatility

In multi-period model I, a smaller volatility leads to a lower value of the price parameter s^i, as shown in Figure C.19. At the same time, s^i is constant among early time periods if allowances cannot be transferred but increasing if the transfer is possible, as it is the case for the higher volatility parameter.

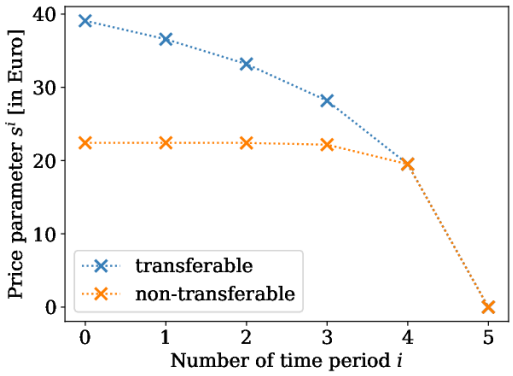

Figure C.19: Price input parameter s^i computed from the price function of the subsequent time period in the simple model variant of multi-period model I with $\sigma = 115.47$.

The trajectories shown in Figures C.20 and C.21 exhibit a more pronounced downward tendency and less fluctuations of X than in the case of a higher volatility, while the behavior of the price process S is largely similar.

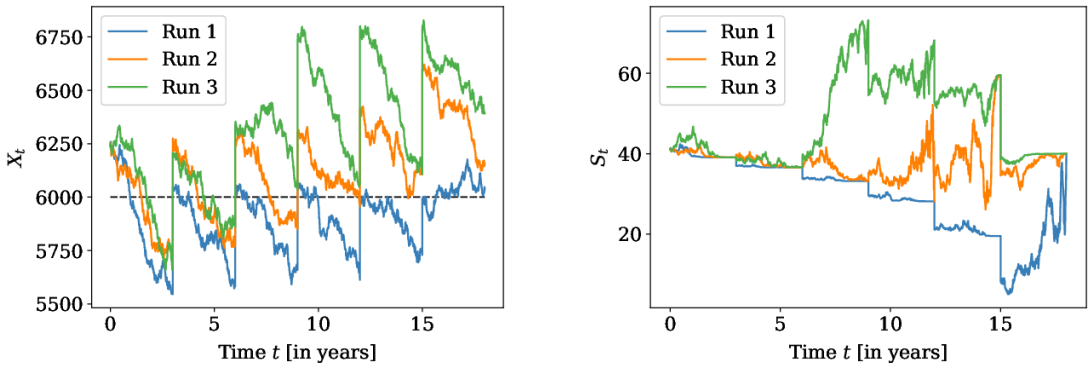

(a) Trajectories of X.

(b) Trajectories of S.

Figure C.20: Three example trajectories of the total expected emissions X with corresponding trajectories of the price process S in the simple variant of multi-period model I where allowances can be transferred. The dashed line represents the threshold e_0. The volatility was set to $\sigma = 115.47$.

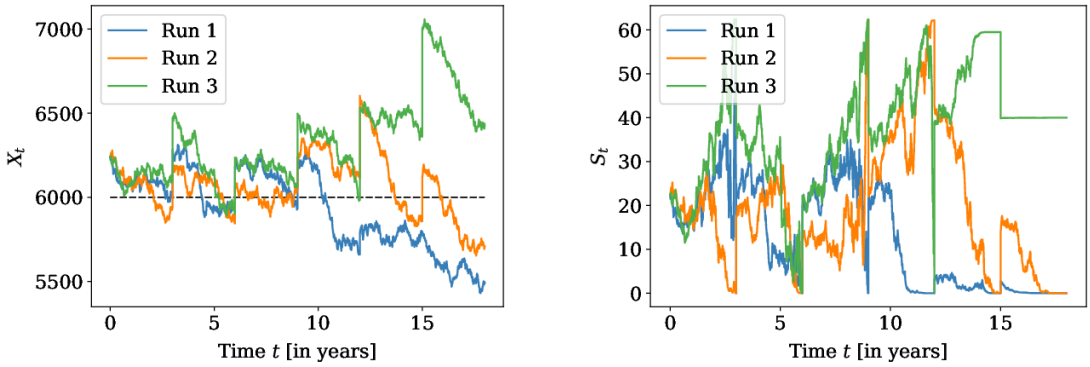

(a) Trajectories of X.

(b) Trajectories of S.

Figure C.21: Three example trajectories of the total expected emissions X with corresponding trajectories of the price process S in the simple model variant of multi-period model I where allowances cannot be transferred. The dashed line represents the threshold e_0. The volatility was set to $\sigma = 115.47$.

Figure C.22 compares the mean trajectories of X and the distributions of the realized emissions X_{T_i} in the case that the transfer of allowances is possible and the case where this is not allowed. These results are again similar to the ones obtained for the higher volatility. The main differences can be found in the exact shape of the distributions; for instance, these are much more narrow.

The relative frequencies of compliance reported in Table C.3 are slightly higher than for the high volatility parameter; but again the frequency of compliance increases remarkably if the transfer of allowances is possible.

Table C.3: Relative frequency of compliance in an ETS with transferable or non-transferable allowances in the simple model variant of multi-period model I with $\sigma = 115.47$.

Time period	0	1	2	3	4	5
Transferable	95.31%	89.51%	84.56%	78.01%	68.73%	50.45%
Non-transferable	64.11%	63.15%	62.51%	60.94%	59.55%	51.07%

The behavior of the allowance price S, as given by its mean and standard deviation trajectories and the distributions of the mean price and the price variability, is visualized in Figure C.23. These results are similar to those obtained with the higher volatility parameter; again the main differences lie in the absolute numbers and the exact shape of the distributions.

Varying Parameters

As in Section 6.2.4, we analyze the impact of varying the penalty p if the volatility parameter is set to $\sigma = 115.47$. The results are shown in Figure C.25; we observe effects very similar to the case of the high volatility parameter, with the impact of allowing for the transfer of allowances being even higher.

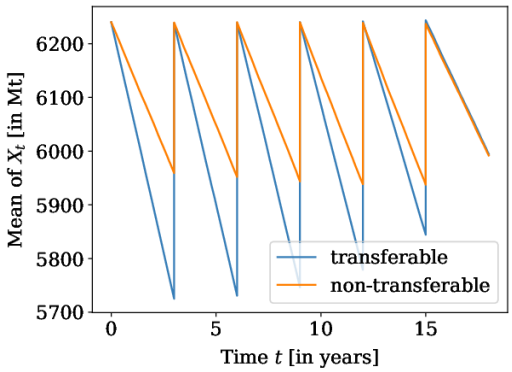

(a) Mean trajectory of X.

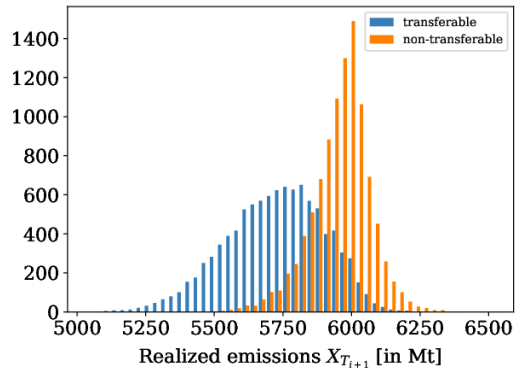

(b) Histogram of realized emissions $X_{T_{i+1}}$ in time period 0.

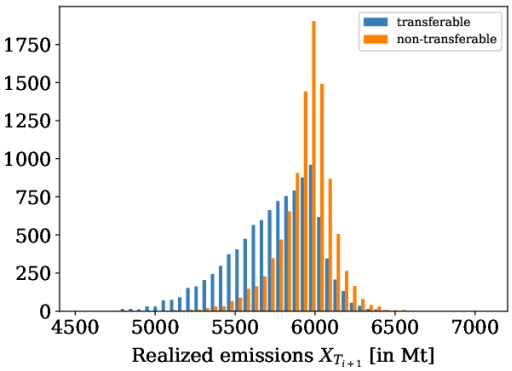

(c) Histogram of realized emissions $X_{T_{i+1}}$ in time period 2.

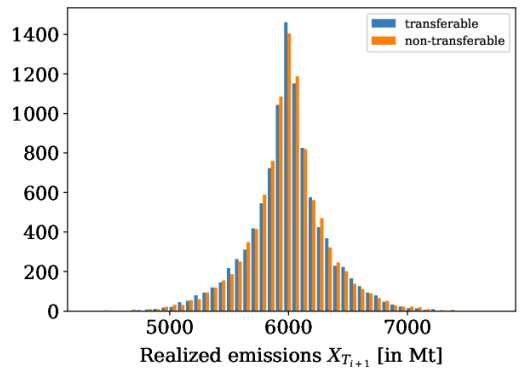

(d) Histogram of realized emissions $X_{T_{i+1}}$ in the last time period.

Figure C.22: Mean trajectory of the process X and distributions of the realized emissions $X_{T_{i+1}}$ in the simple model variant of multi-period model I. The volatility was set to $\sigma = 115.47$. The case of an ETS with transferable allowances is compared to the case where the transfer is not possible.

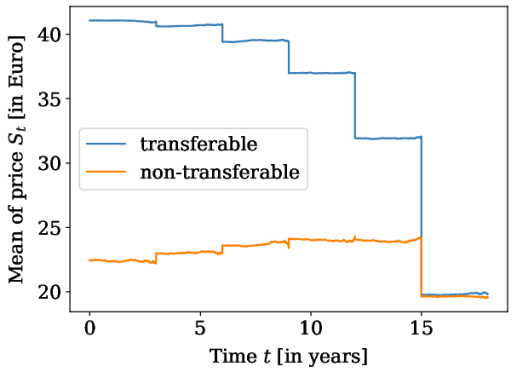

(a) Mean trajectory of S.

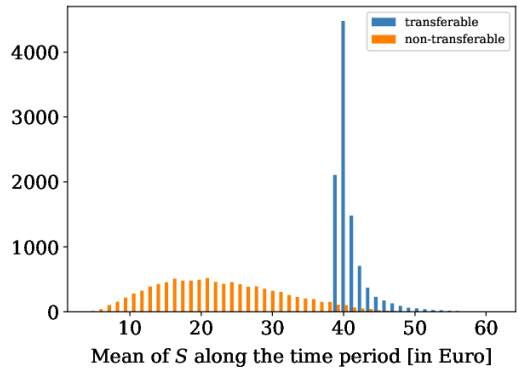

(b) Histogram of mean allowance prices within each run for time period 0.

Figure C.23: Mean trajectory of the process S and distribution of the mean prices within one run in the simple model variant of multi-period model I with volatility $\sigma = 115.47$.

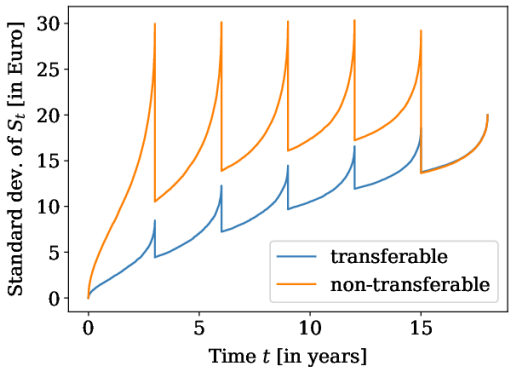

(a) Standard deviation trajectory of S

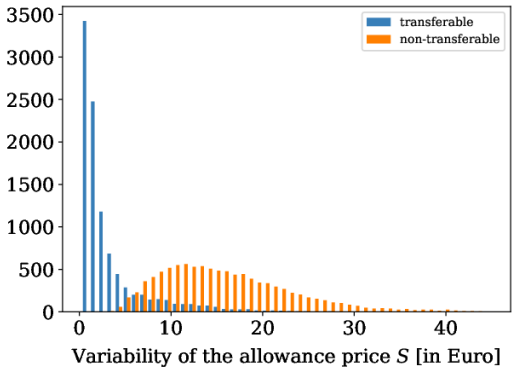

(b) Histogram of the standard deviation of absolute daily returns of S in time period 0, normalized to one year.

Figure C.24: Trajectory of the standard deviation of the allowance price and distribution of its variability in the simple model variant of multi-period model I with volatility $\sigma = 115.47$.

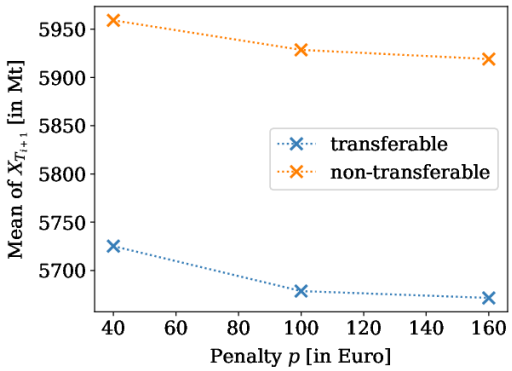

(a) Mean of realized emissions $X_{T_{i+1}}$.

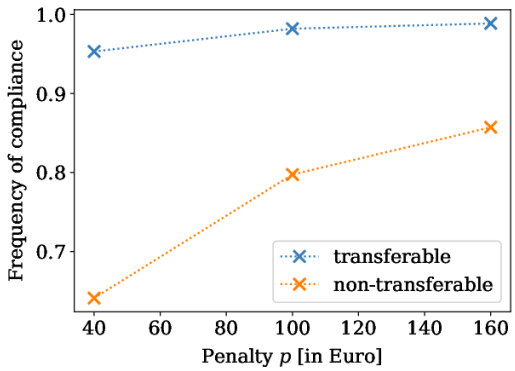

(b) Relative frequency of compliance with the emission target e_0.

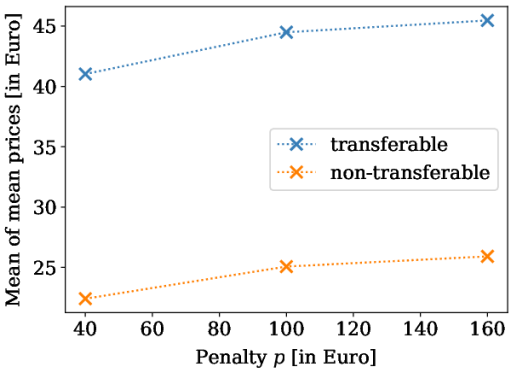

(c) Mean across all runs of the mean prices within one time period.

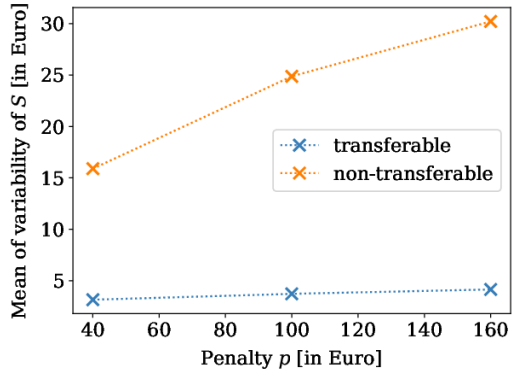

(d) Mean of the variability of the price S.

Figure C.25: Results from time period 0 for varying penalties p in the simple model variant of multi-period model I. The volatility was set to $\sigma = 115.47$.

C.2.3 Multi-Period Model I with Modified Values of x_0

In Figure C.26 the effect of varying the penalty is shown in the case that the initially expected BAU emissions x_0^i amount to 5750 Mt in each time period. Due to the lower BAU emissions, mean realized emissions are lower, whereas the frequency of compliance and the allowance prices are higher; but the impacts of both increasing the penalty and allowing for the transfer of allowances are very similar to the case with default parameters.

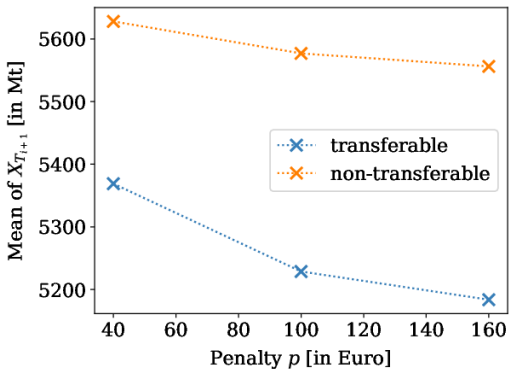

(a) Mean of realized emissions $X_{T_{i+1}}$.

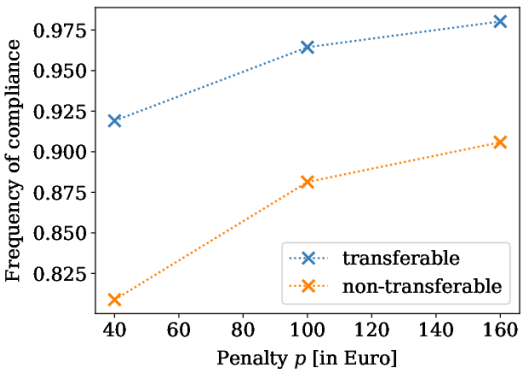

(b) Relative frequency of compliance with the emission target e_0.

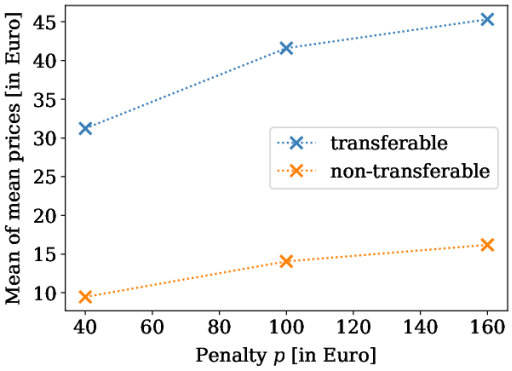

(c) Mean across all runs of the mean prices within one time period.

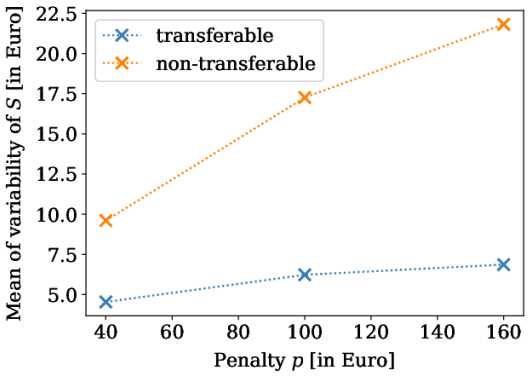

(d) Mean of the variability of the price S.

Figure C.26: Results from time period 0 for varying penalties p in the simple model variant of multi-period model I. The initially expected BAU emissions were set to $x_0 = 5750$. The case of an ETS with transferable allowances is compared to the case where the transfer is not possible.

A similar conclusion can be drawn if the initially expected BAU emissions are increased to $x_0^i = 6750$ in each time period, as shown in Figure C.27. In this case, the mean realized emissions are increased, and the frequency of compliance as well as the mean allowance price decrease; again the impact of increasing the penalty and allowing for the transfer of allowances is very similar to what we observed in default settings.

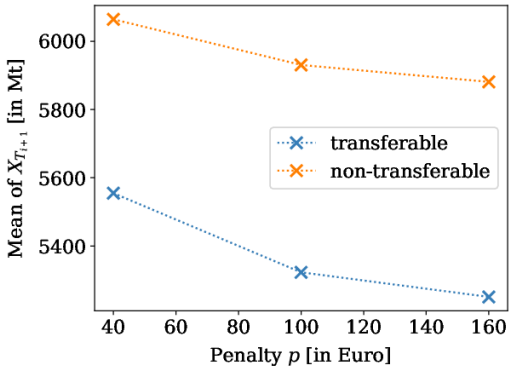

(a) Mean of realized emissions $X_{T_{i+1}}$.

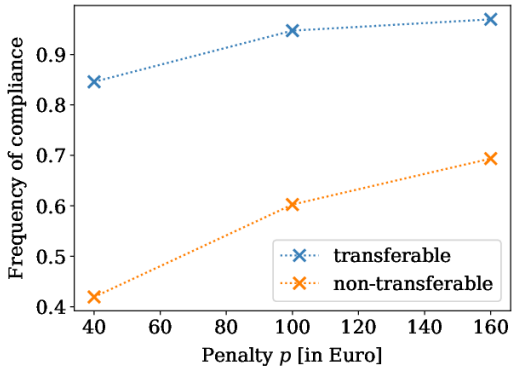

(b) Relative frequency of compliance with the emission target e_0.

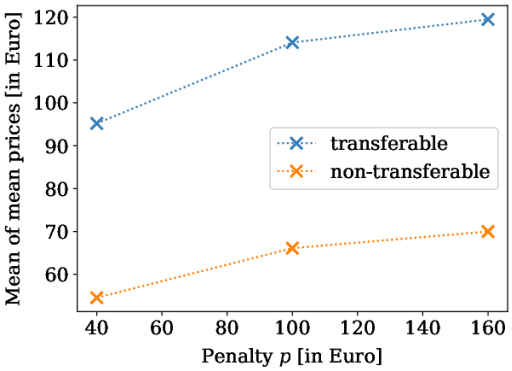

(c) Mean across all runs of the mean prices within one time period.

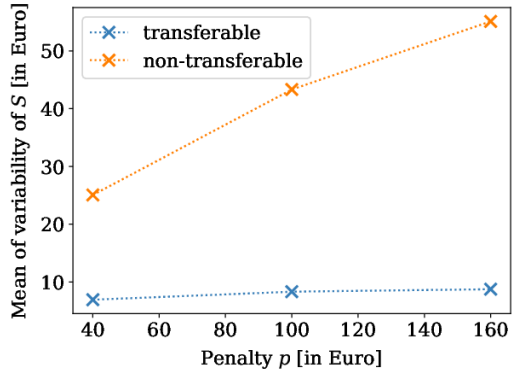

(d) Mean of the variability of the price S.

Figure C.27: Results from time period 0 for varying penalties p in the simple model variant of multi-period model I. The initially expected BAU emissions were set to $x_0 = 6750$. The case of an ETS with transferable allowances is compared to the case where the transfer is not possible.

List of Abbreviations and Notation

List of Frequently Used Notation

$\mathcal{A}(t)$	Admissibility set for controls starting at time t
C	Cost function
D_A	Number of allowances demanded by the agent at the auction
$\mathcal{F}$	Filtration generated by W, augmented by the null sets
G	Volatility function of the process X
H	Volatility function of the process Z
P	Penalty function
S	Allowance price process
S_A	Auction price of an allowance
$\tilde{S}_0^i$	Function to describe the allowance price at the beginning of time period i
T	Final time
T_i	Starting point of time period i
ΔT	Length of one time period in a setting with equidistant time periods
ΔT_i	Length of time period i
$\mathcal{U}$	The set $[0, \infty)$, into which admissible controls are required to map
V	The value function in the stochastic control approach, or the solution of the characteristic PDE
W	A standard Brownian motion
X	Total expected emissions (see Definition 2.1)
$X_{T_i}^+$	Left-sided limit of X at time T_i in the multi-period models; identical to X_0^i.
Y	Mainly: Emission rate process
Z	Mainly: Process to predict the initially expected emissions of the next time period in multi-period model II, given by $X_{T_{i+1}}^+$. Z is also used to denote a given process or random variable in other models.
$Z_{T_i}^+$	Left-sided limit of Z at time T_i in multi-period model II
b	Mainly: Drift term in general formulation of an SDE
c	Cost coefficient
e_0	Emission cap/number of allowances
e_A	Number of allowances distributed by auctioning
e_F	Number of allowances allocated for free in the model with auctioning
erf	Error function
h	Step size in the discretization of the PDE
p	Penalty per ton of surplus emissions
r	Interest rate
s^i	Price of an allowance at the beginning of the next time period, viewed from time period i
u	Abatement rate
x_0	Initially expected BAU emissions for the entire time period
x_0^i	BAU emissions expected for time period i at time 0 in the multi-period models
y_0	Initial value of the emission rate
θ	Mean reversion speed of the Ornstein-Uhlenbeck process
μ	Drift parameter of the emission rate Y in the Brownian model variant and long-term mean of Y in the Ornstein-Uhlenbeck model variant
σ	Volatility parameter of the process X; additionally: Volatility term in general formulation of an SDE

The following superscripts occur in the model extensions:

- Superscript i: Denotes the respective quantity in time period i in the multi-period models; if it is a function in time or a process, then time is measured relative to period i. For example, X_t^i denotes the value of the total expected emissions in time period i at the time point t units after the beginning of time period i.
- Superscript A: Denotes the respective quantity in the auction model.

List of Abbreviations

BAU	Business as usual
CO_2	Carbon dioxide
COP	Conference of the Parties (to the UNFCCC)
ETS	Emission trading system
EUA	Allowance future in the EU ETS
EU ETS	Emission trading system of the European Union
GDP	Gross domestic product
IPCC	Intergovernmental Panel on Climate Change
IR	Infrared
HJB	Hamilton-Jacobi-Bellman
MSR	Market Stability Reserve
Mt	Mega tons
ODE	Ordinary differential equation
PDE	Partial differential equation
SDE	Stochastic differential equation
UNFCCC	United Nations Framework Convention on Climate Change

Bibliography

[AB21] René Aïd and Sara Biagini. "Optimal Dynamic Regulation of Carbon Emissions Market: A Variational Approach". *Université Paris-Dauphine Research Paper No. 3792384* (2021). Available at SSRN: `https://ssrn.com/abstract=3792384`.

[ACD11] Barry Anderson, Frank Convery, and Corrado Di Maria. "Technological Change and the EU ETS: The Case of Ireland". *IEFE Working Paper No. 43* (2011). Available at SSRN: `https://ssrn.com/abstract=1855495`.

[AD11] Barry Anderson and Corrado Di Maria. "Abatement and Allocation in the Pilot Phase of the EU ETS". *Environmental and Resource Economics* 48.1 (2011), pp. 83–103.

[AD13] Peter W. Atkins and Julio De Paula. *Physikalische Chemie*. 5. Auflage. Weinheim: Wiley-VCH, 2013. 1188 pp.

[AS72] Milton Abramowitz and Irene A. Stegun. *Handbook of mathematical functions with formulas, graphs and mathematical tables*. Unabridged, unaltered and corr. republ. of the 1964 ed. New York: Dover Publications, Inc., 1972.

[Axe69] Owe Axelsson. "A class of A-stable methods". *BIT Numerical Mathematics* 9.3 (1969), pp. 185–199.

[BDH11] Konstantin Borovkov, Geoffrey Decrouez, and Juri Hinz. "Jump-Diffusion Modeling in Emission Markets". *Stochastic Models* 27.1 (2011), pp. 50–76.

[BJ15] Germà Bel and Stephan Joseph. "Emission abatement: Untangling the impacts of the EU ETS and the economic crisis". *Energy Economics* 49 (2015), pp. 531–539.

[BK20] Ulrik Beck and Peter K. Kruse-Andersen. "Endogenizing the Cap in a Cap-and-Trade System: Assessing the Agreement on EU ETS Phase 4". *Environmental and Resource Economics* 77.4 (2020), pp. 781–811.

[Boc+19] Johanna Bocklet, Martin Hintermayer, Lukas Schmidt, and Theresa Wildgrube. "The reformed EU ETS - Intertemporal emission trading with restricted banking". *Energy Economics* 84 (2019), p. 104486.

[Bod22] Lena Bodewein. *Starkregen in Australien: Notstand an Ostküste verhängt*. tagesschau. Mar. 9, 2022. `https://www.tagesschau.de/ausland/ozeanien/fluten-australien-101.html` (visited on 06/07/2022).

[BT08] Eva A. Benz and Stefan Trück. "Modeling the Price Dynamics of Co2 Emission Allowances" (2008). Available at SSRN: `https://papers.ssrn.com/abstract=903240`.

[Car+10] René Carmona, Max Fehr, Juri Hinz, and Arnaud Porchet. "Market Design for Emission Trading Schemes". *SIAM Review* 52.3 (2010), pp. 403–452.

[CFH09] René Carmona, Max Fehr, and Juri Hinz. "Optimal stochastic control and carbon price formation". *SIAM Journal on Control and Optimization* 48.4 (2009), pp. 2168–2190.

[CK96] Mark Cronshaw and Jamie Kruse. "Regulated Firms in Pollution Permit Markets with Banking." *Journal of Regulatory Economics* 9 (1996), pp. 179–89.

[Com] The SciPy Community. *SciPy v1.8.1 Manual – scipy.integrate.solve_ivp*. `https://docs.scipy.org/doc/scipy/reference/generated/scipy.integrate.solve_ivp.html` (visited on 05/23/2022).

[CP17] Wugan Cai and Jiafeng Pan. "Stochastic Differential Equation Models for the Price of European CO2 Emissions Allowances". *Sustainability* 9.2 (2017), p. 207.

[DED10] Erik D. Delarue, A. Denny Ellerman, and William D. D'haeseleer. "Short-term CO2 Abatement in the European Power Sector: 2005–2006". *Climate Change Economics* 01.2 (2010), pp. 113–133.

[EB08] A. Denny Ellerman and Barbara K. Buchner. "Over-Allocation or Abatement? A Preliminary Analysis of the EU ETS Based on the 2005–06 Emissions Data". *Environmental and Resource Economics* 41.2 (2008), pp. 267–287.

[ECa] European Commission. *Development of EU ETS (2005-2020)*. Climate Action. `https://ec.europa.eu/clima/eu-action/eu-emissions-trading-system-eu-ets/development-eu-ets-2005-2020_en` (visited on 06/03/2022).

[ECb] European Commission. *European Green Deal*. Climate Action. `https://ec.europa.eu/clima/eu-action/european-green-deal_en` (visited on 06/03/2022).

[ECc] European Commission. *Market Stability Reserve*. Climate Action. `https://ec.europa.eu/clima/eu-action/eu-emissions-trading-system-eu-ets/market-stability-reserve_en` (visited on 06/07/2022).

[ECd] European Commission. *Revision for phase 4 (2021-2030)*. Climate Action. `https://ec.europa.eu/clima/eu-action/eu-emissions-trading-system-eu-ets/revision-phase-4-2021-2030_en` (visited on 06/03/2022).

[EC21] European Commission. *Proposal for a Directive of the European Parliament and of the council amending Directive 2003/87/EC establishing a system for greenhouse gas emission allowance trading within the Union, Decision (EU) 2015/1814 concerning the establishment and operation of a market stability reserve for the Union greenhouse gas emission trading scheme and Regulation (EU) 2015/757*. 2021. `https://eur-lex.europa.eu/legal-content/EN/TXT/?uri=CELEX%3A52021PC0551`.

[ECP10] A. Denny Ellerman, Frank J. Convery, and Christian de Perthuis. *Pricing Carbon: The European Union Emissions Trading Scheme*. Cambridge: Cambridge University Press, 2010.

[EEA] European Environment Agency. *EU Emissions Trading System (ETS) data viewer*. `https://www.eea.europa.eu/data-and-maps/dashboards/emissions-trading-viewer-1` (visited on 10/08/2021).

[EEA07] European Environment Agency. *Annual European Community greenhouse gas inventory 1990-2005 and inventory report 2007*. Available at https://www.eea.europa.eu/publications/technical_report_2007_7. 2007.

[EEA11] European Environment Agency. *EUA future prices 2005–2011*. Oct. 18, 2011. https://www.eea.europa.eu/data-and-maps/figures/eua-future-prices-200520132011 (visited on 03/02/2021).

[Ege+11] Christian Egenhofer, Monica Alessi, Anton Georgiev, and Noriko Fujiwara. "The EU Emissions Trading System and Climate Policy Towards 2050: Real Incentives to Reduce Emissions and Drive Innovation?" *CEPS Special Reports* (2011). Available at SSRN: http://ssrn.com/abstract=1756736.

[Ehl69] Byron L. Ehle. "On Padé approximations to the exponential function and A-stable methods for the numerical solution of initial value problems". PhD thesis. University of Waterloo, Ontario, 1969.

[EK86] Stewart N. Ethier and Thomas G. Kurtz. *Markov Processes: Characterization and Convergence*. Wiley, 1986. 552 pp.

[Em22] *EU Carbon Price Tracker*. Ember. June 7, 2022. https://ember-climate.org/data/data-tools/carbon-price-viewer/ (visited on 06/08/2022).

[EPA16] US Environmental Protection Agency. *Cross-State Air Pollution Rule and Acid Rain Program*. 2016.

[Erb22] Gregor Erbach. *Review of the EU ETS: 'Fit for 55' package*. Available at https://www.europarl.europa.eu/thinktank/en/document/EPRS_BRI(2022)698890. Think Tank European Parliament, July 5, 2022.

[EU03] "Directive 2003/87/EC of the European Parliament and of the Council of 13 October 2003 establishing a scheme for greenhouse gas emission allowance trading within the Community and amending Council Directive 96/61/EC". *Official Journal* L 275 (Oct. 25, 2003), p. 32.

[EU09] "Directive 2009/29/EC of the European Parliament and of the Council of 23 April 2009 amending Directive 2003/87/EC so as to improve and extend the greenhouse gas emission allowance trading scheme of the Community". *Official Journal* L 140 (Apr. 23, 2009), p. 63.

[EU10] "Commission Regulation (EU) No 1031/2010 of 12 November 2010 on the timing, administration and other aspects of auctioning of greenhouse gas emission allowances pursuant to Directive 2003/87/EC of the European Parliament and of the Council establishing a scheme for greenhouse gas emission allowances trading within the Community". *Official Journal* L 302 (Nov. 12, 2010), p. 1.

[EU15] "Decision (EU) 2015/1814 of the European Parliament and of the Council of 6 October 2015 concerning the establishment and operation of a market stability reserve for the Union greenhouse gas emission trading scheme and amending Directive 2003/87/EC". *Official Journal* L 264 (Oct. 6, 2015), p. 1.

[EU18] "Directive (EU) 2018/410 of the European Parliament and of the Council of 14 March 2018 amending Directive 2003/87/EC to enhance cost-effective emission reductions and low-carbon investments, and Decision (EU) 2015/1814". *Official Journal* L 76 (Mar. 14, 2018), p. 3.

[Eva10] Lawrence C. Evans. *Partial differential equations*. 2nd ed. Vol. 19. Graduate Studies in Mathematics. American Math. Soc., 2010.

[Gil+21] Nathan P. Gillett, Elizaveta Malinina, Darrell Kaufman, and Raphael Neukom. *Summary for Policymakers of the Working Group I Contribution to the IPCC Sixth Assessment Report - data for Figure SPM.1*. 2021.

[GK96] István Gyöngy and Nicolai Krylov. "Existence of strong solutions for Itô's stochastic equations via approximations". *Probability Theory and Related Fields* 105.2 (1996), pp. 143–158.

[Gru16] Michael Grubb. "Full legal compliance with the Kyoto Protocol's first commitment period – some lessons". *Climate Policy* 16.6 (2016), pp. 673–681.

[Gyö98] István Gyöngy. "A Note on Euler's Approximations". *Potential Analysis* 8.3 (1998), pp. 205–216.

[Hai14] Corina Haita. "Endogenous market power in an emissions trading scheme with auctioning". *Resource and Energy Economics* 37 (2014), pp. 253–278.

[Har+20] Charles R. Harris, K. Jarrod Millman, Stéfan J. van der Walt, Ralf Gommers, Pauli Virtanen, David Cournapeau, Eric Wieser, Julian Taylor, Sebastian Berg, Nathaniel J. Smith, Robert Kern, Matti Picus, Stephan Hoyer, Marten H. van Kerkwijk, Matthew Brett, Allan Haldane, Jaime Fernández del Río, Mark Wiebe, Pearu Peterson, Pierre Gérard-Marchant, Kevin Sheppard, Tyler Reddy, Warren Weckesser, Hameer Abbasi, Christoph Gohlke, and Travis E. Oliphant. "Array programming with NumPy". *Nature* 585.7825 (2020), pp. 357–362.

[Hin10] Beat Hintermann. "Allowance price drivers in the first phase of the EU ETS". *Journal of Environmental Economics and Management* 59.1 (2010), pp. 43–56.

[Hin20] Martin Hintermayer. "A carbon price floor in the reformed EU ETS: Design matters!" *Energy Policy* 147 (2020), p. 111905.

[HK06] Nikolaos Halidias and P. E. Kloeden. "A note on strong solutions of stochastic differential equations with a discontinuous drift coefficient". *Journal of Applied Mathematics and Stochastic Analysis* 2006 (2006), e73257.

[HK08] Nikolaos Halidias and Peter E. Kloeden. "A note on the Euler–Maruyama scheme for stochastic differential equations with a discontinuous monotone drift coefficient". *BIT Numerical Mathematics* 48.1 (2008), pp. 51–59.

[HMS03] Desmond J. Higham, Xuerong Mao, and Andrew M. Stuart. "Strong Convergence of Euler-Type Methods for Nonlinear Stochastic Differential Equations". *SIAM Journal on Numerical Analysis* 40.3 (2003), pp. 1041–1063.

[HNW93] Ernst Hairer, Syvert Nørsett, and Gerhard Wanner. *Solving Ordinary Differential Equations I: Nonstiff Problems*. 2nd, rev. ed. Springer series in computational mathematics 8. Berlin Heidelberg: Springer-Verlag, 1993.

[Hof21] Caroline Hoffmann. *Dürre in Afrika: Eine lebensbedrohliche Trockenheit*. tagesschau. Dec. 26, 2021. `https://www.tagesschau.de/ausland/afrika/ostafrika-duerre-101.html` (visited on 06/07/2022).

[Hor22] Peter Hornung. *Indien: "Der heißeste Sommer aller Zeiten"*. tagesschau. Apr. 30, 2022. `https://www.tagesschau.de/ausland/indien-hitzewelle-103.html` (visited on 05/30/2022).

[HRW17] Ronald A. Hites, Jonathan D. Raff, and Peter Wiesen. *Umweltchemie*. 1. Auflage. Weinheim: Wiley-VCH Verlag GmbH & Co. KGaA, 2017.

[Hun07] John D. Hunter. "Matplotlib: A 2D Graphics Environment". *Computing in Science & Engineering* 9.3 (2007), pp. 90–95.

[HW96] Ernst Hairer and Gerhard Wanner. *Solving Ordinary Differential Equations II: Stiff and differential-algebraic problems*. 2nd, rev. ed. Springer series in computational mathematics 14. Berlin: Springer-Verlag, 1996. 614 pp.

[ICA] ICAP. *Emissions Trading Worldwide: 2022 ICAP Status Report*. Available at `https://icapcarbonaction.com/en/publications/emissions-trading-worldwide-2022-icap-status-report`.

[Inn03] Robert Innes. "Stochastic pollution, costly sanctions, and optimality of emission permit banking". *Journal of Environmental Economics and Management* 45.3 (2003), pp. 546–568.

[IPC21] IPCC. "Summary for policymakers". *Climate Change 2021: The Physical Science Basis. Contribution of Working Group I to the Sixth Assessment Report of the Intergovernmental Panel on Climate Change*. Ed. by Valérie Masson-Delmotte, Panmao Zhai, Anna Pirani, Sarah L. Connors, C. Péan, Sophie Berger, Nada Caud, Y. Chen, Leah Goldfarb, Melissa I. Gomis, Mengtian Huang, Katherine Leitzell, Elisabeth Lonnoy, J. B. Robin Matthews, Thomas K. Maycock, Tim Waterfield, Özge Yelekçi, R. Yu, and Botao Zhou. Cambridge, United Kingdom and New York, NY, USA: Cambridge University Press, 2021, pp. 3–32.

[IPC22] IPCC. "Summary for Policymakers". *Climate Change 2022: Impacts, Adaptation, and Vulnerability. Contribution of Working Group II to the Sixth Assessment Report of the Intergovernmental Panel on Climate Change*. Ed. by H.-O. Pörtner, D.C. Roberts, E.S. Poloczanska, K. Mintenbeck, M. Tignor, A. Alegría, M. Craig, S. Langsdorf, S. Löschke, V. Möller, and A. Okem. Cambridge University Press, 2022.

[IPC92] IPCC. "Policymaker Summary of Working Group I (Scientific Assessment of Climate Change)". *Climate Change: The IPCC 1990 and 1992 Assessments*. 1992.

[Jac07] Peter Jackson. *From Stockholm to Kyoto: A Brief History of Climate Change*. UN Chronicle. Publisher: United Nations. June 2007. `https://www.un.org/en/chronicle/article/stockholm-kyoto-brief-history-climate-change` (visited on 06/02/2022).

[Kee+01] Charles D. Keeling, Stephen C. Piper, Robert B. Bacastow, Martin Wahlen, Timothy P. Whorf, Martin Heimann, and Harro A. Meijer. *Exchanges of Atmospheric CO2 and 13CO2 with the Terrestrial Biosphere and Oceans from 1978 to 2000. I. Global Aspects*. Vol. 06. SIO Reference Series 01. Scripps Institution of Oceanography, 2001.

[Kor14] Ralf Korn. "Zeitstetige Portfolio-Optimierung". *Moderne Finanzmathematik – Theorie und praktische Anwendung: Band 1 – Optionsbewertung und Portfolio-Optimierung*. Studienbücher Wirtschaftsmathematik. Wiesbaden: Springer Fachmedien, 2014, pp. 253–307.

[KP92] Peter E. Kloeden and Eckhard Platen. *Numerical Solution of Stochastic Differential Equations*. Stochastic Modelling and Applied Probability. Berlin Heidelberg: Springer-Verlag, 1992.

[KS98] Ioannis Karatzas and Steven E. Shreve. "Stochastic Differential Equations". *Brownian Motion and Stochastic Calculus*. 2nd ed. Graduate Texts in Mathematics. New York, NY: Springer Science+Business Media, 1998, pp. 281–398.

[KT16] Sascha Kollenberg and Luca Taschini. "Emissions trading systems with cap adjustments". *Journal of Environmental Economics and Management* 80 (2016), pp. 20–36.

[KT19] Sascha Kollenberg and Luca Taschini. "Dynamic supply adjustment and banking under uncertainty in an emission trading scheme: The market stability reserve". *European Economic Review* 118 (2019), pp. 213–226.

[Kut01] Wilhelm Kutta. "Beitrag zur näherungsweisen Integration totaler Differentialgleichungen". *Zeitschrift für Mathematik und Physik* 46 (1901), pp. 435–453.

[Lai+14] Timothy Laing, Misato Sato, Michael Grubb, and Claudia Comberti. "The effects and side-effects of the EU emissions trading scheme". *WIREs Climate Change* 5.4 (2014), pp. 509–519.

[Lan+05] Jürgen Landgrebe, Regina Betz, Karoline Rogge, Joachim Schleich, Wolfgang Eichhammer, Martin Cames, Stefan Besser, Olaf Hölzer, Sonja Lange, Thomas Langrock, and Christoph Kühleis. *Implementation of emissions trading in the EU: National allocation plans of all EU states*. Berlin: Umweltbundesamt, 2005.

[Len+19] Timothy M. Lenton, Johan Rockström, Owen Gaffney, Stefan Rahmstorf, Katherine Richardson, Will Steffen, and Hans Joachim Schellnhuber. "Climate tipping points — too risky to bet against". *Nature* 575.7784 (2019). Comment, pp. 592–595.

[LH20] Jin Liang and Wenlin Huang. "Optimal Control Strategy of Companies: Inheriting Period and Carbon Emission Reduction". *Mathematical Problems in Engineering* 2020 (2020). Article ID 3461747.

[LH22] Jin Liang and Wenlin Huang. "Optimal control model of an enterprise for single and inheriting periods of carbon emission reduction". *Mathematics and Financial Economics* 16 (2022), pp. 89–123.

[LS18] Gunther Leobacher and Michaela Szölgyenyi. "Convergence of the Euler-Maruyama method for multidimensional SDEs with discontinuous drift and degenerate diffusion coefficient". *Numerische Mathematik* 138.1 (2018), pp. 219–239.

[LSH10] Wietze Lise, Jos Sijm, and Benjamin F. Hobbs. "The Impact of the EU ETS on Prices, Profits and Emissions in the Power Sector: Simulation Results with the COMPETES EU20 Model". *Environmental and Resource Economics* 47.1 (2010), pp. 23–44.

[LST15] Gunther Leobacher, Michaela Szölgyenyi, and Stefan Thonhauser. "On the Existence of Solutions of a Class of SDEs with Discontinuous Drift and Singular Diffusion". *Electronic Communications in Probability* 20.6 (2015), pp. 1–14.

[Mae04] Akira Maeda. “Impact of banking and forward contracts on tradable permit markets”. *Environmental Economics and Policy Studies* 6.2 (2004), pp. 81–102.

[Mar55] Gisiro Maruyama. “Continuous Markov processes and stochastic equations”. *Rendiconti del Circolo Matematico di Palermo* 4.1 (1955), pp. 48–90.

[MMR02] Glenn Marion, Xuerong Mao, and Eric Renshaw. “Convergence of the Euler Scheme for a Class of Stochastic Differential Equation”. *International Mathematical Journal* 1 (2002).

[Mon72] W. David Montgomery. “Markets in licenses and efficient pollution control programs”. *Journal of Economic Theory* 5.3 (1972), pp. 395–418.

[NT16] Hoang Long Ngo and Dai Taguchi. “Strong rate of convergence for the Euler-Maruyama approximation of stochastic differential equations with irregular coefficients”. *Mathematics of Computation* 85.300 (2016), pp. 1793–1819.

[NT17] Hoang-Long Ngo and Dai Taguchi. “On the Euler–Maruyama approximation for one-dimensional stochastic differential equations with irregular coefficients”. *IMA Journal of Numerical Analysis* 37.4 (2017), pp. 1864–1883.

[Øks98] Bernt Øksendal. *Stochastic Differential Equations: An Introduction with Applications*. 5th ed. Universitext. Berlin Heidelberg: Springer-Verlag, 1998.

[Ped+11] Fabian Pedregosa, Gaël Varoquaux, Alexandre Gramfort, Vincent Michel, Bertrand Thirion, Olivier Grisel, Mathieu Blondel, Peter Prettenhofer, Ron Weiss, Vincent Dubourg, Jake Vanderplas, Alexandre Passos, David Cournapeau, Matthieu Brucher, Matthieu Perrot, and Édouard Duchesnay. “Scikit-learn: Machine Learning in Python”. *Journal of Machine Learning Research* 12.85 (2011), pp. 2825–2830.

[Pha09] Huyên Pham. “The classical PDE approach to dynamic programming”. *Continuous-time Stochastic Control and Optimization with Financial Applications*. Berlin Heidelberg: Springer-Verlag, 2009, pp. 37–60.

[Pig13] Arthur Cecil Pigou. *The Economics of Welfare*. 6th ed. Palgrave Macmillan, 2013. 896 pp.

[PW16] Grischa Perino and Maximilian Willner. “Procrastinating reform: The impact of the market stability reserve on the EU ETS”. *Journal of Environmental Economics and Management* 80 (2016), pp. 37–52.

[RH10] Karoline S. Rogge and Volker H. Hoffmann. “The impact of the EU ETS on the sectoral innovation system for power generation technologies – Findings for Germany”. *Energy Policy*. Special Section: Carbon Reduction at Community Scale 38.12 (2010), pp. 7639–7652.

[Rog+16] Joeri Rogelj, Michel den Elzen, Niklas Höhne, Taryn Fransen, Hanna Fekete, Harald Winkler, Roberto Schaeffer, Fu Sha, Keywan Riahi, and Malte Meinshausen. “Paris Agreement climate proposals need a boost to keep warming well below 2 °C”. *Nature* 534.7609 (2016), pp. 631–639.

[Rub96] Jonathan D. Rubin. “A Model of Intertemporal Emission Trading, Banking, and Borrowing”. *Journal of Environmental Economics and Management* 31.3 (1996), pp. 269–286.

[Run95] Carl Runge. “Ueber die numerische Auflösung von Differentialgleichungen”. *Mathematische Annalen* 46.2 (1895), pp. 167–178.

[Sch00] Susanne M. Schennach. “The Economics of Pollution Permit Banking in the Context of Title IV of the 1990 Clean Air Act Amendments”. *Journal of Environmental Economics and Management* 40.3 (2000), pp. 189–210.

[Sch91] William E. Schiesser. *The numerical method of lines*. Academic Press, 1991.

[Sie08] Horst Siebert. *Economics of the Environment*. 7th ed. Berlin Heidelberg: Springer-Verlag, 2008.

[SMB16] Igor Shishlov, Romain Morel, and Valentin Bellassen. “Compliance of the Parties to the Kyoto Protocol in the first commitment period”. *Climate Policy* 16.6 (2016), pp. 768–782.

[SNC06] Jos Sijm, Karsten Neuhoff, and Yihsu Chen. “CO2 cost pass-through and windfall profits in the power sector”. *Climate Policy* 6.1 (2006), pp. 49–72.

[SS16] Anton A. Shardin and Michaela Szölgyenyi. “Optimal control of an energy storage facility under a changing economic environment and partial information”. *International Journal of Theoretical and Applied Finance* 19.4 (2016), p. 1650026.

[SUW08] Jan Seifert, Marliese Uhrig-Homburg, and Michael Wagner. “Dynamic behavior of CO2 spot prices”. *Journal of Environmental Economics and Management* 56.2 (2008), pp. 180–194.

[SV18] Bodo Sturm and Carla Vogt. *Umweltökonomik*. 2nd ed. Springer-Verlag GmbH Deutschland, 2018.

[tag22] tagesschau. *Extreme Temperaturen und viele Brände in Süd- und Westeuropa*. July 19, 2022. `https://www.tagesschau.de/ausland/europa/hitzewelle-europa-103.html` (visited on 07/27/2022).

[UN12] *Doha Amendment to the Kyoto Protocol*. United Nations, Treaty Series, No. 30822. Available at `https://treaties.un.org/Pages/showDetails.aspx?objid=0800000280346e7e&clang=_en`. Aug. 12, 2012.

[UN15] *Paris Agreement*. United Nations, Treaty Series, vol. 3156, No. 54113. Available at `https://treaties.un.org/Pages/showDetails.aspx?objid=0800000280458f37&clang=_en`. Dec. 12, 2015.

[UN22] *Global Stocktake: Spurring Countries to Step up Climate Action*. United Nations Climate Change. Mar. 31, 2022. `https://unfccc.int/news/global-stocktake-spurring-countries-to-step-up-climate-action` (visited on 06/02/2022).

[UN97] *Kyoto Protocol to the United Nations Framework Convention on Climate Change*. United Nations, Treaty Series, vol. 2303, No. 30822, p. 163. Available at `https://treaties.un.org/Pages/showDetails.aspx?objid=0800000280021a16&clang=_en`. Dec. 11, 1997.

[Ver81] A. Yu Veretennikov. “On Strong Solutions and Explicit Formulas for Solutions of Stochastic Integral Equations”. *Mathematics of the USSR-Sbornik* 39.3 (1981), p. 387.

[Ver84] A. Yu Veretennikov. “On Stochastic Equations with Degenerate Diffusion with respect to some of the Variables”. *Mathematics of the USSR-Izvestiya* 22.1 (1984), pp. 173–180.

[Vir+20] Pauli Virtanen, Ralf Gommers, Travis E. Oliphant, Matt Haberland, Tyler Reddy, David Cournapeau, Evgeni Burovski, Pearu Peterson, Warren Weckesser, Jonathan Bright, Stéfan J. van der Walt, Matthew Brett, Joshua Wilson, K. Jarrod Millman, Nikolay Mayorov, Andrew R. J. Nelson, Eric Jones, Robert Kern, Eric Larson, C. J. Carey, İlhan Polat, Yu Feng, Eric W. Moore, Jake VanderPlas, Denis Laxalde, Josef Perktold, Robert Cimrman, Ian Henriksen, E. A. Quintero, Charles R. Harris, Anne M. Archibald, Antônio H. Ribeiro, Fabian Pedregosa, and Paul van Mulbregt. “SciPy 1.0: fundamental algorithms for scientific computing in Python”. *Nature Methods* 17.3 (2020), pp. 261–272.

[WBa] The Worldbank. *CO2 emissions - European Union: Climate Watch. 2020. GHG Emissions. Washington, DC: World Resources Institute.* `https://data.worldbank.org/indicator/EN.ATM.CO2E.KT?locations=EU` (visited on 12/02/2020).

[WBb] The Worldbank. *CO2 emissions - World: Climate Watch. 2020. GHG Emissions. Washington, DC: World Resources Institute.* `https://data.worldbank.org/indicator/EN.ATM.CO2E.KT` (visited on 06/02/2022).

[Wei22] Anna-Lara Weidinger. *Was ist in der Flutnacht passiert? - Ein Protokoll.* SWR Aktuell. July 14, 2022. `https://www.swr.de/swraktuell/rheinland-pfalz/flut-rekonstruktion-ahrtal-protokoll-100.html` (visited on 07/18/2022).

[YM15] Jongmin Yu and Mindy L. Mallory. “An optimal hybrid emission control system in a multiple compliance period model”. *Resource and Energy Economics* 39 (2015), pp. 16–28.

[Zha05] Xicheng Zhang. “Strong solutions of SDES with singular drift and Sobolev diffusion coefficients”. *Stochastic Processes and their Applications* 115.11 (2005), pp. 1805–1818.

[Zvo74] Alexander K. Zvonkin. “A Transformation of the Phase Space of a Diffusion Process that removes the Drift”. *Mathematics of the USSR-Sbornik* 22.1 (1974), p. 129.

Scientific and Professional Career

Education

10/2018 – 11/2022	PhD student of Prof. Dr. Jörn Sass, *TU Kaiserslautern*
04/2015 – 02/2018	Master of Science Mathematics, *TU Kaiserslautern*
10/2011 – 11/2014	Bachelor of Science Mathematics, *Eberhard-Karls-Universität, Tübingen*
10/2010 – 05/2014	Bachelor of Science Biochemistry, *Eberhard-Karls-Universität, Tübingen*
08/2002 – 06/2010	Abitur, *Trave-Gymnasium, Lübeck*

Experience

04/2022 – 09/2022	Researcher in the Financial Mathematics Group, *TU Kaiserslautern*
10/2018 – 03/2022	Research assistant, *TU Kaiserslautern*
01/2012 – 04/2013	Student assistant (intermittently), *Eberhard-Karls-Universität, Tübingen*

Wissenschaftlicher und Beruflicher Werdegang

Ausbildung

10/2018 – 11/2022	Doktorandin bei Prof. Dr. Jörn Sass, *TU Kaiserslautern*
04/2015 – 02/2018	Masterstudium Mathematik, *TU Kaiserslautern*
10/2011 – 11/2014	Bachelorstudium Mathematik, *Eberhard-Karls-Universität, Tübingen*
10/2010 – 05/2014	Bachelorstudium Biochemie, *Eberhard-Karls-Universität, Tübingen*
08/2002 – 06/2010	Abitur, *Trave-Gymnasium, Lübeck*

Erfahrung

04/2022 – 09/2022	Wissenschaftliche Mitarbeiterin in der AG Finanzmathematik, *TU Kaiserslautern*
10/2018 – 03/2022	Wissenschaftliche Hilfskraft, *TU Kaiserslautern*
01/2012 – 03/2013	Studentische Hilfskraft (mit Unterbrechungen), *Eberhard-Karls-Universität Tübingen*